

Synthesis and Characterization of Calixarene-Based Supramolecular Frameworks

by

Philip Osborne Brown

B.Sc. (Highest Honours), *Carleton University*, 2000

A THESIS SUBMITTED in PARTIAL FULFILLMENT of the REQUIREMENTS for
the DEGREE of DOCTOR of PHILOSOPHY

in

THE FACULTY of GRADUATE STUDIES and RESEARCH

DEPARTMENT of CHEMISTRY

CARLETON UNIVERSITY

OTTAWA, CANADA

September 2006

© Copyright

Philip Osborne Brown, 2006



Library and
Archives Canada

Bibliothèque et
Archives Canada

Published Heritage
Branch

Direction du
Patrimoine de l'édition

395 Wellington Street
Ottawa ON K1A 0N4
Canada

395, rue Wellington
Ottawa ON K1A 0N4
Canada

Your file *Votre référence*
ISBN: 978-0-494-18210-9
Our file *Notre référence*
ISBN: 978-0-494-18210-9

NOTICE:

The author has granted a non-exclusive license allowing Library and Archives Canada to reproduce, publish, archive, preserve, conserve, communicate to the public by telecommunication or on the Internet, loan, distribute and sell theses worldwide, for commercial or non-commercial purposes, in microform, paper, electronic and/or any other formats.

The author retains copyright ownership and moral rights in this thesis. Neither the thesis nor substantial extracts from it may be printed or otherwise reproduced without the author's permission.

AVIS:

L'auteur a accordé une licence non exclusive permettant à la Bibliothèque et Archives Canada de reproduire, publier, archiver, sauvegarder, conserver, transmettre au public par télécommunication ou par l'Internet, prêter, distribuer et vendre des thèses partout dans le monde, à des fins commerciales ou autres, sur support microforme, papier, électronique et/ou autres formats.

L'auteur conserve la propriété du droit d'auteur et des droits moraux qui protègent cette thèse. Ni la thèse ni des extraits substantiels de celle-ci ne doivent être imprimés ou autrement reproduits sans son autorisation.

In compliance with the Canadian Privacy Act some supporting forms may have been removed from this thesis.

Conformément à la loi canadienne sur la protection de la vie privée, quelques formulaires secondaires ont été enlevés de cette thèse.

While these forms may be included in the document page count, their removal does not represent any loss of content from the thesis.

Bien que ces formulaires aient inclus dans la pagination, il n'y aura aucun contenu manquant.


Canada

ABSTRACT

The structural and dynamic features of solid-state supramolecular frameworks based on 4-*t*-butylcalix[4]arene, tetrameric resorcinarenes and hexameric resorcinarenes are investigated using a variety of physical methods, including X-ray diffraction (XRD) and solid-state nuclear magnetic resonance (SSNMR) spectroscopy. The complementary features of these techniques allows for detailed studies of how multiple weak interactions can be used to produce new packing schemes that are representative of the hierarchy of forces involved in stabilizing these structures. Through judicious choice of guest, the structural motifs and pseudopolymorphism arising from various combinations of interactions has been systematically investigated.

The inclusion of aliphatic amines in 4-*t*-butylcalix[4]arene gives rise to structural motifs where 3 to 5 guest molecules are enclathrated for each calixarene molecule, with the specific motif tuned for by choice of amine. These motifs are a result of acid-base chemistry of the amines and the calixarene, which results in a reduction in host symmetry. The amines are available as reactive sites, allowing for chemisorption of CO₂, suggesting that this simple host can serve as a suitable building block for producing functional materials.

The amines are also shown to be viable coordinate ligands for Ag⁺ and Zn²⁺, as well as hydrogen bonding partners with solvent molecules. With the metals, the calixarene and certain guests serve as secondary ligands, such that the competition of the various weak interactions in the framework serves to guide the primary coordination sphere. The resulting materials can also be tuned, with removal of the amines allowing

for the production of reduced Ag nanoparticles supported by an unfunctionalized calixarene.

For resorcinarenes, the conformational and configurational flexibility of the host gives rise to a broad range of frameworks. With *C*-methylcalix[4]resorcinarene, acidic conditions and judicious selection of cation and anion gives rise to a family of channelled compounds. Pseudopolymorphism involving simple solvent inclusions allows for the isolation of a guest free form of *C*-methylpyrogall[4]arene. Similarly, enclathration of DMSO by *C*-ethylpyrogall[6]arene gives rise to a channelled 12 guest : 1 host that can be transformed into related pseudopolymorphs through either heating or recrystallization from acetone.

ACKNOWLEDGEMENTS

It's interesting to look at this thesis, and realize that it represents six years of work. So, without further ado, I'd like to thank some of the important people who have made this journey worthwhile.

First of all, I'd like to thank Dr. John Ripmeester for the opportunity to work in such a tremendous group at the NRC, and the guidance on matters scientific and not so scientific he's given me over the years. I also owe many thanks to Drs. Gary Enright and Kostia Udatchin for serving as patient, skilled tutors in the study of X-ray crystallography; Drs. Stephen Lang and Igor Moudrakovski for their assistance regarding solid-state NMR; Dr. Shane Pawsey for his advice regarding NMR in general; and Dr. Dmitriy Soldatov for his insight into metal-organic supramolecular materials and gas adsorption. On the technical side of things, the assistance of both Jamie Bennett and Jeff Farnand was invaluable in keeping things running smoothly.

I'd also like to thank the many students and post-doctoral fellow who have passed through the group, contributing to a lively, diverse group of scientists that were always a pleasure to work with. In particular, I owe considerable debts to fellow students Maria Stancescu and Irene Zuger for keeping good cheer in the office, a tradition that was carried on by Dr. Tara Burchell. I also count myself as fortunate for having had the opportunity to work with Dr. Pierre Desjardins, whose untimely passing was deeply felt.

Finally, I'd like to thank my parents, Ronnie and Jim, for their support throughout my Ph.D. work, and the rest of my life. No matter where I've gone, they've been there.

TABLE OF CONTENTS

TITLE PAGE	i
ABSTRACT	ii
ACKNOWLEDGEMENTS	iv
TABLE OF CONTENTS	v
LIST OF TABLES	ix
LIST OF FIGURES	xi
ABBREVIATIONS AND KEY TO COMPOUND IDENTIFICATION.....	xv
CURRICULUM VITAE.....	xviii

Chapter I: Supramolecular Chemistry and Calixarenes

1. Supramolecular Chemistry	1
Definition	1
Solid-State Supramolecular Chemistry	3
2. A Perspective on Calixarene Chemistry	5
Definition	5
History.....	6
Properties.....	8
Applications.....	11
3. Calixarenes in the Solid-State.....	14
Structural Studies	14
Intermolecular Interactions.....	19
Polymorphism and Pseudopolymorphism.....	22
4. Thesis.....	23
5. References.....	27

Chapter II: Physical Methods

1. Introduction.....	34
2. X-Ray Diffraction (XRD)	36
Crystal Symmetry and the Unit Cell.....	37
Generation of X-rays and the Diffraction Phenomenon	39
SCXRD Structure Solution	41
SCXRD Structure Refinement.....	43
SCXRD in Supramolecular Chemistry	45
Powder X-ray Diffraction.....	46
General Details of SCXRD and PXRD Equipment Used.....	46
3. Solid-State Nuclear Magnetic Resonance (SSNMR) Spectroscopy.....	47
The NMR Phenomenon	48
Key Challenges in SSNMR of Spin $\frac{1}{2}$ Nuclei.....	50
SSNMR of Spin $\frac{1}{2}$ Nuclei in Organic Materials.....	55
High Resolution SSNMR Spectroscopy	62
General Details of SSNMR Equipment Used	64
4. Summary.....	65
5. References.....	65

Chapter III: Alkylamine Clathrates of 4-<i>t</i>-butylcalix[4]arene	
1. Abstract.....	68
2. Introduction.....	69
3. Experimental Section.....	71
4. Results and Discussion.....	77
Polar Clusters: <i>n</i> -butylamine and amylamine	77
Polar Layers: hexylamine and dodecylamine.....	88
Pseudopolymorphism arising from Amine Polar Clusters and Layers	93
CO ₂ Adsorption by <i>n</i> -butylamine clusters in 4tBC4A.....	109
5. Conclusion	119
6. References	121
Chapter IV: The role of secondary interactions in guiding structural motifs of alkylamine clathrates of 4-<i>t</i>-butylcalix[4]arene	
1. Abstract.....	125
2. Introduction.....	125
3. Experimental Section.....	128
4. Results and Discussion.....	133
Water in <i>n</i> -butylamine 4tBC4A Clathrates.....	133
Enclathration of Zn <i>n</i> -butylamine Coordination Compounds by 4tBC4A	136
Flexible Coordination in Ag alkylamine 4tBC4A Clathrates	140
Formation of Ag Nanoclusters by Amine Desorption of 4tBC4A Clathrates	150
Ethylene Adsorption by 4tBC4A Supported Ag Nanoclusters	159
5. Conclusions.....	163
6. References.....	165
Chapter V: Isoalkylamine Clathrates of 4-<i>t</i>-butylcalix[4]arene	
1. Abstract.....	170
2. Introduction.....	171
3. Experimental Section.....	174
4. Results and Discussion.....	181
Inclusion of Isopropylamine in 4tBC4A	181
Secondary Coordination and Isopropylamine Ag Complexes.....	183
Enclathration of isobutylamine by 4tBC4A	186
Desorption behaviour of Isobutylamine 4tBC4A Clathrate 3	192
Supramolecular Solid Solutions of isobutylamine-Ag complexes	196
Fully Loaded Isobutylamine-Ag 4tBC4A Frameworks.....	203
Desorption Behaviour of Isobutylamine-Ag Loaded 4tBC4A Frameworks	208
Enclathration of Isoamylamine and Isoamylamine Ag complexes by 4tBC4A... ..	218
5. Conclusions.....	223
6. References	226

Chapter VI: Inclusion of Difunctional Amines in 4-<i>t</i>-butylcalix[4]arene	
1. Abstract.....	230
2. Introduction.....	231
3. Experimental Section.....	234
4. Results and Discussion.....	238
¹³ C SSNMR and SCXRD of 4tBC4A EtDAOH Clathrate 1	238
Desorption Behaviour of 4tBC4A EtDAOH Clathrate 1	249
CO ₂ Adsorption Behaviour of 4tBC4A EtDAOH Clathrate 1.....	255
¹³ C SSNMR and SCXRD of 4tBC4A EtDA Clathrate 3	262
Desorption Behaviour of 4tBC4A EtDA Clathrate 3.....	268
SCXRD of EtDA Ag 4tBC4A Clathrate 5.....	272
¹³ C SSNMR and PXRD Investigation of EtDA Ag 4tBC4A Clathrate 5.....	277
TEM of Ag Nanoclusters derived from Clathrate 5	285
5. Conclusion	287
6. References.....	289
Chapter VII: Organic Cationic Guests in Inorganic Anion/<i>C</i>-methylcalix[4]resorcinarene frameworks	
1. Abstract.....	294
2. Introduction.....	294
3. Experimental Section.....	297
4. Results and Discussion.....	305
Conformational Control of CMCR inclusions of 4,4'-Bipyridinium salts.....	305
Influence of Guest Geometry on Inorganic Anion/CMCR Frameworks	310
Influence of Solvent on Inorganic Anion/CMCR Frameworks.....	315
Thermal Stability of Inorganic Anion/CMCR Frameworks	321
5. Conclusions.....	324
6. References.....	326
Chapter VIII: Host-Guest Chemistry of <i>C</i>-methylpyrogall[4]arene	
1. Abstract.....	328
2. Introduction.....	329
3. Experimental Section.....	330
4. Results and Discussion.....	335
Isolation of the <i>apo rctt</i> PGR by Molecular Recognition.....	335
Isolation of bulk <i>apo rctt</i> PGR.....	339
Inclusion of Viologens in Anionic Frameworks of <i>rctt</i> PGR.....	342
5. Conclusions.....	347
6. References.....	349

Chapter IX: Pseudopolymorphism in Hexameric Pyrogallarenes	
1. Abstract.....	351
2. Introduction.....	352
3. Experimental Section.....	354
4. Results and Discussion.....	356
Single Crystal X-ray Diffraction (SCXRD) Structure of Clathrate 1	356
Structural Studies of Thermal Transformation Product 2a	359
TGA and SCXRD Studies of Recrystallization Product 2b	364
PXRD, SSNMR, and Microscopic Studies of 2b	369
5. Conclusion	372
6. References.....	374

Chapter X: Conclusions and Future Work

1. Supramolecular Frameworks based on 4-<i>t</i>-butylcalix[4]arene	375
2. Supramolecular Frameworks based on Resorcinarenes	377
3. Summary of Contributions	379

LIST OF TABLES

Chapter I: Supramolecular Chemistry and Calixarenes

1. Potential energy of intermolecular interactions in a liquid or gas 21

Chapter II: Physical Methods

1. The seven crystal systems and fourteen Bravais Lattices 38

Chapter III: Alkylamine Clathrates of 4-*t*-butylcalix[4]arene

1. SCXRD data for clathrates 1 to 8 75-76
2. ¹³C CP/MAS NMR spectral data for clathrates 1, 2 and 3 80
3. TGA data for clathrates 1, 2 and 3 95
4. PXRD Unit cell parameters of clathrates 1, 2 and 3 and their deaminated products.... 98

Chapter IV: The role of secondary interactions in guiding structural motifs of alkylamine clathrates of 4-*t*-butylcalix[4]arene

1. SCXRD data for clathrates 1 to 5 131-132
2. Unit cell parameters of 3*(*n*BA):1*(4tBC4A) clathrate and clathrate 1 136
3. TGA data for Ag *n*-butylamine and Ag amylamine clathrates with 4tBC4A 151
4. ¹³C CP/MAS NMR spectral data for clathrates 3 and 6 153
5. PXRD unit cell parameters for clathrates 3 and 6 154
6. Langmuir constants for the adsorption of ethylene on metal loaded β₀ 4tBC4A. 161

Chapter V: Isoalkylamine Clathrates of 4-*t*-butylcalix[4]arene

1. SCXRD data for Clathrates 2, 3, 5 to 11, 14 and 15 177-180
2. ¹³C CP/MAS NMR spectral data for clathrate 1 182
3. TGA data for clathrate 2 186
4. ¹³C CP/MAS NMR spectral data for clathrates 3 and 4 192
5. TGA data for clathrates 3, 7 and 11 193
6. PXRD unit cell parameters for clathrates 3 and its desorption products 196
7. Structural and synthetic parameters of clathrates 5 to 10 200
8. ¹³C CP/MAS NMR spectral data for clathrates 7 and 12 210
9. PXRD unit cell parameters for clathrate 7 and its desorption products 211
10. Unit cell parameters for clathrate 11 and its desorption product clathrate 13 215

Chapter VI: Inclusion of Difunctional Amines in 4-<i>t</i>-butylcalix[4]arene	
1. SCXRD data for clathrates 1, 3 and 5.....	237
2. ¹³ C CP/MAS NMR spectral data for clathrates 1 and 2.....	240
3. Unit cell parameters of 3 (<i>n</i> -butylamine)*1(4tBC4A) clathrate and Clathrate 1.....	245
4. TGA data for clathrates 1, 3 and 5.....	250
5. PXRD unit cell parameters for clathrates 1 and 2.....	253
6. ¹³ C CP/MAS NMR spectral data for clathrates 3 to 6.....	264
7. PXRD unit cell parameters for clathrate 3 and its desorption products.....	271
8. PXRD unit cell parameters for clathrate 5 and its desorption products.....	280
Chapter VII: Organic Cationic Guests in Inorganic Anion/<i>C</i>-methylcalix[4]resorcinarene frameworks	
1. SCXRD data for clathrates 1 to 7	302-304
Chapter VIII: Host-Guest Chemistry of <i>C</i>-methylpyrogall[4]arene	
1. SCXRD data for clathrates 1, 4 and 5 and compound 2.....	333-334
2. PXRD unit cell parameters for compound 2 and clathrate 3	341
Chapter IX: Pseudopolymorphism in Hexameric Pyrogallarenes	
1. SCXRD data for clathrates 1 and 2b.....	356
2. Comparison of unit cell parameters of clathrate 1 and clathrate 2a	361

LIST OF FIGURES

Chapter I: Supramolecular Chemistry and Calixarenes

1. Synthesis of 4- <i>t</i> -butylcalix[4]arene.....	5
2. Synthesis of resorcin[4]arene.....	5
3. Conformations of 4- <i>t</i> -butylcalix[4]arene	9
4. Conformations of C-methylcalix[4]resorcinarene	9
5. Dimensions of the cavity of the cone conformer of 4- <i>t</i> -butylcalix[4]arene.....	10

Chapter II: Physical Methods

1. A schematic diagram of a crystallographic unit cell.....	37
2. Reflection of X-rays from two crystal lattice planes	40
3. Energy level diagram depicting Zeeman splitting of an $I=1/2$ nucleus	48
4. Definition of the the internuclear vector of a ^{13}C - ^1H heteronuclear pair	52
5. Chemical shift anisotropy of a polycrystalline powder	53
6. The effects of CSA in a carbonyl on the observed NMR spectrum.....	54
7. Definition of the magic angle and its role in averaging out CSA.....	58
8. The cross-polarization pulse sequence.....	60
9. Effects of SSNMR methodologies on the spectrum of MeOH-quinol clathrate	63

Chapter III: Alkylamine Clathrates of 4-*t*-butylcalix[4]arene

1. ^{13}C CP/MAS NMR spectra of clathrates 1, 2 and 3.....	78
2. Structure of clathrate 1 as viewed down the a axis.....	81
3. Capped cavity in clathrate 2 as viewed down the a axis.....	86
4. Structure of clathrate 3 as viewed down the a axis.....	91
5. Diagram of H-bonding between host and guest in clathrate 3.....	92
6. Structure of clathrate 4 as viewed down the a axis.....	93
7. ^{13}C CP/MAS spectra of clathrate 1 after heating	96
8. PXRD patterns of clathrate 1 before and after heating	97
9. A view of the 1:1 guest to host clathrate 5 along the a axis	99
10. A view of the 1:2 guest to host clathrate 6 along the a axis.	100
11. ^{13}C CP/MAS spectra of clathrate 2 after heating	103
12. PXRD patterns of clathrate 2 before and after heating	104
13. A view of the 1:2 guest to host clathrate 7 along the a axis	105
14. ^{13}C CP/MAS spectra of clathrate 3 after heating	107
15. PXRD patterns of clathrate 3 before and after heating	108
16. A view of the 1:2 guest to host clathrate 8 along the a axis	109
17. CO_2 adsorption isotherm for nBA 4tBC4A clathrate 1	111
18. ^{13}C CP/MAS spectra of sealed samples of $^{13}\text{CO}_2$ loaded clathrate 1.....	113
19. ^{13}C CP/MAS and HPDEC spectra of sealed sample A of $^{13}\text{CO}_2$ loaded clathrate 1	114
20. ^{13}C CP/MAS SSNMR spectra of desorption of $^{13}\text{CO}_2$ from clathrate 1	118

Chapter IV: The role of secondary interactions in guiding structural motifs of alkylamine clathrates of 4-*t*-butylcalix[4]arene

1. Packing scheme of <i>n</i> -butylamine in the extended cavity of clathrate 1.....	133
2. Packing scheme of clathrate 2.....	138
3. Packing scheme of clathrate 3 as viewed down the <i>a</i> axis	143
4. The infinite hydrogen bonded chain of Ag ⁺ coordination complexes in clathrate 3 ..	144
5. Packing scheme of clathrate 4 as viewed down the <i>a</i> axis	146
6. Packing scheme of clathrate 5 as viewed down the <i>a</i> axis	149
7. ¹³ C CP/MAS spectra of clathrate 3 as synthesized and after heating	152
8. PXRD patterns of clathrate 3 as synthesized and after heating	153
9. Adsorption isotherm of ethylene on Ag loaded β ₀ 4tBC4A	160
10. ¹³ C CP/MAS spectrum of ethylene adsorbed on Ag supported by β ₀ 4tBC4A	162
11. PXRD pattern of ethylene adsorbed on Ag supported by β ₀ 4tBC4A.....	162

Chapter V: Isoalkylamine Clathrates of 4-*t*-butylcalix[4]arene

1. ¹³ C CP/MAS SSNMR spectrum of clathrate 1	182
2. The extended cavity formed by clathrate 2 in the <i>ab</i> plane	184
3. Asymmetric unit of clathrate 3 as viewed perpendicular to the (110) plane	187
4. Hydrogen bonding in clathrate 3 as viewed along the <i>c</i> axis.....	188
5. Packing diagram depicting the primary channel along the <i>c</i> axis in clathrate 3.....	189
6. ¹³ C CP/MAS NMR spectra of clathrate 3 before and after heating.....	191
7. PXRD patterns of clathrate 3 before and after heating.....	195
8. The distribution of amine sites surrounding the Ag ⁺ centre in clathrate 5	198
9. The substitutional disorder in a cross-section of the channels found in clathrate 5 ...	198
10. Unit cell volume versus silver occupancy for clathrates 5 to 10	202
11. <i>Exo</i> amine occupancy versus silver occupancy for clathrates 5 to 10	203
12. The capped cavity containing the [Ag(iBA) ₂] ⁺ complex in clathrate 11	205
13. The capped cavity containing the [Ag(iBA) ₃] ⁺ complex in clathrate 11	205
14. The overall packing scheme of Ag ⁺ complexes in clathrate 11	207
15. ¹³ C CP/MAS NMR spectra of clathrate 7 before and after heating.....	209
16. PXRD patterns of clathrate 7 before and after heating.....	210
17. ¹³ C CP/MAS NMR spectra of clathrate 11 before and after heating.....	214
18. PXRD patterns of clathrate 11 before and after heating.....	215
19. Packing scheme of clathrate 14 as viewed down the <i>a</i> axis	219
20. Packing scheme of clathrate 15 as viewed down the <i>a</i> axis	222

Chapter VI: Inclusion of Difunctional Amines in 4-*t*-butylcalix[4]arene

1. ¹³ C CP/MAS SSNMR spectrum of clathrate 1	240
2. The asymmetric unit of clathrate 1 as viewed down the <i>a</i> axis	242
3. The threefold disorder of one of the <i>exo</i> amines found in clathrate 1	243
4. The ten molecule EtDAOH cluster in clathrate 1 as viewed down the <i>a</i> axis	244
5. The ten molecule EtDAOH cluster in clathrate 1 as viewed down the (011) plane ...	245
6. ¹³ C HPDEC SSNMR spectra of clathrate 1	248
7. ¹³ C CP/MAS SSNMR spectra of the desorption products of clathrate 1	252
8. PXRDs of the desorption products of clathrate 1	253
9. CO ₂ Langmuir-Freundlich adsorption isotherm for clathrate 1	256
10. ¹³ C CP/MAS SSNMR spectra of ¹³ CO ₂ loaded clathrate 1 (aromatic region)	259
11. ¹³ C CP/MAS SSNMR spectra of ¹³ CO ₂ loaded clathrate 1 (aliphatic region)	260
12. ¹³ C HPDEC SSNMR spectra of ¹³ CO ₂ loaded clathrate 1	261
13. ¹³ C CP/MAS SSNMR spectrum of clathrate 3	263
14. Packing scheme of clathrate 3 as viewed along the <i>a</i> axis	265
15. Packing scheme of clathrate 3 as viewed parallel to the (011) plane	266
16. ¹³ C HPDEC SSNMR spectra of clathrate 3	267
17. ¹³ C CP/MAS SSNMR spectra of the desorption products of clathrate 3	270
18. PXRD patterns of clathrate 3 and its desorption products	271
19. Asymmetric unit of clathrate 5	273
20. Packing scheme of clathrate 5 as seen from a view parallel to the (011) plane	274
21. ¹³ C CP/MAS NMR spectra of clathrate 5 and its desorption products	278
22. PXRD patterns for clathrate 5 and its desorption products	280
23. Colour change of bulk samples of clathrate 5 due to heating	282
24. Bright field TEM image of the nanoparticles derived from clathrate 5	286

Chapter VII: Organic Cationic Guests in Inorganic Anion/*C*-methylcalix[4]resorcinarene frameworks

1. The crown and boat conformers of the <i>rccc</i> isomer of calix[4]resorcinarene	296
2. View along the <i>a</i> axis of the primary channel of clathrate 1	306
3. View down the <i>c</i> axis of the secondary channel of clathrate 1	307
4. View down the major channels of clathrate 2	308
5. View down the <i>b</i> axis of guests in channels of clathrate 3	312
6. View down the <i>a</i> axis of guests in channels of clathrate 3	312
7. View down the <i>b</i> axis of guests in channels of clathrate 4	315
8. View down the <i>c</i> axis of guests in channels of clathrate 4	315
9. The primary channel of clathrate 6	317
10. Secondary assembly of guests connecting primary channels in clathrate 6	317
11. Overall packing scheme of clathrate 7	319
12. A perpendicular view of the layering of guests and hosts in clathrate 7	320
13. ¹³ C CP/MAS SSNMR spectra of clathrate 1 and its desolvation product	323
14. PXRD patterns of clathrate 1 and its desolvation product	324

Chapter VIII: Host-Guest Chemistry of C-methylpyrogall[4]arene

1. Packing scheme of clathrate 1.....	336
2. Packing scheme of clathrate 2 viewed along the (011) direction	338
3. ¹³ C CP/MAS NMR spectra of clathrate 3 before and after heating.....	340
4. PXRD patterns of clathrate 3 before and after heating.....	341
5. The hydrogen bonding scheme of clathrate 4 viewed down the <i>b</i> axis	343
6. Channels in clathrate 4 as viewed at 63.9° to the (001) plane	344
7. Channels in clathrate 4 as viewed down the <i>a</i> axis.....	344
8. Alternate layering of clathrate 5 as viewed down the <i>c</i> axis.....	346
9. Alternate layering of clathrate 5 as viewed down the <i>a</i> axis	346

Chapter IX: Pseudopolymorphism in Hexameric Pyrogallarenes

1. Packing scheme of clathrate 1 as viewed down the <i>c</i> axis.....	357
2. View of the secondary channel in clathrate 1	358
3. Crystal chemical unit of clathrate 1 as viewed down the <i>c</i> axis	359
4. PXRD patterns of the thermal conversion of clathrate 1 to clathrate 2a	361
5. ¹³ C CP/MAS NMR spectra comparing clathrate 1 and clathrate 2a.....	363
6. TGAs of clathrate 2a and clathrate 2b	366
7. Packing diagram of clathrate 2b as viewed down the <i>c</i> axis	367
8. Space-filling packing diagram of clathrate 2b.....	368
9. The disordered DMSO and acetone sites in clathrate 2b.....	368
10. ¹³ C CP/MAS spectrum of clathrate 2b.....	369
11. PXRD patterns of clathrate 1 and clathrate 2b	370
12. Microscopic observation of the transformation of clathrate 1 into clathrate 2b.....	372

ABBREVIATIONS AND KEY TO COMPOUND IDENTIFICATION

Common Abbreviations:

α	Dense Form of <i>apo</i> 4- <i>t</i> -butylcalix[4]arene
β	Open Form of <i>apo</i> 4- <i>t</i> -butylcalix[4]arene
σ	Chemical shift
$ F_C $	Calculated structure factor amplitude
$ F_O $	Observed values structure factor amplitude
1,3-BPTU	1,3-bis(3-pyridylmethyl)-(2-thiourea)
6EPGR	ethylpyrogall[6]arene
B_0	Applied magnetic field
CIS	Complexation-induced shift
CMCR	C-methylcalix[4]resorcinarene
CP	Cross polarization
CP/MAS	Cross polarization/magic angle spinning
CSA	Chemical shift anisotropy
CW	Continuous wave
E_{hkl}	Normalized structure factor
<i>endo</i>	Included within the calixarene cavity
EtDA	Ethylenediamine
EtDAOH	Ethanolamine
<i>exo</i>	Found outside the calixarene cavity
F_{hkl}	Crystallographic structure factor
HPDEC MAS	High powered decoupled magic angle spinning
<i>I, S</i>	Nuclear Spin
iAA	Isoamylamine
iBA	Isobutylamine
iPA	Isopropylamine
K_α	Wavelength of X-radiation arising from the drop of an electron from the L shell to the K shell
MAS	Magic angle spinning
PGR	C-methylpyrogall[4]arene
PXRD	Powder X-ray diffraction
R index, R1, wR2	Residual Index
<i>rccc</i>	<i>r-cis, cis, cis</i>
<i>rcct</i>	<i>r-cis, cis, trans</i>
<i>rectt</i>	<i>r-cis, trans, trans</i>
<i>rtct</i>	<i>r-trans, cis, trans</i>
<i>r-tctct</i>	<i>r-trans, cis, trans, cis, trans</i>
SCXRD	Single crystal X-ray diffraction
SSNMR	Solid-state nuclear magnetic resonance
TEM	Transmission electron microscopy
TGA	Thermogravimetric analysis
U_{ij}	SCXRD Thermal Parameter

XRD	X-ray diffraction
Z	# of formula units per unit cell
γ	Gyromagnetic ratio
ρ_{calc}	Crystal density calculated from SCXRD data

Key to Compounds by Chapter:

Chapter III: Alkylamine Clathrates of 4-*t*-butylcalix[4]arene

3(*n*-butylamine) *1(4tBC4A) clathrate 1 (KU78)
 3(amylamine)*1(4tBC4A) clathrate 2 (POB14)
 3(hexylamine)*1(4tBC4A) clathrate 3 (POB106)
 3(dodecylamine)*1(4tBC4A) clathrate 4 (JR26)
 1(*n*-butylamine) *1(4tBC4A) clathrate 5 (KU88)
 1(*n*-butylamine)*2(4tBC4A) clathrate 6 (KU81)
 1(amylamine)*2(4tBC4A) clathrate 7 (POB48)
 1(hexylamine)*2(4tBC4A) clathrate 8 (POB45)

Chapter IV: The role of secondary interactions in guiding structural motifs of alkylamine clathrates of 4-*t*-butylcalix[4]arene

3(*n*-butylamine)*2(H₂O)*(4-*t*-butylcalix[4]arene) clathrate 1 (KU79)
 2(Zn²⁺)*7(*n*-butylamine)*(H₂O)*2(Cl⁻)*(4-*t*-butylcalix[4]arene)⁻ clathrate 2 (KU82)
 [Ag(*n*-butylamine)₃]⁺*1(*n*-butylamine)*(4-*t*-butylcalix[4]arene)⁻ clathrate 3 (POB109)
 [Ag⁺(propylamine)₃]⁺*(4-*t*-butylcalix[4]arene)⁻ clathrate 4 (POB65)
 [Ag⁺(amylamine)₂]⁺*1(amylamine)*(4-*t*-butylcalix[4]arene)⁻ clathrate 5 (POB88)

Chapter V: Isoalkylamine Clathrates of 4-*t*-butylcalix[4]arene

Isopropylamine*4tBC4A clathrate 1
 [Ag(isopropylamine)₃]⁺*1(H₂O)*1(4tBC4A)⁻ clathrate 2 (POB34)
 3(isobutylamine)*1(4tBC4A) clathrate 3 (POB78)
 1(isobutylamine)*1(4tBC4A) clathrate 4
 Variably loaded silver-*i*BA 4tBC4A clathrates 5-10 (POB79, 80, 100, 98, 96 and 97)
 Fully loaded silver-*i*BA 4tBC4A clathrate 11 (POB 101)
 1(*i*BA)*1(4tBC4A) Partially Ag Loaded clathrate 12
 1(*i*BA)*1(4tBC4A) Fully Ag Loaded clathrate 13
 3(isoamylamine)*1(4tBC4A) clathrate 14 (POB38)
 [Ag(isoamylamine)₃]⁺*1(isoamylamine)*1(4tBC4A)⁻ clathrate 15 (POB23)

Chapter VI: Inclusion of Difunctional Amines in 4-*t*-butylcalix[4]arene

- 5(EtDAOH)*(4tBC4A) clathrate 1 (POB67)
1(EtDAOH)*(4tBC4A) clathrate 2
5(EtDA)*(4tBC4A) clathrate 3 (POB66)
1(EtDA)*(4tBC4A) clathrate 4
3(EtDA)*0.87(Ag⁺)*(4tBC4A)⁻ clathrate 5 (POB62)
1(EtDA)*Ag*1(4tBC4A) clathrate 6

Chapter VII: Organic Cationic Guests in Inorganic Anion/*C*-methylcalix[4]resorcinarene frameworks

- 1(4,4'-bipyridinium)*1(SO₄²⁻)*1(EtOH)*3(H₂O)*1(CMCR) clathrate 1 (POB25)
1(4,4'-bipyridinium)*2.87(MeCN)*2(H₂O)*2(Cl⁻)*1(CMCR) clathrate 2 (POB 4)
1(*trans*-1,2-bis(4-pyridinium)ethylene)*3(H₂O)*1(H₃O⁺)*(1.5 SO₄²⁻)*1(CMCR) clathrate 3
1(1,3-bis(3-pyridiniummethyl)-(2-thiourea))*4(MeCN)*2(Cl⁻)*1(CMCR) clathrate 4 (POB10)
1(1,3-bis(3-pyridiniummethyl)-(2-thiourea))*2(MeCN)*2(Br⁻)*1(CMCR) clathrate 5 (POB 60)
Synthesis of 8(dimethylammonium)*1(DMF)*4.23(H₂O)*4(SO₄²⁻)*1(CMCR) clathrate 6 (POB 46)
0.5*(4,4'-bipyridinium)*1(4-pyridinium-4'-pyridine)*2.5(H₂O)*2(Br⁻)*(CMCR) clathrate 7 (POB70)

Chapter VIII: Host-Guest Chemistry of *C*-methylpyrogall[4]arene

- 1(1,3-bis(3-pyridylmethyl)-2-thiourea)*1(SO₄²⁻)*1(H₂O)*2(*C*-methylpyrogall[4]arene) clathrate 1 (POB57)
apo form of *rcct* isomer of PGR (compound 2, POB58)
PGR DMF clathrate 3
1(methyl viologen)*2(Cl⁻)*1.5(EtOH)*2.69(H₂O)*1(*C*-methylpyrogall[4]arene) clathrate 4 (POB52)
1(ethyl viologen)*2(Br⁻)*1(MeCN)*2(H₂O)*1(*C*-methylpyrogall[4]arene) clathrate 5 (POB56)

Chapter IX: Pseudopolymorphism in Hexameric Pyrogallarenes

- 12(DMSO)*1(6EPGR) Clathrate 1 (POB91)
6(DMSO)* 1(6EPGR) Clathrate 2a
4.26(DMSO)*(1.74 Acetone)*1(6EPGR) Clathrate 2b (POB99)

CURRICULUM VITAE

EDUCATION

B.Sc., Biochemistry (Highest Honours), Carleton University, Ottawa, ON, (1996- 2000)
Thesis title: "An Investigation of Naphthalimide Derivatives and Bacteriorhodopsin for use in Hybrid Electrochromic Devices."
Supervisor: Professor Wayne Z.Y. Wang

Ph.D. Candidate, Chemistry, Carleton University, Ottawa, ON, (2000-2006)
Supervisor: Adjunct Professor John A. Ripmeester

EXPERIENCE

- 1998 Summer Research Assistant, National Research Council Canada
Supervisor: Adjunct Professor John A. Ripmeester
- 1999-2000 Undergraduate Research Assistant, Carleton University
Supervisor: Professor Wayne Z.Y. Wang
- 2000-2006 Graduate Research/Teaching Assistant, Carleton University
Supervisor: Adjunct Professor John A. Ripmeester
- 2001-2003 NUG Graduate Representative, Chemistry

AWARDS and SCHOLARSHIPS

NSERC Undergraduate Student Research Award, Carleton University, 1999
Dean's Honour List, Carleton University, 1997-2000
Senate Medal for Outstanding Academic Achievement, Carleton University, 2000
NSERC Undergraduate Student Research Award, Carleton University, 2000
Molecular Recognition and Inclusion Scholarship, Carleton University, 2000
NSERC Postgraduate Scholarship, Carleton University, 2000-2002
Ontario Graduate Scholarship, Carleton University, 2002-2003
NRC Graduate Student Scholarship Supplement, Carleton University, 2003-2005
Canada Graduate Scholarship (Doctoral), Carleton University, 2003-2005

PUBLICATIONS

1. Udachin, K.A., Enright, G.D., Brown, P.O., Ripmeester, J.A.
Pseudopolymorphism in the *p*-*tert*-butylcalix[4]arene—*n*-butylamine system:
directing the structural motifs. *Chem. Commun.* **2002**, 2162-2163.

2. Brown, P.O., Enright, G.D., Ripmeester, J.A. Cationic Guests in Extended Anionic *C*-methylcalix[4]resorcinarene-Inorganic Frameworks: Further demonstrating the conformational flexibility of *C*-methylcalix[4]resorcinarene. *J. Supramol. Chem.*, **2002**, *2*, 497-500.
3. Brown, P.O., Udachin, K.A., Enright, G.D., Ripmeester, J.A. Supramolecular Stabilization of Polar Clusters and Layers: Extending the Supramolecular Chemistry of *p-t*-butylcalix[4]arene with H-Bonding and Secondary Coordination. *Chem. Commun.*, **2005**, 4402-4404.
4. Brown, P.O., Enright, G.D., Ripmeester, J.A. Pseudopolymorphism of Ethylpyrogall[6]arene: Investigating the Role of Solvent in Guiding Self-Assembly of 3D Networks. *Cryst. Growth & Des.*, **2006**, *6*, 719-725.
5. Brown, P.O., Enright, G.D., Ripmeester, J.A. Resorcinarene Configuration and Inclusion Behaviour: Isolation of a guest free form of pyrogall[4]arene. *CrystEngComm*, **2006**, *8*, 381-383.
6. Brown, P.O., Udachin, K.A., Enright, G.D., Ripmeester, J.A. Pseudopolymorphism of aliphatic amine/4-*t*-butylcalix[4]arene inclusion compounds: Supramolecular Stabilization as a route to Polar Clusters and Layers. *Chem. Eur. J.*, **2006**, DOI: 10.1002/chem.200600434.
7. Brown, P.O., Enright, G.D., Ripmeester, J.A. Nanocrystalline Ag from Supramolecular Stabilization of Metals in 4-*t*-butylcalix[4]arene Lattices. *Chem. Asian J.*, **2006**, *in press*.

REFEREED PRESENTATIONS

Oral Presentations

1. Brown, P.O., Enright, G.D., Ripmeester, J.A. "Extended Ionic Frameworks: Demonstrating the conformational flexibility of *c*-methylcalix[4]resorcinarene." *The 85th Conference of The Canadian Society for Chemistry, Vancouver, BC, Canada, June 4, 2002*.
2. Brown, P.O., Enright, G.D., Udachin, K.A., Ripmeester, J.A. "Anionic and Neutral Frameworks: Self-Assembly Motifs of Resorcinarene and Pyrogallolarene." *The 87th Conference of The Canadian Society for Chemistry, London, ON, Canada, June 1, 2004*.

Poster Presentations

1. Brown, P.O., Udachin, K.A., Enright, G.D., Ripmeester, J.A. "Polar Clusters and Layers—Extending the chemistry of *p-t*-butylcalix[4]arene with amines." *The 35th International Conference on Coordination Chemistry, Heidelberg, Germany, July 23, 2002*.
2. Brown, P.O., Enright, G.D., Ripmeester, J.A. "Organic Ionic Frameworks: Investigations of the Inclusion Properties of Calixresorcinarenes and Pyrogallolarenes." *The 39th IUPAC Congress and the 86th Conference of The Canadian Society for Chemistry, Ottawa, ON, Canada, August 14, 2003*.

3. Brown, P.O., Enright, G.D., Udachin, K.A., Ripmeester, J.A. "Supramolecular Stabilization in Calixarene Frameworks." *Frontiers in Materials Research Workshop, Vina del Mar, Chile, April 27, 2004.*
4. Brown, P.O., Udachin, K.A., Enright, G.D., Ripmeester, J.A. "Supramolecular Stabilization of Polar Clusters and Layers in 4-*t*-butylcalix[4]arene Frameworks." *The 13th International Symposium on Supramolecular Chemistry (ISSC XIII), South Bend, IN, USA, July 25, 2004.*
5. Brown, P.O., Enright, G.D., Udachin, K.A., Ripmeester, J.A. "Directing the inclusion motifs in 4-*t*-butylcalix[4]arene through hydrogen bonding and secondary coordination." *The 2005 International Chemical Congress of Pacific Basin Societies (Pacifichem 2005), Honolulu, HI, USA, December 18, 2005.*

Chapter I: Supramolecular Chemistry and Calixarenes

1. Supramolecular Chemistry	1
Definition	1
Solid-State Supramolecular Chemistry	3
2. A Perspective on Calixarene Chemistry	5
Definition	5
History	6
Properties	8
Applications	11
3. Calixarenes in the Solid-State	14
Structural Studies	14
Intermolecular Interactions	19
Polymorphism and Pseudopolymorphism	22
4. Thesis	23
5. References	27

1. Supramolecular Chemistry

Definition

Supramolecular chemistry is an incredibly dynamic field of study, encompassing a broad range of topics with roots in traditional organic, inorganic and physical chemistry, as well as biochemistry.^[1, 2] At its simplest, it is chemistry beyond the molecule, involving the study of assemblies of molecules through the use of non-covalent intermolecular interactions.^[1] By making use of hydrogen bonding, ionic interactions, coordinate bonds, and the various weak forces classed collectively as non-directional van der Waals interactions, the resulting supramolecular compounds not only serve to further our understanding of the roles of these weak forces in directing structures, but also have intriguing functional properties, such as serving as catalysts, storage materials, or receptors capable of recognizing specific substrates.^[3, 4] Such materials would mirror those found in nature, with biological macromolecules such as proteins proving to be excellent expressions of the power of supramolecular chemistry to produce functional

structures suitable for use as catalysts, structural elements and selective hosts for storing molecules of interest.^[5]

The modern study of supramolecular chemistry as a distinct field only dates back to the 1960s and 70s, arising out of Pedersen's studies of crown ethers,^[6] Cram's investigations of carcerands and spherands,^[7] and Lehn's studies of carcerands.^[8] However, many aspects of supramolecular chemistry actually trace their roots back much further. The study of clathrate hydrates began with Davy's discovery of chlorine hydrate in 1811,^[9] while the origins of supramolecular metal-organic frameworks can be traced back to Werner's studies of coordination compounds.^[10-12] In the realm of organic chemistry, systematic studies of common cyclic host molecules such as cyclodextrins date back to the 1930s (with the molecules themselves being first discovered in 1891).^[13]

Despite these diverse origins in both solution based and solid-state chemistry, collectively these systems represent a different direction from traditional molecular-oriented chemistry. In describing supramolecular chemistry, Lehn noted that "supermolecules are to molecules and the intermolecular bond what molecules are to atoms and the covalent bond."^[8] Much as the maturation of organic chemistry has involved controlling the formation and breakage of covalent bonds, the rational design of supramolecular structures is dependent on being able to predictably control intermolecular interactions in designing a given framework. With modern instrumental techniques, such as NMR and XRD, it has been possible to characterize the structures arising from such interactions, and thereby begin to produce materials with desirable properties.

Solid-State Supramolecular Chemistry

As suggested above, given the incredibly broad nature of supramolecular chemistry, a number of sub-fields have developed almost in isolation of one another. One primary division is that between solution-based assemblies (which are products of equilibrium thermodynamics) and solid-state structures (which arise from a more complex combination of kinetic and thermodynamic factors). Because of these differences in origin, larger, infinite structures based on weak interactions between organics are much more accessible in the field of crystal engineering^[14] than in solution,^[15] as solvent will frequently interfere and disrupt such assemblies (although certain organic compounds have been observed to form large capsules in solution similar to those observed in the solid-state^[16-19]). Most importantly, however, the structures of crystalline compounds can be readily determined using XRD, thereby giving us direct insight into the forces governing the assembly of such structures by presenting the experimenter with a picture representing the final result of the crystallization process, and the balance between kinetic and thermodynamic parameters it represents.

Current research into solid-state supramolecular systems can be readily divided into three broad areas: inorganic, metal-organic, and organic supramolecular compounds. As mentioned above, each of these areas trace their roots back to clathrate hydrate chemistry, coordination chemistry and host-guest chemistry. The inorganic frameworks are among the best known of these systems, with the zeolites^[20, 21] and clathrate hydrates^[22, 23] representing typical compounds in this class, and receiving considerable attention due to their roles in industry as adsorbents, storage materials, and (in the case of

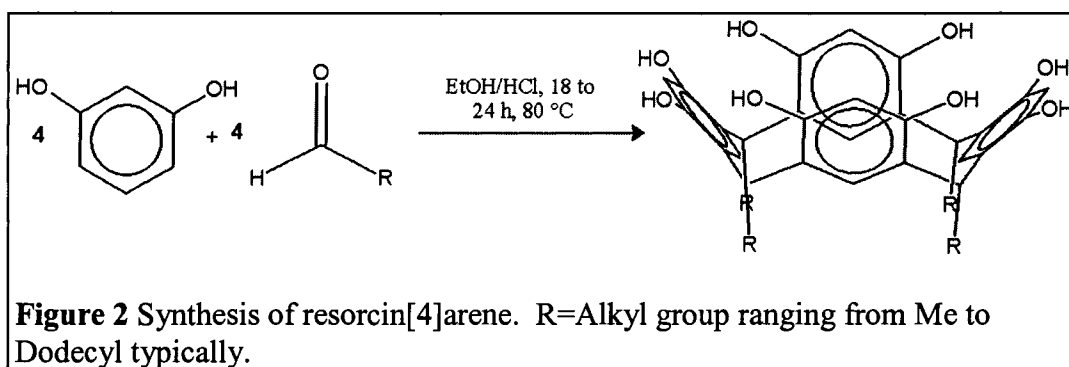
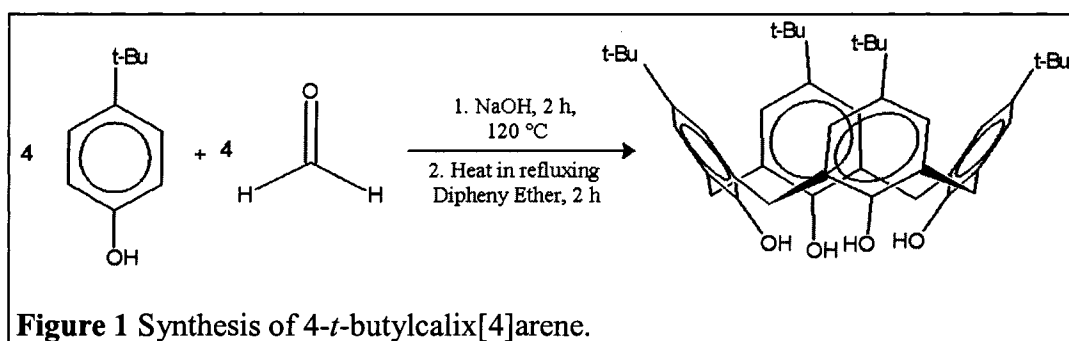
hydrates) undesirable by-products of industrial processes. Similarly, the metal-organic frameworks^[24-27] have risen to considerable prominence, with the advent of molecular tectonics as a method to design various net-like porous materials that mimic the zeolites, such that they have potential applications as adsorbents and catalysts.

In the case of organic frameworks, a broad range of supramolecular compounds has been reported. As hinted at above, the precise control over the structure of an organic compound allows for custom tailoring of a given molecule to include moieties capable of directing the assembly of a structure in the solid-state. In general, the hydrogen bond has proven to be the most readily directed interaction,^[15] based on the inclusion of hydroxyl and amino functionalities, as well as various carbonyl moieties. The versatility offered by such a range of compounds make them ideal for investigating the forces guiding self-assembly, with compounds such as ureas,^[28, 29] tri-*o*-thymotide,^[30, 31] tris(5-acetyl-3-thienyl)methane,^[32-34] and dipeptides^[35-37] forming a broad range of inclusion compounds. In addition to these small molecules, macrocyclic organic systems are particularly prominent in inclusion chemistry, with the calixarenes^[3, 4, 38, 39] having proven to have an exquisite balance of non-directional and directional intermolecular forces guiding the formation of clathrates by these compounds. These properties make them ideal targets for both investigating the balance of intermolecular forces guiding the formation of such compounds, as well as designing functional materials.^[3, 4]

2. A Perspective on Calixarene Chemistry

Definition

The calixarenes are a family of macrocyclic compounds synthesized through the condensation of a phenol with an aldehyde, either through a base catalyzed^[40, 41] (see Figure 1) or acid catalyzed process^[42-44] (see Figure 2).



The number of aromatic units composing the macrocycle varies between 4 and 8, depending on reaction conditions, giving rise to a broad range of cavity sizes. While calixarenes can potentially assume a number of different conformations, the name “calixarene” itself was coined by Gutsche due to the resemblance of the common cone conformer of the cyclic tetramer to a Greek calix crater vase.^[45, 46] With the discovery of the larger hexamers and octamers, as well as substituted calixarenes, this nomenclature was further expanded such that reference was made to both the size of the macrocycle

through the insertion of a number in square brackets, and the insertion of a reference to any groups appended to the calixarene itself. As such, the tetrameric product arising from the base catalyzed condensation of *p-tert*-butyl phenol and formaldehyde is generally referred to as either *p-tert*-butylcalix[4]arene or 4-*tert*-butylcalix[4]arene.

A similar system is used to describe the products arising from acid catalyzed condensations of resorcinols and aldehydes, with the prefix 'C-' used to indicate the substitution at the bridging carbon between phenol rings, and the name of the original resorcinol incorporated into the calixarene name, such that they are referred to as resorcinarenes. Therefore, the tetrameric product arising from acid catalyzed condensation of resorcinol and acetaldehyde is known formally as C-methylcalix[4]resorcinarene. In both cases, the research community, in preference to the burdensome systematic names for such compounds,^[47] has adopted this nomenclature.

History

The discovery of the calixarenes illustrates the intimate connection between physical characterization and innovative syntheses in providing a full understanding of host-guest chemistry (and therefore supramolecular chemistry). The early history of calixarene chemistry has been covered in a number of excellent reviews and monographs.^[38, 46, 48-50] As a result, what follows is only a brief overview of the early developments as they relate to emergence of these compounds as supramolecular hosts, with a particular focus on the simple parent compounds that have lent themselves to investigations of the role of various intermolecular forces in guiding the structures of calixarene clathrate compounds.

The development of phenol-aldehyde chemistry began with Bayer's preparation of polymeric resins through acid catalyzed condensation of the two starting materials in the 1870s.^[51, 52] The inability to characterize these materials, however, caused this area of chemistry to be marginalized until it was revisited by Baekeland in the early 1900s, and the introduction of the phenolic resin derived from a based catalyzed condensation reaction known as Bakelites.^[53] However, once again the resinous nature of the compounds precluded any detailed structural characterization. It was not until the 1940s, when attempting to examine in more detail the process used to produce the Bakelites, that Zinke investigated the base-catalyzed reaction of para-substituted phenols, which surprisingly gave rise to a crystalline product.^[54, 55] At the same time, studies by Niederl and Vogel indicated that acid catalyzed reaction of resorcinols gave rise to similar crystalline products.^[42]

Both of these groups postulated that these compounds were in fact cyclic tetramers, based on the reactivity of the compounds. A step-wise synthesis of a cyclic tetramer by Hayes and Hunter in 1950s subsequently demonstrated that such a structure was feasible,^[56, 57] while Cornforth's crystallographic studies subsequently indicated that the compounds produced by Zinke were clearly cyclic compounds (although the assertion that only the cyclic tetramer was produced was not correct).^[58, 59] It was not until the chemistry of these compounds was revisited 1970s by Gutsche that it became clear that while the base catalyzed condensation of phenols with aldehydes gives rise to cyclic products, the size of the macrocycle is heavily dependent on the base concentration.^[60, 61] Finally, in 1979, Andreetti, Ungaro and Pochini published the first single-crystal X-ray

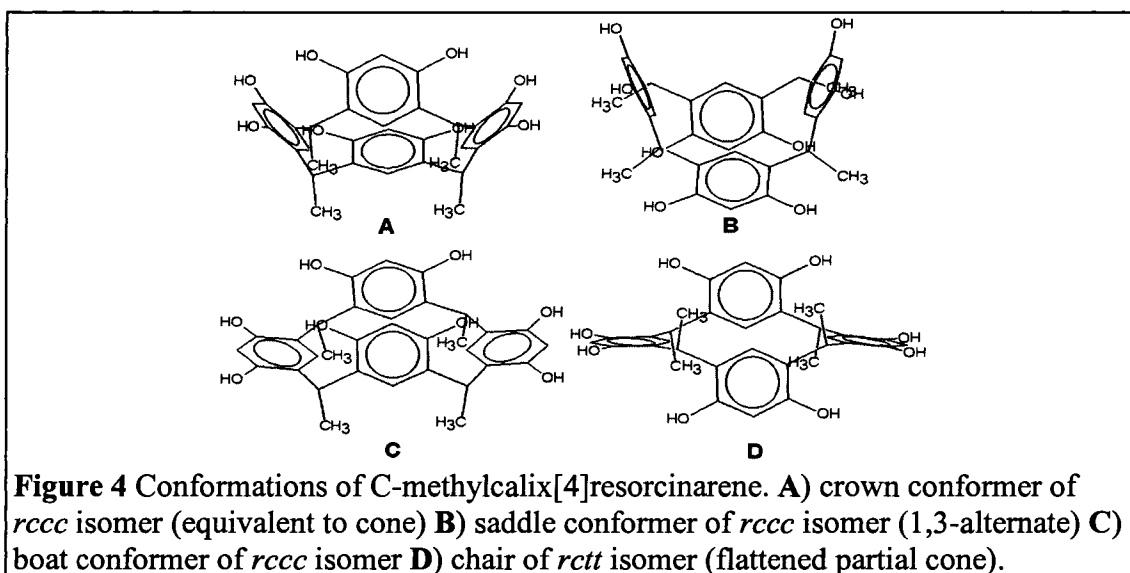
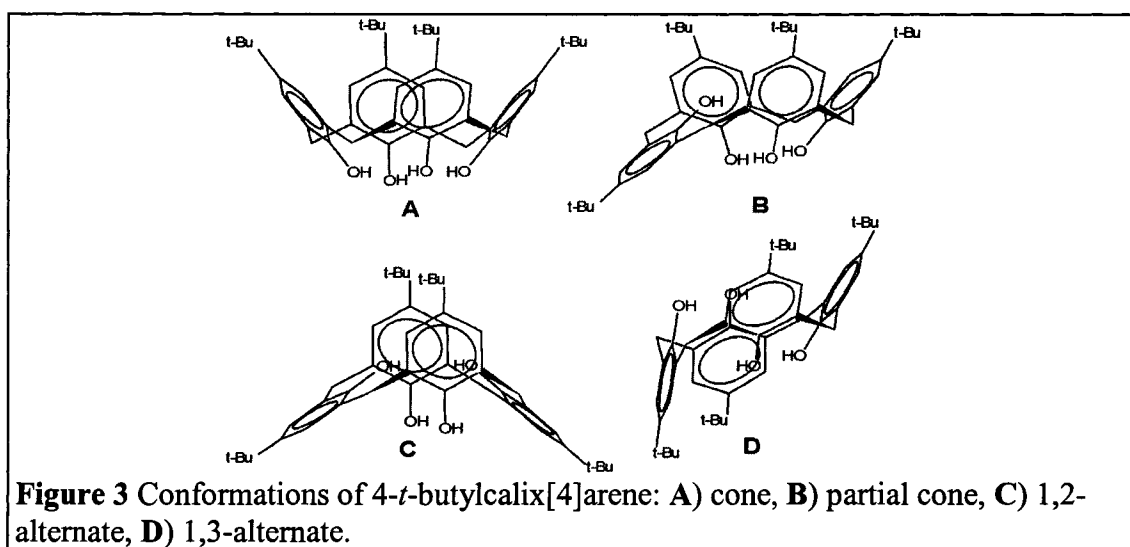
diffraction structure of 4-*t*-butylcalix[4]arene, serving as a host to toluene.^[62] In contrast with this, the initial X-ray studies of derivatives of the products of acid catalyzed condensations of aldehydes and resorcinols occurred in the late 1960s.^[63] Systematic studies of the resorcinarenes in general were not carried out until the 1980s, when Högberg revisited the chemistry of these compounds, and made use of solution NMR studies to elucidate the structures of the parent compounds.^[43, 44]

Properties

As noted above, calixarenes are readily produced through one-pot syntheses, with the specific reaction conditions serving to determine the exact size of the calixarene obtained. The resulting crystalline solids range in colour from white (for the 4-*t*-butylcalixarenes) to light yellow (for the calixresorcinarenes), and decompose at temperatures greater than 300°C. The resulting macrocycles in general exhibit reduced solubilities when compared to the phenolic starting materials from which they are derived.

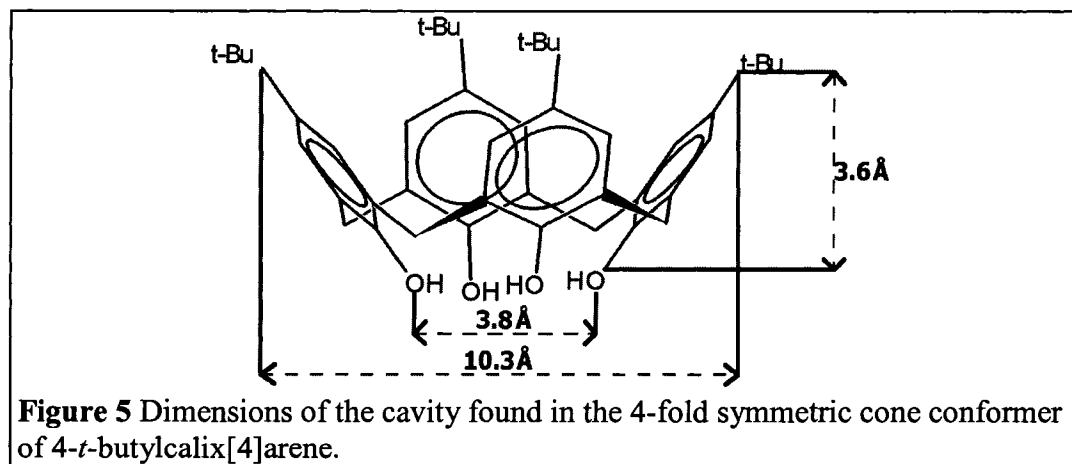
The initial structural investigations of calixarenes in solution, making use of ¹H NMR spectroscopic studies, clearly indicated that the macrocycles exhibited a high degree of conformational flexibility.^[64-66] For 4-*t*-butylcalix[4]arene, four common structural isomers are observed: cone, partial cone, 1,2-alternate, and 1,3-alternate (see Figure 3). A similar situation is observed for the resorcinarenes,^[43, 44, 67] with the increased flexibility of the calixarene also allowing for the aromatic rings to assume planar conformations as well (see Figure 4). The introduction of substitutions on the linking methylene group also introduces the potential for configurational isomers based

on the positions of the substituents, such that *r-cis, cis, cis* (*rccc*), *r-cis, cis, trans* (*rcct*), *r-cis, trans, trans* (*rctt*) and *r-trans, cis, trans* (*rtct*) stereoisomers are possible for the tetramer. In practice, only the *rccc* (Figures 4A-C) and *rctt* isomers (Figure 4D) of resorcinarene tetramers are obtained in large quantities, with the *rccc* isomer being the form generally studied in the literature due to its analogous cavity structure to the base synthesized calixarenes.



For 4-*t*-butylcalix[4]arene and the *rccc* isomer of C-methylcalix[4]resorcinarene, the cone (crown) conformer is the favoured form,^[44, 68] due to the stabilization offered by hydrogen bonding between the phenolic hydroxyl moieties.

The key feature of interest in the most common conformations of both the calixarenes and resorcinarenes is the bowl shaped cavity capable of including a variety of guests. In both cases, the cavity has two openings, with the one at the lower rim being considerably smaller than the one at the upper rim. For the four-fold symmetric 4-*t*-butylcalix[4]arene, the opening at the upper rim is 10.3 Å wide, while the opening at the base is 3.8 Å in diameter, resulting in a hydrophobic cavity 3.6 Å deep (see Figure 5). Crown conformers of resorcinarenes possess similar dimensions, with the hydrogen bonding scheme at the upper rim resulting in asymmetric openings for many inclusion compounds (typical dimensions are 9.6 Å by 6.2 Å for the upper opening, 4.9 Å by 5.3 Å for the lower opening, with the cavity being approximately 3.8 Å deep).



The structures of both the *para*-substituted calixarenes and resorcinarenes contain a number of different sites suitable for post-synthetic modification. For the *para*-substituted calixarenes, the key sites are the *para* carbon on the upper rim of the

calixarene, and the phenolic hydroxides at the base. Upper rim modifications can be carried out using various methods,^[69] thereby introducing a wide range of potential functionalities, such as nitro groups,^[70, 71] sulfonato groups,^[72-74] iodo groups^[75] (which can be used to introduce aryl,^[76] alkynyl^[75] and carboxyalkyl groups^[77]), and acyl derivatives.^[78] Similarly, these sites can be used to introduce other supramolecular receptors, such as substituent macrocycles^[79-81] capable of binding cationic metal centres. Lower rim modifications at the phenolic hydroxide are much more common, as in addition to adding functionalities of interest (such as crown ethers,^[82-84] esters,^[85] amides,^[85] thioureas,^[86] sulfonates^[87] and alkyl chains^[88]) through more efficient alkylation and acylation chemistry, they can also be used to fix the conformation of the calixarene in solution.^[89, 90]

Functionalization of resorcinarenes is typically limited to changes in the methylene linker arising from judicious selection of the aldehyde during the initial synthesis, and alkylation and acylation of the phenolic hydroxides on the upper rim.^[91-97] Again, these modifications can be used to conformationally fix the resorcinarene,^[96, 97] as well as introduce binding sites for various cations and metal centres.^[91, 96] In particular, the resorcinarenes have seen repeated use by numerous groups as natural building blocks for producing cavitands through covalent linking of the hydroxyl groups located on the upper rim to each other and various aromatic groups.^[94, 97-100]

Applications

As might be expected from a conformationally versatile and easily modified compound, the calixarenes have proven to be extremely popular molecules for

researchers interested in designing functional materials. A keyword search on “calixarene” using ISI’s Web of Science indicates that over 2000 publications have appeared since the year 2000, while the U.S. Patent and Trademark Office have now granted 82 patents for calixarene-based systems. Therefore, the following is only a brief survey of some of the applications for calixarenes that researchers have investigated, and once again the reader is directed to the various excellent monographs and reviews available for more detailed accounts of the progress of various areas of applied calixarene chemistry.^[3, 4, 38, 39]

One of the principal applications of calixarenes is the binding of cationic species for either separation or detection as part of a sensor. Patents have been issued for modified calixarene systems suitable for the extraction of actinides and lanthanides from aqueous systems for the purposes of treating radioactive waste,^[101] as well as more general metal binding systems.^[102] Similarly, studies have shown that thiacalix[4]crowns can be used to selectively bind Ra-226 cations,^[103] while nitro-functionalized calix[4]arene rhenium(V) complexes have been investigated as potential radiopharmaceuticals.^[104] Calix[4]arene amide derivatives have been used as ionophores in lead sensing electrodes^[105] and other modified calixarenes have been used in Pb optical sensing membranes.^[106] Modified calix[4]arenes supported on Merrifield resin has been demonstrated to be suitable for preconcentrating toxic metals cations such as Cr(VI), As(III) and Tl(I) for the purposes of trace detection from water samples.^[107] This metal binding activity has also prompted research into the potential catalytic activity of calixarene-transition metal complexes, with one such system patented for the purposes of

olefin polymerization.^[108] Resorcinarene based cavitands have also been demonstrated to catalyze the Menschutkin reaction of quinuclidine.^[109]

The applications of calixarenes as receptors suited for extraction of materials also extend to selective binding of organics from various substrates. Calixarene based solid-phase microextractions to detect propranolol enantiomers in human urine have been reported,^[110] as has a system suitable for detection of chlorobenzenes in soil.^[111] Nitrophenylazo-calix[4]arenes have been investigated as chromogenic sensors of gas phase amines.^[112] Conformationally frozen modified calixarenes have also seen use as stationary phases suitable for HPLC separations of purines, pyrimidines and non-steroidal anti-inflammatory drugs.^[113] Finally, a patent has been issued for the use of calixarenes in the removal of carbonyl sulfide from liquid petroleum.^[114]

A number of researchers are also involved in investigating the potential biological applications of calixarenes. Several studies have examined Zn(II) calixarene complexes as potential model systems for enzymatic phosphate diester transesterification,^[115, 116] as well as acyl and phosphoryl transfer reactions.^[117] The biological properties of *p*-sulphonatocalix[*n*]arenes are under active investigation, and show promise as potential anti-thrombotic agents^[118] with minimal hemolytic activity for certain derivatives.^[119] Amphiphilic calix[4]arenes readily form solid lipid nanoparticles which are under investigation as potential drug delivery vehicles,^[120, 121] while the capsular assemblies formed by resorcinarenes might also be suited to stabilization of pharmaceuticals.^[118, 122, 123] The diversity of applications listed makes it apparent how versatile the calixarenes are for the purposes of constructing functional supramolecular materials.

3. Calixarenes in the Solid-State

As indicated by the selection of applications presented, a large number of studies of calixarenes are focused on covalent modification of selected parent compounds to yield materials with desirable properties. In the case of the *para*-substituted calixarenes, this trend has resulted in the essential chemistry of the simple 4-*t*-butylcalix[4]arene to be largely overlooked save by those interested in investigating how weak forces guide inclusion in such macrocycles. In a similar fashion, physical studies of resorcinarenes in the solid state continue to trail their extensive use as building blocks for carcerands (with the prominent exception of studies of capsule formation). As such, the current knowledge base regarding the supramolecular chemistry of calixarenes is heavily coloured by the use of covalently modified systems to effectively restrict the intermolecular interactions guiding supramolecular self-assembly, thereby negating several of the advantages of the self-assembly approach to designing materials (such as avoiding complex organic syntheses). If rational design of calixarene supramolecular systems relying extensively on intermolecular forces is to become a reality, more thorough physical investigations of self-assembled calixarene systems relying upon multiple interactions are called for.

Structural Studies

The study of calixarene clathrates in the solid state presents considerable challenges to physical chemists. While the initial single crystal X-ray study of toluene inclusion in 4-*t*-butylcalix[4]arene by Andreetti, Ungaro and Pochini^[62] clearly established that the calixarenes as molecular hosts, it (along with subsequent studies of

other simple guests) also highlighted a number of the difficulties involved in such studies. In particular, it demonstrated how the disorder inherent to many host-guest compounds makes it quite difficult to assess the role of specific intermolecular interactions in stabilizing a clathrate compound.

In the case of the toluene inclusion complex of 4-*t*-butylcalix[4]arene, the disorder of both the guest and the host presented serious challenges to understanding the forces governing the inclusion complex. The toluene was observed to be disordered over two positions, such that the four-fold symmetry of the host was maintained, while the *tert*-butyl groups on the calixarene itself exhibited a less readily understood disorder. The resulting *R*-value of the structure (the measure of the agreement of the structural model to the diffraction intensities^[124]) was 0.092. Brouwer^[125] notes that this tendency towards large *R*-values due to disorder in both the host and guest is common amongst the high symmetry *para*-substituted calixarene compounds.^[126-134] Guest disorder is also observed in many of the resorcinarene inclusions reported in the literature.^[16, 19, 135-140]

It was not until more rigorous studies involving complementary physical techniques that many of the structural features of this first calixarene inclusion compound were resolved. Solid state NMR spectroscopic studies by Facey *et al.*^[141] and Brouwer *et al.*^[142, 143] revealed that the disorder in the toluene inclusion compounds of 4-*t*-butylcalix[4]arene at room temperature is the result of molecular motion of the toluene between two positions giving rise to a local two-fold symmetry of the calixarene, which is subsequently spatially averaged to give rise to the observed four-fold symmetry of the XRD structure. At low temperatures, solid state NMR indicated this local disordering

ultimately gives rise to a shift to a highly twinned monoclinic structure involving dynamic disordering, but the observation of this shift through crystallography exhibited a disturbing dependence on the wavelength of radiation used to obtain the structure.^[144] Ultimately, these studies have highlighted the strengths of both of these techniques in probing both the long range and short range ordering of the structure, such that a more accurate model for the inclusion behaviour of the calixarene was reached.

The 4-*t*-butylcalix[4]arene system has subsequently been used to probe the relative importance of various structural factors in guiding the inclusion of guest molecules. The inclusion behaviour of acetone mirrors that of toluene,^[133, 145] as do the clathrates formed with a variety of other guests, such as chloroform,^[146] benzene,^[147] and DMSO.^[148] Of particular note, the inclusion behaviour of a broad range of aliphatic hydrocarbon guests has also been examined in some detail.^[125, 143, 149] In this case, the length of the hydrocarbon chain serves to determine whether a 1 guest : 1 host or 1 guest : 2 host inclusion motif is favoured, with the inclusions shifting to the 1:2 motif for guests larger than pentane.^[149] In both cases, however, the four-fold symmetry of the calixarene host is maintained.

By and large, these systems can be treated as discrete host-guest systems with no extended structure. This is largely a consequence of the high symmetry of the calixarene, for which the most energetically favourable packing arrangement is the formation of *endo* inclusions. However, studies have show that with the disruption of the host symmetry, other more complex structural motifs will emerge. Nitrobenzene forms a 1 guest : 1 host inclusion that crystallizes in the orthorhombic $Pc2_1n$ space group, a result of the off-axis,

static positioning of the guest in order to accommodate the bulk of the nitro group.^[127] This inclusion motif can be tuned through exchange with gaseous guests, such that the symmetry of the calixarene is restored by effectively forcing the nitrobenzene to align with the calixarene molecular axis.^[128] Thus, while the symmetry of the host is disrupted, no extended framework is imposed.

This is not the case for the inclusion of 1,3-butanediamine in 4-*t*-butylcalix[4]arene, where presumed proton transfer from the calixarene to the amine inherently disrupts the symmetry of the calixarene, giving rise to a 3 guest : 1 host inclusion compound.^[130] The amines both hydrogen bond to each other and the calixarenes, such that an infinite framework results, while still being arranged such that one of the amines is also stabilized by inclusion in the calixarene. This makes the system the first example of competition between hydrogen bonding and the van der Waals interactions which dominate the earlier, symmetrical inclusion compounds of 4-*t*-butylcalix[4]arene, suggesting that such competition might be a route to obtaining structurally complex inclusion compounds with a simple host. More recently, similar effects have been reported for the inclusion of fluorobenzenes, where electrostatic interactions compete with the non-directional van der Waals interactions.^[150]

The investigations of resorcinarenes, in contrast, have followed different lines of inquiry. Following the early studies of Högberg, the investigations of Atwood and MacGillivray determined that the hydroxyl groups on the crown conformer of C-methylcalixresorcin[4]arene could be used to non-covalently bind groups to extend the cavity of the resorcinarene to produce inclusion compounds.^[137, 138] By making use of

bipyridines and pyridines, researchers have demonstrated that the cavities of simple resorcinarenes could be expanded to accept a variety of guests, including nitrobenzene,^[16] acetonitrile,^[138] ferrocenes,^[151] and alkyl substituted benzenes.^[152] These compounds exhibit a mixture of discrete capsular assemblies, and wave like polymers, depending on the specific guest and non-covalent linker.

Bipyridines have also been shown to be a route to exploiting the conformational flexibility of C-methylcalixresorcin[4]arene in the solid state. Studies by Coppens *et al.* ultimately demonstrated that bipyridines could also be used to induce conformational shifts in C-methylcalixresorcin[4]arene,^[153] leading to brick wall type supramolecular compounds capable of enclathrating guests such as benzil^[135] and benzophenone.^[154] Much as with 4-*t*-butylcalix[4]arene, the distortion of the host's geometry allows for the formation of multidimensional supramolecular frameworks, although with the elimination of the calixarene cavity, the competition of forces is now between differing hydrogen bonding partners. Similar distortions have been reported for the inclusion of cationic guests in resorcinarenes, where the competition between ionic interactions and hydrogen bonding prompts distortion of the host molecule to yield tubular^[140] and channelled structures.^[19] These developments have been mirrored in the most recent studies of pyrogallarenes, such as the investigations of large capsular assemblies,^[155-157] but further complexity is introduced by the ability to readily access other isomers than the common all-*cis* isomer.^[158-160]

Thus, while the calixarenes are traditionally known for their abilities as receptors, forming discrete inclusion complexes, the potential exists for more complex

supramolecular structures to be based on these receptors. In particular, the studies of both 4-*t*-butylcalix[4]arene and C-methylcalix[4]resorcinarene indicate that the delicate interplay of various directional and non-directional forces can be used to produce quite complex frameworks. With appropriate guest molecules, not only should such frameworks be highly tunable and versatile, sidestepping the disadvantages of covalently modified systems, they would also represent a convergence of the drive to produce functional materials and the need to more fully understand how intermolecular interactions guide self-assembly processes with well-known host molecules.

Intermolecular Interactions

In the solid state, various intermolecular interactions serve to guide the structure of an inclusion compound, such that the structure can be seen as a representation of the balancing of these forces such that an energetic minimum is reached in terms of the enthalpy and entropy of the system. In other words, despite their weakness when compared to covalent bonds, collectively these interactions ultimately determine the structure of a crystalline solid. One of the strengths of calixarenes as supramolecular systems is the ability to examine the influence of nearly any intermolecular interaction on the inclusions they form.

Hydrogen bonding is by far the most commonly used intermolecular interaction in the supramolecular chemistry of organic compounds. Typically, a hydrogen bond can be treated as a special sub-class of electrostatic interaction. The proton on an electronegative atom is attracted to an adjacent electronegative atom, such that the resulting interaction is both highly directional and quite strong (bond energy of 16-60

kJ/mol). The resulting broad array of geometries allowed by such an interaction is key in nature, where it guides both the assembly of proteins and nucleic acids. For the calixarenes, it is particularly prominent in guiding the assembly of resorcinarenes, where, as noted previously, it has been used to bind pyridyl moieties suitable for extending the cavities of these compounds such that they can accommodate larger guests.

Related to the hydrogen bond are ion-ion interactions, which typically range in energy from 100-350 kJ/mol, and can be described by Coulomb's law, such that the strength of the interaction varies inversely with the distance between the two ions (see Table 1). While strong ionic interactions, such as those observed in alkali salts are more properly seen as equivalent to covalent interactions (and therefore not supramolecular in nature), weaker interactions between an anionic host molecule and a cationic guest are also possible.^[2] Similarly, a charged ion can interact favourably with a dipole, giving rise to an interaction that falls off according to the square of the distance between the two.

While strong interactions have dominated the chemistry of the heavily modified *para*-substituted calixarene receptors (such as the ionophores), as well as of the resorcinarenes, the basic studies of calixarene inclusion behaviour for 4-*t*-butylcalix[4]arene have typically involved guests incapable of such interactions. In such studies, various weaker interactions serve to dominate the structural motifs of the calixarene inclusion compounds. These include dipole-dipole interactions, dipole-induced dipole interactions and induced dipole-induced dipole interactions (see Table 1).

Dipole-dipole interactions come into play when two polar molecules are close enough together that they are attracted to each other such that the dipoles become

aligned. Mathematically, such an interaction varies directly with the dipole moments of the two molecules, and inversely with respect to the distance raised to the sixth power. A dipole can also induce a temporary dipole in an adjacent molecule, giving rise to an attractive force which varies directly with the dipole moment of the first molecule and the polarizability of the second molecule, and again inversely with respect to the distance raised to the sixth power. Finally, two molecules can experience temporary alignment due to instantaneous dipoles, with the forces involved estimated by the London equation.

Table 1 Equations describing the average potential energy associated with various intermolecular interactions in a liquid or gas.

Interaction ^[a]	Energy	
Charge-Charge	$E_{C-C} = \left(\frac{1}{4\pi\epsilon_0} \right) \left(\frac{q_1 q_2}{r} \right)$	q ₁ , q ₂ = Point charges ε ₀ = Vacuum Permittivity r = Separation distance
Dipole-Charge	$E_{D-C} = - \left(\frac{1}{4\pi\epsilon_0} \right) \left(\frac{\mu_1 q_2}{r^2} \right)$	q ₁ = Point charge μ ₂ = Dipole moment ε ₀ = Vacuum Permittivity r = Separation distance
Dipole-Dipole ^[b]	$E_{D-D} = - \frac{2}{3kT} \left(\frac{\mu_1 \mu_2}{4\pi\epsilon_0} \right)^2 \left(\frac{1}{r^6} \right)$	μ ₁ , μ ₂ = Dipole moments ε ₀ = Vacuum Permittivity k = Boltzmann Constant r = Separation distance
Dipole-Induced Dipole	$E_{D-ID} = - \left(\frac{\mu_1^2 \alpha_2}{4\pi\epsilon_0} \right) \left(\frac{1}{r^6} \right)$	μ ₁ = Dipole moment α ₂ = Polarizability ε ₀ = Vacuum Permittivity r = Separation distance
Induced Dipole-Induced Dipole	$E_{ID-ID} = \frac{3}{2} \left(\alpha_1 \alpha_2 \frac{I_1 I_2}{I_1 + I_2} \right) \left(\frac{1}{r^6} \right)$	α ₁ , α ₂ = Polarizability I ₁ , I ₂ = Ionization Energies r = Separation distance

^[a]Between two molecules **1** and **2**. ^[b]For two freely rotating dipoles.

Collectively, the attractive van der Waals interactions contribute to the determination of what particular crystal packing motif is favoured. For example, along with repulsive interactions due to electrostatic interactions, the interactions with 1/r⁶ radial dependencies give rise to potential energy curves such as the Lennard-Jones 12,6

potential. In the case of the calixarenes, these interactions have typically been rationalized as resulting in the aromatic hydrophobic cavities acting as a soft base (due to the presence of electron donating substituents), giving rise to attractive CH- π interactions such that the inclusion of hydrocarbons is favoured over that of various heteroatoms.^[161] Crystallographic evidence suggests that such interactions are extremely weak, and are likely subordinate to the needs of space filling interactions in determining the crystal structure of such calixarene inclusions.^[149] Despite this, they remain potentially useful for influencing the inclusion motifs of calixarene compounds in conjunction with other intermolecular interactions.

Polymorphism and Pseudopolymorphism

With the broad range of intermolecular forces at play in the solid state, one of the key concerns in studying crystalline materials is the prevalence of polymorphism. Polymorphism, or the tendency of organic molecules to form crystals with identical chemical compositions, but different crystal structures is quite well known in a variety of systems.^[162, 163] Supramolecular host systems such as tri-*o*-thymotide^[31] and tris(5-acetyl-3-thienyl)methane^[33, 34] have been noted to form polymorphic structures. In general, these compounds are conformationally flexible, and their structures are largely determined by hydrogen bonding, such that a number of energetically equivalent packing schemes are possible.

In the simple calixarenes, which do not depend heavily on hydrogen bonding and lack conformational flexibility in the solid state, polymorphism has rarely been observed. As mentioned, the toluene inclusion of 4-*t*-butylcalix[4]arene undergoes a phase

transition at low temperatures, shifting to a monoclinic space group, but this is the only reported incidence for the host. In addition to this, the *apo* host has three distinct polymorphs, corresponding to a dense α form and a pair of related loose packed β forms, which can be interconverted through heating.^[164, 165] Under these circumstances, deducing the relationship between the polymorphs gave rise to a broader understanding of the forces governing the packing motif of both the inclusion compound, as well as the native host. In particular, it has brought to the fore the concept of using non-porous materials with void spaces as potential adsorbents based on cooperative transfer of molecules between calixarene cavities.^[134, 166-169]

By the same token, while the term remains somewhat controversial, pseudopolymorphism (the formation of crystalline compounds which differ in the nature or stoichiometry of the solvent included) provides an ideal opportunity to investigate how specific intermolecular forces influence the packing of a given structure. As might be inferred from the definition, this phenomenon is quite common in supramolecular chemistry, where the choice of solvent has been frequently observed to have dramatic effects on the structure of a given host system. For the simple calixarenes, however, the potential for pseudopolymorphism as method of both controlling and understanding the forces governing a given inclusion compound has been largely untapped.

4. Thesis

While the calixarenes have been extensively used to produce complex receptors, the simple parent compounds remain underexploited as systems for investigating the forces guiding the formation of multi-dimensional supramolecular frameworks through

self-assembly alone. Both 4-*t*-butylcalix[4]arene and the resorcinarenes present intriguing opportunities to investigate how competition between intermolecular forces can be used to guide the formation of complex frameworks while still using relatively simple host and guest molecules. Such investigations will complement the insights garnered from early studies where a single intermolecular force has been observed to dominate the structural motifs of these compounds.

In part, such studies of the interplay between forces have been hampered in the past by the reliance on single crystal X-ray diffraction as the primary technique for characterizing supramolecular calixarene compounds in the solid state. Such a focus has led to a bias in the literature, such that investigations of compounds that cannot be readily characterized by single crystal X-ray diffraction have been largely overlooked. In Chapter II, the use of two principal complementary techniques, single crystal X-ray diffraction and solid state NMR, to obtain a more complete picture of calixarene inclusion compounds is discussed. Building on the previous studies wherein solid state NMR provided information on the local ordering of calixarene structures to resolve disorder in the long range ordering observed in XRD structures, such a combined methodology also allows for investigations into the role of various forces in guiding such structures by disrupting these forces and structurally characterizing the resulting compounds.

Towards this end of developing a further understanding of how multiple interactions can be used to guide the formation of complex frameworks using simple calixarenes, two classes of host system have been selected: 4-*t*-butylcalix[4]arene and

resorcinarenes. The 4-*t*-butylcalix[4]arene system is well known as a simple system suited for the study of non-directional forces in guiding the inclusion of various organic guests, due to its flexibility and well defined geometry in the solid state. However, the chemistry of amines with 4-*t*-butylcalix[4]arene, and in particular the proton transfer phenomenon, suggests a previously unknown realm of inclusion chemistry involving the formation of larger, channelled structures containing supramolecularly stabilized guests.

The resorcinarenes present an intriguing opportunity to further understand how hydrogen bonding interactions can be affected by the presence of anions and cations. In this case, the combination of guests can potentially be used to direct the conformation of the calixarene, while more subtle interactions serve to tune the resulting motif of the framework. Similar effects are to be expected from different isomers of resorcinarenes, which have been largely ignored, but represent alternative systems in which investigations of the role of solvent and guest to direct the formation of calixarene frameworks can be determined.

The investigations of the inclusion chemistry of amines and 4-*t*-butylcalix[4]arene are presented in Chapters III-VI. The multidimensional structures arising from *n*-alkylamine inclusion is discussed in Chapter III. The competition between hydrogen bonding and stabilization by inclusion in the calixarene cavity, and the investigations of the pseudopolymorphism arising from this through solid state NMR and PXRD, establishes the common theme guiding the formation of amine 4-*t*-butylcalix[4]arene compounds investigated. In Chapter IV, the secondary coordinate role of the calixarene in stabilizing *n*-alkylamine inclusions is examined in more detail, with a particular focus

on how coordinate interactions compete with the other intermolecular forces in the system. Chapter V examines how smaller, substituted amine guests can be used to further tune the inclusion motifs observed, while in Chapter VI, the ability to produce larger complex clusters using difunctional amines is examined. Collectively, these systems are therefore demonstrated to not only be suitable for the essential investigations of intermolecular interactions, but also exhibit potential as functional materials by making use of the supramolecularly stabilized amine for chemistry.

The investigations of multidimensional frameworks based on resorcinarenes are presented in Chapters VII-IX. In Chapter VII, the structure directing ability of inorganic anions and organic cations enclathrated by C-methylcalix[4]arene is investigated. In a counterpoint to the basic amines examined for 4-*t*-butylcalix[4]arene, these frameworks are formed under acidic conditions. Chapter VIII focuses on how alternative inclusion motifs arise from pyrogall[4]arenes, such that the first *apo* form of a resorcinarene can be isolated, and the ability to include bulky cations in channelled structures exhibited by the *rctt* isomer. In Chapter IX, the role of solvent in guiding the structural motif of an uncommon isomer of ethylpyrogall[6]arene is investigated, emphasising the importance of multiple characterization techniques in fully understanding pseudopolymorphism in supramolecular frameworks.

In each chapter, an emphasis is placed on the competition between forces and how this guides the structural motifs, making such systems readily tuned by judicious choice of guest. In the course of such discussion, various opportunities for further studies are briefly mentioned, including the production of functional materials based on simple

calixarenes. An overall summary of the trends observed, and the potential avenues for future work on such systems, is found in Chapter X.

5. References

- [1] J.-M. Lehn, in *Comprehensive Supramolecular Chemistry, Vol. 1* (Eds.: J. L. Atwood, J. E. D. Davies, D. D. MacNicol, F. Vogtle), Pergamon Press, Oxford, 1996, p. vii.
- [2] J. W. Steed, J. L. Atwood, *Supramolecular Chemistry*, John Wiley & Sons, Ltd., Chichester, 2000.
- [3] Z. Asfari, V. Bohmer, J. Harrowfield, J. Vicens, *Calixarenes 2001*, Kluwer Academic Publishers, Dordrecht, 2001.
- [4] L. Mandolini, R. Ungaro, *Calixarenes in Action*, Imperial College Press, London, 2000.
- [5] G. Zubay, *Biochemistry*, 4th ed., Wm. C. Brown Publishers, Dubuque, 1998.
- [6] C. J. Pedersen, *Angew. Chem. Int. Ed. Engl.* **1988**, 27, 1021.
- [7] D. J. Cram, *Angew. Chem. Int. Ed. Engl.* **1988**, 27, 1009.
- [8] J.-M. Lehn, *Angew. Chem. Int. Ed. Engl.* **1988**, 27, 89.
- [9] H. Davy, *Philos. Trans. R. Soc. Lond.* **1811**, 101, 155.
- [10] A. Z. Werner, *Anorg. Chemie* **1893**, 3, 267.
- [11] M. T. Beck, *Coord. Chem. Rev.* **1968**, 3, 91.
- [12] J. Lipkowski, in *Comprehensive Supramolecular Chemistry, Vol. 6* (Eds.: J. L. Atwood, J. E. D. Davies, D. D. MacNicol, F. Vogtle), Pergamon Press, Oxford, 1996, pp. 691.
- [13] J. Szejtli, *Chem. Rev.* **1998**, 98, 1743.
- [14] G. R. Desiraju, *Crystal Engineering. The Design of Organic Solids.*, Elsevier, Amsterdam, 1989.
- [15] G. R. Desiraju, in *Comprehensive Supramolecular Chemistry, Vol. 6* (Eds.: J. L. Atwood, J. E. D. Davies, D. D. MacNicol, F. Vogtle), Pergamon Press, Oxford, 1996, pp. 1.
- [16] L. R. MacGillivray, J. L. Atwood, *Nature* **1997**, 389, 469.
- [17] A. Shivanyuk, J. Rebek, *Chem. Commun.* **2001**, 2424.
- [18] A. Shivanyuk, J. Rebek, *J. Am. Chem. Soc.* **2003**, 125, 3432.
- [19] H. Mansikkamaki, M. Nissinen, C. A. Schalley, K. Rissanen, *New J. Chem.* **2003**, 27, 88.
- [20] S. L. Suib, *Chem. Rev.* **1993**, 93, 803.
- [21] S. I. Zones, M. E. Davis, *Curr. Opin. Solid State Mat. Sci.* **1996**, 1, 107.
- [22] D. W. Davidson, J. A. Ripmeester, in *Inclusion Compounds, Vol. III* (Eds.: J. L. Atwood, J. E. D. Davies, D. D. MacNicol), Academic Press, New York, 1984.
- [23] G. A. Jeffery, in *Inclusion Compounds, Vol. I* (Eds.: J. L. Atwood, J. E. D. Davies, D. D. MacNicol), Academic Press, New York, 1984.
- [24] S. L. James, *Chem. Soc. Rev.* **2003**, 32, 276.
- [25] L. J. May, G. K. H. Shimizu, *Z. Kristall.* **2005**, 220, 364.

- [26] A. M. Beatty, *Coord. Chem. Rev.* **2003**, *246*, 131.
- [27] N. W. Ockwig, O. Delgado-Friedrichs, M. O'Keeffe, O. M. Yaghi, *Acc. Chem. Res.* **2005**, *38*, 176.
- [28] K. D. M. Harris, *J. Solid State Chem.* **1993**, *106*, 83.
- [29] L. C. Fetterly, in *Non-Stoichiometric Compounds* (Ed.: L. Mandelcorn), Academic Press, New York, **1964**, pp. 491.
- [30] R. Gerdil, *Top. Curr. Chem.* **1987**, *140*.
- [31] R. Gerdil, in *Comprehensive Supramolecular Chemistry, Vol. 6* (Eds.: J. L. Atwood, J. E. D. Davies, D. D. MacNicol, F. Vogtle), Pergamon Press, Oxford, **1996**, pp. 239.
- [32] F. H. Herbststein, *Acta Crystallog. B* **1997**, *53*, 168.
- [33] P. S. Sidhu, G. A. Enright, J. A. Ripmeester, G. H. Penner, *J. Phys. Chem. B* **2002**, *106*, 8569.
- [34] P. S. Sidhu, G. D. Enright, K. A. Udachin, J. A. Ripmeester, *Cryst. Growth Des.* **2004**, *4*, 1249.
- [35] D. V. Soldatov, I. L. Moudrakovski, J. A. Ripmeester, *Angew. Chem. Int. Edit.* **2004**, *43*, 6308.
- [36] C. H. Gorbitz, *Acta Crystallog. B* **2002**, *58*, 849.
- [37] C. H. Gorbitz, E. Gundersen, *Acta Crystallog. C* **1996**, *52*, 1764.
- [38] C. D. Gutsche, *Calixarenes*, Royal Society of Chemistry, Cambridge, **1989**.
- [39] C. D. Gutsche, *Calixarenes Revisited*, Royal Society for Chemistry, Cambridge, **1998**.
- [40] C. D. Gutsche, M. Iqbal, D. Stewart, *J. Org. Chem.* **1986**, *51*, 742.
- [41] C. D. Gutsche, M. Iqbal, *Org. Synth.* **1990**, *68*, 234.
- [42] J. B. Niederl, H. J. Vogel, *J. Am. Chem. Soc.* **1940**, *62*, 2512.
- [43] A. G. S. Hogberg, *J. Org. Chem.* **1980**, *45*, 4498.
- [44] A. G. S. Hogberg, *J. Am. Chem. Soc.* **1980**, *102*, 6046.
- [45] C. D. Gutsche, R. J. Muthukrishnan, *J. Org. Chem.* **1978**, *43*, 4905.
- [46] C. D. Gutsche, *Acc. Chem. Res.* **1983**, *16*, 161.
- [47] Formally, 4-*t*-butylcalix[4]arene is referred to as 5,11,17,23-tetra-*tert*-butyl-25,26,27,28-tetrahydroxycalix[4]arene.
- [48] J. Vicens, V. Bohmer, *Calixarenes: A Versatile Class of Macrocyclic Compounds*, Kluwer Academic Publishers, Dordrecht, **1991**.
- [49] C. D. Gutsche, *Aldrichimica Acta* **1995**, *28*, 3.
- [50] P. Timmerman, W. Verboom, D. N. Reinhoudt, *Tetrahedron* **1996**, *52*, 2663.
- [51] A. Bayer, *Chemische Ber.* **1872**, *5*, 25.
- [52] A. Bayer, *Chemische Ber.* **1872**, *5*, 280.
- [53] L. H. Baekeland, United States Patent # 942,699, **1908**.
- [54] A. Zinke, E. Ziegler, *Chemische Ber.* **1941**, *B74*, 1729.
- [55] A. Zinke, E. Ziegler, *Chemische Ber.* **1944**, *77*, 264.
- [56] B. T. Hayes, R. F. Hunter, *Chem. Ind.* **1956**, 193.
- [57] B. T. Hayes, R. F. Hunter, *J. Appl. Chem.* **1958**, *8*, 743.
- [58] J. W. Cornforth, P. D'Arcy Hart, G. A. Nicholls, R. J. W. Rees, J. A. Stock, *Br. J. Pharmacol.* **1955**, *10*, 73.

- [59] J. W. Cornforth, E. D. Morgan, K. T. Potts, R. J. W. Rees, *Tetrahedron* **1973**, *29*, 1659.
- [60] C. D. Gutsche, B. Dhawan, K. H. No, R. J. Muthukrishnan, *J. Am. Chem. Soc.* **1981**, *103*, 3782.
- [61] C. D. Gutsche, B. Dhawan, K. H. No, R. J. Muthukrishnan, *J. Am. Chem. Soc.* **1984**, *106*, 1891.
- [62] G. D. Andreotti, R. Ungaro, A. Pochini, *J. Chem. Soc. Chem. Commun.* **1979**, 1005.
- [63] B. Nilsson, *Acta Chem. Scand.* **1968**, *22*, 732.
- [64] H. Kammerer, G. Happel, F. Caesar, *Makromol. Chem.* **1972**, *162*, 179.
- [65] G. Happel, B. Mathiasch, H. Kammerer, *Makromol. Chem.* **1975**, *176*, 3317.
- [66] C. D. Gutsche, L. J. Bauer, *J. Am. Chem. Soc.* **1985**, *107*, 6052.
- [67] L. Abis, E. Dalcanale, A. Du vosel, S. Spera, *J. Chem. Soc. Perkin Trans. 2* **1990**, 2109.
- [68] L. C. Groenen, E. Steinwender, B. T. G. Lutz, J. H. van der Maas, D. N. Reinhoudt, *J. Chem. Soc. Perkin Trans. 2* **1992**, 1893.
- [69] A. Pochini, R. Ungaro, in *Comprehensive Supramolecular Chemistry, Vol. 2* (Eds.: J. L. Atwood, J. E. D. Davies, D. D. MacNicol, F. Vogtle), Pergamon Press, Oxford, **1996**, pp. 103.
- [70] W. Verboom, A. Durie, R. J. M. Egberink, Z. Asfari, D. N. Reinhoudt, *J. Org. Chem.* **1992**, *57*, 1313.
- [71] E. Kelderman, L. Derhaeg, G. J. T. Heesnik, W. Verboom, J. F. J. Engbersen, N. F. van Hulst, A. Persoons, D. N. Reinhoudt, *Angew. Chem. Int. Ed. Engl.* **1992**, *31*, 1075.
- [72] S. Shinkai, S. Mori, T. Tsubaki, T. Sone, O. Manabe, *Tetrahedron Lett.* **1984**, *25*, 5315.
- [73] S. Shinkai, K. Araki, T. Tsubaki, T. Arimura, O. Manabe, *J. Chem. Soc. Perkin Trans. 1* **1987**, 2297.
- [74] A. Casnati, Y. Ting, D. Berti, M. Fabbi, A. Pochini, R. Ungaro, D. Sciotto, G. g. Lombardo, *Tetrahedron* **1993**, *49*, 9815.
- [75] A. Arduini, A. Pochini, A. R. Sicuri, A. Secchi, R. Ungaro, *Gazz. Chim. Ital.* **1994**, *124*, 129.
- [76] A. Arduini, A. Pochini, A. Rizzi, A. R. Sicuri, R. Ungaro, *Tetrahedron Lett.* **1990**, *31*, 4653.
- [77] P. Timmerman, W. Verboom, D. N. Reinhoudt, A. Arduini, S. Grandi, A. R. Sicuri, A. Pochini, R. Ungaro, *Synthesis* **1994**, 185.
- [78] S. Shinkai, T. Nagasaki, K. Iwamoto, A. Ikeda, G.-X. He, T. Matsuda, M. Iwamoto, *Bull. Chem. Soc. Jpn.* **1991**, *64*, 381.
- [79] J. D. Vanloon, L. C. Groenen, S. S. Wijmenga, W. Verboom, D. N. Reinhoudt, *J. Am. Chem. Soc.* **1991**, *113*, 2378.
- [80] B. R. Cameron, S. J. Loeb, *Chem. Commun.* **1996**, 2003.
- [81] B. R. Cameron, S. J. Loeb, G. P. A. Yap, *Inorg. Chem.* **1997**, *36*, 5498.
- [82] E. Ghidini, F. Ugozzoli, R. Ungaro, S. Harkema, A. Abuelfadl, D. N. Reinhoudt, *J. Am. Chem. Soc.* **1990**, *112*, 6979.

- [83] G. D. Andreotti, O. Ori, F. Uguzzoli, C. Alfieri, A. Pochini, R. Ungaro, *J. Incl. Phenom.* **1988**, *6*, 523.
- [84] W. F. Nijenhuis, E. G. Buitenhuis, F. Dejong, E. J. R. Sudholter, D. N. Reinhoudt, *J. Am. Chem. Soc.* **1991**, *113*, 7963.
- [85] F. Arnaudneu, S. Fanni, L. Guerra, W. McGregor, K. Ziat, M. J. Schwingweill, G. Barrett, M. A. McKervey, D. Marrs, E. M. Seward, *J. Chem. Soc. Perkin Trans. 2* **1995**, 113.
- [86] J. Scheerder, M. Fochi, J. F. J. Engbersen, D. N. Reinhoudt, *J. Org. Chem.* **1994**, *59*, 7815.
- [87] S. Shinkai, H. Kawabata, T. Arimura, T. Matsuda, H. Satoh, O. Manabe, *J. Chem. Soc. Perkin Trans. 1* **1989**, 1073.
- [88] S. G. Bott, A. W. Coleman, J. L. Atwood, *J. Am. Chem. Soc.* **1986**, *108*, 1709.
- [89] C. D. Gutsche, B. Dhawan, J. A. Levine, K. H. No, L. J. Bauer, *Tetrahedron* **1983**, *39*, 409.
- [90] A. Casnati, P. Minari, A. Pochini, R. Ungaro, *J. Chem. Soc. Chem. Commun.* **1991**, 1413.
- [91] D. J. Eisler, R. J. Puddephatt, *Can. J. Chem.-Rev. Can. Chim.* **2004**, *82*, 185.
- [92] P. D. Woodgate, G. M. Horner, N. P. Maynard, *Tetrahedron Letters* **1999**, *40*, 6507.
- [93] O. Lukin, A. Shivanyuk, V. V. Pirozhenko, I. F. Tsymbal, V. I. Kalchenko, *J. Org. Chem.* **1998**, *63*, 9510.
- [94] H. Boerrigter, L. Grave, J. W. M. Nissink, L. A. J. Chrisstoffels, J. H. van der Maas, W. Verboom, F. de Jong, D. N. Reinhoudt, *J. Org. Chem.* **1998**, *63*, 4174.
- [95] H. Konishi, H. Yamaguchi, M. Miyashiro, K. Kobayashi, O. Morikawa, *Tetrahedron Letters* **1996**, *37*, 8547.
- [96] R. J. M. Egberink, P. Cobben, W. Verboom, S. Harkema, D. N. Reinhoudt, *J. Incl. Phenom. Mol. Recogn. Chem.* **1992**, *12*, 151.
- [97] L. M. Tunstad, J. A. Tucker, E. Dalcanale, J. Weiser, J. A. Bryant, J. C. Sherman, R. C. Helgeson, C. B. Knobler, D. J. Cram, *J. Org. Chem.* **1989**, *54*, 1305.
- [98] H. J. Choi, Y. S. Park, C. S. Cho, K. Koh, S. H. Kim, K. Paek, *Org. Lett.* **2004**, *6*, 4431.
- [99] H. Boerrigter, W. Verboom, D. N. Reinhoudt, *J. Org. Chem.* **1997**, *62*, 7148.
- [100] D. J. Cram, L. M. Tunstad, C. B. Knobler, *J. Org. Chem.* **1992**, *57*, 528.
- [101] J.-F. Dozol, H. Rouquette, A. Garcia Carrera, L. Delmau, V. Bohmer, A. Shivanyuk, C. Muzigmann, United States Patent # 6,630,114, **2003**.
- [102] G. P. Nicholson, M. J. Kan, G. Williams, M. G. Drew, B. P. D., United States Patent # 6,342,634, **2002**.
- [103] F. W. B. van Leeuwen, H. Beijleveld, C. J. H. Miermans, J. Huskens, W. Verboom, D. N. Reinhoudt, *Anal. Chem.* **2005**, *77*, 4611.
- [104] K. J. C. van Bommel, W. Verboom, R. Hulst, H. Kooijman, A. L. Spek, D. N. Reinhoudt, *Inorg. Chem.* **2000**, *39*, 4099.
- [105] L. X. Chen, J. Zhang, W. F. Zhao, X. W. He, Y. Liu, *J. Electroanal. Chem.* **2006**, *589*, 106.

- [106] N. J. van der Veen, E. Rozniecka, L. A. Woldering, M. Chudy, J. Huskens, F. van Veggel, D. N. Reinhoudt, *Chem. Eur. J.* **2001**, *7*, 4878.
- [107] V. K. Jain, R. A. Pandya, S. G. Pillai, P. S. Shrivastav, Y. K. Agrawal, *Separation Sci. Tech.* **2006**, *41 (1)*, 123.
- [108] S. Nagy, United States Patent # 6,984,599, **2006**.
- [109] B. W. Purse, A. Gissot, J. Rebek, *J. Am. Chem. Soc.* **2005**, *127*, 11222.
- [110] X. W. Zhou, X. J. Li, Z. R. Zeng, *J. Chromatog. A* **2006**, *1104*, 359.
- [111] X. J. Li, Z. R. Zeng, Y. Xu, *Anal. Bioanal. Chem.* **2006**, *384*, 1428.
- [112] C. Liu, J. T. Lin, S. H. Wang, J. C. Jiang, L. G. Lin, *Sens. Actuator B-Chem.* **2005**, *108*, 521.
- [113] M. Sliwka Kaszynska, K. Jaszczolt, A. Kolodziejczyk, J. Rachon, *Talanta* **2006**, *68*, 1560.
- [114] T. J. Bruno, A. F. Lagalante, United States Patent # 6,334,949, **2002**.
- [115] P. Molenveld, J. F. J. Engbersen, D. N. Reinhoudt, *Eur. J. Org. Chem.* **1999**, 3269.
- [116] P. Molenveld, W. M. G. Stikvoort, H. Kooijman, A. L. Spek, J. F. J. Engbersen, D. N. Reinhoudt, *J. Org. Chem.* **1999**, *64*, 3896.
- [117] R. Cacciapaglia, A. Casnati, L. Mandolini, D. N. Reinhoudt, R. Salvio, A. Sartori, R. Ungaro, *J. Org. Chem.* **2005**, *70*, 624.
- [118] E. De Silva, D. Ficheux, A. W. Coleman, *J. Incl. Phenom. Macrocyc. Chem.* **2005**, *52*, 201.
- [119] E. Da Silva, P. Shahgaldian, A. W. Coleman, *Inter. J. Pharm.* **2004**, *273*, 57.
- [120] J. Gualbert, P. Shahgaldian, A. Lazar, A. W. Coleman, *J. Incl. Phenom. Macrocyc. Chem.* **2004**, *48*, 37.
- [121] J. Gualbert, P. Shahgaldian, A. W. Coleman, *Inter. J. Pharm.* **2003**, *257*, 69.
- [122] A. Shivanyuk, J. C. Friese, S. Doring, J. Rebek, *J. Org. Chem.* **2003**, *68*, 6489.
- [123] A. Shivanyuk, K. Rissanen, E. Kolehmainen, *Chem. Commun.* **2000**, 1107.
- [124] G. H. Stout, L. H. Jensen, in *X-Ray Structure Determination. A Practical Guide*, John Wiley & Sons, New York, **1989**, p. 229.
- [125] E. B. Brouwer, Ph.D. thesis, Carleton University (Ottawa), **1996**.
- [126] E. B. Brouwer, G. D. Enright, C. I. Ratcliffe, G. A. Facey, J. A. Ripmeester, *J. Phys. Chem. B* **1999**, *103*, 10604.
- [127] E. B. Brouwer, G. D. Enright, J. A. Ripmeester, *Supramol. Chem.* **1996**, *7*, 7.
- [128] E. B. Brouwer, G. D. Enright, J. A. Ripmeester, *J. Am. Chem. Soc.* **1997**, *119*, 5404.
- [129] E. B. Brouwer, G. D. Enright, J. A. Ripmeester, *Chem. Commun.* **1997**, 939.
- [130] E. B. Brouwer, K. A. Udachin, G. D. Enright, J. A. Ripmeester, *Chem. Commun.* **2000**, 1905.
- [131] R. Caciuffo, G. Amoretti, C. J. Carlile, F. Fillaux, O. Francescangeli, M. Prager, F. Uguzzoli, *Physica B* **1994**, *202*, 279.
- [132] R. Caciuffo, G. Amoretti, F. Fillaux, O. Francescangeli, S. Melone, M. Prager, F. Uguzzoli, *Chem. Phys. Lett.* **1993**, *204*, 427.
- [133] K. A. Udachin, G. D. Enright, C. I. Ratcliffe, J. A. Ripmeester, *ChemPhysChem* **2003**, *4*, 1059.

- [134] G. D. Enright, K. A. Udachin, I. L. Moudrakovski, J. A. Ripmeester, *J. Am. Chem. Soc.* **2003**, *125*, 9896.
- [135] B.-Q. Ma, Y. Zhang, P. Coppens, *J. Org. Chem.* **2003**, *68*, 9467.
- [136] G. Ferguson, C. Glidewell, A. J. Lough, G. D. McManus, P. R. Meehan, *J. Mater. Chem.* **1998**, *8*, 2339.
- [137] L. R. MacGillivray, J. L. Atwood, *Chem. Commun.* **1999**, 181.
- [138] L. R. MacGillivray, J. L. Atwood, *J. Am. Chem. Soc.* **1997**, *119*, 6931.
- [139] A. Shivanyuk, E. F. Paulus, K. Rissanen, E. Kolehmainen, V. Bohmer, *Chem. Eur. J.* **2001**, *7*, 1944.
- [140] H. Mansikkamaki, M. Nissinen, K. Rissanen, *Angew. Chem. Int. Ed.* **2004**, *43*, 1243.
- [141] G. A. Facey, R. H. Dubois, M. Zakrzewski, C. I. Ratcliffe, J. L. Atwood, J. A. Ripmeester, *Supramol. Chem.* **1993**, *1*, 199.
- [142] E. B. Brouwer, G. D. Enright, C. I. Ratcliffe, J. A. Ripmeester, *Supramol. Chem.* **1996**, *7*, 79.
- [143] E. B. Brouwer, J. A. Ripmeester, G. D. Enright, *J. Incl. Phen. and Molec. Recogn. Chem.* **1996**, *24*, 1.
- [144] G. D. Enright, E. B. Brouwer, K. A. Udachin, C. I. Ratcliffe, J. A. Ripmeester, *Acta Crystallogr. B* **2002**, *58*, 1032.
- [145] F. Benevelli, W. Kolodziejski, K. Wozniak, J. Klinowski, *Phys. Chem. Chem. Phys.* **2001**, *3*, 1762.
- [146] F. Benevelli, A. Bond, M. Duer, J. Klinowski, *Phys. Chem. Chem. Phys.* **2000**, *2*, 3977.
- [147] F. Benevelli, Y. Z. Khimyak, J. Klinowski, *J. Incl. Phenom. Macrocyc. Chem.* **2004**, *49*, 211.
- [148] B. M. Furphy, J. M. Harrowfield, M. I. Ogden, B. W. Skelton, A. H. White, F. R. Wilner, *J. Chem. Soc. Dalton Trans.* **1989**, 2217.
- [149] K. A. Udachin, G. D. Enright, E. B. Brouwer, J. A. Ripmeester, *J. Supramol. Chem.* **2001**, *1*, 97.
- [150] G. D. Enright, K. A. Udachin, J. A. Ripmeester, *Chem. Commun.* **2004**, 1360.
- [151] L. R. MacGillivray, H. A. Spinney, J. L. Reid, J. A. Ripmeester, *Chem. Commun.* **2000**, 517.
- [152] L. R. MacGillivray, J. L. Reid, J. A. Ripmeester, *Chem. Commun.* **2001**, 1034.
- [153] B. Q. Ma, Y. Zhang, P. Coppens, *Cryst. Growth Des.* **2002**, *2*, 7.
- [154] B. Q. Ma, Y. G. Zhang, P. Coppens, *Cryst. Growth Des.* **2001**, *1*, 271.
- [155] G. W. V. Cave, J. Antesberger, L. J. Barbour, R. M. McKinlay, J. L. Atwood, *Angew. Chem. Int. Ed. Engl.* **2004**, *43*, 5263.
- [156] T. Gerkenmeier, W. Iwanek, C. Agena, R. Frohlich, S. Kotila, C. Nather, J. Mattay, *Eur. J. Org. Chem.* **1999**, 2257.
- [157] L. Avram, Y. Cohen, *J. Am. Chem. Soc.* **2004**, *126*, 11556.
- [158] M. Luostarinen, A. Ahman, M. Nissinen, K. Rissanen, *Supramol. Chem.* **2004**, *16*, 505.
- [159] B. W. Purse, A. Shivanyuk, J. Rebek Jr., *Chem. Commun.* **2002**, 2612.

- [160] T. Gerkenmeier, C. Agena, W. Iwanek, R. Frohlich, S. Kotila, C. Nather, J. Mattay, *Z. Naturforsch. B: Chem. Sci.* **2001**, *56*, 1063.
- [161] T. Fujimoto, R. Yanagihara, K. Kobayashi, Y. Aoyama, *Bull. Chem. Soc. Jpn.* **1994**, *68*, 2113.
- [162] M. R. Caira, in *Design of Organic Solids, Vol. 198*, **1998**, pp. 163.
- [163] B. Rodriguez-Spong, C. P. Price, A. Jayasankar, A. J. Matzger, N. Rodriguez-Hornedo, *Adv. Drug Deliv. Rev.* **2004**, *56*, 241.
- [164] J. L. Atwood, L. J. Barbour, A. Jerga, *Chem. Commun.* **2002**, 2952.
- [165] E. B. Brouwer, G. D. Enright, K. A. Udachin, S. Lang, K. J. Ooms, P. A. Halchuk, J. A. Ripmeester, *Chem. Commun.* **2003**, 1416.
- [166] J. L. Atwood, L. J. Barbour, A. Jerga, *Science* **2002**, *296*, 2367.
- [167] J. L. Atwood, L. J. Barbour, A. Jerga, *Angew. Chem. Int. Ed.* **2004**, *43* (22), 2948.
- [168] A. Dubes, I. L. Moudrakovski, P. Shahgaldian, A. W. Coleman, C. I. Ratcliffe, J. A. Ripmeester, *J. Am. Chem. Soc.* **2004**, *126*, 6236.
- [169] P. K. Thallapally, G. O. Lloyd, T. B. Wirsig, M. W. Breidenkamp, J. L. Atwood, L. J. Barbour, *Chem. Commun.* **2005**, (42), 5772.

Chapter II: Physical Methods

1. Introduction	34
2. X-Ray Diffraction (XRD)	36
Crystal Symmetry and the Unit Cell	37
Generation of X-rays and the Diffraction Phenomenon	39
SCXRD Structure Solution	41
SCXRD Structure Refinement	43
SCXRD in Supramolecular Chemistry	45
Powder X-ray Diffraction	46
General Details of SCXRD and PXRD Equipment Used	46
3. Solid-State Nuclear Magnetic Resonance (SSNMR) Spectroscopy	47
The NMR Phenomenon	48
Key Challenges in SSNMR of Spin ½ Nuclei	50
SSNMR of Spin ½ Nuclei in Organic Materials	55
High Resolution SSNMR Spectroscopy	62
General Details of SSNMR Equipment Used	64
4. Summary	65
5. References	65

1. Introduction

As the diversity of supramolecular systems presented in Chapter I indicates, the study of supramolecular chemistry bridges the traditional sub-disciplines of chemistry (such as organic, inorganic and physical chemistry). The tendency of the field to “appropriate” areas of research that have traditionally been the province of a particular sub-discipline is notorious enough that Steed and Atwood specifically comment on the “greed”^[1] of the field as part of their text on the subject. In general, however, the field remains largely dominated by the synthetic organic and inorganic chemistry tradition, with the synthesis of new compounds being the principal goal of most studies.

This focus on the synthesis of new compounds is particularly prominent in the study of calixarenes, as demonstrated by the large numbers of studies focused on chemical modification of these macrocycles.^[2-7] While these complex systems show

interesting properties, from a supramolecular point of view, the covalent modifications of the calixarene sharply constrain the number of potential intermolecular interactions available to guide the self-assembly of a complex. As a result, the physical characterization of the interplay of intermolecular interactions in guiding the self-assembly of calixarene-based supramolecular frameworks, and therefore the understanding of how intermolecular interactions give rise to structural trends and physical properties, has lagged.

Part of the reason for this lack of physical characterization arises from difficulties in structurally characterizing supramolecular frameworks using traditional approaches. For chemists interested in the solid state, single crystal X-ray diffraction (SCXRD) has long been the key method for structural characterization of materials. However, in spite of advances such as diffractometers based on commercial CCD area detectors, the large unit cells and prevalence of disorder present in many supramolecular systems continue to present considerable challenges to accurately determining structures. Even after addressing these problems, SCXRD only provides data about the long-range ordering of a system, such that local, dynamic disordering cannot be effectively modeled with such data alone. It is also significant that many intriguing supramolecular systems do not readily produce diffraction quality crystals (or fail to crystallize at all), such that focusing on SCXRD entails ignoring such promising systems.

The key to physical characterization of supramolecular frameworks therefore lies in the use of multiple complementary techniques. In the case of solid-state studies, an excellent complement to X-ray diffraction has proven to be solid state NMR (SSNMR)

spectroscopy, which provides information about the local symmetry of a system, as allowing one to probe the dynamics of a compound. It also allows one to investigate a much broader range of solids, including polycrystalline materials for which a single crystal may not be available, and amorphous materials. As we will see throughout the following chapters, the use of SSNMR allows for more accurate modeling of structures from diffraction data, as well as providing a means for monitoring structural transformations and comprehending the roles of various structural influences in guiding these transformations.

This chapter discusses the fundamental aspects of X-ray diffraction (XRD), focusing on single crystal structure determination, and solid-state NMR (SSNMR) spectroscopy as they pertain to the characterization of calixarene-based supramolecular systems. It is meant to provide an overview of these techniques suitable to assist in understanding the structural analysis presented in this thesis. In order to do so, the essential theoretical basis of each technique is presented, along with a discussion of the practical aspects of these methods as they are used in the current work.

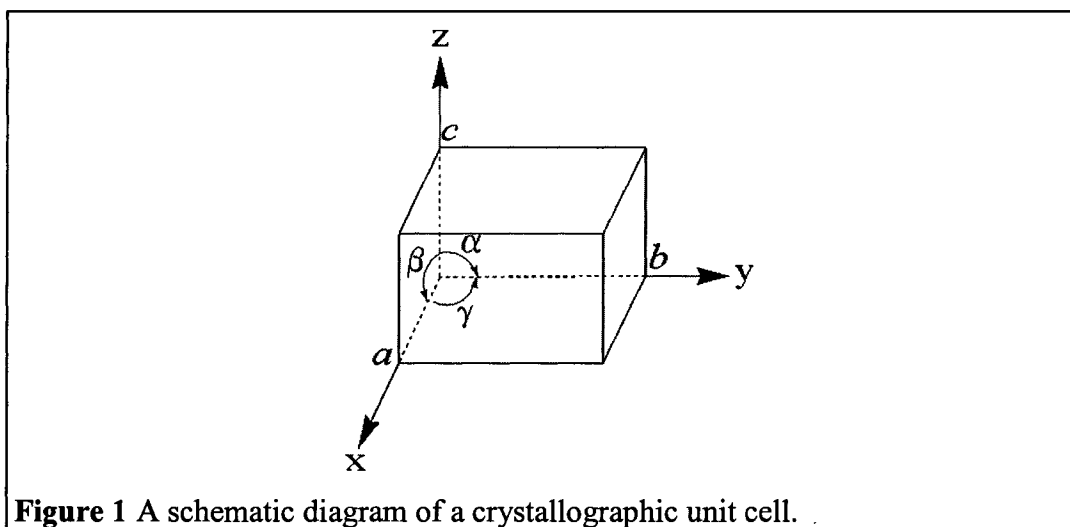
2. X-Ray Diffraction (XRD)

The principal method of characterizing crystalline solids has a long history, entailing the use of a variety of methodologies. In addition to improvements in the instruments used for data collection, the different challenges involved in determining structures of small molecules versus macromolecules and proteins gives rise to a divergence in methods involved in structure solution. What follows therefore is only an overview of the modern, computer-based approach to solving single crystal structures of

small molecules based on data obtained using a diffractometer, and the interested reader is directed to various monographs currently available for more details on the subject.^[8-10]

Crystal Symmetry and the Unit Cell

A crystal consists of a regular, ordered three dimensional structure, such that it can be described in terms of discrete building blocks which are repeated through space.^[11] These building blocks can consist of atoms, ions, molecules, or arrays of molecules. This smallest repeat unit related through translational symmetry is referred to as the unit cell (see Figure 1), and is characterized in terms of the lengths of the cell edges (a, b, c) and the angles between these edges (α, β, γ).



The unit cell is further classified according to the presence of various symmetry elements. Based on the presence of rotation axes and centres of inversion, seven crystal systems are possible (see Table 1). These systems represent the primitive lattices, with the lattice points positioned at the corners of the unit cell such that one point in total is found in each cell. Bravais determined that an additional seven non-primitive lattices

(with two or more lattice points within the unit cell) conforming to the symmetry restrictions of the seven crystal systems exist, such that fourteen Bravais lattices are possible.

Table 1 The seven crystal systems and fourteen Bravais Lattices.

Crystal System	Unit Cell Parameters	Lattice Symmetry	Bravais Lattices ^[a]
Triclinic	$a \neq b \neq c$	-1	<i>P</i>
Monoclinic	$\alpha \neq \beta \neq \gamma$ $a \neq b \neq c$	$2/m$	<i>P, C</i>
Orthorhombic	$\alpha = \gamma = 90^\circ; \beta > 90^\circ$ $a \neq b \neq c$	mmm	<i>P, C, I, F</i>
Tetragonal	$\alpha = \beta = \gamma = 90^\circ$ $a = b \neq c$	$4/mmm$	<i>P, I</i>
Trigonal (rhombohedral)	$a = b = c$ $\alpha = \beta = \gamma \neq 90^\circ$	$\bar{3}m$	<i>R</i>
(hexagonal)	$a = b \neq c$ $\alpha = \beta = 90^\circ; \gamma = 120^\circ$	$6/mmm$	<i>P</i>
Hexagonal	$a = b \neq c$ $\alpha = \beta = 90^\circ; \gamma = 120^\circ$	$6/mmm$	<i>P</i>
Cubic	$a = b = c$ $\alpha = \beta = \gamma = 90^\circ$	$m\bar{3}m$	<i>P, I, F</i>

^[a] *P*-Primitive; *C*-Face centered on *ab* face; *I*-body centered; *F*-Face centered on all faces. *R*-Rhombohedral primitive.

As suggested above, in addition to the translational symmetry described by the Bravais lattices, crystals also possess point symmetry. 32 crystallographic point groups exist, based on various combinations of five symmetry operations (rotation axes, roto-inversion axes, mirror planes, screw axes and glide planes). When combined with the 14 Bravais lattices, this gives rise to 230 crystallographic space groups distributed throughout the seven crystal classes. The resulting combination of symmetry elements also results in many of the space groups being arrayed such that a number of symmetry equivalent atoms or molecules will be located within a single unit cell. The smallest

portion of the unit cell that will generate the entire cell when the symmetry operations are applied to it is known as the asymmetric unit.

Generation of X-rays and the Diffraction Phenomenon

X-rays were first discovered by Röntgen in 1895, with the name being derived from the mysterious origin of this radiation. They are, in fact, electromagnetic radiation with wavelengths ranging from 0.1-100 Å,^[12] such that they occupy a range between UV and gamma rays in the electromagnetic spectrum. Traditionally, they are generated by the bombardment of a metal target with rapidly moving electrons. The electrons are accelerated by making use of a cathode to set up a potential difference, with the voltages required to generate X-rays being on the order of tens of kilovolts. Upon impacting the target, the majority of the energy imparted by this potential difference is converted into waste heat and white radiation, such that only approximately 0.1% of the energy actually serves to produce X-rays useful for crystallographic purposes.^[13]

When the accelerating potential is sufficiently large, however, the electrons become capable of forcing electrons out of the innermost orbital of the metal atoms composing the target (the K shell, corresponding to orbitals with principal quantum number $n=1$). This vacancy is then filled by an electron from a higher energy orbital (the L and M shells, corresponding to orbitals with principal quantum numbers $n=2$ and 3), with the resulting transition resulting in the emission of an X-ray photon. In contrast with the white radiation previously mentioned, this radiation is quite intense and nearly monochromatic in nature. The wavelength of the X-ray depends on the material making up the target, with Mo ($K_{\alpha}=0.71070 \text{ \AA}$) and Cu ($K_{\alpha}=1.54178 \text{ \AA}$) radiation most

commonly being used. The additional resolution and penetrating power afforded by Mo radiation make it well suited for studies of supramolecular compounds containing disordered moieties, such as the systems presented in the current work.

The ability of crystals to cause X-rays to diffract was first reported by von Laue in 1912, which also served to indirectly establish the wave-like nature of X-rays. A year later, W.L. Bragg developed the concept of treating diffraction as reflections of the X-rays from a series of planes of atoms in the crystalline lattice (see Figure 2).

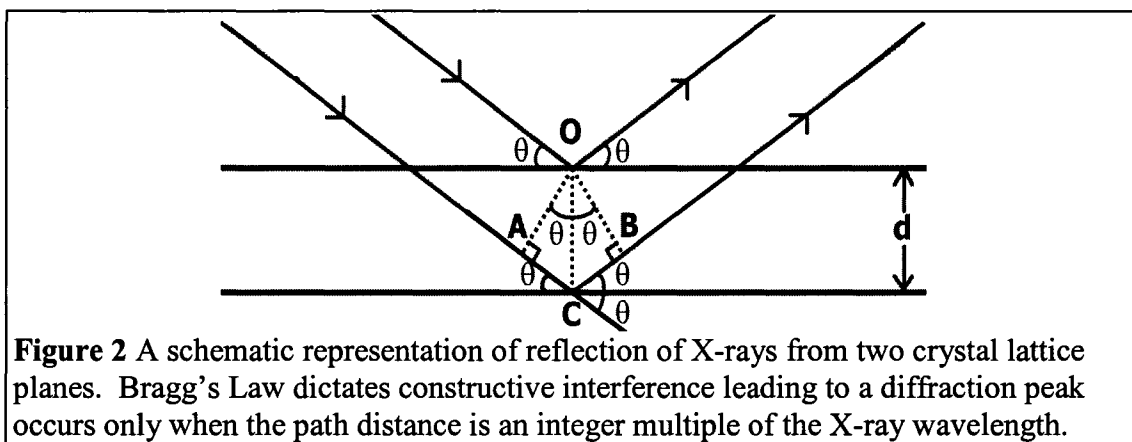


Figure 2 A schematic representation of reflection of X-rays from two crystal lattice planes. Bragg's Law dictates constructive interference leading to a diffraction peak occurs only when the path distance is an integer multiple of the X-ray wavelength.

Given a pair of parallel rays encountering such a lattice at an angle θ , with the distance between layers being a constant value d , the following relationship (based on trigonometric analysis) must be obeyed in order for the X-rays to constructively interfere, giving rise to a diffraction peak:

$$\begin{aligned} \angle AOC &= \angle BOC = \theta \\ AC + CB &= 2AC = n\lambda \\ \text{Since } (AC)/d &= \sin \theta \dots \\ 2d \sin \theta &= n\lambda \end{aligned} \quad (\text{Eq. 1})$$

This final expression is known as Bragg's Law. While the reflection analogy is a rather dramatic simplification of the actual diffraction process of X-rays (which is a combination of scattering and interference effects^[14]), for all practical purposes, it is a

sufficient description of how the various atoms in a crystal will give rise to distinct, sharp diffraction peaks that can be used to extract their position in the crystalline lattice.

Based on the unit cell parameters, planes in the crystals are defined in terms of Miller indices (hkl), with each index simply being the reciprocal of the intercept with the unit cell axes (with distances expressed as fractions of the cell edges). These are the lattice planes that give rise to the reflections observed in a diffraction pattern. As such, the reflections are identified by the Miller index hkl of the plane that produces them. The arrangement of reflections in the diffraction pattern is referred to as the reciprocal lattice, as the spacings in the pattern are reciprocally related to the original lattice. Analysis of the spacing and any systematic absences in the diffraction pattern arising from translational symmetry therefore can be used to deduce the unit cell parameters and crystallographic space group of a crystal.

SCXRD Structure Solution

In order to determine the structure of a crystal through diffraction, it is necessary to relate the various reflections making up the diffraction pattern to the positions of the atoms in the unit cell. The scattering of X-rays making up a given reflection hkl are proportional to the combined scattering factors of all the atoms in the unit cell, giving rise to the structure factor F_{hkl} :

$$F_{hkl} = \sum f_j e^{2\pi i(hx_j + ky_j + lz_j)} \quad (\text{Eq. 2})$$

where f_j is the scattering factor of each atom and x_j, y_j, z_j are the fractional coordinates of each atom.

This expression can be broken down into functions defining the amplitude ($|F_{hkl}|$) and phase (α_{hkl}) of the reflection (in radians):

$$\begin{aligned} |F_{hkl}| &= \sqrt{A_{hkl}^2 + B_{hkl}^2} \\ A_{hkl} &= \sum f_j \cos 2\pi(hx_j + ky_j + lz_j) \\ B_{hkl} &= \sum f_j \sin 2\pi(hx_j + ky_j + lz_j) \quad \text{(Eq. 3)} \\ \alpha_{hkl} &= \tan^{-1} \frac{B_{hkl}}{A_{hkl}} \end{aligned}$$

Finally, by making use of a Fourier synthesis, the structure factor can be related back to the electron density at a given point the unit cell ($\rho(x,y,z)$):^[15]

$$\rho(x, y, z) = \frac{1}{V} \sum_h \sum_k \sum_l |F_{hkl}| \cos 2\pi(hx + ky + lz - \alpha'_{hkl}) \quad \text{(Eq. 4)}$$

where V is the volume of the unit cell, and α'_{hkl} is the phase of the reflection in cycles.

Given that the energy of a cosine wave is proportional to the square of the amplitude of the wave, the intensity of a given reflection is proportional to $|F_{hkl}|^2$, the intensities measured by a diffractometer can be used to determine $|F_{hkl}|$. However, the phase is not directly measurable (a limitation referred to as the phase problem), and must be extracted mathematically. For small molecule structures, the phases are now most commonly deduced initially using direct methods, a complex statistical approach which makes use of normalized structure factors (E_{hkl}) in a probability based determination of an appropriate phase model for the structure.^[8]

While the specific mathematics underlying direct methods is beyond the scope of the current discussion, in general terms the process relies upon certain structure invariant phases serving to subsequently guide the deduction of probable phase relationships

between various reflections (with those between reflections with high E values tending to be true).^[8, 9] In practice, a series of direct methods trials are run, with the best one being selected on the basis of a combined figure of merit (the precise nature of which depends on the structure solution program used). This model is then used to calculate Fourier syntheses of the electron densities in the structure, giving rise to peaks that can then be attributed to various atoms with associated thermal parameters defining their range of motion about the assigned coordinates.

SCXRD Structure Refinement

The solution provided by direct methods (or other phasing methods) serves as the starting point for modeling the crystal structure. The model allows for the calculation of structure factor amplitudes ($|F_C|$) that can then be compared to the observed values ($|F_O|$). However, the initial model typically does not include all of the atoms present in the structure, and the parameters describing those atoms that are present are not optimal. The structural model is completed using difference Fourier syntheses of electron density (so called because the difference between $|F_O|$ and $|F_C|$ is used in place of $|F_C|$ alone), which take advantage of the initial phasing model to locate residual electron density in the unit cell due to these unassigned atoms.

The actual refinement of the structure is carried out through the method of least squares. In order to do so, the following function is minimized:

$$D = \sum_{hkl} w_{hkl} \left(|F_O|^2 - |kF_C|^2 \right)^2 \quad (\text{Eq. 5})$$

where w_{hkl} is a weighting factor, and k is a scale factor. The actual variables involved in such a calculation consist of the coordinates of the various atoms and the thermal

parameters associated with them, which are then used to calculate F_C . The consequence of this is that up to 9 parameters are required to model each crystallographically distinct atom (depending on whether the thermal parameters are treated as being isotropic or anisotropic in nature).

In the ideal case, least squares refinement leads to convergence at a stable minimum, with all large residual electron density peaks accounted for. The quality of the structural model emerging from this refinement can be evaluated in a variety of fashions. Most commonly, a model is evaluated in terms of the residual index (or R value), which measures the agreement between $|F_O|$ and $|F_C|$ (the R1 value), or between $|F_O|^2$ and $|F_C|^2$ (the wR2 value):

$$R1 = \frac{\sum (|F_O| - |F_C|)}{\sum (|F_O|)} \quad (\text{Eq. 6})$$
$$wR2 = \sqrt{\frac{\sum w(|F_O|^2 - |F_C|^2)^2}{\sum w(|F_O|^2)^2}}$$

For a small molecule structure, a good structure will typically have an R1 value < 0.05, with the wR2 value typically being approximately two to three times this. It is important to note that is quite possible to produce a model that agrees quite well with the observed reflection data, but entails a physically impossible arrangement of atoms. Therefore, the truest test of the quality of a converged structure is the chemical reasonability of the overall structure, as indicated by the positioning of the molecules, thermal parameters of the atoms and the bond lengths derived from the resulting model.

SCXRD in Supramolecular Chemistry

The actual process of collecting SCXRD data is highly automated, such that non-expert users can collect solve and refine simple structures as a matter of routine. The structures of supramolecular assemblies are more complex, however, due to conformational flexibility and the dependence on weak intermolecular interactions to guide the structures. In fact, many reported structures of supramolecular compounds have R1 values ranging between 0.05 and 0.15, due to the large atomic thermal parameters arising from unresolved disorder present in these structures. While data collection at low temperature helps to mitigate such effects (by reducing the thermal motion of the atoms), the key to obtaining an accurate single crystal X-ray diffraction structure for a supramolecular system rests in establishing an appropriate model for disordered portions of the structure.

The approach adopted in this thesis to obtain such models consists of a combination of a rigorous data collection strategy, careful consideration of any additional information available regarding the real space orientation of the moiety, and considerable patience. Rigorous data collection entails collecting complete spheres of data to high resolution, in order to be able to distinguish between the various sites a disordered fragment occupies, and accommodate the increased number of atomic parameters associated with modeling disordered sites. Real space information is derived from previous structural studies of guests and hosts, such that appropriate restraints can be applied to distances between nearest neighbour and second nearest neighbour atoms such that the conformations of the molecules are reasonable. Finally, patience is required to

subsequently refine and adjust the initial model of disorder to account for oversights, or to investigate alternative models when the initial model proves to be unreasonable from a chemical or crystallographic point of view.

Powder X-ray Diffraction

Powder XRD (PXRD) follows the same general principles as SCXRD. However, the polycrystalline nature of the powder results in the reflections arising from diffraction to appear as bands of intensity, as opposed to the discrete spots arising from single crystals. For organic supramolecular compounds, which frequently have low symmetry, the resulting powder patterns are quite complex, and not readily indexed by automated means, let alone allowing for structure solution. However, when SCXRD data is available, it is still possible to make use of PXRD for evaluation of supramolecular compounds, basing indexing and structural analysis on predicted powder patterns.^[16, 17] In the current work, this approach has proven to be an excellent supplement for the investigation of pseudopolymorphism of calixarene compounds.

General Details of SCXRD and PXRD Equipment Used

Single Crystal X-ray Diffraction data in this thesis were collected on a Bruker SMART 1K CCD diffractometer (Mo-K α $\lambda=0.71073$ Å) equipped with a graphite monochromator. In general, data were collected at low temperature (either 173 ± 1 K or 125 ± 1 K). Empirical absorption corrections were applied using the SADABS program. Structures were solved using direct methods and refined using full-matrix least squares on F^2 using the SHELXTL suite of programs.^[18] Specific notes regarding the treatment of each data set can be found in the Experimental Section of each chapter and on the CD-

ROM located at the end of the thesis. Relevant parameters are reported with estimated standard deviations in parentheses.

Powder X-ray Diffraction data were collected at room temperature (293 ± 1 K) using either of two instruments. The majority of powder patterns were obtained using a Scintag X-2 Advanced diffractometer ($\text{Cu-K}\alpha=1.54178 \text{ \AA}$) equipped with a graphite monochromator, using the θ - θ scan mode. Such samples were scanned over a 2θ range of 5° to 60° , using a scan rate of $0.02^\circ/\text{sec}$ and a count time of 1 sec. Selected patterns were obtained using a Rigaku Geigerflex vertical goniometer diffractometer ($\text{Co-K}\alpha=1.79021 \text{ \AA}$) equipped with a graphite monochromator, using the θ - θ scan mode. Such samples were scanned over a 2θ range of 5° to 50° , using a scan rate of $0.05^\circ/\text{sec}$ and a count time of 3 sec. When appropriate, the resulting diffraction patterns were manually indexed using the predicted pattern from the SCXRD structures (corrected for appropriate wavelength) as a guide, along with the program Crystal Cracker^[19] and the Powder 4.0 program suite.^[20] Unit cell parameters were then obtained by fitting the calculated 2θ values to the observed peaks (save any angles fixed as a consequence of the space group selection). The uncertainty of individual unit cell parameters is estimated to be $\pm 0.05\%$.

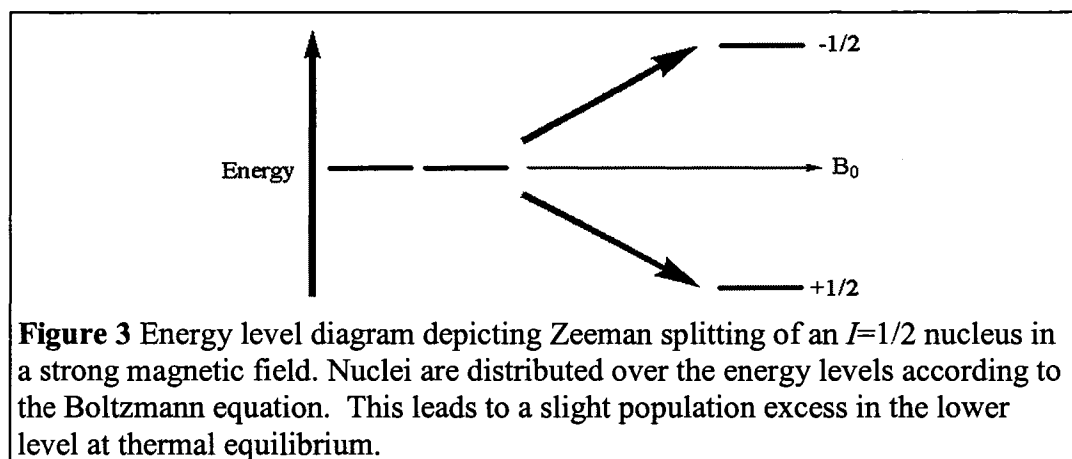
3. Solid-State Nuclear Magnetic Resonance (SSNMR) Spectroscopy

Nuclear magnetic resonance spectroscopy has long been the primary technique for the characterization of organic compounds in solution. In spite of this, solid state NMR (SSNMR) tends to be overlooked by those interested in the behaviour of organics in the solid state. This is largely due to the perception that SSNMR is a complex, labour-intensive technique, unsuitable for use by non-experts. This perception has its roots in

the considerable differences between solution NMR and SSNMR, which indeed are real. However, once these concerns are addressed, a considerable amount of information can be obtained from SSNMR experiments. In this thesis, particular advantage has been taken of the ability to use ^{13}C NMR spectroscopy to complement diffraction data in analysing the inclusion behaviour of calixarenes and the resulting pseudopolymorphism. As such, the following overview focuses on the essential theory underlying the NMR of spin $\frac{1}{2}$ nuclei in the solid state. Readers interested in additional detail regarding SSNMR are directed to the various excellent reviews^[21-24] and monographs^[25-28] currently available.

The NMR Phenomenon

The NMR phenomenon arises out of the interaction of nuclear spin “magnets” with a strong magnetic field, known as the Zeeman effect. In the absence of a magnetic field, the spin states of a particular nucleus with a non-zero spin quantum number are degenerate, showing no differentiation in energy between the various spin states. However, in a strong magnetic field, the orientation of the nuclear spin becomes significant, and this degeneracy vanishes (see Figure 3).



In quantum mechanical terms, the Zeeman interaction is described by the following Hamiltonian:

$$H_z = -\gamma \frac{h}{2\pi} B_0 I \quad (\text{Eq. 7})$$

where γ is a proportionality constant unique to each nucleus (the gyromagnetic ratio), h is Planck's constant, B_0 is the applied magnetic field, and I is the spin of the nucleus. For a given nucleus, quantum theory dictates that $2I+1$ spin energy levels will exist, with the nuclei distributed among these levels according to the Boltzmann equation (i.e., as shown in Figure 3, spin $\frac{1}{2}$ nuclei are distributed over a two-level system as defined by the magnetic quantum number). These populations can be manipulated with resonant radio frequency fields, $\omega = \gamma B$ (where B is the magnetic field experienced by the nucleus) with the subsequent observation of the radio-frequency energy emitted as the nuclei return to thermal equilibrium carrying the information on local magnetic interactions that give rise to the NMR spectrum.

While this means that NMR spectroscopy is a relatively insensitive technique (as the population excess necessary to generate a signal is only on the order of 1 in 10^5 at thermal equilibrium), the resulting spectral lines correlate directly to chemically distinct nuclei. The power of the technique lies in the quantitative, one-to-one correlation of spectral intensity with the number of nuclei involved in giving rise to a particular spectral line. In solution, the spectroscopy is relatively straightforward, with good signal intensity acquired rapidly because thermal equilibrium is reached relatively quickly after an excitation pulse, and the frequency shifts of the observed resonances can be interpreted in a straightforward way. However, this is not the case in the solid-state, where the return to

thermal equilibrium is slow and inherently anisotropic interactions influence the line shape (due to the absence of molecular motions to average these interactions out).

Key Challenges in SSNMR of Spin $\frac{1}{2}$ Nuclei

The NMR line shape can be described by the following Hamiltonian, where the different interactions are treated as perturbations on the Zeeman interaction:

$$H = H_Z + H_Q + H_D + H_\sigma + H_J \quad (\text{Eq. 8})$$

Here H_Q is the quadrupolar interaction, H_D is the nuclear dipolar interaction, H_σ is the chemical shielding interaction, and H_J is the J coupling. In solution, the various terms are treated as scalar interactions lacking directional components, because rapid molecular motions average the directional effects of these interactions relative to the magnetic field. In the solid state, these motions are usually absent, and the various interactions perturbing the Zeeman interaction must be treated as tensors, accounting for the effects of the angular orientation of a nucleus relative to the magnetic field in three-dimensional space.

The J coupling interaction is familiar to most chemists from solution NMR spectroscopy, but in the ^{13}C SSNMR experiment, it is subordinate to a number of other interactions and for experimental reasons is not usually observed. The quadrupolar interaction is only observed for nuclei with spin greater than $\frac{1}{2}$, and is not a concern for the commonly observed nuclei in organic molecules (^1H , ^{13}C , ^{31}P , ^{15}N). However, the effect of the quadrupolar interaction on the NMR line shape has seen considerable application to studies of dynamics in solid-state systems, especially through the use of isotopically labeled materials. As a result, the two dominant perturbing interactions for spin $\frac{1}{2}$ nuclei are the dipolar interaction and the chemical shift interaction.

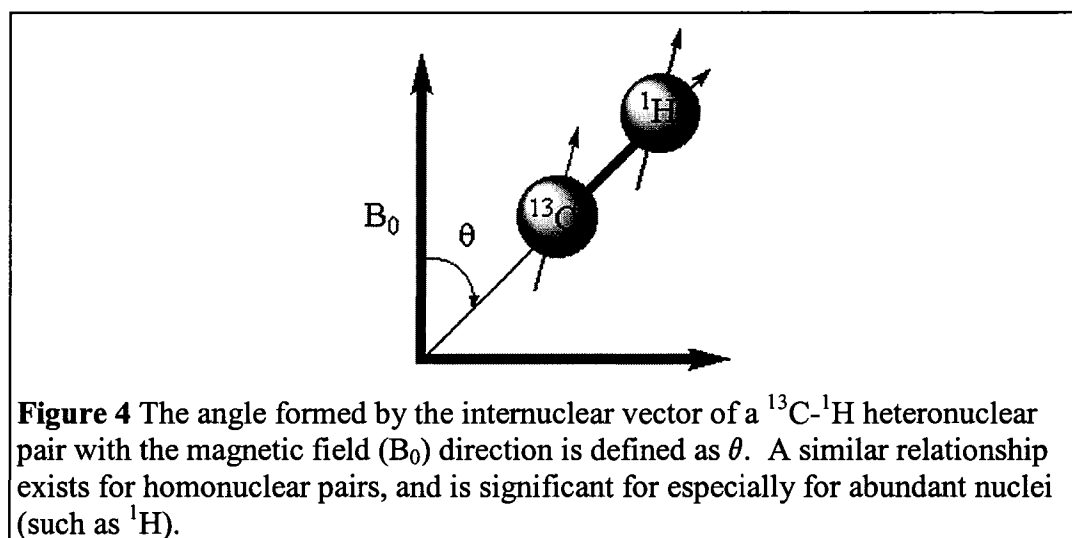
The dipolar interaction results from the through-space interaction of the magnetic moments of two nuclei. The significant terms in the Hamiltonian for dipolar interaction are the dipolar coupling constant and the angular dependence (or orientation) term. The dipolar coupling constant for a typical C-H heteronuclear pair is expressed as:

$$D = \frac{\mu_0}{4\pi} \frac{\gamma_I \gamma_S \hbar}{r^3} \quad (\text{Eq. 9})$$

where μ_0 is the permeability of free space, γ_I is the gyromagnetic ratio of the abundant nucleus (*i.e.*, ^1H), γ_S is the gyromagnetic ratio of the rare nucleus (*i.e.*, ^{13}C) and r is the internuclear distance. For the homonuclear case, the gyromagnetic ratios of the two nuclei are identical, and $(\gamma_I \gamma_S)$ is replaced by (γ^2) in the above expression. It can be readily seen that the dipolar interaction readily drops off with distance, but is highly dependent on the gyromagnetic ratio of the coupled nuclei. As most organic materials have a large number of protons, which have the highest gyromagnetic ratio of the common NMR active nuclei, the dipolar interaction can lead to significant fine structure of both heteronuclear and ^1H spectra in the solid state.

The orientation term simply indicates that the dipolar interaction is proportional to $(3\cos^2\theta - 1)$, where θ is the angle between the internuclear vector and the direction of the external magnetic field (see Figure 4). In solution, molecules tumble rapidly, and this term is averaged to zero. As a result, dipolar coupling is not manifest in solution NMR except as a mechanism for relaxation. In a polycrystalline solid, a distribution of all possible orientations will be observed for the internuclear vectors with respect to the magnetic field for all nuclear magnet pairs, usually obscuring fine structure and giving rise to a very broad spectrum. However, it is important to note that when the orientation

of the internuclear vector relative to the magnetic field is such that $\theta=54.74^\circ$ (the “magic angle”), the orientation term $(3\cos^2\theta-1)=0$, causing the dipolar Hamiltonian for that pair to vanish. By the same token, as a through-space interaction dependent on distance, potentially it can be used to obtain information regarding the structure of a given material.

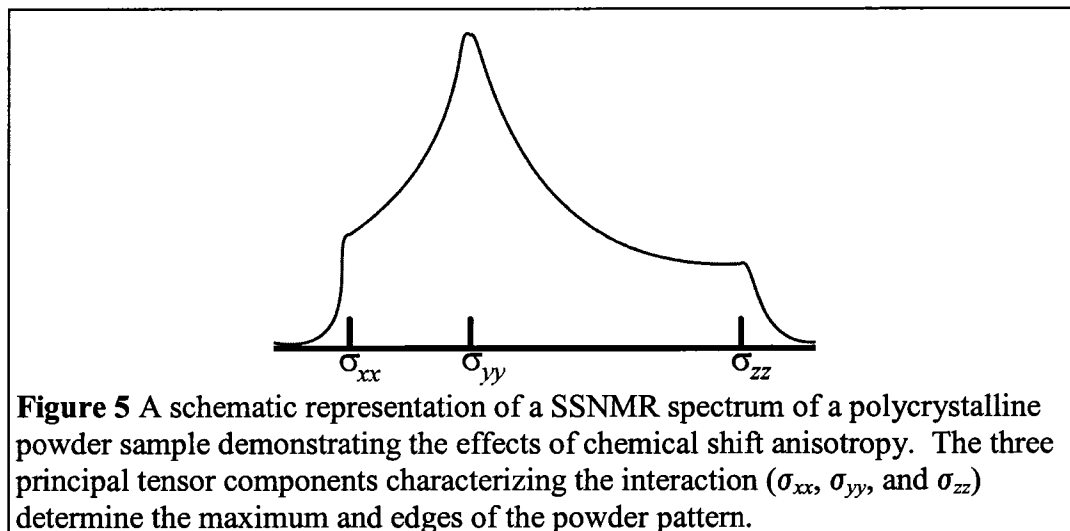


Chemical shielding results from the interactions of the electrons surrounding an atom influencing the net magnetic field experienced by the nucleus. This gives rise to the chemical shift, which, like J coupling, is a phenomenon familiar to organic chemists. Once again, though, the restricted motion of molecules in the solid state results in anisotropy being significant. The Hamiltonian describing this interaction is written as:

$$H_\sigma = I\sigma B \quad (\text{Eq. 10})$$

where I is the spin, σ is the chemical shift and B is the applied magnetic field. In a polycrystalline sample, this gives rise to a range of chemical shifts being observed for each nucleus, depending on the orientation of its shielding tensor with respect to the

magnetic field, producing a broad, structured spectrum known as a powder pattern (see Figure 5).

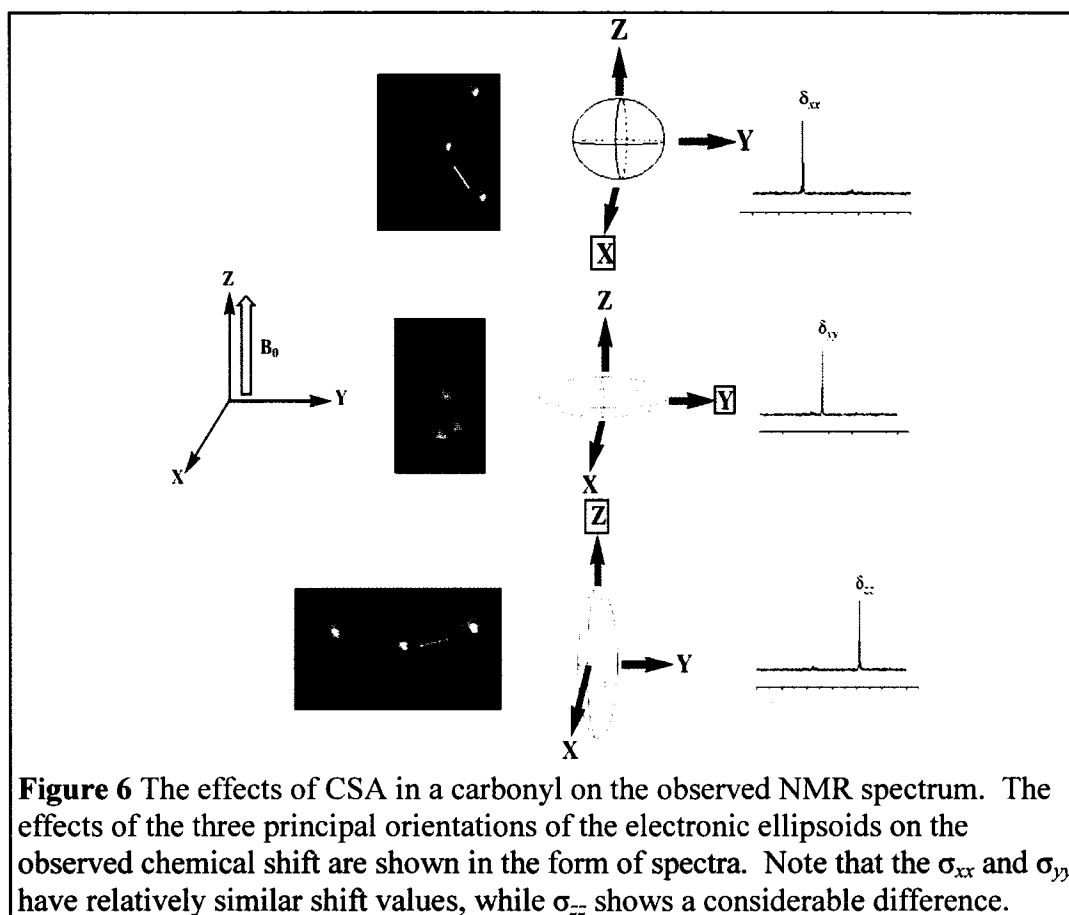


This line shape can be expressed in terms of the angles α and β formed by the tensor with respect to the magnetic field:

$$\omega = \gamma H_0 (\sigma_{xx} \cos^2 \alpha \sin^2 \beta + \sigma_{yy} \cos^2 \alpha \sin^2 \beta + \sigma_{zz} \cos^2 \beta) \quad (\text{Eq. 11})$$

where σ_{xx} , σ_{yy} , and σ_{zz} are the chemical shift tensors arising from the three distinct orientations of the ellipsoids describing the electrons surrounding the nucleus of interest. These orientations are readily apparent in a simple system, such as a carbonyl (see Figure 6). Each of these orientations has a distinct chemical shift that defines the key features in the overall powder pattern. The contributions of the σ_{zz} orientation, which has the highest upfield shift, produces the shoulder that starts the “tail” in the powder pattern depicted in Figure 5, while the other two orientations jointly contribute to produce a relatively sharp peak and a second shoulder. Much like the dipolar interaction, the chemical shift anisotropy (CSA) is also a potential source of information regarding the orientation of

molecules in a solid, but for the purposes of obtaining high-resolution spectra, the spectroscopist must find a way to eliminate its effects.



The final consideration for a SSNMR experiment is the time required for the spin system to return to thermal equilibrium, which is expressed in terms of the spin-lattice relaxation time, T_1 . In solution, the rapid tumbling of molecules results in extensive thermal motion of the nuclear spins, which couples the spins to fluctuating magnetic fields and results in efficient relaxation and relatively small values of T_1 . As might be expected, the lack of mobility in the solid-state can lead to dramatic increases in T_1 values, in particular for low abundance nuclei such as ^{13}C . Since an equilibrium

spectrum requires a waiting time of $\sim 5T_1$ between excitation pulses, this can result in much longer acquisition times for SSNMR spectra.

SSNMR of Spin $\frac{1}{2}$ Nuclei in Organic Materials

It should now be apparent that the standard approach to solution NMR takes advantage of the isotropic averaging of the tumbling of molecules in solution to yield high-resolution spectra. For SSNMR, a wealth of additional anisotropic interactions are present that, while being potential sources of information, are initially frustrating obstacles to obtaining resolved spectra with interpretive value. Fortunately, methods have been developed to effectively deal with the effects of anisotropic interactions, and the technical considerations that these approaches entail have been reviewed by Wasylshen *et al.* [21]

In organic compounds carbon is the most abundant element present (after hydrogen), and ^{13}C is by far the most frequently observed nucleus in SSNMR experiments, and for SSNMR spectroscopists, the standard 1D experiments are routine. Not only is such an experiment the most accessible, but it also forms the foundation for the more advanced methods. With this in mind, the fundamental techniques outlined here, as well as how they are applied, are also suitable for other nuclei commonly encountered in organic chemistry, such as ^{29}Si and ^{15}N .

a) Dipolar Decoupling

For the ^{13}C nucleus, the major obstacles to obtaining high-resolution spectra are heteronuclear dipolar coupling with ^1H , CSA, and the rather long T_1 values.

Heteronuclear dipolar coupling to protons is dealt with by the use of continuous wave

(CW) decoupling after the excitation pulse is applied, much as in liquids spectroscopy, but at much higher power levels (typically ~ 50 kHz for ^{13}C - ^1H). This causes coherent averaging of the ^1H - ^{13}C dipolar couplings. More recent techniques, such as two-pulse phase modulated decoupling (TPPM),^[29] which makes use of an innovative pulse scheme to achieve decoupling at lower power than with comparable CW decoupling, serve to partially overcome the difficulties of putting long, high intensity (and thus, potentially damaging) pulses into the NMR probe.

b) Magic Angle Spinning (MAS)

The broadening of spectral lines arising from CSA is overcome using magic angle spinning (MAS),^[30, 31] which essentially serves to emulate the averaging effects of molecular motion in solution. The CSA line shape arises from the tensor nature of the chemical shift and from the fact that all possible orientations of the molecules are possible in a polycrystalline solid. In order to reduce the shift tensor to its average value, the standard approach is to take advantage of the angular dependence of the chemical shift with respect to the field.

As mentioned previously, when the angle of an interaction tensor in a molecule is aligned with respect to the magnetic field at the magic angle ($\theta=54.74^\circ$), the dipolar as well as the chemical shift tensor Hamiltonians will vanish. Such a method would be of limited utility for polycrystalline powders, with their non-symmetric CSAs and broad distributions of molecular orientations. However, by spinning such a sample at high speed the averaging process can be described by the following equation:

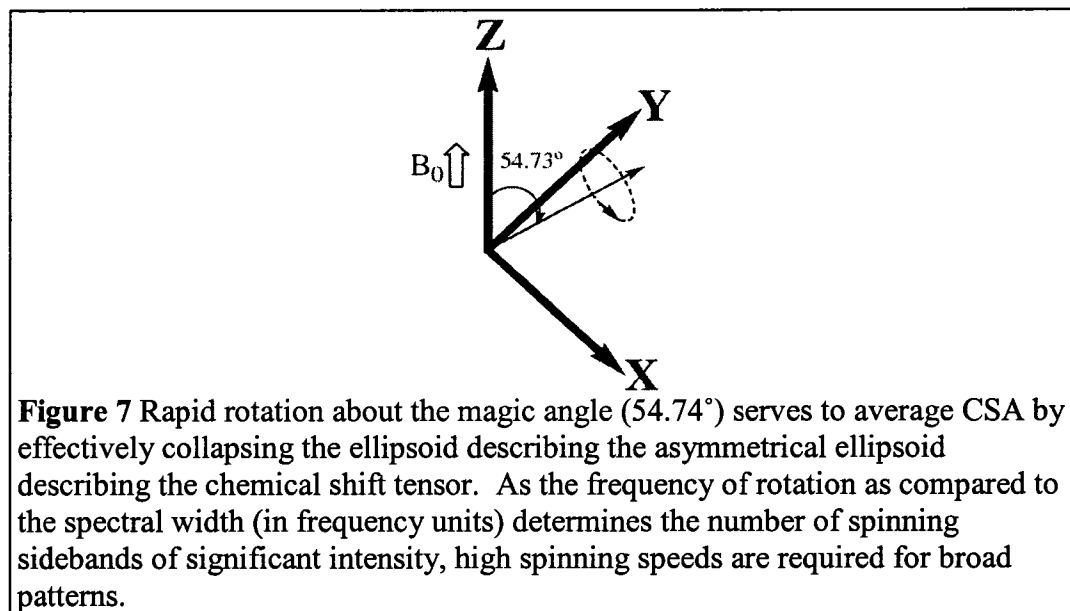
$$\omega = \gamma B_0 [1 - 3/2 \sigma_i \sin^2 \beta + 1/2 (3 \cos^2 \beta - 1) \sum_{ii} \sigma_{ii} \cos^2 \chi_{ii}] \quad \text{(Eq. 12)}$$

such that the anisotropic terms described by the sum of the chemical shifts observed during a given rotation show a dependence on $(3\cos^2\beta-1)$.

As such, MAS relies on rapid spinning of a sample about the magic angle in order to reduce the effects of CSA in a polycrystalline sample (see Figure 7), giving rise to a sharp line at the isotropic shift plus a set of satellite peaks known as spinning sidebands.^[32] The efficacy of the averaging through spinning is dependent on the spinning speed, and at low speeds the sidebands appear at frequency spacings equal to multiples of the spinning frequency. In a MAS spectrum, the integrated intensity of the resonance line must include contributions from all spinning sidebands. However, with modern MAS probes, high enough spinning speeds can be achieved such that the rotational echo amplitudes are minimized (by spinning at rates considerably greater than the spectral width). As well, various pulse sequences exist to suppress the sidebands completely, such as TOSS (total suppression of spinning sidebands).^[33-35] The spectrum obtained under slow spinning conditions will approximate the powder pattern, and can be analyzed by the Herzfeld-Berger method to extract the CSA parameters of each nucleus.^[36]

The resulting isotropic shifts are particularly useful in characterizing inclusion compounds. When a guest is enclathrated in a host molecule, a complexation-induced shift (CIS) from the chemical shift observed for the pure guest in solution is common. This CIS typically arises from close proximity to common shielding functionalities, such as aromatic rings. As a result, qualitative comparisons of inclusion compounds suitable for guiding the creation of structural models can also be derived from analysis of

chemical shift data. The 4tBC4A system is a prime example of how these effects can provide important structural information



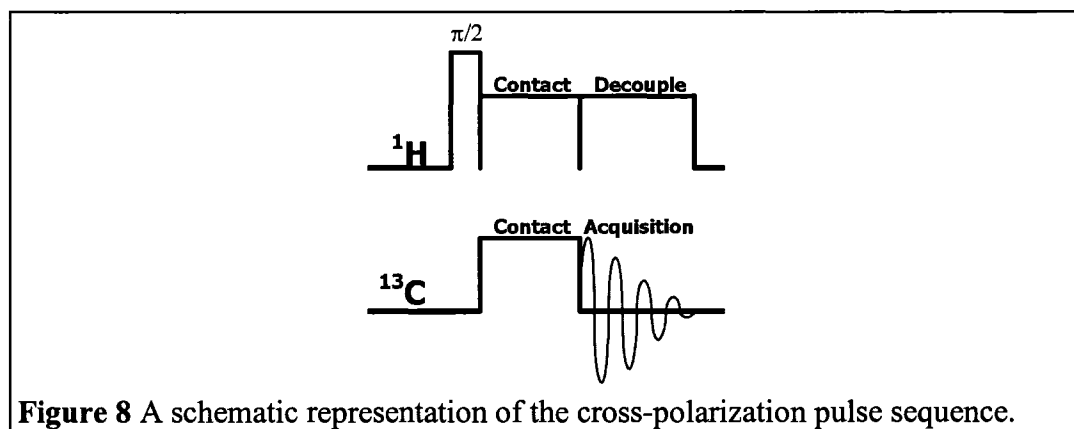
MAS is also useful in averaging out weak dipolar couplings, such as those that might be observed between ^{13}C and NMR active nuclei other than ^1H present in typical organics. However, dipolar coupling to quadrupolar nuclei is frequently not quantized along the magnetic field direction, because of large quadrupolar couplings. In such a case, the dipolar coupling is not averaged completely by MAS, and is magnetic field dependent. Since quadrupolar nuclei such as ^{14}N and $^{35,37}\text{Cl}$ are fairly common in organic materials, one must be aware that resonances due to ^{13}C nuclei adjacent to such species may exhibit broadening or additional fine structure. Alternatively, in the case of sufficiently rapid motion, the fine structure disappears because of self-decoupling (short T_2 of the quadrupolar nucleus).

Finally, it is important to note that even with MAS, ^{13}C SSNMR spectra commonly contain many more resonances than their solution counterparts. As mentioned

previously, packing requirements often reduce molecular symmetry in the solid state that results in increased numbers of crystallographically inequivalent atoms. In SSNMR spectroscopy, these crystallographically inequivalent atoms are also magnetically inequivalent, giving rise to crystallographic splitting of resonances. As such, the number of lines in a ^{13}C spectrum can be used as an indicator of the asymmetric unit, and as such, a probe of the symmetry of a structure. This also has utility in investigating polymorphism and pseudopolymorphism, as the differences in symmetry arising from alternative packing arrangements give rise to different splittings.

c) Cross Polarization (CP)

While the use of dipolar decoupling and MAS results in a sharp-line spectrum, the long T_1 values commonly observed for ^{13}C in the solid state make it difficult to obtain spectra with acceptable signal to noise ratios in a reasonable length of time through direct excitation of carbon nuclei. The protons present in a typical organic compound are considerably easier to polarize than ^{13}C , as represented by their high γ , high natural abundance, and much smaller T_1 values. Through cross polarization (CP), a technique first applied by Waugh and co-workers,^[37] it is possible to enhance the signal obtained and avoid the long T_1 times associated with ^{13}C (see Figure 8).



CP relies upon the tendency for the magnetization of a highly polarized nucleus to be transferred to a less polarized nucleus when such an exchange is energy conserving. Typically, the Hartmann-Hahn method is used for CP experiments, whereby following a $\pi/2$ pulse to magnetize the protons, two RF fields at the resonance frequencies of the nuclei involved are applied for a fixed period of time (the contact time) to allow heteronuclear polarization exchange prior to the use of dipolar decoupling.^[38] In order for this to be energy conserving (and therefore permissible), the Hartmann-Hahn matching condition $H_I\gamma_I = H_S\gamma_S$ (where H_I and H_S are the RF fields experienced by the I and S nuclei, and γ_I and γ_S are the gyromagnetic ratios of said nuclei) must be met.

Given this expression, this matching is accomplished through adjustment of the amplitudes of the applied RF fields, while the contact time is governed by the need to ensure maximum polarization transfer from all nuclei without loss of signal due to relaxation of the nuclei. Taking into account this decay due to relaxation, the maximum possible signal enhancement for a basic Hartmann-Hahn CP experiment due to cross-polarization is γ_I/γ_S , resulting in a factor of ~ 4 for ^1H and ^{13}C . In addition, there is the improvement due to the ability to collect scans more rapidly, as pulse sequence repetition times are governed by ^1H rather than ^{13}C relaxation. Further improvements beyond this

can be obtained through variations on this basic experiment, as briefly reviewed by Wasylishen *et al.*^[21]

However, it is important to remember that as a consequence of this indirect excitation in all CP experiments, the signal intensities observed in the spectra obtained are usually not quantitative, as they are now a product of the kinetics of the cross polarization and relaxation processes. Nuclei which are more readily polarized due to strong dipolar couplings to many protons will frequently show much greater increases in intensity than those nuclei which are not proton-bearing. Quantification of peaks in CP experiments is only possible when all nuclei are polarized to the same degree, or by fitting the intensities in terms of growth (based on contact time) and decay (based on the relaxation rate in the rotating sample, $T_{1\rho}$) parameters.

It is also possible to take advantage of differential signal intensities by reintroducing dipolar couplings after the cross polarization process. A brief interruption in dipolar decoupling causes the signals arising from carbons with strong dipolar couplings that do not rapidly reorient (i.e., especially most CH and CH₂ groups) to be partially or completely eliminated, assisting in spectral assignment. This technique, known as dipolar dephasing,^[39, 40] therefore has the additional benefit of serving as a simple probe of motional dynamics, which is invaluable in assessing the disorder of supramolecular calixarene systems.^[24, 41] More refined “sorting” techniques have been developed as well, such as cross polarization combined with polarization inversion (CPPI)^[42, 43] and separated-local-field experiments (SLF).^[44-46]

High Resolution SSNMR Spectroscopy

The impact of each of these methodologies can be readily seen by the comparison of spectra obtained under various conditions. A simple demonstration of this can be drawn from the clathrate chemistry of quinols.^[24] β -Quinol readily forms a clathrate compound with methanol that is quite suitable for structural characterization by SSNMR. In Figure 9, we can see the effects of the various techniques on the ^{13}C SSNMR spectra of the inclusion compound. As would be expected, standard high-resolution solution NMR methods fail to produce any observable signal (Figure 9a). Application of CP leads to a considerable increase in signal strength (Figure 9b), but the peaks are still not resolved. Combined use of CP and dipolar decoupling of ^1H reveals the outline of the various powder patterns of the magnetically inequivalent nuclei present (Figure 9c). Finally, use of MAS to eliminate the CSA gives rise to a spectrum comparable to the solution state (Figure 9d), which can be compared with that of the parent guest-free compound (Figure 9e). As part of this comparison, the different crystallographic splitting patterns make it apparent that the β polymorph suitable for clathrate formation exhibits higher symmetry than the guest free α polymorph.

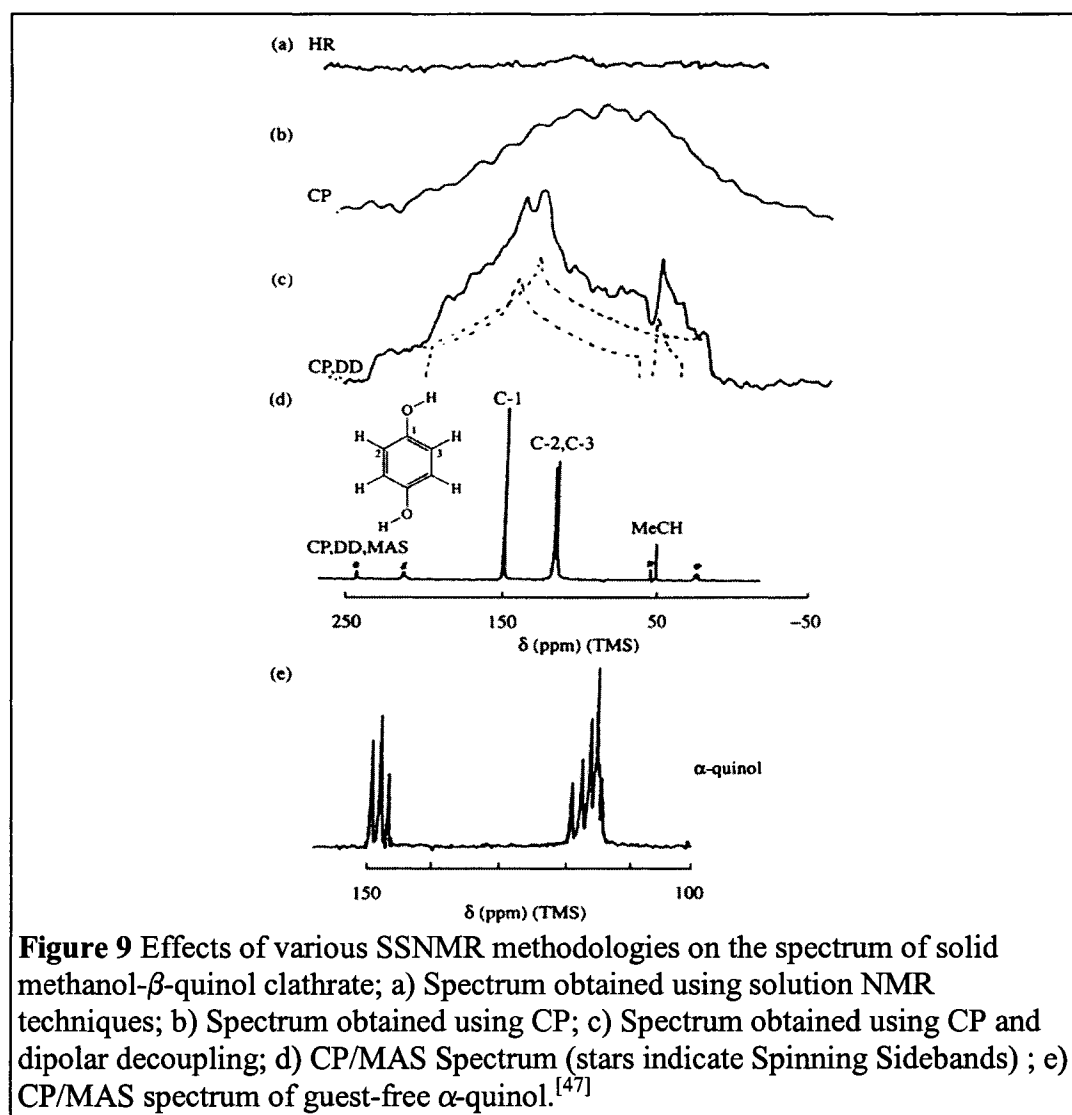


Figure 9 Effects of various SSNMR methodologies on the spectrum of solid methanol- β -quinol clathrate; a) Spectrum obtained using solution NMR techniques; b) Spectrum obtained using CP; c) Spectrum obtained using CP and dipolar decoupling; d) CP/MAS Spectrum (stars indicate Spinning Sidebands) ; e) CP/MAS spectrum of guest-free α -quinol.^[47]

The combined use of these techniques as described above, referred to as CP/MAS spectroscopy, has been a mainstay of SSNMR spectroscopists since its introduction by Schaefer and Stejskal.^[48] Direct excitation high-powered decoupled (HPDEC) MAS spectroscopy also sees extensive use in areas where CP is not feasible (i.e., an absence of protons) or undesirable (i.e., a need for easily integrated peak intensities). It can also serve as a qualitative probe of the mobility of the framework, as moieties with short T_1 will be observed readily with short pulse delays, while the remainder of the supramolecular compound will not. The ease of performing these experiments makes

them quite attractive for the characterization of crystalline materials, particularly those arising from transformations that preclude characterization SCXRD. Even in effectively removing the various anisotropic interactions mentioned to produce solution-like spectra, a wealth of information is still available that is well suited to the characterization of supramolecular compounds in the solid state.

General Details of SSNMR Equipment Used

SSNMR spectra for all compounds investigated in this thesis were collected using one of three spectrometers. The majority of spectra were obtained using a Bruker AMX-300 spectrometer ($^1\text{H}=300.145$ MHz, $^{13}\text{C}=75.483$ MHz) and a Doty 5mm high speed MAS probe. ^{13}C CP/MAS spectra on this instrument were obtained using a pulse delay of 3 sec and a contact time of 2 msec were used, with samples typically spun at approximately 5 kHz. Hexamethylbenzene was used as an external reference with the methyl group signal set to 13.60 ppm.

Selected spectra were obtained using a Tecmag Apollo 200 spectrometer ($^1\text{H}=200.1357$ MHz, $^{13}\text{C}=50.331$ MHz) and a Doty 7mm high speed MAS probe. ^{13}C CP/MAS spectra on this instrument were obtained using a pulse delay of 3 sec and a contact time of 3 msec, with samples typically being spun at approximately 3 kHz. Adamantane was used as an external reference, with the less shielded signal set to 38.56 ppm.

SSNMR spectra of $^{13}\text{CO}_2$ gas adsorption samples were obtained with the assistance of Dr. Igor Moudrakovski, using a Bruker Avance 200 spectrometer ($^1\text{H}=200.495$ MHz, $^{13}\text{C}=50.419$ MHz) and a Chemagnetics Pencil 7.5 mm MAS probe.

CP/MAS spectra were collected using a pulse delay of 3 sec and a contact time of 3 msec, with samples being spun at approximately 3 kHz. HPDEC spectra were obtained using a $\pi/2$ pulse of 5 μ sec, with samples being spun at approximately 3 kHz. To allow for quantitative measurements, suitable pulse delays were determined on the basis T_1 relaxation time measurements. Adamantane was used as an external reference, with the less shielded signal set to 38.56 ppm.

For all spectrometers, dipolar dephased spectra were obtained by inserting a 40 μ s delay between cross polarization and acquisition, during which time the decoupler was switched off. Chemical shifts and the resulting complexation induced shifts (CIS) are accurate to within ± 0.05 ppm.

4. Summary

The theory and practice of XRD and SSNMR as tools for the characterization of solid materials in general, and supramolecular compounds in particular, has been summarized. When used in concert, the two techniques provide complementary information that allow for more detailed structural modeling of materials by allowing one to account for the influences of short-range interactions on long-range ordering. As we will see in the coming chapters, such a combined approach allows for a fuller understanding of the competition between non-covalent forces guiding the assembly of supramolecular frameworks from simple calixarenes, and the pseudopolymorphism that arises from influencing such competition.

5. References

- [1] J. W. Steed, J. L. Atwood, in *Supramolecular Chemistry*, John Wiley & Sons, Ltd., Chichester, **2000**, p. XIX.

- [2] C. D. Gutsche, *Calixarenes*, Royal Society of Chemistry, Cambridge, **1989**.
- [3] C. D. Gutsche, *Calixarenes Revisited*, Royal Society for Chemistry, Cambridge, **1998**.
- [4] J. Vicens, V. Bohmer, *Calixarenes: A Versatile Class of Macrocyclic Compounds*, Kluwer Academic Publishers, Dordrecht, **1991**.
- [5] P. Timmerman, W. Verboom, D. N. Reinhoudt, *Tetrahedron* **1996**, *52*, 2663.
- [6] L. Mandolini, R. Ungaro, *Calixarenes in Action*, Imperial College Press, London, **2000**.
- [7] Z. Asfari, V. Bohmer, J. Harrowfield, J. Vicens, *Calixarenes 2001*, Kluwer Academic Publishers, Dordrecht, **2001**.
- [8] G. H. Stout, L. H. Jensen, *X-Ray Structure Determination. A Practical Guide*, John Wiley & Sons, New York, **1989**.
- [9] C. Giacovazzo, ed., *Fundamentals of Crystallography*, Oxford University Press, Oxford, **1992**.
- [10] M. F. C. Ladd, R. A. Palmer, *Structure Determination by X-ray Crystallography*, 3rd ed., Plenum Press, New York, **1994**.
- [11] G. H. Stout, L. H. Jensen, in *X-Ray Structure Determination. A Practical Guide*, John Wiley & Sons, New York, **1989**, p. 18.
- [12] G. H. Stout, L. H. Jensen, in *X-Ray Structure Determination. A Practical Guide*, John Wiley & Sons, New York, **1989**, p. 7.
- [13] M. F. C. Ladd, R. A. Palmer, in *Structure Determination by X-ray Crystallography*, 3rd ed., Plenum Press, New York, **1994**, p. 494.
- [14] M. F. C. Ladd, R. A. Palmer, in *Structure Determination by X-ray Crystallography*, 3rd ed., Plenum Press, New York, **1994**, p. 134.
- [15] This equation also assumes that Friedel's Law ($F_{hkl}=F_{-h-k-l}$) holds true.
- [16] P. Sidhu, Ph.D. thesis, Carleton University (Ottawa), **2005**.
- [17] P. S. Sidhu, G. D. Enright, K. A. Udachin, J. A. Ripmeester, *Crys. Growth & Design* **2004**, *4*, 1249.
- [18] G. M. Sheldrick, SHELXTL, 6.10, Bruker AXS, Madison, WI, **2000**.
- [19] K. Leinenweber, Crystal Cracker, 186, http://multianvil.asu.edu/Crystal_Cracker/CrystalCracker.html, **2005**.
- [20] N. Drago, *Journal of Applied Crystallography* **2001**, *34*, 535.
- [21] D. L. Bryce, G. M. Bernard, M. Gee, M. D. Lumsden, K. Eichele, R. E. Wasylishen, *Can. J. Anal. Sci. Spect.* **2001**, *46*, 46.
- [22] D. D. Laws, H.-M. L. Bitter, A. Jerschow, *Angew. Chem. Int. Ed.* **2002**, *41*, 3096.
- [23] S. P. Brown, H. W. Spiess, *Chem. Rev.* **2001**, *101*, 4125.
- [24] J. A. Ripmeester, C. I. Ratcliffe, in *Comprehensive Supramolecular Chemistry* (Eds.: J. L. Atwood, J. E. D. Davies, D. D. MacNicol, F. Vogtle), Pergamon Press, Oxford, **1996**.
- [25] C. A. Fyfe, *Solid State NMR for Chemists*, C.F.C. Press, Guelph, ON, **1983**.
- [26] K. Schmidt-Rohr, H. W. Spiess, *Multidimensional Solid-State NMR and Polymers*, Academic Press, London, **1994**.
- [27] E. O. Stejskal, J. D. Memory, *High Resolution NMR in the Solid State: Fundamentals of CP/MAS*, Oxford University Press, Oxford, **1994**.

- [28] M. J. Duer, *ed.*, *Solid-State NMR Spectroscopy: Principles and Applications*, Blackwell Science, Oxford, **2002**.
- [29] A. E. Bennett, C. M. Rienstra, M. Auger, K. V. Lakshmi, R. G. Griffin, *J. Chem. Phys.* **1995**, *103*, 6951.
- [30] E. R. Andrew, A. Bradbury, R. G. Eades, *Nature* **1958**, *182*, 1659.
- [31] I. J. Lowe, *Phys. Rev. Lett.* **1959**, *2*, 285.
- [32] E. R. Andrew, *Phil. Trans. R. Soc. Lond.* **1981**, *A299*, 505.
- [33] W. T. Dixon, J. Schaefer, M. D. Sefcik, E. O. Stejskal, R. A. McKay, *J. Magn. Reson.* **1982**, *49*, 341.
- [34] W. T. Dixon, *J. Chem. Phys.* **1982**, *77*, 1800.
- [35] N. C. Nielsen, H. Bildsoe, H. J. Jakobsen, *J. Magn. Reson.* **1988**, *80*, 149.
- [36] J. Herzfeld, A. E. Berger, *J. Chem. Phys.* **1980**, *73*, 6021.
- [37] A. Pines, M. G. Gibby, J. S. Waugh, *J. Chem. Phys.* **1973**, *59*, 569.
- [38] S. R. Hartmann, E. L. Hahn, *Phys. Rev.* **1962**, *128*, 2042.
- [39] S. J. Opella, M. H. Frey, *J. Am. Chem. Soc.* **1979**, *101*, 5854.
- [40] L. B. Alemany, D. M. Grant, T. D. Alger, R. J. Pugmire, *J. Am. Chem. Soc.* **1983**, *105*, 6697.
- [41] E. B. Brouwer, Ph.D. thesis, Carleton University (Ottawa), **1996**.
- [42] X. Wu, K. W. Zilm, *J. Mag. Res. Ser. A* **1993**, *102*, 205.
- [43] X. Wu, S. T. Burns, K. W. Zilm, *J. Mag. Res. Ser. A* **1994**, *111*, 29.
- [44] E. F. Rybaczewisky, B. L. Neff, J. S. Waugh, J. S. Sherfinski, *J. Chem. Phys.* **1977**, *67*, 1231.
- [45] G. G. Webb, K. W. Zilm, *J. Am. Chem. Soc.* **1989**, *111*, 1455.
- [46] N. K. Sethi, *J. Magn. Reson.* **1991**, *94*, 352.
- [47] Used with permission from J.A. Ripmeester.
- [48] J. Schaefer, E. O. Stejskal, *J. Am. Chem. Soc.* **1976**, *98*, 1031.

Chapter III: Alkylamine Clathrates of 4-*t*-butylcalix[4]arene[†]

1. Abstract.....	68
2. Introduction.....	69
3. Experimental Section.....	71
4. Results and Discussion.....	77
Polar Clusters: <i>n</i> -butylamine and amylamine	77
Polar Layers: hexylamine and dodecylamine.....	88
Pseudopolymorphism arising from Amine Polar Clusters and Layers	93
CO ₂ Adsorption by <i>n</i> -butylamine clusters in 4tBC4A.....	109
5. Conclusion	119
6. References	121

1. Abstract

4-*tert*-butylcalix[4]arene (4tBC4A) is a versatile host capable of forming a variety of 1 guest :1 host and 1 guest :2 host inclusion compounds typically stabilized through van der Waals interactions. However, inclusion of aliphatic amines gives rise to packing motifs that are stabilized by a combination of hydrogen bonding and van der Waals interactions. As exemplified by the inclusion of *n*-butylamine, this competition gives rise to a series of pseudopolymorphic inclusion compounds, including a new 3 guest :1 host inclusion motif. The competition of intermolecular forces results in the structures themselves being representative of the relative strengths of the forces guiding the structural motifs. By using temperature to control the relative dominance of such forces, one can guide the formation of calixarene-based supramolecular frameworks. Such a self-assembled structure can exhibit considerable complexity and include moieties capable of serving as sites for further chemistry, such as CO₂ adsorption.

[†] Portions of this chapter have been previously published: K. A. Udachin, G. D. Enright, P. O. Brown, J. A. Ripmeester, *Chem. Commun.* **2002**, 2162; P. O. Brown, K. A. Udachin, G. D. Enright, J. A. Ripmeester, *Chem. Eur. J.* **2006**, DOI: 10.1002/chem.200600434.

2. Introduction

Much of the research carried out under the banner of supramolecular chemistry ultimately is driven by a desire to develop functional materials for various applications, such as gas adsorption^[1-3] and catalysis.^[4] The vast majority of such studies revolve around the synthesis of increasingly complex molecules to serve as building blocks in organic, inorganic and hybrid metal-organic^[1, 5-13] supramolecular frameworks. As a result, simpler molecules have been marginalized as only suitable for basic studies of intermolecular interactions.

In the area of organic frameworks, the calixarenes,^[14-16] and 4-*t*-butylcalix[4]arene (4tBC4A) in particular, have traditionally been excellent candidates for such essential physical studies. 4tBC4A itself has proven to be an excellent host for investigating the forces guiding self-assembly, with a range of inclusion compounds having been reported.^[17-27] Inclusion of alkanes follow this trend quite well, forming a series of 1 guest : 1 host and 1 guest : 2 host inclusion compounds with four-fold symmetry matching that of the host molecule.^[21]

As a host for use in producing molecular receptors with potential materials applications, 4tBC4A has generally been overlooked due to its relatively low solubility in common organic solvents (and insolubility in aqueous systems) and the relative simplicity of the inclusion motifs it exhibits. However, more recent studies have begun to demonstrate that 4tBC4A has considerable potential as a building block for producing functional materials. A family of interrelated polymorphs and pseudopolymorphs of 4tBC4A and its simple inclusion compounds have been characterized, including a low-

density form which has shown potential as a gas adsorbent.^[2, 3, 28-30] In light of some of the elaborate covalently modified calixarene receptors previously reported,^[16, 31, 32] self-assembly of 4tBC4A frameworks with guest molecules containing different moieties presents an interesting alternative approach to producing more complex functional materials while avoiding complex organic synthetic pathways.

The potential of the self-assembly approach was initially demonstrated with the discovery of a 3.5(1,4-butanediamine):2(4tBC4A) inclusion compound, where the four-fold symmetry of the host was disrupted.^[33] The competition between directional interactions such as H-bonding and dipole-dipole interactions, and non-specific van der Waals interactions with the calix cavity gives rise to a series of amine clusters within a calixarene lattice. Given the strong preference of alkylcalix[4]arenes, and 4tBC4A in particular, for including guests in such a way that the four-fold symmetry of the host is maintained,^[17, 20, 21, 34-36] this packing scheme suggested such combinations of forces could be exploited to produce larger 4tBC4A assemblies containing polar clusters. Amine-containing frameworks could have a variety of applications, including serving as supports for metal centers with potential catalytic activity,^[4, 37] isolated pockets of solvent for reactions,^[38, 39] or as gas adsorbents.^[40]

Studies of the inclusion compounds formed by *n*-butylamine with 4tBC4A have confirmed the potential of using aliphatic amines to produce complex hydrogen-bonded networks, revealing the existence of a series of pseudopolymorphs. Based on this information, it has been possible to investigate how such an approach can be used to design polar clusters and layers in 4tBC4A lattices, and the pseudopolymorphism that

arises out of the competitive forces that guide the formation of such networks. The complementary strengths of solid-state NMR (SSNMR) and X-ray diffraction (XRD) allow both the local and long range ordering of these crystalline solids to be probed, and to demonstrate in detail the relationship among the various pseudopolymorphs observed. The resulting structural data illustrate how subtle changes in the guest can be used to control the nature of the clusters and layers initially formed, and thereby guide the subsequent transformations to other pseudopolymorphs, as well as guest free forms of the host compound.

3. Experimental Section

General Note: Unless otherwise indicated, chemicals were obtained from EMD Chemicals and Sigma-Aldrich, and were used without further purification.

Synthesis of 3(*n*-butylamine) *1(4tBC4A) clathrate **1** (KU78), 3(amylamine)*1(4tBC4A) clathrate **2** (POB14), 3(*n*-hexylamine)*1(4tBC4A) clathrate **3** (POB106), and 3(dodecylamine)*1(4tBC4A) clathrate **4** (JR26): Crystals of these clathrates were all prepared in a similar manner. In a typical synthesis, 0.500 to 1.00 g (7.72×10^{-4} to 1.54×10^{-3} mol) of 4tBC4A was placed in a vial along with 6.0 mL of amine. The resulting mixture was heated to approximately 70°C, and stirred for approximately 15 minutes to dissolve all of the 4tBC4A. The vials were then loosely capped and set aside to allow slow evaporation of the amine. In most cases, after approximately five days, clear crystals were observed to have formed.

Synthesis of 1(*n*-butylamine) *1(4tBC4A) clathrate **5** (KU88): Crystals of this material were prepared through evaporation of the amine at elevated temperatures. Again, 0.500

to 1.50 g of 4tBC4A (7.72×10^{-4} to 2.31×10^{-3} mol) was placed in a vial along with 6.0 mL of amine. The opening of the vial was constricted to slow the rate of evaporation, and placed in an oven at 70°C. After a few days, crystals of the appropriate clathrate were observed to have formed, and the vials were removed from the oven.

Synthesis of 1(*n*-butylamine)*2(4tBC4A) clathrate **6** (KU81), 1(amylamine)*2(4tBC4A) clathrate **7** (POB48), and 1(hexylamine)*2(4tBC4A) clathrate **8** (POB45): Crystals of these clathrates were prepared by recrystallization from dilute amine solutions in tetradecane. Typically, 0.500 to 1.50 g of 4tBC4A (7.72×10^{-4} to 2.31×10^{-3} mol) was placed in a vial along with 3.0 mL of amine and 6.0 mL of tetradecane. The vial was sealed and placed in an oven at 70°C for in order to induce a slow process of dissolution followed by recrystallization. After one to two weeks, crystals of the appropriate clathrate were observed to have formed, and the vials were removed from the oven.

Single Crystal X-ray Diffraction data are summarized in Table 1. For clathrates **2** and **3**, the hydrogen atoms on the disordered groups were placed in calculated positions and refined as riding atoms, with all other hydrogen atoms found from the difference map. For all other clathrates, hydrogen atoms on fully ordered heteroatoms were found from the difference map, with all other hydrogen atoms placed in calculated positions and refined as riding atoms.

Thermogravimetric analysis was carried out using a TA Instruments TGA 2050 instrument, with samples heated from room temperature to 400°C at a rate of 5°C/minute. TGA data were interpreted using TA Instruments' Universal Analysis for Windows 95/NT suite (version 2.3C). The overall host to guest ratio *n* was calculated based on the

weight loss prior to decomposition of the host at $\sim 300^\circ\text{C}$. Based on this, the molar mass of the inclusion compound was calculated, and the proportion of amine lost in each step calculated.

Thermal desorption studies of clathrates **1**, **2**, and **3** were carried out in a stepwise fashion using a vacuum oven to heat bulk samples. In each case, crystals of the clathrate were removed from the mother liquor, blotted dry using filter paper, and gently ground using a mortar and pestle. Samples were heated for 30 minutes at each temperature ($\pm 3^\circ\text{C}$), and then allowed to cool to room temperature. At each temperature, the samples were analyzed using PXRD and ^{13}C CP/MAS solid state NMR.

Powder X-ray Diffraction data were collected on the Scintag X-2 Advanced diffractometer. ^{13}C CP/MAS spectra for clathrates **1**, **2**, **5**, **6**, and the β *apo* form of 4tBC4A were collected using the Bruker AMX-300 spectrometer. ^{13}C CP/MAS Solid State NMR spectra for clathrates **3**, **7** and the α *apo* form of 4tBC4A were collected using the Tecmag Apollo 200 spectrometer.

The CO_2 adsorption isotherm was determined using a custom built volumetric adsorption apparatus constructed from Swagelok VCR components, using a MKS HPS A900 Piezo/MicroPirani pressure gauge with a DualTrans+ transducer. In a typical experiment, 1.19 g (1.37×10^{-3} mol) of clathrate **1** which had been vacuum dried at room temperature overnight was loaded into a 10 mL sample cell, attached to the adsorption line, and immersed in a water bath to maintain constant temperature (293 ± 1 K). The system was then evacuated for approximately 4 hours to remove any adsorbed gas. The volume of the apparatus was calibrated using helium gas (received from Praxair) and a

glass vessel with a known volume, and subsequently evacuated for a further hour. CO₂ (received from Praxair) was then admitted in a stepwise fashion, and the pressure allowed to equilibrate for 18-24 hours. The resulting pressure difference (measured to ± 0.5 mbar) was then used to calculate the number of moles of gas adsorbed based on the ideal gas law (resulting loading ratios have uncertainties of approximately ± 0.05).

¹³C labelled CO₂ gas adsorption experiments for SSNMR were carried out on samples of clathrate 1 derived from the same synthesis. CO₂ gas with 99.1% enrichment in ¹³C was received from ACP Chemicals Inc. For the sealed samples, the crystals of clathrate 1 were removed from the mother liquor, vacuum dried at room temperature overnight, and loaded into 5 mm glass tubes such that each contained approximately 0.12 g of sample. Samples were then pumped down for approximately 2 hours, and a given volume of CO₂ added. The samples were then allowed to equilibrate for 24 hours, and then flame sealed. A similar methodology was used for the desorption experiments, with the sample instead being loaded directly into the rotor, and the rotor placed inside a glass vessel suitable for attachment to the vacuum line. Desorption was carried out by pumping down on a loaded sample for 10 minute intervals. SSNMR on these samples was carried out using the Bruker Avance 200 spectrometer. For the HPDEC spectrum, a pulse delay of 50 s was sufficiently long for quantitative measurements.

Table 1a SCXRD data for clathrates 1 to 4.

Identification code	Clathrate 1 (KU78)	Clathrate 2 (POB14)	Clathrate 3 (POB106)	Clathrate 4 (JR26)
Empirical formula	C ₅₆ H ₈₉ N ₃ O ₄	C ₅₉ H ₉₅ N ₃ O ₄	C ₆₂ H ₁₀₁ N ₃ O ₄	C ₆₈ H ₁₁₀ N ₂ O ₄
Formula weight	868.30	910.38	952.46	1019.58
Temperature	173(2) K	173(2) K	125(2) K	173(2) K
Wavelength	0.71070 Å	0.71070 Å	0.71070 Å	0.71073 Å
Crystal system	Monoclinic	Monoclinic	Triclinic	Triclinic
Space group	<i>P</i> 2 ₁ / <i>c</i>	<i>P</i> 2 ₁ / <i>n</i>	<i>P</i> 1	<i>P</i> -1
Unit cell dimensions	<i>a</i> =12.9405(6) Å <i>b</i> =20.0923(9) Å <i>c</i> =20.7519(9) Å α =90° β =91.1220(1)° γ =90°	<i>a</i> =12.9164(8) Å <i>b</i> =24.9406(16) Å <i>c</i> =18.5354(12) Å α =90° β =107.3670(1)° γ =90°	<i>a</i> =13.3420(15) Å <i>b</i> =14.0770(16) Å <i>c</i> =16.1519(18) Å α =96.248(2)° β =104.320(2)° γ =98.009(2)°	<i>a</i> =13.419(2) Å <i>b</i> =15.599(2) Å <i>c</i> =17.638(3) Å α =108.555(3)° β =107.354(3)° γ =101.963(3)°
Volume	5394.6(4) Å ³	5698.8(6) Å ³	2878.0(6) Å ³	3149.0(8) Å ³
Z	4	4	2	2
ρ_{calc}	1.069 Mg/m ³	1.061 Mg/m ³	1.099 Mg/m ³	1.075 Mg/m ³
Abs. coefficient	0.066 mm ⁻¹	0.065 mm ⁻¹	0.067 mm ⁻¹	0.065 mm ⁻¹
F(000)	1912	2582	1052	1128
Crystal size	0.45 x 0.40 x 0.20 mm ³	0.4 x 0.16 x 0.08 mm ³	0.32 x 0.32 x 0.16 mm ³	0.40 x 0.40 x 0.25 mm ³
θ Range	1.57 to 28.75°	1.41 to 29.62°	1.48 to 29.58°	1.32 to 27.50°
Index ranges	-17<= <i>h</i> <=17 -27<= <i>k</i> <=27 -28<= <i>l</i> <=28	-17<= <i>h</i> <=17 -34<= <i>k</i> <=34 -25<= <i>l</i> <=25	-18<= <i>h</i> <=18 -19<= <i>k</i> <=19 -22<= <i>l</i> <=22	-17<= <i>h</i> <=17 -20<= <i>k</i> <=19 -22<= <i>l</i> <=22
Reflections collected	63744	71636	36360	34741
Ind.. reflections	13978 [R(int) = 0.0554]	16005 [R(int) = 0.0364]	15865 [R(int) = 0.0248]	14408 [R(int) = 0.0595]
Completeness to θ = max	99.7 %	99.7 %	98.1 %	99.5 %
Absorption correction	Multi-scan	Multi-scan	Multi-scan	Multi-scan
Refinement method	Full-matrix least- squares on F ²	Full-matrix least- squares on F ²	Full-matrix least- squares on F ²	Full-matrix least- squares on F ²
Data / restraints / parameters	13978 / 85 / 699	16005 / 58 / 857	15865 / 53 / 1736	14408 / 109 / 989
Goodness-of-fit on F ²	0.943	1.011	1.040	1.065
Final R indices [I>2 σ (I)]	R1 = 0.0564 wR2 = 0.1382	R1 = 0.0509 wR2 = 0.1279	R1 = 0.0418 wR2 = 0.1065	R1 = 0.0759 wR2 = 0.1959
R indices (all data)	R1 = 0.1249 wR2 = 0.1565	R1 = 0.0815 wR2 = 0.1456	R1 = 0.0484 wR2 = 0.1122	R1 = 0.1222 wR2 = 0.2163
Largest diff. peak and hole (e.Å ⁻³)	0.423 and -0.324	0.447 and -0.324	0.354 and -0.216	0.422 and -0.261

Table 1b SCXRD data for clathrates 5 to 8.

Identification code	Clathrate 5 (KU88)	Clathrate 6 (KU81)	Clathrate 7 (POB48)	Clathrate 8 (POB45)
Empirical formula	C ₄₈ H ₆₇ N ₁ O ₄	C ₉₂ H ₁₂₃ NO ₈	C _{23.25} H _{31.25} N _{0.25} O ₂	C _{23.50} H _{31.75} N _{0.25} O ₂
Formula weight	722.03	1370.91	346.24	349.74
Temperature	173(2) K	173(2) K	173(2) K	173(2) K
Wavelength	0.71070 Å	0.71070 Å	0.71073 Å	0.71070 Å
Crystal system	Tetragonal	Tetragonal	Tetragonal	Tetragonal
Space group	<i>P4/n</i>	<i>P4/nnc</i>	<i>P4/nnc</i>	<i>P4/nnc</i>
Unit cell dimensions	<i>a</i> = 12.9816(5) Å <i>b</i> = 12.9816(5) Å <i>c</i> = 12.6459(6) Å $\alpha = 90^\circ$ $\beta = 90^\circ$ $\gamma = 90^\circ$	<i>a</i> = 12.8837(6) Å <i>b</i> = 12.8837(6) Å <i>c</i> = 25.1022(15) Å $\alpha = 90^\circ$ $\beta = 90^\circ$ $\gamma = 90^\circ$	<i>a</i> = 12.8481(6) Å <i>b</i> = 12.8481(6) Å <i>c</i> = 25.2599(19) Å $\alpha = 90^\circ$ $\beta = 90^\circ$ $\gamma = 90^\circ$	<i>a</i> = 12.8201(7) Å <i>b</i> = 12.8201(7) Å <i>c</i> = 25.617(2) Å $\alpha = 90^\circ$ $\beta = 90^\circ$ $\gamma = 90^\circ$
Volume	2131.11(15) Å ³	4166.7(4) Å ³	4169.7(4) Å ³	4210.3(5) Å ³
Z	2	2	8	8
ρ_{calc}	1.125 Mg/m ³	1.093 Mg/m ³	1.104 Mg/m ³	1.104 Mg/m ³
Abs. coefficient	0.070 mm ⁻¹	0.068 mm ⁻¹	0.068 mm ⁻¹	0.068 mm ⁻¹
F(000)	788	1492	1508	1524
Crystal size	0.40 x 0.40 x 0.15 mm ³	0.40 x 0.35 x 0.20 mm ³	0.32 x 0.24 x 0.16 mm ³	0.16 x 0.16 x 0.16 mm ³
θ Range	1.61 to 28.69°.	1.78 to 28.73°.	1.61 to 29.62°.	1.78 to 29.64°.
Index ranges	-17<= <i>h</i> <=17 -17<= <i>k</i> <=17 -17<= <i>l</i> <=17	-16<= <i>h</i> <=17 -17<= <i>k</i> <=17 -33<= <i>l</i> <=33	-17<= <i>h</i> <=17 -17<= <i>k</i> <=17 -35<= <i>l</i> <=34	-17<= <i>h</i> <=17 -17<= <i>k</i> <=16 -35<= <i>l</i> <=35
Reflections collected	24796	45301	48778	48776
Ind.. reflections	2759 [R(int) = 0.0296]	2708 [R(int) = 0.0430]	2959 [R(int) = 0.0582]	2976 [R(int) = 0.0532]
Completeness to $\theta = \text{max}$	99.5 %	99.5 %	99.9 %	99.5 %
Absorption correction	Multi-scan	Multi-scan	Multi-scan	Multi-scan
Refinement method	Full-matrix least-squares on F ²	Full-matrix least-squares on F ²	Full-matrix least-squares on F ²	Full-matrix least-squares on F ²
Data / restraints / parameters	2759 / 37 / 211	2708 / 63 / 160	2959 / 9 / 159	2976 / 11 / 143
Goodness-of-fit on F ²	1.011	1.045	1.041	1.057
Final R indices [I>2 σ (I)]	R1 = 0.0470 wR2 = 0.1350	R1 = 0.0491 wR2 = 0.1378	R1 = 0.0524 wR2 = 0.1405	R1 = 0.0613 wR2 = 0.1746
R indices (all data)	R1 = 0.0608 wR2 = 0.1447	R1 = 0.0640 wR2 = 0.1460	R1 = 0.0763 wR2 = 0.1547	R1 = 0.0888 wR2 = 0.1919
Largest diff. peak and hole (e.Å ⁻³)	0.318 and -0.310	0.331 and -0.230	0.333 and -0.185	0.335 and -0.254

4. Results and Discussion

Polar Clusters: *n*-butylamine and amylamine

In addition to the studies of 1,4-butanediamine, which gives rise to a polar cluster of amines in a calixarene lattice, Brouwer also carried out preliminary investigations into the behaviour of other amines.^[41] Benzylamine also appeared to give rise to proton transfer, thereby disrupting the symmetry of the host. In contrast with this, *t*-butylamine and *sec*-butylamine formed more typical 1 guest : 1 host inclusions. Thus, it appeared that one prerequisite for the formation of polar clusters with aliphatics was that the amine was both flexible and long enough to allow for multiple interactions to effectively compete. As such, the simple alkylamines are ideal compounds for testing the relative dominance of the two interactions in guiding the structural motif of calixarene clathrates.

Recrystallization of 4tBC4A from *n*-butylamine readily yields large, block-like crystals of compound **1** that are suitable for structural characterization by SSNMR and single crystal XRD. Considerable diagnostic information can be derived from analysis of the ¹³C CP/MAS spectra of **1**. The ¹³C CP/MAS spectrum (see Figure 1a) shows complex splitting patterns in both the aromatic and aliphatic regions. This increased complexity is characteristic of a dramatic shift in crystallographic symmetry away from the idealized *C*_{4v} symmetry of the host, similar to that observed for inclusions of nitrobenzene (where interactions with the nitro groups lead to a drop to two fold crystallographic symmetry).^[18] Even so, the majority of these resonances are readily assigned based on previous studies of 4tBC4A inclusion compounds,^[28, 33, 34] the information derived from dipolar dephasing experiments to suppress the signals of CH

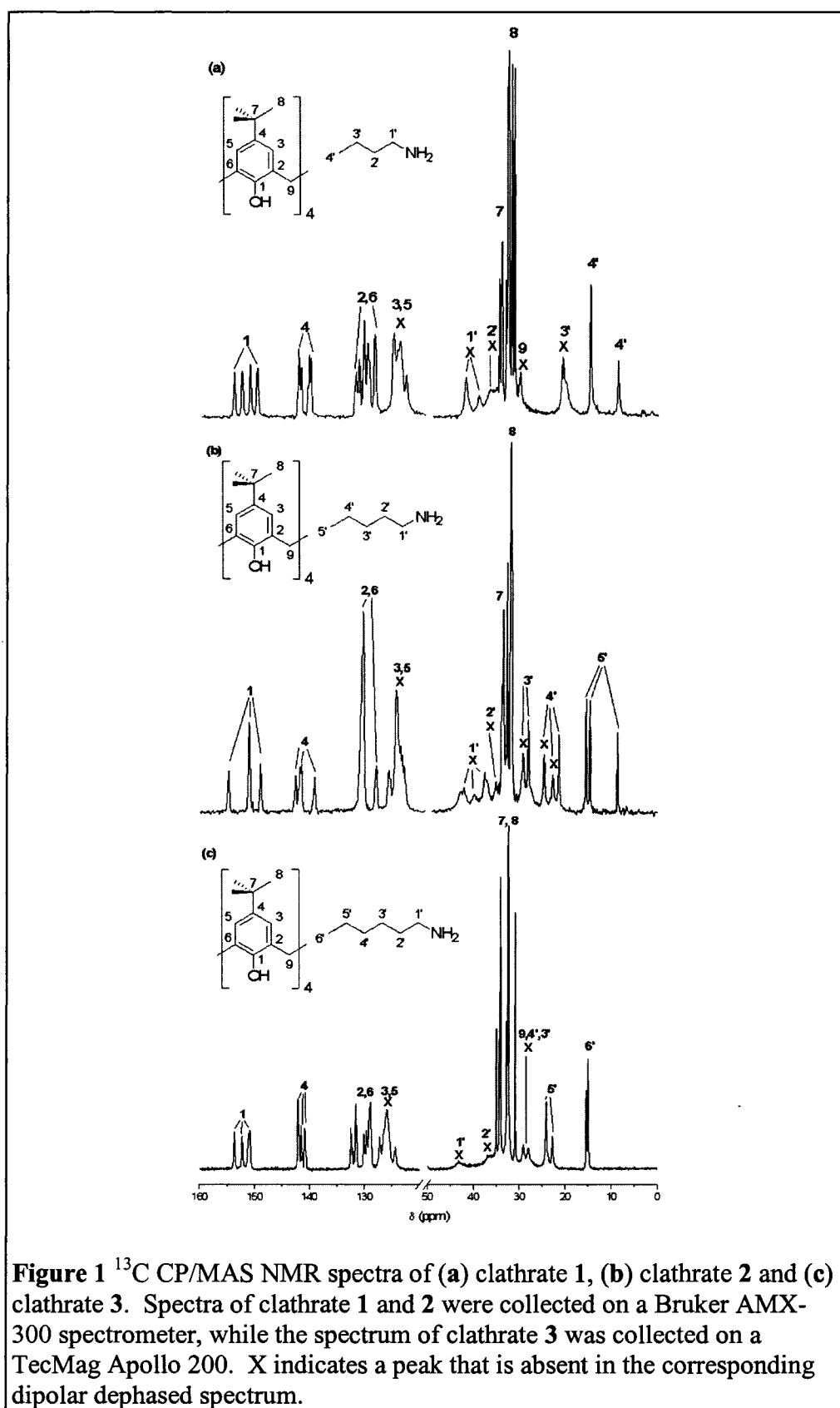


Figure 1 ^{13}C CP/MAS NMR spectra of (a) clathrate 1, (b) clathrate 2 and (c) clathrate 3. Spectra of clathrate 1 and 2 were collected on a Bruker AMX-300 spectrometer, while the spectrum of clathrate 3 was collected on a TecMag Apollo 200. X indicates a peak that is absent in the corresponding dipolar dephased spectrum.

and CH₂ carbons experiencing significant dipolar coupling, and the solution ¹³C spectrum of *n*-butylamine.

The resonances attributed to C1 (154-150 ppm) and C4 (143-140 ppm) in the aromatic ring are of particular diagnostic value. Both carbons show a four-fold splitting, similar to that observed for inclusions of 1,4-butanediamine^[33] or nitrobenzene.^[18] As previously mentioned, the included guest molecules in these systems induce a distortion of the host lattice away from the usual tetragonal symmetry. Given this, a similar guest-induced reduction in calixarene symmetry is expected for clathrate **1**.

In the upfield region, the resonances due to the methylene bridge and *t*-butyl methyls (35-31 ppm) also show considerable splitting, and they partially overlap each other, while the intensity of the peak due to quaternary carbon in the *t*-butyl is too low to make splittings easily observable. In contrast with the spectrum of 1,4-butanediamine:4tBC4A, the guest resonances are well resolved, with the multiplicity suggesting two distinct types of guest. The resonances due to C1', C3' and C4' are clearly split, while the resonances due to C2' partially overlap. Upon dipolar dephasing, all but the C4' resonances disappear, supporting this assignment scheme as well as indicating an absence of dynamic motion in the aliphatic chains (which would result in the C-H dipolar coupling being averaged away such that the CH₂ resonances may be observed).

Further information regarding the structural arrangement of the guest becomes apparent through a comparison of the chemical shifts observed in clathrate **1** with those

observed in solution for *n*-butylamine (see Table 2). The chemical shifts of the stronger signals correspond closely to the reported solution spectrum but with a slight downfield

Table 2 ¹³C CP/MAS NMR spectral data for clathrates 1, 2 and 3.^[a]

Guest	Carbon	δ 4tBC4A ^[b] (\pm 0.05)	δ Solution ^[c]	CIS ^[d] (\pm 0.05)
<i>n</i> -butylamine (1)	C1'	42.84	41.96	+0.88
		39.86		-2.10
	C2'	36.00 (br)	36.07	N/A
	C3'	21.29	20.08	+1.21
		20.45		+0.37
amylamine (2)	C4'	14.95	13.94	+1.01
		8.87		-5.07
	C1'	43.00	42.41	+0.59
		40.83		-1.58
		38.44		-3.97
	C2'	35.98 (br)	33.78	N/A
		29.96		+0.69
	C3'	28.73	29.27	+0.54
		25.24		+2.56
	C4'	23.30	22.68	+0.62
21.94		-0.74		
15.79		14.11		+1.68
15.02		+0.91		
8.94		-5.17		
<i>n</i> -hexylamine (3)	C1'	43.19	42.43	+0.76
	C2'	36.85	34.09	+2.76
	C3', C4'	29.14, 28.04	26.72, 31.88	N/A
	C5'	24.22	22.77	+1.45
		22.82		+0.05
	C6'	15.39	14.09	+1.30
		15.00		+0.91

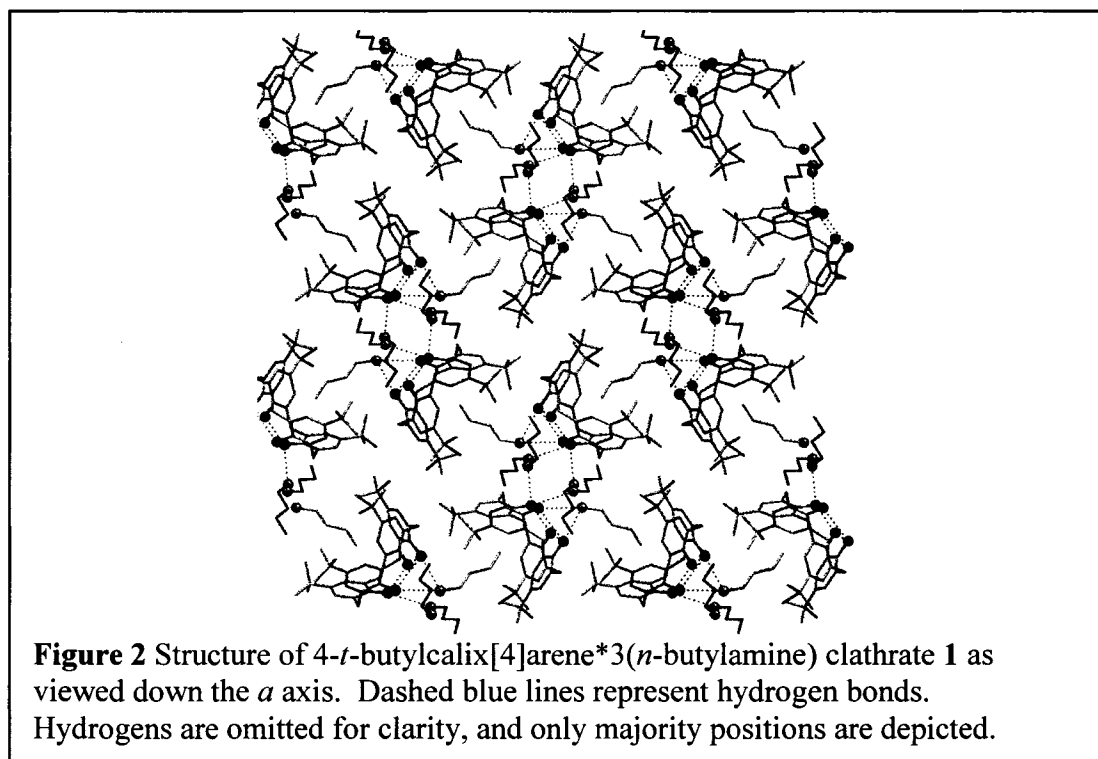
^[a]All values are in ppm. ^[b]Chemical Shift observed in 4tBC4A clathrate. br indicates broad peak. ^[c]Chemical shift of amine in solution, from SDBSWeb.^[42]

^[d]CIS=Complexation-induced shift=(δ 4tBC4A)-(δ Solution)

shift. The weaker signals generally exhibit upfield shifts, with the C4' exhibiting a dramatic complexation induced shift. This suggests that the primary amine site is an *exo*

site, thereby experiencing a small degree of deshielding due to edge-on interactions with the aromatic rings of 4tBC4A. The secondary site is therefore an *endo* site, with the amine positioned such that the methyl is deeply inserted into the cavity, experiencing increased shielding. The relative intensities of the peaks (2:1) also support this.

Given this information, it was expected that the packing scheme of clathrate **1** would consist of at least two distinct types of amine for each host molecule along with a reduction in lattice symmetry. The X-ray diffraction structure of **1** corresponds well to the predictions based on the SSNMR evidence (see Figure 2 and Table 1).



Clathrate **1** crystallizes in the monoclinic spacegroup $P2_1/c$, with three amines observed in the asymmetric unit. One molecule acts as a guest and is deep inside the cavity of 4tBC4A with the amino group pointed outside the cavity. Two other molecules of *n*-butylamine are outside the cavity and are connected by hydrogen bonds to the *n*-

butylamine molecule inside the cage forming a 'T' shaped fragment of three molecules (N...N distances of 2.95-3.08 Å).

All three *n*-butylamine molecules are in the all-*trans* conformation and are disordered over two crystallographically independent positions with site occupancies of 0.68:0.32 for the molecule inside the cavity, and 0.80:0.20 for molecules outside the cavity. One of the *tert*-butyl groups of the calixarene molecule is disordered over three positions with site occupancies 0.37, 0.37 and 0.26. Three of four atoms in each 4tBC4A molecule participate in hydrogen bonding with amine molecules, thus forming a fragment of two hydroxy to hydroxy oriented calix molecules with two 'T'-shaped fragments of three *n*-butylamine molecules between them (O...N distances of 2.85–3.09 Å), giving rise to a capped motif.

This 3 guest : 1 host motif arising from the inclusion of aliphatic amines contrasts dramatically with the simple inclusion compounds formed by the analogous alkanes^[34, 43] This can be attributed to a reduction in host symmetry, leading to poor packing, and which is a consequence of proton transfer from one phenolic hydroxyl to one of the amines, in accord with calixarene pKa values^[44-46] and previous studies.^[24, 47] The X-ray data supports this, as only three of the phenolic oxygens are proton bearing, and excess electron density is found around one of the amino groups. The highly symmetrical and efficient packing schemes observed in 1 guest : 1 host and 1 guest : 2 host inclusion compounds are therefore not available in basic media. The symmetry distorted discrete inclusion compounds seen with guests such as nitrobenzene are disfavoured, as the

presence of a hydrogen bonding guest promotes an alternative arrangement where these directional interactions can stabilize the structure as well.^[18, 41]

This deprotonation and formation of *endo* and *exo* inclusions is a logical extension of the chemistry of amines and calixarenes observed in solution. Early studies suggested that less bulky guests would abstract a proton from the calixarene, forming an *endo* inclusion, while more bulky amines would form *exo* complexes.^[48, 49] This is corroborated by more recent studies confirming only one hydroxyl on 4tBC4A is readily deprotonated under mildly basic conditions (pK_a of ~20 in MeCN).^[50, 51] Therefore, in solution, formation of an *endo* or *exo* complex does not depend on the pK_a of the amine, but rather upon the geometry of the guest. However, in the solid state, efficient packing makes both types of inclusion energetically attractive, presumably overcoming the entropic penalty of organizing the *exo* amines (as observed with modified calixarenes^[52-54]).

The considerable stabilization offered by the formation of an ion-pair therefore directs the overall structural motif to a lower symmetry. While the van der Waals stabilization that directs the inclusion motifs of neutral guests still plays a role in stabilizing the structure, the inclusion of *exo* amines within the structure indicate that hydrogen bonding also has a role to play in these structures. This raises the question as to how larger guests will be accommodated, as increased coiling similar to that observed for neutral guests should compete directly with such directional interactions. Variations in the inclusion motif arising from changes in the guest size should therefore provide insight as to the comparative strengths of these forces.

Recrystallization of 4tBC4A from amylamine gives rise to block-like crystals of clathrate **2**. As with clathrate **1**, the ^{13}C CP/MAS spectrum shows considerable splitting that is characteristic of reduced crystallographic symmetry (see Figure 1b). In the aromatic region, the C4 resonance (139-143 ppm) shows four-fold splitting consistent with a loss of the four-fold symmetry of the calixarene. Interestingly, the C1 carbon only shows a three-fold splitting, with one peak having an intensity approximately twice that of the other two, suggesting that two of the four carbons are nearly identical. This is likely diagnostic of the pseudosymmetry of the calixarene arising from the hydrogen bonding scheme resulting from deprotonation of one of the phenolic hydroxyls. The remaining aromatic carbons give rise to relatively broad resonances that make assessing crystallographic splitting difficult.

In the upfield region (8-45 ppm), the guest resonances show even more extensive splitting than with *n*-butylamine. Three-fold splitting of the resonances attributable to C1', C4' and C5' can be clearly seen, indicating the presence of at least three crystallographically distinct amines in the asymmetric unit. Comparisons of the chemical shifts to solution values indicate that two of these amines are found in the *exo* position, and one in the *endo* position. The intensities of these peaks suggest a similar number of amines in each position. This is most striking for C5', with one peak showing a significant complexation induced shift upfield, indicating the insertion of the methyl group into the calix cavity (see Table 2). The minimal difference between the chemical shifts due to the other two amines suggests the *exo* sites are quite similar, as with *n*-butylamine.

Dipolar dephasing serves to further clarify the assignment of the spectrum. In addition to the methyl C5' resonances, the most shielded resonances, attributed to C3' and C4', are retained upon dephasing. This suggests the presence of dynamic disorder in the *endo* amine. The C1' resonances disappear upon dephasing, suggesting the carbon adjacent to the amine is essentially fixed on the NMR timescale by virtue of the hydrogen bonding of the amine to the rigid calixarene. The modest broadening of these peaks when compared to the other guest resonances is therefore likely due to coupling with the adjacent ^{14}N . Given the NMR data, a 3 amine:1 host inclusion compound similar to that observed for clathrate 1 was expected.

Single crystal X-ray diffraction confirms this hypothesis, while demonstrating that the additional bulk of the amine results in a subtle structural rearrangement. Clathrate 2 crystallizes in the monoclinic $P2_1/n$ space group, displaying essentially the same symmetry as clathrate 1, with 2 amines in *exo* positions and 1 amine in an *endo* position (see Figure 3 and Table 1). The shift in the glide plane results in a more dramatic staggering of the amine pockets, with the capping 4tBC4A showing a 3.29 Å offset from layer to layer. However, the hydrogen bonding calixarene units are nearly in the same plane now, with the larger guest allowing for them to arrange such that each cluster is proximate to the bases of two calixarenes.



Figure 3 Capped cavity in 4-*t*-butylcalix[4]arene*3(amylamine) clathrate **2** as viewed down the *a* axis. Dashed blue lines indicate hydrogen bonds. Protons on carbons are omitted for clarity, with only majority positions being shown.

In contrast with clathrate **1**, the *exo* amines do not display disorder. This explains the improved resolution of the SSNMR of clathrate **2**, with the inability to distinguish between the two sites in clathrate **1** attributable to broadening because of static disorder. As expected from the dipolar dephased spectrum, the *endo* amine displays a 0.60:0.40 disorder over two positions, with the disorder largely confined to an apparent rocking motion involving C3' and C4'. Two *t*-butyl groups exhibit unrelated two-fold disorder with occupancy ratios of 0.87:0.13 and 0.90:0.10.

The absence of disorder in the majority of the amines also leads to a more detailed structural model of clathrate **2** in comparison with clathrate **1**. The quality of the data allows us to determine from the difference map that one *exo* amine bears a proton abstracted from a phenol group of the calixarene. As a result, a series of hydrogen bonded chains consisting of three amines is formed (N...N distances of 3.17, 2.93, and 2.80 Å), with the unprotonated amines hydrogen bonding (N...O distances of 3.17, 3.10, 3.15 Å). Most significantly, the protonated *exo* amines are separated from the O⁻ of the

calixarenes by only 2.78 Å, providing us with direct structural evidence of the formation of an ion pair. The ordering induced in the remaining phenolic hydroxyl groups by this assembly results in two of the phenolic groups being pseudosymmetric, accounting for the three-fold splitting observed in the NMR spectrum.

Furthermore, the lack of significant disorder in the structure makes the influence of steric bulk on the structural motif more readily apparent. The *endo* amine displays a distortion away from the all-*trans* conformation displayed by *n*-butylamine in clathrate **1**, presumably to accommodate the larger guest while maintaining a hydrogen bonded structure. A similar distortion is observed in one of the *exo* amines in order to facilitate the hydrogen bonding scheme. This change in conformation is analogous to that observed for 1 guest : 2 host inclusions of simple alkanes and haloalkanes,^[21] where the energetic costs of assuming such conformations clearly are outweighed by the stabilization offered by the van der Waals interactions with the calixarene. The weakly-interacting alkyl guests show a structural shift from a 1 guest : 1 host to a 2 guest : 1 host inclusion ratio for *n*-hexane and longer alkanes.^[21] Amylamine is approximately the same size as *n*-hexane, indicating that stabilization by hydrogen bonding is strong enough to overcome the influence of guest size in directing the packing motif.

Given the similarity in the conformational accommodation of the amine guest to fit within the calix cavity with that observed for the paraffins, it is reasonable to expect a structural shift due to guest bulk for inclusions of larger aliphatic amines. In addition to the simple 1 guest : 1 host and 2 guest : 1 host inclusions previously mentioned, very large paraffins give rise to pillared structures.^[19] With the clusters formed by *n*-

butylamine and amylamine clearly indicating that hydrogen bonding (particularly the bonds forming between the ions) dominate the selection of the packing scheme, van der Waals interactions with the calixarene cavity and the steric bulk of the guest can be routes to fine tuning the structural motif.

Polar Layers: hexylamine and dodecylamine

The influence of guest size (and thus the steric bulk of the guest) in reduced symmetry systems of 4tBC4A is made apparent by moving to even larger guests. Crystallization of 4tBC4A from hexylamine yields clathrate **3**, with ^{13}C CP/MAS NMR spectroscopy demonstrating quite clearly that there is a significant shift in the structural motif when compared to both clathrates **1** and **2** as well as weakly interacting guests (see Figure 1c). While the aromatic region shows a similar degree of splitting to clathrates **1** and **2**, the lines are broadened. Unlike the previous two structures, the host resonances in the upfield aliphatic region are of considerably greater diagnostic utility.

Eight distinct lines attributable to C7 and C8 are clearly visible from 31-35 ppm, suggesting a further reduction in symmetry such that two crystallographically distinct host molecules are present in the asymmetric unit. For the hexylamine guests, only two crystallographically distinct positions of C5' and C6' can be resolved. Furthermore, the C5' resonance is retained upon dephasing, indicating dynamic motion near the tail of the amine. The resonances due to C1' and C2' are quite broad, and C3' and C4' cannot readily be distinguished because of broadening and overlap with the resonance due to the methylene bridge in the host.

The chemical shifts observed for the guest provide the most significant information regarding the structure. No significant complexation induced shift is observed for any of the resonances, and in most cases, a slight degree of deshielding is observed (see Table 2). This provides strong evidence that all of the amines present are in *exo* positions, presenting a possible explanation for the presence of two calixarenes in the asymmetric unit. Several of the host aliphatic peaks are further upfield in comparison with the corresponding peaks in the spectra of clathrates **1** and **2**, with the resonance at 30.9 ppm exhibiting the most dramatic shielding. In the absence of any *endo* guest, the calixarene should self-include, giving rise to two crystallographically distinct calixarenes, with the *t*-butyl carbons being shielded such that they exhibit a complexation induced upfield shift.

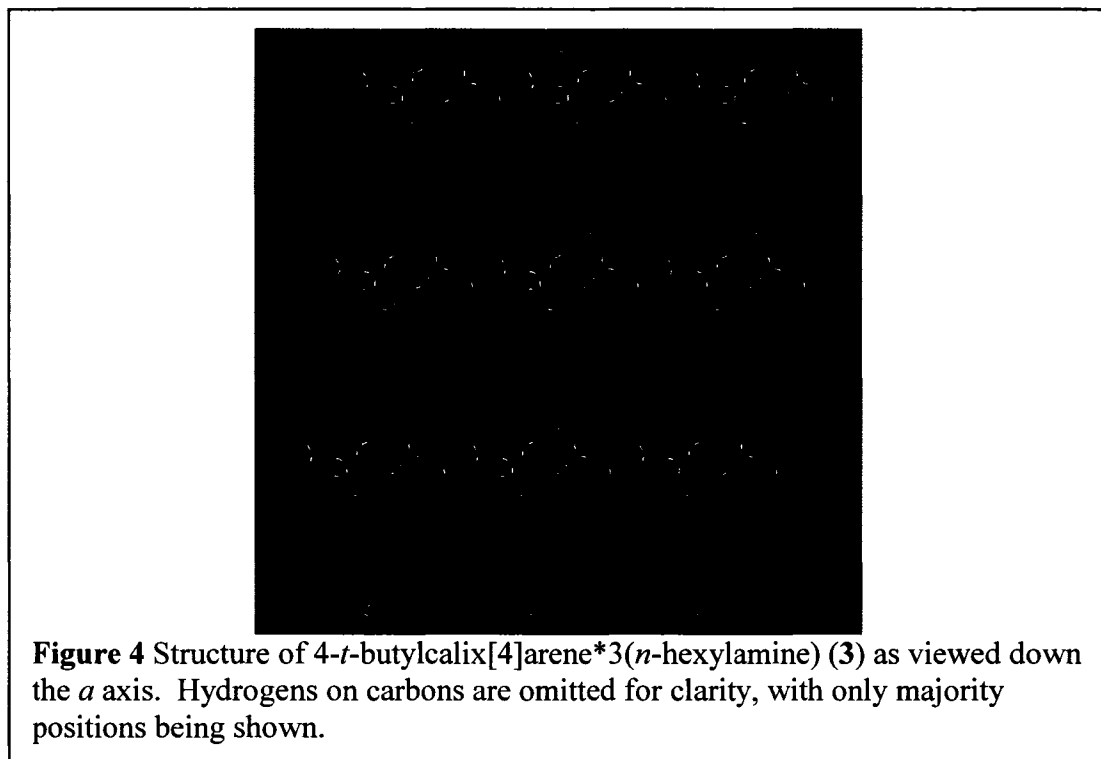
Despite the high quality of the data obtained, initial attempts to solve and refine the structure of **3** in *P*-1 were unsatisfactory. Even after modeling the disorder of the host and guest molecules, the *R* value was 0.1628 with thermal ellipsoids remaining quite large. Furthermore, the resulting unit cell contained only one 4tBC4A molecule, disagreeing with the solid state NMR evidence. Solution in *P*1 gave rise to a much more satisfactory answer, which also shows much better agreement with the NMR spectra obtained.

While the overall 3:1 guest to host ratio observed in other aliphatic amine clathrates is maintained, the packing of the guest molecules is only pseudosymmetrical. The asymmetric unit therefore contains six independent hexylamines and two 4tBC4A units, arranged in alternating layers (see Figure 4 and Table 1). A single *t*-butyl group on

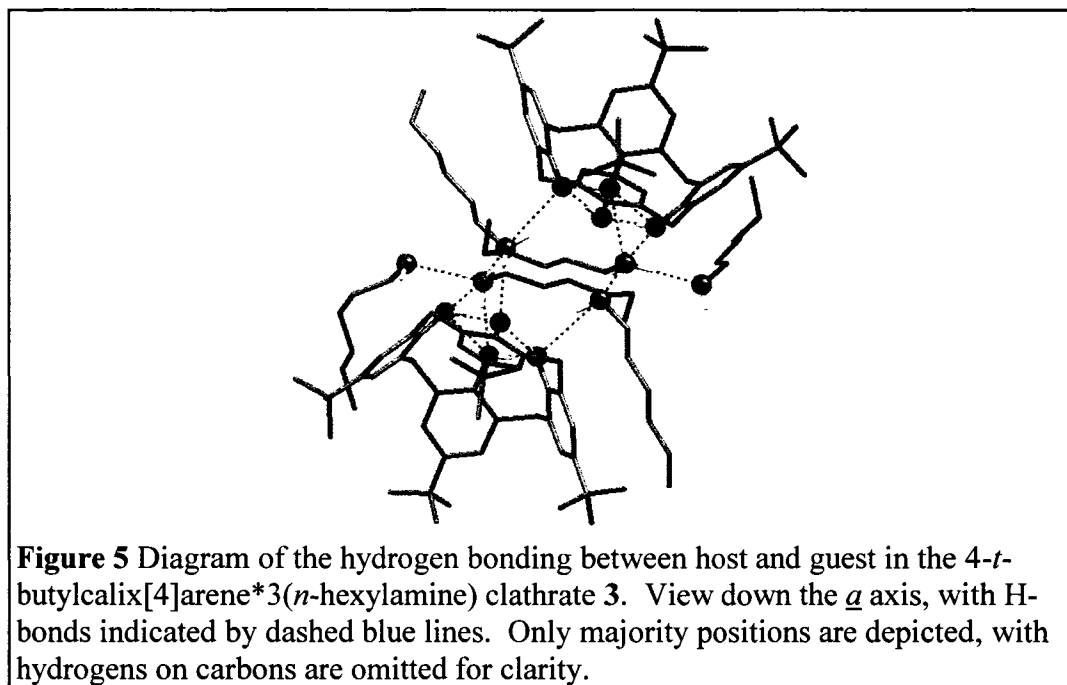
one of the calixarenes exhibits a 0.65:0.35 disorder, while C4', C5' and C6' of three of the amine sites are disordered over two positions (with occupancy ratios of 0.65:0.35, 0.72:0.28 and 0.80:0.20).

Two of the amines reside entirely within the layer defined by the calixarenes, displaying minimal distortions away from the all *trans* conformation. The alkyl tails of the remaining four amines are intercalated between adjacent self-included pairs of 4tBC4A, with three of these amines showing distortions away from an all *trans* conformation. Given this, the two types of amine observed by NMR are likely these two conformationally distinct sets of amines, with most of the splitting lost due to the pseudosymmetrical arrangement of the guest and broadening due to dynamic motion. As seen previously with weakly interacting guests,^[34] this amine clathrate of 4tBC4A (as opposed to all others) shows a correlation of the disorder observed in a guest with that of a *t*-butyl group. In this case, however, it arises from the packing requirements of an exo guest, suggesting the energies involved in the conformational shift of the guest and the *t*-butyl rotation are similar.

This implies that stabilization by inclusion within the calixarene cavity, even with moderate conformational distortion, would interfere with the significant stabilization offered by hydrogen bonding. The guest is now too bulky to allow for coiling while still maintaining the hydrogen bonding network. However, the improved packing arising from intercalation therefore indicates that these weak interactions with the calixarene are sufficient to compensate for the energetic penalty associated with moderately distorted conformations.

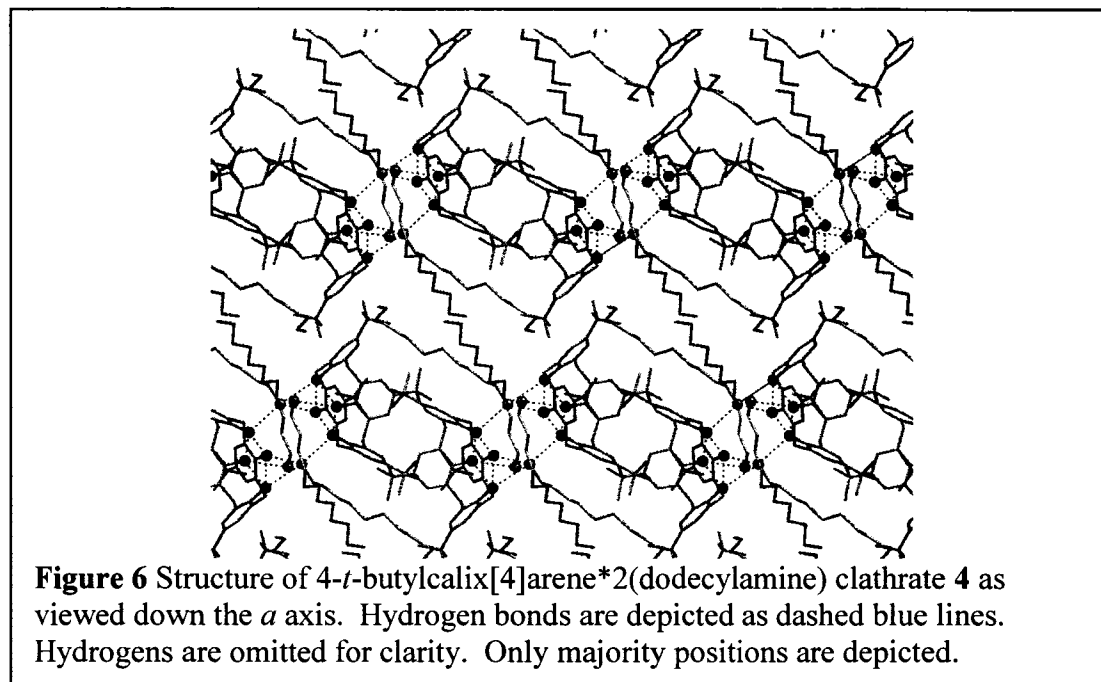


The intermolecular bonding is also more complex than that observed for clathrates **1** and **2** (see Figure 5). The guests are observed to organize into two distinct clusters of three amines, consisting of two neutral and one protonated amine (N...N distances of 2.84, 2.96, 2.79, 2.95 Å). In each case, one neutral and the protonated amine interact with a calixarene in the adjacent layers (N...O distances ranging from 2.79 to 3.16 Å). In contrast with the inclusions formed by the two smaller amines, the protonated amines each interact with two proton-bearing hydroxyls instead of the deprotonated phenol, suggesting that the influence of steric bulk is also sufficient to partially disrupt such an arrangement.



Given the balance of three interactions observed in clathrate **3**, further increases in guest size would be expected to further shift the inclusion motif away from the 3:1 guest to host cluster motif to increasingly distinct layered structures. Recrystallization of 4tBC4A from dodecylamine gives rise to a 2:1 guest to host layered structure without intercalation (clathrate **4**). The bulk of the guest is now too great for stabilization by intercalation to be effective when compared to the hydrophobic environment offered by the chains of adjacent amines. Like clathrate **3**, **4** exhibits triclinic symmetry, but the reduced guest content and lack of conformational variation to accommodate intercalation allows for a centre of inversion (see Figure 6 and Table 1). The guests are disordered over two positions (0.50:0.50 and 0.75:0.25 distributions), while three of the *t*-butyl groups are disordered (with 0.60:0.40, 0.82:0.18 and 0.92:0.08 distributions). As with clathrate **3**, the amino groups on the guests hydrogen bond with the adjacent calixarene

phenolic hydroxyls, serving to bind adjacent calixarene layers together (N...O distances of 2.86 to 3.15 Å).



Pseudopolymorphism arising from Amine Polar Clusters and Layers

The shift in motifs from clathrate **1** to clathrate **4** clearly demonstrate that while the hydrogen bonding between the amino group and the calixarene phenolic group arising from the acid-base chemistry of the compounds dominates the structural motif, the ultimate structural arrangement depends heavily on the balance between stabilization through non-specific interactions and packing concerns arising from increases in guest size. Previous studies of simple 4tBC4A inclusion compounds have clearly demonstrated that by heating such inclusion compounds (as with toluene inclusions) or introduction of an alternative guest (as with nitrobenzene inclusions), the balance between these forces is altered, allowing for control of the structural motif.^[28, 33, 55]

The inclusion of amines in different environments due to the competition of specific and non-specific interactions introduces an intriguing complication when compared with these previous studies. As alluded to above, the competition between these forces gives rise to differing degrees of guest stabilization by the host. This raises the possibility of selectively removing guest amines from the host framework in a controlled fashion, producing related pseudopolymorphs. Given the relative volatility of short chain aliphatic amines, modest increases in temperature should be sufficient to induce such a structural transformation.

Thermogravimetric analysis of clathrate **1** indicates that the material loses guest in two steps separated by about 80°C (see Table 3). The first step, corresponding to the loss of two molecules of *n*-butylamine, occurs just below the boiling point of pure *n*-butylamine (78°C). Given the structural data, such a loss likely corresponds to the loss of the two *exo* amines, which are only stabilized by hydrogen bonding and weak van der Waals interactions between the aliphatic chains (so called hydrophobic interactions) not unlike those the molecules would experience in solution. The resulting 1:1 guest to host inclusion compound, clathrate **5**, would therefore consist of an *endo* stabilized amine that exhibits considerably greater thermal stability.

The nature of this structural transformation is clarified by the combination of NMR spectroscopy and XRD. Comparison of the ¹³C CP/MAS NMR spectra of clathrate **1** before and after heating under conditions similar to that used for TGA indicates that the material remains crystalline, but undergoes a dramatic structural shift (see Figure 7). Heating clathrate **1** at approximately 60°C gives rise to a complex spectrum that indicates

that the original compound has been mostly consumed to give rise to a new phase.

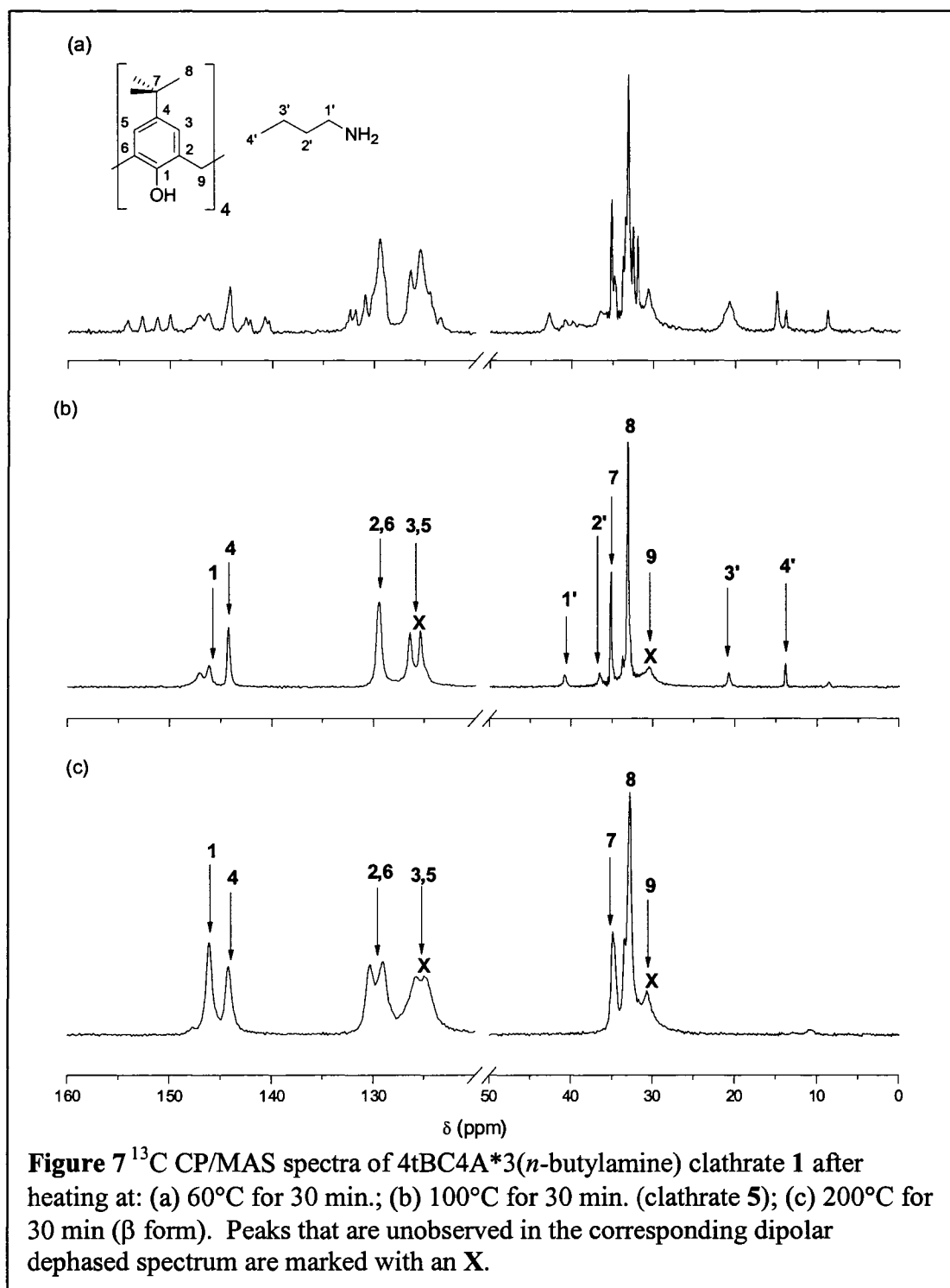
Further heating clarifies the interpretation (Figure 7b) of this new phase, clathrate **5**.

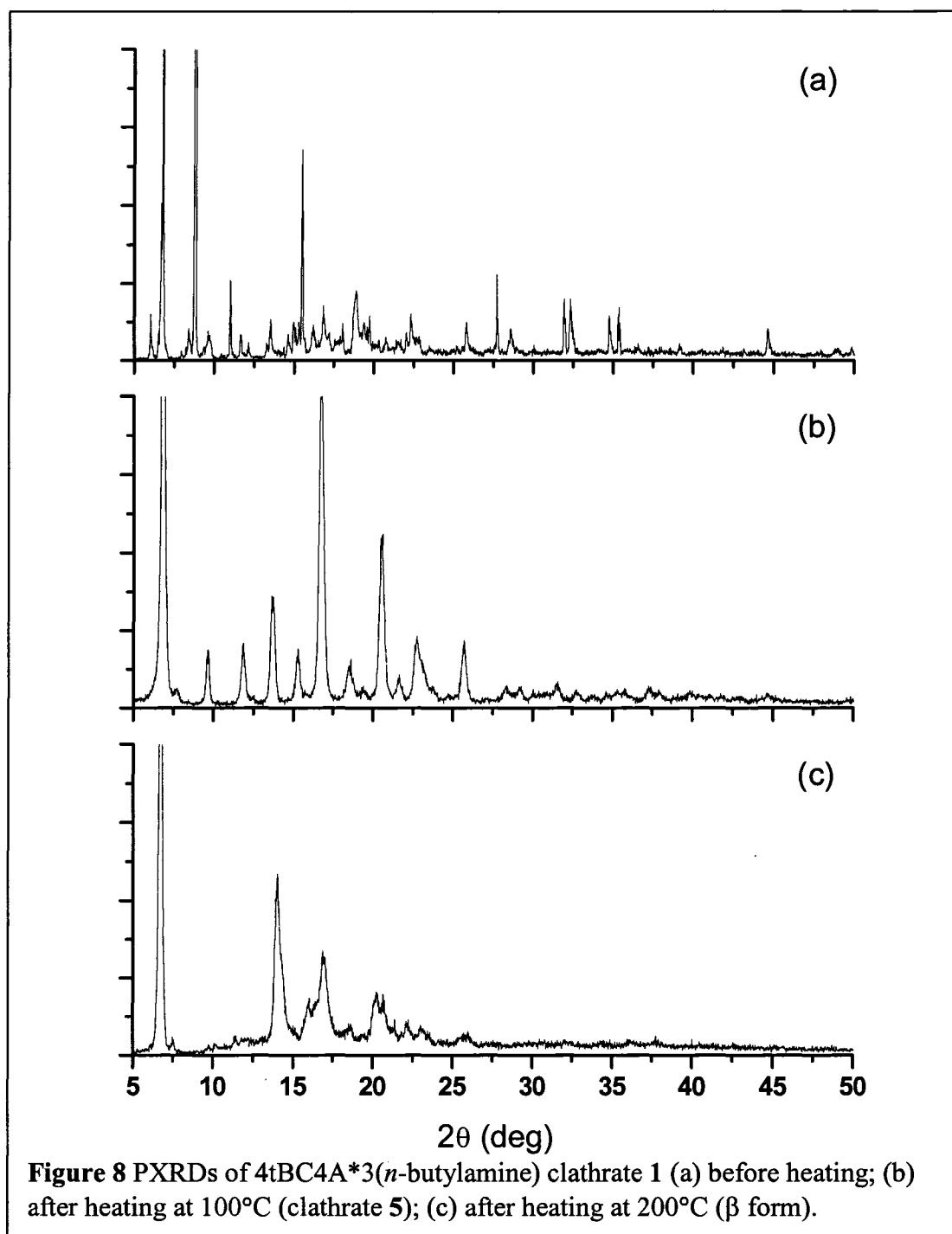
Table 3 TGA data for *n*-butylamine, amylamine and *n*-hexylamine clathrates with 4tBC4A.

Clathrate	Temp. (°C) ^[a] (± 0.1)	% Wt. Lost ^[b] (± 0.01)	Mol. Guest Lost ^[c] (± 0.01)	<i>n</i> ^[d] (± 0.01)
<i>n</i> -butylamine (1)	54.7-71.5	17.60	2.09	2.99
	129.8-156.6	7.60	0.90	
amylamine (2)	64.8-83.5	23.97	2.50	2.99
	151.9-191.8	4.74	0.49	
<i>n</i> -hexylamine (3)	55.4-67.5	25.82	2.43	2.99
	153.6-181.6	5.95	0.56	

^[a]Temperatures are given for the onset and completion of transition. ^[b]Percentage of mass lost by sample. ^[c]Corresponding number of moles of guest lost by host. ^[d]Overall Guest to Host Ratio=(Total % Wt. Lost)/(1-Total % Wt. Lost)*(Mol. Wt. of Host)/(Mol. Wt. of Guest)

In this new compound, the aromatic resonances have collapsed to single peaks, suggesting that the four-fold symmetry of the calixarene has been restored. Only a single set of guest resonances are observed without significant differences from the solvent chemical shifts. The dipolar dephased spectrum suggests that the guest is now dynamic. The PXRD also shows a dramatic simplification consistent with increased symmetry (see Figure 8 and Table 4). In conjunction with the TGA data, this suggests that clathrate **5** is a 1:1 guest to host inclusion compound (similar to that observed for weakly interacting paraffins^[21]) that arises directly from desolvation of clathrate **1**.





Upon further heating to completely remove the remaining guest, the resulting guest free host is obtained. No crystallographic splitting is observed in the aromatic region of the ^{13}C CP/MAS spectrum, with only a two fold splitting observed for the peaks

in the aliphatic region. This is quite similar to the spectra previously reported for the low-density guest free forms of 4tBC4A (β_0 and β_0') as obtained through sublimation^[56] or desolvation of 4tBC4A:toluene inclusion compounds.^[28] Simple visual comparison to spectra and diffractograms obtained for the desorption of toluene from **1** indicate that the *apo* form obtained is the β_0 form previously reported by Atwood *et al.*^[56, 57] and further elaborated upon by Ripmeester *et al.*,^[28] but too few peaks are available to index the cell reliably.

Table 4 Unit cell parameters determined by indexing of PXRD patterns of clathrates **1**, **2** and **3**, and the products arising from removing amine by heating.

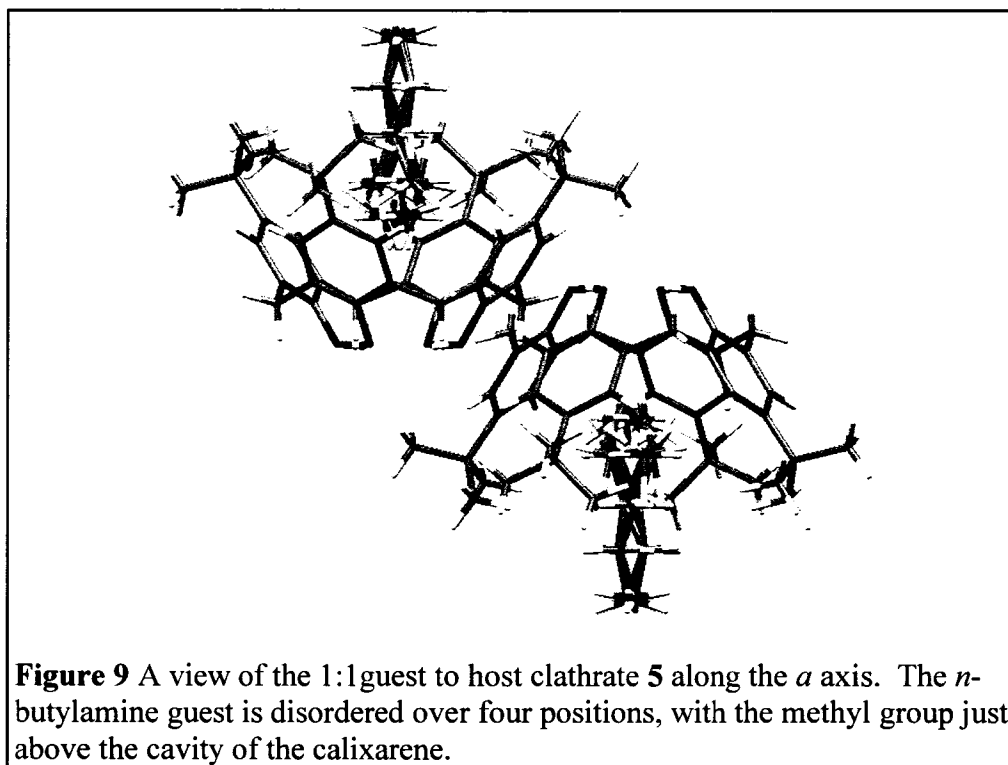
Clathrate	1	5 ^[a]	2	7 ^[b]	3	8 ^[c]	α <i>apo</i> ^[d]
Space Group	<i>P2₁/c</i>	<i>P4/n</i>	<i>P2₁/c</i>	<i>P4/nnc</i>	<i>P-1</i>	<i>P4/nnc</i>	<i>P2₁/c</i>
<i>a</i> (Å)	12.915	12.952	12.851	12.900	13.243	12.891	9.5958
<i>b</i> (Å)	20.019	12.952	25.071	12.900	13.982	12.891	30.416
<i>c</i> (Å)	20.682	12.945	18.607	26.054	16.060	26.133	13.442
α (°)	90	90	90	90	96.25	90	90
β (°)	90.92	90	107.9	90	104.6	90	109.7
γ (°)	90	90	90	90	98.01	90	90
<i>V</i> (Å ³)	5346.2	2171.5	5703.2	4334.9	2818.0	4342.8	3693.4

^[a]Obtained by heating **1** at 100°C. ^[b]Obtained by heating **2** at 100°C. ^[c]Obtained by heating **3** at 70°C. ^[d]Obtained by heating **3** at 185°C.

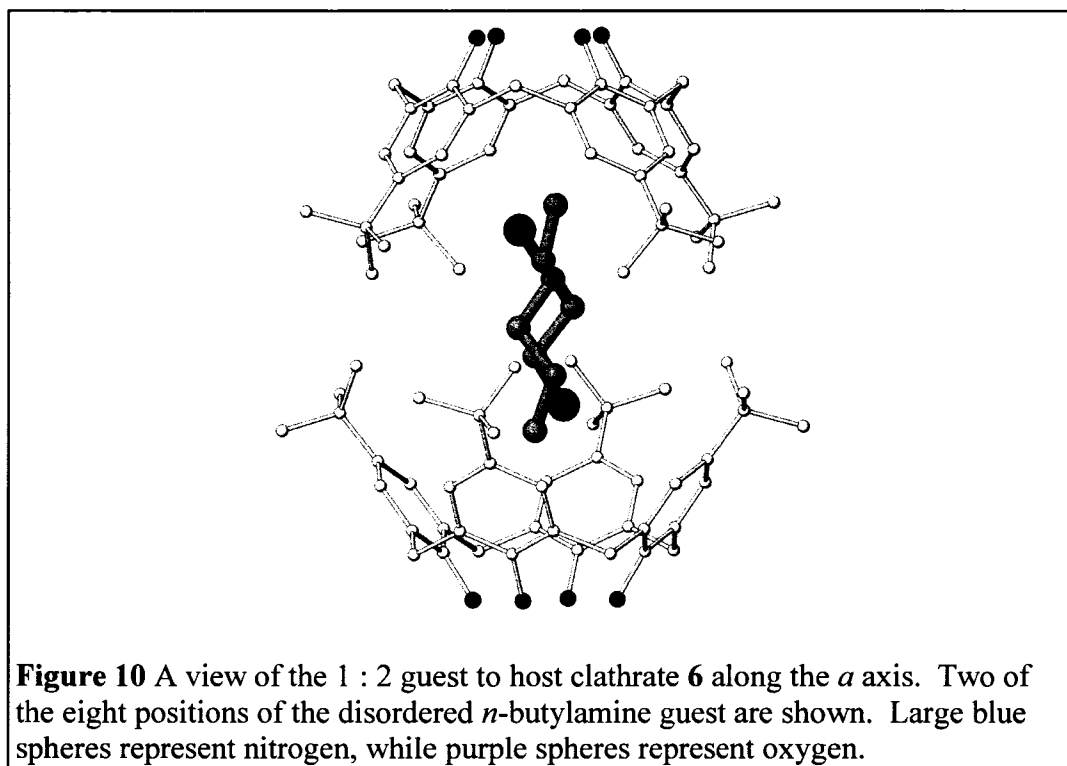
The stability of clathrate **5** prompted us to attempt to obtain crystals of the material by recrystallization through slow evaporation at approximately 70°C. Single crystal X-ray diffraction confirms that the resulting material is a 1 guest : 1 host inclusion compound with *P4/n* symmetry, with the amine guest disordered over four sites within the calixarene cavity. No hydrogen bonding or other directional interactions are observed, with π -CH₃ interactions ruled out by the 3.34 Å distance between the deeply included methyl and the centroid of the nearest phenolic ring (see Figure 9).^[21] The

disorder is a result of the guest attempting to accommodate the four fold symmetry of the host. The PXRD pattern obtained for clathrate **5** can be indexed based on the predicted powder pattern from this data (see Table 4), indicating that the single crystal is representative of the bulk material obtained by heating clathrate **1**.

Interestingly, the related 1:2 guest to host inclusion compound of 4tBC4A and *n*-butylamine (clathrate **6**) can also be isolated by recrystallization at elevated temperatures from a dilute solution of the amine in tetradecane (see Figure 10). This particular compound has *P4/nnc* symmetry, such that the guest is disordered over eight equivalent sites within the calixarene cavity. This disorder results in the guest moving further out of the calixarene cavity, with the NH₂ group being 3.92 Å away from the centroid of the nearest phenolic ring, and the CH₃ group being 3.56 Å distant. Once again, this rules out any π stabilization, such that the guest is stabilized solely by van der Waals interactions.



The ability to form both compounds with a single guest is an intriguing contrast with the studies of the inclusions of simple alkanes in 4tBC4A, where with no such intermediate case being observed in the guest-size correlated shift in motif from 1 host : 1 guest inclusion to 1 guest : 2 host inclusions.^[21] As previously mentioned, the transition between these two motifs was observed upon moving from pentane to hexane. It is clear, however, that the resulting family of three pseudopolymorphs suggests that the *n*-butylamine inclusions represent a convergence of repulsive interactions due to steric hindrance and attractive directional interactions in determining structural motifs in amine-4tBC4A inclusion compounds.



This concentration dependence indicates that the more complex interplay of directional interactions can even influence the formation of such non-directionally stabilized compounds. At high degrees of dilution, it is possible to force a shift in the

inclusion motif away from that which would be predicted from simple alkanes. As such, the hydrogen bonding arising from the presence of the amino functionality interferes with the shift from the 1 guest : 1 host compound to the 1 guest : 2 host compound. Given this, further increases in guest size should drive the resultant pseudopolymorphs towards formation of the 1 guest : 2 host compound.

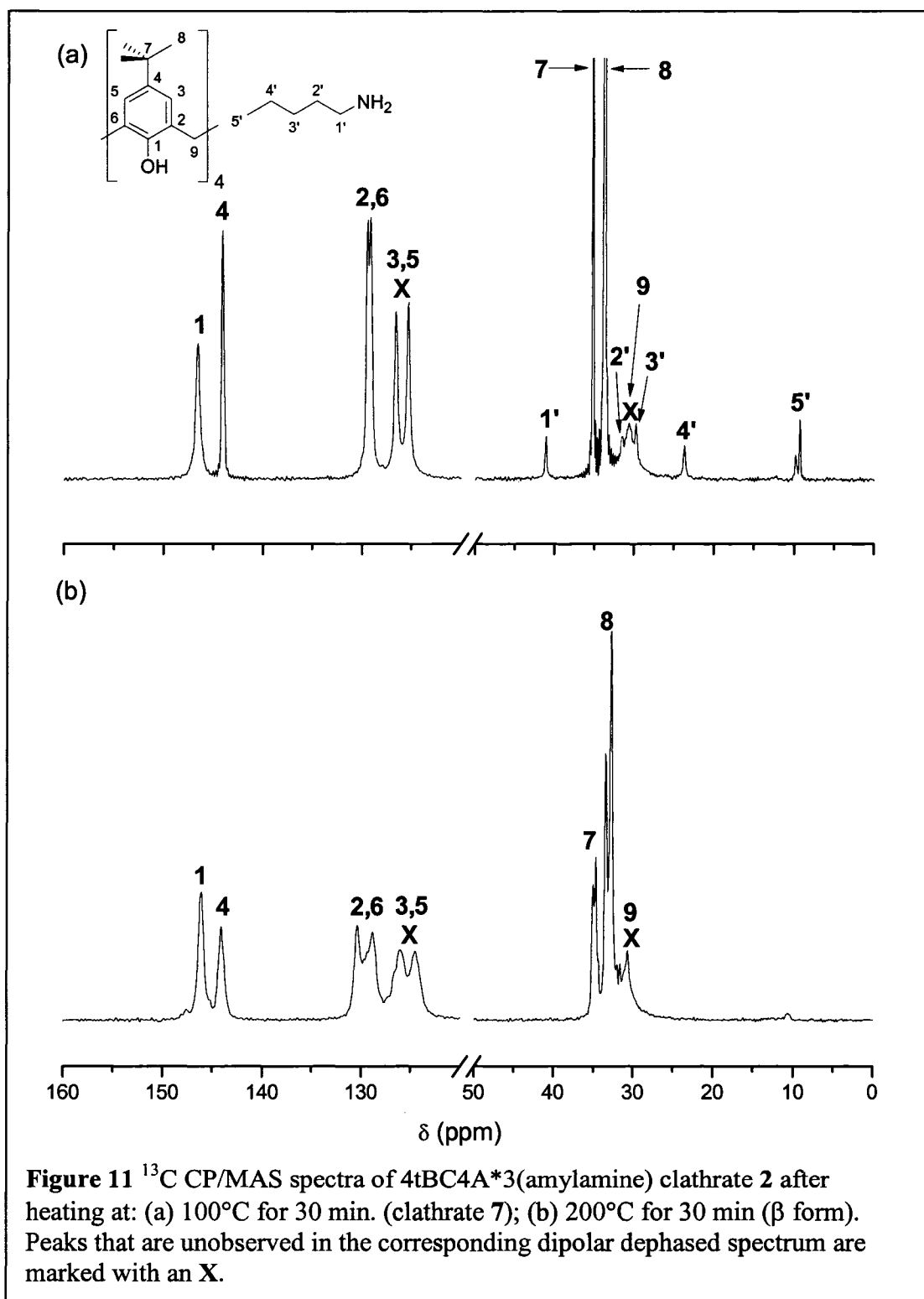
This is confirmed by the thermally induced collapse of clathrate **2** to give rise to the 1 guest : 2 host 4tBC4A:amylamine clathrate **7**. The TGA in this case shows the loss of 2.5 molecules of amine, followed by the loss of 0.5 molecules (see Table 3). There is a noticeable increase in the temperatures required to force the guest out of the host lattice, but the first transition is now well below the boiling point of the free solvent (104°C). The increased bulk of an additional carbon, and the conformational shift away from all *trans* clearly contribute to this comparative increase in the destabilization of the *exo* amines. The increased temperature of the second step is representative of the increased energy required to open the host capsule containing the guest.

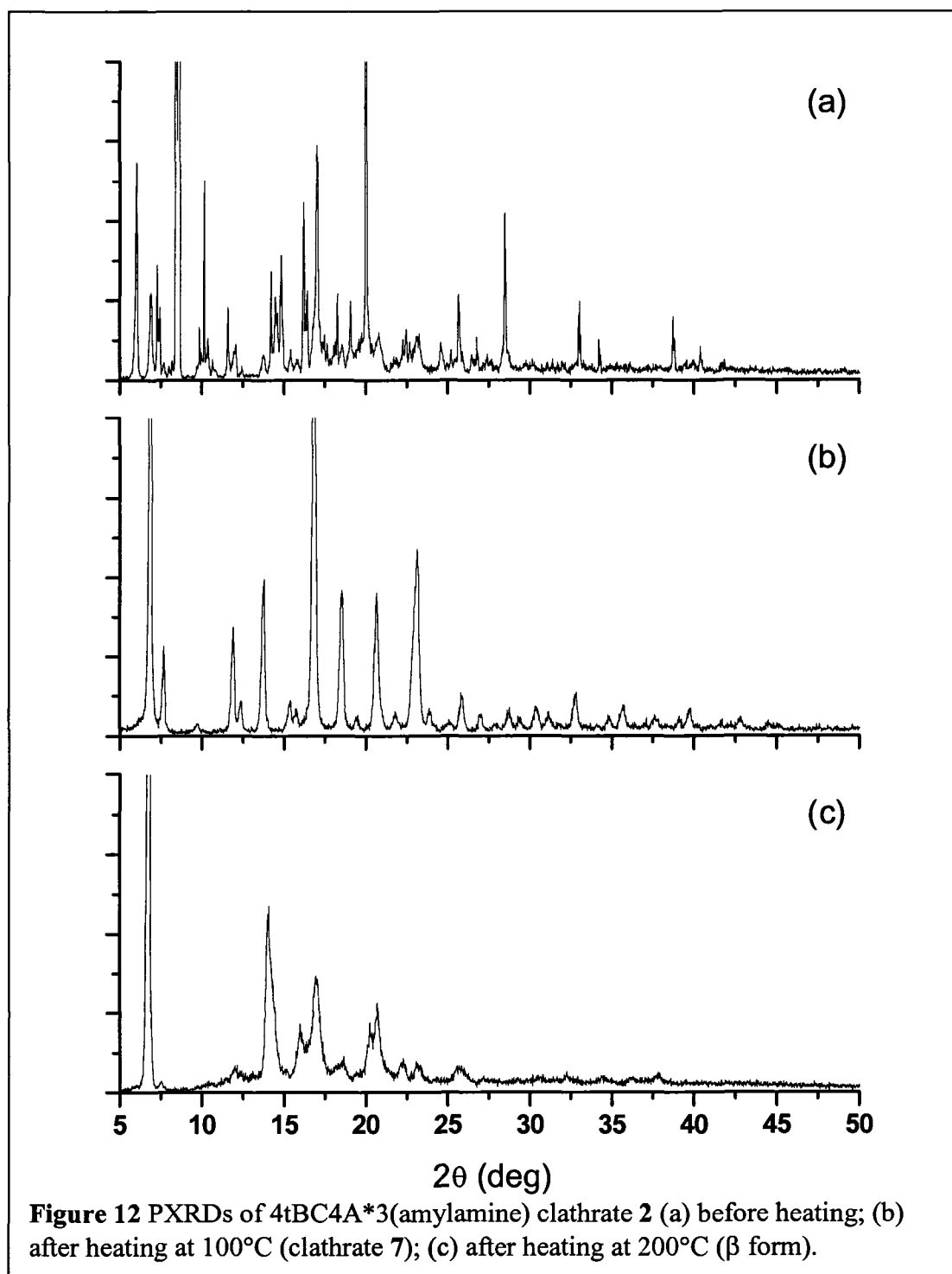
As before, the ¹³C CP/MAS spectrum is able to confirm the structural shift and gives rise to a highly symmetrical structure (see Figure 11). Once again, the splitting in both the aromatic and guest peaks is characteristic of four-fold symmetry, with the guest exhibiting dynamic motion. In addition, it is possible to determine that the transformation does not involve intermediate structures, as a spectrum taken at an intermediate temperature is only a combination of the spectra for **2** and **7**. The loss of amine is also apparent from the dramatic reduction in intensity observed for the guest resonances. It is not possible, however, to distinguish between the 1 guest : 2 host and 1

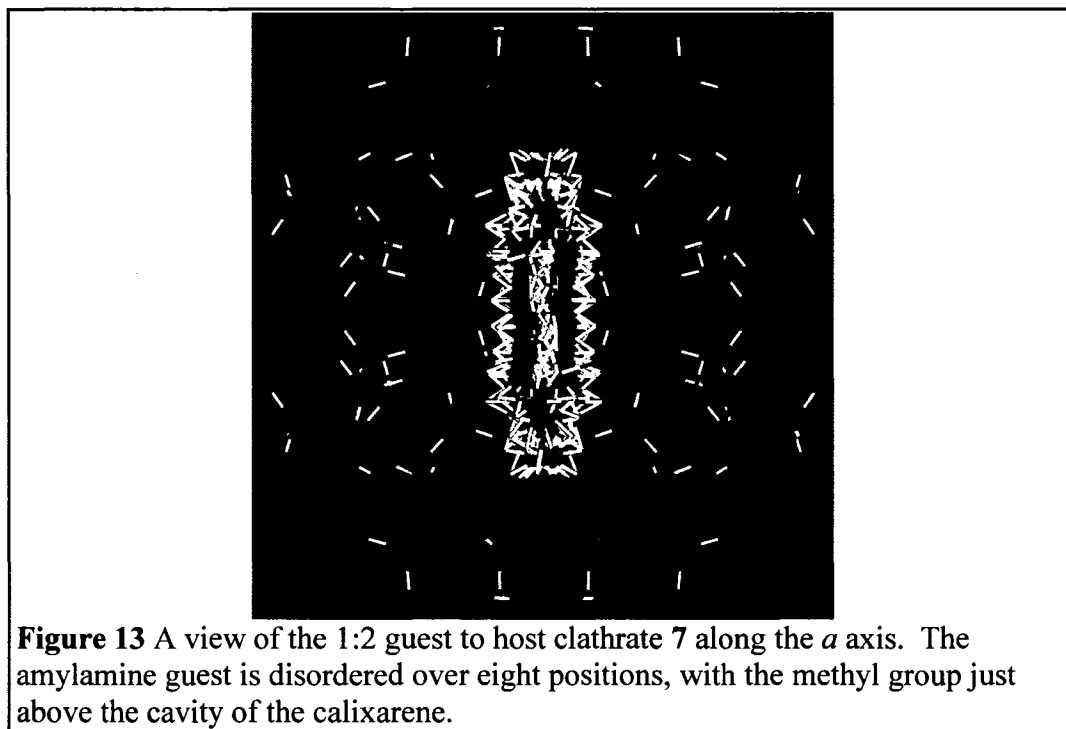
guest : 1 host compounds using NMR, as the splittings arising from the subtle differences between the asymmetric units of the two clathrates are too small to be readily observed.

The symmetry differences do give rise to distinct PXRD patterns, as the additional glide planes give rise to subtle shifts in several indexable peaks (see Figure 12 and Table 4). Single crystals of **7** can be prepared in a fashion similar to that used for preparing the 1 guest : 2 host clathrate of *n*-butylamine, with only a marginal increase in the length of the *c* axis to accommodate the slightly larger guest.^[55] As expected from the absence of any significant complexation induced shift for the guest resonances in the NMR spectrum, the carbons are not deeply included within the calixarene cavity (see Figure 13). The guest is positioned in such a fashion in order to minimize contact between the amino group and the cavity across for the eight guest positions arising from the disorder across the four-fold axis and inversion centre of the structure.

The powder pattern can be indexed in the space group obtained from the SCXRD data set, with slight increases in the unit cell parameters because of expansion of the cell at room temperature. The elevated temperature disrupts the stabilization from hydrogen bonding, such that the size of the guest now guides the structural motif, following the pattern established for paraffins. However, the NMR and PXRD evidence indicate that complete desolvation still results in the formation of the low-density guest free form of 4tBC4A. Despite the presumably greater energy costs in removing the guest from the capsule formed by the two host molecules, it is still more favourable for the compound to remain in an open form rather than to collapse into a dense form.







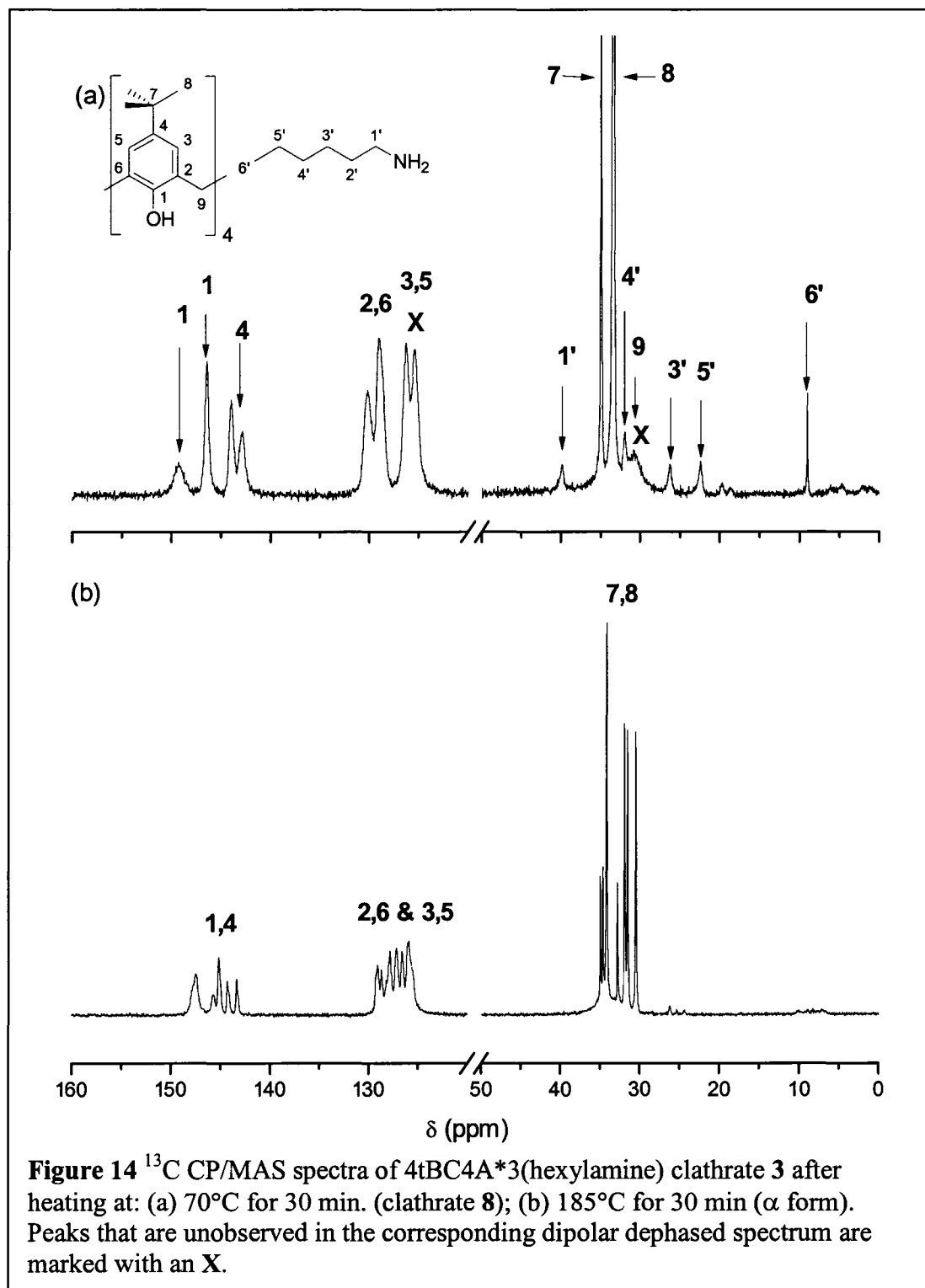
Interestingly, the TGA of clathrate **3** is quite similar to that observed for clathrate

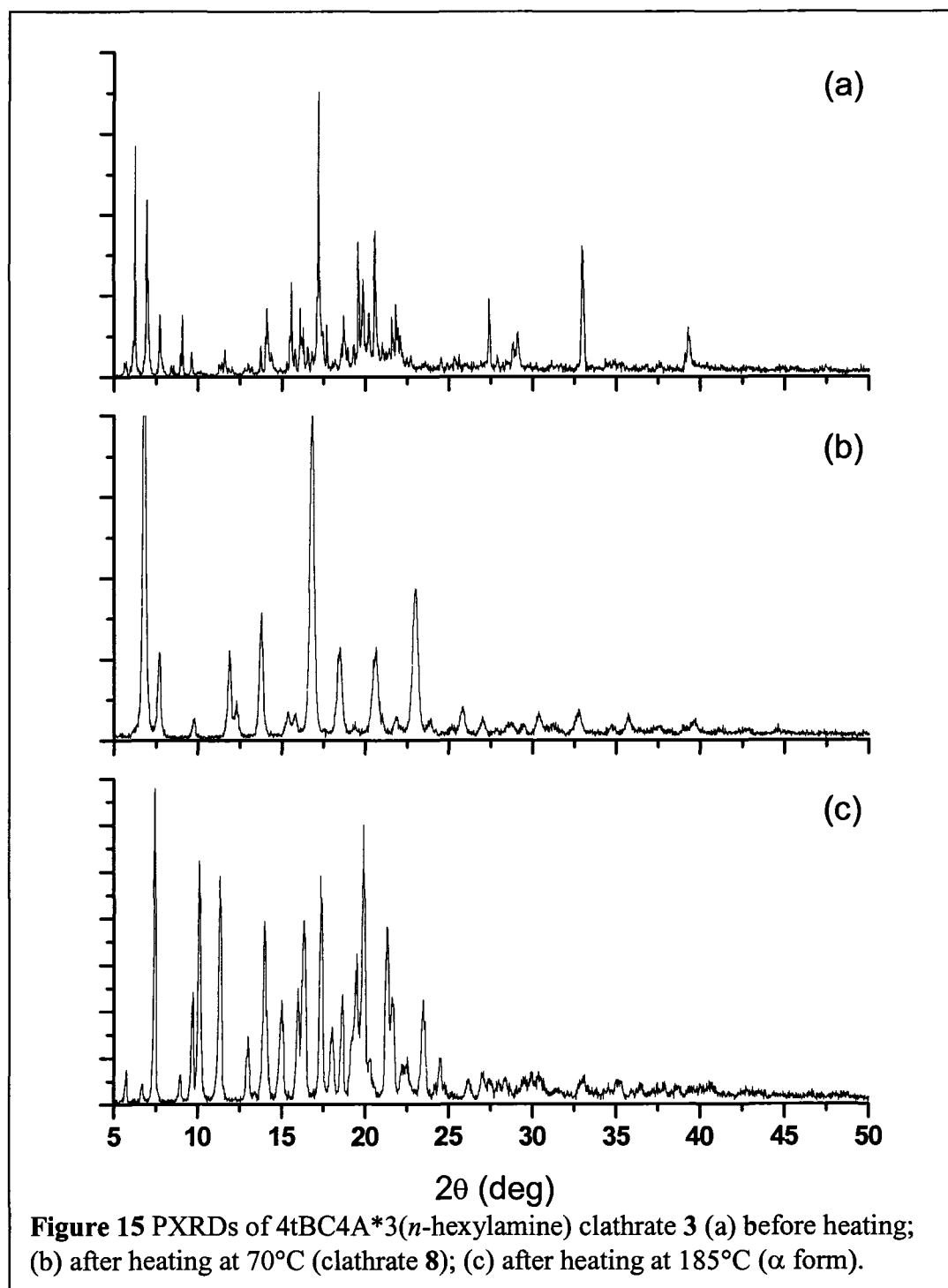
2. The overall trend is identical, with 2.5 equivalents of hexylamine followed by 0.5 equivalents lost with heating. However, the temperature required to eliminate amines in the first transition is less than that observed for clathrate **2** (see Table 3), and is dramatically less than the boiling point of hexylamine (132°C). As with the conformational distortion of the guests observed in the crystal structure clathrate **3**, this is reflective of the fact that the hydrogen bonding and ion-ion interactions are only able to partially compensate for the absence of guest stabilization through van der Waals interactions with the calixarene cavity.

As before, the combination of SCXRD, ¹³C CP/MAS NMR and PXRD make it apparent that the 1 guest : 2 host compound has been isolated. The ¹³C CP/MAS NMR shows the expected decrease in splitting multiplicity from a restoration of four-fold symmetry (see Figure 14), but in this case the guest methyl exhibits a CIS of

approximately 5 ppm. As expected, the single crystal structure indicates that the increased bulk of the guest causes the methyl group to be deeply inserted into the calix cavity (see Figure 15). The PXRD (see Figure 16 and Table 4) pattern agrees well with that based on the predictions from this single crystal structure. This makes it clear that it is not selective removal of *exo* amines from the initial clathrates that guides the formation of the subsequent pseudopolymorphs. Instead, the heat induced disruption of hydrogen bonds results in the van der Waals interactions with the host and guest bulk becoming the primary directors of the structural motif.

Complete desolvation also leads to the formation of a different *apo* host than observed for clathrates 1 and 2. The ^{13}C CP/MAS spectrum clearly shows an increase in splitting in both the aromatic and aliphatic regions consistent with the densely packed guest free form of 4tBC4A (α), while the PXRD pattern is indexable based on the available single crystal data for this form.^[28] Given the lack of *endo* guests in the structure of clathrate 3, this suggests that the guest free form obtained by desolvation at low temperatures is actually guided by the initial inclusion motif observed, altogether avoiding the balancing of temperature and heating rate dictated by the balance of forces in the toluene inclusion system.^[28] Judicious choice of guest size allows one not only to dictate the structure of the inclusion compounds that result, but also that of the empty guest form obtained after desolvation.





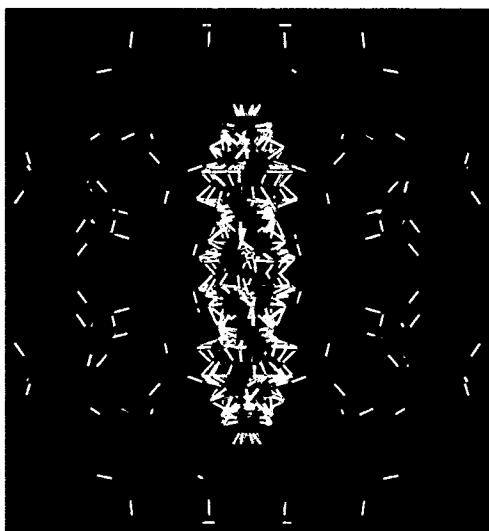


Figure 16 A view of the 1:2 guest to host clathrate **8** along the a axis. The hexylamine guest is disordered over eight positions, with the methyl group of the guest now inserted into the cavity of the calixarene.

CO₂ Adsorption by *n*-butylamine clusters in 4tBC4A

The complex array of pseudopolymorphs is intriguing from a structural point of view, and provides considerable insight into how the competition of two forces will guide a structure towards a compromise packing motif. As we will see in Chapter VI, larger ethanolamine clusters with liquid-like behaviour are enclathrated by 4tBC4A. These clusters are accessible, and chemisorb CO₂ in a fashion not unlike that observed in solution, where amines are of utility in scrubbing industrial gas flows of such greenhouse gases.^[58-60] These materials exhibit no significant structural changes while adsorbing CO₂, a further reflection of the concept that such clusters are essentially droplets contained by an organic lattice.

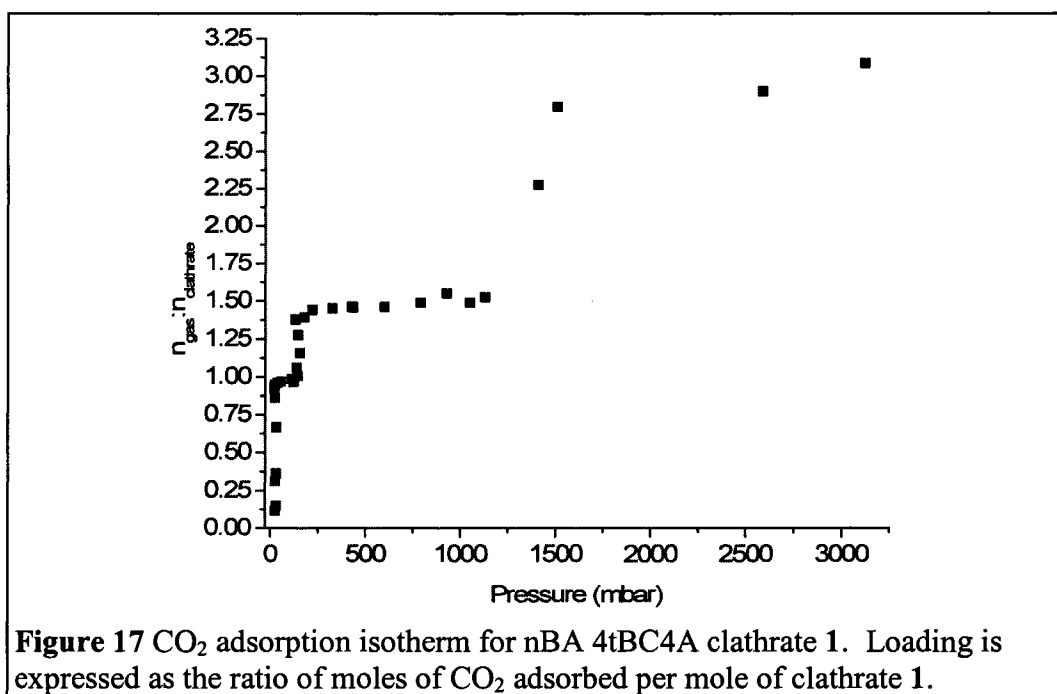
This adsorption behaviour prompted the question as to whether analogous adsorption behaviour would be observed in smaller clusters. Typically, adsorption of CO₂ by amines entails the formation of carbamates,^[61-67] such that as chemisorption

proceeds, more and more amine will react, effectively giving rise to a mixed guest clathrate. Such clathrates are quite common in the clathrate hydrates,^[68] where small help guests are used to promote the formation of gas hydrates suitable for storing hydrogen.^[69] In the case of 4tBC4A, the inclusion geometry of nitrobenzene can be effectively tuned by addition of propane.^[18, 41] Provided they are large enough to still be accessible, chemical modification of the *n*-butylamine through adsorption might have similar effects, given that all of the amines present interact directly with the calixarene framework through hydrogen bonds.

For alkanolamines, the formation of carbamates has been studied intensively, due to their industrial utility. The reaction is typically modeled as being mediated by proton transfer involving water or the alcohol functionality (see Chapter VI).^[62, 64, 65] The chemisorption of CO₂ by pure alkylamines has received considerably less attention, with the chemical equilibria being variations on that proposed for the alkylamines.^[66, 67] In the absence of OH groups, the formation of the anionic carbamate by one amine depends on a second amine forming a corresponding alkylammonium cation.^[67] In a calixarene supported system, presumably the phenolic hydroxyls of the calixarene might also participate in the chemisorption process, along with the formation of alkylammonium-carbamate pairs.

The adsorption isotherm for the nBA 4tBC4A clathrate **1** is shown in Figure 17. Similar to the ethanolamine 4tBC4A system, the amount of CO₂ adsorbed is considerable even at equilibrium pressures below 100 mbar (being an order of magnitude better than the pressures used to adsorb gases on 4tBC4A alone,^[29, 30, 70] and quite comparable to

other solid supported systems^[71-75] where loadings of ~ 130 mg CO₂/g adsorbent are reported^[76]), which is characteristic of a chemisorption process. Unlike that system, however, until a loading ratio of 1 mol CO₂ : 1 mol clathrate **1** is obtained, there is no significant change in the equilibrium pressure required to promote adsorption of the CO₂ (25 mbar), a value which is considerably lower than the 8.5 bar pressure required to obtain a mole CO₂ : 1 mole amine equilibrium adsorption ratio in a 10% ethanolamine solutions.^[77]

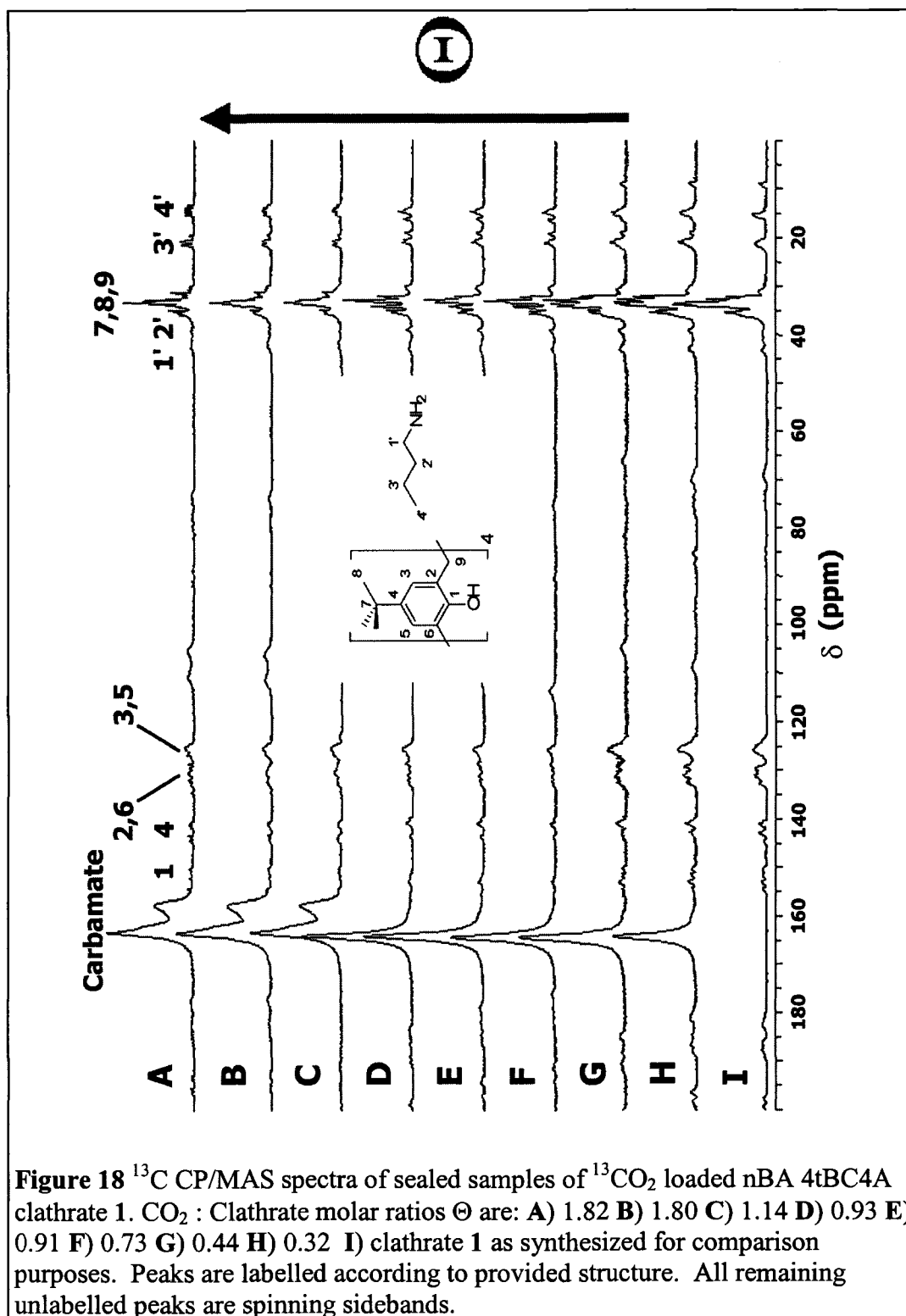


Upon reaching the first plateau, no significant change in CO₂ loading occurs until the pressure increases to 140 mbar, where another spike in adsorption is observed with no change in pressure until a loading ratio of 1.5 mol CO₂ : 1 mol Clathrate is reached. This secondary plateau lasts until the pressure reaches approximately 1200-1400 mbar, upon which time the adsorption behaviour begins to more closely resemble Langmuir behaviour, with the adsorption ratio gradually approaching 3 mol CO₂ : 1 mol Clathrate

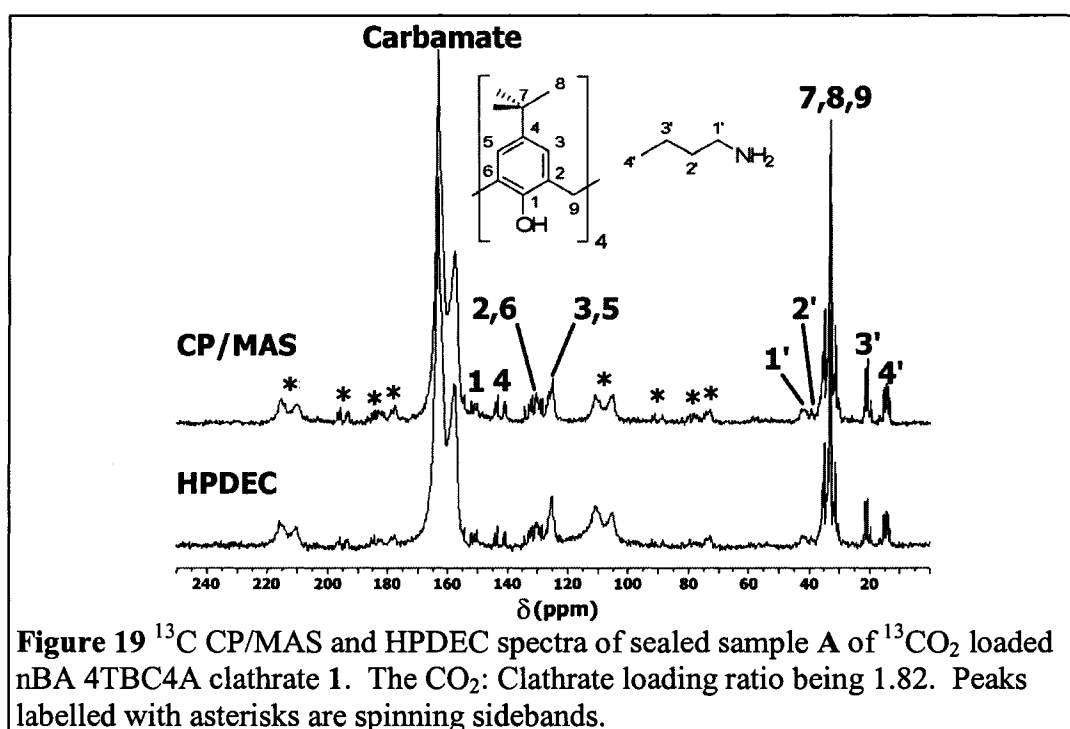
as pressure increases. Clearly, the adsorption process at low pressures is somewhat more complex than in the nanodroplets of ethanolamine supported by 4tBC4A, where the entire adsorption process is adequately modeled using a modified Langmuir equation.

This stepped behaviour has neither been reported in other functionalized solid systems tested for CO₂ adsorption,^[72-75] nor in solution-based systems.^[61-65] The three regions therefore must represent limitations imposed upon the chemisorption process by the intermolecular forces stabilizing the amines within the calixarene structure. Such a situation reconciles well with the absence of any evidence of adsorption of atmospheric CO₂ by clathrate 1. Unlike the ethanolamine 4tBC4A system, where CO₂ has a noticeable impact on both the TGA data and NMR spectra (see Chapter VI), in such a restricted system, the amount of CO₂ present in the atmosphere (~0.3 mbar) is insufficient to introduce the gas and make the molecular interactions guiding chemisorption favoured over continued interaction with the calixarene.

As such, the multi-step adsorption isotherm would appear to represent pressure induced changes to the clathrate. Insight into the nature of these changes can be gleaned from ¹³C CP/MAS spectroscopy of ¹³C labelled CO₂ adsorbed onto clathrate 1. Spectra of sealed samples with a loading ranging from 0.32 to 1.82 mol CO₂ : mol clathrate 1 are depicted in Figure 18. The two broad carbonyl resonances at 160-170 ppm are clearly diagnostic of the formation of carbamates, similar to those observed in both the ethanolamine 4tBC4A clathrate (see Chapter VI), as well as in solution.^[77-79] The various host and guest resonances are also easily identified based on the previously obtained spectrum for clathrate 1 (see Figure 1).



As the CO₂ loading level increases, it is apparent that the symmetry of the both the host and guest change. The peak attributed to the C4' carbon of the *endo* guest disappears rapidly, while the remaining C3' and C4' resonances exhibit increased splitting consistent with the formation of more crystallographically inequivalent sites, with the observed splitting increasing as loading increases. At the same time, the aliphatic resonances due to the host increase in complexity, with the splitting becoming quite fine at higher loadings. The full extent of this structural shift is depicted in Figure 19, which also indicates that the aromatic resonances continue to exhibit extensive splitting. In particular, the resonances due to carbons 1 and 4 continue to exhibit four-fold splitting consistent with deprotonation-induced reduced symmetry of 4tBC4A.



In light of this, it appears that the structure shifts away from the 3 guest : 1 host capped motif seen in the SCXRD structure as carbamates are formed. The initial carbamates can be accommodated in the traditional capped motif, but as the loading approaches 1 mol CO₂ : 1 mol clathrate, such a structure is no longer favoured. With the loss of CIS observed for the *endo* amine, this amine is therefore forced out of calixarene cavity in order to accommodate a new hydrogen bonding scheme. In light of the studies of CO₂ sorption by pure amines,^[67] it seems reasonable to suspect this new packing motif arises partially from the formation of alkylammonium and carbamate pairs through proton transfer from amine to amine.

This suggests that the initial carbamate formation involves the single *endo* amine and one of the *exo* amines. The *endo* amine may in fact represent the initial carbamate-forming moiety, although it is also possible that the *endo* amine shifts position to accommodate further hydrogen bonding to an *exo* carbamate. Either way, such a shift in amine position would also cause the tertiary butyl groups of the calixarene to reorganize to accommodate such a structure, giving rise to the observed change in splitting pattern.

Further structural shifts are observed upon moving to higher loading levels, as seen in both Figures 18 and 19. While the aromatic resonances due to the host do not shift significantly, the aliphatic resonances due to the host continue to exhibit complex splitting that is not readily analyzed. However, examination of the aliphatic guest resonances indicates that as more carbamates form, the various amine sites, despite being located outside of the calixarene cavity now, are now split well enough to produce distinct series of peaks (as opposed to the broad lines observed in lower loaded samples).

Supporting this is the appearance of additional carbamate sites, although the combination of the broadness of the resonances and the fact that the structure itself has changed makes it difficult to assess how many sites are observed.

Comparing the loading ratios of the sealed samples to the adsorption isotherm, these shifts in structure correspond well with the stepped nature of the observed isotherm. Unlike adsorption by the ethanolamine 4tBC4A clathrate, it appears that the small size of the nBA cluster cannot chemisorb CO₂ without a phase change occurring that retains the decreased symmetry of the calixarene due to deprotonation, but results in the guests being reorganized. These phase changes require a certain amount of pressure to overcome the hydrogen bonds binding the structure together in each case, making the carbamate formation more energetically favourable, as well as presumably overcoming any kinetic barriers to CO₂ diffusing through the structure to reach each increasingly isolated site. Such kinetic barriers might also entail spatial restrictions on exchange. These results are quite intriguing, such that further adsorption studies for the purposes of clarifying the observed isotherm and how they relate to the structural changes indicated by NMR are called for. Additional studies to clarify how the gas pressure and sample size affect this process would also be wise, as the pressures required for the sealed samples used in the preliminary NMR studies to reach the highest loadings show increasing divergence from the isotherm of the bulk sample (~200-400 mbar).

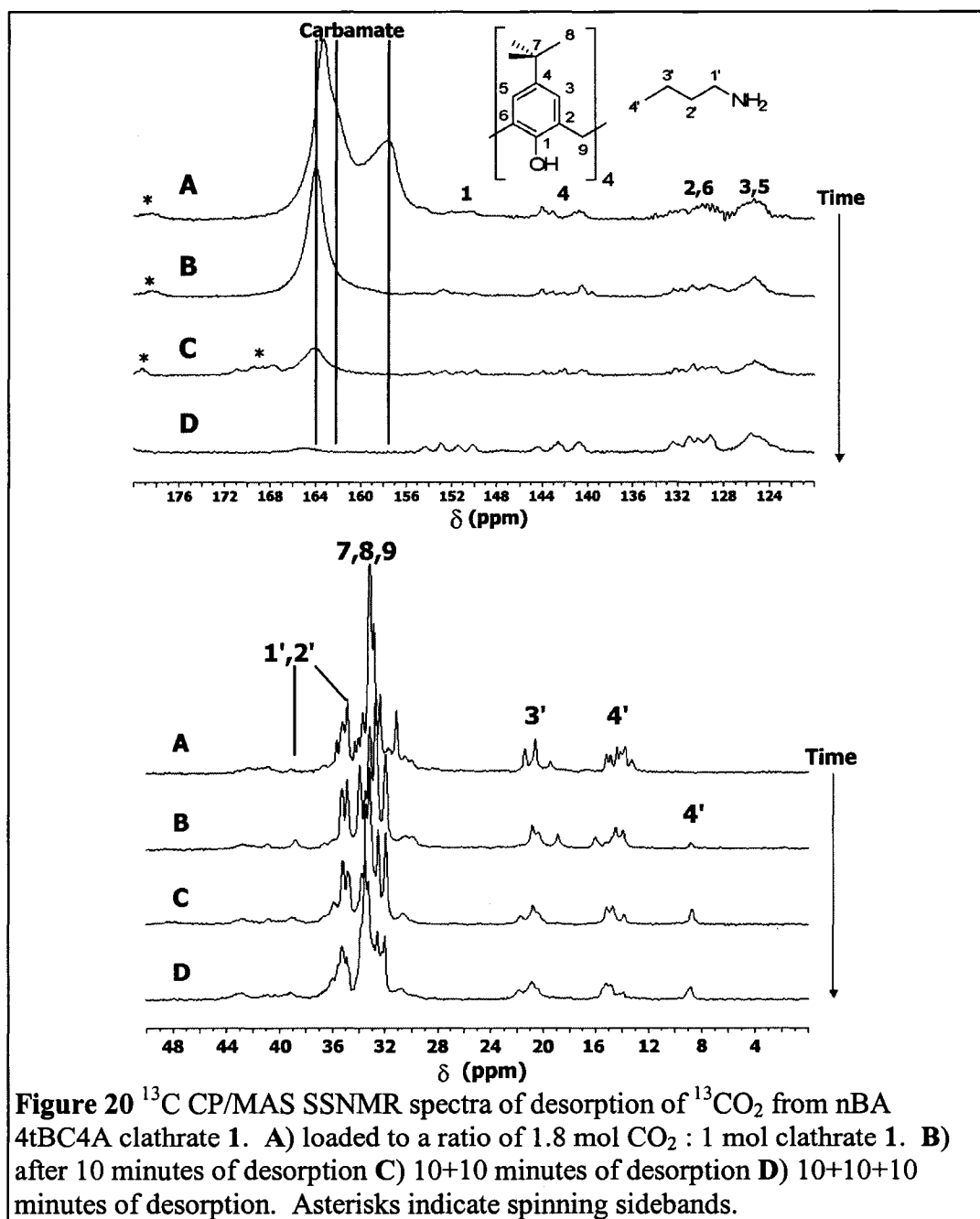
As indicated above, covalent modification of the guest does not lead to any significant shift in the symmetry of the calixarene. This contrasts with studies of propane nitrobenzene 4tBC4A clathrates, where exchange and adsorption of the gaseous guest

within the calixarene cavity leads to increases in host symmetry.^[18, 41] This difference in behaviour due to formation of a covalent linkage raises the question of reversibility regarding the adsorption of CO₂ by this system. While the carbamate linkage is a comparatively weak covalent interaction, the question remains as to whether the van der Waals interactions guiding inclusion of the amine would reassert themselves upon removal of the CO₂ by evacuation.

The structural changes upon vacuum-assisted desorption of CO₂ from a sample with a loading ratio of approximately 1.8 mol CO₂ : 1 mol clathrate 1 are shown in Figure 20. As one can see from the ¹³C SSNMR data, the process does in fact appear to be reversible at these loading levels, as the heavily shielded resonance due to inclusion of carbon 4' in the calixarene reappears as the CO₂ is removed. This also leads to a decrease in the splitting observed for the host aliphatic resonances. Therefore, while the structural changes are different from those observed for physically adsorbed guests, the overall trend of being able to use a gaseous guest to tune the inclusion scheme of a 4tBC4A compound applies even to systems where the symmetry of the host is disrupted due to changes in the host itself.

Unfortunately, the structural evidence currently available is insufficient to allow for a possible adsorption mechanism to be proposed. At the low pressures investigated, physical adsorption can be ruled out, although it would logically contribute as the pressure approached the values known to lead to physical adsorption in 4tBC4A alone.^[30, 70] However, the studies of the kinetics of CO₂ adsorption by amines have focused on solution systems, with water playing a key role as an intermediary. In light of the

formation of pairs of alkylammonium and alkylcarbamate molecules, one would suspect that a similar proton transfer mechanism between amines would have a role in the



calixarene-supported system. Such a shift in protonation would promote alternative hydrogen bonding schemes that would favor the formation of new phases.

It is important to note, though, that the isotherm is not limited to the adsorption of a single molecule of CO₂ for every two molecules of amine, suggesting that such a process is not the only one at work in this system. Indeed, it is also likely that the phenolic groups of the calixarene (and in particular, the O⁻ centre) play a role in the formation of the carbamate in the absence of water to assist,^[61-65, 77-79] as is likely the case for the ethanolamine 4tBC4A clathrate (see Chapter VI). Overall, it is the amine cluster and its size that appears to be the key in directing the system, as demonstrated by the pseudopolymorphism arising from thermal disruption of the hydrogen bonds between the amine and calixarene.

While it is apparent that clathrate **1** readily adsorbs CO₂, further XRD and NMR studies are required to fully understand the nature of the structural transformations, and as such be able to properly model the adsorption behaviour of clathrate **1**. Similarly, it would be of interest to carry out further adsorption and desorption studies to both extract quantitative values for heats of adsorption, as well as obtain a fuller understanding of the kinetics of this system.

5. Conclusion

The introduction of a strong directional interaction has a considerable impact on the structural motifs observed in 4tBC4A:amine inclusions. By disrupting the molecular symmetry of the calix through deprotonation, hydrogen bonding, as exemplified by the ion-ion interaction between the deprotonated calixarene and protonated amine, dominate the structural motifs. As such, all of the fully aminated compounds exhibit complex hydrogen bonding schemes. The van der Waals interactions with the calix cavity and the

steric bulk of the guest are involved in the fine-tuning of the structure. Small guests are stabilized by inclusion, favouring the formation of capped cavities, while larger guests will form layers as self-inclusion of the calix becomes more favourable.

The delicate balance between these forces is most apparent in the desolvation behaviour of these clathrates. Modest heating allows one to disrupt the directional non-covalent interactions, such that non-directional interactions with the calixarene dominate the motif. As a result, the resulting dependence of the inclusion ratio on the guest size mirrors that seen in other paraffins.^[43] More intriguingly, while temperature previously has been shown to play a major role in determining the guest free form obtained,^[28] it is now clear that the guest size also influences which of the two guest free forms can be obtained upon total desolvation, with increased size evidently favouring formation of the dense form.

These materials also have potential as gas adsorbents due to the ability to carry out chemistry using the included guest. The channelled structure arising from the competition of forces also results in the amines being organized into a channel that is accessible to the external environment. In the case of CO₂, the resulting adsorption process also happens to be another method for tuning the structure of the calixarene clathrate lattice. As we will see in Chapter VI, while the structural tuning is not always observed for amine clusters, the adsorption activity does appear to be a common feature of these materials. As such, the perception of 4tBC4A as being unsuitable for producing supramolecular functional materials with 3D structures only holds true if the symmetry of the calixarene remains undisturbed due to interaction with the guest. With amines,

however, non-covalent forces allows for very easy tuning of the structure to obtain desired functionalities and chemical activity towards acid gases.

While supramolecular chemistry is chiefly concerned with non-covalent interactions, a surprising amount of effort is focused on covalent modification of host molecules in attempts to direct structural motifs. Much of this chemistry is a consequence of the difficulties inherent to structural prediction in the face of a broad range of weak interactions. The diversity of inclusion motifs arising from the inclusion of simple aliphatic amines in 4tBC4A clearly demonstrates that self-assembly guided by competing non-covalent interactions is an excellent alternative to covalent modification in producing a diverse range of structures in a controlled manner. As we will see in subsequent chapters, the competition between forces can be further influenced by introduction of hydrogen bonding intermediaries (such as water), metal centres and variation in the amine structure itself.

6. References

- [1] J. L. C. Rowsell, E. C. Spencer, J. Eckert, J. A. K. Howard, O. M. Yaghi, *Science* **2005**, *309*, 1350.
- [2] G. D. Enright, K. A. Udachin, I. L. Moudrakovski, J. A. Ripmeester, *J. Am. Chem. Soc.* **2003**, *125*, 9896.
- [3] P. K. Thallapally, T. B. Wirsig, L. J. Barbour, J. L. Atwood, *Chem. Commun.* **2005**, 4420.
- [4] M. J. Wilkinson, P. van Leeuwen, J. N. H. Reek, *Org. Biomol. Chem.* **2005**, *3*, 2371.
- [5] A. C. Sudik, A. P. Cote, O. M. Yaghi, *Inorg. Chem.* **2005**, *44*, 2998.
- [6] R. M. McKinlay, G. W. V. Cave, J. L. Atwood, *Proc. Natl. Acad. Sci. USA* **2005**, *102*, 5944.
- [7] L. J. May, G. K. H. Shimizu, *Z. Kristall.* **2005**, *220*, 364.
- [8] L. C. Palmer, A. Shivanyuk, M. Yamanaka, J. Rebek, *Chem. Commun.* **2005**, 857.
- [9] J. Antesberger, G. W. V. Cave, M. C. Ferrarelli, M. W. Heaven, C. L. Raston, J. L. Atwood, *Chem. Commun.* **2005**, 892.

- [10] D. V. Soldatov, I. L. Moudrakovski, J. A. Ripmeester, *Angew. Chem. Int. Edit.* **2004**, *43*, 6308.
- [11] D. V. Soldatov, G. D. Enright, J. A. Ripmeester, *Cryst. Growth Des.* **2004**, *4*, 1185.
- [12] A. Shivanyuk, J. Rebek, *J. Am. Chem. Soc.* **2003**, *125*, 3432.
- [13] H. R. Webb, M. J. Hardie, C. L. Raston, *Chem. Eur. J.* **2001**, *7*, 3616.
- [14] C. D. Gutsche, *Calixarenes*, Royal Society of Chemistry, Cambridge, **1989**.
- [15] C. D. Gutsche, *Calixarenes Revisited*, Royal Society of Chemistry, Cambridge, **1998**.
- [16] L. Mandolini, R. Ungaro, *Calixarenes in Action*, Imperial College Press, London, **2000**.
- [17] G. D. Andreotti, R. Ungaro, A. Pochini, *J. Chem. Soc. Chem. Commun.* **1979**, 1005.
- [18] E. B. Brouwer, G. D. Enright, J. A. Ripmeester, *J. Am. Chem. Soc.* **1997**, *119*, 5404.
- [19] E. B. Brouwer, K. A. Udachin, G. D. Enright, J. A. Ripmeester, K. J. Ooms, P. A. Halchuk, *Chem. Commun.* **2001**, 565.
- [20] G. D. Enright, E. B. Brouwer, K. A. Udachin, C. I. Ratcliffe, J. A. Ripmeester, *Acta Crystallogr. Sect. B-Struct. Sci.* **2002**, *58*, 1032.
- [21] K. A. Udachin, G. D. Enright, E. B. Brouwer, J. A. Ripmeester, *J. Supramol. Chem.* **2001**, *1*, 97.
- [22] G. D. Andreotti, A. Pochini, R. Ungaro, *J. Chem. Soc. Perkin Trans. 2* **1983**, 1773.
- [23] S. G. Bott, A. W. Coleman, J. L. Atwood, *J. Am. Chem. Soc.* **1986**, *108*, 1709.
- [24] J. M. Harrowfield, M. I. Ogden, W. R. Richmond, B. W. Skelton, A. H. White, *J. Chem. Soc. Perkin Trans. 2* **1993**, 2183.
- [25] R. Ungaro, A. Pochini, G. D. Andreotti, P. Domiano, *J. Chem. Soc. Perkin Trans. 2* **1985**, 197.
- [26] R. Ungaro, A. Pochini, G. D. Andreotti, V. Sangermano, *J. Chem. Soc. Perkin Trans. 2* **1984**, 1979.
- [27] W. Xu, R. J. Puddephatt, L. Manojlovicmuir, K. W. Muir, C. S. Frampton, *J. Incl. Phenom. Molec. Recogn.* **1994**, *19*, 277.
- [28] E. B. Brouwer, G. D. Enright, K. A. Udachin, S. Lang, K. J. Ooms, P. A. Halchuk, J. A. Ripmeester, *Chem. Commun.* **2003**, 1416.
- [29] J. L. Atwood, L. J. Barbour, P. K. Thallapally, T. B. Wirsig, *Chem. Commun.* **2005**, 51.
- [30] J. L. Atwood, L. J. Barbour, A. Jerga, *Angew. Chem. Int. Edit.* **2004**, *43*, 2948.
- [31] J. D. Vanloon, W. Verboom, D. N. Reinhoudt, *Org. Prep. Proced. Int.* **1992**, *24*, 437.
- [32] Z. Asfari, V. Bohmer, J. Harrowfield, J. Vicens, *Calixarenes 2001*, Kluwer Academic Publishers, Dordrecht, **2001**.
- [33] E. B. Brouwer, K. A. Udachin, G. D. Enright, C. I. Ratcliffe, J. A. Ripmeester, *Chem. Commun.* **2000**, 1905.

- [34] E. B. Brouwer, G. D. Enright, C. I. Ratcliffe, J. A. Ripmeester, *Supramol. Chem.* **1996**, *7*, 79.
- [35] K. A. Udachin, G. D. Enright, C. I. Ratcliffe, J. A. Ripmeester, *ChemPhysChem* **2003**, *4*, 1059.
- [36] G. D. Enright, K. A. Udachin, J. A. Ripmeester, *Chem. Commun.* **2004**, 1360.
- [37] A. Robertson, S. Shinkai, *Coord. Chem. Rev.* **2000**, *205*, 157.
- [38] R. J. Hooley, J. Rebek, *J. Am. Chem. Soc.* **2005**, *127*, 11904.
- [39] B. W. Purse, A. Gissot, J. Rebek, *J. Am. Chem. Soc.* **2005**, *127*, 11222.
- [40] X. C. Xu, C. S. Song, J. M. Andresen, B. G. Miller, A. W. Scaroni, *Micropor. Mesopor. Materials* **2003**, *62*, 29.
- [41] E. B. Brouwer, Ph.D. thesis, Carleton University (Ottawa), **1996**.
- [42] NIAIST, "SDBSWeb", to be found under <http://www.aist.go.jp/RIODB/SDBS/>. **2005**.
- [43] E. B. Brouwer, J. A. Ripmeester, G. D. Enright, *J. Incl. Phenom. Molec. Recogn.* **1996**, *24*, 1.
- [44] K. Araki, K. Iwamoto, S. Shinkai, T. Matsuda, *Bull. Chem. Soc. Japan* **1990**, *63*, 3480.
- [45] S. Shinkai, K. Araki, P. D. J. Grootenhuys, D. N. Reinhoudt, *J. Chem. Soc. Perkin Trans. 2* **1991**, 1883.
- [46] F. F. Nachtigall, M. Lazzarotto, F. Nome, *J. Braz. Chem. Soc.* **2002**, *13*, 295.
- [47] J. M. Harrowfield, W. R. Richmond, A. N. Sobolev, A. H. White, *J. Chem. Soc. Perkin Trans. 2* **1994**, 5.
- [48] C. D. Gutsche, L. J. Bauer, *J. Am. Chem. Soc.* **1985**, *107*, 6063.
- [49] C. D. Gutsche, M. Iqbal, I. Alam, *J. Am. Chem. Soc.* **1987**, *109*, 4314.
- [50] A. F. D. de Namor, R. M. Cleverley, M. L. Zapata-Ormachea, *Chem. Rev.* **1998**, *98*, 2495.
- [51] I. D. Cunningham, M. Woolfall, *J. Org. Chem.* **2005**, *70*, 9248.
- [52] G. D. Andreotti, F. Ugozzoli, Y. Nakamoto, S. I. Ishida, *J. Incl. Phenom. Molec. Recogn.* **1991**, *10*, 241.
- [53] M. Czugler, S. Tisza, G. Speier, *J. Incl. Phenom. Molec. Recogn.* **1991**, *11*, 323.
- [54] C. Bavoux, M. Perrin, *J. Incl. Phenom. Molec. Recogn.* **1993**, *14*, 247.
- [55] K. A. Udachin, G. D. Enright, P. O. Brown, J. A. Ripmeester, *Chem. Commun.* **2002**, 2162.
- [56] J. L. Atwood, L. J. Barbour, A. Jerga, *Chem. Commun.* **2002**, 2952.
- [57] J. L. Atwood, L. J. Barbour, G. O. Lloyd, P. K. Thallapally, *Chem. Commun.* **2004**, 922.
- [58] S. H. Lin, C. T. Shyu, *Environ. Technol.* **2000**, *21*, 1245.
- [59] D. W. Bailey, P. H. M. Feron, *Oil Gas Sci. Technol.* **2005**, *60*, 461.
- [60] O. Erga, O. Juliussen, H. Lidal, *Energy Conv. Manag.* **1995**, *36*, 387.
- [61] E. B. Rinker, S. S. Ashour, O. C. Sandall, *Ind. Eng. Chem. Res.* **1996**, *35*, 1107.
- [62] P. M. M. Blauwhoff, G. F. Versteeg, W. P. M. Van Swaaij, *Chem. Eng. Sci.* **1984**, *39*, 207.
- [63] E. F. Da Silva, H. F. Svendsen, *Ind. Eng. Chem. Res.* **2004**, *43*, 3413.
- [64] M. Caplow, *J. Am. Chem. Soc.* **1968**, *90*, 6795.

- [65] P. V. Danckwerts, *Chem. Eng. Sci.* **1979**, *34*, 443.
- [66] M. B. Jensen, *Acta Chem. Scand.* **1957**, *11*, 499.
- [67] D. B. Dell'Amico, F. Calderazzo, L. Labella, F. Marchetti, G. Pampaloni, *Chem. Rev.* **2003**, *103*, 3857.
- [68] J. A. Ripmeester, C. I. Ratcliffe, in *Inclusion Compounds, Vol. 5* (Eds.: J. L. Atwood, J. E. D. Davies, D. D. MacNicol), Oxford University Press, Oxford, **1991**, pp. 37.
- [69] H. Lee, J. W. Lee, D. Y. Kim, J. Park, Y. T. Seo, H. Zeng, I. L. Moudrakovski, C. I. Ratcliffe, J. A. Ripmeester, *Nature* **2005**, *434*, 743.
- [70] I. L. Moudrakovski, J. A. Ripmeester, Unpublished Results, **2006**.
- [71] Y. D. Chen, J. A. Ritter, R. T. Yang, *Chem. Eng. Sci.* **1990**, *45*, 2877.
- [72] N. Hiyoshi, K. Yogo, T. Yashima, *Chem. Lett.* **2004**, *33*, 510.
- [73] H. Y. Huang, R. T. Yang, D. Chinn, C. L. Munson, *Ind. Eng. Chem. Res.* **2003**, *42*, 2427.
- [74] O. Leal, C. Bolivar, C. Ovalles, J. J. Garcia, Y. Espidel, *Inorg. Chim. Acta* **1995**, *240*, 183.
- [75] R. V. Siriwardane, M. S. Shen, E. P. Fisher, J. A. Poston, *Energy & Fuels* **2001**, *15*, 279.
- [76] X. C. Xu, C. S. Song, J. M. Andresen, B. G. Miller, A. W. Scaroni, *Energy & Fuels* **2002**, *16*, 1463.
- [77] J.-Y. Park, S. J. Yoon, H. Lee, *Environ. Sci. Technol.* **2003**, *37*, 1670.
- [78] T. Suda, T. Iwaki, T. Mimura, *Chem. Lett.* **1996**, *9*, 777.
- [79] J. P. Jakobsen, J. Krane, H. F. Svendsen, *Ind. Eng. Chem. Res.* **2005**, *44*, 9894.

Chapter IV: The role of secondary interactions in guiding structural motifs of alkylamine clathrates of 4-*t*-butylcalix[4]arene[†]

1. Abstract.....	125
2. Introduction.....	125
3. Experimental Section.....	128
4. Results and Discussion.....	133
Water in <i>n</i> -butylamine 4tBC4A Clathrates.....	133
Enclathration of Zn <i>n</i> -butylamine Coordination Compounds by 4tBC4A.....	136
Flexible Coordination in Ag alkylamine 4tBC4A Clathrates.....	140
Formation of Ag Nanoclusters by Amine Desorption of 4tBC4A Clathrates.....	150
Ethylene Adsorption by 4tBC4A Supported Ag Nanoclusters.....	159
5. Conclusions.....	163
6. References.....	165

1. Abstract

The addition of water or transition metal centres results in an additional degree of complexity in the structural motifs of the alkylamine clathrates formed by 4-*t*-butylcalix[4]arene (4tBC4A). Water allows for further expansion of the hydrogen bonding network observed in the pure clathrates, such that the same essential 3 guest : 1 host structural motif is observed. In the case of transition metal complexes, supramolecular stabilization of the complex competes with the previously examined hydrogen bonding and van der Waals interactions in guiding the structural, such that the inclusion motif is dependent on the coordinative flexibility of the metal centre.

2. Introduction

Competition between intermolecular interactions in the solid state is the cornerstone upon which crystal engineering is built. Such a design philosophy is

[†] Portions of this chapter have been previously published: P. O. Brown, K. A. Udachin, G. D. Enright, J. A. Ripmeester, *Chem. Commun.* **2005**, 4402.

frequently cited as an extrapolation of the molecular recognition concept originally proposed by Fischer to describe the binding of a substrate by an enzyme,^[1, 2] However, while natural systems make use of a complex combination of hydrogen bonding, coordinate bonds, and a variety of weaker interactions, such complexity makes rational design of crystalline materials very challenging. This has given rise to the concept of supramolecular synthons, molecules with well defined geometries capable of strong directional interactions.^[3]

For example, the self-assembly of metal-organic frameworks based on tectons to produce reticular (net-like) structures depends on the formation of strong coordinate bonds between well defined metal clusters and rigid organic ligands.^[4, 5] Such an approach is frequently seen in the chemistry of resorcinarenes. Studies have demonstrated how interactions with pyridyl-type ligands have served to extend the cavity of resorcinarenes,^[6-10] and interactions with metal centres have been used to direct formation of capsules.^[11, 12] However, while such frameworks are structurally well defined, the near total dominance of a single intermolecular interaction in defining their structure results in a lack of post-synthetic flexibility.

Such flexible frameworks are of considerable interest due to their inherent versatility, as well as the potential for *in situ* modification leading to smart materials which exhibit structural traits dependent on the nature of a given guest.^[13, 14] By supplementing one type of strong interaction, such as metal coordination, with other competing interactions, new structural motifs become accessible. In addition to resorcinarenes, calixarenes derived from base-catalyzed syntheses^[15-17] have proven to be

excellent ionophores, capable of binding metal cations through mixed coordination to various oxygen containing moieties,^[18-27] amino groups,^[28] and other traditional donor atoms,^[29-36] as well as cation- π interactions.^[37-45] However, the combination of conformational freezing arising from the covalent modification of the calixarene to add the coordinating moieties and the prevalence of cation- π based coordination schemes in many such structures limits their role in producing extended frameworks.

By introducing ligands that are not tied to the calixarene, the potential exists for producing supramolecular systems with novel coordination geometries that would not otherwise be accessible due to the additional stabilization provided by other weak interactions. This has been shown to be the case in the formation of complex coordination polymers dependent on hydrogen bonding,^[46-50] or stabilization of otherwise weak coordinate interactions through secondary coordination.^[51-53] Having demonstrated the diversity of structural motifs beyond the 1 guest :1 host and 1 guest :2 host clathrates^[15-17, 54-57] arising from inclusion of aliphatic amines in 4-*tert*-butylcalix[4]arene (4tBC4A), such a system is ideally suited for further investigations into how intermolecular forces can be used to tune the behaviour of supramolecular materials. The studies of aminocalixarenes by Gutsche *et al.*^[28] make it clear that the amine groups should be quite accessible for coordination chemistry.

This chapter therefore focuses on the introduction of other non-covalent bonding intermediaries, such as water or metal centres, and the impact such modifications have on the structural motif. While water serves to gently expand the hydrogen bonding scheme observed for *n*-butylamine, coordination to silver and zinc induces somewhat more

dramatic structural shifts. Further studies of other alkylamine Ag^+ complexes enclathrated by 4tBC4A suggest that these structural shifts are reflective of the coordinative flexibility of the metal centre allowing for the hydrogen bonding and van der Waals interactions to actually direct the geometry of the complex.

Finally, the potential of this approach for generating functional materials is briefly explored. The Ag^+ *n*-butylamine system is shown to undergo redox chemistry that visually bears some similarities to that observed for Ag zeolites, yielding metallic silver nanoclusters. The resulting metallic Ag 4tBC4A compound is demonstrated to readily adsorb ethylene, suggesting that amine stabilization of metals in 4tBC4A is a potential route to isolating supported metal centres.

3. Experimental Section

General Note: Unless otherwise indicated, chemicals were obtained from EMD Chemicals and Sigma-Aldrich, and were used without further purification.

Synthesis of $3(n\text{-butylamine}) \cdot 2(\text{H}_2\text{O}) \cdot (4\text{-}t\text{-butylcalix[4]arene})$ clathrate 1 (KU79):

Crystals of the clathrate were produced using a methodology similar to that used to obtain the pure alkylamine clathrates of 4tBC4A. 0.695 g (1.07×10^{-3} mol) of 4tBC4A was placed in a vial along with 4.0 mL of *n*-butylamine and 2.0 mL of water. The resulting mixture was heated to approximately 70°C, and stirred for approximately 15 minutes to dissolve all of the 4tBC4A. The vials were then loosely capped and set aside to allow excess solvent to evaporate off. After a few days, blocklike crystals were observed to have formed.

Synthesis of $2(\text{Zn}^{2+}) \cdot 7(n\text{-butylamine}) \cdot (\text{H}_2\text{O}) \cdot 2(\text{Cl}^-) \cdot (4\text{-}t\text{-butylcalix[4]arene})^-$

clathrate **2** (KU82): 0.729 g (1.13×10^{-3} mol) of 4tBC4A was placed in a vial, and dissolved in a solution of 3.0 mL *n*-butylamine and 1.0 mL H₂O. 0.460 g (3.38×10^{-3} mol) of ZnCl₂ was then added, and the mixture stirred gently at room temperature until all solid had dissolved. The solution was then set aside and excess solvent allowed to evaporate off. After approximately one week, clear blocklike crystals had formed.

Synthesis of $[\text{Ag}(n\text{-butylamine})_3]^+ \cdot 1(n\text{-butylamine}) \cdot (4\text{-}t\text{-butylcalix[4]arene})^-$ clathrate **3** (POB109), $[\text{Ag}^+(\text{propylamine})_3]^+ \cdot (4\text{-}t\text{-butylcalix[4]arene})^-$ clathrate **4** (POB65) and $[\text{Ag}^+(\text{amylamine})_2]^+ \cdot 1(\text{amylamine}) \cdot (4\text{-}t\text{-butylcalix[4]arene})^-$ clathrate **5** (POB88):

Crystals of all Ag coordination compounds were prepared in a similar fashion. In a typical synthesis, 0.524 g (3.08×10^{-3} mol) of AgNO₃ was placed in a vial along with 6.0 mL of *n*-butylamine, and gently stirred at room temperature until all of the metal salt had dissolved. 1.002 g (1.55×10^{-3} mol) of 4tBC4A was then added to the solution, and again the solution was gently stirred until dissolution was complete. The vial was then covered with aluminium foil to prevent photoreduction of the silver, and placed aside to allow excess amine to evaporate off. After one week, block-like crystals were observed to have formed.

Single Crystal X-ray Diffraction data are summarized in Table 1. For clathrates **2** and **3**, the hydrogen atoms on the disordered groups were placed in calculated positions and refined as riding atoms, with all other hydrogen atoms found from the difference map and refined independently. For all other clathrates, hydrogen atoms on fully ordered

heteroatoms were found from the difference map and refined independently, with all other hydrogen atoms placed in calculated positions and refined as riding atoms.

Thermogravimetric analysis was carried out following the procedure detailed in Chapter III on pages 72-73. Thermal desorption studies of clathrate **3** (giving rise to 1 host: 1 guest clathrate **6** and the metal loaded β *apo* form of 4tBC4A) were carried following the procedure detailed in Chapter III on page 73. Samples were heated for 30-45 minutes at each temperature, and then allowed to cool to room temperature.

The ethylene adsorption isotherm was determined using the apparatus and methodology detailed in Chapter III on pages 73-74. In a typical experiment, 0.5675 g (7.499×10^{-4} mol) of the metal loaded β *apo* form of 4tBC4A (derived from clathrate **3**) was used. Ethylene was received from Matheson Tri-Gas, and pressures were allowed to equilibrate for 18-24 hours. The experimental isotherm was fit to a Langmuir adsorption isotherm using the non-linear curve fitting routines of OriginLabs Origin 7.0.

Powder X-ray Diffraction data for clathrates **3** and **6** were collected on the Scintag X-2 Advanced diffractometer. Data for the metal loaded β *apo* form of 4tBC4A were collected at 288 K on the Rigaku Geigerflex vertical goniometer diffractometer. For the purposes of crystallite size determination by the Scherrer equation,^[58] the silver 111 peak observed in each case was fit using the Pearson VII model to determine FWHM and peak position. The peak profiles from standard patterns of Si were used to account for instrumental broadening.

¹³C CP/MAS spectra for clathrates **3**, the metal loaded β *apo* form of 4tBC4A, and the 0.78 ethylene loaded metal loaded β *apo* form of 4tBC4A were collected using

the Bruker AMX-300 spectrometer. ^{13}C CP/MAS Solid State NMR spectra for

clathrate 6 were collected using the Tecmag Apollo 200 spectrometer.

Table 1a Single Crystal X-ray data for Clathrates 1-3.

Identification code	Clathrate 1 (KU79)	Clathrate 2 (KU82)	Clathrate 3 (POB109)
Empirical formula	$\text{C}_{56}\text{H}_{93}\text{N}_3\text{O}_6$	$\text{C}_{36}\text{H}_{66.11}\text{C}_{11.16}\text{N}_{3.50}\text{O}_{2.50}\text{Zn}$	$\text{C}_{60}\text{H}_{99.21}\text{AgN}_4\text{O}_4$
Formula weight	904.33	694.53	1048.52
Temperature	173(2) K	173(2) K	125(2) K
Wavelength	0.71070 Å	0.71070 Å	0.71070 Å
Crystal system	Monoclinic	Triclinic	Orthorhombic
Space group	$P2_1/c$	$P-1$	$P2_12_12_1$
Unit cell dimensions	$a = 12.900(1)$ Å $b = 22.2170(17)$ Å $c = 19.4755(15)$ Å $\alpha = 90^\circ$ $\beta = 94.224(2)^\circ$ $\gamma = 90^\circ$	$a = 12.5854(15)$ Å $b = 16.2134(19)$ Å $c = 20.695(2)$ Å $\alpha = 77.408(2)^\circ$ $\beta = 86.846(2)^\circ$ $\gamma = 79.320(2)^\circ$	$a = 12.5555(18)$ Å $b = 17.054(2)$ Å $c = 27.854(4)$ Å $\alpha = 90^\circ$ $\beta = 90^\circ$ $\gamma = 90^\circ$
Volume	$5566.5(7)$ Å ³	$4049.5(8)$ Å ³	$5964.2(15)$ Å ³
Z	4	4	4
ρ_{calc}	1.079 Mg/ m ³	1.139 Mg/ m ³	1.169 Mg/ m ³
Abs. coefficient	0.712 mm^{-1}	0.716 mm^{-1}	0.384 mm^{-1}
F(000)	1992	1505	2268
Crystal size	$0.3 \times 0.3 \times 0.2 \text{ mm}^3$	$0.4 \times 0.3 \times 0.2 \text{ mm}^3$	$0.32 \times 0.24 \times 0.24 \text{ mm}^3$
θ Range	1.58 to 28.76°	1.47 to 28.78°	1.40 to 29.60°
Index ranges	$-17 \leq h \leq 17$ $-30 \leq k \leq 30$ $-26 \leq l \leq 26$	$-16 \leq h \leq 17$ $-21 \leq k \leq 21$ $-27 \leq l \leq 27$	$-17 \leq h \leq 17$ $-23 \leq k \leq 23$ $-38 \leq l \leq 38$
Reflections collected	65010	48385	73978
Ind. reflections	14320	20806	16633
Completeness to $\theta = \text{max}$	[R(int) = 0.0602] 98.8 %	[R(int) = 0.0611] 98.8 %	[R(int) = 0.0466] 99.1 %
Absorption correction	Multi-Scan	Multi-Scan	Multi-Scan
Refinement method	Full-matrix least-squares on F^2	Full-matrix least-squares on F^2	Full-matrix least-squares on F^2
Data / restraints / parameters	14320 / 179 / 803	20806 / 82 / 996	16633 / 114 / 707
Goodness-of-fit on F^2	0.869	1.023	1.032
Final R indices [I > 2 σ (I)]	R1 = 0.0594 wR2 = 0.1462	R1 = 0.0736 wR2 = 0.2077	R1 = 0.0546 wR2 = 0.1331
R indices (all data)	R1 = 0.1352 wR2 = 0.1829	R1 = 0.1257 wR2 = 0.2491	R1 = 0.0830 wR2 = 0.1540
Largest diff. peak and hole ($\text{e.}\text{\AA}^{-3}$)	0.320 and -0.390	3.452 and -0.733	0.948 and -1.886

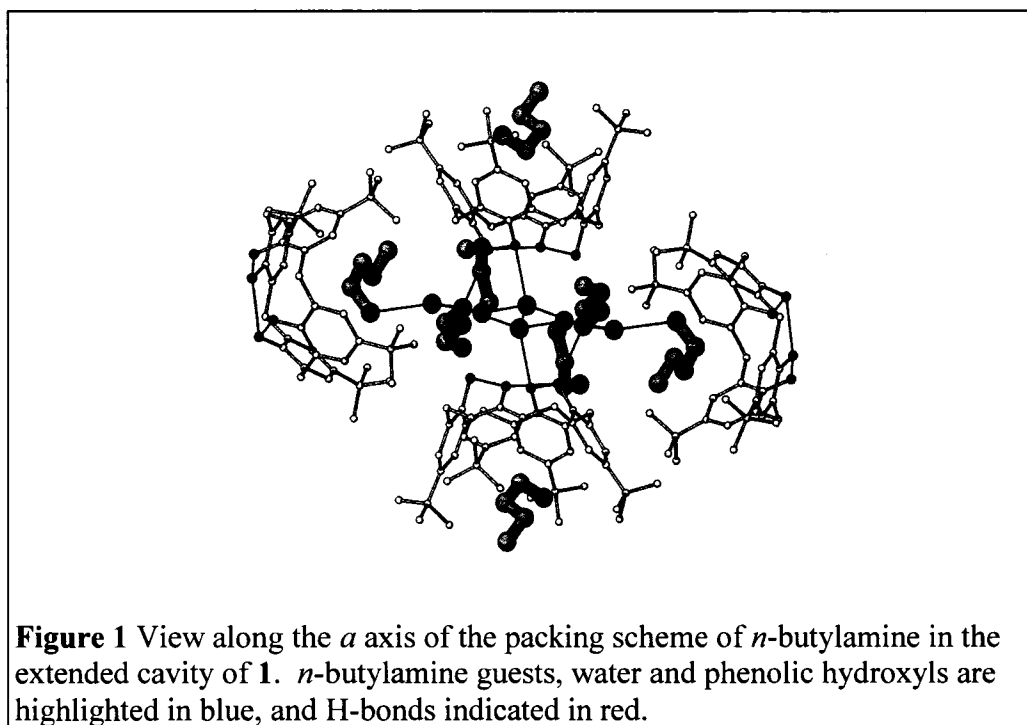
Table 1b Single Crystal X-ray data for Clathrates 4-5.

Identification code	Clathrate 4 (POB65)	Clathrate 5 (POB88)
Empirical formula	C ₅₃ H ₈₂ AgN ₃ O ₄	C ₅₉ H ₉₄ AgN ₃ O ₄
Formula weight	933.09	1017.24
Temperature	173(2) K	125(2) K
Wavelength	0.71073 Å	0.71073 Å
Crystal system	Monoclinic	Monoclinic
Space group	<i>P</i> 2 ₁ / <i>c</i>	<i>P</i> 2 ₁ / <i>c</i>
Unit cell dimensions	<i>a</i> = 13.6184(9) Å <i>b</i> = 21.4481(13) Å <i>c</i> = 18.4954(11) Å α = 90° β = 111.409 (1)° γ = 90°.	<i>a</i> = 13.0509(6) Å <i>b</i> = 21.325 (1) Å <i>c</i> = 19.9729(9) Å α = 90° β = 92.134 (1)° γ = 90°
Volume	5029.5(5) Å ³	5554.8(4) Å ³
Z	4	4
ρ_{calc}	1.232 Mg/ m ³	1.216 Mg/ m ³
Abs. coefficient	0.446 mm ⁻¹	0.409 mm ⁻¹
F(000)	2000	2192
Crystal size	0.32 x 0.16 x 0.16 mm ³	0.48 x 0.48 x 0.48 mm ³
θ Range	1.52 to 29.61°	1.40 to 29.61°
Index ranges	-18 ≤ <i>h</i> ≤ 18 -29 ≤ <i>k</i> ≤ 29 -25 ≤ <i>l</i> ≤ 25	-17 ≤ <i>h</i> ≤ 18 -29 ≤ <i>k</i> ≤ 29 -27 ≤ <i>l</i> ≤ 27
Reflections collected	62753	68271
Ind. reflections	14097 [R(int) = 0.0749]	15421 [R(int) = 0.0309]
Completeness to θ = max	99.6 %	98.6 %
Absorption correction	Multi-Scan	Multi-Scan
Refinement method	Full-matrix least-squares on F ²	Full-matrix least-squares on F ²
Data / restraints / parameters	14097 / 0 / 746	15421 / 24 / 885
Goodness-of-fit on F ²	0.998	0.997
Final R indices [I > 2 σ (I)]	R1 = 0.0505 wR2 = 0.1225	R1 = 0.0323 wR2 = 0.0839
R indices (all data)	R1 = 0.0822 wR2 = 0.1410	R1 = 0.0451 wR2 = 0.0921
Largest diff. peak and hole (e.Å ⁻³)	1.174 and -0.509	0.711 and -0.524

4. Results and Discussion

Water in *n*-butylamine 4tBC4A Clathrates

Recrystallization of 4tBC4A from an aqueous solution of *n*-butylamine by slow evaporation yields crystals of an inclusion compound (clathrate **1**) with a stoichiometric ratio of *n*-butylamine:4tBC4A:water is 3:1:2. As can be seen from Figure 1, the 3:1 amine-calixarene packing motif previously observed for small alkylamines (see Chapter III) [59, 60] is largely preserved in the structure of clathrate **1**. However, the hydrogen bonded clusters are now centred on molecules of included water, giving rise to an extended hydrogen bonding network that leads to subtle shifts in the conformation and ordering of the *n*-butylamine molecules.



As seen in our previous study, one of the three crystallographically independent *n*-butylamine molecules is included within the 4tBC4A's bowl-shaped cavity (*endo*), while two are situated outside the cavity (*exo*). The disordered *exo* amines show

increased electron density surrounding them, which, in conjunction with a single elongated O...O distance in the 4tBC4A molecule (2.92 Å), indirectly indicate proton transfer from the 4tBC4A to the amine, resulting in an anionic 4tBC4A balanced by a cationic amine.

In this case, the terminal carbon of the aliphatic tail of the *endo* amine is directed outwards with the 2' carbon adjacent to the amino group most deeply inserted, such that the terminal methyl carbon now points outward into the rest of the amine cluster (see Figure 1). This partial *cis* conformer is disordered over two positions with a 0.50:0.50 occupancy ratio. Given the 0.63:0.32 disorder observed for the *endo* amine in the pure *n*-butylamine:4tBC4A clathrate, such disordering is again likely the result of the non-directional stabilization offered by the 4tBC4A giving rise to a number of energetically equivalent positions in the calixarene cavity, two of which are favoured due to the hydrogen bonding to the the *exo* components of the structure. In this case, though, the presence of water leads to shifts in the hydrogen bonding moieties, such that an alternate conformation and inclusion is favoured for the *endo* amine. However, as this results in the aliphatic tail of the amine sticking out of the calixarene cavity, this also gives rise to more significant disordering of the *t*-butyl groups, such two groups exhibit the typical 0.50:0.50 disorder, and a third exhibits a broad spectrum of positions (0.37:0.18:0.19:0.26 distribution).

With this conformation, the *endo n*-butylamine is hindered from hydrogen bonding directly to the *exo* amines. Instead, a water molecule forms a hydrogen-bonded bridge (N...O distances of 2.72, 2.73, 3.15 Å) between the *endo n*-butylamine and each of

the two independent *exo n*-butylamine molecules. The water molecule and the two *exo n*-butylamine molecules also form hydrogen bonds with hydroxyl groups of two adjacent 4tBC4A molecules. Additional water molecules form H-bonded bridges cross-linking the *exo n*-butylamine molecules of adjacent asymmetric units.

In order to accommodate this packing scheme, one of the *exo* amines, like the *endo* amine, adopts a partial *cis* conformation, while the second is observed to be all *trans*. The partial *cis* amine is disordered over two positions (0.50:0.50), once again showing similar behaviour to the related pure amine clathrate. The all *trans* amine, however, is fully ordered. Given that it is the sole amine in the structure to hydrogen bond directly to the calixarene framework, this interaction stabilizes the amine to an extent where this particular position is energetically favourable, and since the calixarene exhibits no significant disorder, no corresponding disorder in the amine is expected.

The result is a large H-bonded cluster consisting of six *n*-butylamine and four water molecules all situated within a large cavity bounded by four 4tBC4A molecules. Despite disrupting the clusters and forcing them apart, the overall structural shift is minor. As seen from Table 2, the chief difference is a modest increase in the unit cell volume arising from expansion along the *b* axis and an increase in the β angle. This suggests that the altered conformation of the *endo n*-butylamine is a result of the inclusion of water, whereby the favoured 3 guest : 1 host structural motif that accommodates the two-fold symmetry of the capped motif is preserved. This is further supported by the hydrogen bond distances between the amines and the central water

molecule, which are remarkably similar to those observed in the pure amine clathrate.^[59, 60]

Table 2 Comparison of the unit cell parameters of 3*(*n*-butylamine):1*(4tBC4A) clathrate and Clathrate 1.

Compound	3*(<i>n</i> -butylamine):1*(4tBC4A) ^a	Clathrate 1
Space Group	<i>P</i> 2 ₁ / <i>c</i>	<i>P</i> 2 ₁ / <i>c</i>
<i>a</i> / Å	12.9405(1)	12.900(1)
<i>b</i> / Å	20.0923(1)	22.2170(17)
<i>c</i> / Å	20.7519(1)	19.4755(15)
β / °	91.122(1)	94.224(2)
<i>V</i> / Å ³	5394.5(4)	5566.5(7)

^aFrom Udachin *et. al.*^[59]

As such, the introduction of a solvent as hydrogen bonding intermediary is a potential method for expanding the size of the amine cluster. It also serves to force a rearrangement of the *endo* guest, by shifting the hydrogen bonding scheme such that the conformation of the guest adjusts to accommodate this. However, the shift in structure with water is very small, and the synthesis of clathrate itself proved to be highly dependent on the specific synthetic conditions. As such, attempts to produce bulk samples of the compound for further studies were unsuccessful.

Enclathration of Zn *n*-butylamine Coordination Compounds by 4tBC4A

The suggestion of proton transfer in these and previous studies, led us to consider including cationic metal centres into a framework containing anionic 4tBC4A molecules. Secondary coordination, or intermolecular interactions with a portion of the primary coordination sphere of a metal complex, has been investigated in a variety of host-guest systems.^[61] Studies have focused on well-known macrocyclic systems, ranging from crown ethers,^[62-64] to cyclodextrins^[65, 66] and substituted calixarenes.^[30-33, 35, 36, 51, 67-69] Traditionally, such systems involve relatively small complexes, with only a limited

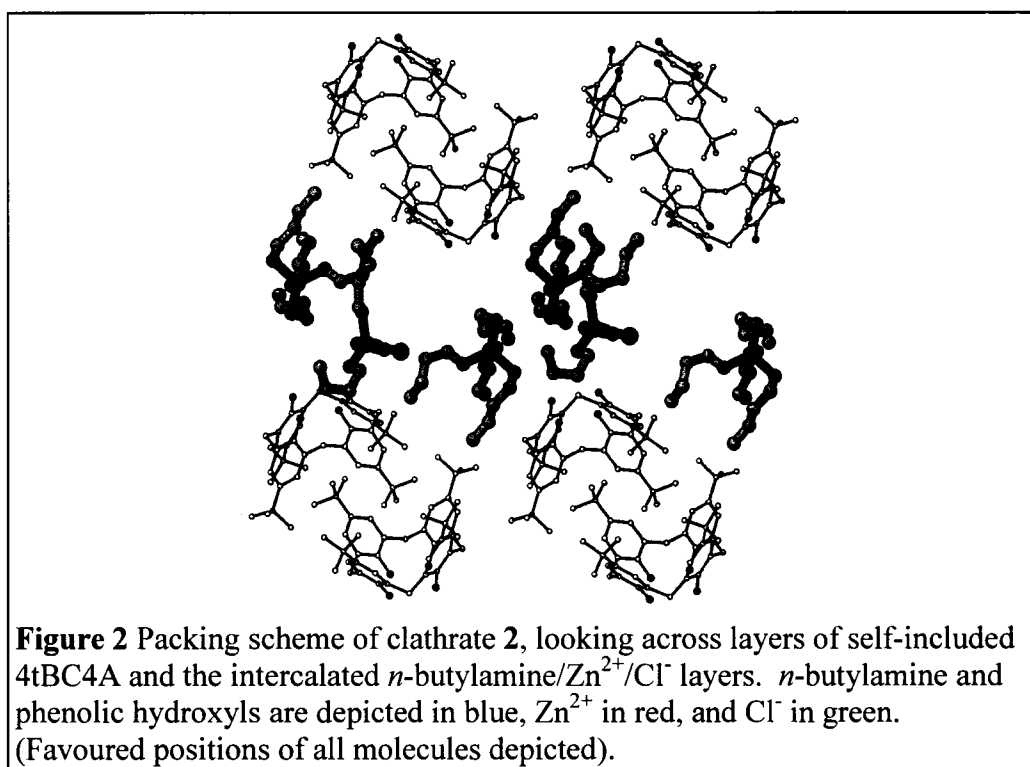
selection of studies examining larger, multifunctional primary and secondary ligands, capable of forming extended structures.^[52, 53, 70]

For the calixarene systems, many of the previously reported systems are discrete receptors, relying upon cation- π interactions or covalently linked ligands. While the lower-rim modified calixarenes typically bind just the metal cation, upper rim modified calixarenes have proven to allow for inclusion of a guest coordinating to the metal centre,^[29-36, 69] taking advantage of the stabilization offered by the calixarene cavity in a fashion not unlike that seen in pure organic inclusions. Clearly, the hydrophobic cavity and phenolic OH groups of 4tBC4A provide ideal sites for secondary coordination, thereby further favouring the introduction of metal centres into a calixarene framework through self-assembly.

Given the confined space of the 4tBC4A clathrates, and the simple nature of the ligands, initial attempts focused on Group 11 and 12 metals in order to restrict the size of the resulting clusters. Clathrate **2** was produced by dissolution of ZnCl_2 in a mixture of *n*-butylamine and water, giving rise to a compound with a stoichiometry of $2(\text{Zn}^{2+}) \cdot 7(n\text{-butylamine}) \cdot (\text{H}_2\text{O}) \cdot 2(\text{Cl}) \cdot (4\text{-}t\text{-butylcalix[4]arene})^-$. The 4tBC4A molecules are arranged in layers of self-included dimers, while two distinct clusters occupy the space between the 4tBC4A layers (see Figure 2).

Each of these clusters contains a tetrahedrally co-ordinated Zn^{2+} centre. One of the clusters consists of a Zn^{2+} centre surrounded by three *n*-butylamine molecules plus a Cl⁻ ion, resulting in an ionic cluster $[\text{Zn}(n\text{-butylamine})_3\text{Cl}]^+$. The second cluster is highly disordered, consisting for the most part (occupancy of 0.68) of Zn^{2+} surrounded by four

n-butylamine molecules, resulting in $[\text{Zn}(\textit{n}\text{-butylamine})_4]^{2+}$, while in the remainder (occupancy of 0.32) one of the *n*-butylamine molecules is replaced by a Cl^- ion weakly interacting with a protonated *n*-butylamine molecule resulting in $[\text{Zn}(\textit{n}\text{-butylamine})_3(\text{Cl}^- \cdot \textit{n}\text{-butylamine}^+)]^{2+}$. In all of the clusters, one *n*-butylamine molecule is observed to have adopted a partial *cis* conformation, presumably to accommodate a more energetically favourable packing scheme. In addition to the two cationic clusters and a deprotonated 4tBC4A molecule, the asymmetric unit contains additional anions, one Cl^- and one hydroxyl, thus attaining charge balance.



These clusters are further stabilized through secondary coordinate interactions with the residual amine and water present, as well as the calixarene framework. The molecules of 4tBC4A form hydrogen bonds directly with two amines from the fully occupied $[\text{Zn}(\textit{n}\text{-butylamine})_3\text{Cl}]^+$ cluster (O...N distances of 2.92 and 2.95 Å), as well as

bonding to the disordered cluster through a molecule of water (O...O distance of 2.80 Å, Water O...N distances of 2.91 and 3.07 Å). In addition, the chloride anions from each cluster also serve as secondary ligands for each adjacent cluster (Cl...N distances of 3.01 and 3.30 Å), forming an infinite chain of Zn^{2+} complexes.

Therefore, the flexibility of using non-covalently bound amines as primary ligands such that the calixarene is a secondary ligand gives rise to much more complicated multidimensional supramolecular frameworks than those observed in the calixarene ionophores previously investigated.^[25, 26, 41-44, 71-75] The inherently limiting cation- π binding mode is ruled out due to the favourability of coordination to the amine, much as coordination to covalently bound ligands appended to the base of the calix^[25, 72-78] are favoured over such interactions. Furthermore, without the ligand being covalently bound to the calixarene, the cluster is organized based on the weak interactions present in the structure, moving beyond the upper rim modified receptors that only peripherally took advantage of inclusion in the cavity.^[29-36] It is therefore structurally significant that while inclusion of *n*-butylamine in 4tBC4A distinctly favours the capped cavity motif that allows for a combination of stabilization by hydrogen bonding and van der Waals interactions, coordination to Zn^{2+} gives rise to complexes that cannot be accommodated in this fashion.^[59]

Instead, a packing scheme similar to the layered motif favoured for aliphatic amines too large to be stabilized by the van der Waals interactions emerges.^[60] Clearly, the geometrical constraints of the coordination compound now dominate the structural motif. Despite the fact that for certain positions of the clusters, only three amines

coordinate to the Zn^{2+} center, the retention of a single chloride as a coordinating ligand results in the coordination compound having a bulky, tetrahedral arrangement. These tetrahedral complexes involving amines alone and amines and chloride are in fact consistent the structures observed for ammine complexes of zinc halides.^[79-83] These complexes, however, are not compatible with the two-fold symmetric capped motif that is observed with the 3 *n*-alkylamine : 1 calixarene systems or the larger clusters formed by small difunctional amines (see Chapter VI).

The ultimate arrangement into layers can therefore be seen as a measure of the dominance of thermodynamic favourability of the coordinate bonds (with bond energies on the order of 50-200 kJ/mol) and hydrogen bonding to various moieties (~20 kJ/mol), as opposed to the non-specific van der Waals forces governing the inclusion of the hydrophobic tail of the amine (<5 kJ/mol).^[84] However, the mixed nature of the inclusion, with the secondary coordinate compound, suggests that even this arrangement is not particularly favourable. Whether this is reflective of the kinetics underlying the formation of the coordination compound given the concentrations of amine used, or of the formation of the inclusion compound is unclear. However, more direct studies of the bulk system are once again precluded due to the difficulties in preparing large quantities of such a solvated system.

Flexible Coordination in Ag alkylamine 4tBC4A Clathrates

The near complete dominance of the coordinate bond in directing the structural motif of clathrate **2** raises the questions as to whether smaller clusters might exhibit behaviour more in line with that seen for the pure amine clathrates. Such compounds

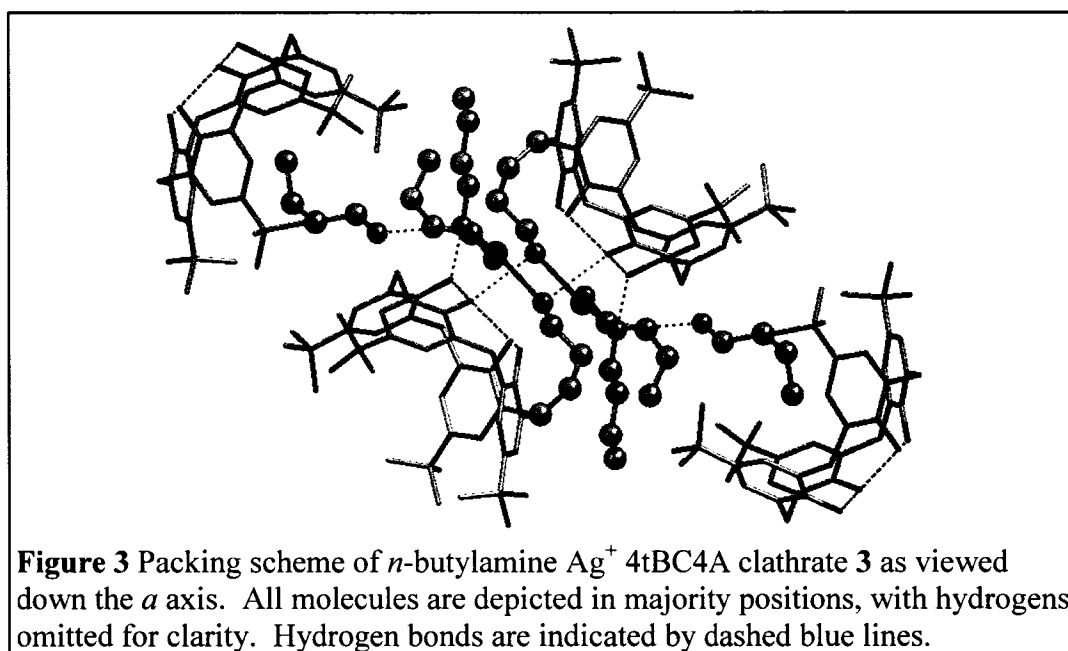
would help to clarify whether it was the coordinative geometry specifically guiding the structural motif towards a layered compound, or if the bulk of the complexes were also playing a role. As well, it was hoped that such compounds would be more tractable to detailed structural studies using techniques other than SCXRD.

Of the group 11 and 12 metals, silver was particularly attractive. Studies of a range of difunctional ligands relying upon nitrogen^[50, 85-88] donors groups established how variation in the coordinating group and the use of non-interacting or minimally interacting counteranions are also useful tools in effectively directing the coordination geometry of the Ag(I) such that infinite multidimensional structures typically involving two, four or six coordinate Ag(I) centres are observed. Shimizu *et al.* have demonstrated how thioether^[89, 90] and sulfonate^[91-93] groups can also be used to produce a broad spectrum of supramolecular coordination compounds. Similarly, Schauer *et al.*^[50] and Puddephatt *et al.*^[46, 94-98] have clearly indicated the potential of Ag(I) as a centre for guiding the formation of coordination polymers with structures mediated by hydrogen bonding. Much of this behaviour is due to the flexible coordination sphere of silver,^[99, 100] which allows for compounds to assume a broad spectrum of geometries, including linear, trigonal and tetrahedral complexes.^[101]

With respect to the calixarenes, much attention has been paid to the binding of silver by various calixarene derivatives. This work was pioneered by Shinkai *et al.*, whose studies of conformationally frozen calixarenes clearly established the importance of the cation- π interaction in binding silver in calixarene-based receptor systems.^[41-43] Since then, various other modifications of the calixarene base have proven to be effective

at binding silver.^[21-23, 40, 72-78, 102] These studies have chiefly focused on the production of discrete, highly discriminatory receptors with highly predictable structures, where the calixarene-cation assemblies are largely discrete. Such structures therefore exhibit none of the extended structure possible in the amine-calixarene frameworks.

Dissolution of AgNO₃ and 4tBC4A in a solution of *n*-butylamine subsequently gave rise to crystals of clathrate **3** (see Figure 3). The stoichiometry of the compound is 4(*n*-butylamine)*1(Ag⁺)*1(4tBC4A)⁻, arising from the formation of an [Ag(*n*-butylamine)₃]⁺ coordination compound and the inclusion of a single uncoordinated molecule of *n*-butylamine. The amines serving as primary ligands are all found *exo* to the calixarene, while the fourth amine is included in the calixarene (*endo*). The silver coordination compound exhibits trigonal planar geometry (Ag...N distances of 2.22, 2.23 and 2.26 Å for majority positions), and is positioned such that it forms an ionic complex with the deprotonated calixarene through the O⁻ formed due to deprotonation (Ag...O distance of 2.83 Å). One of the other calixarene phenolic hydroxyls also serves as a secondary coordinate ligand through a hydrogen bond to two of the coordinating amines (Ag...N distances of 2.90 and 3.13 Å for majority positions). The fourth amine also occupies a position in the secondary coordination sphere of the complex, forming a hydrogen bond with a single adjacent amine in the coordination compound (N...N distance of 3.05 Å for majority positions).

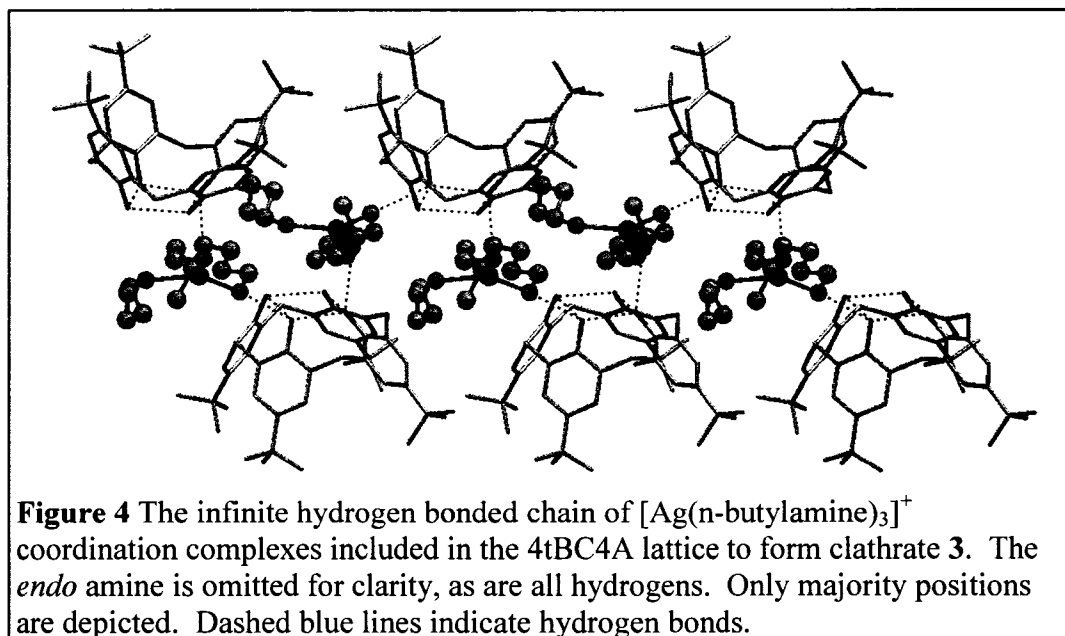


As alluded to above, this structural arrangement gives rise to a considerable degree of disorder in the structure. Only one of the amines coordinated to the silver is fully ordered, assuming an all *trans* conformation (N1A). The remaining two *exo* amines are both disordered over two positions, with one assuming an all *trans* conformation (N1B, 0.74:0.26 distribution) and the second adopting a partial *cis* conformation (N1C, 0.53:0.47 distribution) to accommodate close packing in the structure. The *endo* amine also adopts a partial *cis* conformation such that it is disordered over two positions (N1D, 0.54:0.46 distribution).

The most significant disorder, however, appears to arise out of the ionic interaction with the silver cluster. Two of the phenolic rings of the calixarene exhibit disorder characteristic of the cavity flexing in order to fully accommodate both the *exo* silver cluster and the *endo* amine inclusion. Such a distortion in the cavity of 4tBC4A is reminiscent of the symmetry reduction observed with the inclusion of nitrobenzene,^[56]

but, in this case, the symmetry of the host is already disrupted due to the deprotonation of the calixarene, such that the flexing merely results in increased disorder.

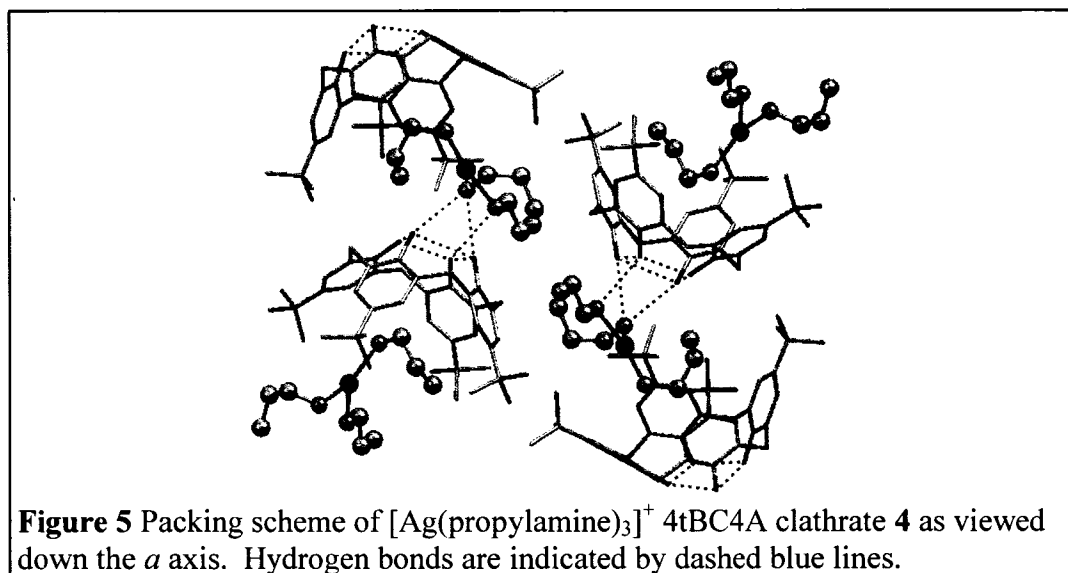
The resulting structural motif is an intriguing hybrid of the capped motif observed for *n*-butylamine and amylamine and the layered motif observed for both hexylamine and clathrate **2**. The *exo* amine silver complex forms distinct layers in the structure, arranged in a plane that forms a 44° angle to the (030) plane (see Figure 4). This causes the adjacent layers of calixarenes forming hydrogen bonds to the *exo* amines to shift by approximately 4.2 Å (the separation between amino groups in N1A and N1B). This induces a similar shift in the capping calixarenes serving as hosts to amine N1D. Thus, coordination, hydrogen bonding and van der Waals interactions all play significant roles in stabilizing portions of the structure to yield a packing arrangement that coincides well with the two fold symmetry of the capped motif.



Previously, trigonal planar coordination schemes with silver have tended to only be observed in coordination polymers based on bulky, rigid tridentate ligands,^[103-109] while structures of amines with simple counteranions tend to consist of ladder like or cubane structures entailing coordination to the counteranion.^[110-112] The motif observed also contrasts with the discrete inclusion complexes of the calixarene ionophores, where primary coordination spheres consisting of complex web-like geometries are observed.^[21-23, 40-43, 76-78, 102] With the Ag^+ complex of clathrate **3** proving to be more compact than the Zn^{2+} complex in clathrate **2**, this strongly implied that the flexible coordination sphere of silver might allow for the geometry of the coordination compound to be partially controlled by the weak forces governing inclusions in the calixarene lattice. Such an arrangement contrasts strikingly with the calixarene ionophores, where covalent attachment of ligands at either the upper or lower rim precludes rearrangements to accommodate improved packing schemes based on weak interactions, again not leading to an extended structure beyond the receptor itself. If the stabilization offered by secondary coordination through a combination of hydrogen bonds and van der Waals interactions is significant, it was suspected that the primary coordination sphere might shift as the bulk of the amine guest increased or decreased in order to allow for inclusion of the amine. In order to test this hypothesis, we also examined the clathrates formed by 4tBC4A with Ag^+ complexes of propylamine and amylamine.

Single crystal X-ray diffraction revealed that crystallization of AgNO_3 and 4tBC4A from propylamine gave rise to a $[\text{Ag}(\text{propylamine})_3]^+ \cdot (4\text{tBC4A})^-$ clathrate **4**. While it was not possible at this time to isolate a pure amine clathrate due to the volatility

of propylamine, coordination to silver gives rise to a complex sufficiently stable for analysis. Much as with the Ag^+ *n*-butylamine clathrate **2**, a trigonal complex is produced ($\text{Ag}\dots\text{N}$ distances 2.22, 2.23 and 2.38 Å), but no additional amine is included (see Figure 5). As a result, one ligand amine is now included within the calixarene (*endo*) and the other two are *exo* amines. The *endo* amine assumes a partial *cis* conformation similar to that observed for clathrate **1**, but the strong interaction to the silver centre appears to fully stabilize the amine in a single position, and no *t*-butyl disorder is observed.



No disorder is observed in the *exo* amines either, which are involved in secondary coordinate interactions with the adjacent calixarene phenolic groups ($\text{N}\dots\text{O}$ distances of 2.97, 2.99, and 3.03 Å). In order to accommodate this, however, the adjacent calixarenes again are forced to shift to adjust for the geometry of the coordination compound. However, unlike clathrate **1**, where the shift was perpendicular to the orientation of the capsule, in this case the calixarenes shift in a direction parallel to the orientation of the capsule, preventing the formation of an infinite hydrogen bonding network to link the

various coordination complexes together. This shift is therefore more akin to a pivot than a true translation.

Therefore, with a smaller guest, the 3 guest : 1 host capped motif is clearly heavily favoured for less bulky complexes. The flexibility of the cluster is sufficiently large to allow for it to be effectively drawn into the favoured lattice of the calixarene, such that the *endo* ligand will assume a distorted conformation to allow for the secondary stabilization due to hydrogen bonding and van der Waals interactions to compensate for additional coordination interactions. Clearly, the coordinative bonding is much weaker in such a system than in clathrate **2**, but it was unclear as to how much distortion such a system would tolerate.

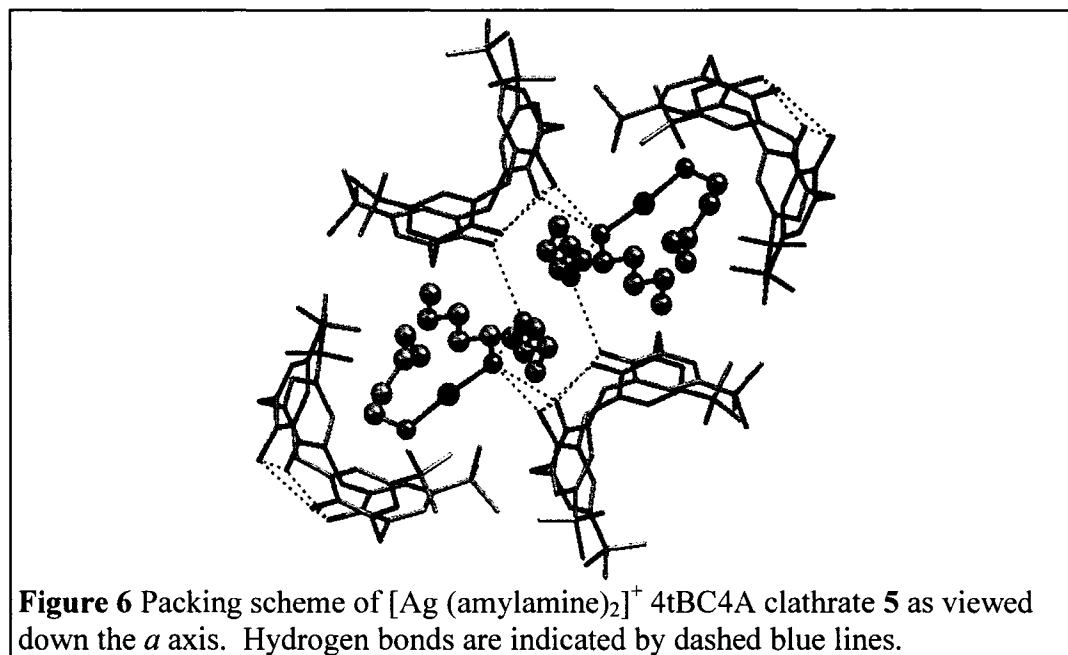
Single crystal X-ray diffraction revealed that crystallization of AgNO₃ and 4tBC4A from amylamine gave rise to a [Ag(amylamine)₂]⁺*1(amylamine)*(4tBC4A)⁻ clathrate (clathrate **5**). The two coordinate silver complex is linear in nature (Ag...N distances of 2.12 and 2.14 Å), but the amine ligands exhibit an intriguing arrangement prompted by the needs to satisfy the symmetry of the overall structure (see Figure 6). Again, one ligand is an *endo* amine with the 1' carbon most deeply included, resulting in a conformation analogous to that observed for clathrate **1**, which again gives rise to a 0.50:0.50 *t*-butyl disorder. The silver therefore serves a similar role in extending the network and tuning the structure at the same time, but in this case, the length of the amine forces a reduction in coordination and a shift in conformation to accommodate the secondary interactions. The second ligand is an *exo* amine in an all *trans* conformation that serves as the basis of a secondary coordination network encompassing the remaining

exo amine and the adjacent calixarenes to stabilize the resulting complex (N...N distance of 2.96 Å, N...O distances of 2.97, 3.02, 3.04 Å).

This lends further support to the hypothesis that hydrogen bonding and Van der Waals interactions generally outweigh stabilization due to coordination, such that the secondary coordination sphere directs the primary sphere. The amine is too bulky now to allow for a trigonal complex to be included, such that an alternative coordination complex is now favoured. Intriguingly, this results in the presence of an uncoordinated *exo* amine serving as a secondary coordinate ligand, an arrangement unique to the amylamine system, with both *n*-butylamine and isoamylamine (see Chapter V) forming structures where the *endo* amine is uncoordinated. This indicates both the importance of van der Waals stabilization of the reduced coordinate complex, as it is great enough for it to be favourable to have the *exo* amine only be stabilized through hydrogen bonds and van der Waals interactions with the other amines.

Given the absence of significant disorder in either clathrates **4** or **5**, one would presume that this particular arrangement gives rise to a selection of interactions which are much more distinct than those governing clathrate **2** or **3**. The energetic compensation from additional coordination of the Ag centre for smaller amines is not as great as that arising from the van der Waals stabilization of the *endo* amine, and the secondary coordinate hydrogen bonding to the calixarene framework. Clearly, the capped motif is a highly favourable energetic compromise, driving the weaker coordinate interactions towards compounds suitable for inclusion in such a structure in order to avoid the layered structure of clathrate **2**. This is consistent with the studies of metalloreceptors based on

upper rim modified calixarenes, where coordination of a final ligand is directed towards the calixarene cavity due to the stabilization offered by such a second sphere interaction.^[29-36]



With the ligands being free, such supramolecular networks could arise from a variety of routes. This is due to the fact that the coordination compounds included are selected for on the basis of their ability to sustain secondary coordinate interactions. Presumably, a dynamic equilibrium of coordination compounds exists in solution, such that the crystallization removing a given complex from solution might serve to drive further formation of the complex according to Le Chatelier's principle. Alternatively, the coordination compound might form after association of the amines with the calixarene. In any case, the nature of such a process cannot be divined from the structural data, which is instead representative of a non-equilibrium process leading to the most readily formed crystalline clathrate.

Formation of Ag Nanoclusters by Amine Desorption of 4tBC4A Clathrates

Recalling the structures of the pure alkylamine clathrates of 4tBC4A, upon heating the structures reverted to simpler pseudopolymorphs reflective of the motifs favoured by 4tBC4A in the absence of hydrogen bonding. Since the metal coordination sphere in the silver amine clathrates is also dependent on these weak interactions, one would expect that similar structural shifts might occur. Thermogravimetric analysis of the *n*-butylamine Ag⁺ clathrate **3** and amylamine Ag⁺ clathrate **4** supports this possibility (reliable data for clathrate **5** was not possible to obtain), with both compounds exhibiting weight loss events corresponding well to the loss of amines in a rational fashion. Each exhibits an initial weight loss event which is quite broad, but ultimately corresponds to the loss of the majority of the amine present, followed by the loss of residual amine (see Table 3). This broadening indicates that much more complex chemistry than previously observed for the pure amine clathrates (see Chapter III) is occurring during desorption, with the increased temperature required to strip away the final amine suggesting that coordination causes the residual amine to be bound more tightly than in the pure amine clathrates. Regardless, the trends observed echo those seen for the pure amine clathrates, with the *n*-butylamine based clathrate **3** forming a 1 host : 1 guest inclusion and the amylamine based clathrate **4** forming a 2 host : 1 guest clathrate after heating.

Given the previous versatility of *n*-butylamine inclusions (see Chapter III), clathrate **3** was therefore selected for further study by solid state NMR and PXRD (see Figures 7 and 8 and Tables 4 and 5). Figure 7a is the ¹³C CP/MAS spectrum for clathrate **3** as synthesized, and exhibits considerable similarities to that of the pure *n*-butylamine

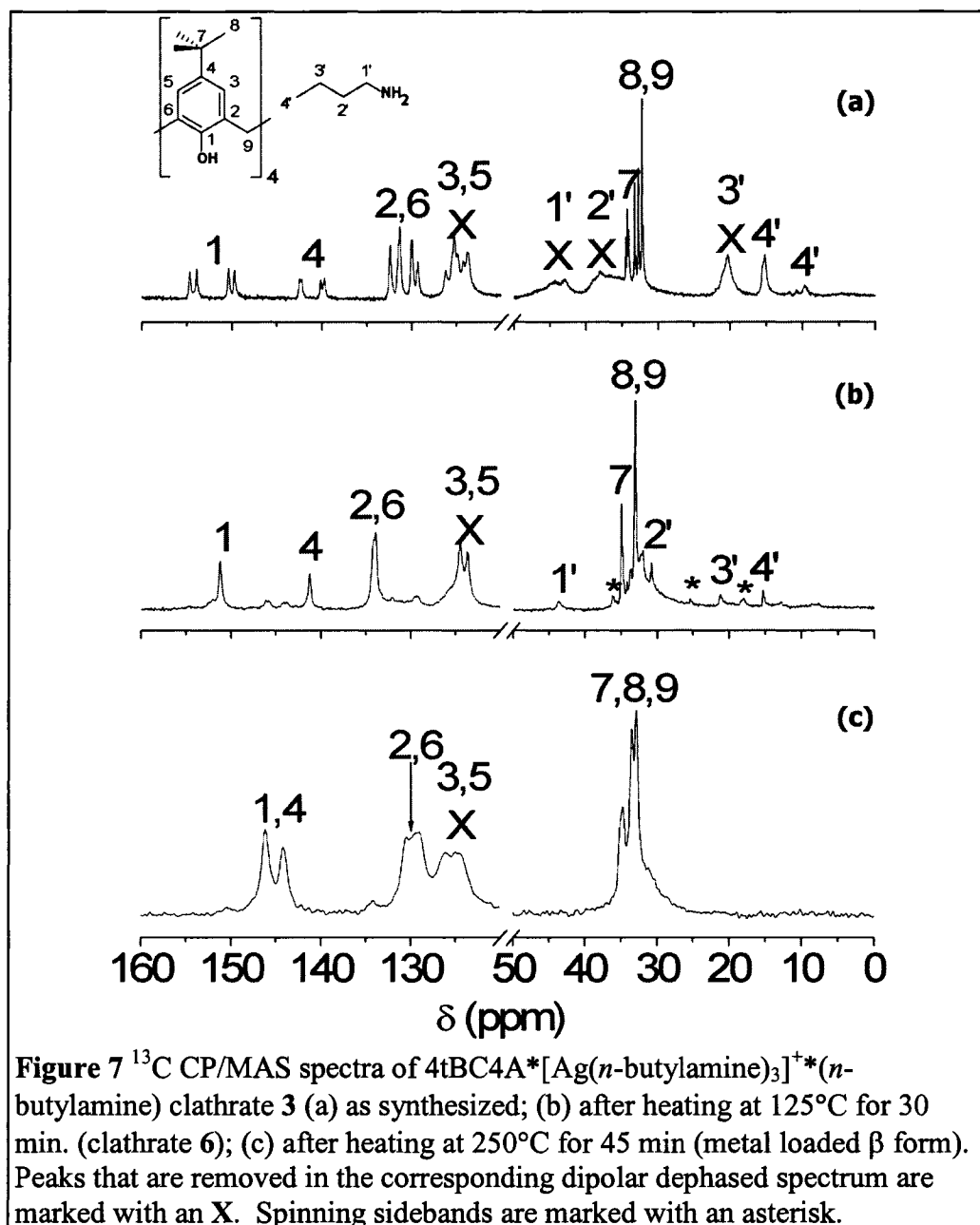
4tBC4A clathrate. As before, the vast majority of the host and guest peaks display crystallographic splitting due to the low symmetry of the crystal structure. While the host resonances in the upfield region from 30 to 35 ppm again are split too extensively to allow for meaningful analysis, the aromatic resonances from 120 to 155 ppm are better resolved and prove to be indicative of several features of the structure.

Table 3 TGA data for Ag⁺ *n*-butylamine and Ag⁺ amylamine clathrates with 4tBC4A.

Clathrate	Temp. (°C) ^[a] (± 0.1)	% Wt. Lost ^[b] (± 0.01)	Mol. Guest Lost ^[c] (± 0.01)	<i>n</i> ^[d] (± 0.01)
Ag ⁺ <i>n</i> -butylamine (3)	73.1-139.4	21.14	3.03	4.02
Ag ⁺ amylamine (4)	218.9-229.7 63.6-150.0	6.88 21.21	0.99 2.48	3.09
	180.5-212.6	5.27	0.61	

^[a]Temperatures are given for the onset and completion of transition. ^[b]Percentage of mass lost by sample. ^[c]Corresponding number of moles of guest lost by host. ^[d]Overall Guest to Host Ratio=(Total % Wt. Lost)/(1-Total % Wt. Lost)*(Mol. Wt. of Host)/(Mol. Wt. of Guest)

The resonances attributed to carbons 1 (155-149 ppm) and 4 (142 ppm-139 ppm), once again clearly exhibit four-fold splitting confirming the presence of a single 4tBC4A molecule in the asymmetric unit of clathrate 3. The range of chemical shifts for these resonances is virtually identical to that observed for the pure *n*-butylamine 4tBC4A clathrate (C1: 154-150 ppm, C4: 143-140 ppm),^[60] but the distribution of the peaks is noticeably different. Instead of the peaks being spaced evenly throughout the chemical shift range, the resonances now form doublets clustered around the extremes of the chemical shift range.



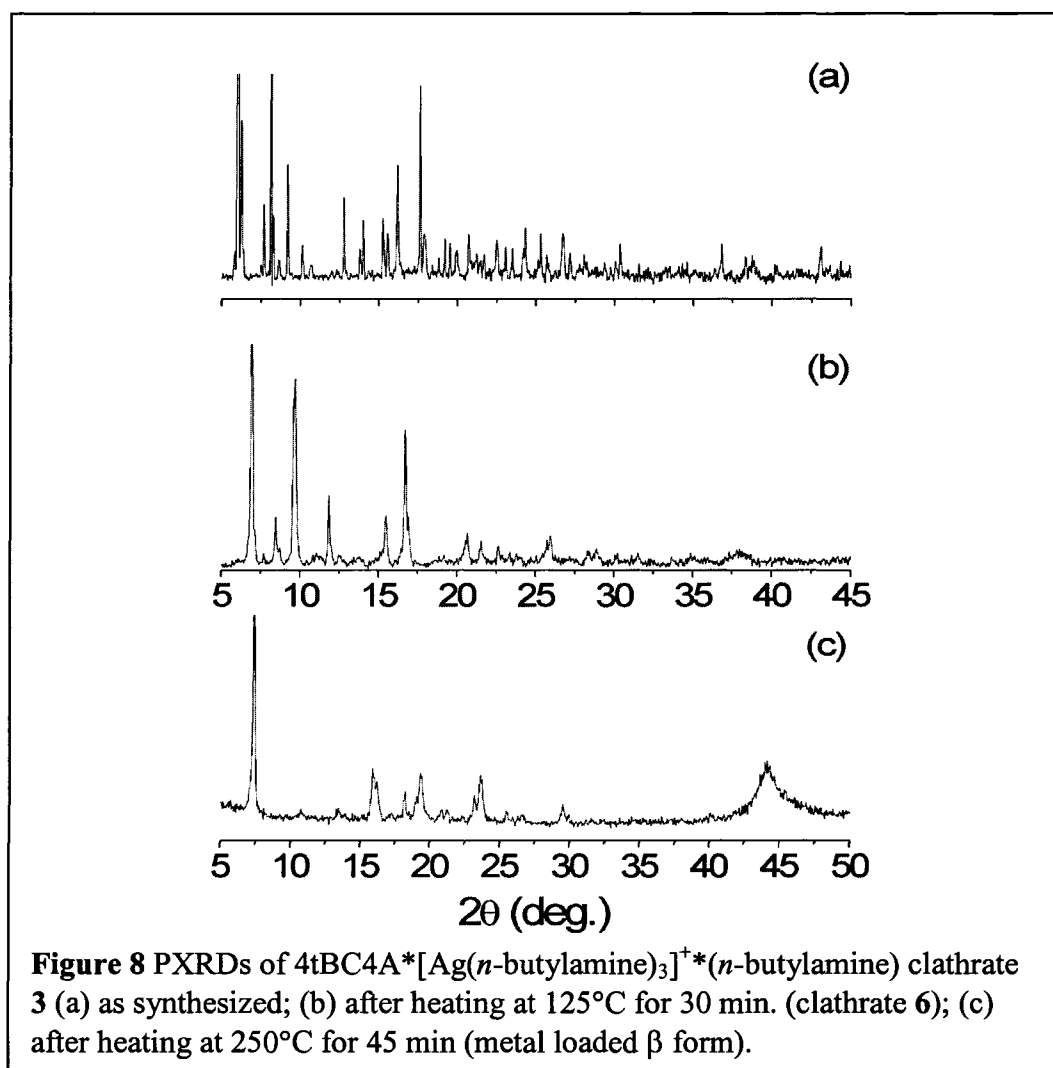


Table 4 Comparison of ¹³C CP/MAS NMR spectral data for clathrates **3** and **6** to solution NMR data.^[a]

Guest	Carbon	δ Solution ^[b]	δ 3 ^[c] (± 0.05)	CIS 3 ^[d] (± 0.05)	δ 6 ^[c] (± 0.05)	CIS 6 ^[d] (± 0.05)
<i>n</i> -butylamine	C1'	41.96	44.77	+2.81	43.69	+1.73
	C2'	36.07	42.94	+0.98	N/A ^e	N/A ^e
			38.03 (br)	+2.04		
	C3'	20.08	20.36	+0.28	21.35	+1.27
	C4'	13.94	15.20	+1.26	15.32	+1.38
			9.70	-4.24		

^[a]All values are in ppm. ^[b]Chemical shift of amine in solution, from SDBSWeb.^[113]

^[c]Chemical Shift observed in 4tBC4A clathrate. (br) indicates broad peak.

^[d]CIS=Complexation-induced shift=(δ clathrate)-(δ Solution). ^[e] Specific shift obscured by host resonances.

Table 5 Unit cell parameters determined by indexing of PXRD patterns of clathrates **3** and **6**.

Clathrate	3	6 ^[a]
Space Group	<i>P2₁2₁2₁</i>	<i>P4/n</i>
<i>a</i> (Å)	12.553	13.003
<i>b</i> (Å)	17.333	13.003
<i>c</i> (Å)	27.532	12.702
α (°)	90	90
β (°)	90	90
γ (°)	90	90
<i>V</i> (Å ³)	5990.2	2147.5

^[a]Obtained by heating **3** at 125°C.

This change in splitting is diagnostic of the influence of silver on the structure of clathrate **3** when compared to the analogous pure amine clathrate. Specifically, the charged silver centre serves to deshield the carbons in the phenolic subunit that interacts closely with it, giving rise to the downfield shift observed. Similarly, the upfield shift must arise from increased shielding of a more remote phenolic group. This is likely due to electronic shifts arising from a combination of hydrogen bonding (introducing additional electron density through N-H...O interactions) and shielding due to the silver complex as a whole. As a result, on a local ordering level, the calixarene can be described as possessing a pseudo-mirror plane, corresponding well to the more dramatic host disorder observed in the SCXRD.

In the upfield aliphatic region of the spectrum, the host carbons are again poorly resolved, as are most of the guest resonances. The resonances due to C1' and C2' of the *n*-butylamine guest are very broad, and given the lack of dynamics indicated by their disappearance upon dipolar dephasing, this is presumably due to coupling to the quadrupolar ¹⁴N of the amine functionality. The resonance to C3' is sharper, but again is

not isotropic, which along with the fact that it only partially dephases, suggests that it consists of multiple overlapping resonances some of which may be dynamic. This is confirmed by the two distinct peaks observed for C4', with the upfield peak exhibiting the complexation induced shift expected of the most deeply included aliphatic carbon in the uncoordinated amine (see Table 4). In contrast, the remaining carbons all exhibit a downfield shift, with C1' and C2' exhibiting the largest degree of deshielding. These resonances are therefore representative of the three amines coordinated to the electron withdrawing silver cation.

The PXRD pattern of clathrate **3** is also complex, confirming the low symmetry of the bulk form of the clathrate. As before, this complexity arises from the extensive overlap of a number of the reflections, such that automated indexing routines cannot be used. However, manual indexing based on the predicted pattern from the SCXRD structure does give rise to a unit cell consistent with that obtained for the single crystal examined (see Table 5), such that it is safe to assume that the SSNMR is representative of the structure model arising from the single crystal X-ray data.

Upon heating clathrate **3** to 125°C, the loss of the majority of the amine results in the transformation of the structure into a higher symmetry form, clathrate **6**. The ¹³C SSNMR spectrum is now quite simple (see Figure 7b), with the host peaks in the aromatic region collapsing into singlets. The aromatic C1 and C4 resonances remain diagnostic of this new structure, indicating that the structure consists of a single symmetrical calixarene. More significantly, the C1 at 151.17 ppm exhibits a 5 ppm downfield shift when compared with the pure *n*-butylamine 4tBC4A 1 host : 1 guest

clathrate (146.01 ppm). This indicates that the silver is still associated with the calixarene in clathrate **6**, likely being stabilized partially by coordination to the hydroxyl base of the calixarene such that the silver serves to deshield C1.

In the aliphatic region, the guest resonances are also simplified considerably, with only a series of comparatively sharp isotropic singlets observed. Intriguingly, while the amine now appears to be undergoing dynamic motion on the NMR timescale, as all of the guest resonances are now observed after dipolar dephasing, each resonance also exhibits a downfield shift instead of a complexation induced shift upfield from the aromatic rings of the calixarene (see Table 4). This indicates that the remaining molecule of *n*-butylamine also appears to continue to be coordinated to the silver centres, but in a fashion such that the amine is not included in the calixarene cavity. Despite this, the PXRD pattern for clathrate **6** is readily indexed in the $P4/n$ to the unit cell of the 1 guest: 1 host *n*-butylamine clathrate of 4tBC4A (see Figure 8b and Table 5). This would suggest that the silver is positioned in such a fashion that it at least obstructs access to the calixarene cavity, and is likely occupying the cavity.

Upon heating clathrate **6** at 240°C, the fully deaminated compound is obtained, with the desorption behaviour continuing to be analogous to that observed for the pure amine clathrates, despite the additional influence of the silver centres. The ^{13}C SSNMR has assumed the simple pattern characteristic of the β_0 forms, with the broadening of the peaks largely due to the increasing polycrystalline character of the heated powder.^[57] By the same token, the PXRD largely matches that previously reported by Atwood *et al.* for

the β_0 form.^[114] The influence of the silver centre is only apparent upon closer examination of the PXRD, and in particular the broad peak at approximately 43° .

This peak is not observed in the PXRD of the pure β_0 form, instead appearing to be characteristic of another phase in the compound. Such a hypothesis is further supported by simple visual observation of the powder following heating. Clathrate 3 takes the form of a white powder, but upon heating to produce the guest free form, the powder turns a deep brown. This clearly suggests that the silver centres are being reduced to form some sort of silver cluster. Similar behaviour has been previously observed in silver loaded zeolites, where the formation of covalent clusters is generally hypothesized to be responsible for a colour change from white to yellow upon heating.^[115-117] As well, a number of systems exist for the production of silver nanoparticles by reduction of silver complexes using chemical or photochemical processes, with a wide variety of sizes and polydispersities.^[118-128] As is well known, such nanoparticles are of considerable interest due to the shifts in physical properties (such as fluorescence^[129-131] and catalytic activity^[121-124, 132-134]) when compared to larger bulk assemblies of similar materials.

Therefore, the additional PXRD peak is most reasonably indexed as the 111 peak of elemental silver (spacegroup F_{m-3m}), indicating that the resulting clusters in this case are metallic in nature. As such, the broadening of the peak is characteristic of the crystallite size of the silver particles thus produced, and can be analyzed using the Scherrer equation to infer the size of the crystallites provided they exhibit perfectly spherical symmetry.^[135-137] Based on this, the resulting silver crystallites are

approximately 57 Å in diameter. Furthermore, the PXRD unit cell parameters suggest these silver clusters, are dispersed throughout the calixarene matrix such that they do not significantly perturb the packing of the 4tBC4A away from ideal *apo* packing, as they are too large to be accommodated within the calixarene itself.

The silver therefore has two significant roles in clathrate **3** and the pseudopolymorphs and guest-free form of 4tBC4A arising from desorption of the amine. The first is to serve as a force for directing the structural motif of the clathrate, by stabilizing the *exo* amines such that additional amines can be included within the capped structure favoured by 4tBC4A under basic conditions. The coordinative interaction does not give rise to such massive stabilization to result in the adoption of alternative schemes, clearly indicating that hydrogen bonding in such a structure is at least comparable to the coordinative interaction. However, upon removing many of the amines and the hydrogen bonding upon such inclusions rely upon, the coordinative interaction asserts itself as superior to van der Waals stabilization of the amine within the calixarene.

The second role for silver is as a site for redox chemistry that ultimately gives rise to metallic silver nanoparticles. As was hoped, the combination of an isolated environment and appropriate functionalities gave rise to unexpected chemistry. As we will see in Chapters V and VI, this reductive behaviour is also observed in other Ag⁺ amine systems, providing a firmer basis for forming a hypothesis as to the nature and origin of the redox chemistry involved. Focusing on the current system, the ¹³C SSNMR spectra are quite similar to that of the pure amine clathrates, suggesting that the primary function of the calixarene is that of a lattice to isolate the silver centres, with no

permanent change to the calixarene itself arising from the reduction of the silver.

Given this, the amines must participate in the reduction of the silver centres, at the very least serving to affect the reduction potential of the silver^[125] such that no permanent chemical modification of the calixarene occurs. While the precise nature of the chemistry and structure of these clusters can only be partially inferred from these studies, it does clearly establish the potential for producing metal functionalized calixarene frameworks through a self-assembly approach.

Ethylene Adsorption by 4tBC4A Supported Ag Nanoclusters

As alluded to above, the formation of silver nanoparticles supported by a calixarene matrix exhibits parallels to silver clusters supported by inorganic and organic substrates. In addition to silver loaded zeolites, a number of studies have examined silver supported on amorphous alumina, silica and carbon.^[121-124] Much of this research is driven by the catalytic activity of silver in such structures, which has been shown to be able to catalyze the epoxidation of ethylene^[121, 123] and other molecules,^[122] as well as oxidation of carbon monoxide.^[124] In addition to these practical studies, a number of computational studies have been carried out to examine the adsorption behaviour of silver nanoparticles in light of their catalytic activity.^[132-134]

However, unlike these systems, the calixarene framework is not inherently porous, raising the question as to whether the silver nanoclusters formed by desorption of the amine would be accessible for appreciable gas adsorption to occur. In the past, studies of the low density β *apo* form of 4tBC4A have clearly demonstrated that porosity is not necessarily required to allow for adsorption, provided the framework will allow for

subtle shifts to pass small molecules through the calixarene cavities of the structure.^[138] Furthermore, if gas adsorption was observed, it would give further validity to the hypothesis that the silver clusters are not arranged in relation to the calixarene in such a fashion to restrict their activity.

Therefore, given the bulk of data relating to adsorption of ethylene on silver as a model system for catalytic oxidation of alkenes,^[121, 123, 139-142] the metal loaded β_0 4tBC4A framework arising from amine desorption of clathrate **3** was investigated as a potential adsorbent for ethylene. The resulting adsorption isotherm for ethylene depicted in Figure 9 is readily fit to a Langmuir adsorption isotherm ($\chi = 0.0002$, $R^2 = 0.994$, see Table 6). The low pressure at which the isotherm plateaus, clearly indicating that the adsorption can be attributed to adsorption of the ethylene by the silver clusters, as opposed to adsorption by the calixarene matrix (which becomes a factor at pressures on the order of tens of bars).^[138, 143] As such, this simple model appears to be quite appropriate in this pressure range, although some deviation from this model would be expected to occur at higher pressures.

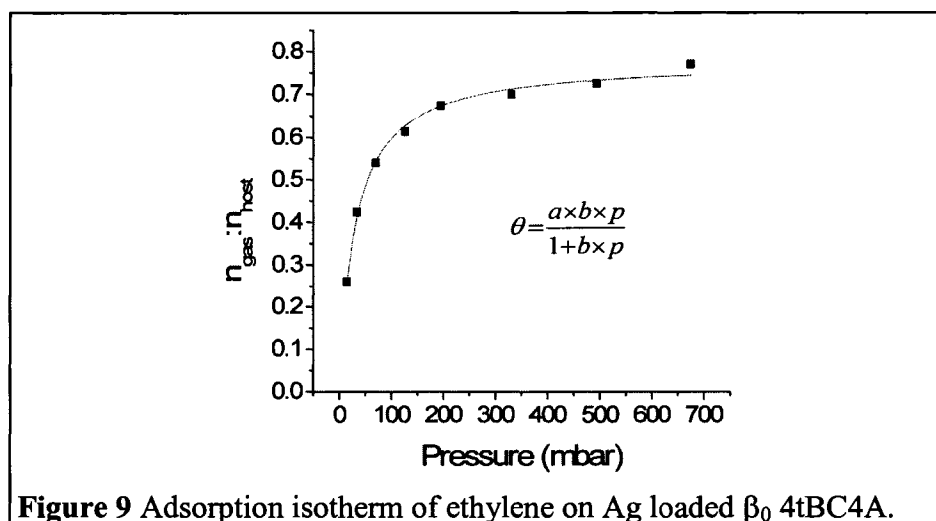


Figure 9 Adsorption isotherm of ethylene on Ag loaded β_0 4tBC4A.

Table 6 Langmuir constants for the adsorption of ethylene on metal loaded β_0 4tBC4A.

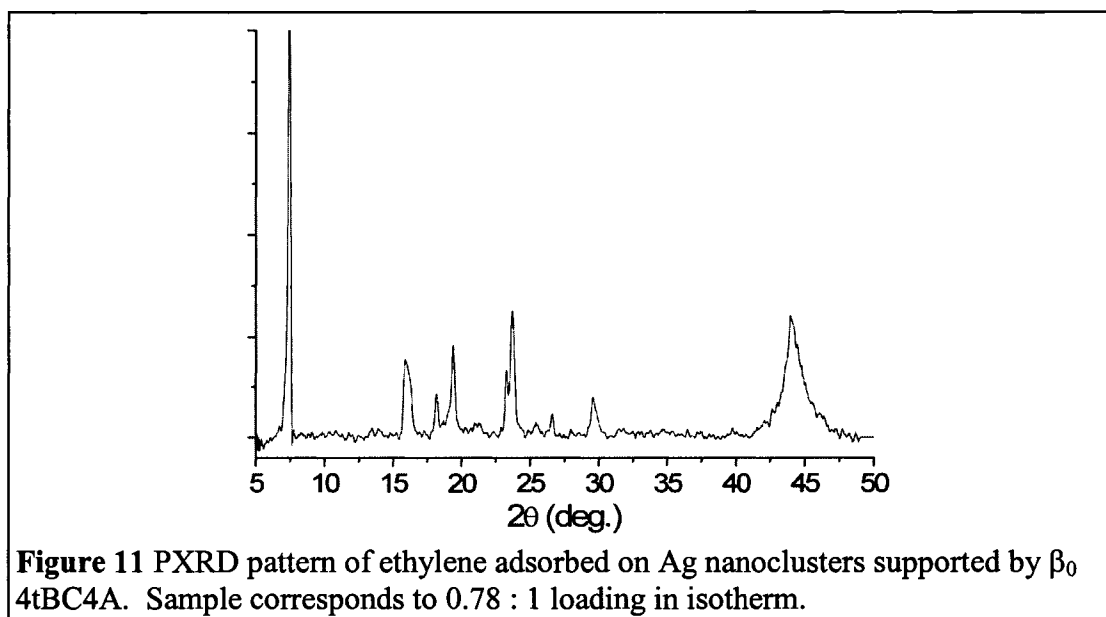
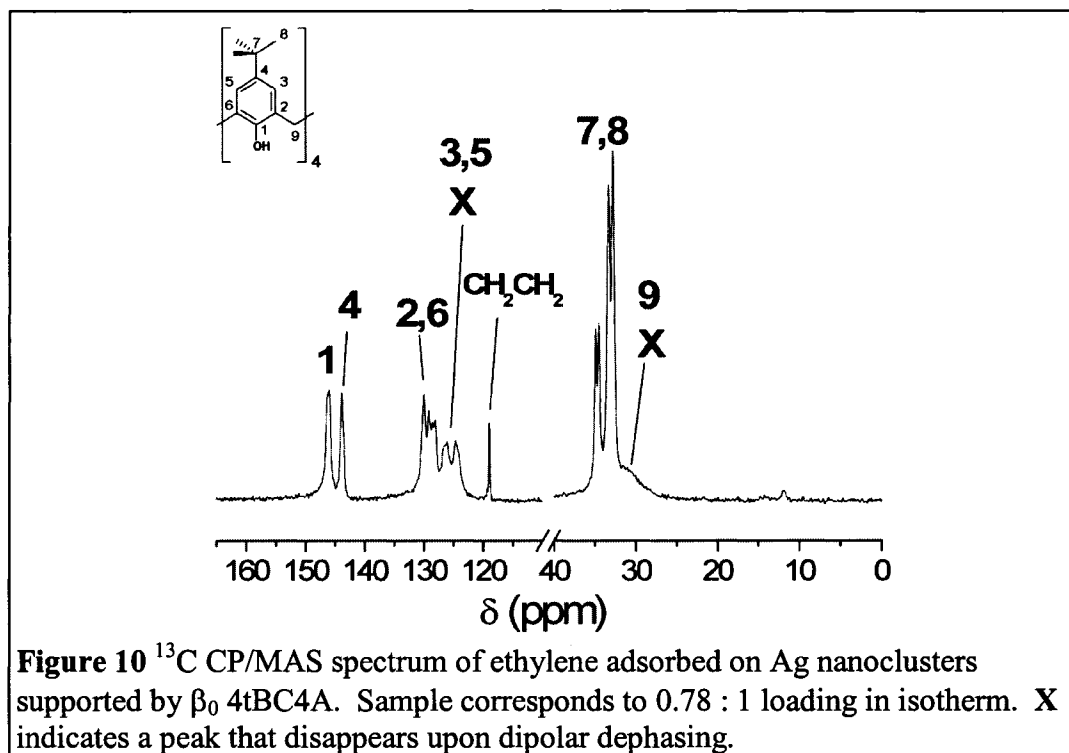
a ($n_{\text{gas}}:n_{\text{host}}$)	0.78 ± 0.01
b (mbar^{-1})	0.033 ± 0.002

The adsorption characteristics of the silver nanoclusters appears quite similar to that observed for other systems, with loadings at low pressures being approximately an order of magnitude less than silicas with 2-8% silver content.^[139, 142] This is attributable to the much more considerable molecular mass of the calixarene in relation to the 1 Ag : 1 host loading. As such, the overall adsorption capacity is quite comparable to the silica-based systems, with the added benefit of the support also being crystalline.

In fact, the ethylene treated sample exhibits sufficient stability to be removed from the adsorption line and used directly for structural studies. The adsorption of ethylene is readily confirmed by ^{13}C SSNMR of the resulting sample (see Figure 10). A single new resonance is observed at 118.89 ppm is due to the adsorbed ethylene. This corresponds well to the values previously observed for ethylene adsorbed on alumina supported silver particles which have been fully reduced.^[139, 142] Thus, the nanoparticles produced through desorption of the amines from calixarene frameworks could reasonably be expected to exhibit catalytic behaviour upon exposure to oxygen.

The various resonances corresponding to the host are virtually identical to those obtained prior to ethylene adsorption, clearly indicating that the adsorption does not result in any structural rearrangement in the carbon framework to accommodate the ethylene. The PXRD data supports this hypothesis, as it does not exhibit significant differences from the pre-adsorption samples (see Figure 11). As such, it appears that the void space within the structure is quite sufficient to allow for adsorption to occur, but in

the absence of more structural data, it is not possible to assess whether this is the result of a cooperative gas transfer process similar to that observed for the *apo* forms of 4tBC4A^[138, 143] or diffusion through a more conventional channelled structure.



5. Conclusions

In the simple amine clathrates, the disruption of the symmetry of the host through the introduction of hydrogen bonding gave rise to novel enclathration schemes with rational desorption behaviour. By introducing additional interactions to these structures, the degree to which these structures are favoured can be probed in greater depth. In the case of the addition of water, the solvent molecules serve to extend the hydrogen bonding network, serving readily as a hydrogen bond acceptor for the amines. However, this only gives rise to a minor perturbation in the structural motif is observed, with the amine guest shifting conformation to accommodate the additional structural elements.

Such a result is representative of the overall equivalence of the hydrogen bonds in the structure and the small size of water. The water is well suited to serve as an intermediary, but the essential stability of the capped motif, arising from the strong hydrogen bonding between the amines and the calixarenes, cannot be overcome by the tenuous stabilization offered by solvent molecules. The water is therefore included because it fits the structural motif, as opposed to forcing a significant shift. In light of this, more significant structural shifts might be observed by attempting to use bulkier alcohols as hydrogen bonding intermediaries.

The introduction of coordinate interactions by using the amines as ligands for metal centres makes it quite apparent that stronger interactions can perturb the favourability of a given motif. In the case of coordination to Zn^{2+} centres, the resulting tetrahedral complexes are too bulky to be accommodated in the capped motif that allows for *endo* inclusion of amines. Such strong coordinate interactions provide sufficient

stabilization to the amines such that van der Waals stabilization of the amine is not necessary. In such a case, as might be expected; the coordinate interaction dominates the structure. Even so, the calixarenes play a key role through secondary coordination; clearly indicating that hydrogen bonding to such a large anion gives rise to significant stabilization of the coordination compound.

Intriguingly, the roles of the coordination compound and calixarene in guiding the structures are reversed when silver is used. In this case, the coordinative flexibility of the metal centre allows for the coordination compound to be effectively selected for by the constraints of the calixarene lattice. As such, now hydrogen bonding and van der Waals interactions become ascendant again in directing the structure of the overall clathrate. More significantly, it indicates that for silver, the coordinate interaction can be used to tune the structural motif, again by using the calixarene as a secondary ligand. As we will see in subsequent chapters, this near balance between hydrogen bonding, van der Waals interactions and coordination can be used to tune how silver is included in such structures through adjustment of the amine ligand.

Finally, the self-assembly of silver coordination compounds in calixarene lattices is a route to the formation of metallic silver nanoclusters capable of serving as ethylene adsorbents. This appears to be a result of secondary coordinate stabilization of the silver centres providing a suitable environment for the amines to reduce the silver centres. As a result, the crystalline nature of the support in this case has allowed for preliminary structural characterization of both the silver clusters and its support framework. Again,

the subsequent chapters will show how this behaviour can be tuned through the choice of the ligand, allowing for further exploration of these materials.

6. References

- [1] E. Fischer, *Ber. Dtsch. Chem. Ges.* **1894**, *27*, 2985.
- [2] F. W. Lichtenthaler, *Angew. Chem. Int. Ed. Engl.* **1994**, *33*, 2364.
- [3] G. R. Desiraju, *Angew. Chem. Int. Ed. Engl.* **1995**, *34*, 2311.
- [4] A. M. Beatty, *Coord. Chem. Rev.* **2003**, *246*, 131.
- [5] N. W. Ockwig, O. Delgado-Friedrichs, M. O'Keeffe, O. M. Yaghi, *Accounts Chem. Res.* **2005**, *38*, 176.
- [6] L. R. MacGillivray, J. L. Atwood, *J. Am. Chem. Soc.* **1997**, *119*, 6931.
- [7] C. L. Barnes, E. Bosch, *Cryst. Growth Des.* **2005**, *5*, 1049.
- [8] I. Georgiev, E. Bosch, *Cryst. Growth Des.* **2004**, *4*, 235.
- [9] M. Nissinen, K. Rissanen, *Supramol. Chem.* **2003**, *15*, 581.
- [10] B. Q. Ma, Y. Zhang, P. Coppens, *Crys. Growth Des.* **2002**, *2*, 7.
- [11] R. M. McKinlay, G. W. V. Cave, J. L. Atwood, *Proc. Nat. Acad. Sci. USA* **2005**, *102*, 5944.
- [12] R. M. McKinlay, P. K. Thallapally, G. W. V. Cave, J. L. Atwood, *Angew. Chem. Int. Ed. Engl.* **2005**, *44*, 5733.
- [13] D. V. Soldatov, *J. Incl. Phenom. Macrocycl. Chem.* **2004**, *48*, 3.
- [14] D. V. Soldatov, J. A. Ripmeester, in *Nanoporous Materials Iv, Vol. 156*, **2005**, pp. 37.
- [15] C. D. Gutsche, *Calixarenes*, Royal Society of Chemistry, Cambridge, **1989**.
- [16] L. Mandolini, R. Ungaro, ed., *Calixarenes in Action*, Imperial College Press, London, **2000**.
- [17] C. D. Gutsche, *Calixarenes Revisited*, Royal Society of Chemistry, Cambridge, **1998**.
- [18] P. D. Beer, J. P. Martin, M. G. B. Drew, *Tetrahedron* **1992**, *48*, 9917.
- [19] W. Xu, R. J. Puddephatt, L. Manojlovicmuir, K. W. Muir, C. S. Frampton, *J. Incl. Phenom. Mol. Recogn. Chem.* **1994**, *19*, 277.
- [20] B. R. Cameron, F. Vanveggel, D. N. Reinhoudt, *J. Org. Chem.* **1995**, *60*, 2802.
- [21] A. Arduini, A. Pochini, S. Reverberi, R. Ungaro, *Tetrahedron* **1986**, *42*, 2089.
- [22] F. Arnaud-Neu, E. M. Collins, M. Deasy, G. Ferguson, S. J. Harris, B. Kaitner, A. J. Lough, M. A. McKervey, E. Marques, B. L. Ruhl, M. J. Schwing-Weill, E. M. Sewardt, *J. Am. Chem. Soc.* **1989**, *111*, 8681.
- [23] W. I. I. Bakker, W. Verboom, D. N. Reinhoudt, *J. Chem. Soc. Chem. Commun.* **1994**, 71.
- [24] A. F. D. de Namor, A. Aguilar-Cornejo, R. Soualhi, M. Shehab, K. B. Nolan, N. Ouazzani, L. Mandi, *J. Phys. Chem. B* **2005**, *109*, 14735.
- [25] J. M. Harrowfield, M. Mocerino, B. W. Skelton, C. R. Whitaker, A. H. White, *Aust. J. Chem.* **1994**, *47*, 1185.
- [26] S. G. Bott, A. W. Coleman, J. L. Atwood, *J. Am. Chem. Soc.* **1986**, *108*, 1709.

- [27] S. J. Dalgarno, J. Fisher, C. L. Raston, *Chem. Eur. J.* **2006**, *12*, 2772.
- [28] C. D. Gutsche, K. C. Nam, *J. Am. Chem. Soc.* **1988**, *110*, 6153.
- [29] I. A. Bagatin, D. Matt, H. Thonnessen, P. G. Jones, *Inorg. Chem.* **1999**, *38*, 1585.
- [30] B. R. Cameron, S. J. Loeb, *Chem. Commun.* **1996**, 2003.
- [31] B. R. Cameron, S. J. Loeb, G. P. A. Yap, *Inorg. Chem.* **1997**, *36*, 5498.
- [32] P. D. Harvey, *Coord. Chem. Rev.* **2002**, *233*, 289.
- [33] C. Jeunesse, D. Armspach, D. Matt, *Chem. Commun.* **2005**, 5603.
- [34] S. Kim, J. S. Kim, S. K. Kim, I. H. Suh, S. O. Kang, J. Ko, *Inorg. Chem.* **2005**, *44*, 1846.
- [35] M. Lejeune, C. Jeunesse, D. Matt, N. Kyritsakas, R. Welter, J. P. Kintzinger, *J. Chem. Soc. Dalton Trans.* **2002**, 1642.
- [36] C. Wieser-Jeunesse, D. Matt, A. De Cian, *Angew. Chem. Int. Ed.* **1998**, *37*, 2861.
- [37] J. M. Harrowfield, M. I. Ogden, W. R. Richmond, A. H. White, *J. Chem. Soc. Chem. Commun.* **1991**, 1159.
- [38] W. Xu, J. J. Vittal, R. J. Puddephatt, *J. Am. Chem. Soc.* **1993**, *115*, 6456.
- [39] H. F. Ji, Y. M. Yang, X. H. Xu, G. Brown, *Org. Biomol. Chem.* **2006**, *4*, 770.
- [40] J. S. Kim, S. H. Yang, J. A. Rim, J. Y. Kim, J. Vicens, S. Shinkai, *Tetrahedron Lett.* **2001**, *42*, 8047.
- [41] A. Ikeda, H. Tsuzuki, S. Shinkai, *J. Chem. Soc. Perkin Trans. 2* **1994**, 2073.
- [42] A. Ikeda, S. Shinkai, *Chem. Rev.* **1997**, *97*, 1713.
- [43] A. Ikeda, S. Shinkai, *J. Am. Chem. Soc.* **1994**, *116*, 3102.
- [44] R. Ungaro, A. Casnati, F. Ugozzoli, A. Pochini, J.-F. Dozol, C. Hill, H. Rouquette, *Angew. Chem. Int. Ed. Engl.* **1994**, *33*, 1506.
- [45] A. B. Rozhenko, W. W. Schoeller, M. C. Letzel, B. Decker, C. Agena, J. Mattay, *Theochem-J. Mol. Struct.* **2005**, *732*, 7.
- [46] T. J. Burchell, D. J. Eisler, R. J. Puddephatt, *Chem. Commun.* **2004**, 944.
- [47] H. Y. An, Y. G. Li, E. B. Wang, D. R. Xiao, C. Y. Sun, L. Xu, *Inorg. Chem.* **2005**, *44*, 6062.
- [48] G. D. Andreotti, L. Cavalca, P. Sgarabot, *Gazz. Chim. Ital.* **1971**, *101*, 494.
- [49] M. R. Sundberg, *Inorg. Chim. Acta* **1994**, *218*, 151.
- [50] C. L. Schauer, E. Matwey, F. W. Fowler, J. W. Lauher, *Mater. Res. Bull.* **1998**, *213*.
- [51] J. L. Atwood, G. W. Orr, F. Hamada, R. L. Vincent, S. G. Bott, K. D. Robinson, *J. Incl. Phenom. Mol. Recogn. Chem.* **1992**, *14*, 37.
- [52] S. A. Dalrymple, M. Parvez, G. K. H. Shimizu, *Chem. Commun.* **2001**, 2672.
- [53] S. A. Dalrymple, G. K. H. Shimizu, *Supramol. Chem.* **2003**, *15*, 591.
- [54] G. D. Andreotti, R. Ungaro, A. Pochini, *J. Chem. Soc. Chem. Commun.* **1979**, 1005.
- [55] R. Ungaro, A. Pochini, G. D. Andreotti, P. Domiano, *J. Chem. Soc. Perkin Trans.* **1985**, *2*, 197.
- [56] E. B. Brouwer, G. D. Enright, J. A. Ripmeester, *J. Am. Chem. Soc.* **1997**, *119*, 5404.
- [57] E. B. Brouwer, K. A. Udachin, G. D. Enright, J. A. Ripmeester, K. J. Ooms, P. A. Halchuk, *Chem. Commun.* **2001**, 565.

- [58] P. Scherrer, *Nachr. Ges. Wiss. Gottingen* **1918**, 26 Sept., 98.
- [59] K. A. Udachin, G. D. Enright, P. O. Brown, J. A. Ripmeester, *Chem. Commun.* **2002**, 2162.
- [60] P. O. Brown, K. A. Udachin, G. D. Enright, J. A. Ripmeester, *Chem. Eur. J.* **2006**, DOI: 10.1002/chem.200600434.
- [61] F. M. Raymo, J. F. Stoddart, *Chem. Berichte* **1996**, 129, 981.
- [62] J. E. Kickham, S. J. Loeb, *Inorg. Chem.* **1994**, 33, 4351.
- [63] I. Batinic-Haberle, I. Spasojevic, A. L. Crumbliss, *Inorg. Chem.* **1996**, 35, 2352.
- [64] S. Kannan, S. S. Raj, H. K. Fun, *Polyhedron* **2001**, 20, 2145.
- [65] D. R. Alston, A. M. Z. Slawin, J. F. Stoddart, D. J. Williams, *J. Chem. Soc., Chem. Commun.* **1985**, 1602.
- [66] L. Caron, H. Bricout, S. Tilloy, A. Ponchel, D. Landy, S. Fourmentin, E. Monflier, *Adv. Synth. Catal.* **2004**, 346, 1449.
- [67] Q. L. Guo, W. X. Zhu, S. J. Dong, S. L. Ma, X. Yan, *J. Mol. Struct.* **2003**, 650, 159.
- [68] H. R. Webb, M. J. Hardie, C. L. Raston, *Chem. Eur. J.* **2001**, 7, 3616.
- [69] J. L. Atwood, L. J. Barbour, M. J. Hardie, C. L. Raston, *Coord. Chem. Rev.* **2001**, 222, 3.
- [70] D. A. Beauchamp, S. J. Loeb, *Chem. Eur. J.* **2002**, 8, 5084.
- [71] J. M. Harrowfield, M. I. Ogden, W. R. Richmond, A. H. White, *J. Chem. Soc. Chem. Commun.* **1991**, 1159.
- [72] W. Xu, R. J. Puddephatt, K. W. Muir, A. A. Torabi, *Organometallics* **1994**, 13, 3054.
- [73] W. Xu, J. J. Vittal, R. J. Puddephatt, *Can. J. Chem.* **1996**, 74, 766.
- [74] N. Singh, M. Kumar, G. Hundal, *Tetrahedron* **2004**, 60, 5393.
- [75] G. Barrett, M. A. McKervey, J. F. Malone, A. Walker, F. Arnaudne, L. Guerra, M. J. Schwingweill, C. D. Gutsche, D. R. Stewart, *J. Chem. Soc. Perkin Trans. 2* **1993**, 1475.
- [76] K. Ohto, H. Yamaga, E. Murakami, K. Inoue, *Talanta* **1997**, 44, 1123.
- [77] J. Xie, Q. Y. Zheng, Y. S. Zheng, C. F. Chen, Z. T. Huang, *J. Incl. Phenom. Macrocycl. Chem.* **2001**, 40, 125.
- [78] X. J. Hu, Z. G. Pan, L. Wang, X. F. Shi, *Spectroc. Acta Pt. A-Molec. Biomolec. Spectr.* **2003**, 59, 2419.
- [79] R. H. Prince, in *Comprehensive Coordination Chemistry*, Vol. 5, 1st ed. (Ed.: G. Wilkinson), Pergamon Press, Oxford, **1987**, pp. 925.
- [80] T. Yamaguchi, H. Ohtaki, *Bull. Chem. Soc. Jpn.* **1978**, 51, 3227.
- [81] K. F. Tebbe, *Z. Kristall.* **1980**, 153, 297.
- [82] T. Yamaguchi, O. Lindqvist, *Acta Chem. Scand. A* **1981**, 35, 811.
- [83] R. Essmann, *J. Mol. Struct.* **1995**, 356, 201.
- [84] J. W. Steed, J. L. Atwood, *Supramolecular Chemistry*, John Wiley & Sons, Ltd., Chichester, **2000**.
- [85] L. Carlucci, G. Ciani, D. M. Proserpio, A. Sironi, *Angew. Chem. Int. Ed. Engl.* **1995**, 34, 1895.

- [86] L. Carlucci, G. Ciani, D. M. Proserpio, A. Sironi, *J. Am. Chem. Soc.* **1995**, *117*, 4562.
- [87] D. Venkataraman, S. Lee, J. S. Moore, P. Zhang, K. A. Hirsch, G. B. Gardner, A. C. Covey, C. L. Prentice, *Chem. Mat.* **1996**, *8*, 2030.
- [88] D. Venkataraman, G. B. Gardner, S. Lee, J. S. Moore, *J. Am. Chem. Soc.* **1995**, *117*, 11600.
- [89] G. K. H. Shimizu, G. D. Enright, C. I. Ratcliffe, J. A. Ripmeester, *Chem. Commun.* **1999**, 461.
- [90] G. K. H. Shimizu, G. D. Enright, C. I. Ratcliffe, J. A. Ripmeester, D. D. M. Wayner, *Angew. Chem. Int. Ed.* **1998**, *37*, 1407.
- [91] D. J. Hoffart, S. A. Dalrymple, G. K. H. Shimizu, *Inorg. Chem.* **2005**, *44*, 8868.
- [92] S. K. Makinen, N. J. Melcer, M. Parvez, G. K. H. Shimizu, *Chem. Eur. J.* **2001**, *7*, 5176.
- [93] L. J. May, G. K. H. Shimizu, *Chem. Mat.* **2005**, *17*, 217.
- [94] N. L. S. Yue, M. C. Jennings, R. J. Puddephatt, *Chem. Commun.* **2005**, 4792.
- [95] D. J. Eisler, R. J. Puddephatt, *Inorg. Chem.* **2005**, *44*, 4666.
- [96] D. J. Eisler, R. J. Puddephatt, *Cryst. Growth Des.* **2005**, *5*, 57.
- [97] D. J. Eisler, C. W. Kirby, R. J. Puddephatt, *Inorg. Chem.* **2003**, *42*, 7626.
- [98] T. J. Burchell, R. J. Puddephatt, *Inorg. Chem.* **2006**, *45*, 650.
- [99] L. Tei, V. Lippolis, A. J. Blake, P. A. Cooke, M. Schroder, *Chem. Commun.* **1998**, 2633.
- [100] D. Venkataraman, Y. Du, S. R. Wilson, K. A. Hirsch, P. Zhang, J. S. Moore, *J. Chem. Ed.* **1997**, *74*, 915.
- [101] R. J. Lancashire, in *Comprehensive Coordination Chemistry, Vol. 5*, 1st ed. (Ed.: G. Wilkinson), Pergamon Press, Oxford, **1987**, pp. 777.
- [102] S.-K. Chang, I. Cho, *J. Chem. Soc. Perkin Trans. 1* **1986**, 211.
- [103] R. P. Feazell, C. E. Carson, K. K. Klausmeyer, *Inorg. Chem.* **2005**, *44*, 996.
- [104] M. O. Awaleh, A. Badia, F. Brisse, X. H. Bu, *Inorg. Chem.* **2006**, *45*, 1560.
- [105] K. H. Li, Z. T. Xu, H. H. Xu, P. J. Carroll, J. C. Fettinger, *Inorg. Chem.* **2006**, *45*, 1032.
- [106] S. Hiraoka, T. Yi, M. Shiro, M. Shionoya, *J. Am. Chem. Soc.* **2002**, *124*, 14510.
- [107] A. B. Mallik, S. Lee, E. B. Lobkovsky, *Cryst. Growth Des.* **2005**, *5*, 609.
- [108] R. S. Rarig, J. Zubieta, *Inorg. Chim. Acta* **2002**, *340*, 211.
- [109] L. Zhang, X. Q. Lu, C. L. Chen, H. Y. Tan, H. X. Zhang, B. S. Kang, *Cryst. Growth Des.* **2005**, *5*, 283.
- [110] L. M. Engelhardt, S. Gotsis, P. C. Healy, J. D. Kildea, B. W. Skelton, A. H. White, *Aust. J. Chem.* **1989**, *42*, 149.
- [111] C. Nather, A. Beck, *Z.Naturforsch.(B)* **2004**, *59*, 992.
- [112] P. G. Jones, C. Wolper, *Dalton Trans.* **2005**, 1762.
- [113] NIAIST, "SDBSWeb", to be found under <http://www.aist.go.jp/RIODB/SDBS/>. **2005**.
- [114] J. L. Atwood, L. J. Barbour, G. O. Lloyd, P. K. Thallapally, *Chem. Commun.* **2004**, 922.
- [115] T. Sun, K. Seff, *Chem. Rev.* **1994**, *94*, 857.

- [116] R. Seifert, A. Kunzmann, G. Calzaferri, *Angew. Chem. Int. Ed* **1998**, *37*, 1521.
- [117] R. Seifert, R. Rytz, G. Calzaferri, *J. Phys. Chem. A* **2000**, *104*, 7473.
- [118] Y. Zhou, H. J. Liu, S. H. Yu, Z. Y. Chen, Y. R. Zhu, W. Q. Jiang, *Mater. Res. Bull.* **1999**, *34*, 1683.
- [119] Y. Yin, Z.-Y. Li, Z. Zhong, B. Gates, Y. Xia, S. Venkateswaran, *J. Mater. Chem.* **2002**, *12*, 522.
- [120] L. Rodriguez-Sanchez, M. C. Blanco, M. A. Lopez-Quintela, *J. Phys. Chem. B* **2000**, *104*, 9683.
- [121] B. S. Bal'zhinimaev, *Kinet. Catal.* **1999**, *40*, 795.
- [122] R. J. Chimentao, I. Kirm, F. Medina, X. Rodriguez, Y. Cesteros, P. Salagre, J. E. Sueiras, J. L. G. Fierro, *Appl. Surf. Sci.* **2005**, *252*, 793.
- [123] R. B. Grant, R. M. Lambert, *J. Chem. Soc. Chem. Commun.* **1983**, 662.
- [124] D. C. Lim, I. Lopez-Salido, Y. D. Kim, *Surf. Sci.* **2005**, *598*, 96.
- [125] A. Frattini, N. Pellegri, D. Nicastro, O. de Sanctis, *Mater. Chem. Phys.* **2005**, *94*, 148.
- [126] D. K. Lee, Y. S. Kang, *ETRI Journal* **2004**, *26*, 262.
- [127] J. Widoniak, S. Eiden-Assmann, G. Maret, *Colloids & Surfaces A: Physiochem. Eng. Aspects.* **2005**, *270-271*, 340.
- [128] M. Yamamoto, M. Nakamoto, *J. Mater. Chem.* **2003**, *13*, 2064.
- [129] T. L. Jennings, M. P. Singh, G. F. Strouse, *J. Am. Chem. Soc.* **2006**, *128*, 5462.
- [130] C. Hempen, U. Karst, *Anal. Bioanal. Chem.* **2006**, *384*, 572.
- [131] X. H. Gao, L. L. Yang, J. A. Petros, F. F. Marshal, J. W. Simons, S. M. Nie, *Curr. Opin. Biotechnol.* **2005**, *16*, 63.
- [132] A. Kokalj, A. Dal Corso, S. de Gironcoli, S. Baroni, *J. Phys. Chem. B* **2002**, *106*, 9839.
- [133] A. Kokalj, A. Dal Corso, S. de Gironcoli, S. Baroni, *Surf. Sci.* **2003**, *532*, 191.
- [134] S. Linic, H. Piao, K. Adib, M. A. Barteau, *Angew. Chem. Int. Ed.* **2004**, *43*, 2918.
- [135] H. Borchert, E. V. Shevchenko, A. Robert, I. Mekis, A. Kornowski, G. Grubel, H. Weller, *Langmuir* **2005**, *21*, 1931.
- [136] J. I. Langford, A. J. C. Wilson, *J. Appl. Cryst.* **1978**, *11*, 102.
- [137] $d=(K\lambda)/(B\cos\theta)$, where d =Crystallite Diameter, λ = Wavelength of radiation, K =Scherrer Constant (0.9), B =Broadening of Peak at FWHM, corrected for instrumental broadening, θ =Diffraction Angle in Radians.
- [138] J. L. Atwood, L. J. Barbour, A. Jerga, *Angew. Chem. Int. Ed.* **2004**, *43*, 2948.
- [139] J. K. Plischke, A. J. Benesi, M. A. Vannice, *J. Catalysis* **1992**, *138*, 223.
- [140] E. Hughes, J. M. Koons, J. X. Wang, P. D. Ellis, *J. Catalysis* **1999**, *183*, 182.
- [141] N. Giordano, J. C. J. Bart, R. Maggiore, *Z. Physik. Chem. (Wiesbaden)* **1981**, *127*, 109.
- [142] E. F. Fernandes, A. J. Benesi, M. A. Vannice, *J. Phys. Chem.* **1994**, *98*, 8498.
- [143] I. L. Moudrakovski, J. A. Ripmeester, Unpublished Results, **2006**.

Chapter V: Isoalkylamine Clathrates of 4-*t*-butylcalix[4]arene[†]

1. Abstract.....	170
2. Introduction.....	171
3. Experimental Section.....	174
4. Results and Discussion.....	181
Inclusion of Isopropylamine in 4tBC4A	181
Secondary Coordination and Isopropylamine Ag Complexes.....	183
Enclathration of Isobutylamine by 4tBC4A	186
Desorption behaviour of Isobutylamine 4tBC4A Clathrate 3	192
Supramolecular Solid Solutions of isobutylamine-Ag complexes	196
Fully Loaded Isobutylamine-Ag 4tBC4A Frameworks.....	203
Desorption Behaviour of Isobutylamine-Ag Loaded 4tBC4A Frameworks	208
Enclathration of Isoamylamine and Isoamylamine Ag complexes by 4tBC4A... ..	218
5. Conclusions.....	223
6. References	226

1. Abstract

In order to further investigate the effects of guest size and coordinative ability, studies of the inclusion of *iso*-substituted amines in 4-*t*-butylcalix[4]arene (4tBC4A) were carried out. Inclusion of isobutylamine (iBA) or isoamylamine (iAA) results in a dramatic distortion of the common capped motif observed for small amines. This guest-induced distortion carries over to the clathrates of isobutylamine-Ag complexes. Competition between supramolecular stabilization and direct coordination gives rise to a family of calixarene frameworks that have a silver loading level dictated by the synthetic conditions, such that a solid solution forms for loadings from 0.2 to 0.4 Ag. In contrast with this, coordination of isopropylamine (iPA) to silver gives rise to an ideal capped structure, while coordination of isoamylamine results in a structure analogous to that formed by *n*-butylamine and silver.

[†] Portions of this chapter have been previously published: P. O. Brown, K. A. Udachin, G. D. Enright, J. A. Ripmeester, *Chem. Commun.* **2005**, 4402.

2. Introduction

The concept of a cooperative fit between a guest and a receptor is a central theme in host-guest chemistry. In the case of 4-*t*-butylcalix[4]arene (4tBC4A), this has typically been seen in the form of various organic guests arranging themselves within the cavity of the calixarene such that the four-fold symmetry of the host is preserved.^[1-18] Under such circumstances, the hydrogen bonding interaction at the base of the calixarene is highly favourable, such that the guest must adapt to fit within the heavily favoured cone conformation of the calixarene.

However, upon disrupting this hydrogen bonding at the base, lower host symmetries for calixarenes are observed. Traditionally, such disruption has been the result of covalent or coordinate modification of the hydroxyl groups forming the base of 4tBC4A,^[19-28] but as we have seen in Chapters III and IV, simple deprotonation due to basic conditions is sufficient as well.^[29-33] Under such conditions, the resulting structures are rightly seen as the result of a structural compromise between the two-fold symmetry of the calixarene receptor, and the various forces stabilizing the amine guest.

This concept of a single centre directing the geometrical arrangement of a supramolecular structure, and thus its symmetry, is not unique to organic systems. Both inorganic frameworks, such as zeolites,^[34] and metal-organic frameworks,^[35-37] rely heavily on the distinct geometries dictated by the coordination chemistry of metal centres. The structures of the various calix ionophores also are directed largely by the coordinative demands of the included metal centre, with the cation- π interactions in particular serving to determine which conformers are favoured.^[38-40] The strength of

coordination bonding is such that the production of reticular metal-organic frameworks is largely a matter of selecting the appropriate metal centre and a rigid, well defined ligand to produce the geometry desired.^[41]

However, in the case of coordinatively flexible metal centers, such as silver, the reality of designing such supramolecular compounds is somewhat more complicated, as exhibited by the intriguing coordination polymers formed with Ag(I) centres.^[42-44] The resulting structures are heavily dependent on the geometry and bulk of the ligand, allowing for the formation of the otherwise uncommon three coordinate trigonal planar geometry.^[45-53] However, as demonstrated with the *n*-alkylamines and ethylenediamine (see Chapters III and VI), an alternative to controlling the ligand geometry to control the coordination about the metal centre is to make use of weak interactions to stabilize a given geometry through molecular recognition, giving rise to trigonal planar geometry derived from supramolecular secondary coordination.

The diversity of structures observed with simple linear *n*-alkylamines suggests that, much like the simple amine inclusions, it should be possible to further tune both the host and the guest in these frameworks in a relatively rational fashion. It was suspected that altering the bulk and length of the amine might have dramatic effects on the favourability of the capped inclusion scheme of the smaller amines. Furthermore, coordination to silver allows for the use of amines that otherwise are too volatile to produce inclusion compounds suited to crystallographic study, while the guest's bulk might also allow for further tuning of the coordination scheme.

The current chapter therefore focuses on the inclusion chemistry of *iso*-substituted amines, and how this subtle shift in bulk and chain length affects both the simple amine inclusion compounds and the compounds arising from coordination to silver. In the case of isopropylamine (iPA), the amine alone is too small to result in the formation of a capped motif, but upon coordination to silver, the capped motif is observed. This demonstrates the strength of the coordination bond in guiding the inclusion of very small guests while still being influenced by the secondary coordinate interactions.

In the case of isobutylamine (iBA), a much more complex set of interactions is observed, giving rise to a dramatic shift in the inclusion motifs observed for both types of compounds when compared to the studies of the inclusion of *n*-alkylamines. Upon coordination to silver, this system gives rise to the first reported supramolecular solid solution derived from a self-assembled hybrid organic-inorganic framework. As such, coordination to iBA thereby represents a route to producing simple, unfunctionalized calixarene frameworks with variable silver loading.

Finally, inclusion of isoamylamine (iAA) causes similar distortions to iBA, with the increased length of the amine reducing the magnitude of the shift. Coordination to silver has a similar effect, such that the resulting structure is analogous to that observed for *n*-butylamine. As such, iBA represents the optimal length of amine under these conditions to yield a supramolecularly stabilized amine cluster that is sufficiently stable to compete with the stabilization offered by coordination to silver.

3. Experimental Section

General Note: Unless otherwise indicated, chemicals were obtained from EMD Chemicals and Sigma-Aldrich, and were used without further purification.

Synthesis of isopropylamine*4tBC4A clathrate **1**: 0.250 g (3.85×10^{-4} mol) of 4tBC4A was weighed out into a scintillation vial. 5.0 mL iPA was then added to the vial, and the calixarene and amine were gently mixed for approximately 1 minute. The resulting clear solution was then set aside to allow excess amine to evaporate. After approximately one day, large colourless block-like crystals had formed.

Synthesis of $[\text{Ag}(\text{isopropylamine})_3]^+ \cdot 1(\text{H}_2\text{O}) \cdot 1(4\text{tBC4A})^-$ clathrate **2** (POB34): 0.065 g (3.83×10^{-4} mol) of AgNO_3 was weighed out into a scintillation vial. Following this, 5.0 mL of iPA was then added, such that all of the metal salt dissolved immediately. 0.248 g (3.82×10^{-4} mol) of 4tBC4A was then added, and the solution mixed for approximately 5 minutes, at which point all calixarene had dissolved. The samples were then set aside, and excess amine allowed to evaporate over two days resulting in the formation of clear, block-like crystals suitable for SCXRD.

Synthesis of 3(isobutylamine)*1(4tBC4A) clathrate **3** (POB78): In a typical synthesis, 1.128 g (1.74×10^{-3} mol) of 4tBC4A was placed in a vial along with 4.5 mL of iBA. The resulting mixture was gently mixed for approximately 10 minutes, and then heated to approximately 50°C to speed the dissolution of any remaining particles of 4tBC4A. The resulting solution was then set aside and excess solvent allowed to slowly evaporate over the course of a few days, giving rise to large, block like crystals suitable for structural analysis.

Synthesis of variably loaded silver-iBA clathrates of 4tBC4A: For clathrates **5-10** (POB79, 80, 100, 98, 96 and 97), a typical synthesis entailed weighing out 0.275 g (1.64×10^{-3} mol) of AgNO₃ into a scintillation vial. Following this, 6.0 mL of iBA was then added, and the resulting solution mixed over the course of approximately 10 minutes, such that all of the metal salt was dissolved. At this point, between 0.525 g (8.10×10^{-4} mol) and 2.101 g (3.24×10^{-3} mole) of 4tBC4A was added, such that the resulting ratio of Ag : 4tBC4A ranged from 1.28:1 and 2:1. The samples were then stored in the dark, and excess amine allowed to evaporate. For clathrate **11** (POB101), the amount of silver used was increased to ensure sufficient amounts of clathrate were produced, with 0.419 g (2.48×10^{-3} mol) of AgNO₃ and 0.401 g (6.19×10^{-4} mol) of 4tBC4A dissolved in 4.5 mL of iBA, resulting in an Ag : 4tBC4A ratio of 4:1. In both cases, it was preferred to hold the amount of AgNO₃ used constant while varying the amount of 4tBC4A to avoid difficulties with photoreduction of the materials.

Synthesis of 3(isoamylamine)*1(4tBC4A) clathrate **14** (POB38): Synthesis was carried out in according to the procedure outlined for clathrate **1**, using 0.251 g (3.87×10^{-4} mol) of 4tBC4A and 3.0 mL of iAA.

Synthesis of [Ag(isoamylamine)₃]⁺*1(isoamylamine)*1(4tBC4A)⁻ clathrate **15** (POB23): Synthesis was carried out according to the procedure outlined for clathrate **2**, using 0.054 g AgNO₃ (3.2×10^{-4} mol), 3.0 mL of iAA and 0.204 g (3.15×10^{-4} mol) of 4tBC4A.

Single Crystal X-ray Diffraction data are summarized in Table 1. For clathrates **3** and **14**, the hydrogen atoms on the disordered groups were placed in calculated positions and refined as riding atoms, with all other hydrogen atoms found from the difference

map. For all other clathrates, hydrogen atoms on fully ordered heteroatoms were found from the difference map, with all other hydrogen atoms placed in calculated positions and refined as riding atoms. In general, disordered moieties were modeled anisotropically provided the site occupancy was greater than 0.40, with the thermal parameters of adjacent atoms constrained when they approached each other closer than 0.7 Å. Anisotropic refinement of the endo amine in Clathrate **15** was not possible due to the extensive disorder observed in this case.

Thermogravimetric analysis was carried out following the procedure detailed in Chapter III on page 72-73. Thermal desorption studies of clathrates **3**, **7** and **11** were carried following the procedure detailed in Chapter III on page 73.

Powder X-ray Diffraction data for clathrates **3** and its desorption products (clathrate **4** and the α *apo* form of 4tBC4A), partially loaded clathrate **7** and clathrate **12** were collected on the Scintag X-2 Advanced diffractometer. All other powder patterns were collected on the Rigaku Geigerflex vertical goniometer diffractometer. In the case of clathrates **3**, **7**, **11**, and the α *apo* form of 4tBC4A, the actual SCXRD structures of the compounds were used to guide the indexing, while for clathrates **4**, **12**, **13** the SCXRD data from the 1 Guest: 1 Host n-butylamine:4tBC4A clathrate were used.^[32] Crystallite size determination was carried out as described in Chapter IV on page 130.

¹³C CP/MAS spectra for all compounds were collected using the Bruker AMX-300 spectrometer (¹H=300.145 MHz, ¹³C=75.483 MHz).

Table 1a SCXRD data for clathrates **2**, **3**, and **5**.

Identification code	Clathrate 2 (POB34)	Clathrate 3 (POB78)	Clathrate 5 (POB79)
Empirical formula	C ₁₂₀ H _{149.50} Ag ₂ N ₇ O ₁₀	C ₅₆ H ₈₉ N ₃ O ₄	C _{27.87} H _{43.79} Ag _{0.11} N _{1.47} O ₂
Formula weight	2065.71	868.30	443.27
Temperature	173(2) K	125(2) K	125(2) K
Wavelength	0.71073 Å	0.71073 Å	0.71073 Å
Crystal system	Monoclinic	Monoclinic	Orthorhombic
Space group	<i>P</i> 2 ₁ / <i>c</i>	<i>P</i> 2 ₁ / <i>c</i>	<i>Pnma</i>
Unit cell dimensions	<i>a</i> = 22.133(3) Å <i>b</i> = 20.811(3) Å <i>c</i> = 23.420(3) Å α = 90° β = 103.438(2)° γ = 90°	<i>a</i> = 11.5224(7) Å <i>b</i> = 19.9406(13) Å <i>c</i> = 23.3234(15) Å α = 90° β = 93.881(1)° γ = 90°	<i>a</i> = 19.8789(9) Å <i>b</i> = 23.4375(11) Å <i>c</i> = 11.2218(5) Å α = 90° β = 90° γ = 90°
Volume	10492(2) Å ³	5346.6(6) Å ³	5228.4(4) Å ³
Z	4	4	8
ρ _{calc}	1.308 Mg/m ³	1.079 Mg/m ³	1.126 Mg/m ³
Abs. coefficient	0.437 mm ⁻¹	0.066 mm ⁻¹	0.148 mm ⁻¹
F(000)	4370	1912	1940
Crystal size	0.5 x 0.3 x 0.2 mm ³	0.48x0.32x0.32 mm ³	0.48x0.32x0.32 mm ³
θ Range	1.33 to 21.15°	1.34 to 29.57°	1.74 to 29.60°
Index ranges	-22 ≤ <i>h</i> ≤ 22, -20 ≤ <i>k</i> ≤ 20, -23 ≤ <i>l</i> ≤ 23	-15 ≤ <i>h</i> ≤ 13, -27 ≤ <i>k</i> ≤ 27, -32 ≤ <i>l</i> ≤ 32	-27 ≤ <i>h</i> ≤ 27, -32 ≤ <i>k</i> ≤ 32, -15 ≤ <i>l</i> ≤ 15
Reflections collected	63280	47208	62623
Ind. reflections	63527 [R(int) = 0.0966]	14806 [R(int) = 0.0363]	7479 [R(int) = 0.0454]
Completeness to θ = max	97.3 %	98.9 %	99.4 %
Absorption correction	Multi-scan	Multi-scan	Multi-scan
Refinement method	Full-matrix least-squares on F ²	Full-matrix least-squares on F ²	Full-matrix least-squares on F ²
Data / restraints / parameters	63527 / 66 / 1250	14806 / 44 / 747	7479 / 20 / 418
Goodness-of-fit on F ²	0.979	1.028	1.041
Final R indices [I > 2σ(I)]	R1 = 0.0771 wR2 = 0.1916	R1=0.0540, wR2=0.1325	R1=0.0610, wR2=0.1488
R indices (all data)	R1 = 0.1480 wR2 = 0.2342	R1=0.0816, wR2=0.1473	R1=0.0833, wR2=0.1622
Largest diff. peak and hole (e.Å ⁻³)	0.576 and -0.653	0.483 and -0.517	0.753 and -0.246

Table 1b SCXRD data for Clathrates **6**, **7**, and **8**.

Identification code	Clathrate 6 (POB80)	Clathrate 7 (POB100)	Clathrate 8 (POB98)
Empirical formula	C ₂₈ H _{44.35} Ag _{0.11} N _{1.50} O ₂	C _{27.82} H _{44.13} Ag _{0.15} N _{1.45} O ₂	C ₂₈ H _{44.25} Ag _{0.17} N _{1.48} O ₂
Formula weight	446.13	446.84	452.14
Temperature	125(2) K	125(2) K	125(2) K
Wavelength	0.71073 Å	0.71073 Å	0.71073 Å
Crystal system	Orthorhombic	Orthorhombic	Orthorhombic
Space group	<i>Pnma</i>	<i>Pnma</i>	<i>Pnma</i>
Unit cell dimensions	<i>a</i> = 19.884(4) Å <i>b</i> = 23.455(5) Å <i>c</i> = 11.225(2) Å $\alpha = 90^\circ$ $\beta = 90^\circ$ $\gamma = 90^\circ$	<i>a</i> = 19.8865(13) Å <i>b</i> = 23.4792(15) Å <i>c</i> = 11.2026(7) Å $\alpha = 90^\circ$ $\beta = 90^\circ$ $\gamma = 90^\circ$	<i>a</i> = 19.8812(16) Å <i>b</i> = 23.5305(19) Å <i>c</i> = 11.1940(9) Å $\alpha = 90^\circ$ $\beta = 90^\circ$ $\gamma = 90^\circ$
Volume	5235.2(18) Å ³	5230.7(6) Å ³	5236.7(7) Å ³
Z	8	8	8
ρ_{calc}	1.132 Mg/m ³	1.135 Mg/m ³	1.147 Mg/m ³
Abs. coefficient	0.150 mm ⁻¹	0.175 mm ⁻¹	0.192 mm ⁻¹
F(000)	1953	1953	1973
Crystal size	0.48x0.32x0.32 mm ³	0.35x0.20x0.20 mm ³	0.35x0.30x0.20 mm ³
θ Range	1.74 to 29.57°.	1.73 to 29.59°.	1.73 to 29.58°.
Index ranges	-27 ≤ <i>h</i> ≤ 27, -32 ≤ <i>k</i> ≤ 32, -15 ≤ <i>l</i> ≤ 15	-27 ≤ <i>h</i> ≤ 27, -32 ≤ <i>k</i> ≤ 32, -15 ≤ <i>l</i> ≤ 15	-27 ≤ <i>h</i> ≤ 27, -32 ≤ <i>k</i> ≤ 32, -15 ≤ <i>l</i> ≤ 15
Reflections collected	62754	63210	63523
Ind. reflections	7483 [R(int) = 0.0368]	7458 [R(int) = 0.0323]	7482 [R(int) = 0.0389]
Completeness to $\theta = \text{max}$	99.5 %	99.1 %	99.4 %
Absorption correction	Multi-scan	Multi-scan	Multi-scan
Refinement method	Full-matrix least-squares on F ²	Full-matrix least-squares on F ²	Full-matrix least-squares on F ²
Data / restraints / parameters	7483 / 19 / 396	7458 / 16 / 375	7482 / 16 / 366
Goodness-of-fit on F ²	1.015	1.049	1.032
Final R indices [I > 2 σ (I)]	R1=0.0501, wR2=0.1322	R1=0.0461, wR2=0.1183	R1=0.0500, wR2=0.1272
R indices (all data)	R1=0.0710, wR2=0.1482	R1=0.0678, wR2=0.1378	R1=0.0708, wR2=0.1446
Largest diff. peak and hole (e.Å ⁻³)	0.804 and -0.246	0.662 and -0.269	0.603 and -0.447

Table 1c SCXRD data for Clathrates **9**, **10** and **11**.

Identification code	Clathrate 9 (POB96)	Clathrate 10 (POB97)	Clathrate 11 (POB101)
Empirical formula	C _{27.74} H _{43.69} Ag _{0.19} N _{1.44} O ₂	C ₂₈ H _{44.22} Ag _{0.21} N _{1.50} O ₂	C ₁₁₂ H ₁₇₆ Ag ₂ N ₆ O ₈
Formula weight	450.20	456.66	1950.33
Temperature	125(2) K	125(2) K	125(2) K
Wavelength	0.71073 Å	0.71073 Å	0.71073 Å
Crystal system	Orthorhombic	Orthorhombic	Triclinic
Space group	<i>Pnma</i>	<i>Pnma</i>	<i>P</i> -1
Unit cell dimensions	<i>a</i> = 19.8944(13) Å <i>b</i> = 23.5816(16) Å <i>c</i> = 11.1924(8) Å α = 90° β = 90° γ = 90°	<i>a</i> = 19.901(3) Å <i>b</i> = 23.604(4) Å <i>c</i> = 11.1945(18) Å α = 90° β = 90° γ = 90°	<i>a</i> = 13.210(4) Å <i>b</i> = 20.308(6) Å <i>c</i> = 21.335(7) Å α = 91.457(7)° β = 106.273(7)° γ = 96.738(8)°
Volume	5250.8(6) Å ³	5258.7(14) Å ³	5446(3) Å ³
Z	8	8	2
ρ _{calc}	1.139 Mg/m ³	1.154 Mg/m ³	1.189 Mg/m ³
Abs. coefficient	0.207 mm ⁻¹	0.221 mm ⁻¹	0.415 mm ⁻¹
F(000)	1962	1989	2096
Crystal size	0.32x0.32x0.32 mm ³	0.40x0.30x0.15 mm ³	0.32x0.15x0.08 mm ³
θ Range	1.73 to 28.31°	1.73 to 29.53°	1.00 to 29.55°
Index ranges	-26 ≤ <i>h</i> ≤ 26, -31 ≤ <i>k</i> ≤ 31, -14 ≤ <i>l</i> ≤ 14	-27 ≤ <i>h</i> ≤ 25, -32 ≤ <i>k</i> ≤ 32, -15 ≤ <i>l</i> ≤ 15	-18 ≤ <i>h</i> ≤ 18, -28 ≤ <i>k</i> ≤ 27, -29 ≤ <i>l</i> ≤ 29
Reflections collected	58317	63229	66681
Ind. reflections	6673 [R(int) = 0.0360]	7479 [R(int) = 0.0448]	29565 [R(int) = 0.0316]
Completeness to θ = max	99.7 %	99.3 %	97.0 %
Absorption correction	Multi-scan	Multi-scan	Multi-scan
Refinement method	Full-matrix least-squares on F ²	Full-matrix least-squares on F ²	Full-matrix least-squares on F ²
Data / restraints / parameters	6673 / 18 / 480	7479 / 16 / 361	29565 / 103 / 1464
Goodness-of-fit on F ²	1.047	1.041	1.026
Final R indices [I > 2σ(I)]	R1=0.0455, wR2=0.1163	R1=0.0471, wR2=0.1184	R1=0.0505, wR2=0.1297
R indices (all data)	R1=0.0649, wR2=0.1348	R1=0.0780, wR2=0.1446	R1=0.0804, wR2=0.1458
Largest diff. peak and hole (e.Å ⁻³)	0.790 and -0.315	0.831 and -0.329	2.444 and -2.644

Table 1d SCXRD data for Clathrates 14 and 15.

Identification code	Clathrate 14 (POB38)	Clathrate 15 (POB23)
Empirical formula	C ₅₉ H ₉₅ N ₃ O ₄	C ₆₄ H ₁₀₇ AgN ₄ O ₄
Formula weight	910.38	1104.41
Temperature	173(2) K	173(2) K
Wavelength	0.71073 Å	0.71073 Å
Crystal system	Monoclinic	Monoclinic
Space group	<i>P</i> 2 ₁ / <i>c</i>	<i>P</i> 2 ₁ / <i>n</i>
Unit cell dimensions	<i>a</i> = 13.5699(6) Å <i>b</i> = 20.2516(9) Å <i>c</i> = 20.5933(9) Å α = 90° β = 94.093 (1)° γ = 90°	<i>a</i> = 12.9351(10) Å <i>b</i> = 27.642(2) Å <i>c</i> = 19.1574(15) Å α = 90° β = 107.856 (1)° γ = 90°
Volume	5644.9(4) Å ³	6519.9(9) Å ³
Z	4	4
ρ_{calc}	1.071 Mg/m ³	1.125 Mg/m ³
Abs. coefficient	0.066 mm ⁻¹	0.354 mm ⁻¹
F(000)	2008	2392
Crystal size	0.48 x 0.48 x 0.32 mm ³	0.64 x 0.64 x 0.48 mm ³
θ Range	1.41 to 29.63°.	1.69 to 28.29°.
Index ranges	-18 ≤ <i>h</i> ≤ 18, -28 ≤ <i>k</i> ≤ 28, -28 ≤ <i>l</i> ≤ 28	-17 ≤ <i>h</i> ≤ 17, -36 ≤ <i>k</i> ≤ 36, -25 ≤ <i>l</i> ≤ 25
Reflections collected	70771	74767
Ind. reflections	15864 [R(int) = 0.0354]	16176 [R(int) = 0.0872]
Completeness to $\theta = \text{max}$	99.6 %	99.9 %
Absorption correction	Multi-Scan	Multi-Scan
Refinement method	Full-matrix least-squares on F ²	Full-matrix least-squares on F ²
Data / restraints / parameters	15864 / 0 / 947	16176 / 75 / 736
Goodness-of-fit on F ²	1.054	1.022
Final R indices [I > 2 σ (I)]	R1 = 0.0514, wR2 = 0.1376	R1 = 0.0802, wR2 = 0.2115
R indices (all data)	R1 = 0.0864, wR2 = 0.1557	R1 = 0.1134, wR2 = 0.2483
Largest diff. peak and hole (e.Å ⁻³)	0.467 and -0.364	1.270 and -1.067

4. Results and Discussion

Inclusion of Isopropylamine in 4tBC4A

As previously noted, our efforts to investigate the inclusion chemistry of small amines such as propylamine had been hampered by the volatility of the amine (see Chapter III). Upon trying to produce an isopropylamine clathrate of 4tBC4A, we encountered similar problems. Preliminary diffraction data indicated the formation of a layered structural motif, suggesting the isopropylamine was too small to form the proton abstraction directed structures previously observed. Unfortunately, crystals suitable for a full structure determination could not be obtained.

The ^{13}C CP/MAS data, however, does tend to support this preliminary model of the inclusion of isopropylamine in 4tBC4A (see Figure 1). The spectrum is indicative of a highly symmetric structure, without crystallographic splitting observed in any of the host peaks. As a result, it is possible to resolve the resonances for all of the host carbons, although the resonance due to carbon 9 of 4tBC4A is extremely broad (which typically experiences minimal cross-polarization). Examination of the guest resonances suggests that the entire amine is included within the calixarene cavity, but the complexation induced shift is quite small in each case (see Table 2), such that this inclusion is likely quite shallow. Furthermore, the guest appears to be undergoing dynamic motion, as the 1' carbon resonance is retained upon dipolar dephasing. This also serves to explain the equivalence of the 2' carbons, which are likely indistinguishable due to rapid exchange on the NMR timescale due to rotation of the amine about the symmetry axis of the calixarene.

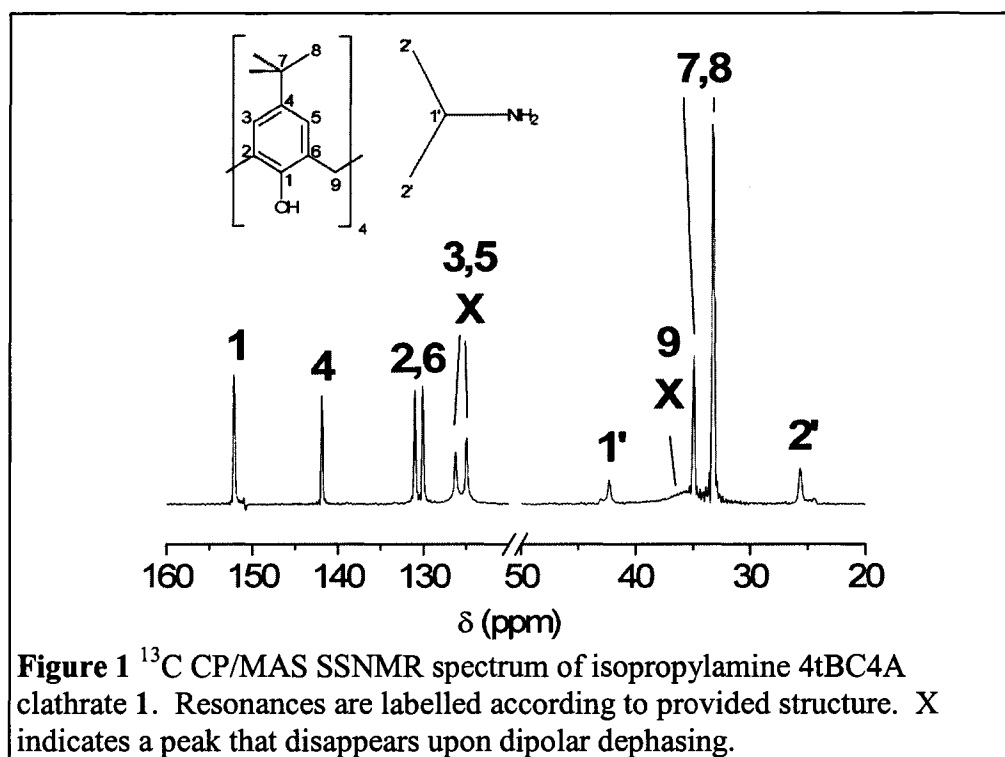


Table 2 ^{13}C CP/MAS NMR spectral data for clathrate 1.^[a]

Guest	Carbon	δ 4tBC4A ^[b] (± 0.05)	δ Solution ^[c]	CIS ^[d] (± 0.05)
Isopropylamine (1)	C1'	42.33	42.83	-0.50
	C2'	25.66	26.21	-0.55

^[a]All values are in ppm. ^[b]Chemical Shift observed in 4tBC4A clathrate. ^[c]Chemical shift of amine in solution, from SDBSWeb.^[54] ^[d]CIS=Complexation-induced shift=(δ 4tBC4A)-(δ Solution)

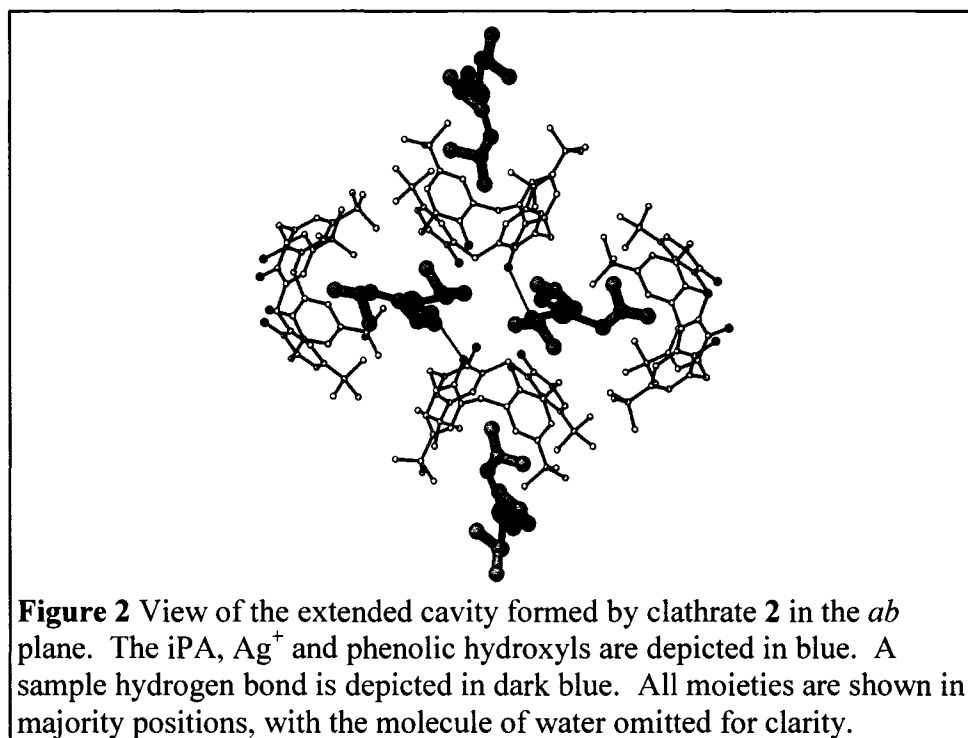
While the instability of the sample also served to prevent accurate PXRD and TGA analysis, a simple comparison of the SSNMR spectrum makes it quite apparent that a typical tetragonal 1:1 or 2:1 inclusion compound has been formed. Given the absence of host splitting and the small size of the amine, it would be reasonable to assume that the 1:1 form has been produced in this case. However, structural investigations at low temperature would serve to further clarify whether this structure is a result of a highly unstable hydrogen bonded amine clathrate, or whether the small size of the amine is totally insufficient to produce such a packing scheme. Regardless, it is clear that

hydrogen bonding with the calixarene alone at room temperature is insufficient to stabilize smaller amines in a capped motif.

Secondary Coordination and Isopropylamine Ag Complexes

Given the apparent need for additional stabilization to induce the inclusion of smaller amines in a capped motif, coordination to a metal centre appeared to be an ideal route to direct the structure towards such a motif. Unlike the neat isopropylamine clathrate, slow evaporation of 4tBC4A and AgNO₃ from isopropylamine (iPA) yielded large crystals that were suitable for single crystal X-ray diffraction. The resulting amine/silver-4tBC4A compound (clathrate **2**) has an asymmetric unit consisting of two silver cations coordinated by three molecules of isopropylamine each, with two 4tBC4A molecules, each serving as a host to a single isopropylamine from one cluster (see Figure 2). As before, in each cluster, one amine is included in an *endo* fashion, while the other two are found *exo* to the calixarene cavity.

As predicted, the structure assumes the distinctive capped motif previously observed for the *n*-alkylamines (see Chapters III and IV). The singly charged silver cations are balanced by the deprotonated 4tBC4A molecules, without any evidence of proton transfer to the amines. Only one of the six amines exhibits disorder, with two energetically equivalent conformers being observed (0.63:0.37 distribution). A single molecule of water is located at the centre of the structure, serving to further stabilize the resulting calixarene assembly (O...O distances of 2.91 and 3.04 Å), but does not interact with the silver coordination compounds. The silver centres, however, exhibit significant disorder over a number of positions.



Each coordination complex consists of a single site with approximately 0.90 occupancy, such that an [Ag(iPA)₃]⁺ compound is observed. For these majority positions, the coordination geometry is trigonal planar (Ag...N distances of 2.24, 2.25, and 2.34 Å), with hydrogen bonding between the *exo* amine and the capping calixarenes serving to further stabilize the complex (N...O distances of 2.91-3.06 Å). However, the silver occupies two sites in one cluster and three sites in the second corresponding to the formation of [Ag(iPA)₂]⁺ complexes (Ag...N distances of 1.80-2.00 Å), such that the *endo* amine is stabilized solely by inclusion in the calixarene. Given the low occupancies of these sites, such complexes are clearly disfavoured, but their existence make it apparent that the stabilization offered by coordination to silver is still not considerably greater than that to be offered by inclusion in the calixarene cavity.

Even in the face of coordination bonds, the stabilization through van der Waals interactions with the calixarene cavity is still sufficient to drive the motif towards the 3

guest : 1 host motif favoured to allow the maintenance of a two-fold axis of symmetry, instead of an anion induced tetrahedral arrangement similar to those formed by Ag(I) with halides.^[55, 56] The small size of the guest coordination compound is quite appropriate for maximizing each interaction in order of degree of stabilization: coordination to silver, followed by hydrogen bonding, followed by inclusion in the calixarene. This also indicates that the cation- π interactions characteristic of the calixarene ionophores^[38-40] are disfavoured even with a small guest which only minimally interacts with the calixarene cavity, such that the resulting structures are more similar to the metalloreceptors described by Loeb and others (where secondary coordination through van der Waals interactions partially guides the coordination geometry).^[57-64] Clearly, it is not the decreased symmetry of the compound, which is observed in most calixarene ionophores and metalloreceptors, but rather the favourability of amino-metal interactions and secondary coordination through hydrogen bonding and van der Waals interactions that prevent any such aromatic complexes from forming. In light of this, it is unlikely that any amine-metal complex based on free amine ligands would produce structures with discrete receptors like the calixarene ionophores, as the stabilization offered by the combination of primary and secondary coordination is much greater than that of primary coordination alone.

It would still be expected that for compound **2**, the four molecules of iPA not included within a specific 4tBC4A cavity in each asymmetric unit would be quite labile. Thermogravimetric analysis of dried crystals of clathrate **2** showed three regions of guest loss prior to sublimation of 4tBC4A at approximately 300°C with the weight percentage

lost corresponding to the loss of approximately 1 molecule of iPA each time (see Table 3). This suggests that as the *exo* amines are stripped away, the silver centres bind the remainder more tightly, such that the *endo* amines are only released just before the 4tBC4A sublimes, in fashion similar to *n*-butylamine-Ag⁺ clathrates. However, despite the increased stabilization due to coordination to the silver centre, as represented by the high temperatures required to desorb the amine when compared to the boiling point of isopropylamine (35°C), systematic investigation of the desorption process proved to be impossible due to the inability to obtain high quality PXRD and SSNMR data for the initial silver inclusion compound and desorption products.

Table 3 TGA data for isopropylamine Ag⁺ clathrate **2** with 4tBC4A.

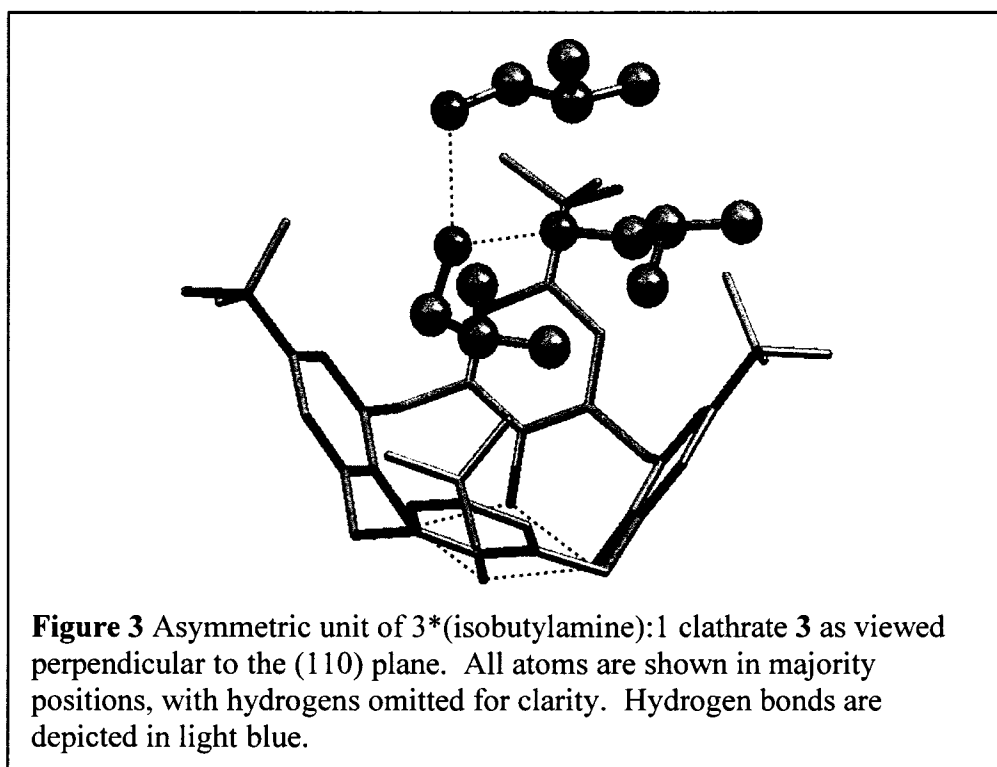
Clathrate	Temp. (°C) ^[a] (± 0.1)	% Wt. Lost ^[b] (± 0.01)	Mol. Guest Lost ^[c] (± 0.01)	<i>n</i> ^[d] (± 0.01)
IPA Ag ⁺ (2)	83.8-102.7	7.34	1.32	3.13
	161.2-181.8	5.99	0.95	
	256.3-259.2	6.29	1.00	

^[a]Temperatures are given for the onset and completion of transition. ^[b]Percentage of mass lost by sample. ^[c]Corresponding number of moles of guest lost by host. ^[d]Overall Guest to Host Ratio=(Total % Wt. Lost)/(1-Total % Wt. Lost)*(Mol. Wt. of Host)/(Mol. Wt. of Guest)

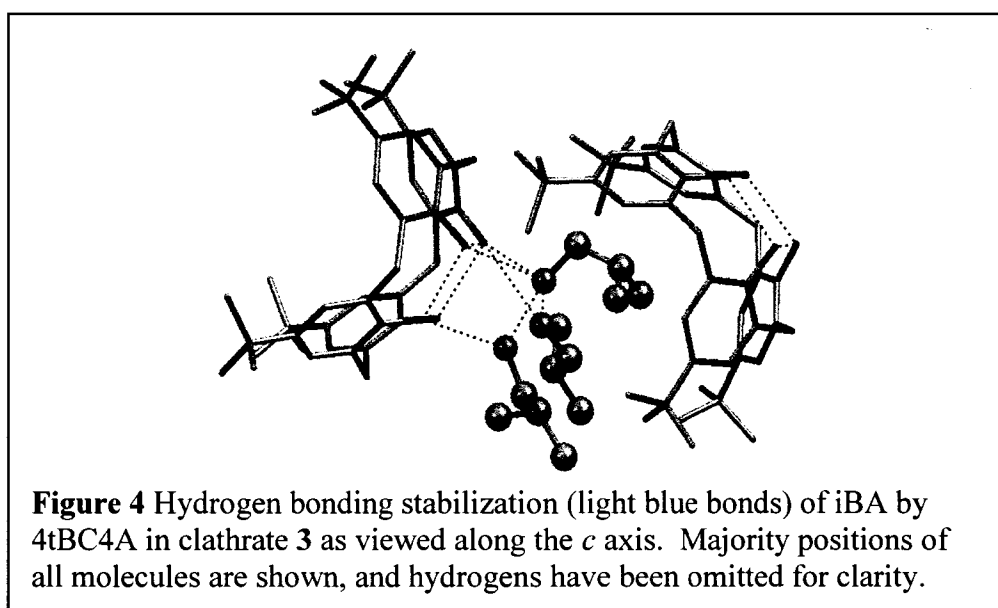
Enclathration of Isobutylamine by 4tBC4A

Given the difficulties in working with isopropylamine, it was hoped that larger amines might prove to produce more stable, and therefore, more easily studied clathrates. More importantly, the apparent effect of the small size of the guest in driving the packing scheme towards a motif where all forces were satisfied, as opposed to one merely being ignored in favour of the stronger interactions, suggested that such compounds would be quite useful in tuning the capped motif, by forcing the calixarene lattice to shift to accommodate the three competing forces simultaneously.

Recrystallization of 4tBC4A from iBA results in the formation of blocky crystals of clathrate **3**, with the details of the crystal structure of **3** and its refinement found in Table 1. The 3 Guest:1 Host stoichiometry is consistent with the previous studies of enclathration of *n*-alkylamines by 4tBC4A (see Chapter III).^[29] As with the inclusion of *n*-butylamine and *n*-amylamine, this stoichiometry is the result of the inclusion of a single *endo* amine located within the calixarene cavity and two additional *exo* amines found outside of the calixarene (see Figure 3). Both the *endo* amine and a single *exo* amine are disordered over two positions with occupancy ratios of 0.53:0.47 and 0.86:0.14 respectively. One of the tertiary butyl groups of the calixarene is also disordered over two positions, with an occupancy ratio of 0.59:0.41, suggesting that this disorder is induced by the motion of the *endo* amine.

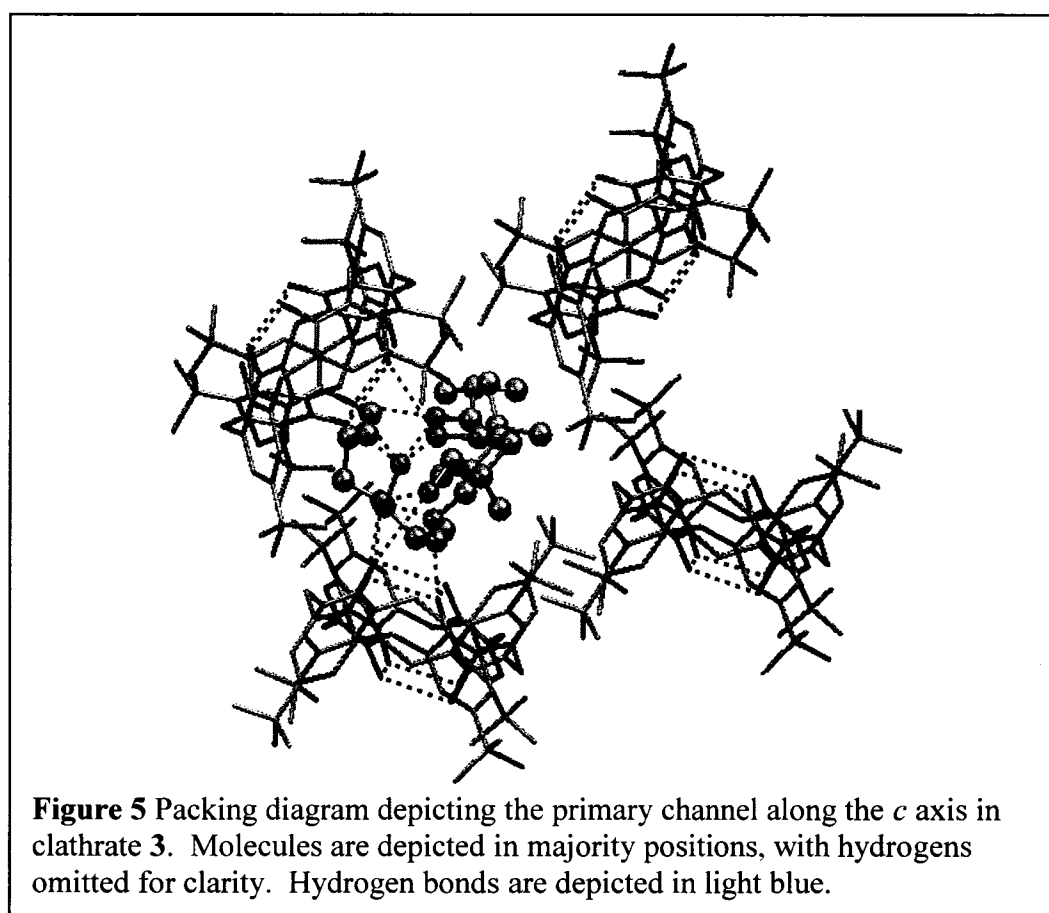


Once again, a single phenolic hydroxyl is observed to have been deprotonated by the *endo* amine, destroying the host symmetry such that the four fold symmetric 1:1 and 2:1 inclusions are precluded. Instead, an extensive hydrogen bonded network is formed to stabilize the resulting clusters. The *endo* amine serves as a hydrogen bond donor to both of the *exo* amines (N...N distances of 2.89 and 2.94 Å). These amines also form a series of hydrogen bonds to the phenolic hydroxyl groups of an adjacent calixarene (N...O distances of 2.76, 2.92, 3.00 and 3.03 Å, see Figure 4). In order to accommodate this bonding, the NH₃ of the *endo* amine is twisted upward out of the plane formed by the carbon backbone, unlike those of the *exo* amines.



While the dual stabilization by van der Waals interactions and hydrogen bonding is consistent with the structural trends observed for the *n*-alkylamines, the overall packing scheme only bears a passing resemblance to the one previously observed for comparable *n*-alkylamines, where capped cavities formed a channel along the *a* axis.^[29] The amine clusters are assembled in an infinite channel along the *c* axis with a cross-section of

approximately 10.7 by 11.3 Å. While each segment is defined by four molecules of 4tBC4A (see Figure 5), no true capping is observed in this case. Only two calixarenes serve as a van der Waals host and a hydrogen bond donor, respectively. The phenyl rings of a second pair of calixarenes form the other walls of the channel. Unlike the motifs observed with difunctional amines, there is no interaction between the individual amine clusters.^[31]



This new channelled structure is directly attributable to the decrease in overall length when compared to the *n*-alkylamines. The three crystallographically distinct amines in the 3(*n*-butylamine):1(4tBC4A) clathrate are all found in an all *trans* configuration, such that distance from the N to the terminal C of the three

crystallographically unique amines are all approximately 5 Å, while the three unique isobutylamine molecules in **3** have lengths of 3.80, 3.81 and 2.97 Å. The resulting clusters are too small to support hydrogen bonding to two distinct calixarenes, resulting in the contracted capping. This also gives rise to twisting of the channel along the *c* axis, as now the neighbouring units of 4tBC4A have opposite orientations, causing the hydrophobic calixarene cavity serving as host to the *endo* amine to be staggered around the channel.

These structural insights are also supported by the ¹³C CP/MAS NMR spectrum of the compound as synthesized, indicating that the SCXRD structure is reflective of the bulk sample (see Figure 6A). The upfield resonances due to the aromatic portion of 4tBC4A show considerable splitting, which is indicative of the decreased symmetry of the host. In particular, the four-fold split resonances due to carbon 1 (156.2-150.0 ppm) and carbon 4 (142.8-138.6 ppm) characteristic of the presence of a single calixarene unit in the crystallographic asymmetric unit. The resonances due to carbons 2 and 6 show no splitting due to near magnetic equivalence arising from their similarity, while the resonances due to carbons 3 and 5 are assigned in light of their disappearance upon dipolar dephasing.

Similarly, the guest resonances exhibit splitting representative of the two environments the amines reside in. Dipolar dephasing results in the effective elimination of almost all but the methyl peaks upon dipolar dephasing. However, small residual signals due to 1' and 2' are observed, suggesting possibly some small motion that interferes with dephasing, suggesting that while the disorder is largely static on the NMR

timescale, some dynamics may be at play. A three fold splitting of the resonance due to carbon 1' is observed, with the two upfield resonances assigned readily to the deshielded *exo* amines, and the downfield resonance to the shielded *endo* amine (see Table 4).

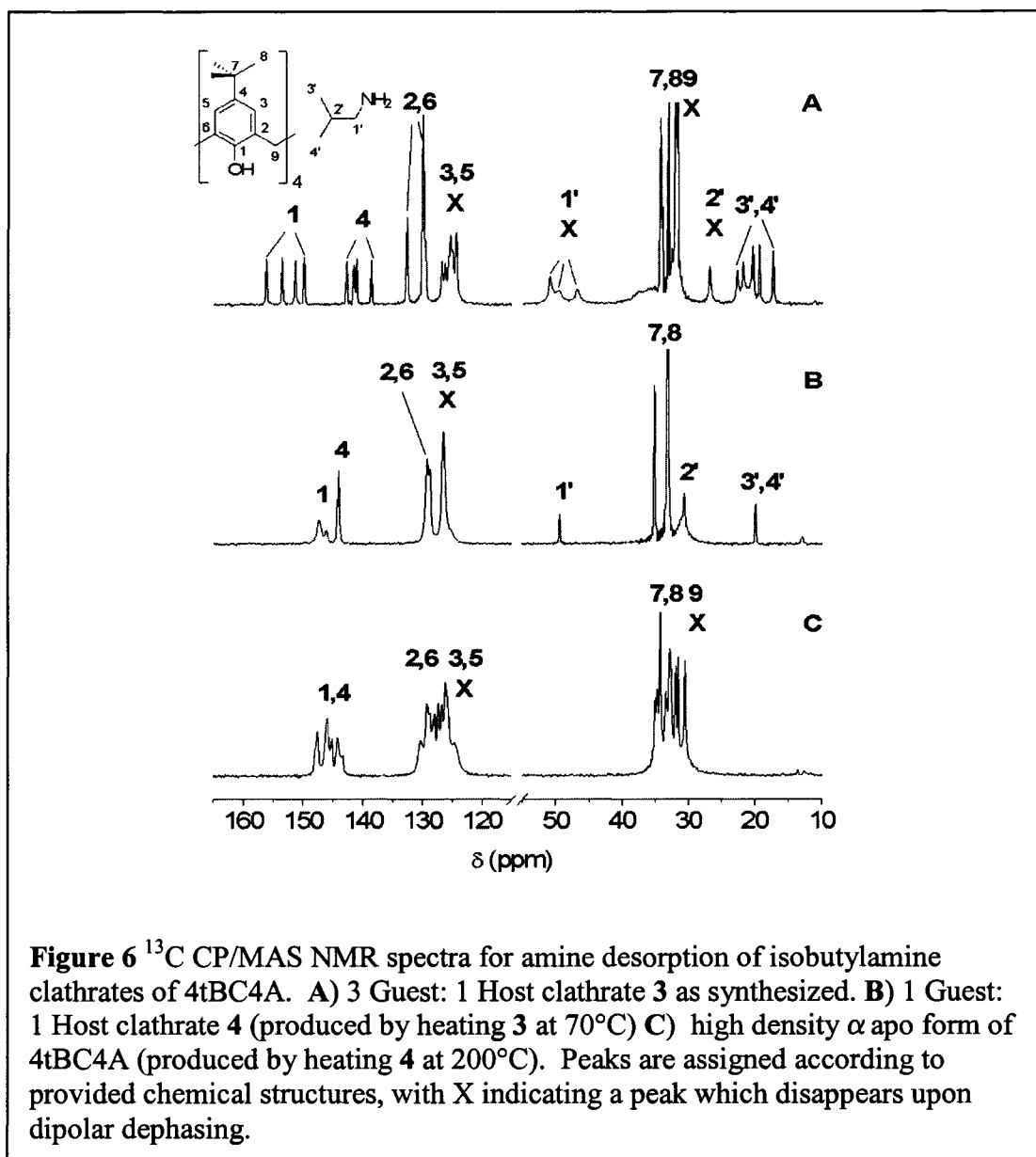


Table 4 Comparison of ^{13}C CP/MAS NMR spectral data for clathrates 3 and 4 to solution NMR data.^[a]

Guest	Carbon	δ Soln. ^[b]	δ 3 ^[c] (± 0.05)	CIS for 3 ^[d] (± 0.05)	δ 4 ^[c] (± 0.05)	CIS for 4 ^[d] (± 0.05)
Isobutylamine	C1'	50.22	50.88	+0.66	49.40	-0.82
			49.71	-0.51		
			46.81	-3.41		
	C2'	31.57	26.81	-4.76	30.70	-0.87
	C3',C4'	20.02	22.67	+2.65	19.89	-0.13
			21.84	+1.82		
			20.34	+0.32		
19.37			-0.65			
		17.31	-2.71			

^[a]All values are in ppm. ^[b]Chemical shift of amine in solution, from SDBSWeb.^[54]

^[c]Chemical Shift observed in 4tBC4A clathrate. ^[d]CIS=Complexation-induced shift=(δ clathrate)-(δ Solution)

Given the apparent lack of significant dynamic motion, the broadening of the resonance is likely due to coupling to the nitrogen. The resonances due to carbon 2' are largely obscured by the aliphatic resonances of the host, such that only the heavily shielded *endo* amine peak is observed. This corresponds well to the crystal structure, which indicated that the 2' carbon is the most deeply included carbon in the amine. For the 3' and 4' carbons, both resonances can be distinguished for the *exo* amines, while only one methyl peak is observed for the *endo* amine, which is also likely due to the fact that the two groups are nearly mirror images of each other (resulting in pseudo-crystallographic equivalence).

Desorption behaviour of Isobutylamine 4tBC4A Clathrate 3

As demonstrated previously, there is a clear relationship between the degree of stabilization experienced by amine guests and the desorption behaviour of the clathrate (see Chapters III and IV).^[30, 32] However, in spite of the shift in structural motif, thermogravimetric analysis shows an overall desorption pattern comparable to that

observed for the *n*-alkylamines (see Table 5). Two major transitions are observed, with the weight percentages lost corresponding well to the loss of two molecules of iBA, followed by the subsequent loss of one more molecule. Furthermore, the Ag⁺ coordinated amines exhibit further stabilization above that experienced by the pure amine clathrate, as represented by the increased temperature required to remove the amines. However, upon carrying out thermal desorption upon bulk samples of **3**, it immediately became apparent that the shift in structural motif also has an impact on the desorption process.

Table 5 TGA data for isobutylamine clathrate **3** and isobutylamine Ag⁺ Clathrates **7** and **11** with 4tBC4A.

Clathrate	Temp. (°C) ^[a] (± 0.1)	% Wt. Lost ^[b] (± 0.01)	Mol. Guest Lost ^[c] (± 0.01)	<i>n</i> ^[d] (± 0.01)
Isobutylamine (3)	49.8-64.3	17.19	2.04	2.99
Partially Loaded iBA Ag ⁺ (7)	143.0-162.4 57.9-86.6	8.01 17.19	0.95 2.15	3.20
Fully Loaded iBA Ag ⁺ (11)	178.6-196.9 58.2-107.6	8.40 14.64	1.05 1.97	3.17
	144.8-242.1	8.92	1.20	

^[a]Temperatures are given for the onset and completion of transition. ^[b]Percentage of mass lost by sample. ^[c]Number of moles of guest lost by host. ^[d]Overall Guest to Host Ratio=(Total % Wt. Lost)/(1-Total % Wt. Lost)*(Mol. Wt. of Host)/(Mol. Wt. of Guest)

The ¹³C CP/MAS NMR spectra of the desorbed samples are shown in Figures 6B and 6C. Upon heating to 70° C, a considerable degree of simplification in the peak splitting of both the host and the guest is observed. This suggests that the system has been transformed into a highly symmetrical form (clathrate **4**), consistent with the disruption of the stabilizing hydrogen bonds which led to the destruction of the four-fold symmetry favoured by the calixarene.^[32] Given the absence of splitting of the host or guest peaks,

this suggests the asymmetric unit of **4** contains only one molecule of 4tBC4A for each molecule of iBA. This lone amine does not appear to be deeply included in the calixarene cavity, with only a marginal CIS observed for each guest resonance (see Table 4). Given the persistence of all the guest peaks in the dipolar dephased spectrum, this is likely the result of the dynamic motion of the guest to accommodate this new four-fold symmetry.

The PXRD pattern arising from this clathrate is readily indexed to the $P4/n$ tetragonal unit cell of a 1 Guest: 1 Host inclusion compound of 4tBC4A. The cell exhibits a modest amount of expansion along the *c* axis due to the poorly included molecule of iBA forcing the layers apart (see Figure 7B and Table 6). Upon further heating at 200°C (see Figure 7C), the resulting PXRD pattern exhibits an increase in complexity when compared to that of clathrate **3**. Qualitative analysis indicates that this pattern is that of the two fold symmetric, densely packed α *apo* form of 4tBC4A first produced through recrystallization of 4tBC4A from tetradecane.^[7] Indeed, this pattern is easily indexed to the unit cell parameters of the α *apo* form of 4tBC4A (see Table 6).^[65]

At first glance, this behaviour is a rather dramatic contrast with that previously observed for the *n*-alkylamines (see Chapter III),^[29] where *endo* inclusions showed a preference for forming the four-fold symmetric, low density β *apo* form of 4tBC4A. However, it can be rationalized upon closer examination of the structure of clathrate **3**. The arrangement of the channels in clathrate **3** results in a motif where the calixarenes are ideally positioned to fold into each other, introducing a predisposition towards such close packing as seen with the layered *exo* inclusions of *n*-alkylamines. The *endo* inclusions of *n*-alkylamines lack this structural arrangement, presumably making the crystalline

transformation to a layered low density packing scheme much more favourable.

Therefore, amine size as a director of *endo* or *exo* inclusion behaviour is not the sole factor which determines the desorption behaviour. Instead, it is the more general application of amine size as one of the forces competing to influence the overall packing motif that appears to guide the selection of the *apo* form.

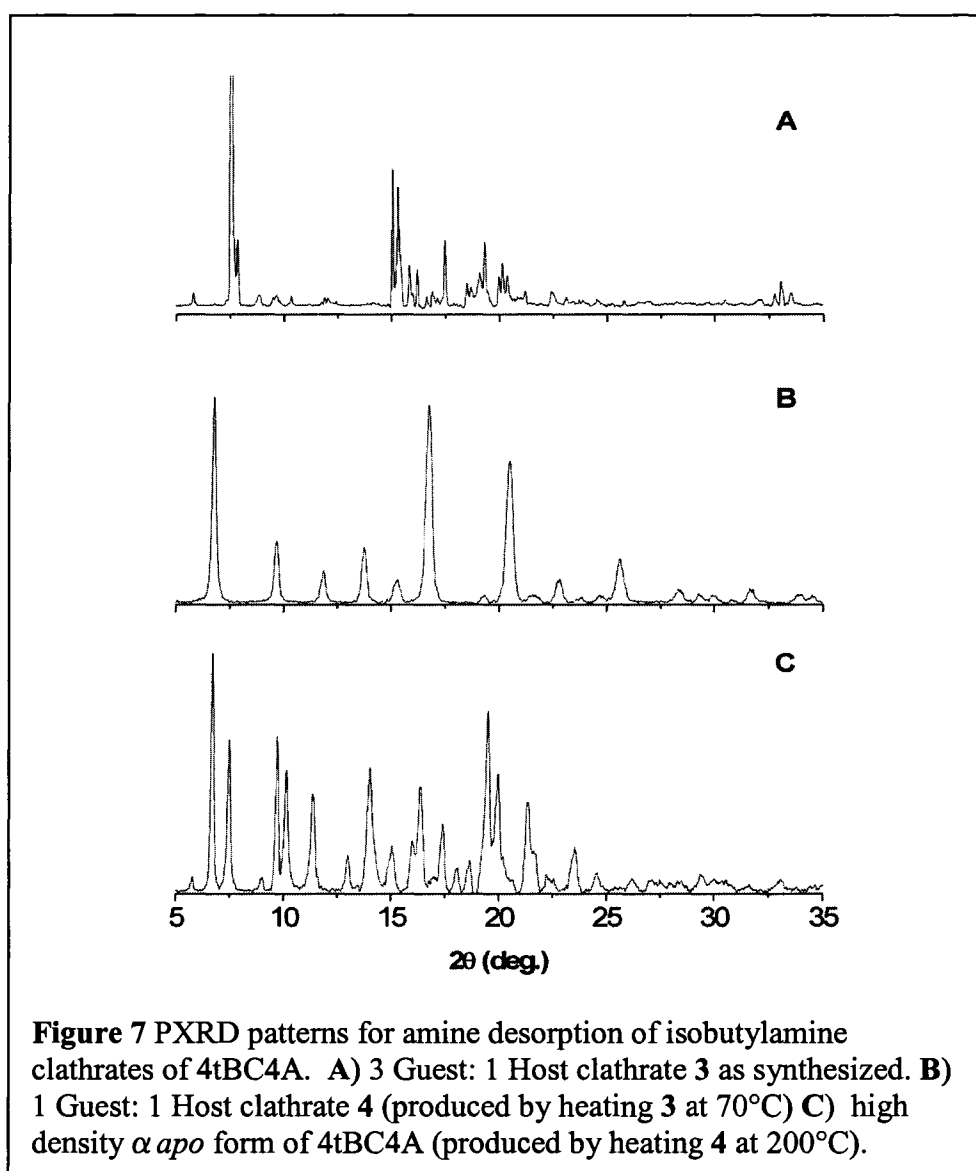


Table 6 Unit cell parameters for clathrates **3**, and its desorption products **4** and the α *apo* form of 4tBC4A as determined by PXRD.

	Clathrate 3	Clathrate 4	α <i>apo</i> form of 4tBC4A
Space Group	<i>P2</i> ₁ / <i>c</i>	<i>P4</i> / <i>n</i>	<i>P2</i> ₁ / <i>c</i>
<i>a</i> /Å	11.476	12.972	9.7327
<i>b</i> /Å	19.998	12.972	30.920
<i>c</i> /Å	23.347	13.085	13.556
α /deg.	90	90	90
β /deg.	93.74	90	109.9
γ /deg.	90	90	90
<i>V</i> /Å ³	5346.8	2201.8	3836.6

Supramolecular Solid Solutions of isobutylamine-Ag complexes

The influence of the size and geometry of the amine in dictating the structural motif of clathrate **3** raised intriguing questions as to how isobutylamine-Ag⁺ coordination complexes would be enclathrated by 4tBC4A. For the pure amine compound, the hydrogen bonding is more limited due to the small size of the amine forcing contraction of the calixarene lattice, while van der Waals stabilization has been retained in preference to forming layered structures that allow for inclusion of Ag(I) halide type infinite networks.^[55, 56] Given the structural shifts in the iPA-Ag⁺ 4tBC4A clathrate structure, a coordination complex involving iBA would also adapt to the small size of the amine and the constraints this places on the calixarene packing. Alternatively, the addition of metal coordinative interactions to a collapsed calixarene system like this might force the packing motif to finally resemble the discrete receptor motifs of calixarene ionophores^[38-40] and metalloreceptors,^[57-64] if the framework can not withstand any further distortions due to additional forces. The inclusion of an analogous flexible silver complex presented an ideal opportunity to investigate how significant these secondary coordinate

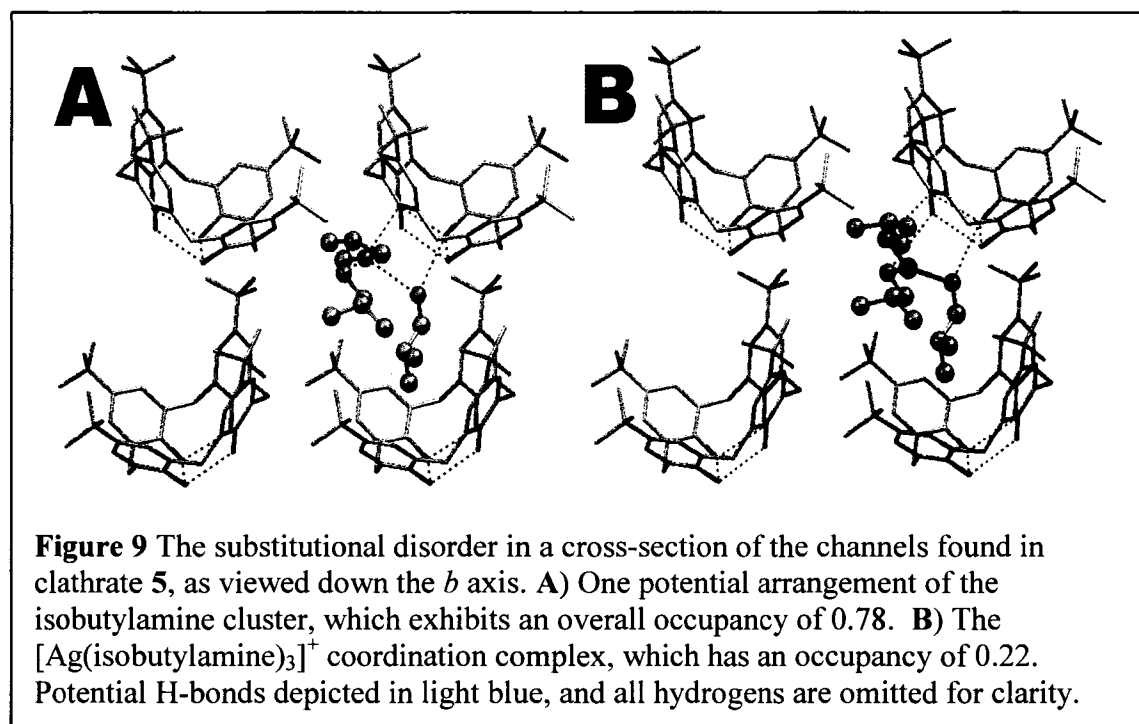
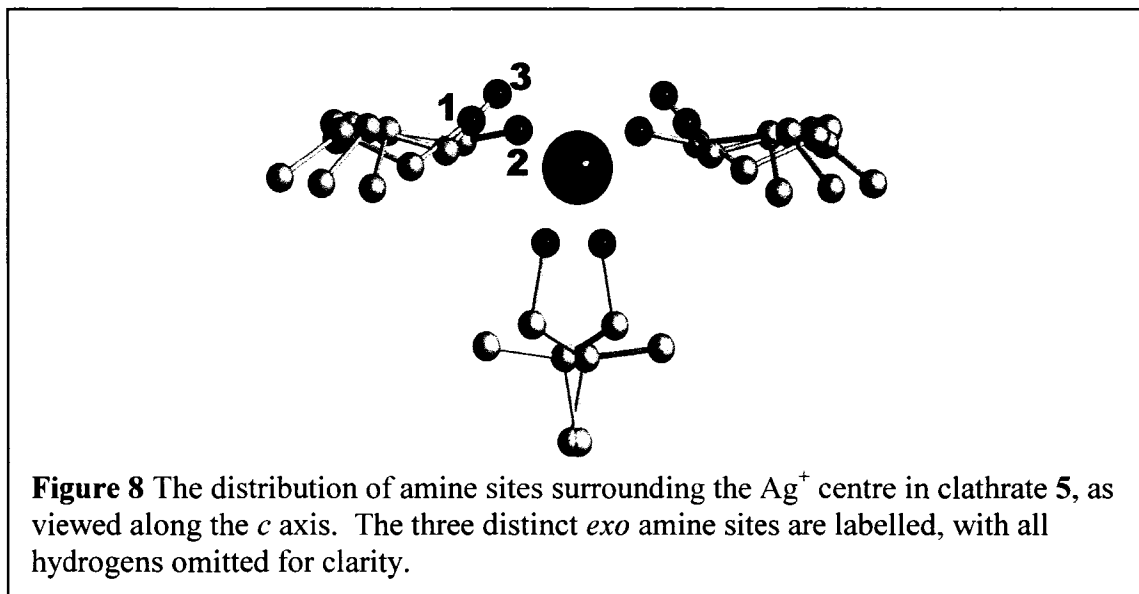
interactions are in directing the structures, and determining the stability of such compounds.

Crystals of clathrate **5** were readily produced by evaporation of a solution of 4tBC4A and AgNO₃ in iBA. However, initial attempts to understand the structure of **5** by SCXRD were frustrating. While the host and amine guests were readily identified, there was a region of electron density located between the amines that could not be adequately described using a fully occupied Ag⁺ atom as a model. After ruling out the possibility of other atoms accounting for this density, it became apparent that it was, in fact, a silver site with an occupancy of only 22%.

Clathrate **5** crystallizes in the *Pnma* space group (see Table 1), such that the silver site lies on a mirror plane. This mirror plane also bisects the calixarene, such that only two crystallographically unique molecules of iBA are observed. The *endo* guest lies across the mirror plane, such that it exhibits a 50:50 disorder over two positions. The second guest is *exo* to the calixarene and is disordered over three positions (in addition to being reflected across the mirror plane), with occupancy ratios of 0.33:0.32:0.33 (sites 1, 2 and 3, see Figure 8). However, the overall stoichiometry of clathrate **5** is 3(iBA):0.22(Ag⁺):1(4tBC4A)⁻, such that the structural motif observed in the silver-free clathrate **3** is maintained.

Once again, one *endo* and two *exo* amines are included in a series of channels arising from the staggered arrangement of the calixarenes serving as the host to the *endo* amine, such that only one other molecule of 4tBC4A can serve as a hydrogen bond acceptor (N...O distances of 2.72 to 3.10 Å). The two remaining units of 4tBC4A are

turned such that their phenyl rings serve as non-interacting walls (see Figure 9). With the increased symmetry of the framework, this channel is now located parallel to the (011) plane, such that a new secondary channel just large enough to accommodate the *exo* amines (3.75 Å across, ignoring hydrogens) is formed down the *c* axis.



A closer examination of the crystallographically unique guests helps to reveal the origin of this low level of silver loading. The *endo* guest is easily positioned to coordinate to the Ag⁺ centre when it is present, with an Ag...N bond distance of 2.19 Å observed. The same is true for site 1 and 3 of the *exo* amine, which have Ag...N bond distances of 2.30 and 2.38 Å. However, site 2 is positioned too close to the silver centre (predicted Ag...N bond distance of 1.34 Å) to allow for it to be present at the same time as the silver. The structure is therefore the result of substitutional disorder, with clathrate 4 consisting of a mixture of enclathrated [Ag(iBA)₃]⁺ and clusters of three molecules of iBA, where one molecule of iBA in the cluster is protonated in order to maintain charge balance.

This prompted the question as to whether the loading of the silver within a calixarene framework could be controlled through substitutional disorder involving complexes with iBA. The initial attempts focused on simply varying the ratio of Ag to 4tBC4A between 1.28:1 (the conditions under which clathrate 5 was synthesized) and 2.00:1. Impressively, not only did the increase in silver concentration lead to significantly increased silver content in clathrates 6 through 10 (see Tables 1 and 7), the intermolecular interactions also remain intact, such that the resulting structures are isostructural to clathrate 5. This relationship is largely linear, with increased silver concentration giving rise to increased silver loading from 0.22 to 0.42 silver occupancy (with only slight variations within individual syntheses observed). Given this, it appears that this family of clathrates arises from the formation of a solid solution between the amine clusters and silver coordinate complexes.

Table 7 Comparison of the structural and synthetic parameters of the family of clathrates **5** to **10**, which together represent the formation of a supramolecular solid solution.

	5 (POB79)	6 (POB80)	7 (POB100)	8 (POB98)	9 (POB96)	10 (POB97)
Ag:Calix Ratio for Synth.	1.28:1	1.28:1	1.54:1	1.43:1	2.00:1	2.00:1
Ag % in Structure	0.219	0.226	0.295	0.343	0.388	0.423
<i>a</i> (Å)	19.879	19.884	19.887	19.881	19.894	19.902
<i>b</i> (Å)	23.438	23.455	23.479	23.531	23.582	23.604
<i>c</i> (Å)	11.222	11.225	11.203	11.194	11.192	11.195
<i>V</i> (Å ³)	5228.4	5235.2	5230.7	5236.7	5250.8	5258.7
Site 1 Occup.	0.33	0.36	0.41	0.46	0.55	0.55
Site 2 Occup.	0.32	0.34	0.30	0.27	0.23	0.23
Site 3 Occup.	0.33	0.30	0.27	0.25	0.19	0.22

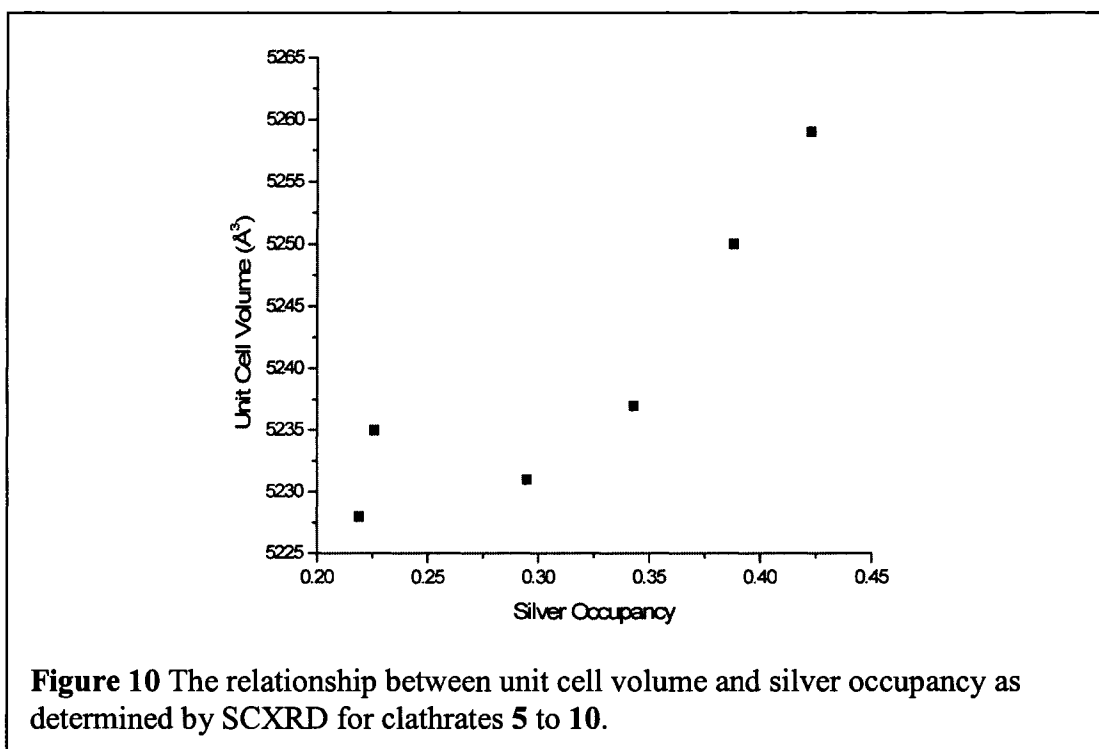
Solid solutions arise when components of a crystal lattice can be randomly

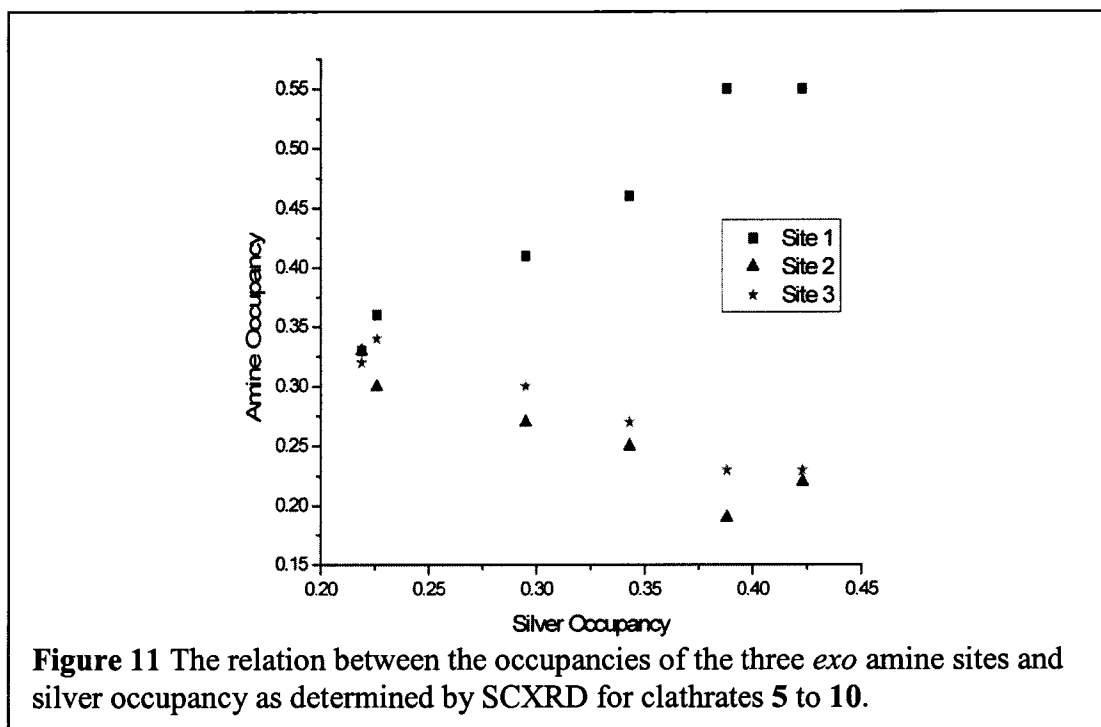
substituted for each other without significantly distorting the structure. In practical terms, this means that the components have very similar volumes and geometries such that the structural motif remains largely unchanged, as well as identically charged. As a result, solid solutions are quite commonly observed in clathrate hydrates,^[66, 67] minerals^[68] and certain pharmaceutical formulations,^[69] but have rarely been seen in supramolecular organic frameworks.^[70, 71] In particular, no such behaviour has been reported in the calixarene ionophores and metalloreceptors, which, while typically being designed to have an affinity for specific metal centres, might be expected to exhibit such behaviour. However, solid-state studies of such systems typically do not examine potential arrays of cations for inclusion, and thus the substitutional disorder that might give rise to a solid solution is not possible. Therefore, these clathrates represent the first example of solid solutions in such a hybrid organic-inorganic framework.

This solid solution also indicates that even in a framework where the calixarene packing motif is heavily constricted, suggesting possible instabilities due to reduced interactions between the calixarene and the amine complex, discrete receptors similar to calixarene ionophores or metalloreceptors will not result. Despite the energetic equivalence of the metal complex and amine complex, even the reduced number of secondary interactions observed to stabilize these guests is favoured over any of the discrete motifs relying upon cation- π interactions^[38-40] or other direct interactions between the calixarene and the metal.^[57-64, 72-74] Once again, this indicates that while the calixarene ionophores and metalloreceptors are well suited to metal binding, their efficiency is a result of sacrificing structural complexity and versatility, such that the role of the calixarene as secondary coordinate ligand is restricted.

In this case, the small size of the amine gives rise to a structural motif that restricts the maximum number of calixarene units capable of stabilizing the resulting structures. Therefore, the inclusion of the coordination complex over the amine cluster is not favoured on either an enthalpic or entropic basis, as both will be stabilized in an identical fashion, rendering them identical for the purposes of substitution. Therefore, the ensuing substitutional disorder represents the relative availability of silver in the bulk solution, with an increased concentration of silver leading to increased silver loading in the calixarene framework. In such a case, the subtle shifts in the structure arising from the changes in substitution provide us with insight as to the forces involved in guiding the formation of the clathrates, as well as helping to distinguish between the structures favoured by each type of cluster.

This can most easily be visualized by comparisons of the volume and *exo* amine occupancies in relation to the silver loading. As can be seen from Figure 10, the volume of the unit cell increases modestly with increased silver loading. This arises from an expansion along the *b* axis attributable to the silver clusters forcing the structure to expand to better accommodate secondary coordinate interactions with the cluster. Similarly, increased silver loading results in *exo* amine site 1 being preferred over sites 2 and 3 (see Figure 11), indicating that coordination also leads to increased ordering of the amines to facilitate structural stabilization through directional secondary interactions (*i.e.*, hydrogen bonding). It also clarifies that sites 2 and 3 are likely representative of the structure of the pure amine complex.





Fully Loaded Isobutylamine-Ag 4tBC4A Frameworks

While solid solutions of many binary alloys extend across the entire range of composition, such behaviour is not expected in this system. For this solid solution, the two clusters must remain structurally similar, such that the supramolecular stabilization of the two by the calixarene framework remains largely indistinguishable. However, as the concentration of silver increases in the amine solution, one would expect that it would become increasingly energetically favourable for the calixarene framework to shift to fully accommodate the large number of silver complexes being generated, leading to the exclusion of the amine clusters from such structures. This is also alluded to by the subtle shifts in the structural parameters of the solid solutions with increasing silver loading.

Upon moving to even higher concentrations of silver, the solid solution is indeed disrupted, and new phases emerge. In order to obtain a clathrate with full silver loading,

it is necessary to use a comparatively large amount of AgNO₃ in the synthesis, such that the ratio of Ag to Calix is 4:1. The resulting clathrate **11** exhibits the expected stoichiometry of 3(iBA):1(4tBC4A):1(Ag⁺). However, it crystallizes in the triclinic *P*-1 space group, exhibiting a dramatic drop in symmetry when compared to both the simple amine clathrate **3** and the solid solutions as represented by clathrates **5-10**. The actual asymmetric unit of the compound consists of two molecules of 4tBC4A, six molecules of iBA and two Ag⁺ centres.

This drop in symmetry is the result of inclusion of two types of Ag⁺ coordination compounds: a three coordinate complex, and a two coordinate complex. The [Ag(iBA)₃]⁺ complex consists of a single *endo* amine and two *exo* amines coordinated to the silver, with a trigonal planar geometry similar to that observed for clathrates **3** and **5** (see Figure 12). All three amines are fully ordered, and the Ag...N distances are somewhat shorter than those in clathrate **5** (2.27 to 2.29 Å). The [Ag(iBA)₂]⁺ complex is composed of two *exo* amines bound to the silver, with the resulting Ag...N distances proving even shorter (2.09 and 2.16 Å). The single *endo* amine associated with the calixarene endcap of the cavity serves as a secondary coordinate ligand, hydrogen bonding to one *exo* amine (N...N distance of 3.09 Å, see Figure 13), as well as serving as an intermediary for secondary stabilization by van der Waals interactions with the calixarene cavity. All three of these amines are disordered over two positions, with the *exo* amines having 0.79:0.21 and 0.81:0.19 occupancy distributions, and the *endo* amine sites having a 0.61:0.39 distribution.

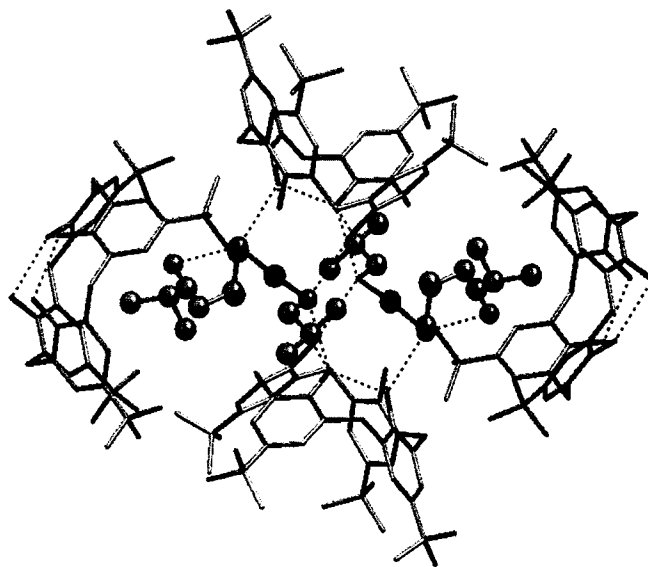


Figure 12 The capped cavity containing the $[\text{Ag}(\text{iBA})_2]^+$ complex in clathrate **11**, as seen from a viewpoint perpendicular to the (110) plane. Only majority positions are shown, with hydrogen bonds are depicted in light blue, with hydrogen omitted for clarity.

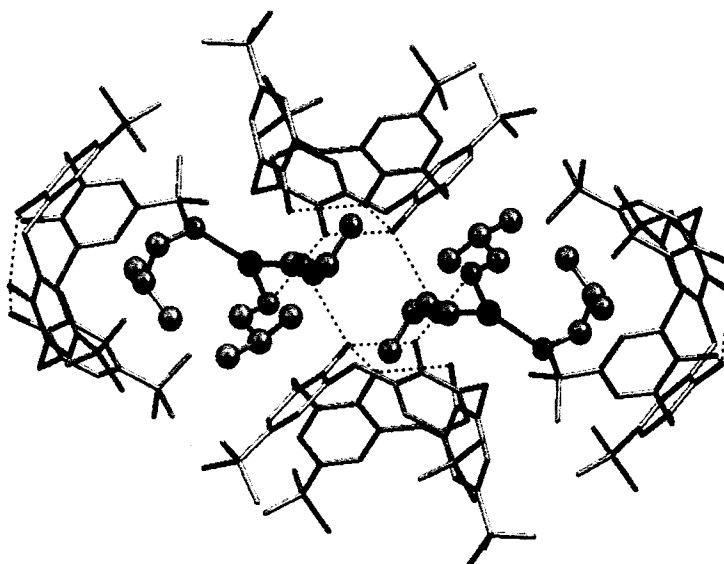
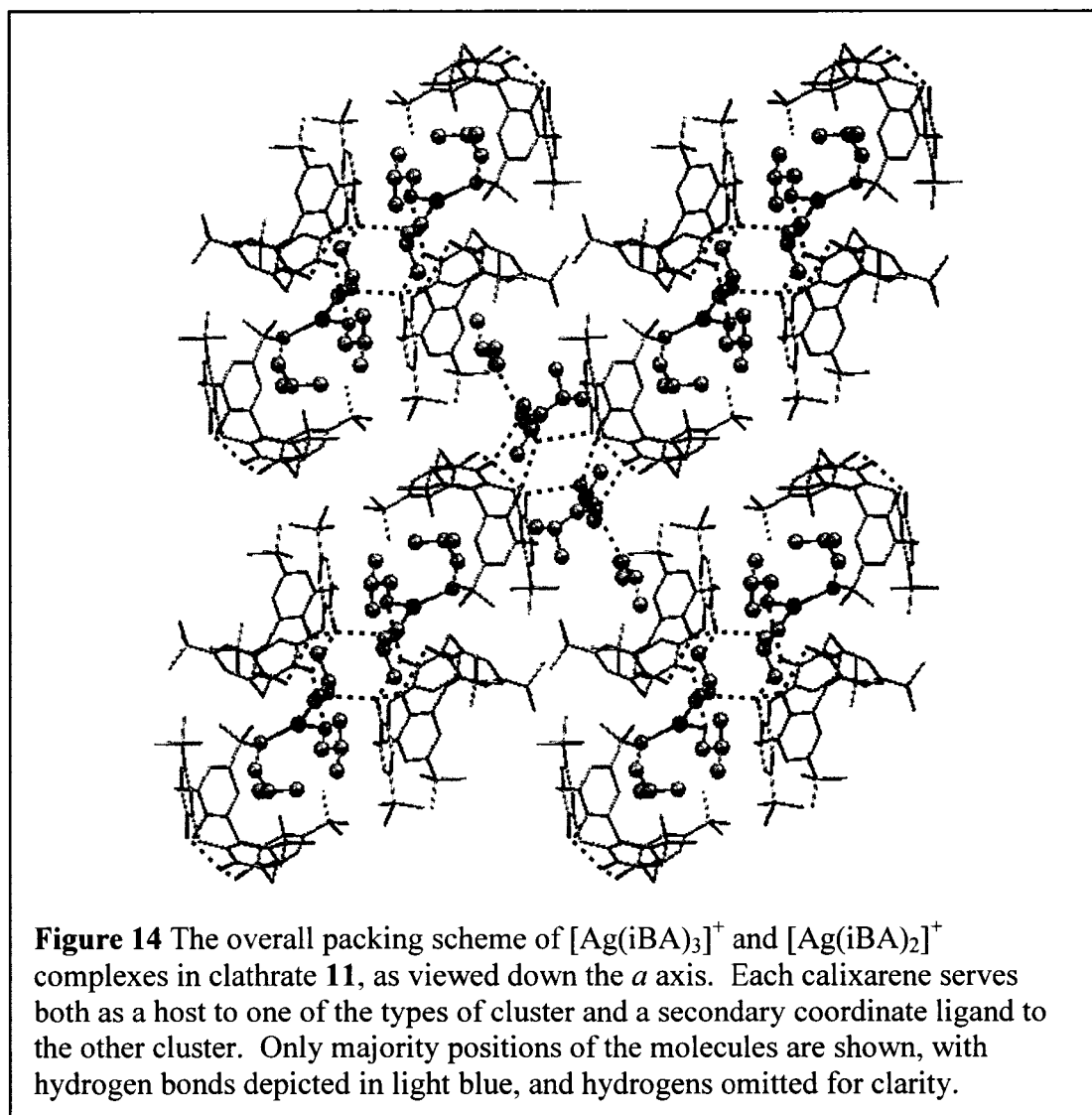


Figure 13 The capped cavity containing the $[\text{Ag}(\text{iBA})_3]^+$ complex in clathrate **11**, as seen along the (011) plane: Only majority positions are shown, with hydrogen bonds are depicted in light blue, with hydrogen omitted for clarity.

In both cases, the cavities containing the amine clusters are aligned along the *a* axis, such that a series of channels are formed. In each case, a pair of complexes is found in each cavity, with the phenolic hydroxyls from two calixarenes forming hydrogen bonds with four amines (O...N distances of 3.02 and 3.06 for [Ag(iBA)₃]⁺; 2.85 and 2.95 Å for [Ag(iBA)₂]⁺), such that they serve as secondary coordinate ligands. Each of these hydrogen bonding calixarenes also serve as van der Waals hosts to the endo amine of the opposing coordination complex, such that the two coordinate and three coordinate complexes are juxtaposed consistently throughout the structure (see Figure 14). The resulting overall packing scheme is consistent with the capped structure previously observed in other alkylamines (see Chapters III and IV).^[30, 31]

It therefore appears that the phase shift at higher loadings is the combined result of a structural shift to fully accommodate secondary coordination through both hydrogen bonding and van der Waals interactions to stabilize the complexes, as well as the introduction of a second coordination compound, completing the shift predicted by the iPA Ag⁺ 4tBC4A clathrate **2**. While such mixed coordination compounds are well known for various flexible transition metals and amine ligands,^[75-78] again this is a behaviour not observed in the calixarene ionophores and metalloreceptors, the closest related calixarene based metal coordination systems. Presumably, the inclusion of the second coordination compound is the result of a packing compromise to maximize the efficient filling of void space within the structure, which is not necessary in the discrete receptor structures formed by the calixarene ionophores. Given the previously observed structures, one would assume that the three coordinate complex forms initially to

template the self-assembled framework, with the two coordinate complex then being prompted to form in order to complete the formation of the observed framework. The self-assembly process therefore is both controlled by and involved in controlling the formation of the coordination complexes, giving rise to a rather intriguing example of molecular recognition dependent on the coordinative flexibility of silver.



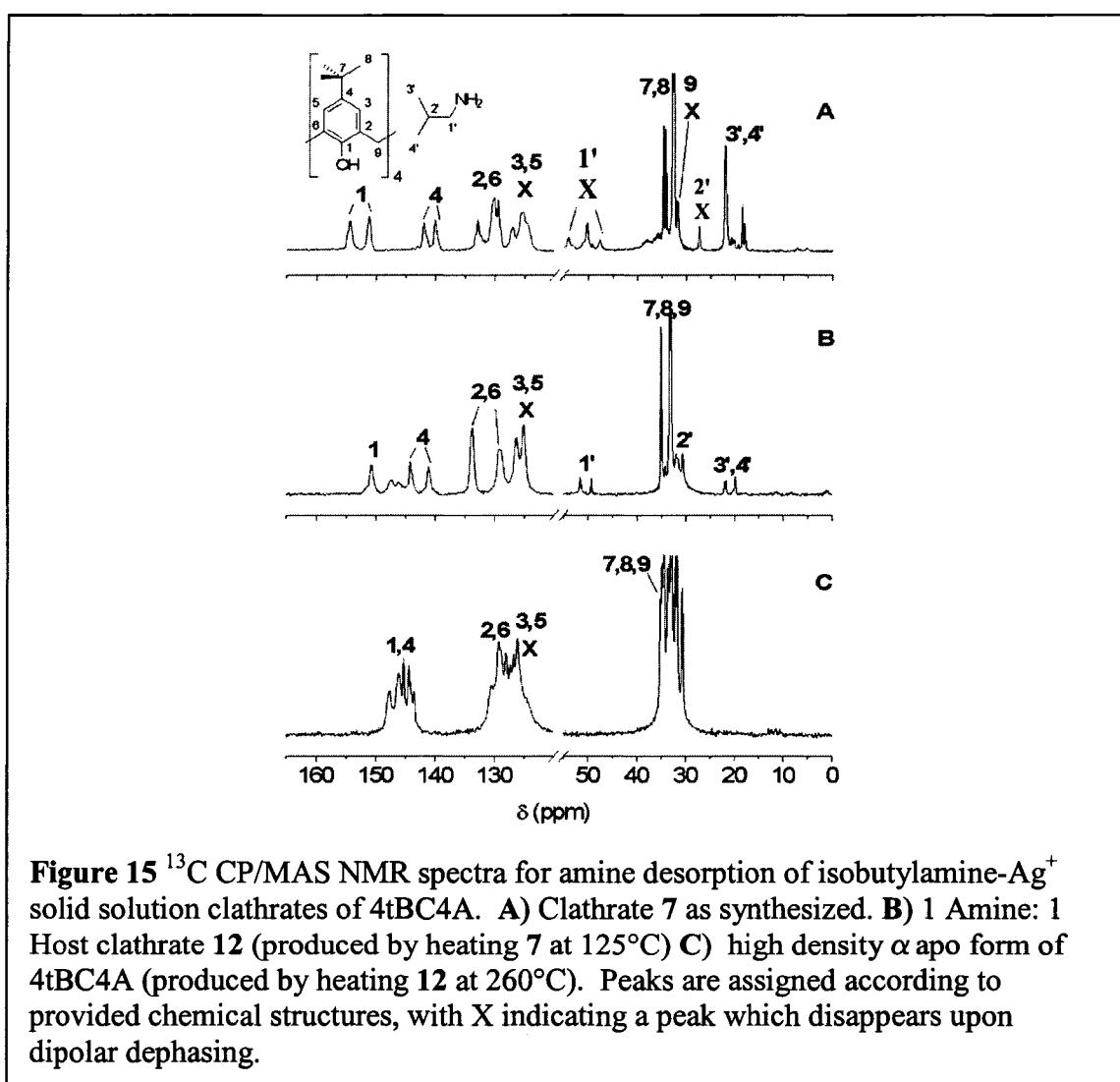
Desorption Behaviour of Isobutylamine-Ag Loaded 4tBC4A Frameworks

In light of the previous studies of the enclathration of *n*-butylamine-Ag⁺ that suggested that removal of the amine moieties through heating not only allows for selective control over the structural motif observed (see Chapter IV), but also gives rise to redox behaviour that has parallels to that observed for silver zeolites,^[79-81] the multiple phases observed for isobutylamine-Ag⁺ inclusions immediately raise intriguing questions. Would the phases desorb in a similar fashion, yielding identical materials? Or would the structural differences once again serve to direct them towards different desorbed calixarene forms loaded with metallic nanoparticles?

TGAs of the partially loaded clathrate **7** and the fully loaded clathrate **11** proved to be remarkably similar. Both exhibit two major steps, corresponding to the loss of approximately 2 amines followed by the loss of a single amine (see Table 5). The increased temperature required to desorb the first amine indicates a modest increase in stabilization of the *exo* amines via coordination to silver. As before, this temperature increase becomes more dramatic for the desorption of the final amine. Furthermore, the transitions are much broader for clathrate **11**, suggesting the presence of additional silver complicates desorption, such that the structural differences arising from the increased coordination are in fact influencing the structural shifts observed.

Using these results, it was therefore possible to clarify the nature of these structural shifts by carrying out desorption experiments on bulk samples of two of the silver loaded clathrates. For clathrate **7**, the ¹³C CP/MAS NMR spectrum of the initial sample is consistent with the SCXRD structure (see Figure 15A and Table 8). The PXRD

pattern of the initial sample is indexed with some difficulty to the expected orthorhombic unit cell, although the cause in the expansion of unit cell parameters is not immediately evident (see Figure 16A and Table 9). In particular, two lines at 6 and 6.5° cannot be indexed by such a cell, which is troubling. Given that such peaks correspond poorly with those expected of clathrate 3, this may be indicative of another minor phase that fails to perturb the TGA, or is a function of the solid solution's make up in the bulk..



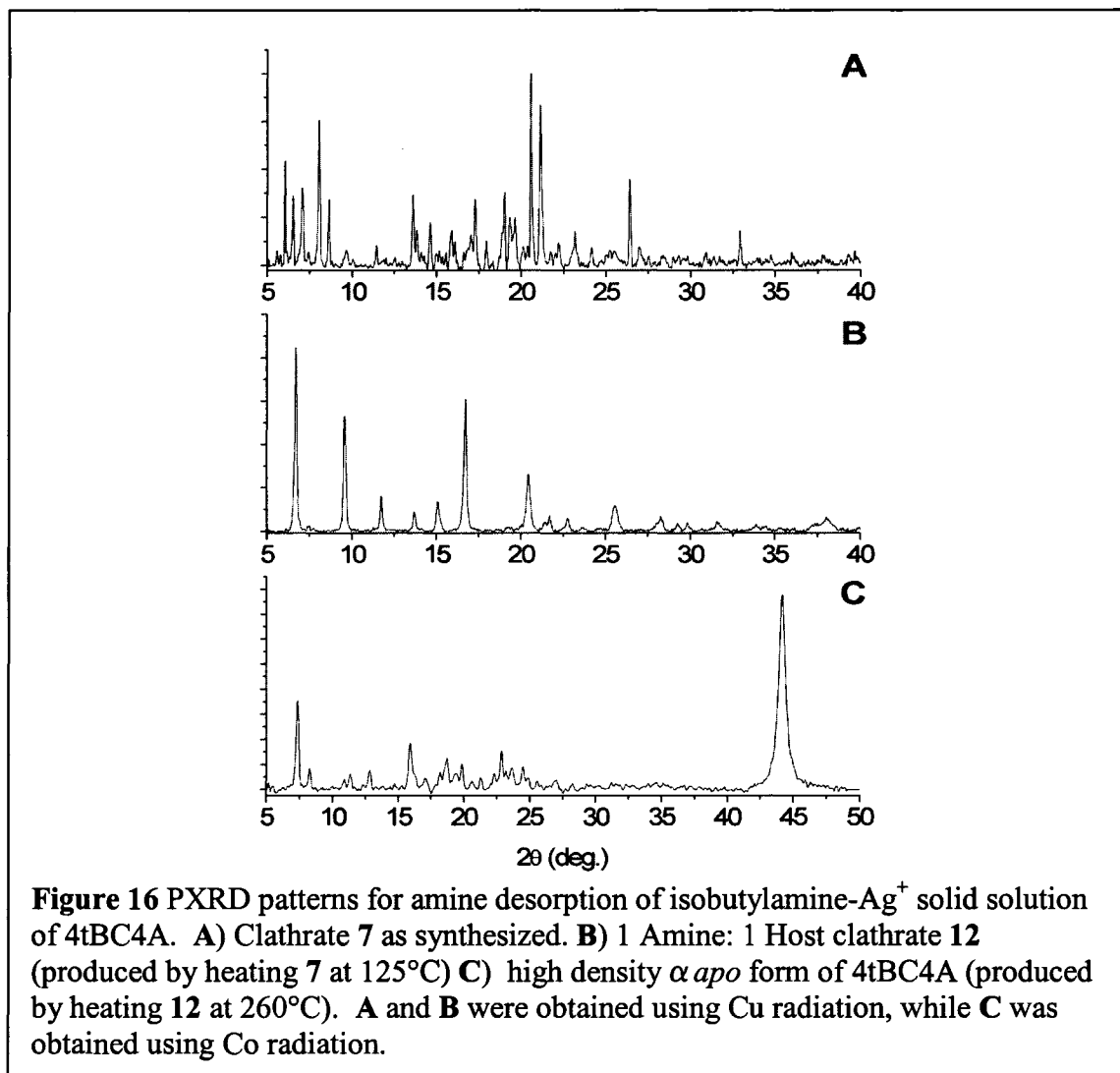


Table 8 Comparison of ^{13}C CP/MAS NMR spectral data for clathrates **7** and **12** to solution NMR data.^[a]

Guest	Carbon	δ Soln. ^[b]	δ 7 ^[c] (± 0.05)	CIS for 7 ^[d] (± 0.05)	δ 12 ^[c] (± 0.05)	CIS for 12 ^[d] (± 0.05)
Isobutylamine	C1'	50.22	54.10	3.88	51.49	1.27
			50.19	-0.03	49.12	1.10
			47.82	-2.40		
	C2'	31.57	27.34	-4.23	N/A	N/A
C3',C4'	20.02	22.10	2.08	21.84	1.79	
		18.43	1.59	19.73	1.30	

^[a]All values are in ppm. ^[b]Chemical shift of amine in solution, from SDBSWeb.^[54]

^[c]Chemical Shift observed in 4tBC4A clathrate. ^[d]CIS=Complexation-induced shift=(δ clathrate)-(δ Solution)

Table 9 Unit cell parameters for clathrate **7**, and its desorption products clathrate **12** and the α *apo* form of 4tBC4A as determined by PXRD.

	Clathrate 7	Clathrate 12	α <i>apo</i> form of 4tBC4A
Space Group	<i>Pnma</i>	<i>P4/n</i>	<i>P2₁/c</i>
<i>a</i> /Å	20.453	12.946	9.6016
<i>b</i> /Å	24.890	12.946	27.721
<i>c</i> /Å	13.035	13.008	15.031
α /deg.	90	90	90
β /deg.	90	90	109.7
γ /deg.	90	90	90
<i>V</i> /Å ³	6636.0	2180.0	3766.2

Despite the unusual PXRD data, the SSNMR is generally consistent with the SCXRD data. While the splitting of the various peaks is less than expected from the asymmetric unit, the peaks are much broader than in clathrate **3**. This suggests that the disorder in the structure is such that the fine peak splittings are obscured and lost, with only large differences arising from the influence of the silver centre being observed. This is particularly pronounced for the aromatic host carbons 1 and 4, which are the closest to the silver centres. The broadening is somewhat less pronounced for the guest resonances, with the 1' carbon exhibiting the expected three-fold splitting. Carbons 1' and 2' are almost completely dephased, suggesting the amines are experiencing minimal motion on this timescale at best. The CIS of the guest resonances are similar to that observed for **3**, indicating that once again, the 2' carbon is most deeply included, while at least one *exo* amine experiences considerable deshielding due to the silver (see Table 8).

Upon heating to 125°C, clathrate **7** transforms into clathrate **12**, yielding a much simplified ¹³C CP/MAS NMR spectrum (see Figure 15B). Unlike clathrate **3**, both the aromatic 1 and 4 carbons of the host and the various guest resonances exhibit a two fold splitting, making the initial assignment of the structural shift uncertain. The PXRD

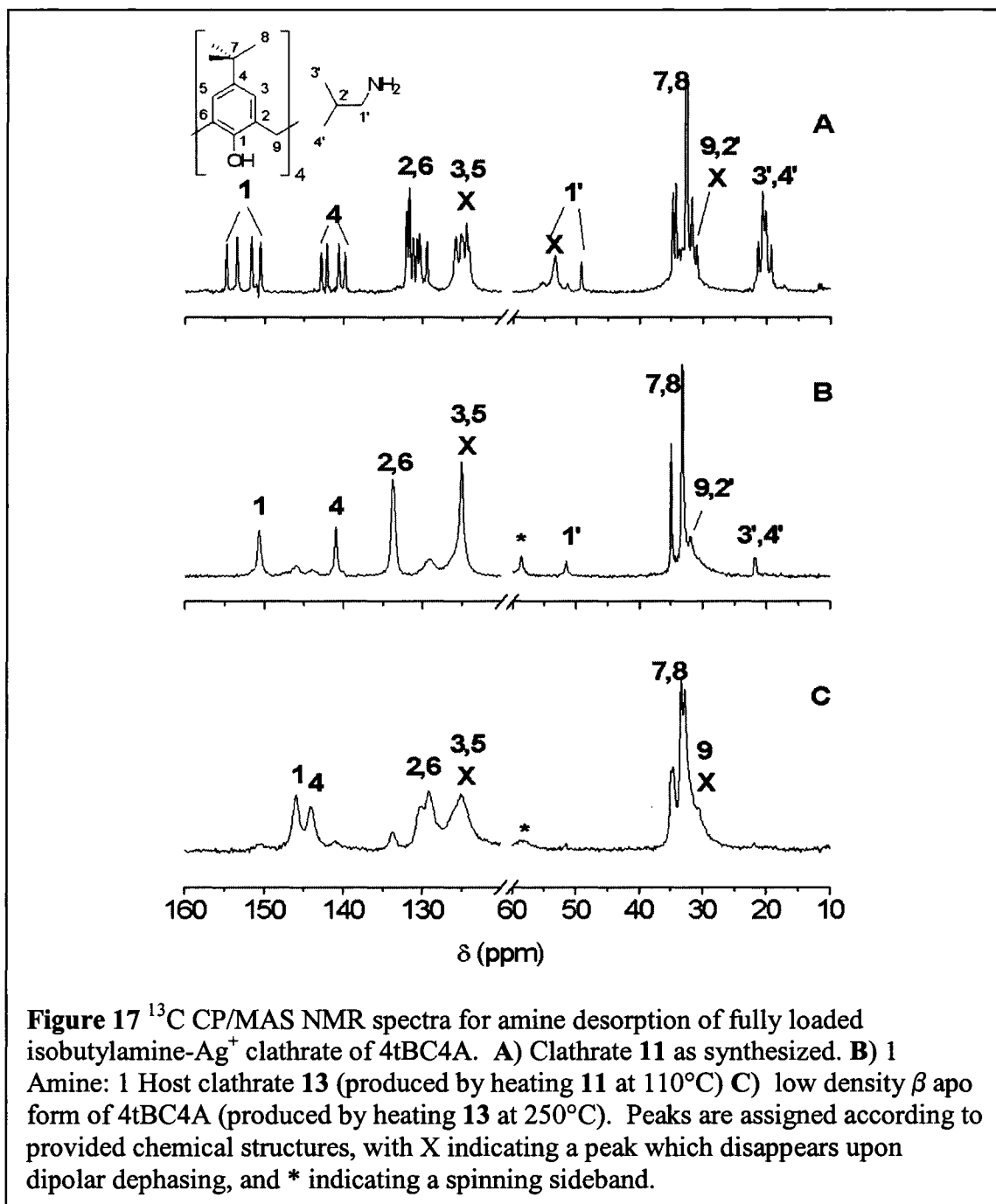
pattern exhibits the simplification anticipated for the formation of a tetragonal 1 Guest: 1 Host clathrate of 4tBC4A, and is readily indexed in the $P4/n$ spacegroup, with cell parameters consistent with previous such compounds (see Figure 16B and Table 9, and Chapter III). As such, instead of being representative of the asymmetric unit, the splitting in the NMR spectrum is diagnostic of two distinct local environments within the structure of clathrate 12. This is consistent with the random distribution expected of a solid solution. Presumably, the deshielded resonances are representative of the silver sites within the solid solution, while the shielded resonances are representative of the simple amine sites in the clathrate. In both cases, it appears that the amine interacts minimally with the calixarene cavity, as no significant CIS due to aromatic shielding can be determined for either site.

The remaining amine is fully removed upon heating to 250°C, such that the powder goes from white to a deep red-brown, indicating the silver ions have been oxidized similar to other 4tBC4A amine-Ag⁺ systems (see Chapters IV and VI). The ¹³C CP/MAS NMR spectrum indicates a dramatic drop in symmetry (see Figure 15C). With no guest peaks observable, the various aromatic host resonances are heavily split and overlap each other extensively. As a result, the spectrum can only be assigned in a very general fashion. However, qualitative comparison of the spectrum to that previously obtained for the *apo* forms of 4tBC4A clearly indicate that the calixarene is now in the densely packed α *apo* form, suggesting that the remaining silver in the structure is located outside of the calixarene itself.

The PXRD derived unit cell parameters do not match the analogous *apo* form exactly, suggesting that the calixarene layers have been forced to shift to accommodate a residual guest. In contrast with our studies of ethylenediamine-Ag⁺ compounds (see Chapter VI),^[31] where the framework appeared to expand, the *b* axis has collapsed by about 3 Å, presumably to accommodate favourable interactions with the silver. As with the other amine-Ag⁺ compounds (see Chapters IV and VI), the high-angle peak with $d=2.3-2.4$ Å is observed corresponds to the peak is the 111 peak of elemental silver, as indexed in the F_{m-3m} spacegroup, indicating that a silver cluster has been formed within the calixarene matrix. Analyzing the broadening of the line by way of the Scherrer equation,^[82-84] these silver clusters have a crystallite size of approximately 181 Å, which is almost 3 times the size of the 57 Å clusters arising from the *n*-butylamine-Ag⁺ calixarene clathrate system (see Chapter IV), and twice as large as the clusters arising from the ethylenediamine-Ag⁺ system (see Chapter VI).

A similar set of transformations is observed for clathrate **11**, although the temperatures involved in the transformations are slightly different. The ¹³C CP/MAS NMR spectrum and PXRD of the compound as synthesized again correspond well to predictions from the SCXRD structure (see Figures 17A and 18A and Table 10), with the NMR spectrum contributing the most information. The decreased disordering of the overall structure make it again possible to resolve the full splitting of the aromatic resonances for host carbons 1 and 4, with the triclinic symmetry also resulting in carbons 2 and 6 exhibiting increased splitting in comparison with clathrate **3**. With regards to the guest, all of the resonances attributed to 2' carbons are now obscured by the host's

resonances, a situation consistent with the methyls now being the most deeply included moieties in the structure. However, the methyl resonances are now heavily overlapping, such that it is not possible to effectively analyze the CIS.



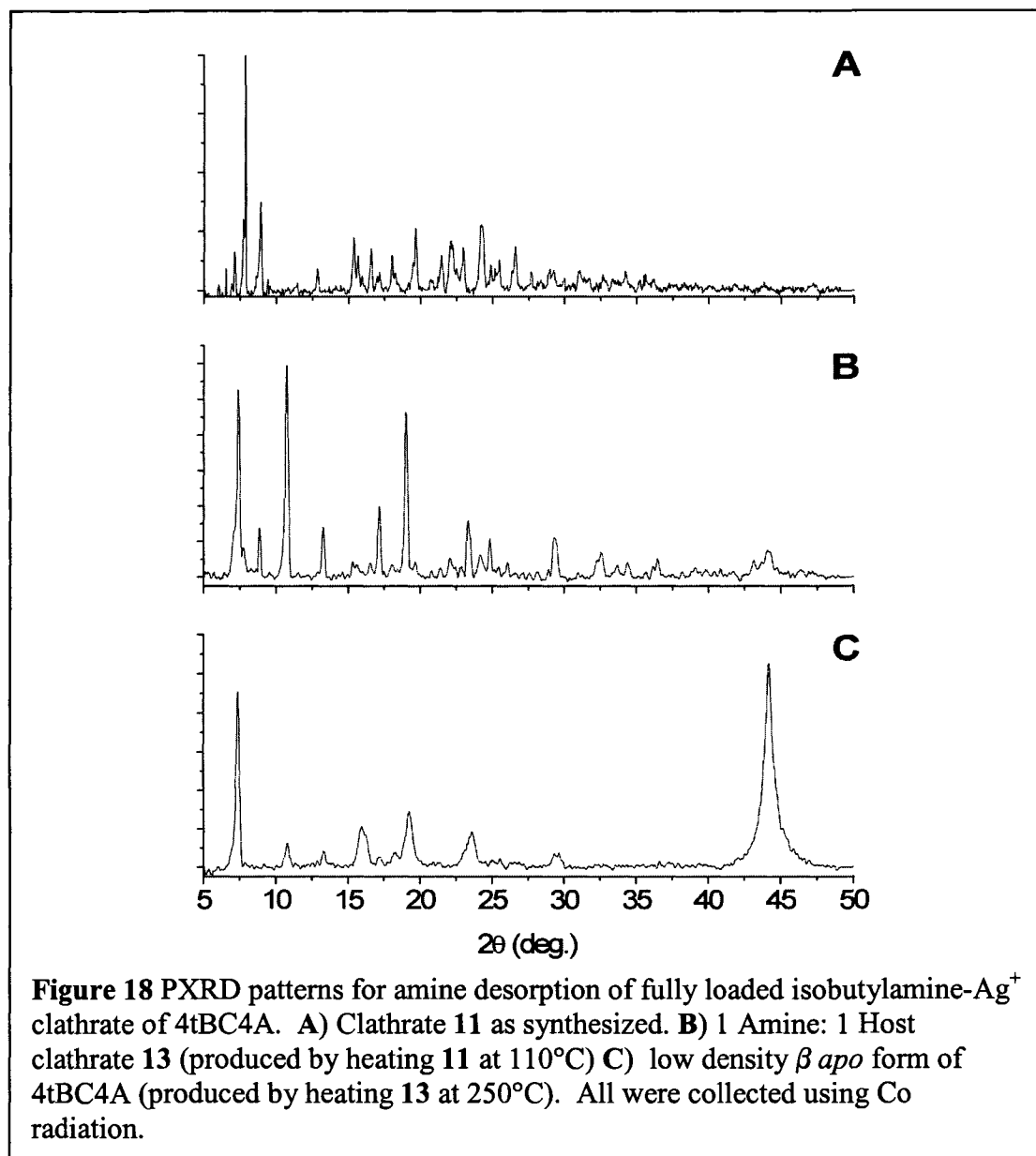


Table 10 Unit cell parameters for clathrate 11 and its desorption product clathrate 13 as determined by PXR D.

	Clathrate 11	Clathrate 13
Space Group	<i>P</i> -1	<i>P</i> 4/ <i>n</i>
<i>a</i> /Å	13.988	13.261
<i>b</i> /Å	22.093	13.261
<i>c</i> /Å	21.147	14.188
α /deg.	91.35	90
β /deg.	106.7	90
γ /deg.	96.68	90
<i>V</i> /Å ³	6206.0	2495.2

Heating at 110°C gives rise to the expected 1 Guest: 1 Host clathrate **13**, with the ^{13}C NMR spectrum now being entirely representative of the four-fold symmetry of the structure (see Figure 17B). None of the host peaks are split, and only a single set of guest peaks are observed. No CIS is observed for these peaks, indicating that the amine interacts minimally with the calixarene itself. Even so, the PXRD pattern is readily indexed in the $P4/n$ space group (see Figure 18B and Table 10), suggesting that stabilization of the amines through van der Waals interactions with the calixarene cavity is precluded due to the energetic favourability of interaction with the silver centres. This is also supported by the distortion of the unit cell parameters, where once again an expansion of the structure is evident.

Upon complete removal of the amine at approximately 260°C, once again the powder becomes brown, suggesting reduction of the silver ions to produce clusters. However, the symmetry in this case remains high, with no splitting observed, suggesting that the *apo* form obtained in this case is the low density β_0' form previously observed upon removal of toluene from 4tBC4A,^[6] and upon full removal of *n*-butylamine from the *n*-butylamine 4tBC4A clathrate.^[29] The ^{13}C CP/MAS spectrum closely corresponds to that reported for this precursor to the lower symmetry β_0 form (see Figure 17C), while the PXRD pattern is consistent with a $P4/n$ unit cell with similar dimensions to the pseudo-orthorhombic β_0 form (see Figure 18C). However, complete indexing of the pattern is precluded due to the small number of reflections, which are quite broad. As before, an intense silver 111 peak is also observed, with the analysis of the broadening indicating

the formation of silver crystals with crystallite sizes of 132 Å, a size comparable to that obtained for the ethylenediamine-Ag⁺ system (see Chapter VI).

The spectra and diffraction patterns clearly indicate that the redox chemistry occurring in the isobutylamine system is analogous to that observed in the *n*-butylamine-Ag⁺ 4tBC4A clathrate in Chapter IV and ethylenediamine-Ag⁺ 4tBC4A clathrate in Chapter VI. Again this indicates that the calixarene serves largely as a lattice for isolating the silver centres, undergoing no structural changes. The amine presumably promotes reductive chemistry not generally observed in simple amine-Ag⁺ coordination compounds, giving rise to complex redox chemistry. Qualitatively, therefore, the process remains similar to that of reduction of silver in zeolites, where confinement gives rise to unusual redox chemistry,^[79-81] but ultimately leading to a different final product.

Structurally, however, these two different deaminated structures clearly indicate that just as the amount of silver plays a significant role also in directing the self-assembly of the frameworks, it also plays a significant role in directing the desorption behaviour. For clathrate **7**, the high amine cluster content gives rise to behaviour that is the same as that observed for the pure amine clathrate **3**, yielding a densely packed 4tBC4A network. The fully loaded clathrate **12** collapses to yield the open β type 4tBC4A structure. This is likely the result of the structure directing influence of the silver nanocrystals themselves, with the densely packed form better suited to accommodating larger silver clusters. The smaller amines also appear to favour formation of larger silver crystallites, although this could also be a result of dynamics or other factors. Regardless, the practical implication of the structural data is that the silver centres in all cases are still likely located between

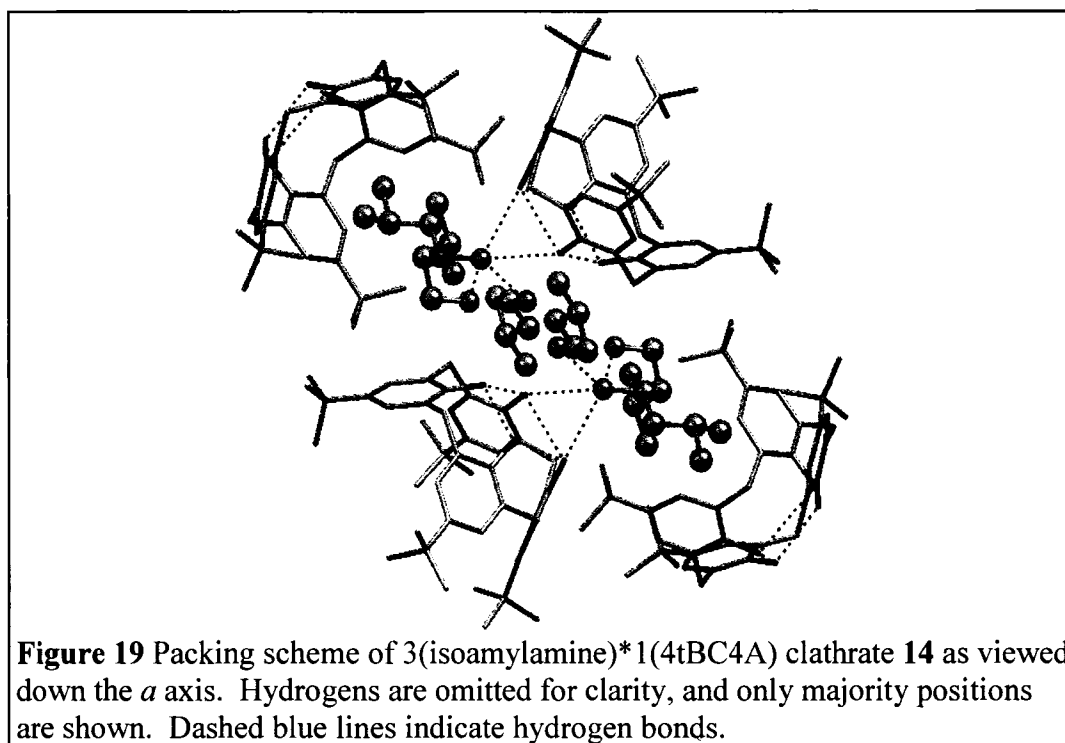
layers of calixarene, as they remain too large to be accommodated within the calixarene cavity. However, at the present time, it is not possible to determine whether the switch between the two packing schemes for accommodating silver clusters necessarily involves the initial structure undergoing a phase change from the solid solution to a lower symmetry form, or is just a simple consequence of the overall silver concentration in the framework.

Enclathration of Isoamylamine and Isoamylamine Ag complexes by 4tBC4A

While isobutylamine is both more bulky due to the terminal dimethyl group and smaller in length than *n*-butylamine, the four carbon backbone of isoamylamine is sufficient to give it a length that is comparable to *n*-butylamine. As such, the inclusion of isoamylamine is an ideal test of how significant the terminal dimethyl group is in directing the structural motif observed. Despite the relatively small increase in bulk associated with such a substitution, initial SCXRD investigations clearly dimethyl substitution pattern does indeed have a subtle, but observable, effect on the inclusion motif observed.

As expected, recrystallization of 4tBC4A from isoamylamine readily yielded crystals suitable for SCXRD. The resulting clathrate **14** has the expected stoichiometry of 3(isoamylamine)*1(4tBC4A), such that it is clearly isostructural with the previously observed *n*-butylamine 4tBC4A clathrate (see Table 1 and Chapter III). Once again, a single amine is included within the calixarene cavity (*endo*), while the other two amines are *exo* to the calixarene (see Figure 19). The amines are bound together through a series of hydrogen bonds centred on the *endo* amine (N...N distances of 2.84 and 2.85 Å). This

cluster is further stabilized through hydrogen bonding between the *endo* amine and an adjacent molecule of 4tBC4A (N...O distances of 2.82 and 3.10 Å). The resulting staggering of the 4tBC4A to accommodate the hydrogen bonding, such that only one can interact with each amine cluster is identical to the *n*-alkylamines, where *n*-butylamine forced a similar arrangement.



Intriguingly, unlike the *n*-butylamine clathrate, only the *endo* amine exhibits any disorder. This amine is disordered over two positions (0.75:0.25 distribution of occupancies), with the amino group remaining fixed in one position. As such, the disordering is representative of only subtle shifts within the calixarene cavity, and has no impact on the host itself. As such, no disorder is observed in any of the *t*-butyl groups of the calixarene. Clearly, in contrast with the disorder observed for the *n*-butylamine inclusions, the bulk of the dimethyl substitution is sufficient to lead to only a single

energy minimum for the *exo* guests by way of non-specific interactions between the hydrophobic chains of the amine.

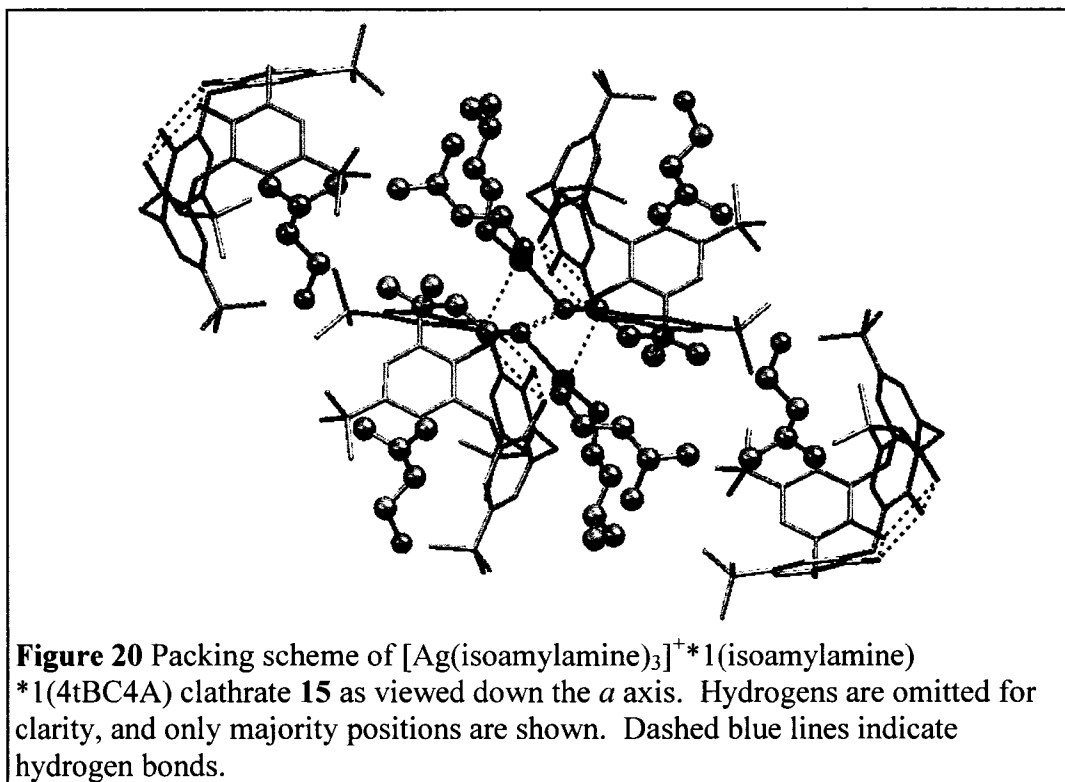
The dimethyl tail of isoamylamine is also observed to have an effect when coordination to silver is introduced to guide the structural motif. Recrystallization of 4tBC4A from a solution of AgNO₃ and isoamylamine gives rise to clathrate **15**, which was also suitable for SCXRD analysis (see Table 1). Once again, while the resulting clathrate is isostructural to that obtained for *n*-butylamine-Ag⁺, with a stoichiometry of [Ag(isoamylamine)₃]⁺*1(isoamylamine)*1(4tBC4A)⁻, the specific intermolecular interactions exhibit clear deviations arising from the difference in guest bulk.

As with *n*-butylamine, a trigonal planar silver complex is formed *exo* to the calixarene cavity (Ag...N distances of 2.26, 2.28 and 2.33 Å), while a fourth amine serves as an *endo* guest (see Figure 20). Secondary coordination to the calixarene further stabilizes the complex, by way of hydrogen bonds between two of the *exo* amines and the phenolic hydroxyl groups of the calixarene (N...O distances of 2.95 and 3.00 Å). This forces the hydrogen bonding calixarenes to be staggered off the axis of the cavity defined by the two capping calixarenes by approximately 2.7 Å, with the silver clusters remaining discrete entities. Two of the *exo* amines assume an all *trans* conformation, while the third exhibits a partial *cis* conformation, giving rise to a twofold disordering (0.51:0.49 occupancy ratio). This marked decrease in disorder for *exo* amines further confirms the stabilizing influence of hydrophobic interactions and restricted rotation due to additional bulk on the amine hydrocarbon chain for such sites.

In contrast, the *endo* amine exhibits extensive disorder that proved difficult to model appropriately. Modeling the amine isotropically, three major positions are observed (0.46:0.35:0.18 occupancy ratio), with the comparatively large thermal parameters observed ($U_{\text{iso}} \sim 0.15$) clearly indicating that such sites are likely representative of a broad range of energetically equivalent orientations for the amine within the calixarene cavity. As can be seen from Figure 20, the majority position is such that the *endo* amine does not hydrogen bond with the *exo* amine Ag^+ complex, such that the secondary coordinate role of the calixarene is restricted to hydrogen bonding. Only the *endo* amine is predominantly stabilized through van der Waals interactions with the calixarene alone, partially explaining the lack of one particular preferred orientation of the *endo* amine. A similar degree of disordering is observed in the calixarene, with one *t*-butyl group disordered over two positions (0.82:0.18 occupancy ratio), and the remaining three exhibiting signs of thermal motion.

The inclusion of the dimethyl tail of isoamylamine is therefore more energetically favourable for the *endo* amine than serving as a secondary coordinate ligand to the *exo* amine Ag^+ complex. Under such conditions, the metalloreceptor analogy fails, as the potential secondary interactions are more effective at stabilizing the amine alone than an amine bound to the coordination complex. While the amine is enclathrated no deeper in the calixarene cavity than the corresponding *n*-butylamine or *n*-butylamine- Ag^+ clathrates (distance from the terminal guest carbon to the phenolic base of the calixarene in each case is approximately 4 Å), the increased bulk of the dimethyl tail presumably interferes with the free orientation of the amine due to potential collisions with the *t*-butyl groups at

the rim. As such, any potential stabilization by hydrogen bonding to the silver complex is largely offset by the energetic costs of steric disruption of the *t*-butyl groups. In this case, the *endo* amine serves solely as a space-filling guest, inhabiting a broad range of sites, although whether this amine is truly dynamic cannot be determined in the absence of NMR data.



The isoamylamine based clathrates are similar to those observed for *n*-butylamine, indicating the amine's length is the key determining factor in the structural motif in this case. However, while the constricted capped motif observed for isobutylamine is no longer favoured, the addition of a terminal methyl group still influences the resulting motif in a distinct fashion, suggesting that this may be yet another route to controlling the structural motif in a rational fashion. Further studies of the influence of guest bulk should serve to clarify the extent to which these substitutions

affect the structural motif. By the same token, detailed NMR and PXRD studies of bulk samples of such systems would serve to clarify whether these subtle changes have any significant effects on the formation of daughter pseudopolymorphs.

5. Conclusions

Clearly, a number of forces are at work in guiding the inclusion of isobutylamine based compounds in 4tBC4A. The acid-base chemistry that has largely been the province of solution-state chemists^[85] has significant impacts on the solid structure formed in this case. Not only does the symmetry of the host change dramatically, deprotonation of the calix also gives rise to even more favourable hydrogen bonding interactions between the amine and the host. In this chapter, by further controlling both the length of the amine and its bulk, it is possible to make use of various forces to control the structural motifs.

For inclusion of isopropylamine, the amine itself is too small to simultaneously support stabilization by hydrogen bonding and inclusion in the calixarene. Under such circumstances, the inclusion scheme favoured is the typical 1:1 motif of a non-interacting guest. However, upon introducing coordination as another force competing to direct the structure, the lower symmetry capped motif is adopted in order to allow for increased stabilization of the guest through three distinct routes.

In the case of isobutylamine, the amine is still too small to allow the full capped motif to be observed, but is large enough to force the calixarene framework to assemble such that one unit of 4tBC4A will be available to hydrogen bond, giving rise to a competitively stabilized structure that can be seen as a partially collapsed variation on the

capped motif previously described. This collapsed structure, as result, highly favours the formation of the densely packed *apo* form upon complete desorption of the amine.

However, the significance of the collapse induced by the competition between interactions is truly highlighted by the inclusion behaviour of 4tBC4A with regards to silver coordination compounds of isobutylamine. With the amine cluster being effectively equivalent to a trigonal planar silver complex for the purposes of inclusion, crystallization proceeds to produce a partially loaded framework. This solid solution indicates that the collapsed channelled structural motif observed is clearly favoured for a much broader range of amine-silver inclusions than for other examined systems (see Chapters IV and VI).^[30, 31] This structure must represent a rather dramatic energetic minimum for the purposes of efficient packing in the solid state, such that relatively strong stabilizing interactions (such as coordinative bonding) are overwhelmed by hydrogen bonding and van der Waals interactions. It is not until a much larger concentration of silver is present that a shift in the favoured motif for stabilizing the silver complexes present is observed.

Finally, the bulk and length of isoamylamine is sufficient to fully establish the capped motif observed for *n*-butylamine. Under such circumstances, the modest increase in bulk arising from the dimethyl tail results in only a slight increase in the overall unit cell volume. Similarly, coordination to silver gives rise to an analogous inclusion scheme involving *exo* amines coordinating to the metal centre and a single *endo* amine. However, the *endo* isoamylamine exhibits considerable disorder, with a majority position that does not interact with the silver complex, suggesting that unlike the *n*-alkylamines,

its role is restricted to serving as a space filling element that allows the adoption of a favoured calixarene lattice to accommodate the complex.

In conclusion, the inherent flexibility of the concept of using simple components and competing interactions to guide the formation of an organic self-assembled framework has been demonstrated by showing how small changes in an amine guest can tune a calixarene framework in very dramatic ways. The resulting materials are natural extensions of the metalloreceptor concept, with the ligands now fully organized on the basis of secondary coordination interactions as well as interactions with a metal centre. When compared to the customized design of complex tectons for organic and metal-organic frameworks, such simplicity is a considerable advantage. In this particular case, the size and capacity for hydrogen bonding of the amine has been used to produce frameworks tuned to yield compact inclusions and dense packing of the calixarene. It also allowed for the custom loading of an organic compound with a transition metal, which, upon desorption, gave rise to supported silver clusters clearly analogous to those previously shown to exhibit catalytic behaviour.^[86-89]

However, more detailed systematic investigations are required to clarify the relationship between the amine and cluster size, as well as the relationship between cluster size and the calixarene packing scheme. Such studies would also entail further examination as to what effect the heating conditions and time have on the formation of the nanoparticles. Such future studies would therefore further clarify the hierarchy of forces guiding the formation of these interrelated frameworks, as well as the intriguing chemistry of the guest clusters that are formed.

6. References

- [1] C. D. Gutsche, *Calixarenes*, Royal Society of Chemistry, Cambridge, **1989**.
- [2] C. D. Gutsche, *Calixarenes Revisited*, Royal Society for Chemistry, Cambridge, **1998**.
- [3] Z. Asfari, V. Bohmer, J. Harrowfield, J. Vicens, *Calixarenes 2001*, Kluwer Academic Publishers, Dordrecht, **2001**.
- [4] L. Mandolini, R. Ungaro, ed., *Calixarenes in Action*, Imperial College Press, London, **2000**.
- [5] E. B. Brouwer, G. D. Enright, C. I. Ratcliffe, J. A. Ripmeester, *Supramol. Chem.* **1996**, *7*, 79.
- [6] E. B. Brouwer, G. D. Enright, K. A. Udachin, S. Lang, K. J. Ooms, P. A. Halchuk, J. A. Ripmeester, *Chem. Commun.* **2003**, 1416.
- [7] E. B. Brouwer, K. A. Udachin, G. D. Enright, J. A. Ripmeester, K. J. Ooms, P. A. Halchuk, *Chem. Commun.* **2001**, 565.
- [8] E. B. Brouwer, J. A. Ripmeester, G. D. Enright, *J. Incl. Phenom. Molec. Recogn.* **1996**, *24*, 1.
- [9] J. L. Atwood, L. J. Barbour, A. Jerga, *Chem. Commun.* **2002**, 2952.
- [10] G. D. Andreotti, R. Ungaro, A. Pochini, *J. Chem. Soc. Chem. Commun.* **1979**, 1005.
- [11] W. Xu, R. J. Puddephatt, L. Manojlovicmuir, K. W. Muir, C. S. Frampton, *J. Incl. Phenom. Molec. Recogn.* **1994**, *19*, 277.
- [12] J. M. Harrowfield, M. I. Ogden, W. R. Richmond, B. W. Skelton, A. H. White, *J. Chem. Soc. Perkin Trans. 2* **1993**, 2183.
- [13] J. M. Harrowfield, M. I. Ogden, W. R. Richmond, A. H. White, *J. Chem. Soc. Chem. Commun.* **1991**, 1159.
- [14] J. L. Atwood, G. W. Orr, F. Hamada, R. L. Vincent, S. G. Bott, K. D. Robinson, *J. Am. Chem. Soc.* **1991**, *113*, 2760.
- [15] B. M. Furphy, J. M. Harrowfield, M. I. Ogden, B. W. Skelton, A. H. White, F. R. Wilner, *J. Chem. Soc. Dalton Trans.* **1989**, 2217.
- [16] R. Ungaro, A. Pochini, G. D. Andreotti, P. Domiano, *J. Chem. Soc. Perkin Trans. 2* **1985**, 197.
- [17] R. Ungaro, A. Pochini, G. D. Andreotti, V. Sangermano, *J. Chem. Soc. Perkin Trans. 2* **1984**, 1979.
- [18] G. D. Andreotti, A. Pochini, R. Ungaro, *J. Chem. Soc. Perkin Trans. 2* **1983**, 1773.
- [19] R. Ungaro, A. Arduini, A. Casnati, A. Pochini, F. Ugozzoli, *Pure Appl. Chem.* **1996**, *68*, 1213.
- [20] A. Arduini, M. Fabbi, M. Mantovani, L. Mirone, A. Pochini, A. Secchi, R. Ungaro, *J. Org. Chem.* **1995**, *60*, 1454.
- [21] A. Casnati, Y. H. Ting, D. Berti, M. Fabbi, A. Pochini, R. Ungaro, D. Sciotto, G. G. Lombardo, *Tetrahedron* **1993**, *49*, 9815.
- [22] W. Verboom, S. Datta, Z. Asfari, S. Harkema, D. N. Reinhoudt, *J. Org. Chem.* **1992**, *57*, 5394.

- [23] L. C. Groenen, J. D. Vanloon, W. Verboom, S. Harkema, A. Casnati, R. Ungaro, A. Pochini, F. Ugozzoli, D. N. Reinhoudt, *J. Am. Chem. Soc.* **1991**, *113*, 2385.
- [24] E. Ghidini, F. Ugozzoli, R. Ungaro, S. Harkema, A. Abuelfadl, D. N. Reinhoudt, *J. Am. Chem. Soc.* **1990**, *112*, 6979.
- [25] P. J. Dijkstra, J. A. J. Brunink, K. E. Bugge, D. N. Reinhoudt, S. Harkema, R. Ungaro, F. Ugozzoli, E. Ghidini, *J. Am. Chem. Soc.* **1989**, *111*, 7567.
- [26] G. Calestani, F. Ugozzoli, A. Arduini, E. Ghidini, R. Ungaro, *J. Chem. Soc. Chem. Commun.* **1987**, 344.
- [27] S. G. Bott, A. W. Coleman, J. L. Atwood, *J. Am. Chem. Soc.* **1986**, *108*, 1709.
- [28] M. M. Olmstead, G. Sigel, H. Hope, X. J. Xu, P. P. Power, *J. Am. Chem. Soc.* **1985**, *107*, 8087.
- [29] P. O. Brown, K. A. Udachin, G. D. Enright, J. A. Ripmeester, *Chem. Eur. J.* **2006**, DOI: 10.1002/chem.200600434.
- [30] P. O. Brown, K. A. Udachin, G. D. Enright, J. A. Ripmeester, *Chem. Commun.* **2005**, 4402.
- [31] P. O. Brown, G. D. Enright, J. A. Ripmeester, *Chem. Asian J.* **2006**, in press.
- [32] K. A. Udachin, G. D. Enright, P. O. Brown, J. A. Ripmeester, *Chem. Commun.* **2002**, 2162.
- [33] E. B. Brouwer, K. A. Udachin, G. D. Enright, C. I. Ratcliffe, J. A. Ripmeester, *Chem. Commun.* **2000**, 1905.
- [34] D. Bruhwiler, G. Calzaferri, *Microporous Mesoporous Mat.* **2004**, *72*, 1.
- [35] A. M. Beatty, *Coord. Chem. Rev.* **2003**, *246*, 131.
- [36] D. V. Soldatov, G. D. Enright, J. A. Ripmeester, *Cryst. Growth Des.* **2004**, *4*, 1185.
- [37] A. C. Sudik, A. P. Cote, O. M. Yaghi, *Inorg. Chem.* **2005**, *44*, 2998.
- [38] A. Ikeda, S. Shinkai, *Chem. Rev.* **1997**, *97*, 1713.
- [39] A. Ikeda, H. Tsuzuki, S. Shinkai, *J. Chem. Soc. Perkin Trans. 2* **1994**, 2073.
- [40] A. Ikeda, S. Shinkai, *J. Am. Chem. Soc.* **1994**, *116*, 3102.
- [41] N. W. Ockwig, O. Delgado-Friedrichs, M. O'Keeffe, O. M. Yaghi, *Accounts Chem. Res.* **2005**, *38*, 176.
- [42] S. Muthu, J. H. K. Yip, J. J. Vittal, *J. Chem. Soc., Dalton Trans.* **2001**, 3577.
- [43] C. L. Schauer, E. Matwey, F. W. Fowler, J. W. Lauher, *J. Am. Chem. Soc.* **1997**, *119*, 10245.
- [44] T. J. Burchell, D. J. Eisler, R. J. Puddephatt, *Chem. Commun.* **2004**, 944.
- [45] R. P. Feazell, C. E. Carson, K. K. Klausmeyer, *Inorg. Chem.* **2005**, *44*, 996.
- [46] M. O. Awaleh, A. Badia, F. Brisse, X. H. Bu, *Inorg. Chem.* **2006**, *45*, 1560.
- [47] K. H. Li, Z. T. Xu, H. H. Xu, P. J. Carroll, J. C. Fettinger, *Inorg. Chem.* **2006**, *45*, 1032.
- [48] S. Hiraoka, T. Yi, M. Shiro, M. Shionoya, *J. Am. Chem. Soc.* **2002**, *124*, 14510.
- [49] A. B. Mallik, S. Lee, E. B. Lobkovsky, *Cryst. Growth Des.* **2005**, *5*, 609.
- [50] R. S. Rarig, J. Zubieta, *Inorg. Chim. Acta* **2002**, *340*, 211.
- [51] L. Zhang, X. Q. Lu, C. L. Chen, H. Y. Tan, H. X. Zhang, B. S. Kang, *Cryst. Growth Des.* **2005**, *5*, 283.

- [52] G. F. Swiegers, T. J. Malefetse, *Chemical Reviews* **2000**, *100*, 3483.
- [53] C. Y. Su, Y. P. Cai, C. L. Chen, M. D. Smith, W. Kaim, H. C. Z. Zoye, *J. Am. Chem. Soc.* **2003**, *125*, 8595.
- [54] NIAIST, "SDBSWeb", to be found under <http://www.aist.go.jp/RIODB/SDBS/> **2005**.
- [55] L. M. Engelhardt, S. Gotsis, P. C. Healy, J. D. Kildea, B. W. Skelton, A. H. White, *Aust. J. Chem.* **1989**, *42*, 149.
- [56] C. Nather, A. Beck, *Z.Naturforsch.(B)* **2004**, *59*, 992.
- [57] C. Jeunesse, D. Armspach, D. Matt, *Chem. Commun.* **2005**, 5603.
- [58] S. Kim, J. S. Kim, S. K. Kim, I. H. Suh, S. O. Kang, J. Ko, *Inorg. Chem.* **2005**, *44*, 1846.
- [59] P. D. Harvey, *Coord. Chem. Rev.* **2002**, *233*, 289.
- [60] M. Lejeune, C. Jeunesse, D. Matt, N. Kyritsakas, R. Welter, J. P. Kintzinger, *J. Chem. Soc. Dalton Trans.* **2002**, 1642.
- [61] I. A. Bagatin, D. Matt, H. Thonnessen, P. G. Jones, *Inorg. Chem.* **1999**, *38*, 1585.
- [62] C. Wieser-Jeunesse, D. Matt, A. De Cian, *Angew. Chem. Int. Edit.* **1998**, *37*, 2861.
- [63] B. R. Cameron, S. J. Loeb, G. P. A. Yap, *Inorg. Chem.* **1997**, *36*, 5498.
- [64] B. R. Cameron, S. J. Loeb, *Chem. Commun.* **1996**, 2003.
- [65] Intriguingly, the peak at approximately 6.5 degrees does not index to this cell. It is unclear if this peak is the result of non-random alignment, or possibly a small amount of clathrate 3.
- [66] D. W. Davidson, J. A. Ripmeester, in *Inclusion Compounds, Vol. 3* (Eds.: J. L. Atwood, D. D. MacNicol, J. E. D. Davies), Academic Press, London, **1984**, pp. 69.
- [67] J. A. Ripmeester, C. I. Ratcliffe, in *Inclusion Compounds, Vol. 5* (Eds.: J. L. Atwood, J. E. D. Davies, D. D. MacNicol), Oxford University Press, Oxford, **1991**, pp. 37.
- [68] F. C. Hawthorne, S. V. Krivovichev, P. C. Burns, in *Sulfate Minerals - Crystallography, Geochemistry and Environmental Significance, Vol. 40*, **2000**, pp. 1.
- [69] J. Sangster, *J. Phys. Chem. Ref. Data* **1999**, *28*, 889.
- [70] E. Lamcharfi, G. Kunesch, C. Meyer, B. Robert, *Spectroc. Acta Pt. A-Molec. Biomolec. Spectr.* **1995**, *51*, 1861.
- [71] A. Anthony, M. Jaskolski, A. Nangia, *Acta Crystallogr. Sect. B-Struct. Sci.* **2000**, *56*, 512.
- [72] J. M. Harrowfield, M. Mocerino, B. W. Skelton, C. R. Whitaker, A. H. White, *Aust. J. Chem.* **1994**, *47*, 1185.
- [73] W. Xu, J. J. Vittal, R. J. Puddephatt, *Can. J. Chem.* **1996**, *74*, 766.
- [74] W. Xu, R. J. Puddephatt, K. W. Muir, A. A. Torabi, *Organometallics* **1994**, *13*, 3054.
- [75] G. D. Andreotti, L. Cavalca, P. Sgarabot, *Gazz. Chim. Ital.* **1971**, *101*, 494.
- [76] G. Ciani, M. Moret, A. Sironi, S. Bruni, F. Cariati, A. Pozzi, T. Manfredini, L. Menabue, G. C. Pellacani, *Inorg. Chim. Acta* **1989**, *158*, 9.

- [77] R. P. Feazell, C. E. Carson, K. K. Klausmeyer, *Eur. J. Inorg. Chem.* **2005**, 3287.
- [78] R. Horikoshi, K. Okazawa, T. Mochida, *J. Organomet. Chem.* **2005**, 690, 1793.
- [79] T. Sun, K. Seff, *Chem. Rev.* **1994**, 94, 857.
- [80] R. Seifert, A. Kunzmann, G. Calzaferri, *Angew. Chem. Int. Ed* **1998**, 37, 1251.
- [81] R. Seifert, R. Rytz, G. Calzaferri, *J. Phys. Chem. A* **2000**, 104, 7473.
- [82] H. Borchert, E. V. Shevchenko, A. Robert, I. Mekis, A. Kornowski, G. Grubel, H. Weller, *Langmuir* **2005**, 21, 1931.
- [83] J. I. Langford, A. J. C. Wilson, *J. Appl. Cryst.* **1978**, 11, 102.
- [84] $d=(K\lambda)/(B\cos\theta)$, where d =Crystallite Diameter, λ = Wavelength of radiation, K =Scherrer Constant (0.9), B =Broadening of Peak at FWHM, corrected for instrumental broadening, θ =Diffraction Angle in Radians.
- [85] A. F. Danil de Namor, R. M. Cleverly, M. L. Zapata-Ormachea, *Chem. Rev.* **1998**, 98, 2495.
- [86] B. S. Bal'zhinimaev, *Kinet. Catal.* **1999**, 40, 795.
- [87] R. J. Chimentao, I. Kirm, F. Medina, X. Rodriguez, Y. Cesteros, P. Salagre, J. E. Sueiras, J. L. G. Fierro, *Appl. Surf. Sci.* **2005**, 252, 793.
- [88] R. B. Grant, R. M. Lambert, *J. Chem. Soc. Chem. Commun.* **1983**, 662.
- [89] D. C. Lim, I. Lopez-Salido, Y. D. Kim, *Surf. Sci.* **2005**, 598, 96.

Chapter VI: Inclusion of Difunctional Amines in 4-*t*-butylcalix[4]arene[†]

1. Abstract.....	230
2. Introduction.....	231
3. Experimental Section.....	234
4. Results and Discussion.....	238
¹³ C SSNMR and SCXRD of 4tBC4A EtDAOH Clathrate 1	238
Desorption Behaviour of 4tBC4A EtDAOH Clathrate 1	249
CO ₂ Adsorption Behaviour of 4tBC4A EtDAOH Clathrate 1.....	255
¹³ C SSNMR and SCXRD of 4tBC4A EtDA Clathrate 3	262
Desorption Behaviour of 4tBC4A EtDA Clathrate 3.....	268
SCXRD of EtDA Ag 4tBC4A Clathrate 5.....	272
¹³ C SSNMR and PXRD Investigation of EtDA Ag 4tBC4A Clathrate 5	277
TEM of Ag Nanoclusters derived from Clathrate 5	285
5. Conclusion	287
6. References	289

1. Abstract

The influence of multiple hydrogen bonding moieties on a single amine on the enclathration behaviour of 4-*t*-butylcalix[4]arene (4tBC4A) is investigated, focusing on the difunctional amines ethanolamine (EtDAOH) and ethylenediamine (EtDA). In contrast with the clathrates formed by *n*-alkylamines and isoalkylamines, the resulting pure amine clathrates give rise to 5 Guest : 1 Host structures, indicating that the addition of a second hydrogen bonding moiety (be it NH₂ or OH) allows for the formation of a more extensive hydrogen bonding motif capable of stabilizing larger clusters that are functionally pseudo-liquid droplets. In the case of EtDAOH, these droplets are accessible, and the parent compound can be subsequently used to adsorb CO₂, with a mixture of chemisorption and physisorption occurring. For EtDA, the constrained geometry of the calixarene inclusion can be used to produce Ag⁺ complexes with

[†] Portions of this chapter have been previously published: P. O. Brown, G. D. Enright, J. A. Ripmeester, *Chem. Asian J.* 2006, in press.

distorted tetrahedral geometries such that the amine is both a chelating and non-chelating ligand. Visual, XRD and TEM studies of amine desorption from this Ag loaded structure confirms the formation of Ag nanoparticles similar to those reported in Chapters IV and V.

2. Introduction

In the course of synthesizing complex supramolecular materials that are not based on pre-organized receptors with distinct molecular cavities (such as the calixarenes^[1-4]), chemists typically do not rely on monofunctional organic molecules as templates. This common thread is observed in hydrogen bonded organic systems, such as the inclusions formed by Dianin's compound,^[5-9] urea,^[10-14] tri-*o*-thymotide,^[15-18] and peptide-based nanotubes,^[19] as well as inorganic and hybrid systems relying on coordination chemistry, such as Werner clathrates^[20] and reticular metal-organic frameworks.^[21] When making use of strong directional interactions, monofunctional building blocks cannot serve as linkers between vertices in a lattice, such that discrete molecular compounds not exhibiting inclusion chemistry result instead.

In the presence of competing forces (as are present in the 4tBC4A amine system) such polyfunctional linkers are not strictly necessary to produce complex frameworks, but they do offer the opportunity to further extend these frameworks. The 4tBC4A clathrate of 1,4-butanediamine^[22] gave rise to a complex array of hydrogen bonding interactions, such that the amine molecules were effectively part of an infinite hydrogen bonded layer. Alternatively, the inclusion of water in an *n*-butylamine 4tBC4A clathrate^[23] (see Chapter III) clearly indicates that the discrete amine clusters formed in

such compounds could also potentially be extended further with additional sites for hydrogen bonding. Small difunctional aliphatic amines would serve to avoid the inherent difficulties associated with the synthesis of such mixed solvent clathrates, such as the need to carefully control the concentration of water to produce a given structure, while still giving rise to semi-isolated clusters.

As solvent-based hydrogen bonded clusters grow in size, it is important to consider the potential implications for the structure. Studies of zeolites have demonstrated how the localization of small guests in large cavities is a significant challenge which can only be adequately addressed using a variety of techniques, including XRD and NMR.^[24-29] Similarly, XRD studies of proteins frequently require careful consideration of the impact of bulk solvent on the structural parameters.^[30-32] For organics, however, investigations of capsular compounds with large void spaces^[33-40] have focused heavily on the structures of the capsules themselves, while the solvent trapped within such structures being poorly characterized at best due to the inherent disorder in such assemblies. Given that one of the most frequently cited goals for the production of such materials is the production of isolated environments suitable for carrying out reactions away from bulk solvent, a better understanding of the structural arrangement and accessibility of hydrogen bonded clusters of enclathrated guests in such systems is called for.

Difunctional guests also provide an opportunity to examine how significant the symmetry and packing demands of the amine-induced low symmetry of 4tBC4A are in guiding the formation of guest clusters. In particular, the variation in coordination

observed for both the *n*-alkylamine and isoalkylamines suggest that unusual coordination of Ag⁺ will be adopted in order to accommodate framework geometries that maximize a wide range of weak interactions. For a difunctional amine, such packing schemes would be obliged to compete with the formation of polymeric structures, such that the calixarene framework might again be used to direct the formation of coordination compounds with novel geometries.

The current chapter therefore focuses on investigations of the 4tBC4A clathrates formed by two difunctional amines, ethanolamine (EtDAOH) and ethylenediamine (EtDA). Given the apparent versatility of these structures, and the well-known chemistry of ethanolamines in their role as CO₂ scrubbers,^[41, 42] we were curious as to whether stabilized EtDAOH nanoclusters might be suitable gas adsorbents without exhibiting the structural shifts observed with *n*-butylamine (see Chapter III). Similarly, the well-known Ag⁺ coordination chemistry of ethylenediamine^[43] makes it an ideal candidate for investigation of the potential of using 4tBC4A to guide the formation of coordination compounds in a fashion similar to that observed in Chapters IV and V.

The clathrates formed from the pure amines do indeed contain an expanded hydrogen bonded cluster, giving rise to a 5 guest : 1 host stoichiometry, while retaining the essential features of the capped motif previously observed for monofunctional amines. Based on single-crystal X-ray diffraction (SCXRD) and ¹³C CP/MAS NMR data, these clusters are highly dynamic, such that they can be described as liquid nanodroplets of amine. In the case of ethanolamine, these clusters are, as hoped, available for use as CO₂ adsorbents, serving as the first system suitable for structural

characterization of ethanolamine-mediated adsorption of CO₂ in the solid state. For ethylenediamine, coordination to Ag⁺ gives rise to an unusual distorted tetrahedral complex, which clearly represents the influence of van der Waals stabilization and hydrogen bonding to the calixarene framework in directing the formation of a coordination compound, as opposed to the coordination compound completely shaping the framework around it.

3. Experimental Section

General Note: Unless otherwise indicated, chemicals were obtained from EMD Chemicals and Sigma-Aldrich, and were used without further purification.

Synthesis of 5(EtDAOH)*4tBC4A clathrate 1 (POB67): In a typical synthesis, 0.248 g (3.84×10^{-4} mol) of 4tBC4A was placed in a vial along with 4.5 mL of EtDAOH. The resulting mixture was gently mixed for approximately 10 minutes, and then heated to approximately 60°C to speed the dissolution of any remaining particles of 4tBC4A. The resulting solution was then set aside and excess solvent was allowed to slowly evaporate over the course of two weeks, giving rise to large, block like crystals suitable for structural analysis.

Synthesis of 5(EtDA)*(4tBC4A) clathrate 3 (POB66): 0.484 g (7.47×10^{-4} mol) of 4tBC4A was weighed out into a vial with 3.0 mL of EtDA. The resulting mixture was heated at 70°C until the calixarene was completely dissolved. The vial was then loosely capped and set aside to allow slow evaporation of the amine. After approximately two days, clear crystals were observed to have formed.

Synthesis of $3(\text{EtDA}) \cdot 0.87(\text{Ag}^+) \cdot (4\text{tBC4A})^-$ clathrate **5** (POB62): 0.840 g (1.29×10^{-3} mol) of 4tBC4A was weighed out into a vial with 4.5 mL of EtDA. The resulting mixture was heated at 70°C until the calixarene was completely dissolved. The solution was allowed to cool, and 0.118 g AgNO_3 (6.98×10^{-4} mol) was then dissolved in the amine. The vial was then loosely capped and set aside to allow slow evaporation of the amine. After approximately five days, clear crystals were observed to have formed.

Single Crystal X-ray Diffraction data are summarized in Table 1. For clathrates **1** and **5**, hydrogen atoms on fully ordered heteroatoms were found from the difference map, with all other hydrogen atoms placed in calculated positions and refined as riding atoms. For the disordered amine residues and tertiary butyl group, the majority positions were refined anisotropically, as were any minority positions with occupancies greater than 0.40. Anisotropic displacement parameters were constrained to be equal for disordered fragments when interatomic distances were too short to allow for independent refinement (<0.7 Å separation). For clathrate **3**, the extensive guest disorder required alternative modeling of the structure. All hydrogens were placed in calculated positions and refined as riding atoms for the *endo* amine and three of the *exo* amines. No hydrogens were placed on the fourth *exo* amine due to the large thermal parameters of both sites.

Thermogravimetric analysis was carried out following the procedure detailed in Chapter III on page 72-73, save that samples were heated from room temperature to 350°C at a rate of 5°C/minute. Thermal desorption studies of clathrate **1** (yielding $1(\text{EtDAOH}) \cdot 1(4\text{tBC4A})$ clathrate **2** and the β_0 *apo* form of 4tBC4A), clathrate **3** (yielding $1(\text{EtDA}) \cdot 1(4\text{tBC4A})$ clathrate **4** and the α *apo* form of 4tBC4A), and clathrate

5 (yielding 1(EtDA)*Ag*1(4tBC4A) clathrate **6** and the Ag loaded β_0 *apo* form of 4tBC4A), were carried following the procedure detailed in Chapter III on page 73, with the exception that the final sample was heated to 245°C in the vacuum oven, and then transferred to a high temperature furnace for heating at 270°C to remove residual amine. TEM images were obtained by Dr. K. Yu, with the powders deposited on a TEM grid by suspending them in an acetone solution.

PXRD data for the β_0 *apo* form of 4tBC4A arising from desorption of **1** was collected on the Rigaku Geigerflex vertical goniometer diffractometer. Data for all other compounds were collected at on the Scintag X-2 Advanced diffractometer. In the case of clathrates **1**, **3**, **5**, and the α *apo* form of 4tBC4A, the actual SCXRD structures of the compounds were used to guide the indexing, while for clathrates **2**, **4** and **6**, the SCXRD data from the 1 Guest: 1 Host *n*-butylamine:4tBC4A clathrate were used.^[44] Crystallite size determination was carried out as described in Chapter IV on page 127.

¹³C spectra for all clathrates as synthesized and thermal desorption experiments were collected using the Bruker AMX-300 spectrometer. The high-power decoupled (HPDEC) spectra were collected using pulse delays ranging from 5 s to 30 s.

The CO₂ adsorption isotherm was determined using using the apparatus and methodolgy detailed in Chapter III on page 73-74. In a typical experiment, 1.08 g (1.06 x 10⁻³ mol) of clathrate **1** was used. The experimental isotherm was fit to a Sips adsorption isotherm using the non-linear curve fitting routines of OrginLabs Origin 7.0. ¹³C labelled CO₂ gas adsorption experiments for SSNMR were carried out on sealed samples of clathrate **1**, using the general procedure described in Chapter III on page 72. Spectra of

these samples were obtained using the Avance 200 spectrometer. For the HPDEC spectra, a pulse delay of 30 s was sufficiently long for quantitative measurements.

Table 1 Single Crystal X-Ray Diffraction data for Clathrates 1, 3 and 5.

Identification code	Clathrate 1 (POB67)	Clathrate 3 (POB66)	Clathrate 5 (POB62)
Empirical formula	C ₅₄ H ₉₁ N ₅ O ₉	C ₅₄ H ₇₂ N ₁₀ O ₄	C ₅₀ H _{78.88} Ag _{0.87} N ₆ O ₄
Formula weight	954.32	925.22	921.92
Temperature	173(2) K	125(2) K	173(2) K
Wavelength	0.71073 Å	0.71073 Å	0.71073 Å
Crystal system	Monoclinic	Monoclinic	Monoclinic
Space group	<i>P</i> 2 ₁ / <i>n</i>	<i>P</i> 2 ₁ / <i>n</i>	<i>P</i> 2 ₁ / <i>n</i>
Unit cell dimensions	<i>a</i> = 12.6601(7) Å <i>b</i> = 20.0210(11) Å <i>c</i> = 21.9037(12) Å α = 90° β = 92.646 (1)° γ = 90°	<i>a</i> = 12.9059(6) Å <i>b</i> = 19.6917(10) Å <i>c</i> = 22.2135(11) Å α = 90° β = 93.305(1)° γ = 90°	<i>a</i> = 13.3739(6) Å <i>b</i> = 21.1368(10) Å <i>c</i> = 18.5147(9) Å α = 90° β = 109.652 (1)° γ = 90°
Volume	5546.0(5) Å ³	5635.9(5) Å ³	4928.9(4) Å ³
Z	4	4	4
ρ _{calc}	1.143 Mg/m ³	1.090 Mg/m ³	1.242 Mg/m ³
Abs. coefficient	0.077 mm ⁻¹	0.070 mm ⁻¹	0.407 mm ⁻¹
F(000)	2088	1992	1975
Crystal size	0.48 x 0.24 x 0.16 mm ³	0.40 x 0.25 x 0.15 mm ³	0.48 x 0.16 x 0.16 mm ³
θ Range	1.38 to 29.61°	1.78 to 26.41°	1.51 to 29.61°
Index ranges	-17 ≤ <i>h</i> ≤ 17 -27 ≤ <i>k</i> ≤ 27 -30 ≤ <i>l</i> ≤ 30	-16 ≤ <i>h</i> ≤ 16 -24 ≤ <i>k</i> ≤ 24 -27 ≤ <i>l</i> ≤ 27	-18 ≤ <i>h</i> ≤ 18 -29 ≤ <i>k</i> ≤ 29 -25 ≤ <i>l</i> ≤ 25
Reflections collected	63557	55865	61547
Ind. reflections	15577	11548	13857
Completeness to θ = max	[R(int) = 0.0568] 99.7 %	[R(int) = 0.0482] 99.7 %	[R(int) = 0.0373] 99.9 %
Abs. correction	Multi-Scan	Multi-Scan	Multi-Scan
Refinement method	Full-matrix least-squares on F ²	Full-matrix least-squares on F ²	Full-matrix least-squares on F ²
Data / restraints / parameters	15577 / 60 / 805	11548 / 262 / 845	13857 / 73 / 679
Goodness-of-fit on F ²	1.021	1.030	1.033
Final R indices [I > 2σ(I)]	R1 = 0.0655 wR2 = 0.1702	R1 = 0.0896 wR2 = 0.2545	R1 = 0.0471 wR2 = 0.1182
R indices (all data)	R1 = 0.1249 wR2 = 0.1963	R1 = 0.1395 wR2 = 0.2946	R1 = 0.0827 wR2 = 0.1328
Largest diff. peak and hole (e.Å ⁻³)	0.332 and -0.458	0.737 and -0.363	0.944 and -0.349

4. Results and Discussion

¹³C SSNMR and SCXRD of 4tBC4A EtDAOH Clathrate 1

The adsorption of acid gases, such as CO₂ and H₂S, is of critical importance to a variety of industrial applications. Many natural gas streams contain significant fractions of such gases thus requiring efficient, selective removal by adsorbents.^[45] Because of its status as a greenhouse gas, CO₂ in exhaust flue gas has received attention for post-combustion treatment.^[46, 47] Commercially, the majority of processes currently used for scrubbing acid gases rely upon aqueous mixtures of ethanolamines to sequester the CO₂ through the formation of carbamates and carbonates.^[41, 42, 48-51] However, the process is quite expensive, given that the regeneration of the ethanolamine is energy intensive, and that the process liquids are corrosive makes them undesirable from an engineering standpoint.

One strong alternative is the use of appropriate porous solid materials for adsorption of CO₂. The majority of solid state systems with potential for industrial applications have been inorganic, for instance, various unmodified zeolites.^[52-54] More recently, polyethyleneimine-modified MCM-41 has been shown to adsorb CO₂ readily,^[55] while amine-modified MCMs and xerogels,^[56] amorphous silicas,^[57] zeolites^[58] and polymer beads^[59] have also proven to well suited to CO₂ adsorption. However, these approaches have significant limitations, with the zeolites exhibiting comparatively low selectivity, and the structures of the modified materials being difficult to control from a synthetic point of view. Even so, the studies of the modified materials indicate the potential strength of making use of an organic functionality to introduce the

desired specificity. Given the ease with which amines are included in frameworks of 4tBC4A, it was natural to attempt to include EtDAOH in order to attempt to produce a solid-supported ethanolamine adsorbent.

Recrystallization of 4tBC4A from ethanolamine (EtDAOH) readily produces large crystals of an ethanolamine 4-*t*-butylcalix[4]arene clathrate (clathrate 1). An examination of the ^{13}C CP/MAS NMR spectrum makes it immediately apparent that the structural motif resulting from this inclusion is based on the elimination of the four-fold symmetry for the host molecule (see Figure 1). All of the resonances are readily assigned in light of previous studies of low-symmetry inclusion compounds of 4tBC4A, such as those arising from enclathration of other aliphatic amines^[23, 44, 60] (see Chapter III) or nitrobenzene.^[61] The resonances due to carbons 1 and 4 in the host are particularly well defined, with the four-fold splitting exhibited by each suggesting that the asymmetric unit contains a single calixarene unit. The other aromatic host resonances are less well defined due to increased overlap between split peaks, suggesting that the structural shifts due to inclusion are less dramatic for these atoms.

In the aliphatic region of the spectrum, the host resonances again are extensively split such that the various peaks overlap with each other. In particular, the weak resonances due to carbon 9 are almost completely overwhelmed by those from carbons 7 and 8, such that their existence can only be readily deduced from a decrease in intensity in this region of the spectrum upon dipolar dephasing. In light of the solution spectrum of ethanolamine,^[62] the two remaining broad resonances are assigned to the carbons of the guest. Comparison of the chemical shifts of these peaks indicates a modest

complexation-induced shift (see Table 2), suggesting that these resonances arise from guest molecules included within the calixarenes cavity such that the aromatic phenol groups shield them.

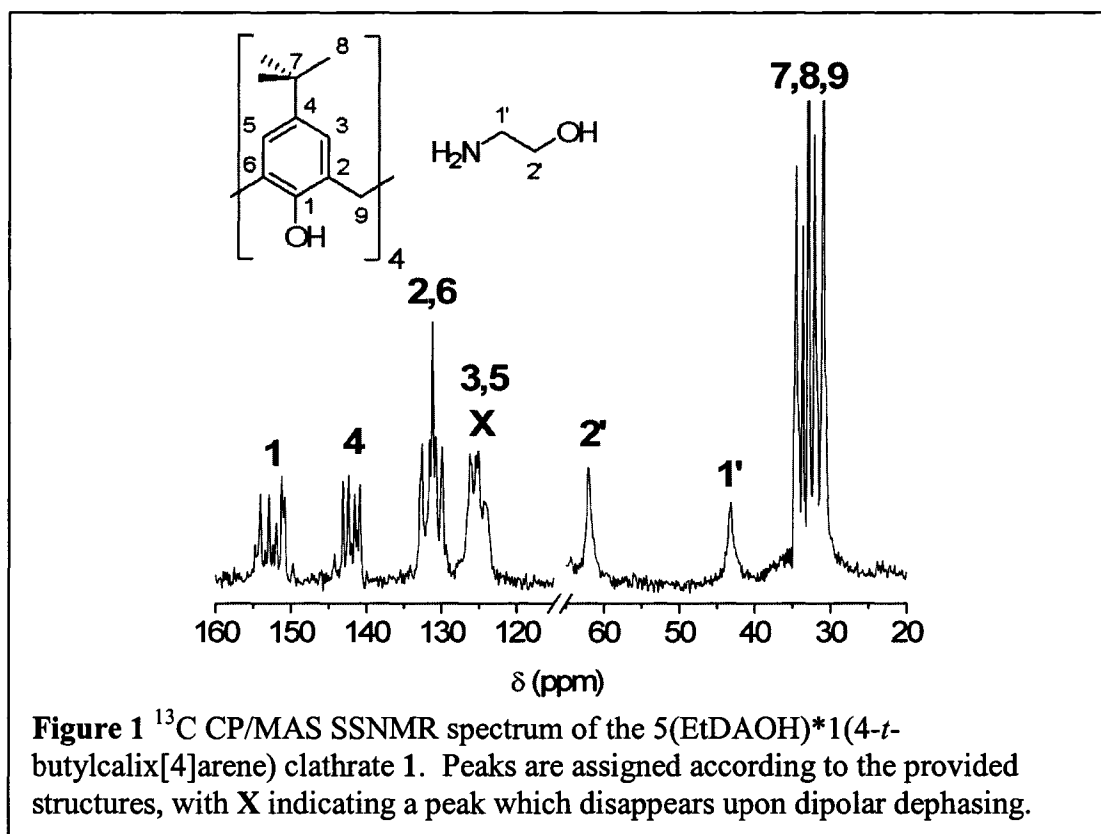


Table 2 Comparison of ^{13}C chemical shift values obtained by CP/MAS spectroscopy for ethanolamine in clathrates 1 and 2 with that observed in solution.^[a]

Guest	Carbon	δ Soln. ^[b]	δ 3 ^[c] (± 0.05)	CIS for 3 ^[d] (± 0.05)	δ 4 ^[c] (± 0.05)	CIS for 4 ^[d] (± 0.05)
Ethanolamine	C1'	43.96	43.19	-0.77	41.87	-2.09
	C2'	63.18	61.95	-1.23	62.18	-1.00

^[a]All values are in ppm. ^[b]Chemical shift of amine in solution, from SDBSWeb.^[62]

^[c]Chemical Shift observed in 4tBC4A clathrate. ^[d]CIS=Complexation-induced shift=(δ clathrate)-(δ Solution)

The broadening of these guest peaks may arise from a combination of factors.

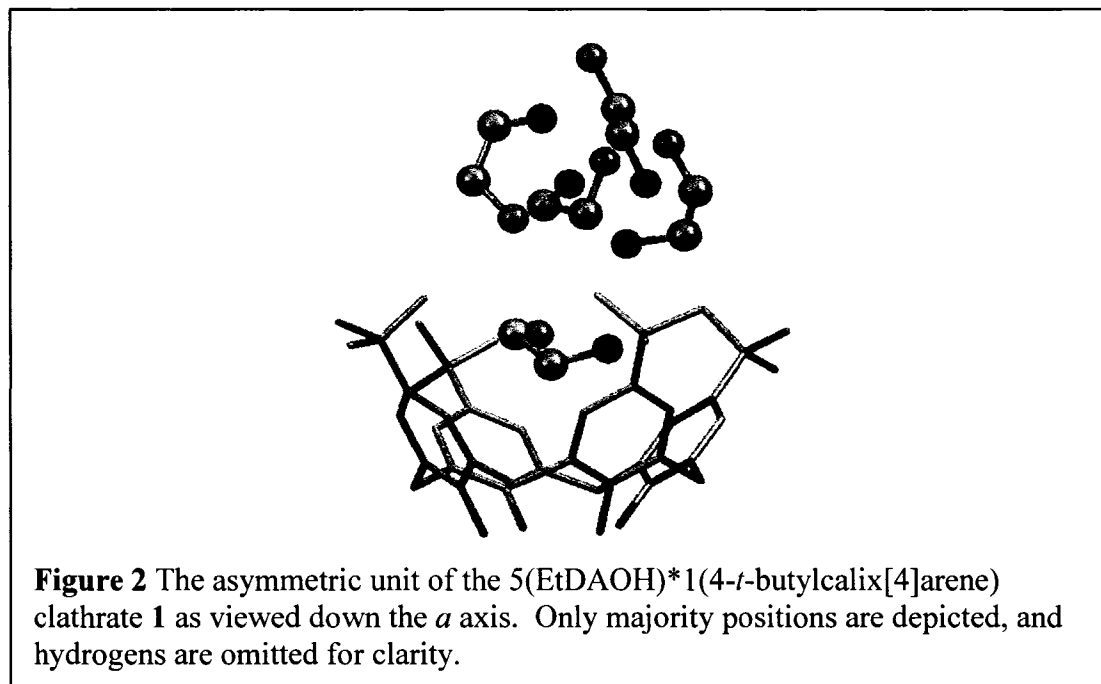
Neither carbon exhibits a decrease in intensity upon dipolar dephasing suggesting that they undergo sufficiently rapid motion to reduce the dipolar couplings significantly.

Therefore we can state that, unlike the 3 Guest: 1 Host amine clusters formed by *N*-alkylamines like *n*-butylamine,^[44, 60] a much broader range of hydrogen bonding interactions exist within the amine cluster enclathrated by units of 4tBC4A. While the broadening makes it difficult to determine what the potential ratio of amine to calixarene is exactly, the restricted geometries observed for the 3 Guest :1 Host compounds suggests that such dynamics inherently entails the formation of a larger amine cluster than previously observed.

The structural model obtained from SCXRD data confirms this hypothesis, with the stoichiometric ratio of clathrate 1 shown to be 5 units of ethanolamine for each molecule of 4tBC4A. In the resulting asymmetric unit, a single amine is included within the calixarene (*endo*), while the remaining four amines are located *exo* to the calixarene cavity (see Figure 2). As seen in previous structures of amine clathrates formed by 4tBC4A, the symmetry of the host molecule clearly is reduced because of the abstraction of a proton from one of the phenol groups by a single, fully ordered *exo* amine. The resulting structure now contains only a two-fold roto-inversion axis, crystallizing in the monoclinic $P2_1/n$ space group.

In order to accommodate even this reduced symmetry, a number of the moieties in the asymmetric unit are disordered, with the amines assuming a variety of conformations to accommodate the extensive hydrogen bonding scheme stabilizing the cluster. The *endo* amine assumes a *gauche* conformation in order to accommodate the inclusion of the hydrophobic carbon backbone in the calixarene cavity. It exhibits a disorder that can be modeled as being over two sites (occupancy ratio of 0.73:0.27), with the reversal of the

positions of the heteroatoms being the chief difference between the two sites. This shift in the positions of the heteroatoms also appears to induce a two-fold disorder in a single *t*-butyl group (occupancy ratio of 0.78:0.22), with the shift in the group presumably occurring to accommodate the increased bulk of the oxygen centre.



Of the remaining *exo* amines, two exhibit disorder, while the other two are fully ordered. One of the fully ordered amines assumes a *gauche* conformation similar to that observed for the *endo* amine, while the other amine (which bears the abstracted proton) is found in a *trans* conformation. Of the two disordered amines, one is found in a *gauche* conformation, with the disorder consisting of two positions (occupancy ratio of 0.70:0.30) reflective of a subtle rotation about the carbon-carbon bond. The other amine exhibits more significant disorder modeled as being over three distinct positions (occupancy ratios of 49:30:20) that appears to be reflective of two processes (see Figure 3).

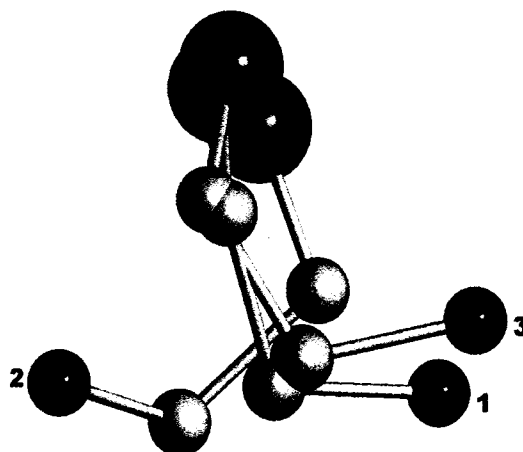
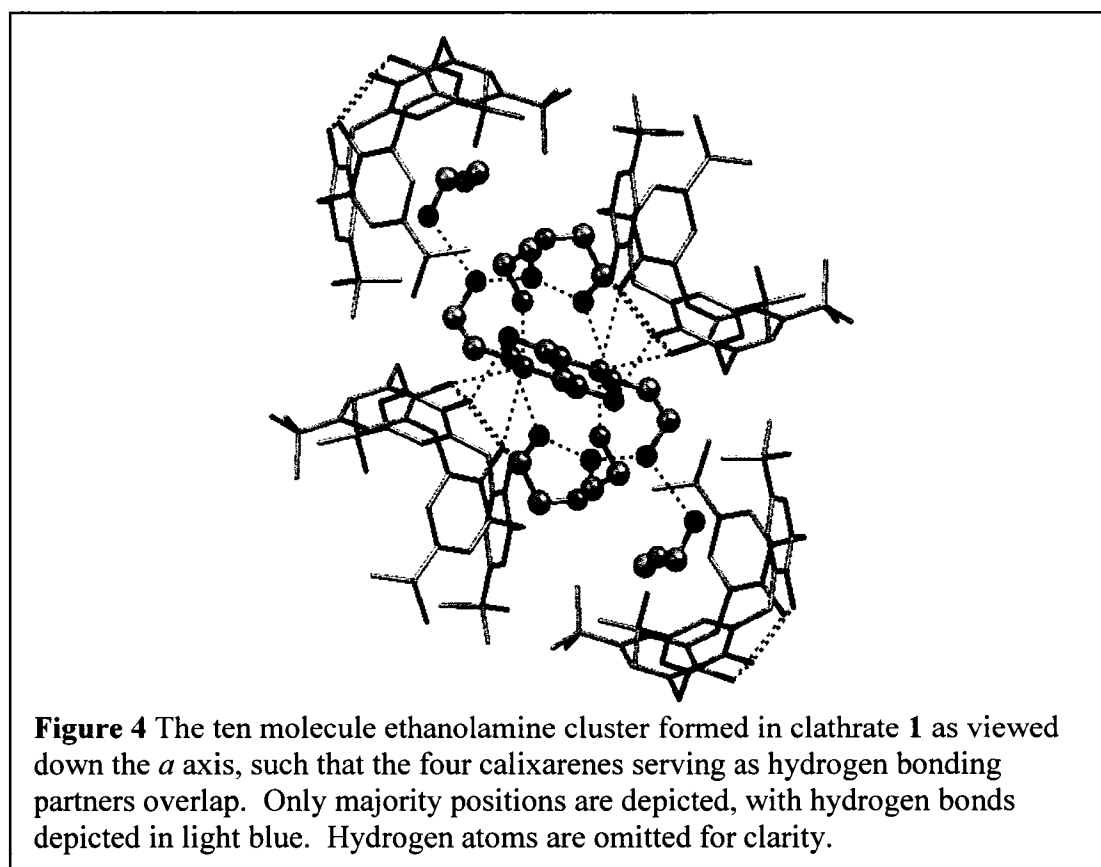


Figure 3 The threefold disorder of one of the *exo* amines found in 5(EtDAOH)*1(4-*t*-butylcalix[4]arene) clathrate **1**. Based on the thermal parameters, the nitrogens experience considerable motion. Each of the positions is labelled according to its relative occupancy (1=0.49, 2=0.30, 3=0.20).

The first and third positions appear to arise out of minor shifts to accommodate variations in the hydrogen bonding scheme, while the second position is reflective of a more significant rotation about the carbon-oxygen bond. This rotation results in the nitrogen exhibiting comparatively large thermal parameters (isotropic U_{11} of approximately 0.08), suggesting the two positions are likely reflective of a broader range of potential sites.

These disordered ethanolamine molecules assemble with 4tBC4A in a fashion similar to that observed for the 3:1 amine compounds (see Chapter III).^[60] In fact, the unit cell parameters of clathrate **1** and the 3(*n*-butylamine)*1(4tBC4A) clathrate are virtually identical, with only an expansion of 151.41 Å³ arising from a slight increase in the β angle (see Table 3). The amines reside in a channel defined by an assembly of capping calixarene units, with the larger 6 × 8 × 14 Å clusters found in clathrate **1** composed of 10 molecules of ethanolamine. Instead of four capping calixarenes defining each portion of the channel, each cluster interacts with six units of 4tBC4A. Two of these calixarenes

serve as hosts for two *endo* amines, while the other four calixarenes interact with the clusters by way of hydrogen bonds formed between the phenolic groups at the bottom of each molecule of 4tBC4A and two crystallographically equivalent *exo* ethanolamine molecules (N...O distances of 2.94 and 3.02 Å, O...O' distance of 2.70 Å). The remaining *exo* ethanolamine molecules form an intricate web of hydrogen bonds between each other (N...N and N...O distances ranging from 2.67 to 3.27 Å, see Figures 4 and 5). Therefore, even with the increased prevalence of hydrogen bonding in such structures, the role of the calixarene as host suitable for van der Waals stabilization of the *endo* amines is still quite significant.



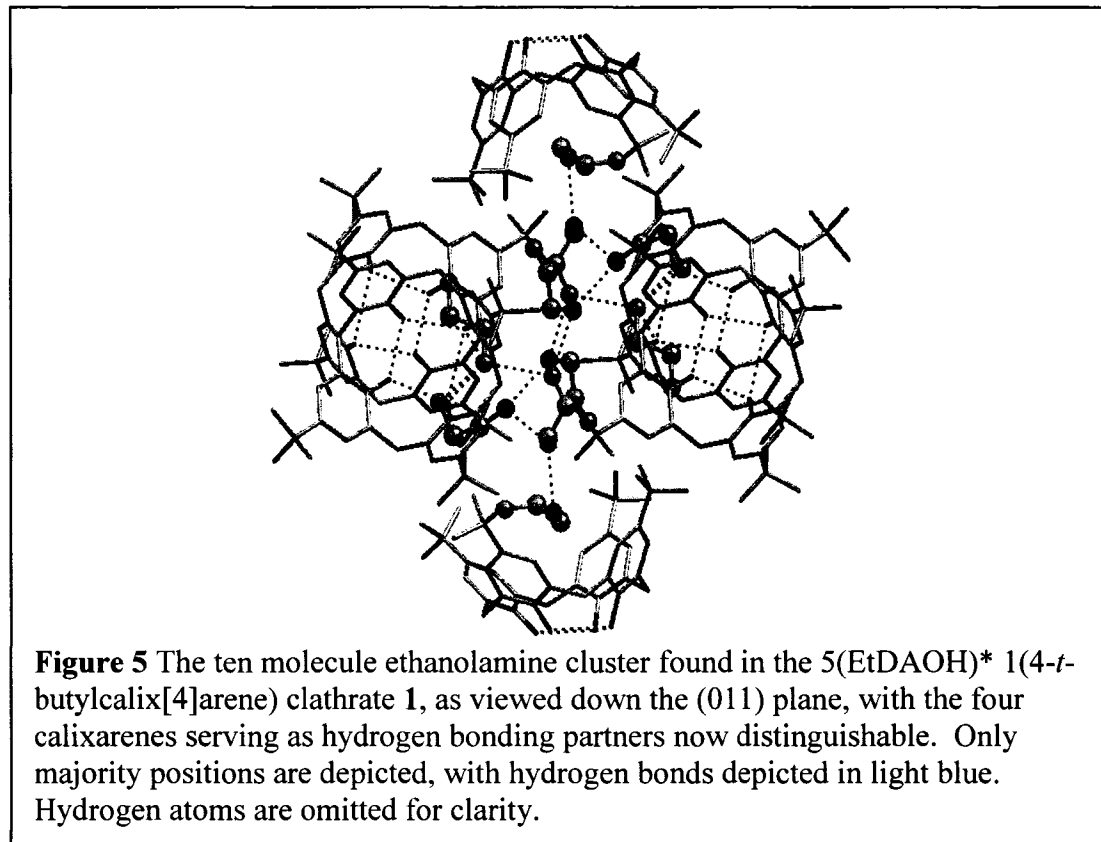


Table 3 Comparison of the unit cell parameters of 3 (*n*-butylamine)*1(4tBC4A) clathrate and Clathrate **1**.

Compound	3*(<i>n</i> -butylamine):1*(4tBC4A) ^a	Clathrate 1
Space Group	$P2_1/c$	$P2_1/n$
$a / \text{Å}$	12.9405(1)	12.6601(7)
$b / \text{Å}$	20.0923(1)	20.0210(11)
$c / \text{Å}$	20.7519(1)	21.9037(12)
$\beta / ^\circ$	91.122(1)	92.656(1)
$V / \text{Å}^3$	5394.6(4)	5546.0(5)

^aFrom Udachin *et. al.*^[44]

However, as suggested by the shift in the β angle, the exact geometry of this interaction has undergone a change when compared to previous studies. This can be attributed to the fact that the capping calixarenes are shifted off the axis defined by the units of 4tBC4A serving as hosts to *endo* amines by approximately 5.00 and 7.54 Å respectively. This distortion arises from the ability of the difunctional guest to support a

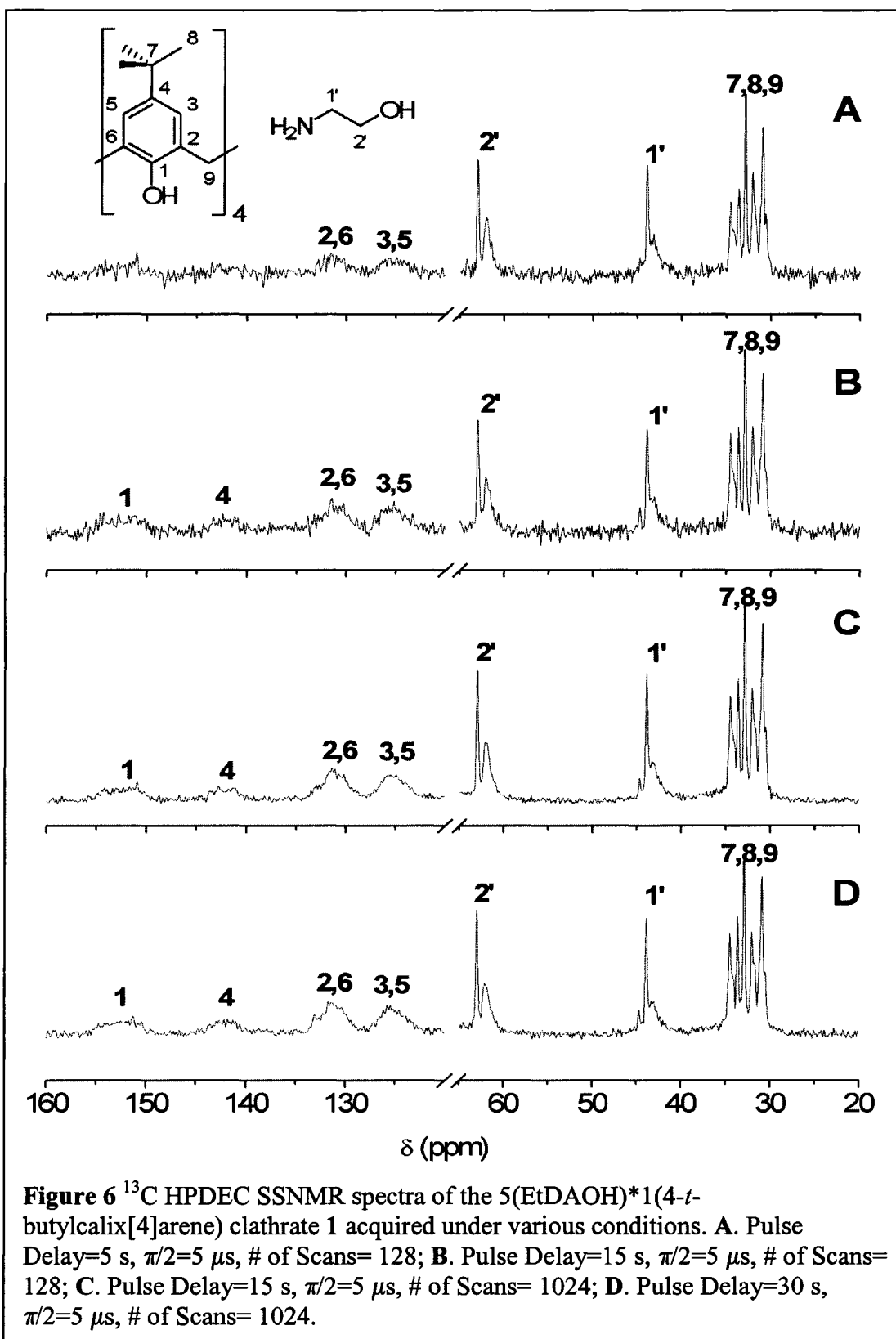
broader range of hydrogen bonding schemes, such that large clusters can offer a similar degree of stabilization as that arising from interactions between the 3 guest : 1 host clusters favoured by the monofunctional alkylamines. The capping calixarenes are now free to act as linkers between clusters, interacting only with amines on the periphery of the cluster that would otherwise be coordinatively unsatisfied. Thus, while the hydrogen bonding scheme remains dependent on the combination of forces serving to stabilize the amines, it is possible to drive the structure towards more complex, infinitely linked motifs by introducing guests that will favour more extensive hydrogen bonding.

The disorder observed in this hydrogen bonded cluster, along with the evidence from the CP/MAS spectra of dynamics fast on a time scale determined by dipolar couplings, raises intriguing questions as to the nature of the amine cluster formed. As previously mentioned, for 3 guest : 1 Host amine inclusions, the motion of the guests was inherently restricted by the fact that each amine in the cluster interacted with the calixarene lattice. For clathrate 1, only four ethanolamine molecules out of the ten present in a cluster interact directly with the calixarene framework (the *endo* amines through limited van der Waals stabilization, and the *exo* amines serving as linkers to form the infinite hydrogen bonding network), with the remainder only interacting with other ethanolamine molecules. Presumably, these free amines experience an environment much more similar to that observed for liquids than that experienced by those bound to the framework.

In order to test this hypothesis, we therefore obtained high-power ^1H decoupled Bloch decay ^{13}C SSNMR spectra. If the amines experience a liquid-like environment, it

would be expected that the relaxation times of the carbons would be quite short as compared to those not involved in fast dynamics. In the absence of cross-polarization (as is the case for the standard Bloch decay), this would be observable by comparison of the relative peak intensities of the guest and host for short pulse delays. As can be seen from Figure 6, even with comparatively short pulse delays (5 to 15 s), the two amine signals observed in the ^{13}C CP/MAS spectra are readily observed, as are the aliphatic host carbons (which are subject to significant relaxation through modulation of dipolar coupling by methyl and *t*-butyl rotation). Clearly, the ethanolamine molecules represented by these resonances experience considerable motion. It is only upon making use of a much longer pulse delay (and the accumulation of additional transients) that the immobile carbons in the aromatic rings begin to appear.

More significantly, two additional, isotropic ethanolamine resonances appear in the high-power decoupled Bloch decay spectra. Since the sample powders were well dried prior to obtaining the spectra, these resonances presumably represent amines experiencing such extensive motions that the dipolar interactions with the protons around them are averaged out. As such, they do not undergo effectively cross polarization, much as a liquid fails to undergo cross polarization. The signals appearing in both the CP and direct excitation experiments are those attributable to those amines on the periphery of the cluster experiencing somewhat restricted motion, while the resonances appearing only through direct excitation arise from the highly dynamic, liquid-like amines at the center of the cluster. This is also supported by comparison of the peak areas of the guest and the aliphatic host carbons, which give rise to the expected ratio of 5:5:20.



It therefore appears that an appropriate model for stabilization of larger amine clusters within frameworks formed by 4tBC4A would be that of a liquid droplet supported by an organized framework. The addition of another hydrogen bonding moiety allows for a much more fluid inclusion scheme, as predicted by the mixture of finite and infinite hydrogen bonded chains of 1,4-butanediamine included in 4tBC4A.^[22] The amines closely associated with the calixarene framework (through directional hydrogen bonding) experience a degree of ordering similar to that observed for other amine inclusions, while the remainder undergo tumbling that effectively mimics the interactions experienced in the liquid phase. However, it is likely that on some slow timescale even the various distinguishable amines undergo exchange. The resulting material gives us access to the diverse amine chemistry of the liquid clusters, while allowing one to operate in the solid state.

Desorption Behaviour of 4tBC4A EtDAOH Clathrate 1

As demonstrated previously, one of the key traits of the amine clathrates of 4tBC4A is the ability to use heating to adjust the primacy of hydrogen bonding and van der Waals stabilization in directing the structural motif.^[44] With the addition of more hydrogen bonding moieties giving rise to stabilized droplets, it seemed possible that the 5:1 inclusion motif was only one representative structure, with smaller clusters forming at higher temperatures. Alternatively, the cluster could depend on the overall stabilization provided by the entire web of interactions, such that disrupting one would inevitably lead to the disruption of the cluster (yielding behaviour similar to that observed for smaller clusters).

Thermogravimetric analysis indicates only two major weight loss events prior to the sublimation of 4tBC4A at approximately 300°C (see Table 4). The first major transition corresponding to the loss of four amines occurs at a temperature considerably lower than the boiling point of ethanolamine (170°C), clearly representing the tenuous nature of the hydrogen bonded cluster. However, the final amine is not lost until the sample is heated to 175°C, clearly indicating the resulting 1:1 inclusion compound is quite stable. It is important to note, however, that immediately upon heating a gradual weight loss is observed that corresponds to the loss of at least one additional molecule of amine. It is unclear as to whether this indicates that the clusters are in fact even larger than indicated by the XRD and NMR data, or if this merely corresponds to excess solvent trapped between the particles of the clathrate such that this amine is lost while preparing **1** for structural analysis. However, as we will see later, part of this weight loss can also be attributed to CO₂ chemisorbed from the atmosphere.

Table 4 TGA data for EtDAOH, EtDA and EtDA-Ag⁺ clathrates with 4tBC4A.

Clathrate	Temp. (°C) ^[a] (± 0.1)	% Wt. Lost ^[b] (± 0.01)	Mol. Guest Lost ^[c] (± 0.01)	<i>n</i> ^[d] (± 0.01)
EtDAOH (1)	65.0-96.5	26.50	4.15	5.08
	161.9-201.8	5.92	0.93	
EtDA (3)	27.0-90.5	25.49	4.13	5.22
	146.8-176.2	6.75	1.09	
EtDA Ag ⁺ (5)	76.1-100.6	7.47	1.14	3.01
	134.0-146.9	6.97	1.07	
	233.3-244.2	5.22	0.80	

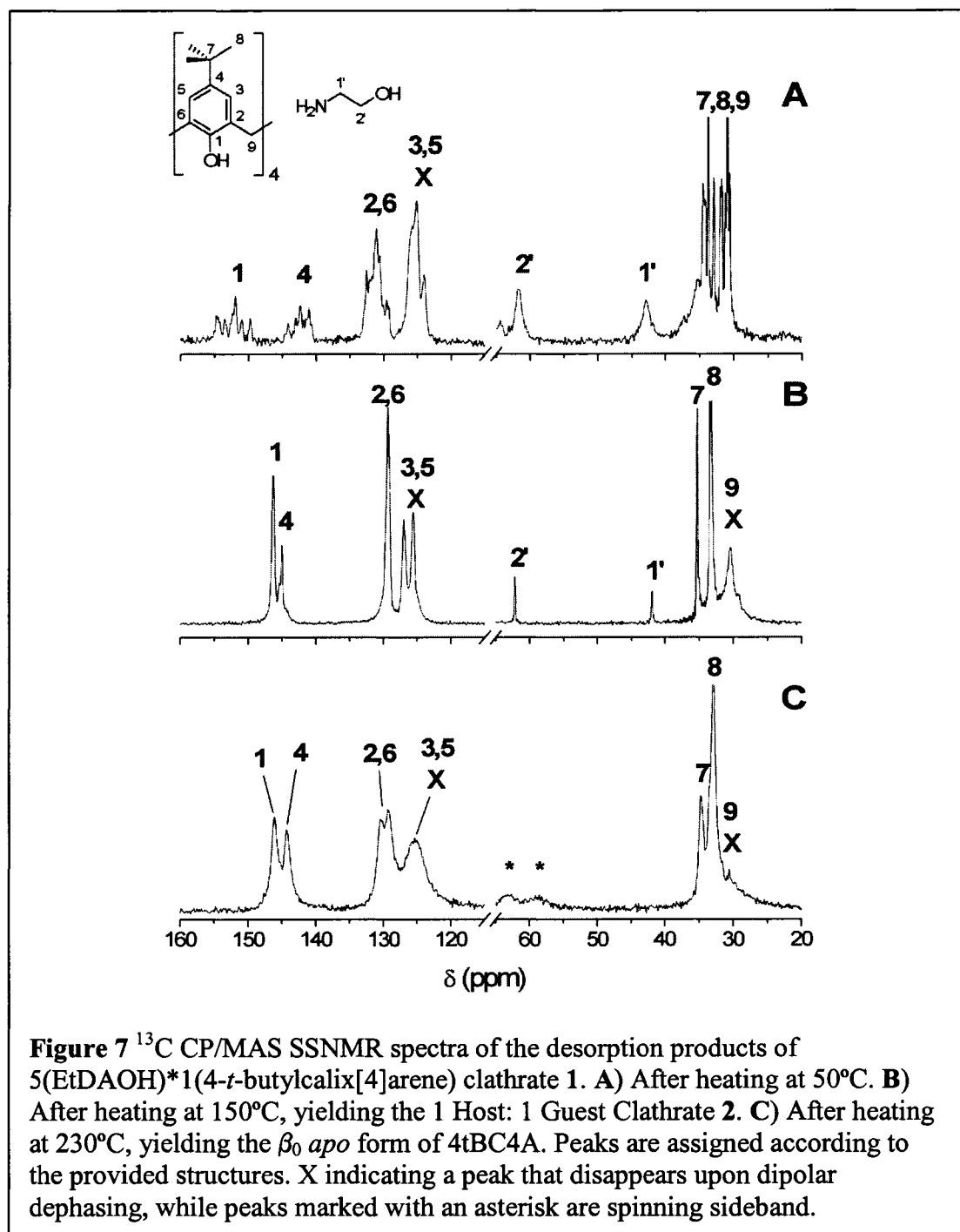
^[a]Temperatures are given for the onset and completion of transition. ^[b]Percentage of mass lost by sample. ^[c]Corresponding number of moles of guest lost by host. ^[d]Overall Guest to Host Ratio=(Total % Wt. Lost)/(1-Total % Wt. Lost)*(Mol. Wt. of Host)/(Mol. Wt. of Guest)

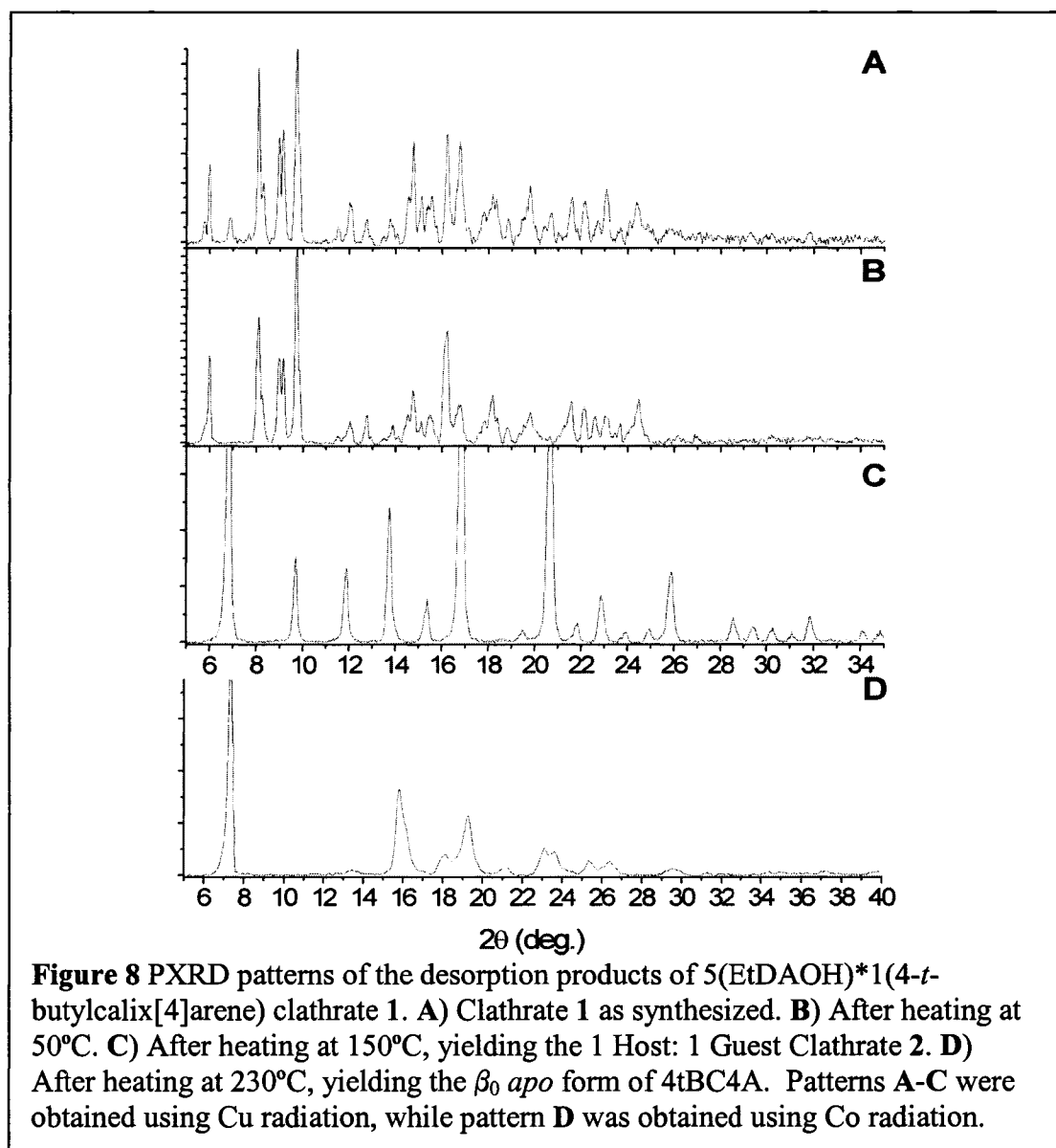
As before, the structural transformations arising from desorption of the amine from clathrate **1** can most easily be monitored using solid state NMR and PXRD. After

heating at 50°C for 30 minutes under vacuum, significant changes are not observed in the solid-state NMR spectrum or PXRD (see Figures 7A, 8B and Table 5). This suggests that the gradual loss of amine observed in the TGA has no impact on the structure of the clathrate. Presumably, this amine is included in such a fashion that the cluster either can readily rearrange itself to maintain the structural motif, suggesting that the parent clathrate can in fact accommodate additional amine either within the cluster, or in a secondary location. However, the broadness of the amine signals precludes identifying any particular sites for these amines.

Upon heating to 150°C, passing the first major transition, the structural evidence confirms the assumptions based on the TGA data (see Figures 7B and 8C). The ¹³C solid state NMR spectrum is now quite simple, with the various host resonances collapsing down to singlets. This indicates that only one calixarene is present in the asymmetric unit, such that the spectrum corresponds well to that expected of a 1 Host : 1 Guest inclusion compound (clathrate **2**). Furthermore, carbons 2 and 6 are functionally magnetically equivalent due to the local symmetry of the host molecule, such that their lines are indistinguishable. Two sharp singlets are observed for the guest, and the persistence of these resonances upon dipolar dephasing confirms the dynamic nature of the 1 Host: 1 Guest inclusion. However, comparison of the complexation induced shifts for these resonances to those observed for clathrate **1** (see Table 2) indicate that, on average, the 1' carbon adjacent to the OH group in the ethanolamine is now most deeply included in the calixarene cavity. Such an arrangement presumably accommodates interactions between the NH₂ group and the OH groups of the calixarene serving as host,

not unlike that predicted for solution inclusions.^[63, 64] Finally, the PXRD pattern obtained is readily indexed in the expected $P4/n$ space group, with unit cell parameters similar to that observed for other 1 : 1 inclusions in 4tBC4A (see Table 5).^[44, 60, 65, 66]



**Table 5** PXR D unit cell parameters for clathrates 1 and 2.

Clathrate	1 (as synthesized)	1 (after heating at 50°C)	2
Space Group	$P2_1/n$	$P2_1/n$	$P4/n$
$a / \text{Å}$	12.637	12.669	12.900
$b / \text{Å}$	20.077	20.273	12.900
$c / \text{Å}$	22.032	21.922	12.849
$\alpha / ^\circ$	90	90	90
$\beta / ^\circ$	92.44	92.45	90
$\gamma / ^\circ$	90	90	90
$V / \text{Å}^3$	5584.6	5626.2	2138.1

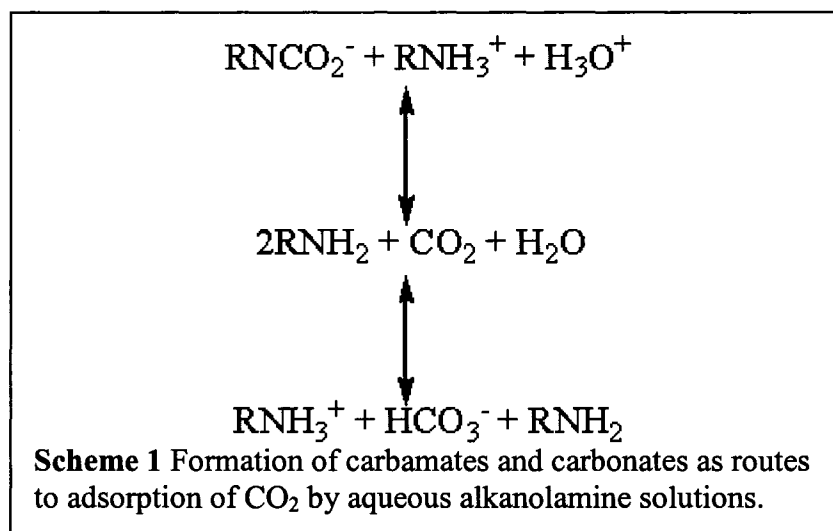
After heating to 230°C, all amine is removed from the clathrate. The resulting *apo* form continues to exhibit high symmetry, as evidenced by the ¹³C solid state NMR spectrum (see Figure 7C). The PXRD is also indicative of a crystalline, high-symmetry phase, but indexing cannot be reliably undertaken with so few distinct reflections (see Figure 8D). However, a simple visual comparison to the NMR spectra and powder patterns obtained for the desorption of toluene from 4tBC4A indicate that the *apo* form obtained is the β_0 form previously reported by Atwood *et al.* and further elaborated upon by Ripmeester *et al.*^[65, 66] This follows the previous studies of *n*-alkylamines, where a similar preference for the β_0 form was observed for the desorption of *n*-butylamine and amylamine.^[44, 60]

Given the similarity in desorption behaviour to monofunctional *n*-alkylamines, it would seem that the size of the cluster has no significant impact on the overall desorption behaviour. While the difunctional guest allows for additional hydrogen bonds to form such that the stabilization of larger clusters becomes possible, these clusters exhibit stability similar to that seen for the previously reported smaller clusters. In light of this, the fluid nature of the cluster as represented by the dynamic motion and disorder observed for the parent compounds clearly indicates that the individual hydrogen bonds are reasonably weak. Furthermore, they are all approximately equivalent in energy, as no intermediate cluster is observed upon heating the clathrate to remove the amine. As such, it appears that while the limitations of hydrogen bonding to the framework is much more significant than any guest-guest interactions in determining the stability of the structure,

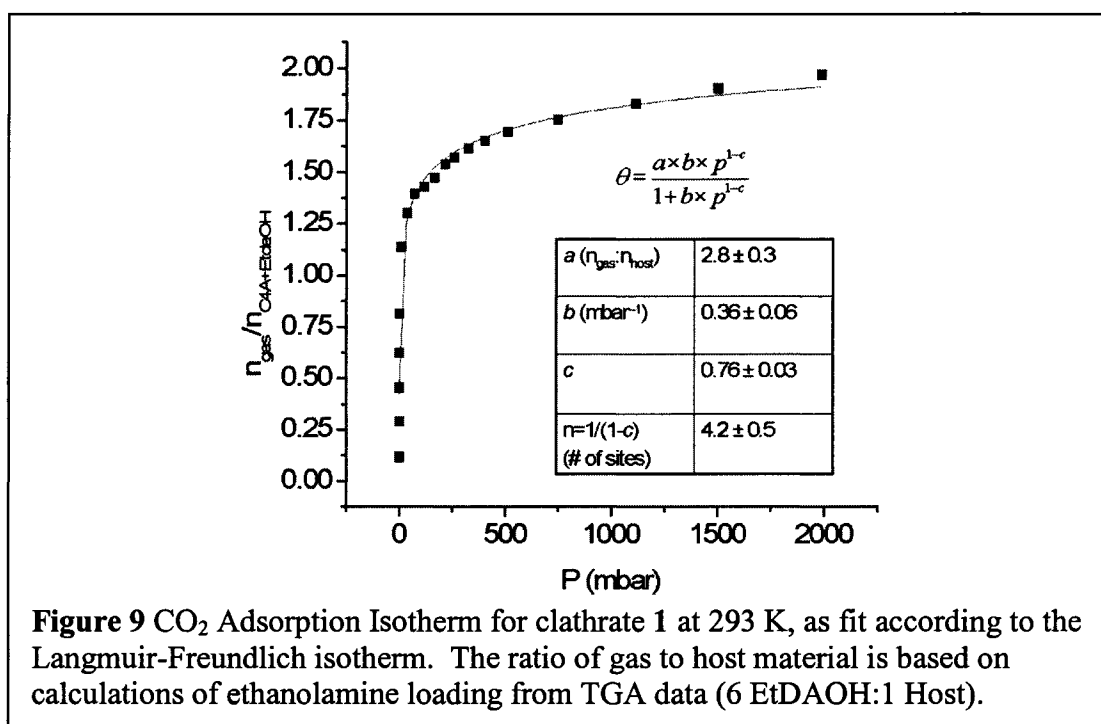
those guest-guest interactions can be used to tune the inclusion motif to allow for larger clusters.

CO₂ Adsorption Behaviour of 4tBC4A EtDAOH Clathrate 1

As mentioned, the use of alkanolamines to treat acid gas streams is well known, with a number of studies having examined adsorption of CO₂ by aqueous mixtures of ethanolamine and related compounds. This chemistry is based upon the reaction of CO₂ with the amine functionality and water to produce a carbamate or carbonate, thereby sequestering the gas (see Scheme 1). This process is essentially the same as that mentioned in Chapter I for pure amines, with the water serving as an additional site for proton transfer. The favoured mechanisms for explaining how this adsorption occurs revolve around the formation of a zwitterionic intermediate that is subsequently deprotonated to yield a carbamate,^[42, 48] or a single-step, third order reaction leading directly to carbamate formation.^[49] While the zwitterionic mechanism has been held as the preferred mechanism,^[41, 50] recent *ab initio* calculations suggest that the formation of zwitterionic species is less likely than previously thought.^[51]



The channelled structure of clathrate **1** clearly suggests that the ethanolamine droplets are available for adsorption in a fashion similar to that observed in solution. Therefore, a bulk sample of clathrate **1** was prepared and volumetric gas adsorption measurements with CO₂ were carried out. As seen from the adsorption isotherm at 293K (see Figure 9), clathrate **1** has a considerable affinity for carbon dioxide even at extremely low pressures. In comparison to the adsorption behaviour exhibited by the low-density *apo* form of 4tBC4A, clathrate **1** adsorbs comparable amounts of CO₂ at pressures which are an order of magnitude less.^[67] Therefore, the ethanolamine molecules are available as adsorbents, further suggesting that the supramolecular support of the amines within the calix framework gives rise to a droplet like structure.



Direct comparison to aqueous ethanolamine systems is somewhat more awkward, due to the wide range of sample compositions and experimental procedures. NMR studies of the equilibrium adsorption of CO₂ by 10% ethanolamine solutions indicated a 1

mole CO₂ : 1 mole amine loading ratio at approximately 8.5 bar.^[68] Clearly, the supramolecularly stabilized ethanolamine droplets in clathrate 1 exhibit a massive improvement in adsorption capacity at low pressures. This is likely due to the elimination of the bulk aqueous phase, thereby avoiding difficulties in solubilizing CO₂ such that it can now react with the ethanolamine. Furthermore, the adsorption capacity is also enhanced due to the fact that the solid adsorbent is considerably more compact than a comparable aqueous volume of amine, and is quite comparable to that observed for other solid supported systems,^[53, 56-58] such as polyethyleneimine loaded MCMs (~130 mg CO₂/ g of adsorbent).^[55]

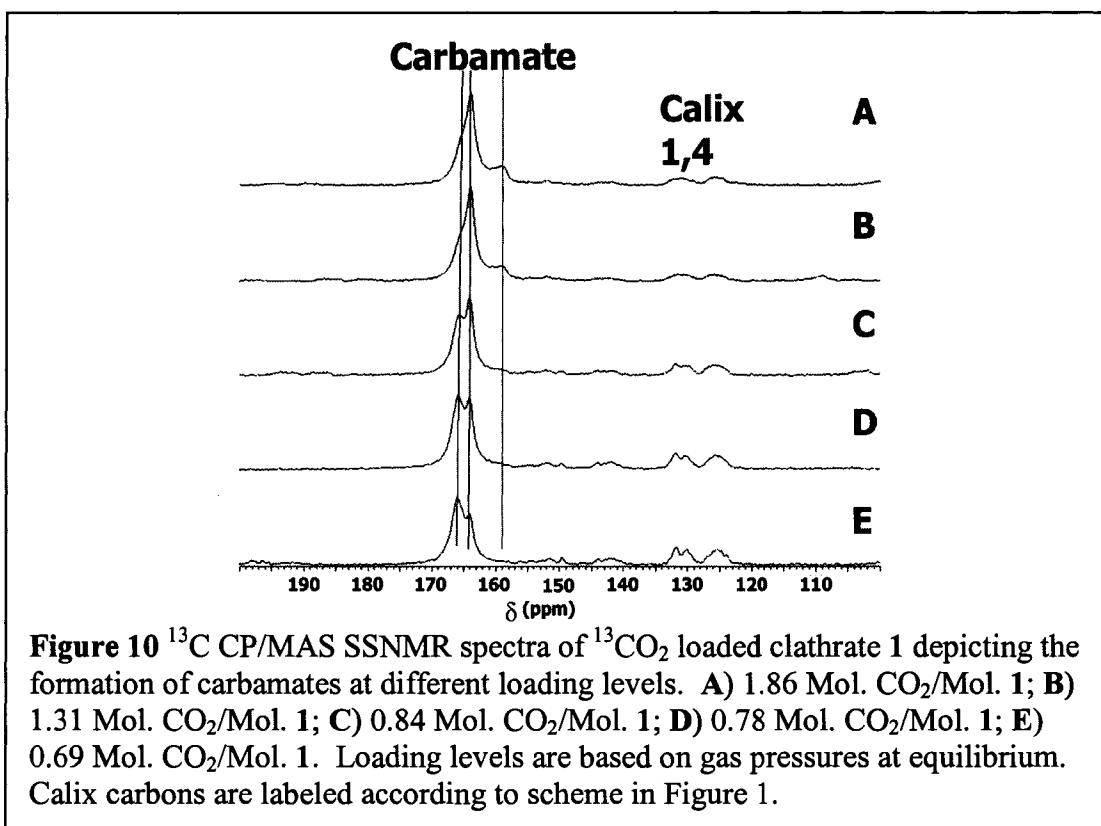
In light of the TGA evidence, it is also important to consider the potential impact on weight loss adsorbed carbon dioxide might have. It was previously stated that an additional gradual weight loss was observed at low temperatures. Examination of the observed weight loss at low temperatures cannot be entirely accounted for by adsorbed carbon dioxide given the partial pressure of CO₂ in the atmosphere (~0.3 mbar) although a carbamate peak can be observed in the HPDEC spectrum of the material as synthesized (165 ppm, not shown). The adsorption data therefore confirm the presence of an additional molecule of ethanolamine, which is accounted for in the determination of loading in the isotherm. Given the TGA data, this amine is very loosely held by the clathrate, such that it has not been possible to determine the specific location of this amine using XRD or SSNMR.

Despite this, given the distinct nature of the chemical species arising from such chemisorption, a number of studies have been carried out to clarify these mechanisms by

observing the formation of the carbamates and carbonates. Solution NMR studies have been shown to be quite suitable for monitoring the effects of pH and concentration on the species formed and the kinetics of the reaction.^[68-70] By making use of ¹³C labelled CO₂, it was possible to observe the species formed by adsorption of CO₂ by clathrate 1 directly using solid state NMR. While TGA indicates that evacuation to prepare the samples does result in some amine loss (resulting ratio is 4.2 guest : 1 host), as we will see, the structural motif is maintained, such that the spectra can be seen as representative of the processes occurring in the system described by the SCXRD structure. At the time of writing, this is the first attempt to structurally characterize the adsorption of CO₂ by alkanolamines in the solid state.

As can be seen from the ¹³C CP/MAS spectra, the inference from the adsorption isotherm that high loading at low pressures arises from chemisorption is correct (see Figure 10). At least three intense, distinct peaks are observed in the range between 160 and 170 ppm (overwhelming those from the calix framework) and consistent with the formation of a carbamate similar to that observed in solution spectra.^[68-70] It is important to note that while the furthest upfield peak at 159 ppm could also be potentially identified as a carbonate, the formation of such a species in the absence of water is highly unlikely. Such a resonance is more likely from carbamate formation with the difficult to access, shielded *endo* amine. The peaks observed therefore represent three distinct carbamate sites arising from the crystallographic inequivalence of the various amines in the structure. This inequivalence also appears to give rise to differences in accessibility, as the upfield peaks increase in intensity as overall loading increases.

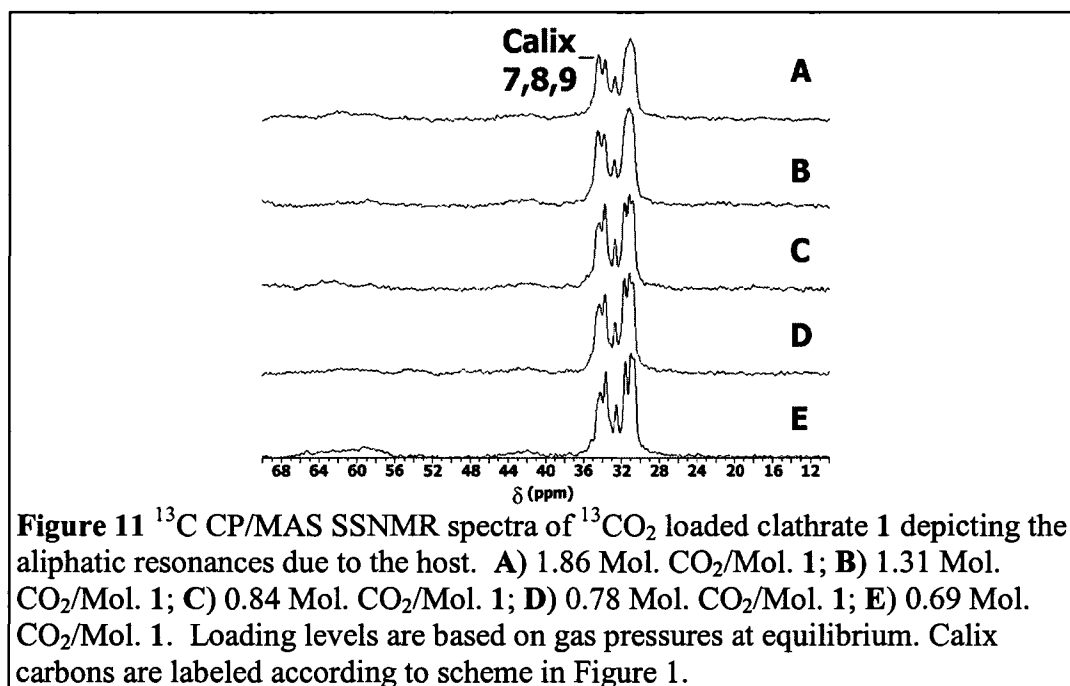
This adsorption behaviour can be rationalized as a consequence of the channelled structure observed in the SCXRD structure. The one dimensional nature of the channels requires that CO₂ diffuse through the structure, presumably resulting in the most accessible amine sites becoming saturated throughout the structure prior to carbamate formation at other sites. Without water present to mediate the reaction, presumably those ethanolamine molecules in close proximity to hydroxyls on either the



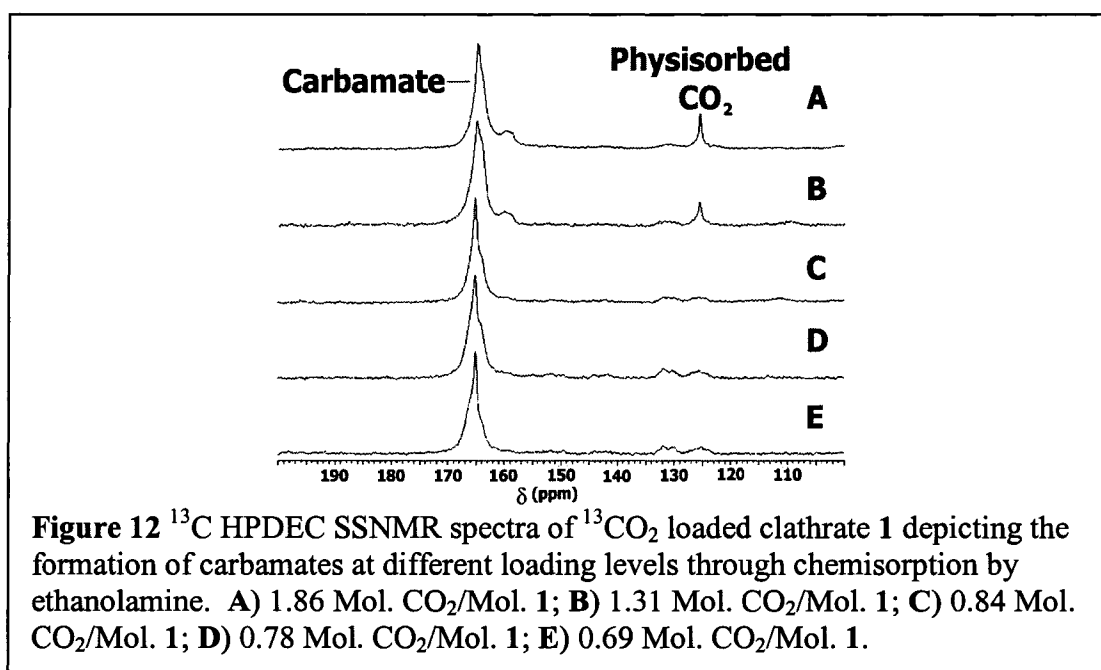
calix or adjacent amines will form carbamates more rapidly. Such amines are represented by the peak furthest downfield, which does not change appreciably in intensity over the range of loadings examined. As these amines are converted, the dynamic nature of the droplets allows for the other amines to serve as adsorption sites, giving rise to the upfield

peaks. Given the intensities observed, one of these upfield sites consists of the majority of the amines present in the system.

As with *n*-butylamine, it is reasonable to expect that carbamate formation is likely accompanied by the formation of alkylammonium cations, but again the overall adsorption capacity indicates that this is not the sole route for CO₂ adsorption. Furthermore, the solid state NMR data in the aliphatic region indicates that any structural shifts to accommodate chemisorption do not dramatically impact the packing motif (see Figure 11). However, it is important to note that the relatively broad peaks observed due to the inevitable loss of crystallinity arising from the initial vacuum degassing of the samples renders it difficult to assess if any smaller changes in chemical environment occur for either host or guest. Even so, PXRD analysis of a selection of adsorption samples provided no additional information. As such, the increased size of the droplet likely insulates the system against the shifts in motif observed for *n*-butylamine.



In addition to the three chemisorption sites, there is at least one physical adsorption site available for the uptake of CO₂ (possibly arising from the decreased amine content). This site is only apparent upon examination of the HPDEC spectra, whereupon a peak at approximately 125 ppm is observed in the same region as that of the now suppressed calix aromatic resonances (see Figure 12). While this physisorption is expected from the absorption behaviour observed for the *apo* form of 4tBC4A,^[67] it is important to note that the isotropic lineshape indicates that the physical adsorption site is found outside of the calixarene cavity, indicating a different overall mechanism of adsorption. As such, while the overall adsorption isotherm appears to be comparatively simple, it is actually the result of a combination of two adsorption processes across a series of energetically distinct sites.



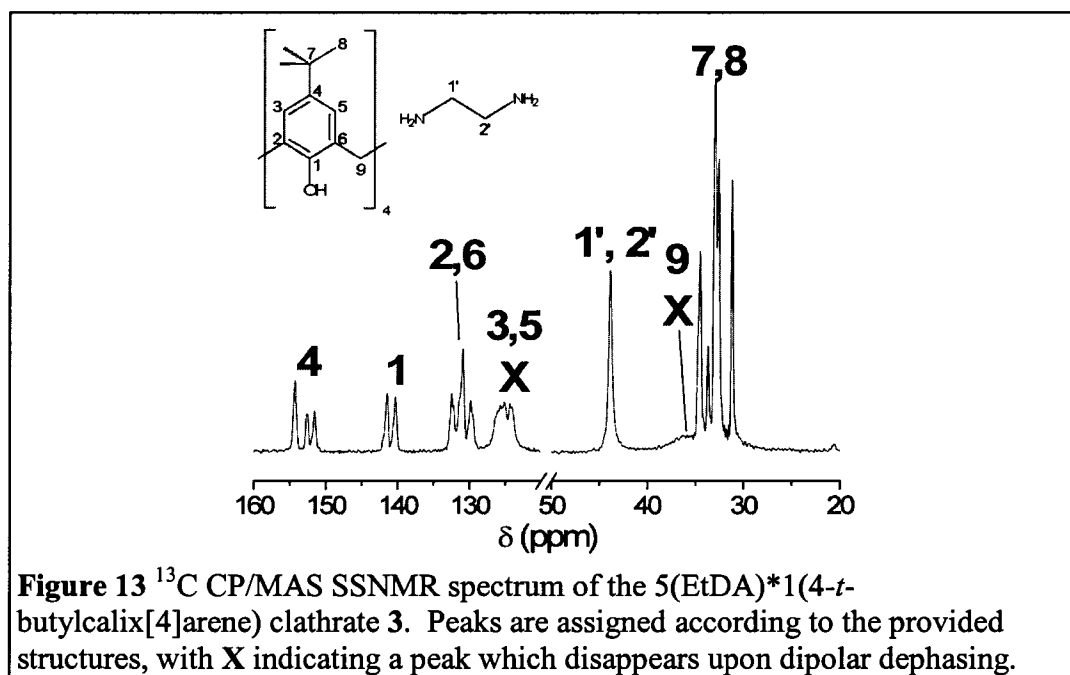
The resulting isotherm can be modeled adequately ($\chi^2=0.0035$, $R^2=0.988$) as a four site system using an extended Langmuir model (Langmuir-Freundlich isotherm, see

Figure 9), with an approximate maximum loading of 3 moles of CO₂ per mole of clathrate 1. This suggests that at least three of the amines serve as energetically equivalent sites, which, given the structural data, are likely the highly mobile three *exo* amines located at the heart of the droplet. Again, the specific mechanism of adsorption is unclear, likely involving a mixture of chemisorption and physisorption unlike that seen in liquid systems, including the formation of alkylammonium cations and proton transfer involving calixarene hydroxyl moieties. Therefore, at higher pressures, it might be expected that significant deviation from such a model may occur due to the combination of different adsorption processes. By the same token, the massive adsorption at low pressures gives rise to considerable difficulty in obtaining equilibrium adsorption values, such that further studies of the system are called for, including kinetic and thermodynamic studies.

¹³C SSNMR and SCXRD of 4tBC4A EtDA Clathrate 3

The inclusion of ethanolamine gave rise to nanodroplets that exhibited only partial ordering of the amine centres. Given the natural hydrogen bond donor-acceptor relationship between alcohols and amines, such stabilization is unsurprising.^[71] Indeed, the boiling point of ethanolamine (170°C) when compared to that of ethylenediamine (118°C) clearly indicates the high degree of stabilization that arises from such interactions. If this hypothesis holds true, one would expect to see a much greater degree of disorder in an ethylenediamine 4tBC4A clathrate, where the amino groups will be much more dependent on interactions with the calixarene than with neighbouring amine molecules.

Intriguingly, preparation of ethylenediamine 4tBC4A clathrate **3** is much easier than that of the corresponding ethanolamine clathrate. The less viscous ethylenediamine readily dissolves 4tBC4A, suggesting that the decreased competition between guest-guest and guest-host hydrogen bonding gives rise to greater solubility of 4tBC4A. ^{13}C CP/MAS of the resulting crystals, however, has many features in common with the spectrum of ethanolamine 4tBC4A clathrate **1** (see Figure 13). Once again, the characteristic multiple splitting of a capped *endo-exo* amine clathrate is observed in the aromatic host region. However, only the resonances due to carbon 4 of the host are readily resolved for detailed analysis, with three distinct peaks observed. This suggests, much as with the inclusion of amylamine, that two of the carbons are virtually magnetically equivalent, despite a lack of symmetry in the overall host molecule.



In contrast, the aliphatic host region exhibits a rather high degree of resolution, with at least six distinct host peaks attributable to carbons 7 and 8. In particular, one

resonance exhibits significant shielding (being observed at 31.21 ppm), further supporting the concept that one of the phenolic rings exhibits a rather dramatic distortion away from the other three rings. More intriguingly, only a single isotropic guest resonance is observed exhibiting only a minimal complexation induced shift (see Table 6). Given that the peak is retained upon dipolar dephasing, indicating the guest is undergoing dynamic motion, but the host symmetry is still reduced as in the capped amine clathrates, this clearly suggests that the guest resonance observed is actually an average of a number of positions undergoing rapid exchange. Thus, once again, the amine cluster appears to have been extended by virtue of the difunctional nature of the guest.

Table 6 Comparison of ^{13}C chemical shift values obtained by CP/MAS spectroscopy for ethylenediamine in clathrates 3-6 with that observed in solution.^[a]

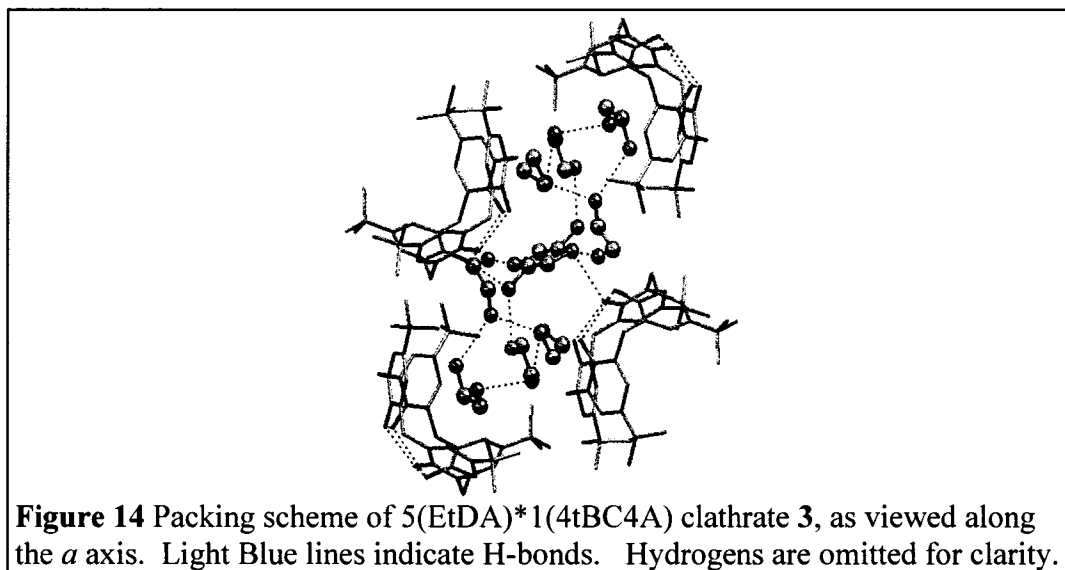
Clathrate	Carbon	δ 4tBC4A ^[b] (± 0.05)	δ Solution ^[c]	CIS ^[d] (± 0.05)
EtDA as Synth. (3)	C1',C2'	43.82	44.87	-1.05
EtDA 1:1 Form (4)	C1',C2'	37.85	44.87	-7.02
EtDA Ag ⁺ as Synth. (5)	C1',C2'	48.29	44.87	3.42
		46.91		2.04
		41.17		-3.70
EtDA Ag 1:1 Form (6)	C1',C2'	43.57	44.87	-1.30

^[a]All values are in ppm. ^[b]Chemical Shift observed in 4tBC4A clathrate. ^[c]Chemical shift of amine in solution, from SDBSWeb.^[62] ^[d]CIS=Complexation-induced shift=(δ clathrate)-(δ Solution)

The SCXRD data supports this supposition of a highly dynamic, large guest cluster. Clathrate 5 is observed to have a stoichiometry of 5(EtDA)*1(4tBC4A), with the calixarene framework exhibiting an even more dramatic distortion of the capped motif than that observed for ethanolamine clathrate 1. While the amine guests again consist of

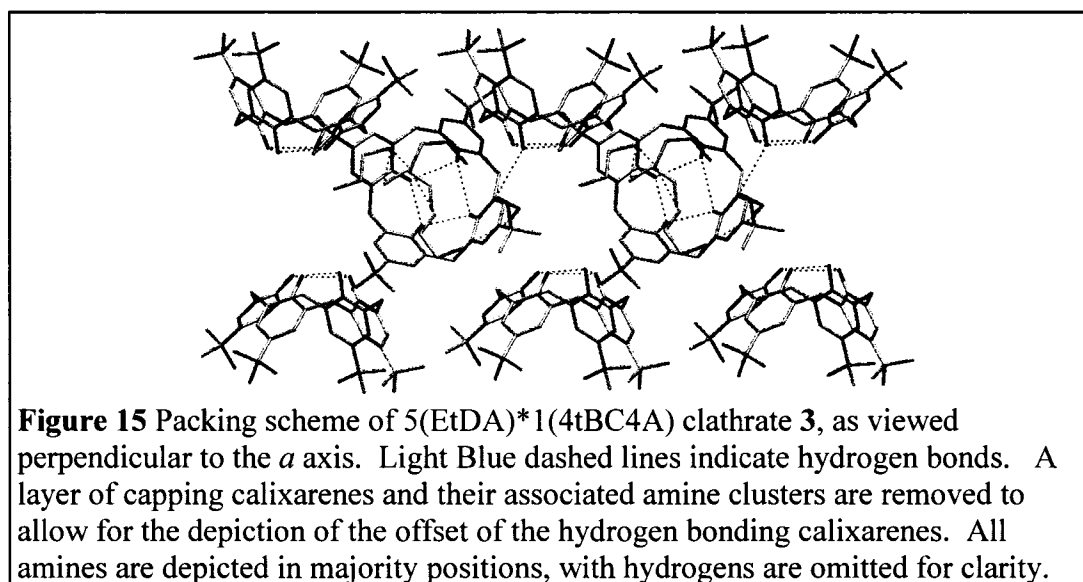
a single *endo* included amine and four *exo* amines, all of the amines in clathrate **5** are heavily disordered. The *endo* amine exhibits a two fold 0.50:0.50 disorder, while the *exo* amines are best modeled as a series of two-fold disordered molecules, with occupancy ratios of 0.52:0.48, 0.53:0.47, 0.56:0.44, and 0.78:0.22. Even with such modeling, the thermal parameters of the carbons and nitrogens of the guest molecules are quite large (U_{eq} ranging from ~ 0.08 to 0.3 typically), such that these two-fold models are only representative of the two major positions of the guest. Given the indications of dynamic motion observed in the SSNMR spectra, and the suggestion of exchange induced averaging, the disorder clearly suggests that the ethylenediamine included in 4tBC4A is also forming a liquid nanodroplet.

The ethylenediamine guests are largely stabilized through a broad network of hydrogen bonds (see Figure 14). A series of hydrogen bonds between the guests themselves (N...N distances of 2.90, 2.91, 2.92, 3.02, and 3.13 Å) results in two clusters of 5 EtDA molecules assembling to fill the capped cavity formed by the calixarenes, such



that the droplet is approximately $6 \times 9 \times 13 \text{ \AA}$ in size. A single *exo* amine also serves to link together the layers of calixarene (N...O distance of 2.96 and 3.15 \AA), such that an infinite hydrogen bonded chain is formed parallel to the (011) plane (see Figure 15).

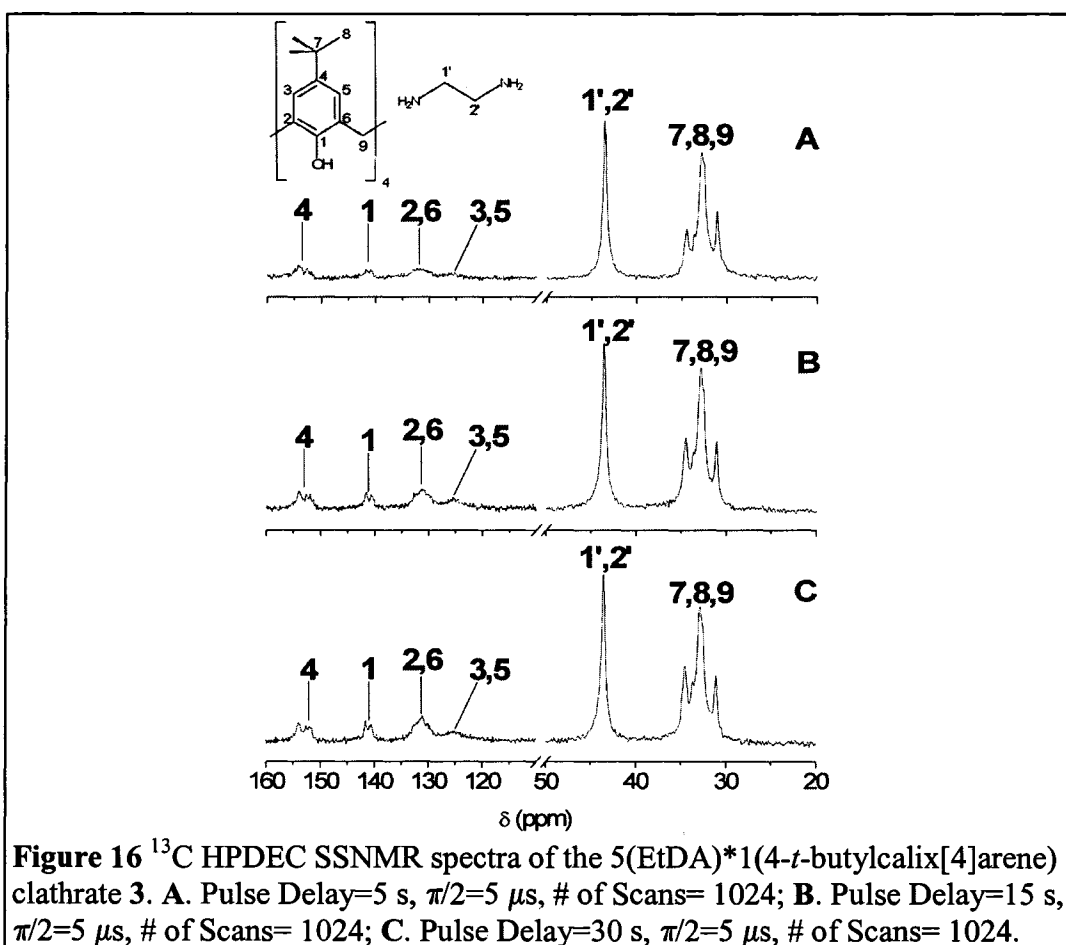
Much as before with clathrate 1, this gives rise to an amine filled channel along the *a* axis of the structure with each cluster interacting with six 4tBC4A units in total.



This hydrogen bonding motif presumably gives rise to the aforementioned distortion of the capped motif. The molecules of 4tBC4A are arranged such that two of the phenolic subunits form much shorter intramolecular hydrogen bonds at the base than the bond between the other pair (O...O distances of 2.45 and 2.96 \AA), giving rise to the magnetic and chemical equivalence predicted by the SSNMR spectrum. Furthermore, this results in the hydrogen bonding calixarene units being offset from each other by a distance equivalent to the diameter of the calixarene ($\sim 10.4 \text{ \AA}$). This shift is likely to accommodate hydrogen bonding to the large, dynamic nanodroplet. In addition to this, one

of the *t*-butyl groups exhibits a 0.77:0.23 disorder over two positions, presumably induced by the motion of the *endo* amine.

The extent of the dynamic motion of the ethylenediamine guest is qualitatively shown by ^{13}C HPDEC spectra of clathrate **5** (see Figure 16). As would be expected by a system undergoing rapid exchange in a liquid-like droplet, the guest resonances are readily observed even with short pulse delays. Unlike clathrate **1**, no additional peaks appear, with the ratio of guest to aliphatic host resonances consistent with a 5 to 1 inclusion ratio. Thus, the mobility of the ethylenediamine at room temperature is greater



than ethanolamine, due to the decreased strength of the hydrogen bond interactions in stabilizing a specific orientation, such that they are more liquid-like and readily exchange.

Desorption Behaviour of 4tBC4A EtDA Clathrate **3**

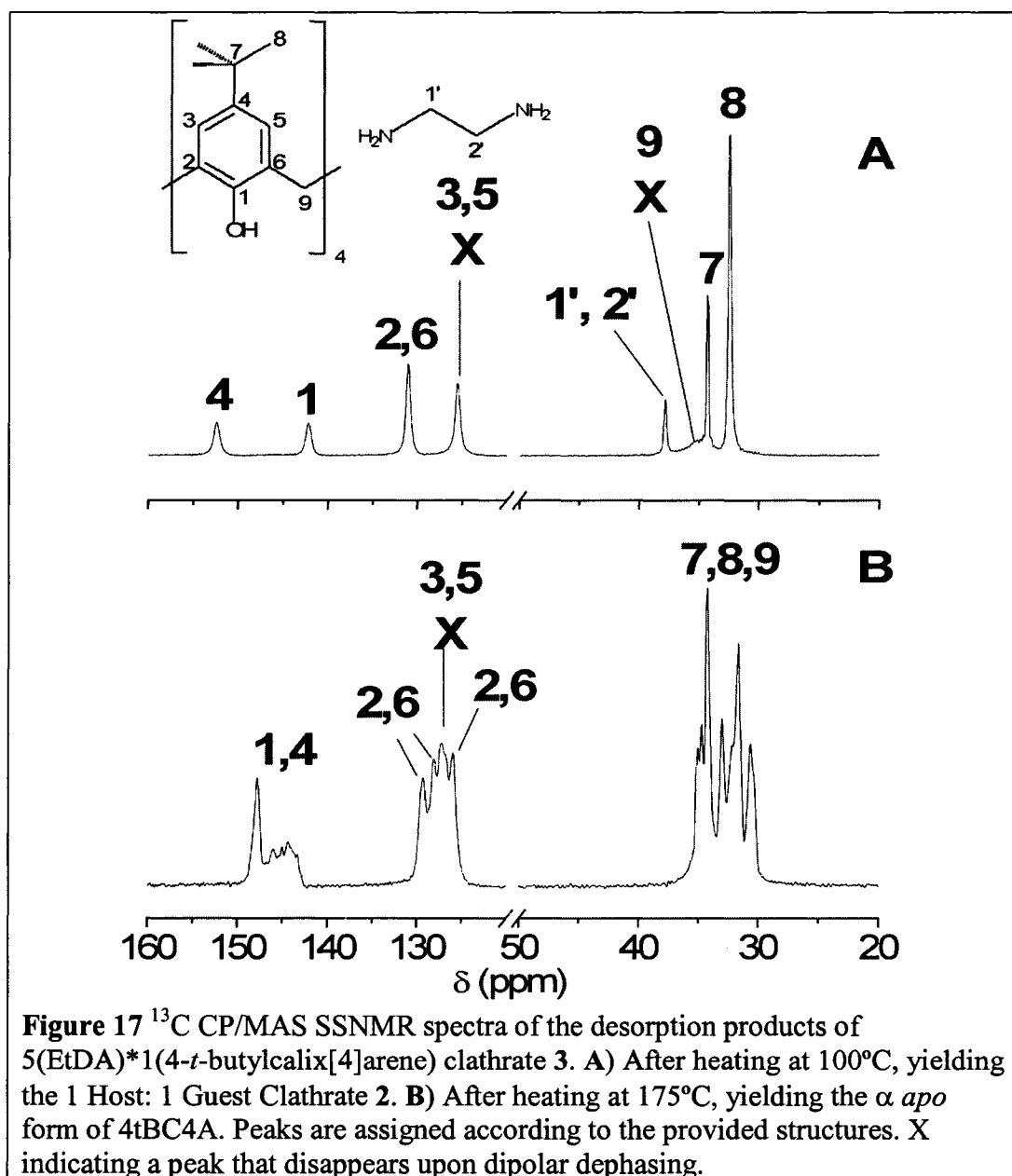
Given the extremely high mobility of the ethylenediamine molecules in clathrate **3** inferred from the structural evidence, suggesting only minimal stabilization of the cluster, it was expected that the *exo* amines would be relatively easily removed from the clathrate. As seen from the TGA data, the initial amines in fact begin desorbing at room temperature (see Table 4), ultimately forming a 1 guest : 1 host inclusion before collapsing into an *apo* form. While this precludes using clathrate **3** as a gas adsorbent in a fashion similar to ethanolamine clathrate **1**, the more dramatic distortion of the capped motif also suggested the potential for a shift in the structures of the desorption products analogous to that observed for the hexylamine 4tBC4A clathrate (see Chapter III).

Structural characterization of the desorption products of bulk samples of clathrate **3** confirmed this suspicion. Upon heating at 100°C, the expected 1 guest : 1 host clathrate **4** is obtained. The ¹³C CP/MAS NMR spectrum (see Figure 17) undergoes the simplification characteristic of the elimination of hydrogen bonding interactions in favour of stabilization of a single amine through non-specific interactions with the calixarene cavity. Furthermore, while the amine remains dynamic (as indicated by dipolar dephasing), it is now clearly localized to a site deep within the calixarene cavity similar to that predicted for solution complexes,^[63, 64] as evidenced by the large complexation induced shift observed (see Table 6).

However, the structural shift is not entirely consistent with that previously observed for the *n*-alkylamines^[60] and isoalkylamines (see Chapters III and IV). As seen from the PXRD pattern for clathrate 4 (see Figure 18 and Table 7), the unit cell parameters exhibit a certain degree of expansion. While part of this is attributable to the higher collection temperature of the PXRD pattern, it would also appear that the ethylenediamine complex is arrayed such that the calixarenes are precluded from packing together tightly. The specific structural origin of such a shift in packing can only be speculated upon given the current data, with the most compelling explanation being that the significant shift in the arrangement of calixarene subunits in clathrate 3 preventing a collapse to a more compact form due to difficulties in rearranging the lattice. Such a situation would be an intriguing counterpoint to the co-operative shift observed in the single crystal to single crystal transformations of 4tBC4A clathrates of toluene^[72] and vinyl bromide.^[73]

This structural perturbation carries over to directing the structure of the final *apo* form. Much as with the preference exhibited by the hexylamine 4tBC4A clathrate^[60] (see Chapter III), the renewed complexity of both the ¹³C CP/MAS NMR spectrum (see Figure 17) and PXRD pattern (see Figure 18 and Table 7) clearly indicate that the removal of the final amine results in the low-symmetry α *apo* form of 4tBC4A being isolated. Presumably, the initial alignment of the calixarene in opposing caps without any interfering hydrogen bonding calixarene moieties in the way allows for the 4tBC4A molecules to simply close in on one another, and self-include readily. As such, the large, disordered ethylenediamine droplet serves a similar role as the bulky hexylamine tails in

forcing the calixarene lattice into an arrangement where self-inclusion is easily achieved, precluding the formation of the low density, energetically unfavourable β *apo* forms.



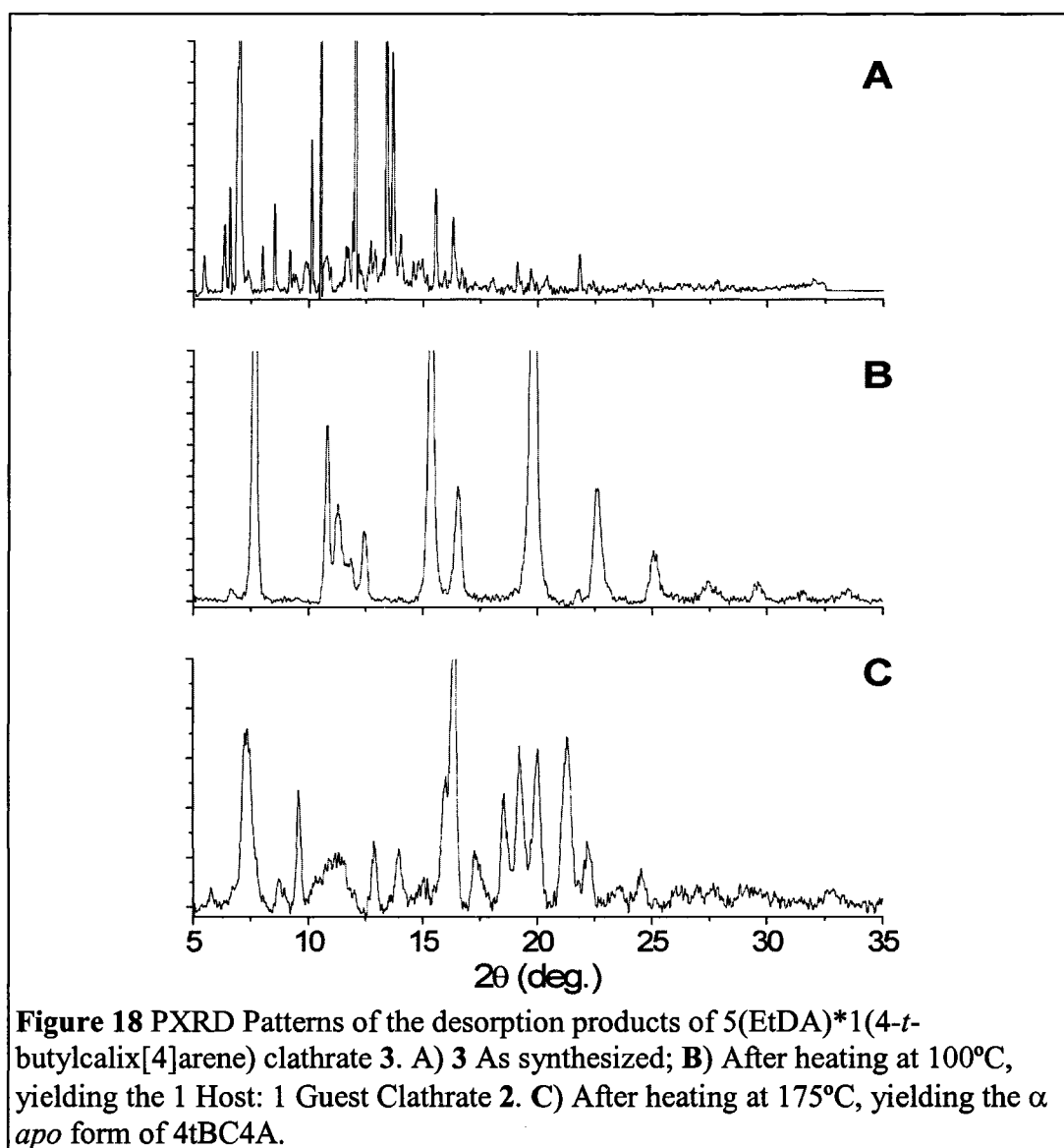


Table 7 PXR D unit cell parameters for clathrates **3**, **4** and the α *apo* form of 4tBC4A derived from clathrate **3**.

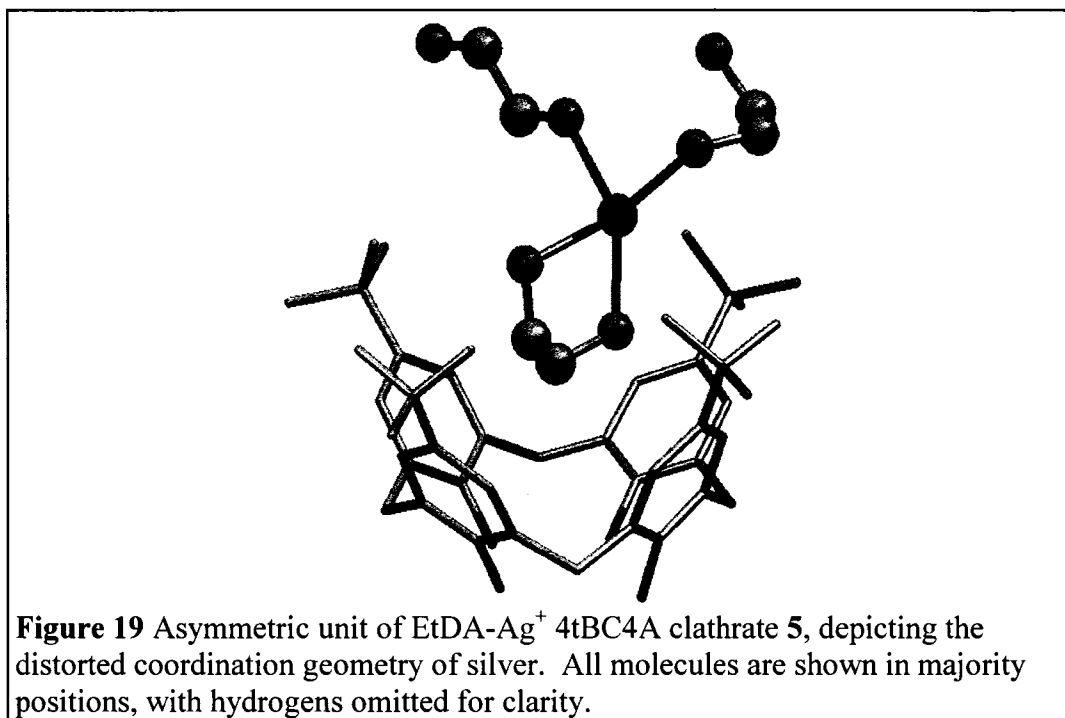
Compound	EtDA 4tBC4A Clathrate 3	EtDA 4tBC4A Clathrate 4	α <i>apo</i> form of 4tBC4A derived from clathrate 3
Space Group	$P2_1/n$	$P4/n$	$P2_1/c$
$a / \text{Å}$	12.921	16.301	9.8639
$b / \text{Å}$	19.698	16.301	31.157
$c / \text{Å}$	22.183	14.135	13.677
$\alpha / ^\circ$	90	90	90
$\beta / ^\circ$	93.43	90	109.7
$\gamma / ^\circ$	90	90	90
$V / \text{Å}^3$	6635.8	3755.9	3957.6

SCXRD of EtDA Ag 4tBC4A Clathrate 5

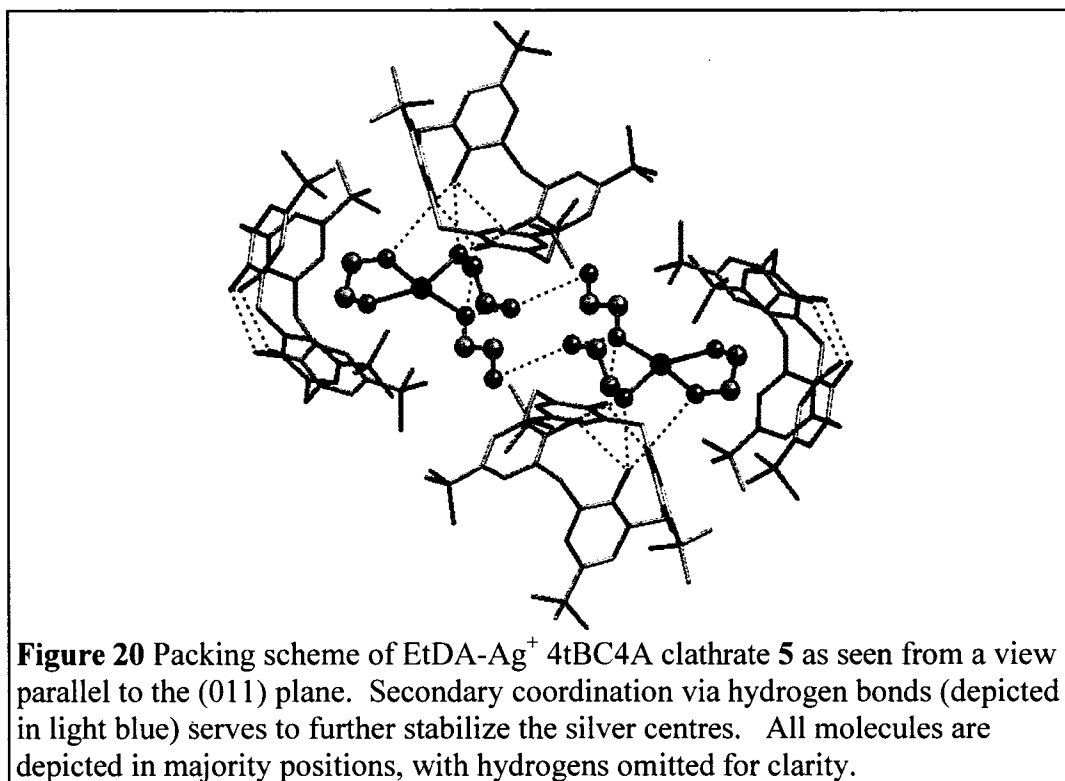
As mentioned above, difunctional amine guests present an intriguing opportunity to investigate how guests capable of serving as bidentate ligands might influence the packing motif of such compounds. The resulting motif would be representative of the relative importance of increased coordination of silver (which is well-known to be coordinatively flexible^[74, 75]) via chelation versus the formation of an extended hydrogen bond network in stabilizing such inclusions. Furthermore, the high mobility of EtDA in clathrate 3 suggests that a corresponding silver compound might have the same delicate balance between coordination and hydrogen bonding that gave rise to the solid solutions of isobutylamine-Ag⁺ 4tBC4A clathrates (see Chapter V). Dissolution of AgNO₃ and 4tBC4A in Ethylenediamine (EtDA) gives rise to a solution that, upon evaporation of excess solvent, readily produces crystals of a silver-amine calixarene clathrate suitable for SCXRD.

The resulting clathrate 5 has a stoichiometry of 3(EtDA)*0.87(Ag⁺)*1(4tBC4A)⁻, such that each silver is coordinated by three molecules of EtDA, giving rise to a distorted tetrahedral coordination geometry. (see Figure 19). As a result, rather extensive disorder is observed in the structure. The silver is disordered over three positions (48:32:7 distribution), along with one of the *exo* amines (0.67:0.27:0.6 distribution), while the *endo* amine is disordered over two positions (0.72:0.28 distribution). The *endo* amine also appears to induce disorder in at least one of the *t*-butyl groups (two fold disorder with 0.72:0.28 distribution). The two singly coordinated molecules of EtDA are found

outside the calixarene cavity (*exo*), while the single bidentate chelating molecule of EtDA resides within the calixarene (*endo*).



The complex is further stabilized through a network of hydrogen bonds not unlike that seen in previous amine-metal-calixarene compounds^[23] and silver coordination polymers^[76-78] (see Figure 20). The coordinating amines interact with the phenolic hydroxyls of the calixarene framework (N...O distances 2.94, 2.98, 3.03, 3.09 Å). The free amino groups of the two *exo* molecules of EtDA form weak hydrogen bonds to an adjacent silver-amine unit (N...N distance of 3.51 Å). In conjunction with the altered geometry of the silver-amine complex, this gives rise to a dramatic distortion of the capped structural motif previously observed for amine-4tBC4A complexes, with the cavities of the terminal calixarenes offset by 7.48 Å.



As with the other amine-Ag⁺ 4tBC4A frameworks (see Chapters IV and V), the hybrid coordination geometry of the guest complex is reminiscent of the calixarene-metal complexes previously reported, where a range of interactions, such as cation- π stabilization^[79-83] or complexation to covalently bound ligand moieties,^[84-89] serve to bind the metal centre, while secondary coordination ultimately directs only small segments of the primary coordination sphere. However, as mentioned previously, these strategies fail to produce multidimensional supramolecular structures as the pre-organization of the calixarene which serves to make the receptor suitable for taking up the metal cation also restricts its structural flexibility, and therefore its ability to accommodate the multiple weak interactions upon which a supramolecular framework is built.

Given this, more appropriate comparisons can be drawn from examinations of other supramolecular coordination compounds. As mentioned earlier, recent studies have

clearly demonstrated that secondary interactions such as hydrogen bonding play a significant role in directing the structure (and therefore the coordination geometry) of various Ag(I) coordination polymers.^[76-78] Earlier studies of a range of difunctional ligands relying upon nitrogen,^[90-95] thioether,^[96, 97] and sulfonate^[93, 98, 99] donor groups demonstrated how variation in the coordinating group and the use of non-interacting or minimally interacting counteranions are also useful tools in effectively directing the coordination geometry of the Ag(I) such that infinite multidimensional structures typically involving two, four or six coordinate Ag(I) centres are observed.

The calixarene is both a hydrogen bonding partner and non-interacting counteranion, and as such is well suited to directing the coordination geometry observed for the silver. Even accounting for this, however, the included complex is an intriguing contrast with the Ag(I) coordination compounds typically formed by EtDA and a variety of simple counteranions in the solid state, which generally take the form of coordination polymers where each Ag(I) is coordinated by two units of EtDA^[100-102] (although exceptions do exist where chelation is observed^[103, 104]). It also contrasts with what might be expected based off of studies of Ag(I) chemistry in pure bases, where Ag halides dissolved in neat monofunctional bases have been shown to produce predominantly 1 ligand : 1 AgX compounds with a tetrahedral geometry.^[105, 106] One would expect similar geometries to be favoured even with crystals derived from neat ethylenediamine, with the difunctional nature of the amine leading to crosslinked polymer chains without any chelation. However, with the calixarene as counteranion, such a structure is not observed.

Ultimately, one must also consider the stabilization offered by inclusion in the calixarene in order to explain the geometry of the observed complex. Previous studies indicated that tetrahedral amine-Zn clusters^[26] (see Chapter IV) can not be accommodated in a capped structure, such that all amines are found *exo* to the calixarene cavity. When viewed in light of the fact that similar behaviour is observed for clusters composed of amines larger than hexylamine^[42] enclathrated by 4tBC4A (see Chapter III), the unusual coordination geometry is therefore a structural compromise in order to allow the formation of a capped motif (albeit in a distorted form). Only small clusters suitable for simultaneous *endo* inclusion and hydrogen bonding to adjacent calixarene units can take full advantage of the calixarene as a secondary ligand, a situation that is allowed for by the coordinative flexibility of Ag(I). This means that the stabilization offered by inclusion and hydrogen bonding with the calixarene can overwhelm the potential for stabilization through the formation of a more extensive coordination network where the ethylenediamine molecules each coordinate to two silver centers.

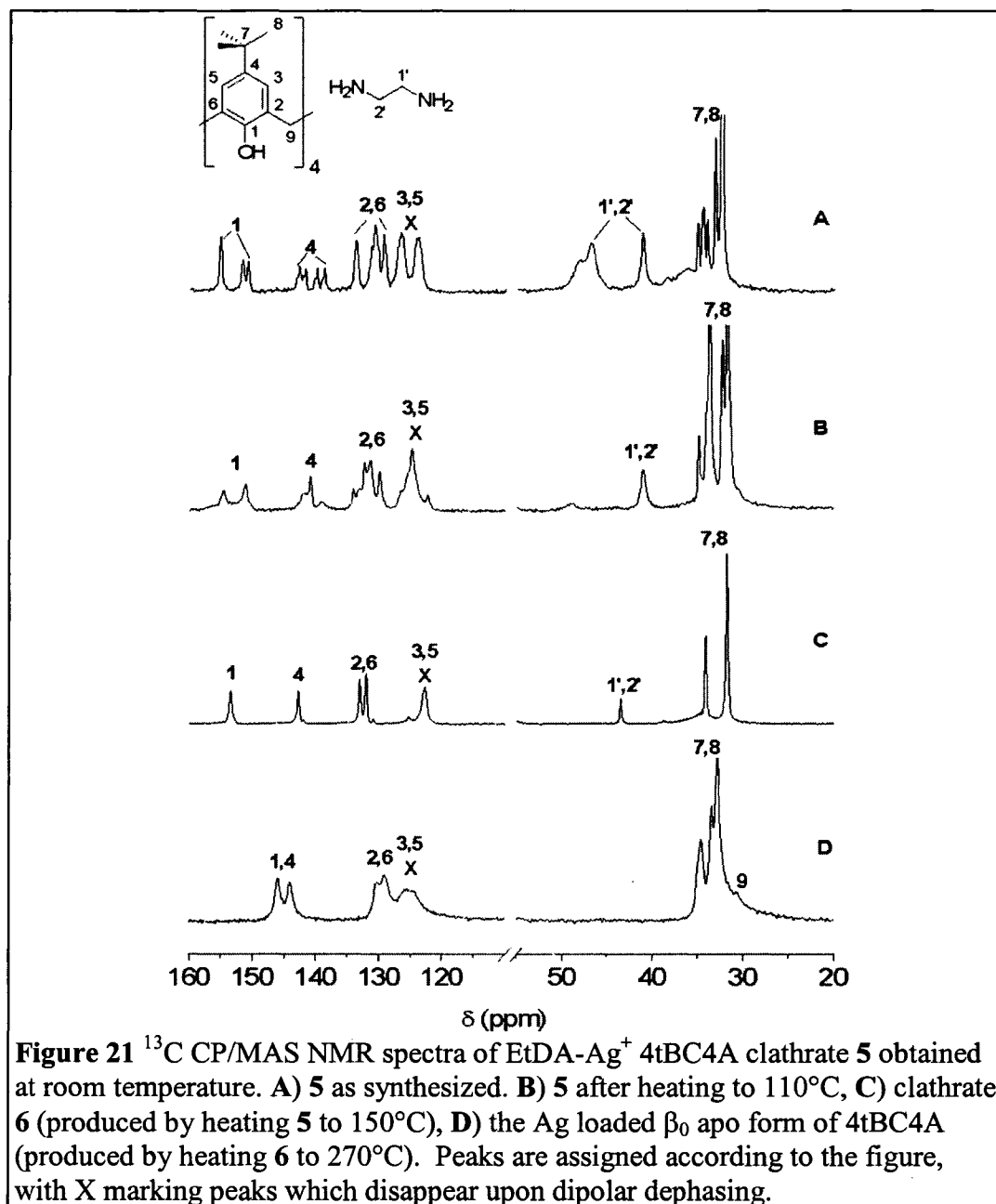
As such, it can be said that the stabilization offered by inclusion and hydrogen bonding with the calixarene can overwhelm the potential for stabilization by more extensive coordination to Ag⁺ in such a situation. It is important to note that both the disorder in the structure and the range of Ag...N distances observed make it clear that a number of energetically equivalent conformations exist for the guest, indicating that various subtly different combinations of these forces are suitable for stabilizing this particular motif.

¹³C SSNMR and PXRD Investigation of EtDA Ag 4tBC4A Clathrate 5

Much as was the case with the solid solution formed by isobutylamine (see Chapter IV), the resulting balance of forces responsible for stabilizing this structure is quite delicate. However, the distorted geometry of the complex raises intriguing questions regarding the potential routes for removing the amine to yield an Ag loaded calixarene framework. Given the rather significant distortions of the intermediate 1 guest : 1 host structure observed for the desorption of EtDA from clathrate 3, it might be expected that similar distortions would be observed for the desorption of clathrate 5, with the resulting silver clusters exhibiting an even more significant effect on the framework. As it turns out, thermogravimetric analysis of 5 indicated that guest was lost during three major transitions at ending at approximately 100°C, 150°C and 260°C, with the resulting decreases in mass corresponding to the loss of approximately one amine at each step (see Table 4). A small amount of residual amine is also present, as will be observed in the SSNMR spectrum. As with other amine-Ag⁺ clathrates of 4tBC4A, these increased temperatures to desorb the amine correspond well with more extensive stabilization due to coordination to the metal centre.

The ¹³C CP/MAS NMR spectrum of clathrate 5 as synthesized corresponds well with the SCXRD structure (see Figure 21A). The host portion of the spectrum of clathrate 5 exhibits the high degree of splitting that would be expected from the large asymmetric unit found from SCXRD data where none of the carbons in the calixarene molecule are crystallographically equivalent. Furthermore, three ethylenediamine peaks are observed (see Table 6), with the upfield peak attributable to the shielded *endo* guest

and the downfield peaks due to the silver deshielded *exo* amines. These peaks persist upon dipolar dephasing, indicating the crystallographic disorder is likely due to dynamic processes of sufficient amplitude to reduce dipolar coupling to hydrogen.



The spectra clearly indicate that significant structural shifts occur as amine is removed from the system (see Figure 21). After heating to 110°C, the *exo* amine peaks disappear, but the overall low symmetry of the structure is retained. While specific details regarding the asymmetric unit are difficult to assess due to broadening of the aromatic peaks, the low symmetry observed presumably still corresponds to an *exo* and *endo* inclusion, where the amines experience a combination of shielding due to the calixarene and deshielding due to coordination that render them nearly equivalent. The exact structure of such an arrangement, however, cannot be deduced from the current data, although, as we will see later, visual observations hint at a possible explanation.

However, upon heating at 150°C, peak splittings are no longer observed for the host or guest, so that the spectrum now reflects those observed for the high symmetry tetragonal 1:1 Host:Guest compounds of 4tBC4A.^[107, 108] Furthermore, the complexation induced shift of the guest is greatly reduced, suggesting the amine now resides outside the calix cavity, coordinated to the silver atom. The high symmetry appears to be retained upon final removal of the amine guest at 270°C. Throughout this process, dipolar dephasing indicates that the amine present is undergoing dynamic motion.

These structural shifts are also quite clear from the powder x-ray diffraction (PXRD) data (see Figure 22). The powder pattern for the bulk sample of compound **5** is readily indexed based on the predictions from the SCXRD structure (see Table 8). The pattern of the sample heated to 110°C is also readily indexed to this initial cell, indicating the structure of **5** is robust enough to survive the loss of the first amine as indicated by TGA and NMR. As expected from the NMR data, though, upon heating to 150°C, the pattern

simplifies considerably. Preliminary indexing of this pattern in the $P4/n$ space group suggested by the NMR spectrum and previous studies^[44, 65, 109] yields an expanded cell compared to structures of all other amine clathrates of 4tBC4A (see Table 8).

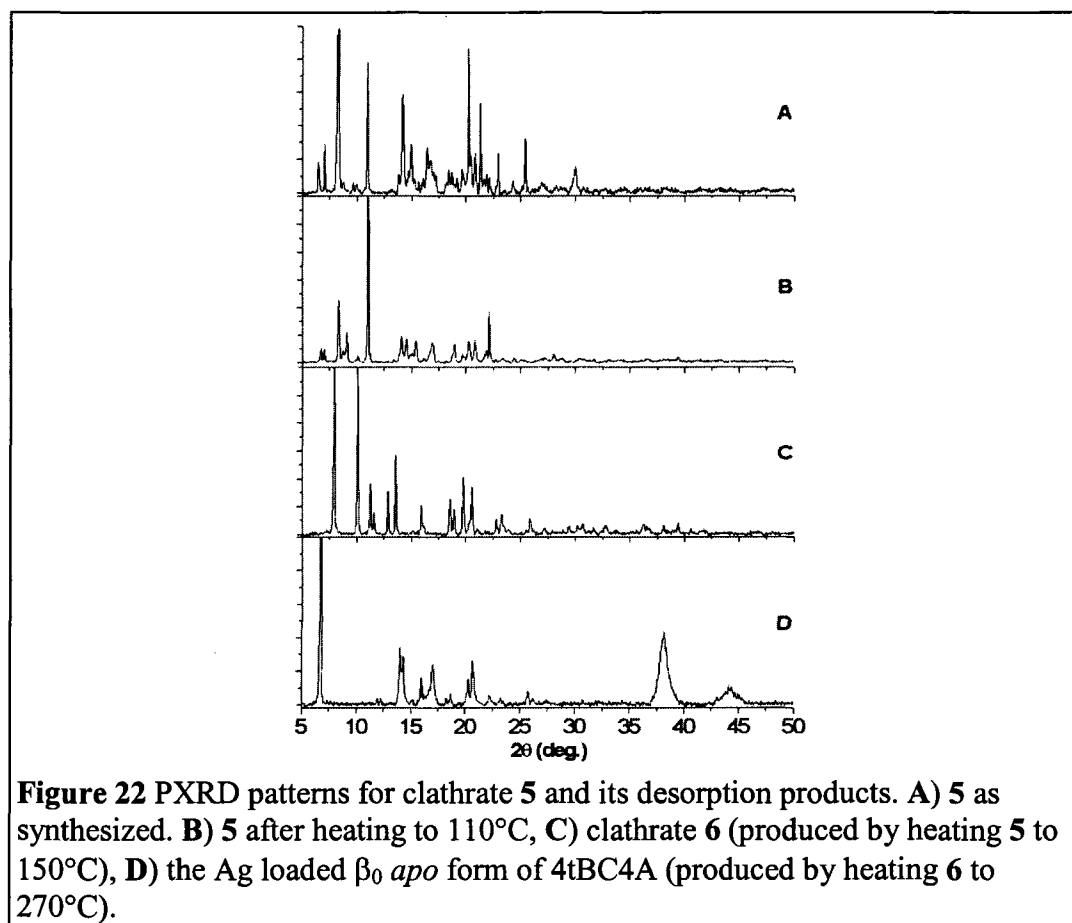


Figure 22 PXR D patterns for clathrate **5** and its desorption products. **A)** **5** as synthesized. **B)** **5** after heating to 110°C, **C)** clathrate **6** (produced by heating **5** to 150°C), **D)** the Ag loaded β_0 *apo* form of 4tBC4A (produced by heating **6** to 270°C).

Table 8 PXR D unit cell parameters for clathrate **5** as synthesized and after heating at 110°C, and clathrate **6**.

	5 (as synth.)	5 (Heated at 110°C)	6
Space Group	$P2_1/n$	$P2_1/n$	$P4/n$
a (Å)	13.357	13.568	13.733
b (Å)	21.090	21.314	13.733
c (Å)	18.498	18.642	22.076
α (°)	90	90	90
β (°)	109.7	109.9	90
γ (°)	90	90	90
V (Å ³)	4905.4	5070.2	4163.2

The unit cell of the corresponding ethylenediamine clathrate **5** also exhibits considerable expansion, in this case, the shift in the *c* axis is much more dramatic in this case (see Table 7). Given the NMR evidence, this would seem to indicate that the silver clusters are forcing the calixarene layers apart. By the same token, the absence of a complexation induced shift of the resonance assigned to ethylenediamine for the 1 Guest: 1 Host complex, it would appear that coordination to silver precludes inclusion. However, we cannot rule out at this time the formation of an alternative high symmetry phase due to the absence of a few low angle reflections predicted for such a tetragonal cell. Full removal of the amine gives rise to a relatively simple pattern similar to those observed for amine-4tBC4A complexes,^[44, 60] with the exception of two broad high angle peaks at $2\theta=38.26^\circ$ ($d=2.35 \text{ \AA}$) and 44.23° ($d=2.05 \text{ \AA}$), suggesting a second phase is now present.

Visual observation of the samples during the heating process provides a reasonable suggestion as to the origin of these high angle peaks. As can be seen from Figure 23, as the sample is heated, a dramatic colour change in the sample is observed, going from white to yellow-orange to deep brown, suggesting that the silver undergoes reduction. In fact, these reflections can readily be indexed as the 111 and 200 peaks of metallic silver (spacegroup F_{m-3m}). The broad peak widths therefore arise from the small size of the spherical silver crystallites, and are representative of the minimum size of the silver clusters (provided each such domain is composed of a single cluster). Using the Scherrer equation to quantitate this,^[110] the crystallites are found to have an average

diameter of 94 Å, which corresponds to a cross-section composed of approximately 29 Ag atoms (based on an atomic radius of 1.6 Å).

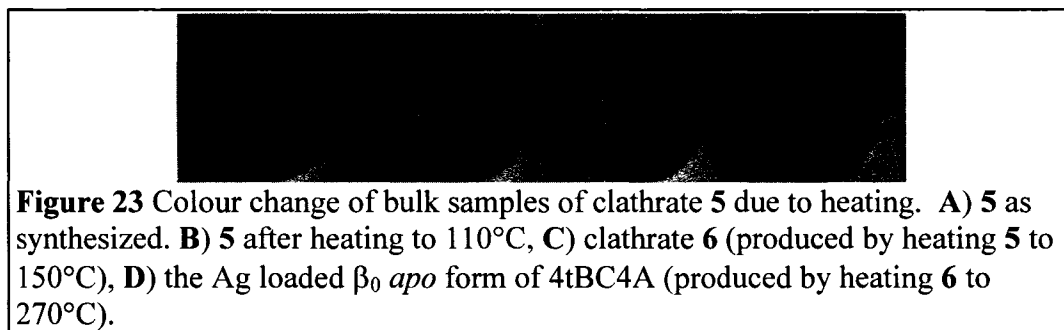


Figure 23 Colour change of bulk samples of clathrate **5** due to heating. **A)** **5** as synthesized. **B)** **5** after heating to 110°C, **C)** clathrate **6** (produced by heating **5** to 150°C), **D)** the Ag loaded β_0 *apo* form of 4tBC4A (produced by heating **6** to 270°C).

The changes in colour observed upon heat treatment in this particular case raises intriguing questions as to how this reduction might progress, providing the clearest possible link to the reduction of silver in zeolite. Previous studies of syntheses of silver nanoparticles based on comparable simple primary ligands do not exhibit this progression of colours.^[111-114] Along with the colours observed for the final products in the other amine-Ag⁺ 4tBC4A systems (see Chapters IV and V), this suggests the supramolecular nature of the assembly, and in particular, this tends to confirm the hypothesis that the calixarene plays a key role in the reduction process. As suggested earlier, the two major roles for the calixarene that most easily come to mind are that of a reducing agent and that of a framework serving to isolate the silver complex such that the reduction process is carried out in a novel fashion.

Despite the fact that similar behaviour is observed for three types of amine-Ag⁺ 4tBC4A clathrate, even when considering all the data accumulated for these systems, it is not possible to establish a specific mechanism for the process. However, certain routes can be ruled out in light of the structural evidence available. The oxidation of the hydroxyl groups on 4-*t*-butylcalixarenes to form spirodienone derivatives^[115-118] related

to calixquinones^[119, 120] is well known, and is the most plausible method by which the calixarene would serve to reduce the silver centres. Furthermore, such a transformation would likely give rise to the colour changes reported. However, as the ¹³C SSNMR makes clear in this and all the other cases, no disruption of the aromaticity related to the formation of an ene-one occurs, nor is a resonance corresponding to a keto carbon observed at ~180 ppm. Furthermore, such a transformation would give rise to a massive increase in crystallographic splitting due to the low symmetry of such a compound.^[116] It therefore appears that the calixarene alone does not reduce the silver centre.

Given previous observations suggesting that amine coordination serves to decrease the reduction potential of Ag(I),^[114] it would appear that a more complex reduction mechanism involving the amine is at play, such that the calixarene only has a peripheral role that does not result in structural changes. As previously mentioned, one of the roles of the calixarene satisfying such a restriction would be its role as a framework isolating the silver centres. In doing so, the resulting environment might be conducive to amine oxidization by the silver in a fashion analogous to previously reported catalytic systems involving Ag⁺,^[121, 122] or undergo chemistry similar to that carried out in biological systems by amine oxidases.^[123] However, once again, the absence of any unassigned resonances in the ¹³C SSNMR spectra indicate that if such chemistry occurs, the amine would also have to be eliminated from the system in the course of oxidation.

Qualitatively, the colour changes observed are quite similar to another supramolecular system where confinement has been shown repeatedly to give rise to unusual redox chemistry: heat treated silver-loaded zeolites. In such systems, the silver

centres have been proposed to undergo partial reduction to form charged silver clusters with covalent character,^[124, 125] such that a number of competing models for structural features leading to the yellow Ag zeolites have been proposed.^[126] At this time, however, we have no direct evidence to confirm any of the models, as the PXRD data provides no evidence of large covalent clusters having been formed for this or any of the other amine-Ag⁺ 4tBC4A systems (although small clusters would not be possible to observe by this technique). It is also important to recall that the end product in each case is the formation of metallic nanocrystals of silver, indicating that while the process of reduction of Ag⁺ in the molecular based supramolecular calixarene framework does take place, it is likely to involve different mechanisms from those hypothesized to occur in the vast majority of zeolites.

Structurally, the location of the silver nanoparticles in this particular case can be partially inferred from the spectroscopic and XRD data. The size of the silver crystals does suggest that silver in a certain volume can agglomerate, so that again dynamics plays a role in guiding the formation of these nanocrystals. As mentioned above, the final form of the amine desorbed calixarene is essentially that of the high symmetry β *apo* form, indicating that the silver nanoparticles are included in the calixarene matrix such that they do not perturb the favoured packing scheme of the pure calixarene. This is not particularly surprising, as the inclusion motifs observed for silver in the various conformationally locked calixarenes previously studied^[80-83] could not possibly accommodate silver particles of the size predicted from the Scherrer equation. The logical alternative to such an arrangement would be the formation of an intercalated

structure, a supposition in this case supported by the PXRD unit cell expansion along the *c* axis when compared to the normal β *apo* form (although part of this expansion must also be due to the influence of ethylenediamine itself).^[60]

TEM of Ag Nanoclusters derived from Clathrate 5

While the spectroscopic and XRD data indicate that the calixarene assumes a high symmetry structure similar to that of the β_0 *apo* form, it is not possible to deduce the position of the silver from this information. The available data suggest that the silver crystals are a distinct phase dispersed throughout the calixarene, but so far it is not possible to say if there are still interactions between calixarenes and silver. The diffraction data, as stated previously, gives us some insight as to the average size of the crystallites composing the sample, but the Scherrer equation is highly dependent on both the shape and particle size distribution of the resulting powder.^[127, 128] However, transmission electron microscopy (TEM) provides an opportunity to examine whether such effects are at play in the Ag nanoparticles formed in the 4tBC4A matrix.^[129] Given the particularly intriguing chemistry exhibited by the EtDA-Ag⁺ system, it was selected for preliminary analysis by TEM.

A sample bright-field TEM image of the 4tBC4A supported silver nanoparticles derived from the EtDA-Ag⁺ system is shown in Figure 24. As can be clearly seen, a range of particle sizes can be observed in this section of the sample. The majority of the particles are approximately 5 nm in size, suggesting the Ag nanoparticles and calixarene units are interspersed with each other evenly. However, these preliminary images are insufficient for the purposes of obtaining an accurate sample to calculate a quantitative

particle size distribution. On a qualitative level, however, these particles are only one half the size determined by PXRD, and the source of this discrepancy is not immediately clear.

It is possible that the preparation of the sample results in disruption of the nanoparticles, although given the extreme temperatures used to prepare the materials, such a scenario is unlikely. It is much more likely that the size determined by XRD is representative of an uneven particle size distribution and non-spherical character of the particles (which would cause the Scherrer Constant used in the equation to be less than 0.9).^[129] However, most intriguingly, it is possible that the smaller nanoparticles observed are in fact representative of the covalent clusters suggested by the colour changes observed in the sample, which would not appear in the XRD pattern readily, and thus would not be represented in analysis of the peak widths. Clearly, in order to resolve these questions, further TEM, PXRD and spectroscopic studies of 4tBC4A supported Ag nanoparticles are required.

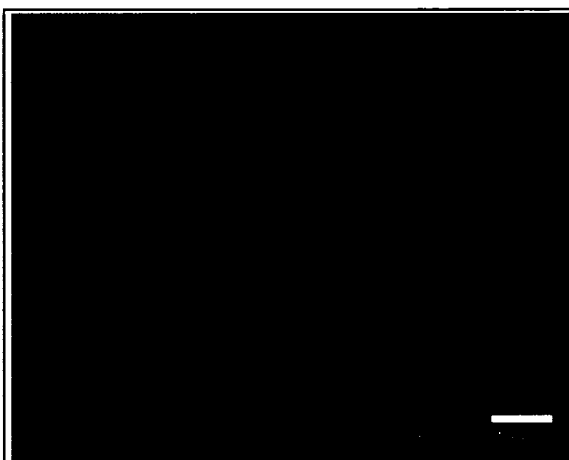


Figure 24 A bright field TEM image of the Ag-4tBC4A nanoparticles derived from amine desorption of EtDA-Ag⁺ 4tBC4A clathrate **5**.

5. Conclusion

In comparing the structural motifs observed in both EtDAOH 4tBC4A clathrate 1 and EtDA 4tBC4A clathrate 3 with other amine inclusion compounds of 4tBC4A,^[22, 23, 44] the increase in cluster size and shift in calixarene lattice makes it readily apparent that even the introduction of additional hydrogen bonding moieties on the guest can have significant impacts on the structure. Our previous studies of *n*-butylamine complexes of Zn have shown that relatively strong interactions (such as metal coordination) can lead to further distortions of the frequently observed 3 guest : 1 host inclusion motif.^[23] Clearly, the significantly distorted calixarene lattices observed in 5 guest : 1 host amine clusters formed with difunctional amines make it apparent that even additional hydrogen bonding interactions between guests can be expected to lead to new motifs.

The droplet like behaviour of the amines found in these clathrates confirms that it is possible to use such a self-assembly approach to produce isolated solvent clusters. Given the high mobility of the resulting amine clusters, this presents yet another way to tune such calixarene framework structures. It also suggests that larger guest ratios are not precluded by packing concerns arising from molecular symmetry (as might be thought based on the inclusion of *n*-alkylamines), but are a function of the presence of sufficiently strong interactions to stabilize the clusters. Furthermore, these inter-guest interactions can be easily tuned by including an appropriate hydrogen bond donor and acceptor to maximize the stabilization of the cluster and reduce dynamic liquid-like behaviour.

By the same token, multifunctional guests can also be used to direct the coordination of metal centres. As demonstrated by the structure of EtDA-Ag⁺ clathrate 5,

the distinct favourability of hydrogen bonding to the calixarene and inclusion in the calixarene cavity actually results in the supramolecular secondary coordination effects directing the geometry of the coordination compound. This clearly indicates the near equivalence of the three forces in guiding the structural motif, as was predicted based on the studies of the coordination compounds formed by monofunctional amines. As such, it is possible with a flexible ligand and metal centre to actually reverse the traditional roles of organic ligands and metal centres in supramolecular chemistry,^[20, 130] wherein the metal centre typically dictates what form a framework will take.

Finally, the solvent clusters have proven to be accessible sites for carrying out chemistry. The significant CO₂ adsorption of EtDAOH clathrate **1** makes it clear that the channelled structure, while restricting access to the amine clusters, does not prevent it. The resulting chemisorption process gives rise to the carbamates expected from solution studies of ethanolamine, while the calix framework also appears to be capable of physical adsorption of the gas. As indicated by the hybrid adsorption isotherm, the resulting process is quite different from that observed in solution, with the crystallographic inequivalence of the amines giving rise to different sites with different accessibilities. While further studies will be required to clarify the exact nature of the relationship between the various carbamate resonances observed in the SSNMR and the amine sites SCXRD data, it currently seems reasonable to assume that the deshielded resonances represent the *exo* amines which are most easily accessed by CO₂, while the shielded resonances are reflective of the less accessible *endo* amine.

In conclusion, we have demonstrated how the introduction of a secondary hydrogen bonding moiety can be used to produce larger, solvent like clusters in clathrates of simple calixarenes, or to direct the coordination geometry of a metal centre. The pure amine droplets are accessible to carry out chemistry, such as CO₂ adsorption, while the silver coordinated system gives rise to an isolated environment suitable for carrying out reduction on silver centres, rendering them suitable sites for catalysis. Difunctional amines therefore present both another route for tuning the structures of calixarene frameworks, as well as another self-assembly approach for the generation of materials with potential industrial applications.

6. References

- [1] Z. Asfari, V. Bohmer, J. Harrowfield, J. Vicens, *Calixarenes 2001*, Kluwer Academic Publishers, Dordrecht, **2001**.
- [2] C. D. Gutsche, *Calixarenes*, Royal Society of Chemistry, Cambridge, **1989**.
- [3] C. D. Gutsche, *Calixarenes Revisited*, Royal Society for Chemistry, Cambridge, **1998**.
- [4] V. Böhmer, *Angew. Chem. Int. Ed.* **1995**, *34*, 713.
- [5] T. Bernhard, H. Zimmermann, U. Haeberlen, *Mol. Phys.* **1992**, *77*, 1123.
- [6] A. P. Dianin, *J. Russ. Phys. Chem. Soc.* **1914**, *31*, 1310.
- [7] G. D. Enright, C. I. Ratcliffe, J. A. Ripmeester, *Mol. Phys.* **1999**, *97*, 1193.
- [8] G. O. Lloyd, M. W. Bredenkamp, L. J. Barbour, *Chem. Commun.* **2005**, 4053.
- [9] J. G. Selbo, J. M. Desper, C. J. Eckhardt, *J. Incl. Phenom. Macrocycl. Chem.* **2003**, *45*, 73.
- [10] J. Merchan, N. Yutronic, M. T. Garland, R. Baggio, *Supramol. Chem.* **2004**, *16*, 147.
- [11] J. E. D. Davies, V. A. Tabner, *J. Incl. Phenom. Molec. Recogn.* **1998**, *31*, 99.
- [12] M. Brustolon, A. L. Maniero, U. Segre, *J. Chem. Soc. Perkin Trans. 2* **1997**, 2519.
- [13] M. Brustolon, A. L. Maniero, A. Marcomini, U. Segre, *J. Mater. Chem.* **1996**, *6*, 1723.
- [14] K. D. M. Harris, *J. Solid State Chem.* **1993**, *106*, 83.
- [15] R. Gerdil, *Top. Curr. Chem.* **1987**, *140*, 71.
- [16] R. Aradyellin, B. S. Green, M. Knossow, G. Tsoucaris, *J. Am. Chem. Soc.* **1983**, *105*, 4561.
- [17] R. Aradyellin, B. S. Green, M. Knossow, *J. Am. Chem. Soc.* **1980**, *102*, 1157.

- [18] W. Baker, B. Gilbert, W. D. Ollis, *J. Chem. Soc.* **1952**, 1443.
- [19] D. V. Soldatov, I. L. Moudrakovski, J. A. Ripmeester, *Angew. Chem. Int. Ed.* **2004**, *43*, 6308.
- [20] J. Lipkowski, in *Comprehensive Supramolecular Chemistry, Vol. 6* (Eds.: J. L. Atwood, J. E. D. Davies, D. D. MacNicol, F. Vogtle), Pergamon Press, Oxford, **1996**, pp. 691.
- [21] N. W. Ockwig, O. Delgado-Friedrichs, M. O'Keeffe, O. M. Yaghi, *Accounts Chem. Res.* **2005**, *38*, 176.
- [22] E. B. Brouwer, K. A. Udachin, G. D. Enright, J. A. Ripmeester, *Chem. Commun.* **2000**, 1905.
- [23] P. O. Brown, K. A. Udachin, G. D. Enright, J. A. Ripmeester, *Chem. Commun.* **2005**, 4402.
- [24] C. A. Fyfe, D. H. Brouwer, *Microporous Mesoporous Mat.* **2000**, *39*, 291.
- [25] C. A. Fyfe, A. C. Diaz, H. Grondey, A. R. Lewis, H. Forster, *J. Am. Chem. Soc.* **2005**, *127*, 7543.
- [26] V. V. Tersikh, I. L. Moudrakovski, C. I. Ratcliffe, J. A. Ripmeester, C. J. Reinhold, P. A. Anderson, P. P. Edwards, *J. Am. Chem. Soc.* **2001**, *123*, 2891.
- [27] V. V. Tersikh, C. I. Ratcliffe, J. A. Ripmeester, C. J. Reinhold, P. A. Anderson, P. P. Edwards, *J. Am. Chem. Soc.* **2004**, *126*, 11350.
- [28] M. Sanchez-Sanchez, T. Blasco, *J. Am. Chem. Soc.* **2002**, *124*, 3443.
- [29] A. E. Aliev, K. D. M. Harris, *J. Phys. Chem. A* **1997**, *101*, 4541.
- [30] B. W. Lepore, F. J. Ruzicka, P. A. Frey, D. Ringe, *Proc. Nat. Acad. Sci. USA* **2005**, *102*, 13819.
- [31] C. Mattos, C. R. Bellamacina, E. Peisach, A. Pereira, D. Vitkup, G. A. Petsko, D. Ringe, *J. Mol. Biol.* **2006**, *357*, 1471.
- [32] M. Unciuleac, M. Boll, E. Warkentin, U. Ermler, *Acta Crystallog. Sect. D: Biol. Cryst.* **2004**, *60*, 388.
- [33] L. J. Barbour, G. W. Orr, J. L. Atwood, *Nature* **1998**, *393*, 671.
- [34] G. W. V. Cave, J. Antesberger, L. J. Barbour, R. M. McKinlay, J. L. Atwood, *Angew. Chem. Int. Ed.* **2004**, *43*, 5263.
- [35] L. C. Palmer, J. Rebek Jr., *Org. Letters* **2005**, *7*, 787.
- [36] D. A. Makeiff, J. C. Sherman, *J. Am. Chem. Soc.* **2005**, *127*, 12363.
- [37] L. R. MacGillivray, J. L. Atwood, *Nature* **1997**, *389*, 469.
- [38] A. Shivanyuk, J. C. Friese, S. Doring, J. Rebek Jr., *J. Org. Chem.* **2003**, *68*, 6489.
- [39] A. Shivanyuk, J. Rebek Jr., *Chem. Commun.* **2002**, 2326.
- [40] M. Yamanaka, A. Shivanyuk, J. Rebek Jr., *J. Am. Chem. Soc.* **2004**, *126*, 2939.
- [41] P. M. M. Blauwhoff, G. F. Versteeg, W. P. M. Van Swaaij, *Chem. Eng. Sci.* **1984**, *39*, 207.
- [42] P. V. Danckwerts, *Chem. Eng. Sci.* **1979**, *34*, 443.
- [43] D. A. House, in *Comprehensive Coordination Chemistry, Vol. 2* (Ed.: G. Wilkinson), Pergamon Press, Oxford, **1987**.
- [44] K. A. Udachin, G. D. Enright, P. O. Brown, J. A. Ripmeester, *Chem. Commun.* **2002**, 2162.
- [45] S. H. Lin, C. T. Shyu, *Environ. Technol.* **2000**, *21*, 1245.

- [46] D. W. Bailey, P. H. M. Feron, *Oil Gas Sci. Technol.* **2005**, *60*, 461.
- [47] O. Erga, O. Juliussen, H. Lidal, *Energy Conv. Manag.* **1995**, *36*, 387.
- [48] M. Caplow, *J. Am. Chem. Soc.* **1968**, *90*, 6795.
- [49] J. E. Crooks, J. P. Donnellan, *J. Chem. Soc. Perkin Trans. 2* **1989**, 331.
- [50] E. B. Rinker, S. S. Ashour, O. C. Sandall, *Ind. Eng. Chem. Res.* **1996**, *35*, 1107.
- [51] E. F. Da Silva, H. F. Svendsen, *Ind. Eng. Chem. Res.* **2004**, *43*, 3413.
- [52] R. T. Yang, *Gas Separation by Adsorption Processes*, Imperial College Press, London, **1997**.
- [53] Y. D. Chen, J. A. Ritter, R. T. Yang, *Chem. Eng. Sci.* **1990**, *45*, 2877.
- [54] R. V. Siriwardane, M.-S. Shen, E. P. Fisher, J. A. Poston, *Energy & Fuels* **2001**, *15*, 279.
- [55] X. Xu, C. Song, J. M. Andresen, B. G. Miller, A. W. Scaroni, *Micropor. Mesopor. Mat.* **2003**, *62*, 29.
- [56] H. Y. Huang, R. T. Yang, D. Chinn, C. L. Munson, *Ind. Eng. Chem. Res.* **2003**, *42*, 2427.
- [57] O. Leal, C. Bolivar, C. Ovalles, J. J. Garcia, Y. Espidel, *Inorg. Chim. Acta* **1995**, *240*, 183.
- [58] N. Hiyoshi, K. Yogo, T. Yashima, *Chem. Lett.* **2004**, *33*, 510.
- [59] T. Filburn, J. J. Helble, R. A. Weiss, *Ind. Eng. Chem. Res.* **2005**, *44*, 1542.
- [60] P. O. Brown, K. A. Udachin, G. D. Enright, J. A. Ripmeester, *Chem. Eur. J.* **2006**, DOI: 10.1002/chem.200600434.
- [61] E. B. Brouwer, G. D. Enright, J. A. Ripmeester, *J. Am. Chem. Soc.* **1997**, *119*, 5404.
- [62] NIAIST, "SDBSWeb", to be found under <http://www.aist.go.jp/RIODB/SDBS/> **2005**.
- [63] C. D. Gutsche, L. J. Bauer, *J. Am. Chem. Soc.* **1985**, *107*, 6063.
- [64] C. D. Gutsche, M. Iqbal, I. Alam, *J. Am. Chem. Soc.* **1987**, *109*, 4314.
- [65] E. B. Brouwer, G. D. Enright, K. A. Udachin, S. Lang, K. J. Ooms, P. A. Halchuk, J. A. Ripmeester, *Chem. Commun.* **2003**, 1416.
- [66] J. L. Atwood, L. J. Barbour, G. O. Lloyd, P. K. Thallapally, *Chem. Commun.* **2004**, 922.
- [67] J. L. Atwood, L. J. Barbour, A. Jerga, *Angew. Chem. Int. Ed.* **2004**, *43*, 2948.
- [68] J.-Y. Park, S. J. Yoon, H. Lee, *Environ. Sci. Technol.* **2003**, *37*, 1670.
- [69] T. Suda, T. Iwaki, T. Mimura, *Chem. Lett.* **1996**, *9*, 777.
- [70] J. P. Jakobsen, J. Krane, H. F. Svendsen, *Ind. Eng. Chem. Res.* **2005**, *44*, 9894.
- [71] J. W. Steed, J. L. Atwood, *Supramolecular Chemistry*, John Wiley & Sons, Ltd., Chichester, **2000**.
- [72] G. D. Enright, I. L. Moudrakovski, J. A. Ripmeester, Unpublished Data, **2006**.
- [73] J. L. Atwood, L. J. Barbour, A. Jerga, B. L. Schottel, *Science* **2002**, *298*, 1000.
- [74] D. Venkataraman, Y. Du, S. R. Wilson, K. A. Hirsch, P. Zhang, J. S. Moore, *J. Chem. Ed.* **1997**, *74*, 915.
- [75] L. Tei, V. Lippolis, A. J. Blake, P. A. Cooke, M. Schroder, *Chem. Commun.* **1998**, 2633.

- [76] L. Zhang, X. Q. Lu, C. L. Chen, H. Y. Tan, H. X. Zhang, B. S. Kang, *Cryst. Growth Des.* **2005**, *5*, 283.
- [77] T. J. Burchell, R. J. Puddephatt, *Inorg. Chem.* **2006**, *45*, 650.
- [78] T. J. Burchell, D. J. Eisler, R. J. Puddephatt, *Chem. Commun.* **2004**, 944.
- [79] J. M. Harrowfield, M. I. Ogden, W. R. Richmond, A. H. White, *J. Chem. Soc. Chem. Commun.* **1991**, 1159.
- [80] A. Ikeda, H. Tsuzuki, S. Shinkai, *J. Chem. Soc. Perkin Trans. 2* **1994**, 2073.
- [81] A. Ikeda, S. Shinkai, *J. Am. Chem. Soc.* **1994**, *116*, 3102.
- [82] W. Xu, R. J. Puddephatt, K. W. Muir, A. A. Torabi, *Organometallics* **1994**, *13*, 3054.
- [83] A. Ikeda, S. Shinkai, *Chem. Rev.* **1997**, *97*, 1713.
- [84] A. Arduini, A. Pochini, S. Reverberi, R. Ungaro, *Tetrahedron* **1986**, *42*, 2089.
- [85] S.-K. Chang, I. Cho, *J. Chem. Soc. Perkin Trans. 1* **1986**, 211.
- [86] F. Arnaud-Neu, E. M. Collins, M. Deasy, G. Ferguson, S. J. Harris, B. Kaitner, A. J. Lough, M. A. McKervey, E. Marques, B. L. Ruhl, M. J. Schwing-Weill, E. M. Sewardt, *J. Am. Chem. Soc.* **1989**, *111*, 8681.
- [87] E. Ghidinio, F. Ugozzoli, R. Ungaro, S. Harkema, A. Abu El-Fadl, D. N. Reinhoudt, *J. Am. Chem. Soc.* **1990**, *112*, 6979.
- [88] N. Singh, M. Kumar, G. Hundal, *Tetrahedron* **2004**, *60*, 5393.
- [89] J. M. Harrowfield, M. Mocerino, B. W. Skelton, C. R. Whitaker, A. H. White, *Aust. J. Chem.* **1994**, *47*, 1185.
- [90] C. L. Schauer, E. Matwey, F. W. Fowler, J. W. Lauher, *Mater. Res. Bull.* **1998**, 213.
- [91] L. Carlucci, G. Ciani, D. M. Proserpio, A. Sironi, *Angew. Chem. Int. Ed. Engl.* **1995**, *34*, 1895.
- [92] L. Carlucci, G. Ciani, D. M. Proserpio, A. Sironi, *J. Am. Chem. Soc.* **1995**, *117*, 4562.
- [93] L. J. May, G. K. H. Shimizu, *Chem. Mat.* **2005**, *17*, 217.
- [94] D. Venkataraman, S. Lee, J. S. Moore, P. Zhang, K. A. Hirsch, G. B. Gardner, A. C. Covey, C. L. Prentice, *Chem. Mat.* **1996**, *8*, 2030.
- [95] D. Venkataraman, G. B. Gardner, S. Lee, J. S. Moore, *J. Am. Chem. Soc.* **1995**, *117*, 11600.
- [96] G. K. H. Shimizu, G. D. Enright, C. I. Ratcliffe, J. A. Ripmeester, D. D. M. Wayner, *Angew. Chem. Int. Ed.* **1998**, *37*, 1407.
- [97] G. K. H. Shimizu, G. D. Enright, C. I. Ratcliffe, J. A. Ripmeester, *Chem. Commun.* **1999**, 461.
- [98] D. J. Hoffart, S. A. Dalrymple, G. K. H. Shimizu, *Inorg. Chem.* **2005**, *44*, 8868.
- [99] S. K. Makinen, N. J. Melcer, M. Parvez, G. K. H. Shimizu, *Chem. Eur. J.* **2001**, *7*, 5176.
- [100] E. Bang, *Acta. Chem. Scand.* **1978**, *32*, 555.
- [101] B. Magyar, G. Schwarzenbach, *Acta Chem. Scand. A* **1978**, *32*, 943.
- [102] G. Schwarzenbach, H. Ackermann, B. Maissen, G. Anderegg, *Helv. Chim. Acta* **1952**, *35*, 2337.

- [103] Z. D. Liu, H. L. Zhu, *Acta Crystallogr. Sect. E.-Struct Rep. Online* **2004**, *60*, M1883.
- [104] T. Pretsch, H. Hartl, *Inorg. Chim. Acta* **2005**, *358*, 1179.
- [105] L. M. Engelhardt, S. Gotsis, P. C. Healy, J. D. Kildea, B. W. Skelton, A. H. White, *Aust. J. Chem.* **1989**, *42*, 149.
- [106] C. Nather, A. Beck, *Z.Naturforsch.(B)* **2004**, *59*, 992.
- [107] E. B. Brouwer, J. A. Ripmeester, G. D. Enright, *J. Incl. Phenom. Molec. Recogn.* **1996**, *24*, 1.
- [108] E. B. Brouwer, G. D. Enright, C. I. Ratcliffe, J. A. Ripmeester, *Supramol. Chem.* **1996**, *7*, 79.
- [109] J. L. Atwood, L. J. Barbour, A. Jerga, *Chem. Commun.* **2002**, 2952.
- [110] $d=(K\lambda)/(B\cos\theta)$, where d =Crystallite Diameter, λ = Wavelength of radiation, K =Scherrer Constant (0.9), B =Broadening of Peak at FWHM, corrected for instrumental broadening, θ =Diffraction Angle in Radians.
- [111] D. K. Lee, Y. S. Kang, *ETRI Journal* **2004**, *26*, 262.
- [112] J. Widoniak, S. Eiden-Assmann, G. Maret, *Colloids & Surfaces A: Physiochem. Eng. Aspects.* **2005**, *270-271*, 340.
- [113] M. Yamamoto, M. Nakamoto, *J. Mater. Chem.* **2003**, *13*, 2064.
- [114] A. Frattini, N. Pellegri, D. Nicastro, O. de Sanctis, *Mater. Chem. Phys.* **2005**, *94*, 148.
- [115] O. Aleksyuk, F. Grynszpan, A. M. Litwak, S. E. Biali, *New J. Chem.* **1996**, *20*, 473.
- [116] F. Grynszpan, O. Aleksyuk, S. E. Biali, *J. Org. Chem.* **1994**, *59*, 2070.
- [117] F. Grynszpan, O. Aleksyuk, S. E. Biali, *Pure & Appl. Chem.* **1996**, *68*, 1249.
- [118] A. M. Litwak, F. Grynszpan, O. Aleksyuk, S. Cohen, S. E. Biali, *J. Org. Chem.* **1993**, *58*, 393.
- [119] Y. Morita, T. Agawa, Y. Kai, N. Kanehisa, N. Kasai, E. Nomura, H. Taniguchi, *Chem. Lett.* **1989**, 1349.
- [120] Y. Morita, T. Agawa, E. Nomura, H. Taniguchi, *J. Org. Chem.* **1992**, *57*, 3658.
- [121] R. G. R. Bacon, D. Stewart, *J. Chem. Soc. C Org.* **1966**, 1384.
- [122] N. A. Hampson, J. B. Lee, J. R. Morley, B. Scanlon, *Can. J. Chem.* **1969**, *47*, 3729.
- [123] P. Chaudhuri, K. Wieghardt, T. Weyhermuller, T. K. Paine, S. Mukherjee, C. Mukherjee, *Biol. Chem.* **2005**, *386*, 1023.
- [124] T. Sun, K. Seff, *Chem. Rev.* **1994**, *94*, 857.
- [125] R. Seifert, R. Rytz, G. Calzaferri, *J. Phys. Chem. A* **2000**, *104*, 7473.
- [126] R. Seifert, A. Kunzmann, G. Calzaferri, *Angew. Chem. Int. Ed* **1998**, *37*, 1521.
- [127] P. Scherrer, *Nachr. Ges. Wiss. Gottingen* **1918**, *26 Sept.*, 98.
- [128] J. I. Langford, A. J. C. Wilson, *J. Appl. Cryst.* **1978**, *11*, 102.
- [129] H. Borchert, E. V. Shevchenko, A. Robert, I. Mekis, A. Kornowski, G. Grubel, H. Weller, *Langmuir* **2005**, *21*, 1931.
- [130] A. M. Beatty, *Coord. Chem. Rev.* **2003**, *246*, 131.

Chapter VII: Organic Cationic Guests in Inorganic Anion/C-methylcalix[4]resorcinarene frameworks[†]

1. Abstract.....	294
2. Introduction.....	294
3. Experimental Section.....	297
4. Results and Discussion.....	305
Conformational Control of CMCR inclusions of 4,4'-Bipyridinium salts.....	305
Influence of Guest Geometry on Inorganic Anion/CMCR Frameworks	310
Influence of Solvent on Inorganic Anion/CMCR Frameworks	315
Thermal Stability of Inorganic Anion/CMCR Frameworks	321
5. Conclusions.....	324
6. References.....	326

1. Abstract

Under acidic conditions and in the presence of appropriate inorganic ions, bipyridyl-type molecules will self-assemble with C-methylcalix[4]resorcinarene to yield a host-guest supramolecular structure in which the resorcinarene adopts the open boat conformation, with the resorcinarene chains linked by the inorganic ions, and bipyridinium-type molecules included as guests. Such structures arise from the disruption of the hydrogen bonding at the rim of the resorcinarene by the introduction of the anions as stronger hydrogen bonding partners. These structural motifs can be tuned by judicious choice of anion, guest, and solvent conditions. In particular, the bulk and directionality of the various ions play a key role in determining the structural motif.

2. Introduction

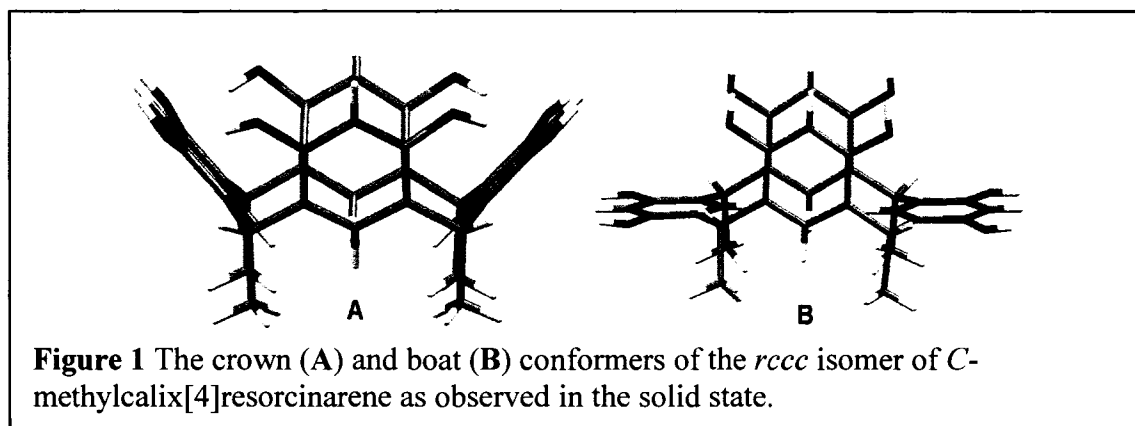
Continuing investigations of the calixarenes and calixresorcinarenes have demonstrated the versatility of these molecules in supramolecular host-guest

[†] Portions of this chapter have been previously published: P. O. Brown, G. D. Enright, J. A. Ripmeester, *J. Supramol. Chem.* **2002**, *2*, 497.

chemistry.^[1-3] For amine inclusions of 4-*t*-butylcalix[4]arene, the competition between non-covalent forces gives rise to a family of pseudopolymorphs that can be controlled using a variety of methods. With numerous phenolic hydroxyl functionalities along their upper rims, the resorcinarenes have been shown repeatedly to be excellent building blocks for supramolecular frameworks, such as capsules^[4-11] and channelled motifs.^[12-17] Further versatility is introduced through binding ligands such as 4,4'-bipyridine to these functionalities, resulting in the formation of an extended cavity capable of taking up large guests such as ferrocene.^[18, 19] The availability of such moieties makes these related compounds also well suited for studies of how combinations of various intermolecular forces can direct calixarene structural motifs towards multidimensional structures.

Investigations have been focused on the readily synthesized *C*-methylcalix[4]resorcinarene (CMCR), and in particular, the crown conformer of this host. As a result, while a number of supramolecular inclusion compounds of the thermodynamically favoured crown conformation (see Figure 1) of CMCR have been reported,^[1, 20] the other possible conformers have received less attention. Despite this, it is possible to induce conformational shifts in CMCR, a phenomenon most commonly observed by the inclusion of bipyridyl/bipyrimidyl linkers^[9, 10, 13, 15, 16] or ammonium cations^[8, 12, 17] which provide stabilization above and beyond that offered by intermolecular hydrogen bonding of the phenolic hydroxyls.

With regards to the role of bipyridyl linkers in CMCR frameworks, Coppens *et al.*^[13] have noted that 4,4'-bipyridine is capable of forming a variety of inclusion



compounds with CMCR. The CMCR molecules assume any of four conformations: crown, boat, chair and scoop. In nearly all examples of CMCR in the open boat conformation, either the CMCR forms a discrete complex with an inorganic ion,^[21] or each CMCR molecule hydrogen bonds directly to at least one adjacent CMCR, resulting in “brick wall” motifs, while the bipyridine serves to link these “walls” together.^[11, 13, 22, 23]

During their investigation of the inclusion properties of triethylammonium chloride in modified resorcinarenes, however, Shivanyuk *et al.*^[12] reported the ability of CMCR to adopt the boat conformation without forming the brick walls described by Coppens in his investigations of bipyridyl-type ligands. Instead, the chloride ions serve to extend the boat shaped cavity to allow accommodation of the triethylammonium ion. As suggested earlier, subsequent studies have demonstrated that various other cations can be included in resorcinarene capsules that form both in solution^[24-27] as well as the solid state.^[8, 17, 28, 29] Use of such inorganic ions presents an interesting alternative route to yielding extended resorcinarene structures.

These studies raised the question as to how bipyridines might be introduced into a CMCR framework without serving as hydrogen bond acceptors, thereby giving rise to a set of structural motifs distinct from those previously reported. Investigations of 4,4'-bipyridinium salts as supramolecular synthons have demonstrated the utility of such molecules as hydrogen bond donors, yielding stable, predictable periodic networks with both chloride anions and metal chloride complexes.^[30-32] Extrapolating from this, judicious choice of anion, pH and guest could be used to control the conformation of CMCR. This competition of forces would be similar to that observed for 4tBC4A and amines.

In this chapter, the structural motifs arising from the inclusion of nitrogen-containing molecules under acidic conditions are examined. In the case of bipyridyl-type guests, the introduction of inorganic anions proves to be sufficient to disrupt the intramolecular hydrogen bonding of the CMCR, yielding channelled structures occupied by the now-protonated guest. Furthermore, it is demonstrated that sufficiently large anions with distinct directional interactions will yield these channelled structures even with a less bulky aliphatic cationic guest. The position of organic cations can be further tuned provided the guests are capable of forming hydrogen bonds in two dimensions. Finally, the stability of a representative framework is examined, leading to comments on the difficulties in analyzing such complex systems.

3. Experimental Section

General Note: Unless otherwise indicated, chemicals were obtained from EMD Chemicals and Sigma-Aldrich, and were used without further purification.

Synthesis of C-methylcalix[4]resorcinarene (CMCR): Synthesis of the host was carried out based on literature procedures.^[33] In a typical synthesis, 18.004 g (0.1635 mol) of resorcinol was placed in a three necked round bottom flask and dissolved in a solution of 30.0 mL H₂O, 30.0 mL EtOH and 15.0 mL concentrated hydrochloric acid. The flask was fitted with a condenser, placed under an N₂ purge and cooled to 0°C with an ice bath. Over the course of approximately 10 minutes, 9.0 mL (0.16 mol) of acetaldehyde was added using a dropping funnel. The resulting mixture was then heated at 80°C for approximately 1 day, at which point a bright yellow precipitate was observed to have formed. This precipitate was filtered off by vacuum and washed with chilled water. After drying overnight at 150°C, 16.886 g (0.03104 mol, 77% yield) of light yellow CMCR was isolated. ¹H NMR (DMSO-*d*₆, 400.130 MHz) δ 1.31 (d, J= 7.03 Hz, 12H, CHCH₃), 4.46 (q, J=7.03 Hz, 4H, CHCH₃), 6.15 (s, 4H, ArH ortho to OH), 6.78 (s, 4H, ArH meta to OH), 8.55 (s, 8H, Ar OH). ¹³C NMR (DMSO-*d*₆, 100.613 MHz) δ 22.48, 29.44, 109.98, 123.97, 126.16, 152.75. ESI-MS (ES⁺, m/z, C₃₂H₃₂O₈H⁺) 545.3.

Synthesis of 1(4,4'-bipyridinium)*1(SO₄²⁻)*1(EtOH)*3(H₂O)*1(CMCR) clathrate **1** (POB25): In a typical synthesis, 0.108 g of CMCR (1.98×10^{-4} mol) and 0.062 g of 4,4'-bipyridine (3.96×10^{-4} mol) were weighed out into a scintillation vial, and dissolved in 10 mL ethanol, giving rise to a light yellow solution. Subsequently, 5.0 mL 10% (w/w) sulphuric acid was added to this solution, causing the colour to change to deep red. This red solution was then capped loosely and set aside to allow excess solvent to evaporate for approximately 5 days, at which point orange platelike crystals had formed.

Synthesis of $1(4,4'-bipyridinium) $*2.87(\text{MeCN})*2(\text{H}_2\text{O})*2(\text{Cl}^-)*1(\text{CMCR})$ clathrate **2**$

(POB 4): 0.250 g (1.60×10^{-3} mol) of 4,4'-bipyridine was weighed out into an Erlenmeyer flask and dissolved in 5 mL of EtOH, 50 mL of MeCN and 10 mL of 10% (w/w) hydrochloric acid. The resulting solution was heated to approximately 70°C, and 0.436 (8.01×10^{-4} mol) of CMCR was added, yielding a red-orange solution. The solution was stirred at 70°C for a further four hours, and cooled to room temperature. The excess solvent was allowed to evaporate over the next 5 days, giving rise to blocklike orange crystals.

Synthesis of $1(\text{trans-1,2-bis(4-pyridinium)ethylene})*3(\text{H}_2\text{O})*1(\text{H}_3\text{O}^+)*(1.5 \text{SO}_4^{2-})$

$*1(\text{CMCR})$ clathrate **3** (POB25): A solution of 10.0 mL MeCN, 2.5 mL EtOH and 3.0 mL 10% (w/w) sulphuric acid was placed in an Erlenmeyer flask and heated to approximately 70°C. 0.019 g (0.104×10^{-3} mol) of *trans*-1,2-bis(4-pyridyl)ethylene was then dissolved in this hot solution. 0.109 g (0.200×10^{-3} mol) of CMCR was then added, yielding an orange solution. This solution was stirred at 70°C for a further two hours, and then cooled to room temperature. The excess solvent was allowed to evaporate over the next five days, giving rise to red prismatic crystals.

Synthesis of $1(1,3\text{-bis(3-pyridiniummethyl)-(2-thiourea)})*4(\text{MeCN})*2(\text{Cl}^-)*1(\text{CMCR})$

clathrate **4** (POB10) and $1(1,3\text{-bis(3-pyridiniummethyl)-(2-thiourea)})*2(\text{MeCN})*2(\text{Br}^-)*1(\text{CMCR})$ clathrate **5** (POB 60): Both compounds were produced in a similar manner.

In a typical synthesis, a solution of 20.0 mL MeCN and 5.0 mL of 20% w/w HBr was placed in an Erlenmeyer flask and heated to 70°C. 0.387g (7.11×10^{-4} mol) of CMCR was then dissolved in the hot solvent, yielding a yellow solution. 0.365 g (1.41×10^{-3}

mol) of 1,3-bis(3-pyridylmethyl)-(2-thiourea) was then added, causing the yellow colour to further deepen. This solution was heated for a further 30 minutes, and then cooled to room temperature. The excess solvent was allowed to evaporate over the next five days, giving rise to yellow platelike crystals.

Synthesis of $8(\text{dimethylammonium}) \cdot 1(\text{DMF}) \cdot 4.23(\text{H}_2\text{O}) \cdot 4(\text{SO}_4^{2-}) \cdot 1(\text{CMCR})$ clathrate **6** (POB 46): A solution of 15.0 mL DMF and 5.0 mL 10% (w/w) sulphuric acid was placed in a vial and heated to approximately 70°C. 0.107 g (1.97×10^{-4} mol) of CMCR was then dissolved in the hot solvent, yielding a yellow solution. 0.061 g (3.91×10^{-4} mol) of 4,4'-bipyridine was then added, causing the solution to turn deep orange. This solution was heated for a further 30 minutes, and then cooled to room temperature. The excess solvent was allowed to evaporate over the next five days, giving rise to clear platelike crystals.

Synthesis of $0.5(4,4'\text{-bipyridinium}) \cdot 1(4\text{-pyridinium-}4'\text{-pyridine}) \cdot 2.5(\text{H}_2\text{O}) \cdot 2(\text{Br}^-) \cdot (\text{CMCR})$ clathrate **7** (POB70): 35.0 mL of ethanol and 5.0 mL of 20% (w/w) hydrobromic acid was placed in an Erlenmeyer flask and heated to approximately 70°C. 0.696 g (1.28×10^{-3} mol) of CMCR was then dissolved in the hot solution, yielding a yellow solution. 0.397 g (2.54×10^{-3} mol) of 4,4'-bipyridine was then added, resulting in the solution turning bright red. A 5 mL portion of this solution was pipetted into a small vial, and set inside a second vial along with ~5 mL of isopropyl ether. The second vial was then capped and set aside to allow the ether to diffuse into the reaction mixture. After approximately one month, small red block-like crystals were observed to have formed.

SCXRD data are summarized in Table 1. In general, all atoms with occupancies greater than 0.4 were refined anisotropically, while the remainder were refined isotropically. For clathrates **1**, **4** and **5**, all hydrogens save those on the acetonitrile were found from the difference map. For clathrate **2**, all hydrogens were placed in calculated positions and refined as riding atoms. For clathrates **3** and **6**, hydrogens on fully ordered heteroatoms were found from the difference map, while all others were placed in calculated positions and refined as riding atoms. For clathrate **7**, the pyridinium hydrogens were found from the difference map, with all others placed in calculated positions and refined as riding atoms.

Thermogravimetric analysis was carried out as described in Chapter III on pages 72-73. ^{13}C CP/MAS spectra for clathrate **1** were collected using the Bruker AMX-300 spectrometer. Powder X-ray Diffraction (PXRD) data were collected on the Scintag X-2 Advanced diffractometer.

Table 1a Single Crystal X-Ray Diffraction data for Clathrates 1-3.

Identification code	Clathrate 1 (POB40)	Clathrate 2 (POB4)	Clathrate 3 (POB25)
Empirical formula	C ₄₄ H ₅₄ N ₂ O ₁₆ S	C _{47.74} H _{54.61} Cl ₂ N _{4.87} O ₁₀	C ₄₄ H _{50.75} N ₂ O ₁₈ S _{1.50}
Formula weight	898.95	927.52	943.71
Temperature	173(2) K	173(2) K	173(2) K
Wavelength	0.71073 Å	0.71073 Å	0.71073 Å
Crystal system	Monoclinic	Triclinic	Monoclinic
Space group	<i>P</i> 2 ₁ / <i>n</i>	<i>P</i> -1	<i>P</i> 2 ₁ / <i>n</i>
Unit cell dimensions	<i>a</i> = 9.5725(6) Å <i>b</i> = 14.6280(9) Å <i>c</i> = 30.2164(19) Å α = 90° β = 98.484 (1)° γ = 90°	<i>a</i> = 12.8602(13) Å <i>b</i> = 14.8584(15) Å <i>c</i> = 15.2379(15) Å α = 117.254(2)° β = 90.827(2)° γ = 113.466(2)°	<i>a</i> = 17.5184(1) Å <i>b</i> = 13.1681(7) Å <i>c</i> = 18.5684(1) Å α = 90° β = 91.166 (1)° γ = 90°
Volume	4184.8(5) Å ³	2304.2(4) Å ³	4282.5(4) Å ³
Z	4	2	4
ρ _{calc}	1.427 Mg/m ³	1.337 Mg/m ³	1.464 Mg/m ³
Abs. coefficient	0.156 mm ⁻¹	0.205 mm ⁻¹	0.183 mm ⁻¹
F(000)	1904	978	1987
Crystal size	0.48 x 0.16 x 0.13 mm ³	0.30 x 0.25 x 0.10 mm ³	0.48 x 0.48 x 0.24 mm ³
θ Range	1.36 to 29.60°	1.55 to 23.33°	1.58 to 30.54°
Index ranges	-13 ≤ <i>h</i> ≤ 13 -20 ≤ <i>k</i> ≤ 20 -42 ≤ <i>l</i> ≤ 41	-14 ≤ <i>h</i> ≤ 14 -16 ≤ <i>k</i> ≤ 16 -16 ≤ <i>l</i> ≤ 16	-25 ≤ <i>h</i> ≤ 24 -18 ≤ <i>k</i> ≤ 18 -26 ≤ <i>l</i> ≤ 26
Reflections collected	52086	17988	55223
Ind. reflections	11736 [R(int) = 0.0341]	6669 [R(int) = 0.0761]	12891 [R(int) = 0.0872]
Completeness to θ = max	99.6 %	99.8 %	98.2 %
Absorption correction	Multi-Scan	Multi-Scan	Multi-Scan
Refinement method	Full-matrix least-squares on F ²	Full-matrix least-squares on F ²	Full-matrix least-squares on F ²
Data / restraints / parameters	11736 / 0 / 772	6669 / 0 / 589	12891 / 0 / 830
Goodness-of-fit on F ²	1.031	0.926	1.182
Final R indices [I > 2σ(I)]	R1 = 0.0411 wR2 = 0.1037	R1 = 0.0578 wR2 = 0.1235	R1 = 0.0891 wR2 = 0.2082
R indices (all data)	R1 = 0.0575 wR2 = 0.1111	R1 = 0.1232 wR2 = 0.1449	R1 = 0.1074 wR2 = 0.2185
Largest diff. peak and hole (e.Å ⁻³)	0.433 and -0.445	0.345 and -0.351	0.590 and -0.738

Table 1b Single Crystal X-Ray Diffraction data for Clathrates 4-6.

Identification code	Clathrate 4 (POB10)	Clathrate 5 (POB60)	Clathrate 6 (POB46)
Empirical formula	C ₅₃ H ₆₀ Cl ₂ N ₈ O ₈ S	C ₅₃ H ₆₀ Br ₂ N ₈ O ₈ S	C ₅₁ H _{106.75} N ₉ O _{29.25} S ₄
Formula weight	1040.05	1128.97	1442.44
Temperature	173(2) K	173(2) K	173(2) K
Wavelength	0.71073 Å	0.71073 Å	0.71073 Å
Crystal system	Monoclinic	Monoclinic	Triclinic
Space group	C2/c	C2/c	P-1
Unit cell dimensions	<i>a</i> = 21.0245(11) Å <i>b</i> = 13.4310(7) Å <i>c</i> = 18.2187(10) Å α = 90° β = 92.400(1)° γ = 90°	<i>a</i> = 21.2602(9) Å <i>b</i> = 13.6759(6) Å <i>c</i> = 18.1235(8) Å α = 90° β = 92.838(1)° γ = 90°	<i>a</i> = 13.0490(8) Å <i>b</i> = 17.2834(11) Å <i>c</i> = 17.7815(11) Å α = 87.555(1)° β = 83.740(1)° γ = 67.968(1)°
Volume	5140.1(5) Å ³	5263.0(4) Å ³	3695.3(4) Å ³
Z	4	4	2
ρ_{calc}	1.344 Mg/m ³	1.425 Mg/m ³	1.296 Mg/m ³
Abs. coefficient	0.230 mm ⁻¹	1.641 mm ⁻¹	0.212 mm ⁻¹
F(000)	2192	2336	1548
Crystal size	0.24 x 0.16 x 0.08 mm ³	0.32 x 0.32 x 0.16 mm ³	0.32 x 0.16 x 0.13 mm ³
θ Range	1.94 to 29.69°	1.77 to 29.58°	1.69 to 29.59°
Index ranges	-29 ≤ <i>h</i> ≤ 29 -18 ≤ <i>k</i> ≤ 18 -25 ≤ <i>l</i> ≤ 25	-29 ≤ <i>h</i> ≤ 29, -18 ≤ <i>k</i> ≤ 18, -25 ≤ <i>l</i> ≤ 25	-18 ≤ <i>h</i> ≤ 18 -23 ≤ <i>k</i> ≤ 24 -24 ≤ <i>l</i> ≤ 24
Reflections collected	32071	32724	46727
Ind. reflections	7261 [R(int) = 0.0468]	7389 [R(int) = 0.0272]	20463 [R(int) = 0.0231]
Completeness to $\theta = \text{max}$	99.4 %	99.9 %	98.7 %
Absorption correction	Multi-Scan	Multi-Scan	Multi-Scan
Refinement method	Full-matrix least-squares on F ²	Full-matrix least-squares on F ²	Full-matrix least-squares on F ²
Data / restraints / parameters	7261 / 0 / 425	7389 / 0 / 424	20463 / 43 / 1038
Goodness-of-fit on F ²	0.906	1.012	1.043
Final R indices [I > 2 σ (I)]	R1 = 0.0425 wR2 = 0.0983	R1 = 0.0298 wR2 = 0.0798	R1 = 0.0398 wR2 = 0.1048
R indices (all data)	R1 = 0.0811 wR2 = 0.1076	R1 = 0.0418 wR2 = 0.0835	R1 = 0.0599 wR2 = 0.1134
Largest diff. peak and hole (e.Å ⁻³)	0.346 and -0.391	0.672 and -0.387	0.418 and -0.376

Table 1c Single Crystal X-Ray Diffraction data for Clathrates 7.

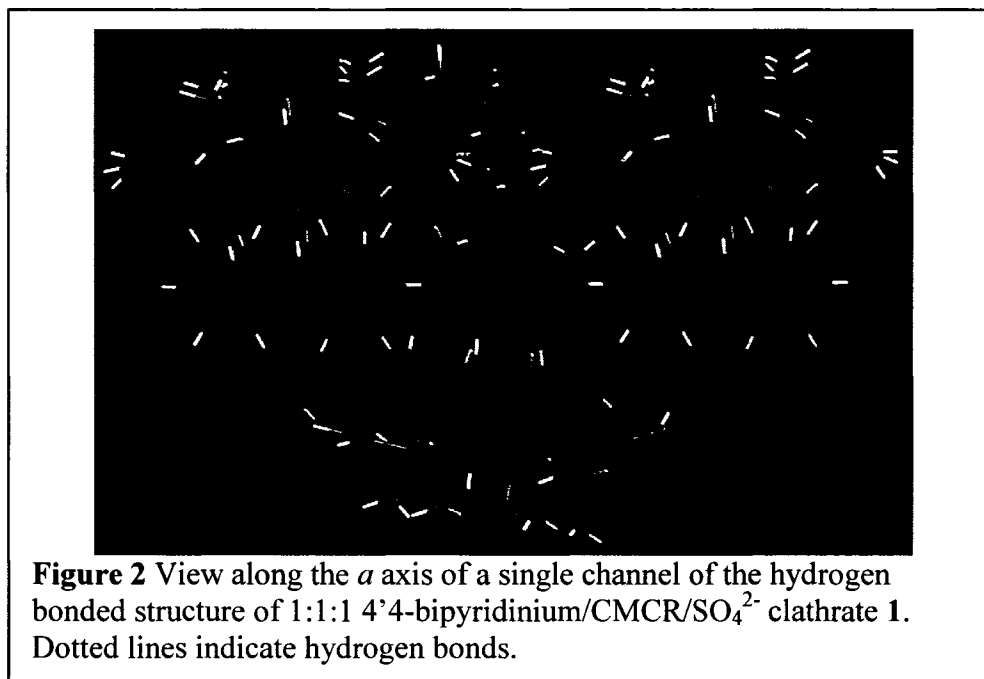
Identification code	Clathrate 7 (POB70)
Empirical formula	$C_{47}H_{46}Br_2N_3O_{11}$
Formula weight	988.69
Temperature	173(2) K
Wavelength	0.71070 Å
Crystal system	Triclinic
Space group	P-1
Unit cell dimensions	$a = 12.5437(6)$ Å $b = 12.8192(6)$ Å $c = 14.8509(7)$ Å $\alpha = 75.356(1)^\circ$ $\beta = 76.361(1)^\circ$ $\gamma = 78.048(1)^\circ$
Volume	2217.51(18) Å ³
Z	2
ρ_{calc}	1.481 Mg/m ³
Abs. coefficient	1.893 mm ⁻¹
F(000)	1014
Crystal size	0.48 x 0.32 x 0.32 mm ³
θ Range	1.69 to 29.55°.
Index ranges	-17 ≤ h ≤ 17 -17 ≤ k ≤ 17 -20 ≤ l ≤ 20
Reflections collected	25851
Ind. reflections	12124 [R(int) = 0.0243]
Completeness to $\theta = \text{max}$	97.6 %
Absorption correction	Multi-Scan
Refinement method	Full-matrix least-squares on F ²
Data / restraints / parameters	12124 / 4 / 624
Goodness-of-fit on F ²	1.014
Final R indices	R1 = 0.0420
[I > 2σ(I)]	wR2 = 0.1028
R indices (all data)	R1 = 0.0659 wR2 = 0.1127
Largest diff. peak and hole (e.Å ⁻³)	0.690 and -0.440

4. Results and Discussion

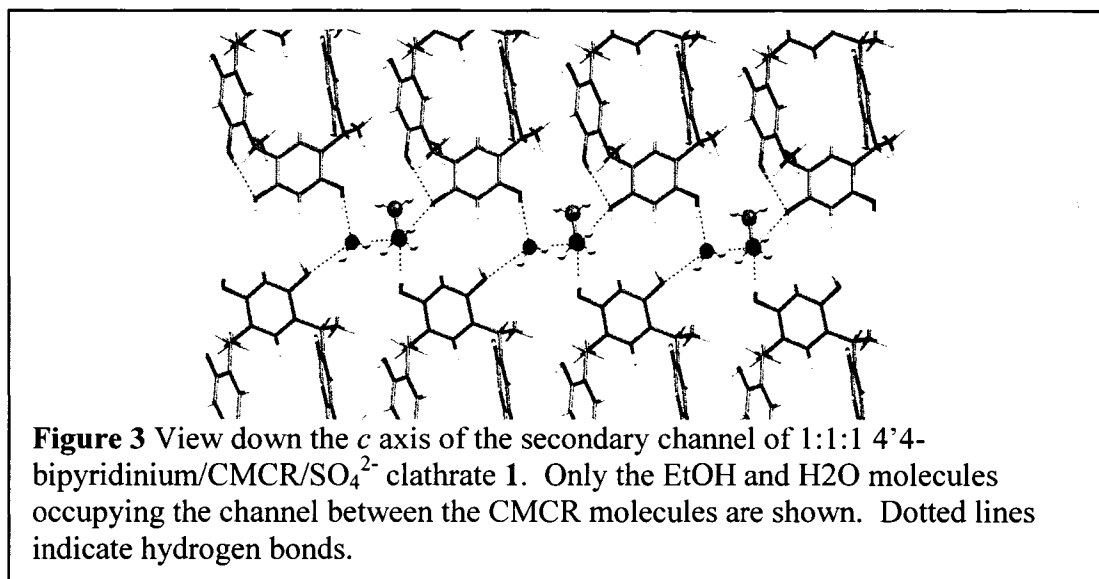
Conformational Control of CMCR inclusions of 4,4'-Bipyridinium salts

The pKa of bipyridinium type compounds is ~ 4.2 ,^[34] such that given recrystallization under typical reaction conditions, bipyridines will only serve as hydrogen bonding acceptors for CMCR in the resulting crystalline compounds. By using strong mineral acids to adjust the pH of the reaction media, and thereby forcing the protonation of the bipyridine, it was expected that the common hydrogen bonded structural motifs would be precluded. Upon slow evaporation of a solution of CMCR and 4,4'-bipyridine in ethanol and 10% (w/w) sulphuric acid, large orange crystals were obtained and subjected to single crystal X-ray diffraction analysis.

Upon solution of the structure, these crystals proved to be a 1(4,4'-bipyridinium)*1(SO₄²⁻)*1(EtOH)*3(H₂O)*1(CMCR) clathrate (clathrate 1). As can be seen from Figure 2, the 4,4'-bipyridinium cation arising from the acid-base chemistry serves as a guest within a channel formed by molecules of CMCR in the scoop conformation. This cation is incapable of serving as a hydrogen bond acceptor, ruling out any interactions between the phenolic hydroxyls of the CMCR as seen in the extended cavities^[18, 19, 23] and the frameworks^[13] previously reported for 4,4'-bipyridine. Similarly, the arrangement of the guest precludes cation- π interactions similar to those seen in the discrete resorcinarene capsules.^[7, 8, 17, 26-29] Instead, these cations form a strong hydrogen bond with a SO₄²⁻ anion (O...N bond distance of 2.71 Å), forming an infinite one-dimensional chain along the crystallographic *b* axis.

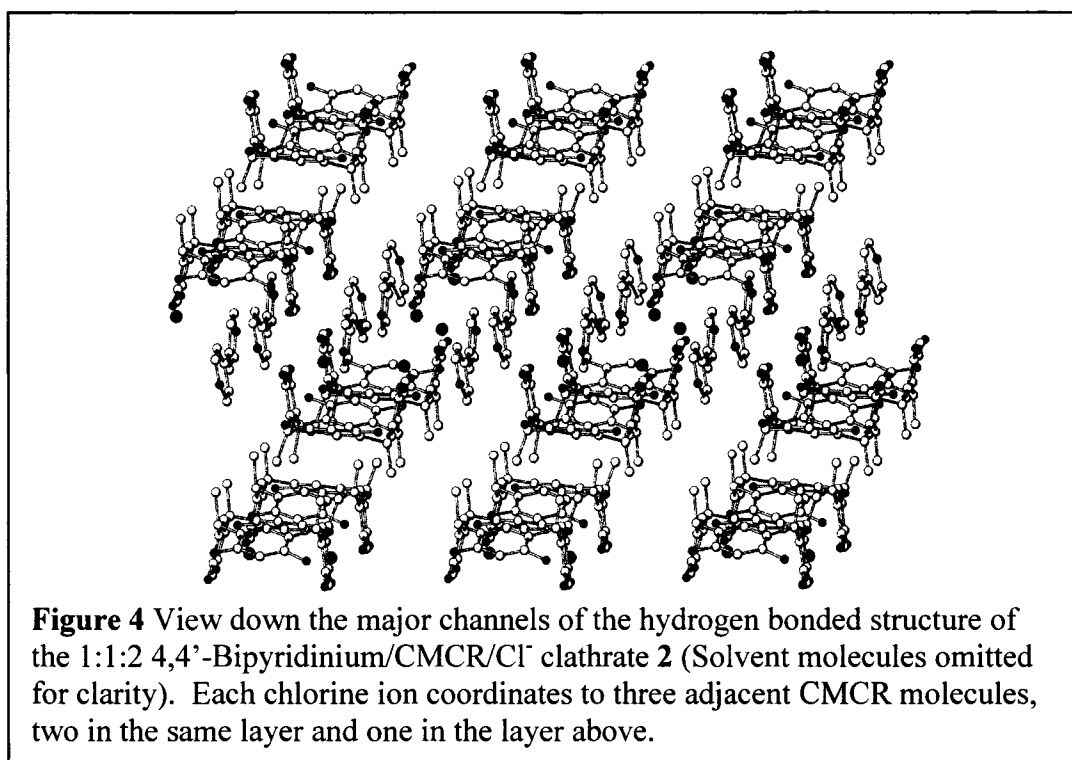


This SO₄²⁻ anion also serves as the centre of an extensive network of hydrogen bonds that serves to link together the molecules of CMCR to form the channels observed. The SO₄²⁻ anion forms hydrogen bonds between molecules of CMCR in a given layer, as well as linking together adjacent layers along the *c* axis (O...O bond distance of 2.61, 2.70 Å 2.74 Å). Further linkages between channels along the *b* and *c* axes are mediated by two molecules of H₂O (O...O bond distances of 2.67-2.81 Å). Adjacent channels along the *a* axis are stabilized by virtue of a hydrogen bonding chain formed by a combination of water and EtOH molecules in a secondary channel perpendicular to the primary channel (O...O bond distances of 2.67-2.84 Å, see Figure 3). As a result, each layer of CMCR molecules along the *b* axis is offset by 5.71 Å along the *a* axis, giving rise to an AB packing scheme.



Using a similar synthesis, with ethanol and acetonitrile together with 10% (w/w) hydrochloric acid, crystals were obtained of a related 1(4,4'-bipyridinium)*2.87(MeCN)*2(H₂O)*2(Cl⁻) clathrate (clathrate **2**). Once again, a doubly channelled structure is produced, with the chloride ions found at the edges of each CMCR (see Figure 4) each linking three CMCR molecules together in the extended structure (Cl...O distances of 2.98-3.11 Å). Much as how the geometric constraints of the directional hydrogen bonding interactions of SO₄²⁻ resulted in the distortion away from the idealized boat conformer of CMCR, the smaller size of the chloride anion results in a smaller distortion of the boat conformation of the CMCR molecule.

The primary channel again is occupied by bipyridinium cations stabilized by an extensive hydrogen bonded network involving CMCR, chloride anions, and residual solvent molecules, although the shift in symmetry results in this channel now being nearly perpendicular to the (001) plane. As well, the smaller chloride ion forces the layers of CMCR molecules to pack more closely, such that one pair of phenolic groups



interact with each other (O...O distance of 2.97 Å). Even so, each bipyridinium molecule is stabilized by hydrogen bonding with a fully ordered acetonitrile molecule (N...N distance of 2.73 Å) as well as two molecules of water (N...O and O...O distances of 2.72 and 2.62 Å), one of which is disordered over two positions (0.81:0.19 occupancy ratio), such that cation- π interactions are again ruled out as a significant source of stabilization.

The secondary channel is instead occupied by a series of paired acetonitrile molecules that do not interact with any other components of the structure. Their role in linking adjacent channels appears to have been supplanted by the chloride anions, resulting in the previously mentioned shift in the channel structure, as well as the overall contraction in the framework suggested by the decreased volume of the unit cell. This suggests they only play a peripheral, space-filling role in stabilizing the framework. Such

a hypothesis is further supported by the fact that one of these non-interacting acetonitrile molecules is only partially occupied (0.87 occupancy), suggesting that the framework can survive partial desolvation.

The conformational shifts observed in these two structures arise out of alterations in the hydrogen bonding scheme of the phenolic hydroxyls on the rim of CMCR. Much as with 4-*t*-butylcalix[4]arene (4tBC4A), the presence of phenolic hydroxyl groups on CMCR presents an opportunity to make use of combinations of weak interactions to control the inclusion behaviour of the host (see Chapters III to VI).^[35, 36] In the case of 4tBC4A, addition of a simple base will disrupt the symmetry of the host since only one hydroxyl can be easily deprotonated (pK_a of ~ 20 in MeCN).^[37, 38] However, the much more acidic character of CMCR is such that four of the eight phenolic hydrogens are readily removed (pK_a of approximately 11.4 in DMF/H₂O),^[39, 40] maintaining the symmetry of the host. This results in symmetrical, 1 Guest: 1 Host inclusion compounds being observed for small organic cations.^[20]

In order to perturb the inclusion scheme, a more favourable interaction, such as hydrogen bonding with an inorganic anion, must be introduced. This requires that the anion is a good hydrogen bond acceptor (such as Cl⁻ and Br⁻), since attempts to use weaker anions such as I⁻ have failed (a failure echoed in recent studies of capsular assemblies^[17]). However, this is not the only factor, as studies by Rissanen *et al.*^[8, 17, 28] and others^[7, 26, 27, 29] clearly show that small anions when paired with small organic cations will still form discrete capsular structures. As such, formation of channelled compounds through opening of the CMCR molecule is also partially predicated on the

cation being capable of multiple hydrogen bonds suitable for the formation of hydrogen bonded polymers. In the case of pyridyl type compounds and larger difunctional quaternary cations,^[17] such cationic guests are rigid enough to lead to formation of such polymers, prompting a conformational shift which either small (Cl⁻) or large (SO₄²⁻) anions will serve to stabilize. However, as we will see later, the larger anions can play a role in allowing smaller cations to be used to form channelled CMCR frameworks.

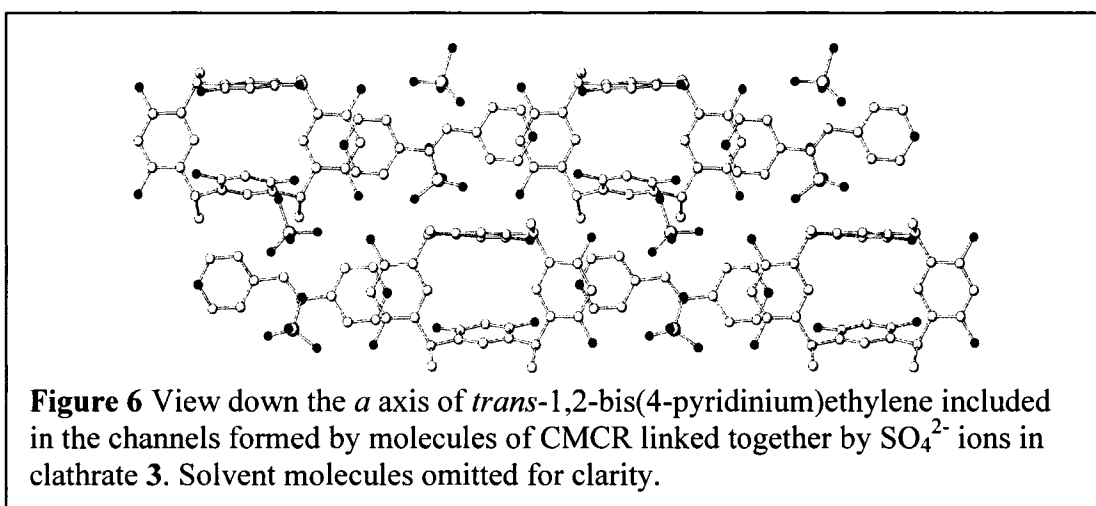
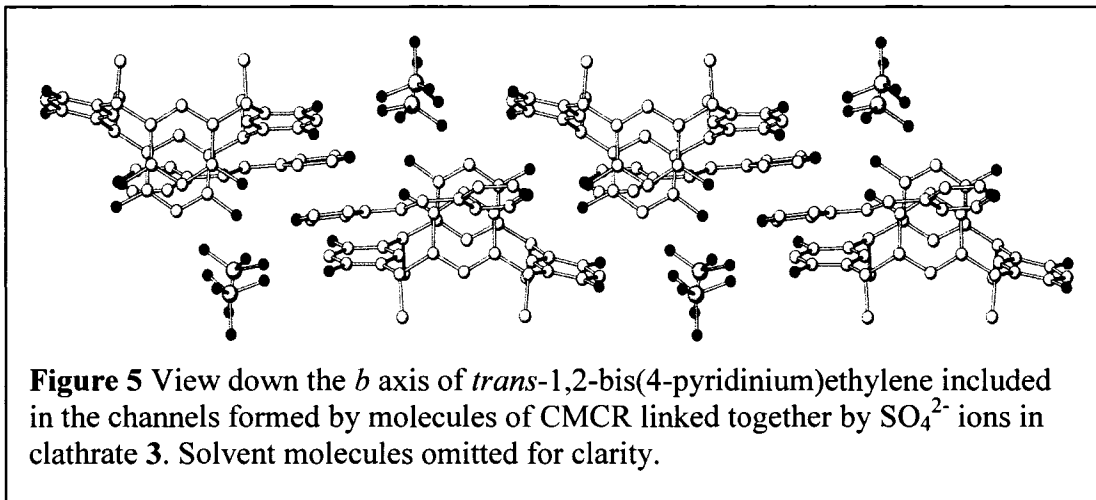
The resulting packing schemes are considerably more complex than that observed for CMCR clathrates involving 4,4'-bipyridine at neutral pH.^[13] Despite this, no disorder is observed in the first structure, and only minor disorder is observed in the second, indicating the various interactions guiding the structure are quite carefully balanced. In the case of the solvent molecules, the strong hydrogen bonds implied by the short bond lengths likely lock these molecules in place. This dependence on solvent hydrogen bonds has obvious consequences for the robustness of these frameworks.

Influence of Guest Geometry on Inorganic Anion/CMCR Frameworks

Given the relatively open nature of the channels in these initial structures, further attempts were made to include other bipyridyl-type molecules. In particular, it appeared that the geometry of the guest molecule might be useful in directing the arrangement of the channels, much as had been observed in moving from the larger SO₄²⁻ anion to the smaller chloride anion. By introducing larger, more flexible linker units between the pyridyl functionalities, it was hoped that further control might be exerted over the formation of the channels in the structure.

Previous studies had indicated that hydrothermal synthesis using *trans*-1,2-bis(4-pyridyl)ethylene and CMCR results in a hydrogen bonded compound, with CMCR in the chair conformation.^[41] Again, using ethanol and acetonitrile as solvent with a small amount of 10% (w/w) sulphuric acid, red crystals were obtained again suitable for crystallographic analysis (clathrate **3**). The resulting channelled structure with stoichiometry of 1(*trans*-1,2-bis(4-pyridinium)ethylene)*3(H₂O)*1(H₃O⁺)*(1.5 SO₄²⁻)*1(CMCR) is depicted in Figures 5 and 6. While this clathrate similar to that observed with 4,4'-bipyridine under acidic conditions, the orientation of the bispyridylethylene is now such that the aromatic rings are parallel to the opened phenolic rings in the boat conformation of CMCR. This allows for cation- π interactions (Aromatic Centroid...N distance of 3.10 Å) similar to that frequently observed for smaller capsular clathrates of organic cations.

As a result, the bispyridiniumethylene simply serves as a spacer between units of CMCR, directly hydrogen bonding to the host through one pyridinium moiety (N...O distance of 2.86 Å), and indirectly through a water molecule (N...O distance of 2.88 Å, O...O distance of 2.74 Å). Under these conditions, the SO₄²⁻ anions are shifted such that they now occupy the secondary channel perpendicular to the primary channel, and solely serve to bind both adjacent layers and channels together through a complex network of hydrogen bonds with a series of disordered water molecules (O...O distances 2.61-3.06 Å). In order to accommodate this broad range of interactions, one of the two SO₄²⁻ anions is disordered over two positions (0.5:0.5 occupancy ratio), while the upright phenolic rings on the CMCR molecule are pinched inwards slightly.



By moving to a slightly larger guest, the inclusion motif undergoes a subtle shift, while retaining conformational control due to the directional, bulky SO_4^{2-} anion. The size of the guest also contributes to causing the conformation to shift, in order to allow for stabilizing cation- π interactions as well as hydrogen bonding. The planar arrangement of the bispyridiniumethylene bears considerable resemblance to that of 4,4'-bipyridine in Coppens' water-mediated CMCR framework resulting from hydrothermal syntheses^[13], where adjacent calixarene layers interact. However, with an anion serving as hydrogen

bond acceptor, direct hydrogen bonding interactions between CMCR molecules are disfavoured. As such, while the increase in guest length was sufficient to promote a shift in the orientation of the bispyridyl-type molecule, the fixed geometry of the *trans* linker precluded any significant shifts in the channel motif.

It would be expected that moving to a larger guest with more sites for interactions, as well as a more flexible linker between the pyridyl rings, might further guide the structural motif away from the brick wall motif observed in hydrothermal syntheses towards. Bispyridylthioureas, which have received attention as potential receptors for enantioselective recognition of amino acids,^[42, 43] and various pharmaceutical applications,^[44-46] appeared to be promising candidates. In addition to exhibiting a high degree of conformational flexibility,^[47] such molecules contain two additional nitrogens suitable as sites capable of directing the anions in a second dimension. The readily available 1,3-bis(3-pyridylmethyl)-(2-thiourea) (1,3-BPTU) was therefore selected to examine how such a ligand might both direct the conformation of CMCR as well as control the placement of the anion.

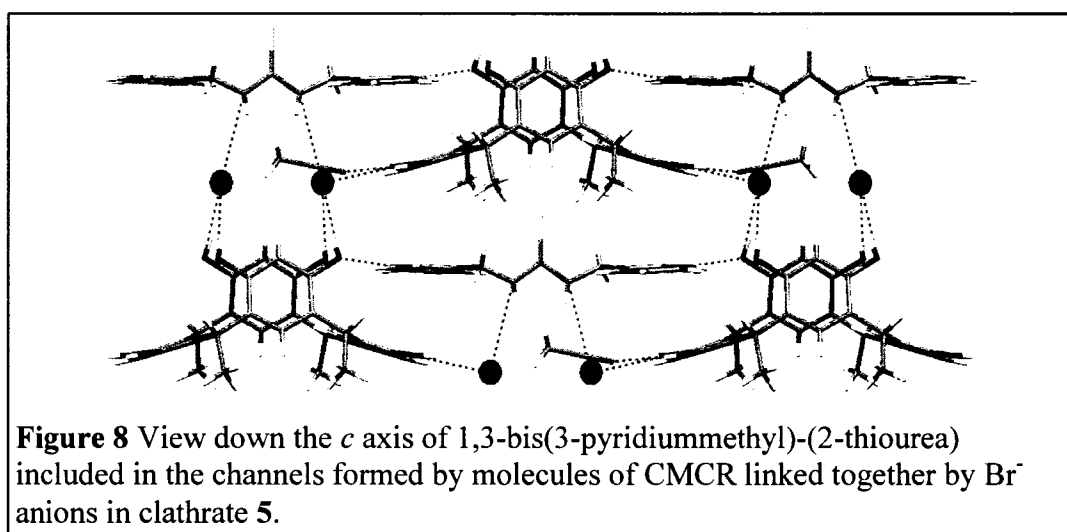
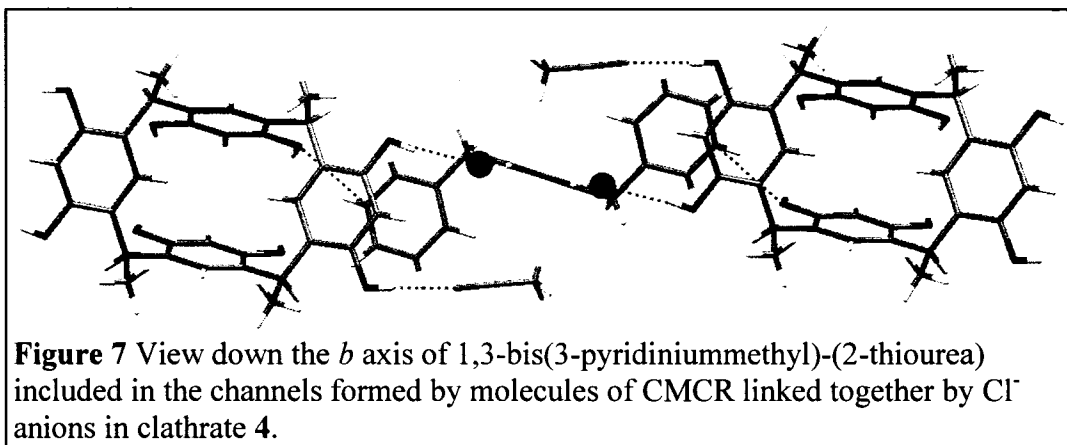
Recrystallization from acidic acetonitrile solutions containing chloride or bromide ions resulted in a pair of isostructural clathrates **4** and **5**, with stoichiometries of 1(1,3-bis(3-pyridiniummethyl)-(2-thiourea))*4(MeCN)*2(Halide⁻)*1(CMCR) (see Figures 7 and 8). As with the inclusion of the bispyridyl ethylene, the length of 1,3-BPTU and the favourability of the interactions between the pyridinium moieties and the phenolic hydroxyls of the resorcinarene result in the thiourea serving as a linker in the resulting framework. Furthermore, once again, cation- π interactions with the aromatic rings of

CMCR (Aromatic Centroid...N distance of 3.04 Å) also serve to facilitate the conformational shift of the host. The urea amides direct the anion such that it serves to bind each molecule of 1,3-BPTU to the molecules of CMCR forming the channel it resides in (Cl...O distance 3.25 Å, Br...O distance 3.38 Å), but also to a molecule of CMCR in the adjacent layer (Cl...O distance 3.11, 3.13 Å, Br...O distances 3.26, 3.29 Å).

As expected, the bispyridylthiourea adopts a staggered conformation in order to maximize the number of interactions with the various anions present in the structure, as well as enabling favourable cation- π interactions. In the case of 1,3-BPTU, this is due to the stronger thiourea nitrogens serving as ligands to the anions, resulting in the cationic pyridinium moieties seeking alternative stabilization sites. The resulting packing scheme is much more efficient than that observed in any of the other CMCR anion frameworks involving bipyridyl type moieties, such that no secondary channels are formed. Much as in the studies of calixarene ionophores, the conformation of the host will adapt to maximize cation- π interactions. However, such interactions are only favoured in this case when the cation is prevented from directly interacting with an anion.

Furthermore, only two of the eight phenolic moieties on each molecule of CMCR present do not interact directly with an anion, instead forming a hydrogen bond with acetonitrile (N...O distance of 2.94 Å in both cases). This is reflected by the fact that all attempts to exchange the anions in crystalline bulk samples of the two BPTU clathrates through exposure to appropriate solutions failed. Given this, the resulting structures are clearly dependent on the stabilization arising from such phenol-anion hydrogen bonds. Any potential exchange would involve significant shifts in the structural motif, possibly

giving rise to new polymorphs or pseudopolymorphs. However, no such transformation resulting in crystals suited for SXCRD was found.



Influence of Solvent on Inorganic Anion/CMCR Frameworks

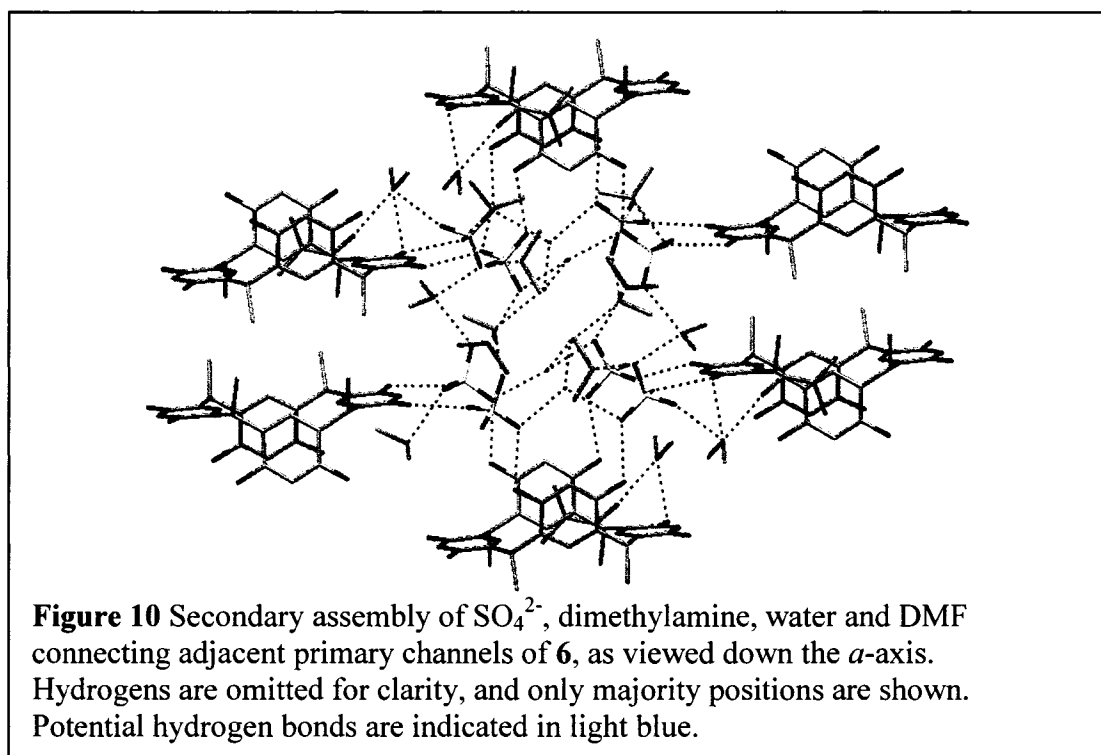
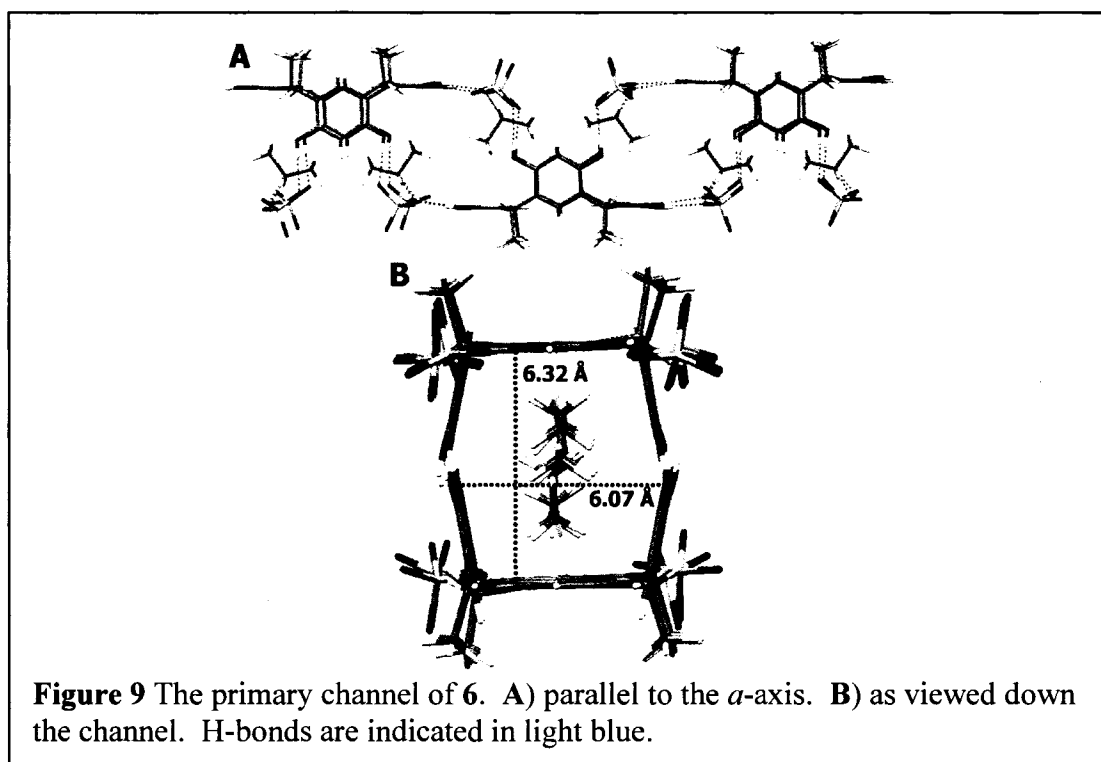
The investigations of guest geometries clearly indicated that while structural modifications could be partially directed through judicious choice of guest, a more complex interplay of factors had to be accounted for in order to fully control the formation of such charged frameworks. Even in the presence of strong ionic interactions, a significant quantity of solvent was still included in these frameworks. In order to

clarify how significant solvent inclusion was, potentially alternative solvent and recrystallization conditions were examined.

When using 4,4'-bipyridine as the base, DMF as the solvent, and H₂SO₄ as the acid, unusual clear block-like crystals were obtained. As suggested by the lack of colour, the 4,4'-bipyridine had not been included in the framework. Instead, dimethylamine, a stronger base on the basis of pK_a data^[48] and one of the products of acid induced cleavage of DMF, was enclathrated (as a dimethylammonium cation, (CH₃)₂NH₂⁺). The resulting multi-channelled structure (clathrate **6**, POB46) has a stoichiometry of 1(CMCR):4(SO₄²⁻):8((CH₃)₂NH₂⁺):1(DMF):4.23(H₂O).

The primary channel is formed parallel to the (011) plane by layers of CMCR in the boat conformation with opposite orientations (see Figures 9). This channel is 6.32 by 6.07 Å in size, allowing for two crystallographically distinct, fully ordered dimethylamine molecules to serve as guests. The assembly of CMCR into channels is mediated by four SO₄²⁻ anions (O...O distances of 2.64 to 2.72 Å), which also serve to stabilize the dimethylamine guests (O...N distances of 2.77 to 2.85 Å).

A secondary hydrogen bonded cluster is involved in the binding of adjacent channels formed by CMCR (see Figure 10). Again, this is mediated principally by the SO₄²⁻ anions, through a complex web of hydrogen bonds with six dimethylamine molecules (O...N distances of 2.70 to 2.89 Å) and three water molecules (O...O distances of 2.78 to 3.00 Å). Interestingly, a single molecule of DMF disordered over three positions (distribution is 51:28:20, with an amine N...O distance of 2.97 Å for the majority position) is also located in a secondary channel. This indicates that despite the



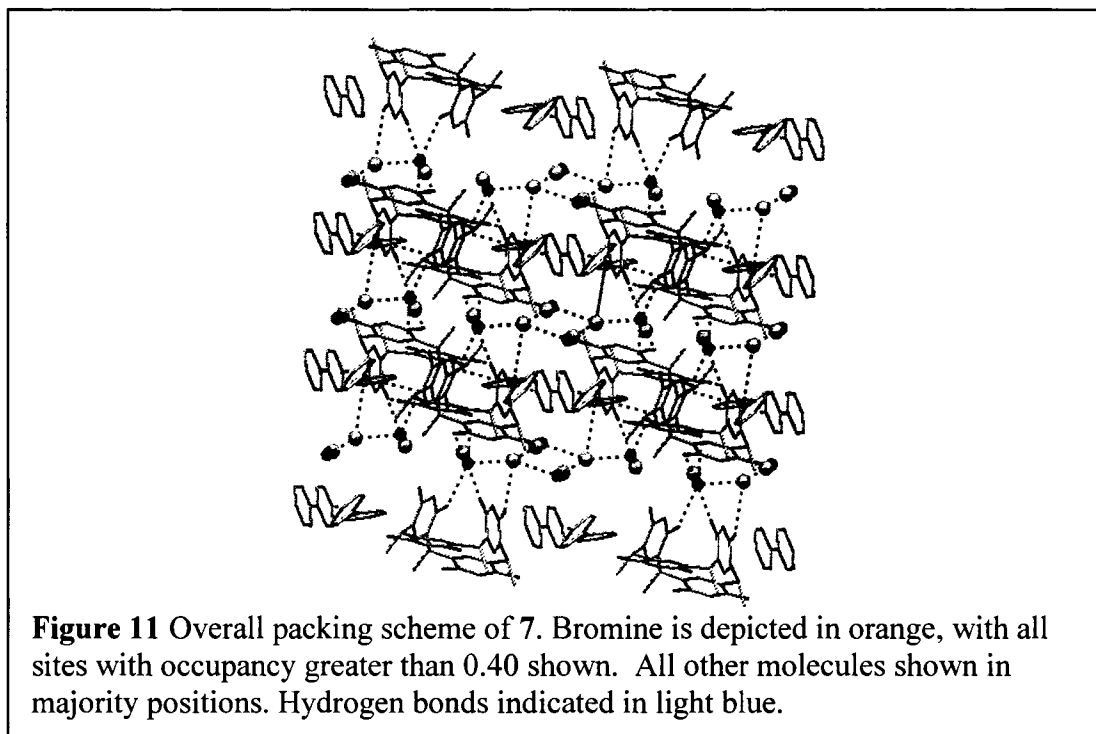
use of acid to catalyze the hydrolysis of the DMF, some remains available for inclusion in the framework. This suggests that manipulating the reaction conditions could allow for the isolation other pseudopolymorphic structures with higher DMF content.

As a result, the overall assembly is considerably more complex than might be anticipated from previous studies of ammonium ion inclusion in frameworks of CMCR.^[12, 17] Once again, in the case of small quaternary alkyl ammonium ions and small, spherical anions (such as Cl^- and Br^-), the most commonly observed inclusion scheme within CMCR is a dimeric capsule.^[8, 17] Despite the fact that dimethylamine is a similar size to such cations, the channelled inclusion motif arising from its inclusion is that of the larger quaternary ammonium cations and bipyridinium cations.^[12]

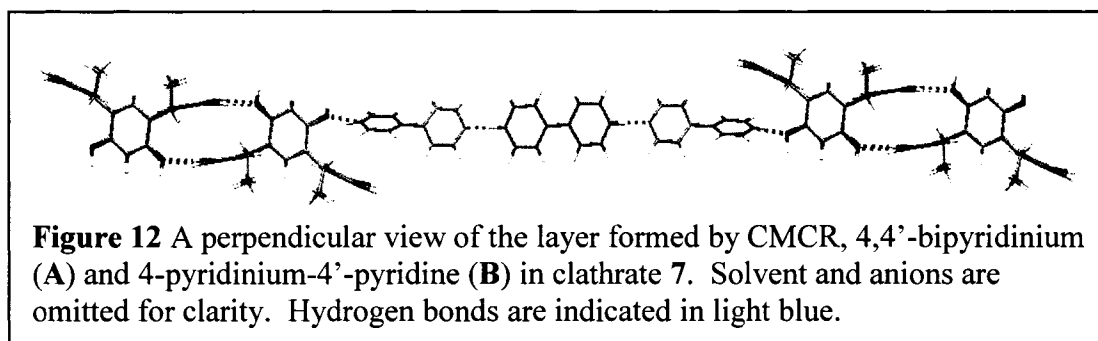
This suggests that, in this case, the anion dominates the self-assembly process, and, thus, the resulting structural motif. It is apparent that the size and geometry of the SO_4^{2-} anion make a capsular motif unfavourable. Instead, the strong hydrogen bonding between the SO_4^{2-} anions and the phenolic hydroxyls of CMCR give rise to the boat conformer. Further stabilization of the structure arises from the comparatively strong ionic interactions between the protonated amines and the SO_4^{2-} anions, which also leads to the cation- π interaction again being rendered largely irrelevant.

This structural insight, along with the role the solvent played in obtaining this structure, suggested that control of the crystallization conditions might also allow us to control the cation, and therefore the packing scheme of such anionic frameworks. In order to test this theory, a mixture of 4,4'-bipyridine and CMCR dissolved in an

EtOH/10% HBr solution was recrystallized by allowing isopropyl ether to diffuse into the aqueous solution, producing crystals of clathrate **7**. This structure consists of layers of CMCR assembled in a brick wall motif (see Figure 11), with two distinct molecules of 4,4'-bipyridine included.^[13]



The plane defined by these chains is nearly perpendicular to the (110) plane, with a dihedral angle between the planes of 70.19° . Only one molecule of 4,4'-bipyridine is fully protonated, with the second only protonated on the nitrogen interacting with the adjacent molecule of CMCR. The resulting 4,4'-bipyridinium (**A**) and 4-pyridinium-4'-pyridine (**B**) molecules form chains composed of two units of **A** and one unit of **B**, with an N...N distance of 2.62 \AA (see Figure 12). These chains, which are approximately 26 \AA in length, serve to link the brick wall sections of CMCR together (N...O distances of 2.92 and 2.95 \AA). The resulting framework has a stoichiometry of $2(\text{CMCR}):1(\text{A})^{2+}:2(\text{B})^+ :4(\text{Br}^-):5(\text{H}_2\text{O})$.



As with the previous structures studied, an intricate web of intramolecular hydrogen bonds and ionic interactions serves to bind adjacent layers of CMCR together (see Figure 11). These interactions are chiefly mediated by two crystallographically distinct bromide anions, one of which is fully ordered and the other of which is disordered over three sites (47:45:8 distribution). In addition to bonding directly to the phenolic hydroxyls of CMCR (Br...O distances of 3.19, 3.24, 3.36 Å), these anions also form an infinite network of hydrogen bonds (Br...O distances of 2.68 to 3.56 Å) with the two crystallographically distinct disordered molecules of water (40:30:30 and 27:26:26:21 distribution) present in the channels arising from the layers formed by the chains of CMCR, **A** and **B**.

This structural motif contrasts with the previous structures where 4,4'-bipyridine was fully protonated, serving as a non-interacting guest molecule within a channel. Instead, the structure is a hybrid of the anionic frameworks previously mentioned,^[12, 17] and the bipyridine frameworks studied extensively by Coppens *et al.*^[13] This is due to the presence of the partially protonated bipyridine molecule, which can serve as both a hydrogen bond donor and acceptor. Furthermore, as predicted previously, with the terminal bipyridinium moieties precluded from interacting directly with the anions in the structure, cation- π interactions instead serve to stabilize the cation (Aromatic

Centroid...N distance of 3.12 Å), causing the bipyridinium to align itself parallel to the opened CMCR molecule.

While this structural data can only provide limited information as to the process behind the formation of such a difunctional species, it is apparent that it arises as a consequence of the diffusion-based recrystallization using a non-polar solvent. One can safely assume that the resulting shift in the acid-base equilibrium clearly favours the production of **B**. At the same time, this process likely competes with the self-assembly of the overall structure. The resulting hybrid structure represents the balance of these competing forces, such that the packing scheme is an energetic compromise between efficient packing of CMCR and the cationic bipyridinium units to minimize their exposure to the non-polar environment. The *in situ* formation of **B** is therefore the key to controlling the motif in this system.

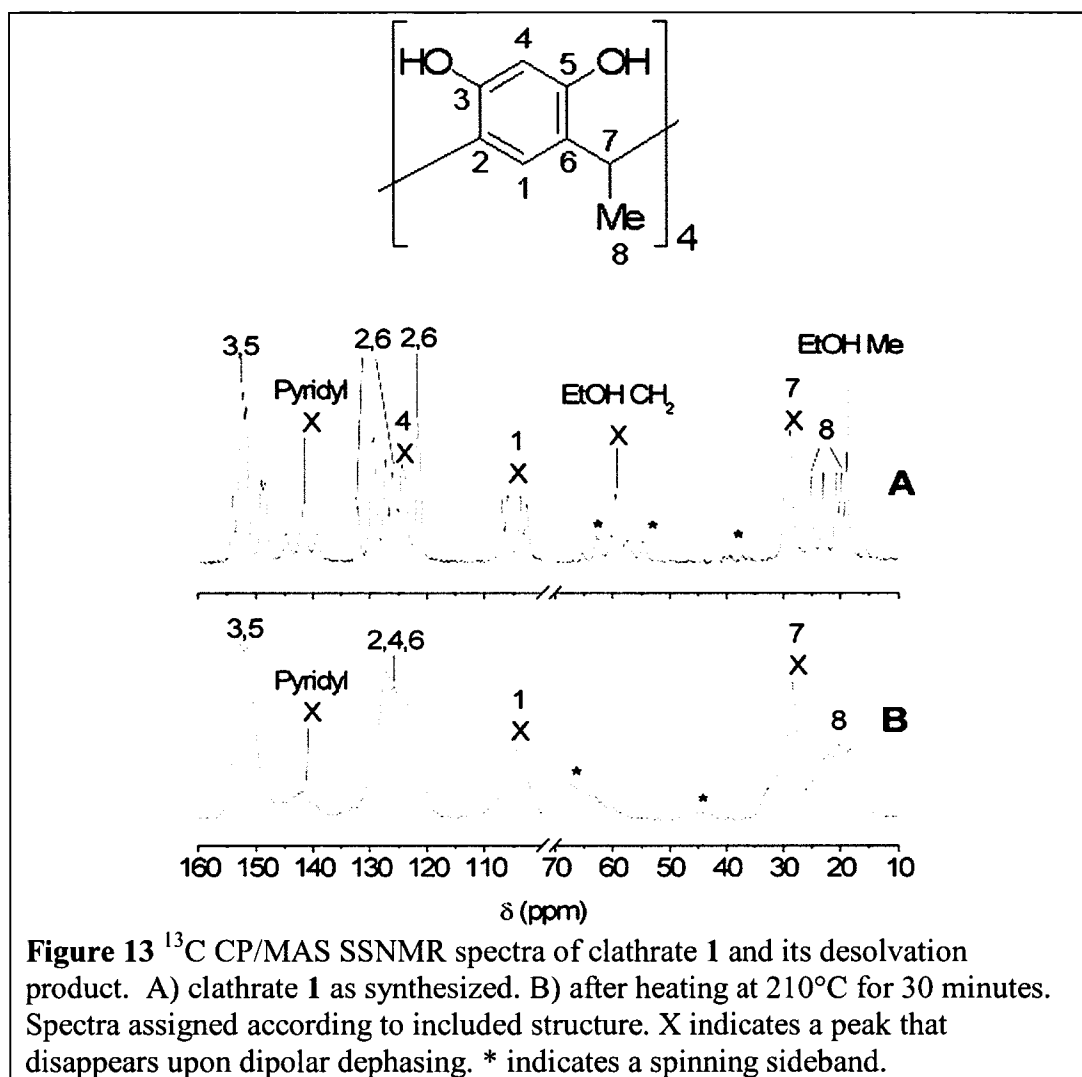
Thermal Stability of Inorganic Anion/CMCR Frameworks

Given the importance of solvent conditions in further tuning the alignment and generation of the ions dominating these structures, the complex array of forces involved in guiding the formation of these structures is quite delicately balanced. Much like the pseudopolymorphism observed in the 4tBC4A amine systems arising from disruption of the hydrogen bonding scheme (see Chapters III to VI), the studies of Coppens *et al.*^[13, 15, 16] also demonstrate how temperature can be used to guide the weak interactions determining the structural motifs in CMCR frameworks. In these cases, using hydrothermal syntheses results in subtle shifts in the favoured hydrogen bonding pattern

such that the CMCR assumes various conformations to accommodate the strongest intermolecular interactions available under such conditions.

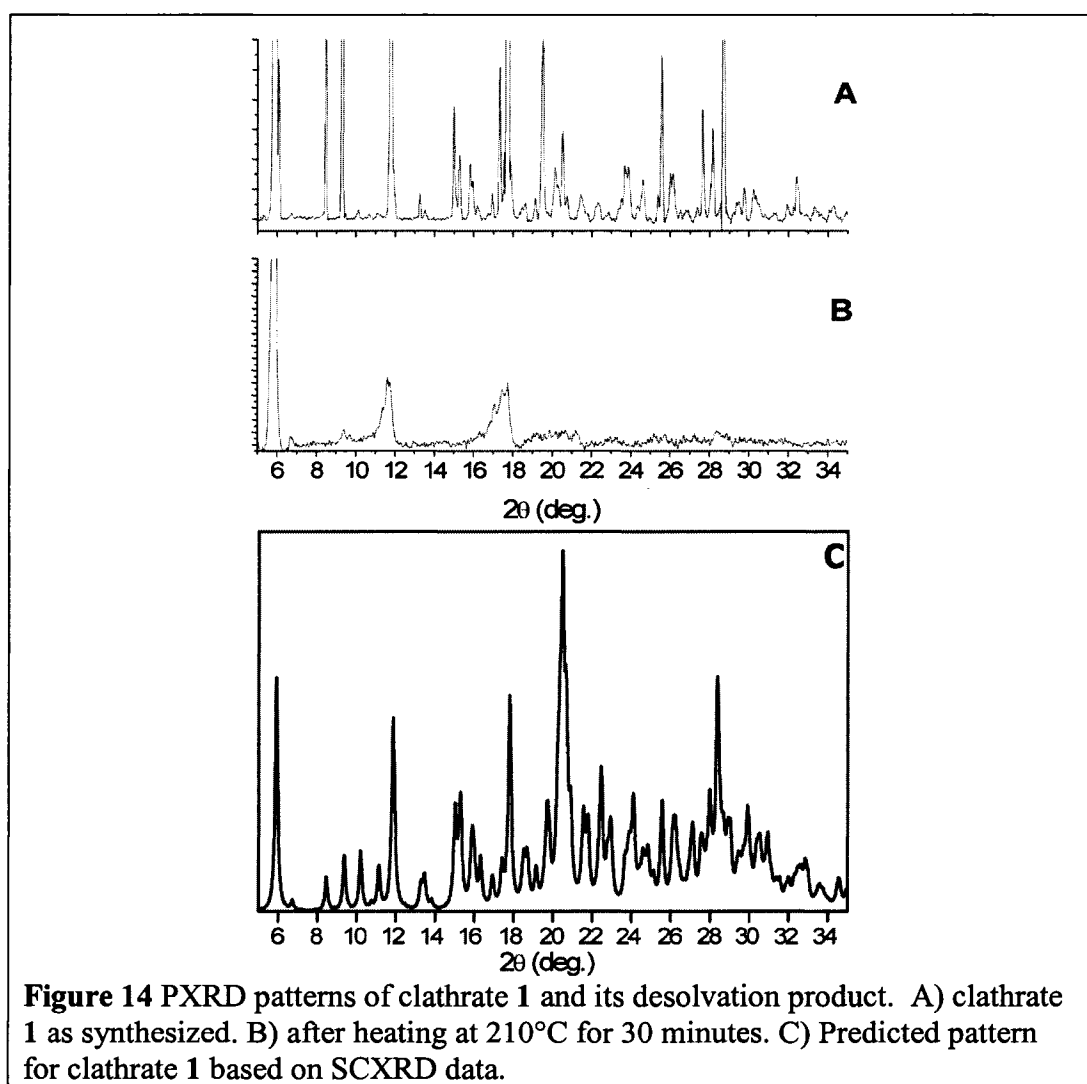
In the case of the ionic frameworks, however, the degree of dependence on solvent in these structures make rational rearrangements such as these unlikely.^[17] In order to test this supposition, the change in structure clathrate **1** upon complete removal of solvent was investigated. Thermogravimetric analysis indicated that all solvent had been removed upon heating to 210°C, the majority of which was lost in a single major transition with an onset temperature of 60°C. As the complex nature of the clathrate precluded specific identification of the solvent molecules removed at any given temperature, the study was limited to a preliminary comparison of the fully solvated and completely desolvated frameworks.

A comparison of the ¹³C CP/MAS solid-state NMR spectra of clathrate **1** as synthesized and after heating to 210°C is shown in Figure 13. The spectrum of clathrate **1** clearly corresponds well with the SCXRD structure, although the overlap of a number of the resonances prevents a thorough analysis of the peak splitting. However, the four fold splitting of both the aliphatic methyl resonance due to carbon 8, and the aromatic resonance due to carbon 1 clearly indicate the presence of the single CMCR molecule in the asymmetric unit. Furthermore, the splitting of carbon 1 into a shielded pair and deshielded pair of resonances corresponds well to the shift in shielding environment due to the conformational shift observed for the resorcinarene. As expected, dipolar dephasing indicates no dynamic motion in any portion of the carbon framework.



Upon heating to 200°C, the spectrum undergoes considerable simplification, with the majority of the resonances exhibiting extreme broadening. This clearly indicates that while the material remains crystalline, the removal of the solvent causes a massive disruption in the structural motif observed. A comparison of the PXRD data obtained for the two compounds confirms this analysis (see Figure 14), with the diffraction pattern for the heated product providing little information regarding the structure of the compound. While a significant orientation effect is observed in the PXRD of clathrate **1**, with the

intensities of many peaks showing significant differences from the predicted pattern, this is readily attributed to the plate-like morphology of the crystals, which is ultimately a result of the channelled packing scheme. Even so, visual comparisons of the patterns indicate the structure is highly dependent on the presence of the solvent, to the point that its removal results in a collapse of the crystalline structure.



5. Conclusions

In conclusion, it has been demonstrated that under acidic conditions, protonation of bipyridyl-type molecules forces the adoption of alternative packing schemes for

CMCR frameworks. The resulting structures incorporating the open boat conformation of CMCR also differ from the “brick wall” motifs most commonly observed with 4,4'-bipyridine at neutral pH, yielding a much more compact packing scheme. These packing schemes are dominated by the ionic interactions between cations and anions in the framework, but can be tuned through choice of solvent conditions and the geometry of the bispyridyl containing moiety.

It is quite clear that the balance of intermolecular forces in these systems is quite delicate. In the case of SO_4^{2-} , the highly directional nature of the anion is the key factor in determining the overall inclusion scheme, such that less bulky guest cations are required. On the other hand, the smaller, spherical anions such as Cl^- and Br^- are essentially interchangeable, such that it is possible to make use of multifunctional guests such as 1,3-BPTU to establish a common inclusion motif. Furthermore, when one of several factors preclude the bipyridinium moiety from directly interacting with the anions in the structure (such as the bulk of the bipyridinium guest, or the inclusion of additional, preferred binding sites for the anion), cation- π interactions analogous to those seen in capsular complexes of organic cations^[7, 25-27] also begin to play a role in directing the conformation of the cation. All the frameworks are heavily dependent on hydrogen bonding solvent molecules to completely stabilize the frameworks, rendering the frameworks unable to survive desolvation.

As with 4tBC4A,^[35, 36] acid base chemistry provides a route to altering the symmetry of the host calixarene, and thereby control the inclusion motif. In this case, both the cation and anion are guests, but the competition between forces is quite similar

in driving the conformational shift of CMCR. Given the ease in varying the anion, cation and solvent used for crystallization of such systems, such syntheses are a promising avenue for producing ionic frameworks for further study to clarify the dominance of the forces involved in the self-assembly of such structures. Further studies will hopefully focus on the competition between the formation of cations and inclusion of the anions, as well as fully explore how selection of solvent might be used to control such interactions.

6. References

- [1] C. D. Gutsche, *Calixarenes*, Royal Society of Chemistry, Cambridge, **1989**.
- [2] L. Mandolini, R. Ungaro, *Calixarenes in Action*, Imperial College Press, London, **2000**.
- [3] C. D. Gutsche, *Calixarenes Revisited*, Royal Society of Chemistry, Cambridge, **1998**.
- [4] L. R. MacGillivray, J. L. Atwood, *J. Am. Chem. Soc.* **1997**, *119*, 6931.
- [5] L. R. MacGillivray, J. L. Atwood, *Nature* **1997**, *389*, 469.
- [6] W. Iwanek, R. Frohlich, M. Urbaniak, C. Nather, J. Mattay, *Tetrahedron* **1998**, *54*, 14031.
- [7] A. Shivanyuk, J. Rebek, *J. Am. Chem. Soc.* **2003**, *125*, 3432.
- [8] H. Mansikkamaki, M. Nissinen, C. A. Schalley, K. Rissanen, *New J. Chem.* **2003**, *27*, 88.
- [9] I. Georgiev, E. Bosch, *Cryst. Growth Des.* **2004**, *4*, 235.
- [10] C. L. Barnes, E. Bosch, *Cryst. Growth Des.* **2005**, *5*, 1049.
- [11] Y. G. Zhang, C. D. Kim, P. Coppens, *Chem. Commun.* **2000**, 2299.
- [12] A. Shivanyuk, E. F. Paulus, K. Rissanen, E. Kolehmainen, V. Bohmer, *Chem. Eur. J.* **2001**, *7*, 1944.
- [13] B. Q. Ma, Y. Zhang, P. Coppens, *Cryst. Growth Des.* **2002**, *2*, 7.
- [14] M. Nissinen, K. Rissanen, *Supramol. Chem.* **2003**, *15*, 581.
- [15] B. Q. Ma, L. F. V. Ferreira, P. Coppens, *Org. Lett.* **2004**, *6*, 1087.
- [16] B. D. Ma, P. Coppens, *Cryst. Growth Des.* **2004**, *4*, 1377.
- [17] H. Mansikkamaki, M. Nissinen, K. Rissanen, *CrystEngComm* **2005**, *7*, 519.
- [18] L. R. MacGillivray, P. R. Diamente, J. L. Reid, J. A. Ripmeester, *Chem. Commun.* **2000**, 359.
- [19] L. R. MacGillivray, H. A. Spinney, J. L. Reid, J. A. Ripmeester, *Chem. Commun.* **2000**, 517.
- [20] P. Timmerman, W. Verboom, D. N. Reinhoudt, *Tetrahedron* **1996**, *52*, 2663.

- [21] M. Munakata, L. P. Wu, T. Kuroda-Sowa, M. Maekawa, Y. Suenaga, K. Sugimoto, I. Ino, *J. Chem. Soc. Dalton Trans.* **1999**, 373.
- [22] L. R. MacGillivray, J. L. Atwood, *Supramol. Chem.* **2000**, *11*, 293.
- [23] L. R. MacGillivray, J. L. Reid, J. A. Ripmeester, *Chem. Commun.* **2001**, 1034.
- [24] L. Avram, Y. Cohen, *J. Am. Chem. Soc.* **2004**, *126*, 11556.
- [25] A. Shivanyuk, J. C. Friese, S. Doring, J. Rebek, *J. Org. Chem.* **2003**, *68*, 6489.
- [26] A. Shivanyuk, J. Rebek, *Proc. Natl. Acad. Sci. U. S. A.* **2001**, *98*, 7662.
- [27] A. Shivanyuk, K. Rissanen, E. Kolehmainen, *Chem. Commun.* **2000**, 1107.
- [28] H. Mansikkamaki, C. A. Schalley, M. Nissinen, K. Rissanen, *New J. Chem.* **2005**, *29*, 116.
- [29] K. Murayama, K. Aoki, *Chem. Commun.* **1997**, 119.
- [30] G. R. Lewis, A. G. Orpen, *Chem. Commun.* **1998**, 1873.
- [31] A. L. Gillon, G. R. Lewis, A. G. Orpen, S. Rotter, J. Starbuck, X. M. Wang, Y. Rodriguez-Martin, C. Ruiz-Perez, *J. Chem. Soc. Dalton Trans.* **2000**, 3897.
- [32] B. Dolling, A. L. Gillon, A. G. Orpen, J. Starbuck, X. M. Wang, *Chem. Commun.* **2001**, 567.
- [33] A. G. S. Hogberg, *J. Am. Chem. Soc.* **1980**, *102*, 6046.
- [34] A. Albert, R. Goldacre, J. Phillips, *J. Chem. Soc.* **1948**, 2240.
- [35] E. B. Brouwer, K. A. Udachin, G. D. Enright, J. A. Ripmeester, *Chem. Commun.* **2000**, 1905.
- [36] P. O. Brown, K. A. Udachin, G. D. Enright, J. A. Ripmeester, *Chem. Eur. J.* **2006**, DOI: 10.1002/chem.200600434.
- [37] I. D. Cunningham, M. Woolfall, *J. Org. Chem.* **2005**, *70*, 9248.
- [38] A. F. D. de Namor, R. M. Cleverley, M. L. Zapata-Ormachea, *Chem. Rev.* **1998**, *98*, 2495.
- [39] H.-J. Schneider, D. Guttes, U. Schneider, *Angew. Chem. Int. Ed. Engl.* **1986**, *25*, 647.
- [40] H.-J. Schneider, D. Guttes, U. Schneider, *J. Am. Chem. Soc.* **1988**, *110*, 6449.
- [41] B. Q. Ma, Y. G. Zhang, P. Coppens, *CrystEngComm* **2001**, art. no. 20.
- [42] G. M. Kyne, M. E. Light, M. B. Hursthouse, J. de Mendoza, J. D. Kilburn, *J. Chem. Soc. Perkin Trans. 1* **2001**, 1258.
- [43] G. M. Kyne, M. E. Light, M. B. Hursthouse, J. de Mendoza, J. D. Kilburn, *J. Chem. Soc., Perkin Trans. 1* **2001**, 1258.
- [44] P. W. Manley, U. Quast, *J. Med. Chem.* **1992**, *35*, 2327.
- [45] T. K. Venkatachalam, S. Qazi, P. Samuel, F. M. Uckun, *Bioorg. Med. Chem.* **2003**, *11*, 1095.
- [46] O. Vajragupta, A. Pathomsakul, C. Matayatsuk, L. Ruangreangyingyod, Y. Wongkrajang, W. O. Foye, *J. Pharm. Sci.* **1996**, *85*, 258.
- [47] N. C. Singha, D. N. Sathyanarayana, *J. Chem. Soc. Perkin Trans. 2* **1997**, 157.
- [48] H. K. Hall, Jr., *J. Am. Chem. Soc.* **1957**, *79*, 5441.

Chapter VIII: Host-Guest Chemistry of *C*-methylpyrogall[4]arene[†]

1. Abstract.....	328
2. Introduction.....	329
3. Experimental Section.....	330
4. Results and Discussion.....	335
Isolation of the <i>apo rctt</i> PGR by Molecular Recognition.....	335
Isolation of bulk <i>apo rctt</i> PGR.....	339
Inclusion of Viologens in Anionic Frameworks of <i>rctt</i> PGR.....	342
5. Conclusions.....	347
6. References:.....	349

1. Abstract

Both single crystals and bulk powder of the *apo* form of the *rctt* isomer of *C*-methylpyrogall[4]arene (PGR) can be obtained, the former by molecular recognition in solution, the latter by desolvation of a clathrate. Preliminary investigations into the inclusion chemistry of the *rctt* form indicate that, like *c*-methylcalix[4]resorcinarene (CMCR), PGR readily forms anionic frameworks. However, with the shift in molecular symmetry, a different set of structural motifs is favoured in such compounds. The resulting structures tend towards formation of channels without any conformational changes, but can still be mediated by judicious choice of anion and cation. In such structures, bipyridinium-type cations incapable of engaging in hydrogen bonding, such as viologens, can be included, such that the cation is reduced to serving as a space filling guest suitable for establishing charge balance.

[†] Portions of this chapter have been previously published: P. O. Brown, G. D. Enright, J. A. Ripmeester, *CrystEngComm* **2006**, *8*, 381.

2. Introduction

As mentioned previously, the OH groups found on the upper rim of the *rccc* isomers of resorcinarenes are natural sites for guiding the formation of various extended structures through directional interactions.^[1-4] These structures can be quite complex, as exemplified by the well known snub-cube capsule formed by *c*-methylcalix[4]resorcinarene (CMCR) in the solid state,^[5] simpler dimeric capsules observed in both solution^[6-10] and the solid state^[11], and the numerous channelled supramolecular assemblies based on resorcinarene and bipyridines under neutral^[1, 4, 12-19] and acidic^[3] pH conditions. Most recently, a number of studies have appeared detailing the self-assembled structures arising from pyrogallarenes, as the addition of another OH group provides additional opportunities for intermolecular bonding.

Such a subtle shift in the structure of the host has proven to give rise to rather dramatic differences in the self-assembly behaviour of pyrogallarenes. Particular attention has been paid to the formation of large hexameric capsules in the solids state by pyrogallarenes bearing long alkyl chain substituents. While similar to the snub-cube formed by resorcinarenes, these structures can be formed through direct hydrogen bonding between the pyrogallarenes,^[20-22] or mediated by metal ions.^[23, 24] Once again, this research has focused on the *rccc* isomers of pyrogallarenes.

Very little research had been conducted on the inclusion properties of the direct analogue of CMCR, *C*-methylpyrogall[4]arene (PGR), beyond initial reports of simple inclusions of solvent.^[25] Given the tunable frameworks formed by CMCR and organic cations (see Chapter VII), and 4tBC4A and amines, the question was raised as to whether

any significant differences would be observed in anionic frameworks of PGR. In fact, the differences in inclusion properties between two isomers of PGR are such that they allow for isolation of the guest free form of the *rctt* isomer. This isomer inherently lacks the four fold symmetry of the common *rccc* pyrogallarenes, making it eminently suited for the formation of extended frameworks with complex hydrogen bonded structures. While no channelled clathrates including the smaller bipyridinium guests examined in Chapter VII were isolated, anionic frameworks based on this isomer do readily include viologens, resulting in a new series of channelled structures.

3. Experimental Section

General Note: Unless otherwise indicated, chemicals were obtained from EMD Chemicals and Sigma-Aldrich, and were used without further purification.

Synthesis of *C*-methylpyrogall[4]arene (PGR): Synthesis of the host was carried out based on literature procedures.^[25] In a typical synthesis, 20.304 g (0.16100 mol) of pyrogallol was placed in a three necked round bottom flask and dissolved in a solution of 35.0 mL H₂O, 35.0 mL EtOH and 8.0 mL concentrated hydrochloric acid. The flask was fitted with a condenser, placed under an N₂ purge and cooled to 0°C with an ice bath. Over the course of approximately 25 minutes, 9.0 mL (0.16 mol) of acetaldehyde was added using a dropping funnel. The resulting mixture was then heated at 100°C for approximately 1 day, at which point an off-white precipitate was observed to have formed. This precipitate was filtered off by vacuum and washed with chilled water. After air-drying overnight, 12.685 g (0.02084 mol, 52% yield) of crude PGR was isolated. Recrystallization of 2.637 g (4.33×10^{-3} mol) of the crude from DMF/Acetone

yielded 1.612 g of the DMF clathrate (clathrate **3**) of the *rctt* isomer of PGR (1.54 mol, 35% yield), giving a net yield of 18.5%. ^1H NMR (DMSO- d_6 , 400.130 MHz) δ 1.18 (d, $J=7.03$ Hz, 12H, CHCH_3), 2.73 (s, 18H, DMF- CH_3), 2.89 (s, 18H, DMF- CH_3), 3.35 (Water), 4.48 (q, $J=7.03$ Hz, 4H, CHCH_3), 5.76 (s, 2H, ArH equatorial), 6.42 (s, 2H, ArH axial), 7.39&7.76-7.91 (m, 12H, Ar OH), 7.96 (s, DMF-CHO). ^{13}C NMR (DMSO- d_6 , 100.613 MHz) δ 21.75, 31.11, 31.63, 36.64, 115.97, 117.12, 122.99, 126.33, 132.85, 141.81, 142.58, 163.17. ESI-MS (ES^+ , m/z , $\text{C}_{32}\text{H}_{32}\text{O}_{12}\text{H}^+$) 609.4.

Synthesis of 1(1,3-bis(3-pyridylmethyl)-2-thiourea)*1(SO_4^{2-})*1(H_2O)*2(*C*-methylpyrogall[4]arene) clathrate (clathrate **1**, POB57) and isolation of the *apo* form of *rctt* isomer of PGR (compound **2**, POB58): 0.202 g (3.32×10^{-4} mol) of crude PGR was added to a 70°C solution of 25.0 mL EtOH, 5.0 mL 10% w/w H_2SO_4 and 5 mL Acetone. 0.170 g (6.58×10^{-4} mol) of 1,3-bis(3-pyridylmethyl)-2-thiourea was then added to the solution, and the resulting yellow solution heated for a further 30 minutes to facilitate complete dissolution of the solids. The solution was then filtered and set aside to allow excess solvent to evaporate off. After approximately two weeks, clear needle-like crystals and orange plate like crystals were observed to have formed.

Synthesis of 1(methyl viologen)*2(Cl^-)*1.5(EtOH)*2.69(H_2O)*1(*C*-methylpyrogall[4]arene) clathrate (clathrate **4**, POB52) and 1(ethyl viologen)*2(Br^-)*1(MeCN)*2(H_2O)*1(*C*-methylpyrogall[4]arene) clathrate (clathrate **5**, POB56): Both clathrates were prepared using the same procedure. In a sample synthesis, 0.115 g (1.90×10^{-4} mol) of crude PGR was dissolved in a 70°C solution of 30.0 mL EtOH and 10.0 mL 10% w/w HCl. 0.097 g (3.77×10^{-4} mol) of methyl viologen dichloride was then

added to this solution, causing it to turn deep red. The solution was heated for a further 30 minutes to ensure complete dissolution of the solids. The solution was then set aside to allow excess solvent to evaporate off. After approximately one week, orange block-like crystals were observed to have formed.

Single Crystal X-Ray Diffraction data are summarized in Table 1. For compounds **1**, **2** and **5**, all hydrogens were found from the difference electron density map, except for those found on the disordered portion of the 1,3-BPTU in **1** (which were placed in calculated positions and refined as riding atoms). For compound **4**, all hydrogens were placed in calculated positions and refined as riding atoms.

Thermogravimetric analysis was carried out as described in Chapter III on pages 72-73. ^{13}C CP/MAS spectra for clathrate **1** were collected using the Bruker AMX-300 spectrometer. Powder X-ray Diffraction (PXRD) data were collected on the Scintag X-2 Advanced diffractometer.

Table 1a SXCRD Data for Clathrate 1, Compound 2 and Clathrate 4.

Identification code	Clathrate 1 (POB57)	Compound 2 (POB58)	Clathrate 4 (POB52)
Empirical formula	C ₇₇ H ₈₂ N ₄ O ₂₉ S ₂	C ₁₆ H ₁₆ O ₆	C ₄₇ H ₅₆ C _{12.01} N ₂ O _{16.19}
Formula weight	1591.59	304.29	979.22
Temperature	173(2) K	173(2) K	173(2) K
Wavelength	0.71073 Å	0.71073 Å	0.71073 Å
Crystal system	Triclinic	Triclinic	Monoclinic
Space group	<i>P</i> -1	<i>P</i> -1	<i>P</i> 2/ <i>c</i>
Unit cell dimensions	<i>a</i> = 9.5012(6) Å <i>b</i> = 18.1017(12) Å <i>c</i> = 21.8277(14) Å α = 70.056(1)° β = 82.320(1)° γ = 83.134(1)°	<i>a</i> = 8.8592(17) Å <i>b</i> = 9.3271(18) Å <i>c</i> = 9.4416(18) Å α = 106.968(4)° β = 104.650(4)° γ = 104.616(4)°	<i>a</i> = 19.1493(10) Å <i>b</i> = 12.4273(6) Å <i>c</i> = 19.3936(10) Å α = 90° β = 91.582(1)° γ = 90°
Volume	3486.3(4) Å ³	675.6(2) Å ³	4613.4(4) Å ³
Z	2	2	4
ρ_{calc}	1.516 Mg/m ³	1.496 Mg/m ³	1.410 Mg/m ³
Abs. coefficient	0.173 mm ⁻¹	0.115 mm ⁻¹	0.217 mm ⁻¹
F(000)	1672	320	2063
Crystal size	0.48 x 0.20 x 0.16 mm ³	0.20 x 0.18 x 0.08 mm ³	0.48 x 0.16 x 0.10 mm ³
θ Range	1.20 to 29.64°.	2.41 to 29.59°.	1.64 to 29.60°.
Index ranges	-13 ≤ <i>h</i> ≤ 13 -25 ≤ <i>k</i> ≤ 25 -30 ≤ <i>l</i> ≤ 30	-12 ≤ <i>h</i> ≤ 12 -12 ≤ <i>k</i> ≤ 12 -13 ≤ <i>l</i> ≤ 13	-26 ≤ <i>h</i> ≤ 26 -17 ≤ <i>k</i> ≤ 17 -26 ≤ <i>l</i> ≤ 26
Reflections collected	44480	7490	57484
Ind. reflections	19416 [R(int) = 0.0542]	3722 [R(int) = 0.0234]	12929 [R(int) = 0.0325]
Completeness to θ = max	98.6 %	98.1 %	99.6 %
Absorption correction	Multi-scan	Multi-scan	Multi-scan
Refinement method	Full-matrix least-squares on F ²	Full-matrix least-squares on F ²	Full-matrix least-squares on F ²
Data / restraints / parameters	19416 / 42 / 1376	3722 / 15 / 273	12929 / 2 / 649
Goodness-of-fit on F ²	0.887	0.996	1.029
Final R indices [I > 2σ(I)]	R1 = 0.0508 wR2 = 0.0866	R1 = 0.0465 wR2 = 0.1174	R1 = 0.0469 wR2 = 0.1268
R indices (all data)	R1 = 0.1249 wR2 = 0.1039	R1 = 0.0706 wR2 = 0.1286	R1 = 0.0707 wR2 = 0.1407
Largest diff. peak and hole (e.Å ⁻³)	0.288 and -0.344	0.401 and -0.219	0.568 and -0.530

Table 1b SCXRD data for Clathrate **5**.

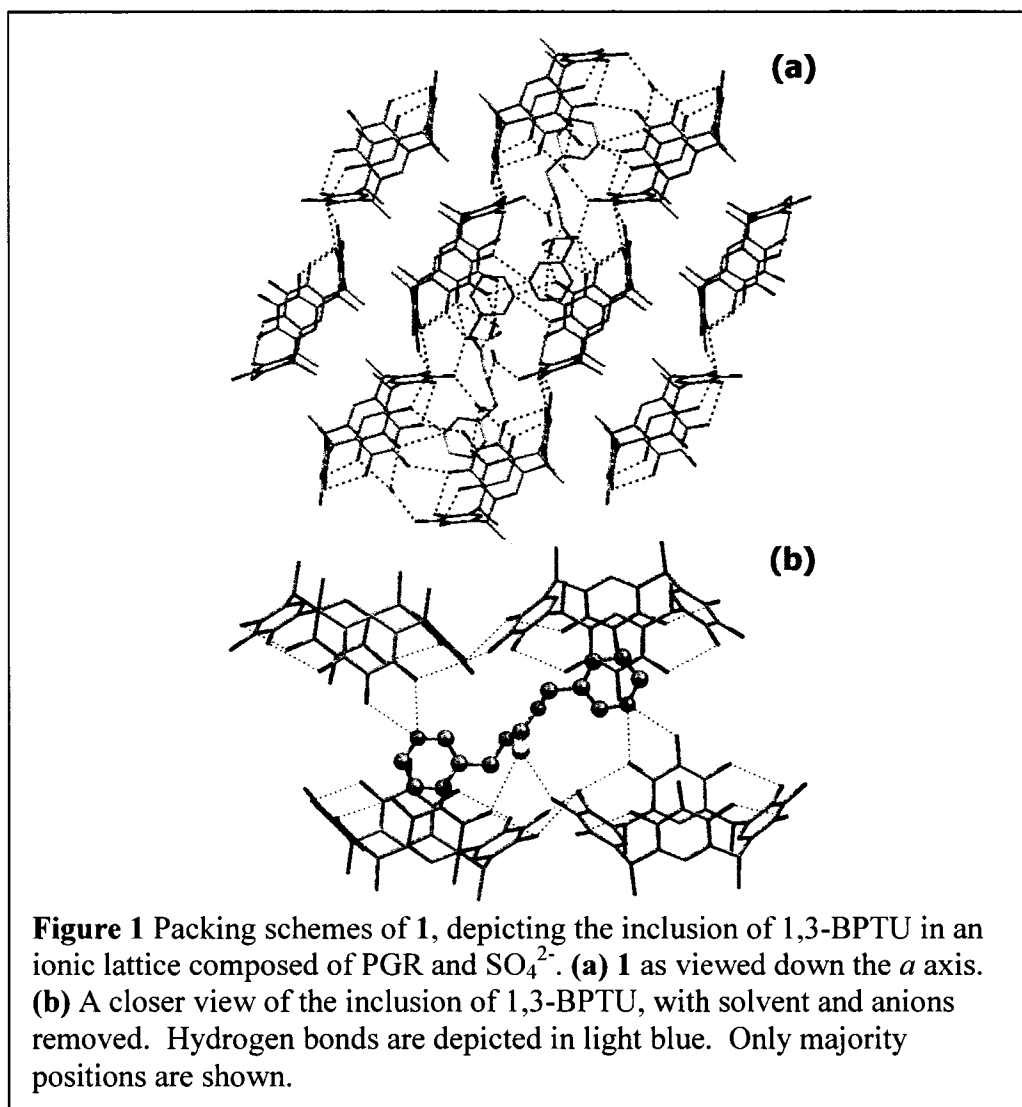
Identification code	Clathrate 5 (POB56)
Empirical formula	C ₄₈ H ₅₇ Br ₂ N ₃ O ₁₄
Formula weight	1059.79
Temperature	173(2) K
Wavelength	0.71073 Å
Crystal system	Triclinic
Space group	<i>P</i> -1
Unit cell dimensions	<i>a</i> = 12.6849(5) Å <i>b</i> = 12.7803(5) Å <i>c</i> = 17.5141(8) Å α = 76.477(1)° β = 74.678(1)° γ = 61.916(1)°
Volume	2395.92(17) Å ³
Z	2
ρ_{calc}	1.469 Mg/m ³
Abs. coefficient	1.761 mm ⁻¹
F(000)	1096
Crystal size	0.32 x 0.32 x 0.16 mm ³
θ Range	1.22 to 29.59°.
Index ranges	-17 ≤ <i>h</i> ≤ 17 -17 ≤ <i>k</i> ≤ 17 -24 ≤ <i>l</i> ≤ 24
Reflections collected	30439
Ind. reflections	13282 [R(int) = 0.0203]
Completeness to $\theta = \text{max}$	98.7 %
Absorption correction	Multi-scan
Refinement method	Full-matrix least-squares on F ²
Data / restraints / parameters	13282 / 0 / 675
Goodness-of-fit on F ²	0.966
Final R indices [I > 2σ(I)]	R1 = 0.0293 wR2 = 0.0729
R indices (all data)	R1 = 0.0421 wR2 = 0.0768
Largest diff. peak and hole (e.Å ⁻³)	0.837 and -0.313

4. Results and Discussion

Isolation of the *apo rectt* PGR by Molecular Recognition

As the existence of both isomers in the crude product was suspected, an investigation as to whether the capabilities of *rccc* and *rectt* isomers were different in respect to the formation of anionic frameworks was carried out. Recrystallization of the crude condensation product along with 1,3-bis(3-pyridylmethyl)-(2-thiourea) (1,3-BPTU) from EtOH/Acetone/10% H₂SO₄ gave rise to two morphologically distinct crystals: clear needles and orange plates. Single crystal diffraction revealed that the PGR frameworks of the two crystals do, in fact, derive from the two different isomers, and can be discriminated by their abilities to serve as hosts to the bispyridyl thiourea guest.

The clear needles were shown to be a layered supramolecular framework consisting of the *rccc* isomer of PGR with 1,3-BPTU as a guest (clathrate **1**, see Figure 1). As with the ionic frameworks formed by CMCR (see Chapter VII),^[3, 26] an SO₄²⁻ anion serves as a linker in the structure, interacting with the nitrogens of the thiourea group (O...N distances of 2.93 and 2.99 Å), as well as adjacent pyrogallarenes (O...O distances of 2.58 to 3.01 Å) and a single molecule of water. However, in contrast with the structures of CMCR and 1,3-BPTU previously examined, the SO₄²⁻ is disordered over two positions (0.71:0.29 occupancy ratio). In order to accommodate this, one of the urea linkers to the pyridyl rings in the 1,3-BPTU is also disordered (0.53:0.47 occupancy ratio).

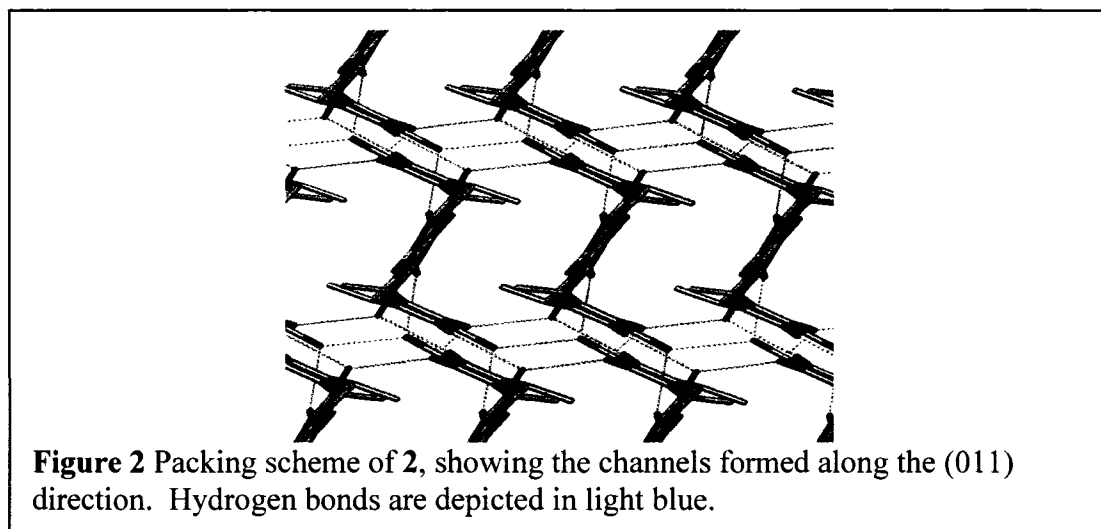


With the pyridyl nitrogen in the 3 position, the guest is stabilized by van der Waals interactions with the calix cavity, while still serving as a base capable of hydrogen bonding with adjacent PGR units (N...O distances of 2.78, 2.80, 2.87 and 3.00 Å). The guest is also further stabilized through weak hydrogen bonds involving the sulphur in the thiourea functionality and adjacent PGR molecules (S...O distances of 3.24 and 3.31 Å). While the staggered conformation of the guest causing the host molecules to arrange themselves in diagonal chains, as observed with CMCR (see Chapter VII),^[26] the host

remains in the crown conformation. Thus, the presence of an additional OH beyond that in CMCR allows for the hydrogen bonding motif giving rise to the crown conformer to be retained, since additional hydrogen bonding moieties are now available to engage in the energetically favourable interactions arising from the inclusion of ionic species.

This situation is clearly analogous to the differences in capsule formation ability of CMCR and PGR,^[20-22] where the additional OH groups allowed for the formation of additional strong intermolecular hydrogen bonds as well as the intramolecular hydrogen bonds responsible for guiding the conformation of the host. Furthermore, such interactions are apparently more favourable than cation- π interactions similar to those seen in Chapter VII, which, unlike the cations which can be included in small capsules,^[9-11, 27, 28] would also require the disruption of the intramolecular hydrogen bonding array at the top of PGR. Such a situation would also explain the difficulty in isolating any other channeled clathrates including the bipyridinium moieties examined in Chapter VII using this synthetic methodology.

Surprisingly, the orange plates are the *rctt* form of PGR without any guest incorporated (compound **2**, see Figure 2). At the time of writing, this is the first reported *apo* form of a resorcinarene-type host. Interactions between the phenolic hydroxyls gives rise to an elaborate hydrogen bonding scheme (O...O distances ranging from 2.74 to 2.82 Å). In order to satisfy this scheme, hydrogens on three of the six crystallographically unique phenol groups exhibit 50:50 disorder over two positions. As expected from the geometry of the host, **2** assumes a stepped packing motif, producing a three dimensional hydrogen bonded lattice. A series of primary channels are found parallel to the (011)



plane, and are occupied by the methyl groups of the PGR molecules. Secondary channels are found parallel to the (100) plane, and are again obstructed by self-inclusion. In both cases, the channels are approximately 4.5 Å at their widest points, with the secondary channels tilting as a result of the staggering of the hosts.

The *rccc* isomers of resorcinarenes are by far the most commonly seen in the literature, as they are the thermodynamically favoured form generally obtained from the acid-catalyzed condensation reaction typically used to produce these compounds.^[29] However, under appropriate conditions, alternative isomers can be obtained. In the case of PGR, which lacks long alkyl chains to enhance its solubility in aqueous media, the kinetically favoured *rctt* isomer precipitates prior to conversion to the *rccc* form.^[25] Manipulation of the acid-base equilibrium allows for both forms to be dissolved, such that the two compounds crystallize as dictated by their potential for interaction with the components present in the solution. Under such conditions, the crystallization is at least partially reflective of the proportions of the isomers present in the materials as synthesized, since no interconversion is possible under such conditions.^[25, 29] This

molecular recognition phenomenon could therefore be used in future studies of such compounds to evaluate the relative importance of given intermolecular interactions in stabilizing the structural motifs favoured by each isomer.

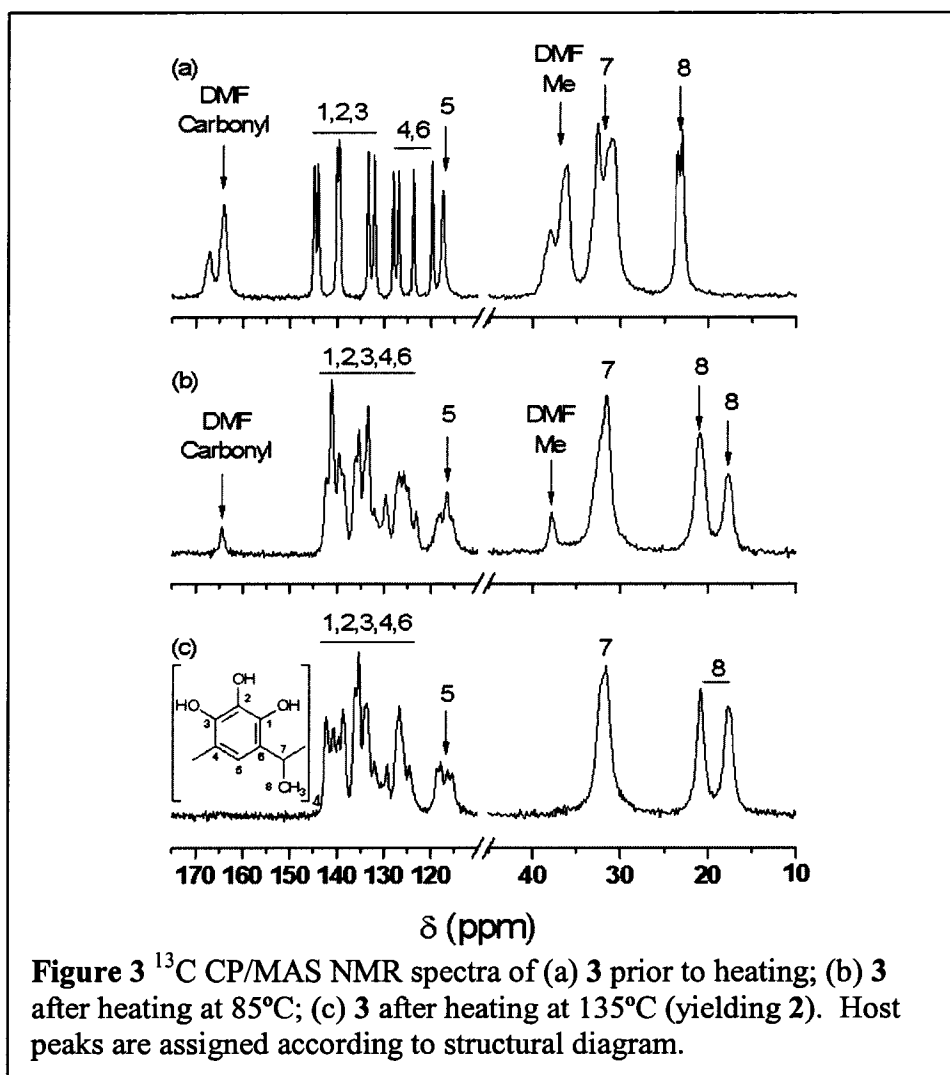
Isolation of bulk *apo rctt* PGR

Given that the structure of an *apo* form can be used as a basis for studies of polymorphism and pseudopolymorphism, interest shifted to finding a route to obtaining this isomer in bulk form. Mattay *et al.* had previously reported the isolation of a 6:1 guest - host DMF clathrate of *rctt* PGR (clathrate **3**).^[25] The single crystal structure they reported is structurally similar to that of the *apo* form **2**, suggesting that it is, in fact, a daughter pseudopolymorph. If this was true, recrystallization under similar conditions, followed by desolvation would be a route to obtaining the *apo* form observed by SCXRD in a bulk form.

Recrystallization of the crude product under similar conditions gave rise to a crystalline solid suitable for NMR and PXRD. The ¹³C CP/MAS solid-state NMR spectrum clearly shows the enclathration of DMF (see Figure 3). The twofold splitting of the aromatic host peaks agrees well with the SCXRD data, indicating an asymmetric unit containing one half of a host molecule. The PXRD is consistent with that predicted from the SCXRD of **3**, and can be indexed to the same unit cell (see Figure 4 and Table 2). The solution NMR is also consistent with that reported by Mattay.^[25,30]

Thermogravimetric analysis indicated that **3** exhibited a weight loss at 85 °C consistent with the elimination of approximately 6 DMF molecules per host molecule.

This transformation was subsequently monitored by PXRD and solid state NMR, heating samples of **3** in a vacuum oven for 30 minute intervals. After heating at 85°C, the PXRD exhibits considerable simplification, but does not correspond well to the predicted pattern for **2**. Examination of the ^{13}C CP/MAS spectrum makes it clear that the transformation is incomplete, with some DMF remaining.



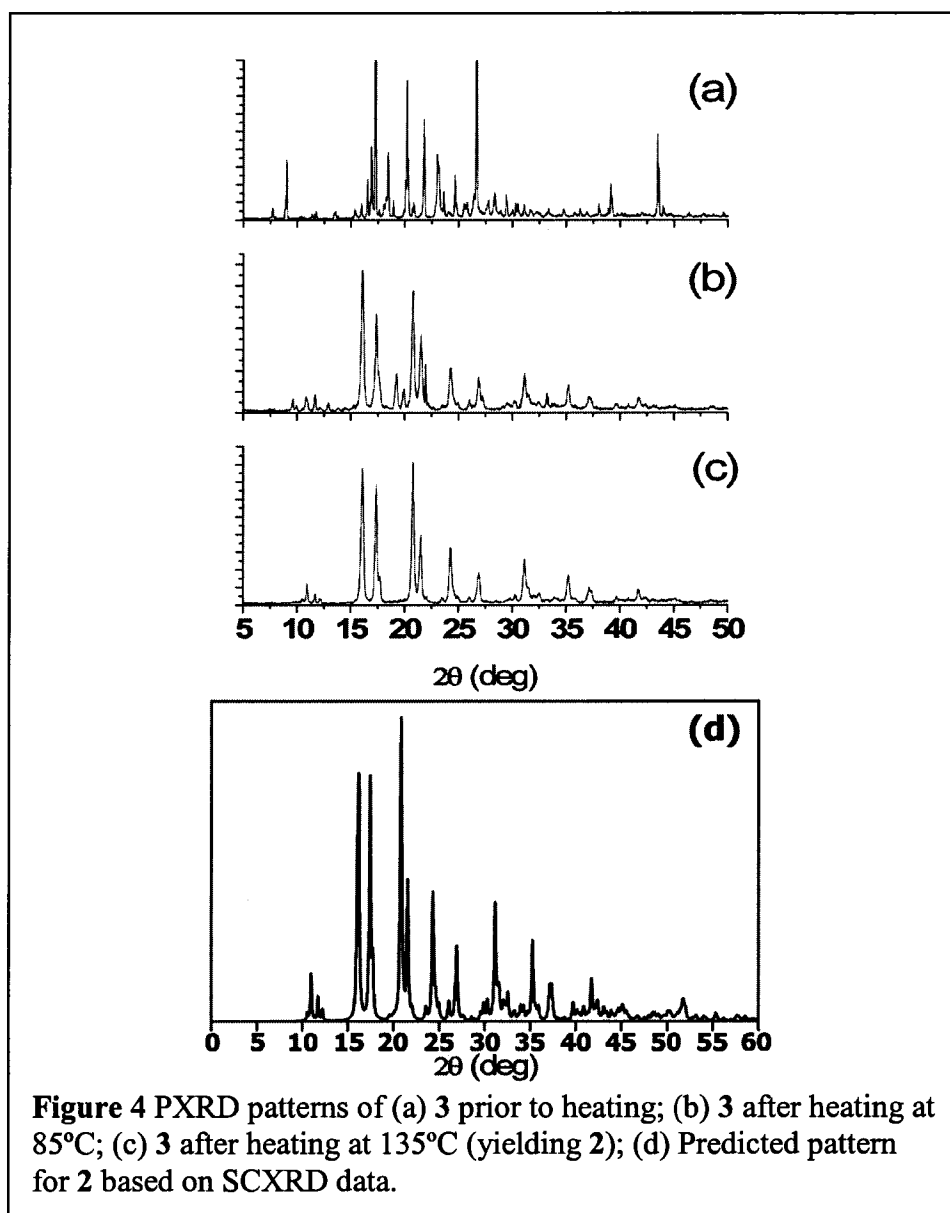


Table 2 PXRD unit cell parameters for the *apo rctt* PGR host (compound 2) and the PGR/DMF clathrate at room temperature (clathrate 3).

	Compound 2	Clathrate 3
Space Group	<i>P</i> -1	<i>P</i> -1
<i>a</i> (Å)	8.8940	10.201
<i>b</i> (Å)	9.3547	11.670
<i>c</i> (Å)	9.4694	11.648
α (°)	106.7	81.44
β (°)	104.6	73.49
γ (°)	104.7	83.68
<i>V</i> (Å ³)	683.52	1311.1

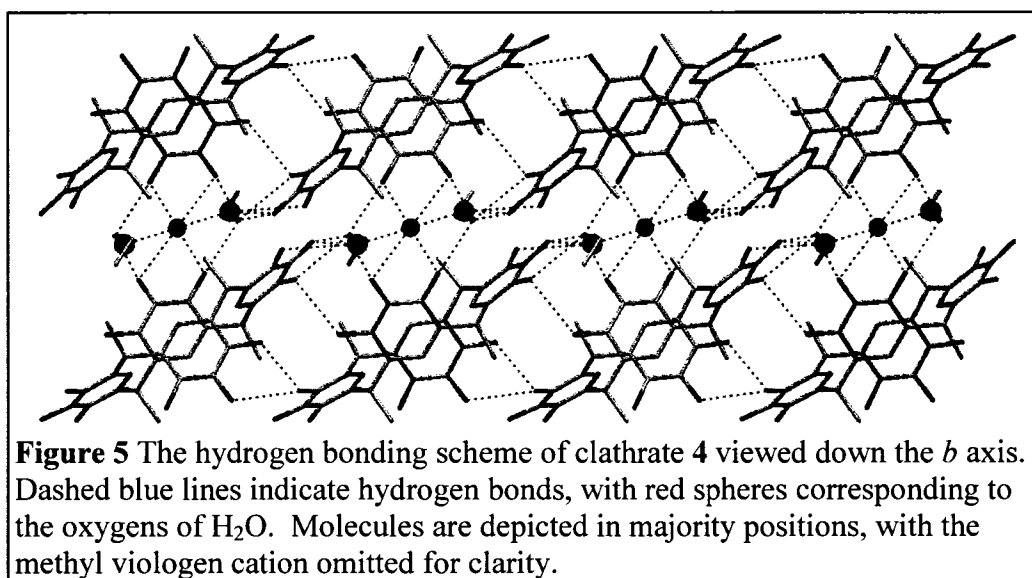
Upon further heating at 135°C to ensure removal of all DMF, the PXRD is now consistent with that predicted for **2**, and is readily indexed to the appropriate unit cell (see Table 2). The ^{13}C CP/MAS spectrum is consistent with a low-symmetry structure, with the extensive crystallographic splitting making assignment of the aromatic region difficult. However, the two-fold splitting of the CH_3 resonance is consistent with the alternate arrangement of the methyl groups expected of the *rctt* isomer.

Inclusion of Viologens in Anionic Frameworks of *rctt* PGR

Unlike the *rccc* isomers of resorcinarenes, the *rctt* isomer has an inherent preference for formation of channelled structures, as demonstrated by both the *apo* forms and DMF clathrates.^[25] It was anticipated that the anionic frameworks arising from such inclusions would display different motifs from CMCR (see Chapter VII). In light of the structure of the *apo* form, such frameworks appeared to be suitable for inclusion of larger pyridinium species. The viologens are well known materials analogous to the bipyridinium cations previously examined, capable of serving as electron donors in materials,^[31, 32] giving rise to spectroelectrochemical activity in inorganic,^[33] polymeric^[34] and supramolecular systems.^[35-39] It had proven not to be possible to readily include these materials in CMCR, presumably due to the lack of sufficient hydrogen bonding moieties to stabilize a 3D framework. Given the discrimination previously observed with recrystallization of the crude for producing the *rctt* isomer, we made further attempts to use this methodology to investigate inclusions of the *rctt* isomer.

Recrystallization of PGR and methyl viologen dichloride from an ethanol solution acidified with HCl readily gave rise to crystals of clathrate **4**, which has a stoichiometry

of 1(methyl viologen)*2(Cl⁻)*1.5(EtOH)*2.69(H₂O)*1(*C*-methylpyrogall[4]arene) clathrate. As expected, the methyl viologen is included within the framework formed by the interactions of the chloride ions with the PGR molecules and solvent (Cl...O distances of 2.80 to 3.15 Å, see Figures 5 and 6). Unlike the discrete resorcinarene capsules and tubular structures formed with small organic cations,^[3, 11] or the channelled structures arising from inclusions of pyridinium cations (see Chapter VII), one of the chloride anions is disordered over three distinct sites (0.52:0.40:0.8 distribution), with these sites occupied by water when chloride anions are not present.



Ethanol serves to fill the voids between viologen molecules, with one molecule being fully ordered and a second disordered over two sites due to its placement on a centre of symmetry. This packing scheme results in two perpendicular channels being formed. The channel bearing the closest resemblance to that observed in CMCR anionic frameworks is defined by pairs of PGR molecules with opposite orientations, forming planes at 63.9° to the crystallographic (001) plane, such that it is approximately 4.9 by

7.8 Å in size (see Figure 6). The viologen, as well as the previously mentioned ethanol molecules, occupy this channel. The second channel is parallel with the a axis and is occupied by the viologen and the disordered chloride anions (see Figure 7), resulting in it having somewhat larger dimensions (6.8 by 9.9 Å at its widest points).

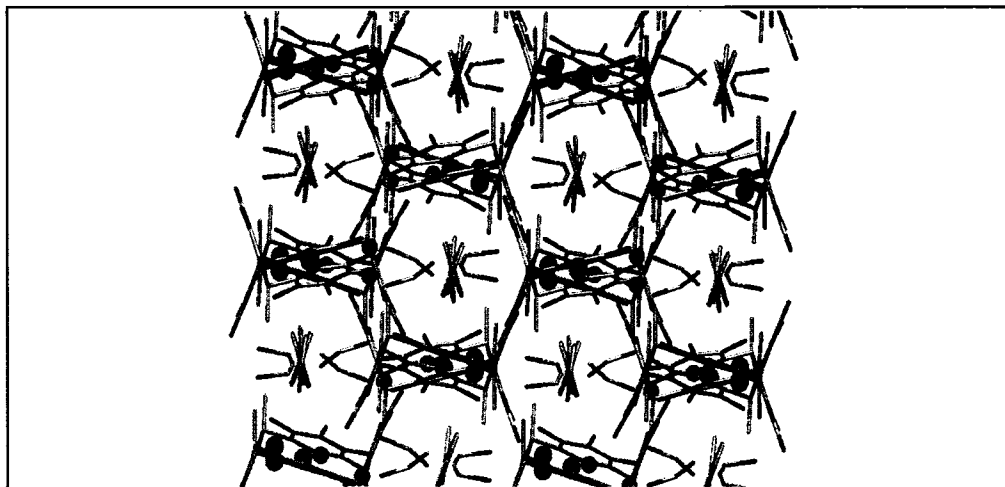


Figure 6 One of two major channels in clathrate 4 as viewed at 63.9° to the crystallographic (001) plane. PGR dimers define the channels containing the combination of solvent and methyl viologen. Molecules are depicted in majority positions with red spheres corresponding to the oxygens of H_2O .

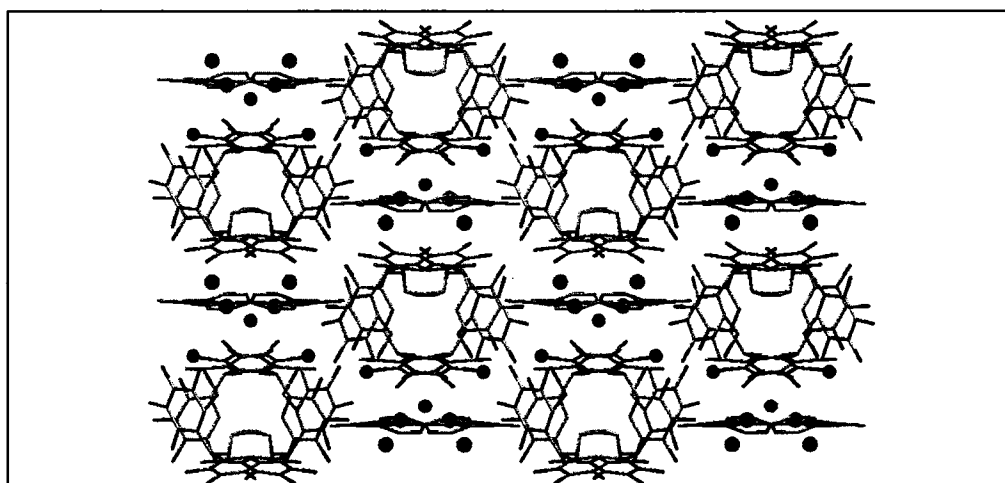


Figure 7 One of two major channels in clathrate 4 as viewed down the a axis. Alternate stacking of the PGR molecules results in staggering of the cations. Molecules are depicted in majority positions with red spheres corresponding to the oxygens of H_2O .

Therefore, while the viologen guest is still capable of directing the formation of a channelled structure, the increased number of potential interactions between the molecules of *rctt* PGR actually results in increased disorder and greater segregation of the components of the structure. Furthermore, the packing scheme also appears to compensate partially for the decreased symmetry of the host by forming the columns of PGR observed along the *a* axis, such that they resemble *rccc* isomers over long ranges. Even so, the high degree of disorder and comparatively large content of solvent implies that this structural compromise is extremely tenuous.

In contrast with this highly solvent dependent structure, inclusion of ethyl viologen in PGR from an acetonitrile solution acidified with HBr gives rise to a 1(ethyl viologen)*2(Br⁻)*1(MeCN)*2(H₂O)*1(*C*-methylpyrogall[4]arene) clathrate (clathrate **5**) which exhibits no disorder. Instead of packing to allow formation of a pseudo *rccc* arrangement, the asymmetrical *rctt* PGR molecules are packed such that each layer is orthogonal to its neighbouring layer (see Figures 8 and 9). A complex network of hydrogen bonds to bromide anions stabilizes this arrangement (Br...O distances of 3.22 to 3.37 Å), with the lack of disorder indicating that this particular structural motif represents a distinct energy minimum (as opposed to the multiple equivalent structural motifs that appear to be represented by the structure of **4**). Concomitant with this appears to be a loss of true channels in the structure, with the ethyl viologens packed along the central axes of the PGR molecules obstructed from moving from site to site by the terminal aromatic hydrogens (not depicted).

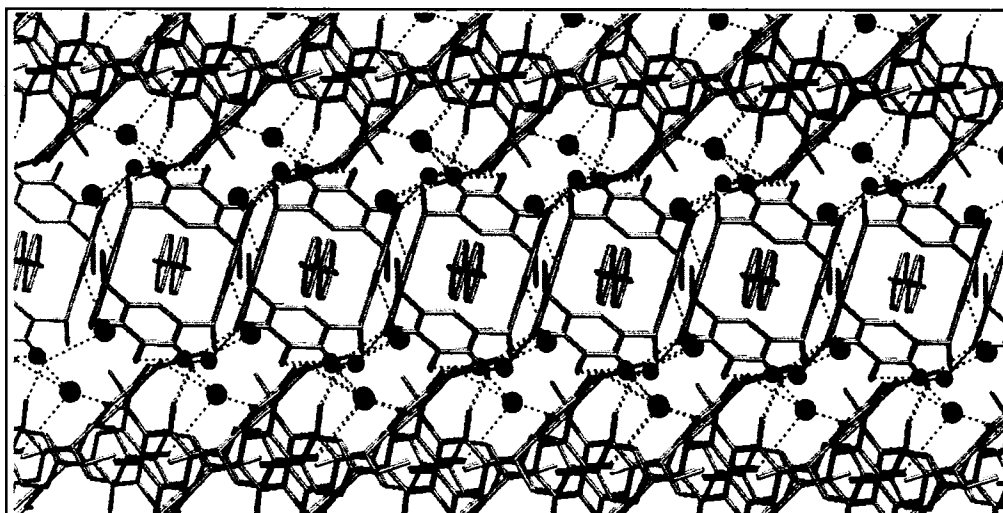


Figure 8 Alternate layering of clathrate **5** as viewed down the *c* axis. Dashed blue lines indicate hydrogen bonds with light red spheres corresponding to the oxygens of H₂O.

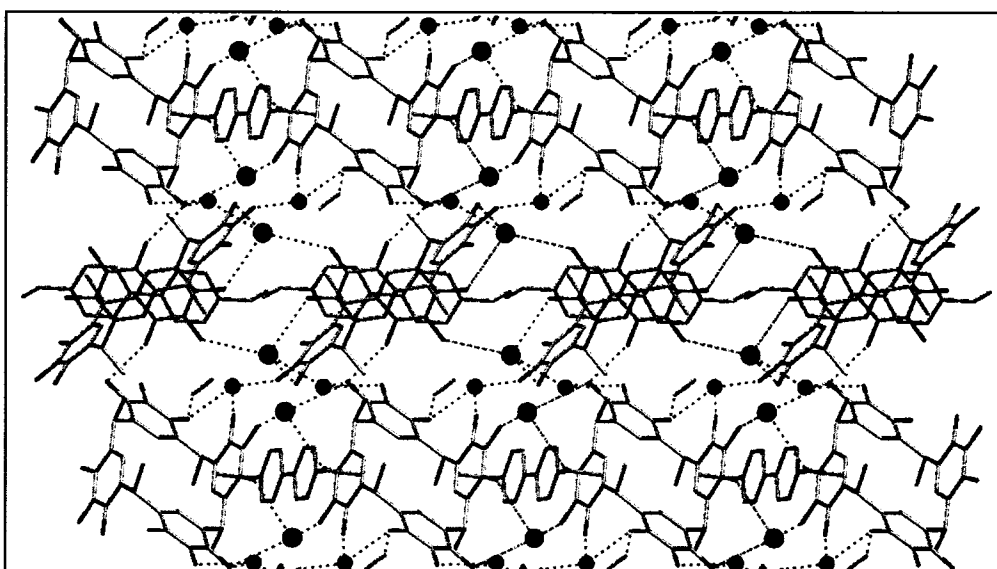


Figure 9 Alternate layering of clathrate **5** as viewed down the *a* axis. Dashed blue lines indicate hydrogen bonds with light red spheres corresponding to the oxygens of H₂O.

In light of these two structures, it appears that the inclusion chemistry of anionic frameworks of the *rcft* form of PGR exhibits a level of complexity beyond that observed for CMCR. Once again, a reduction in host symmetry leads to structural compromises in producing inclusion compounds, while allowing the inclusion of larger organic cations

that do not engage in any directional interactions with the rest of the frameworks.

This particular isomer clearly is unsuited for even cation- π interactions with guests of even modest bulk, which partially explains the current inability to isolate clathrates including smaller bipyridinium cations at this time. As such, it falls to solvent selection and anion choice to guide such structures. Using a small anion, it appears that the flexible hydrogen bonding of ethanol in clathrate **4** allows for a highly disordered structure with distinct channels, while the acetonitrile in clathrate **5** cannot serve such a role. However, further studies with other solvents and a broader range of anions will be required to fully assess how important these factors are in guiding these structures.

5. Conclusions

Shifts in configuration give rise to new geometries with distinct inclusion characteristics. In this case, such differences gives rise to two methods by which to isolate the *apo* form of *rctt* PGR, and carried out preliminary investigations of the inclusion behaviour of such a material when coordinated to anions. The first involves taking advantage of the difference in molecular recognition properties between the *rccc* and *rctt* isomers arising from comparatively weak interactions. The crown conformation favoured by the *rccc* isomer makes it an excellent host under acidic conditions for 1,3-BPTU, while the *rctt* cannot offer a similar degree of van der Waals stabilization to such a guest, and therefore crystallizes separately. This is similar to the stabilization offered by 4tBC4A to amines after elimination of hydrogen bonding interactions.

The second relies on the differential solubility of the two isomers, such that the *rctt* isomer can be recrystallized from polar organics that are considerably better solvents

for the *rccc* isomer. The subsequent desolvation step yields the *apo* host. The common element between the two methods appears to be the massive preference of the *rctt* isomer to exclude polar solvents in order to facilitate a tightly packed, hydrogen bonded motif. While the methyl groups obstruct the channels nominally observed in the SCXRD structure, it is still important to further investigate the flexibility and porosity of the *apo* form, and its relationships to other inclusion compounds. Methods such as ^{129}Xe NMR and pycnometry would further clarify whether additional linker units would be required to produce a porous PGR framework.

Along these lines, preliminary studies of the formation of anionic frameworks from *rctt* PGR were carried out. While the resulting frameworks exhibit considerable similarities to those formed by CMCR (see Chapter VII), the inherent asymmetry of the host and the wider range of hydrogen bonding capabilities result in altered channelled structural motifs to account for these factors. With the altered symmetry of the host preventing the formation of a typical calixarene cavity, the anions now serve to disrupt the intermolecular hydrogen bonds, giving rise to more subtle shifts (between types of channelled structures) that observed in CMCR compounds (where disruption of intramolecular hydrogen bonds causes a shift from discrete inclusions to channelled structures). This allows for inclusion of non-interacting pyridinium cations, such that solvent and anion selection appear to play much more significant roles in guiding these structural motifs. At the same time, however, the predisposition to formation of channels by this isomer might discriminates against inclusion of smaller bipyridinium cations capable of hydrogen bonding, explaining the current inability to isolate such structures at

this time. If this were true, one would suspect that such interactions interfere with the formation of the channels (resulting in alternative structural motifs). Clearly, further systematic study of these anionic compounds is therefore called for to clarify these relationships.

6. References:

- [1] L. R. MacGillivray, J. L. Atwood, *J. Am. Chem. Soc.* **1997**, *119*, 6931.
- [2] L. R. MacGillivray, J. L. Reid, J. A. Ripmeester, *CrystEngComm* **1999**, *1*.
- [3] A. Shivanyuk, E. F. Paulus, K. Rissanen, E. Kolehmainen, V. Bohmer, *Chem. Eur. J.* **2001**, *7*, 1944.
- [4] B. Q. Ma, Y. Zhang, P. Coppens, *Cryst. Growth. Des.* **2002**, *2*, 7.
- [5] L. R. MacGillivray, J. L. Atwood, *Nature* **1997**, *389*, 469.
- [6] B. W. Purse, J. Rebek, *Proc. Nat. Acad. Sci. USA* **2005**, *102*, 10777.
- [7] J. Rebek, *Angew. Chem. Int. Edit.* **2005**, *44*, 2068.
- [8] L. C. Palmer, A. Shivanyuk, M. Yamanaka, J. Rebek, *Chem. Commun.* **2005**, 857.
- [9] A. Shivanyuk, J. Rebek, *J. Am. Chem. Soc.* **2003**, *125*, 3432.
- [10] A. Shivanyuk, J. Rebek, *Chem. Commun.* **2001**, 2424.
- [11] H. Mansikkamaki, M. Nissinen, C. A. Schalley, K. Rissanen, *New J. Chem.* **2003**, *27*, 88.
- [12] B. Q. Ma, Y. G. Zhang, P. Coppens, *Cryst. Growth Des.* **2001**, *1*, 271.
- [13] B. Q. Ma, Y. G. Zhang, P. Coppens, *CrystEngComm* **2001**, art. no. 20.
- [14] L. R. MacGillivray, J. L. Atwood, *Supramol. Chem.* **2000**, *11*, 293.
- [15] L. R. MacGillivray, P. R. Diamente, J. L. Reid, J. A. Ripmeester, *Chem. Commun.* **2000**, 359.
- [16] L. R. MacGillivray, J. L. Reid, J. A. Ripmeester, *Chem. Commun.* **2001**, 1034.
- [17] M. Nissinen, K. Rissanen, *Supramol. Chem.* **2003**, *15*, 581.
- [18] C. L. Barnes, E. Bosch, *Cryst. Growth Des.* **2005**, *5*, 1049.
- [19] I. Georgiev, E. Bosch, *Cryst. Growth Des.* **2004**, *4*, 235.
- [20] T. Gerkenmeier, W. Iwanek, C. Agena, R. Frohlich, S. Kotila, C. Nather, J. Mattay, *Eur. J. Org. Chem.* **1999**, 2257.
- [21] G. W. V. Cave, J. Antesberger, L. J. Barbour, R. M. McKinlay, J. L. Atwood, *Angew. Chem. Int. Ed. Engl.* **2004**, *43*, 5263.
- [22] L. Avram, Y. Cohen, *J. Am. Chem. Soc.* **2004**, *126*, 11556.
- [23] R. M. McKinlay, G. W. V. Cave, J. L. Atwood, *Proc. Nat. Acad. Sci. USA* **2005**, *102*, 5944.
- [24] R. M. McKinlay, P. K. Thallapally, G. W. V. Cave, J. L. Atwood, *Angew. Chem. Int. Ed. Engl.* **2005**, *44*, 5733.
- [25] T. Gerkenmeier, C. Agena, W. Iwanek, R. Frohlich, S. Kotila, C. Nather, J. Mattay, *Z. Natur. B Chem. Sci.* **2001**, *56*, 1063.
- [26] P. O. Brown, G. D. Enright, J. A. Ripmeester, *J. Supramol. Chem.* **2002**, *2*, 497.

- [27] H. Mansikkamaki, C. A. Schalley, M. Nissinen, K. Rissanen, *New J. Chem.* **2005**, *29*, 116.
- [28] H. Mansikkamaki, M. Nissinen, K. Rissanen, *CrystEngComm* **2005**, *7*, 519.
- [29] A. G. S. Hogberg, *J. Am. Chem. Soc.* **1980**, *102*, 6046.
- [30] It is important to note that the ^{13}C NMR data as presented is clearly incorrect, given it is identical to that of the *rccc* isomer.
- [31] P. S. Braterman, J. I. Song, *J. Org. Chem.* **1991**, *56*, 4678.
- [32] C. L. Bird, A. T. Kuhn, *Chem. Soc. Rev.* **1981**, *10*, 49.
- [33] M. Otake, M. Itou, Y. Araki, O. Ito, H. Kido, *Inorg. Chem.* **2005**, *44*, 8581.
- [34] V. Balzani, H. Bandmann, P. Ceroni, C. Giansante, U. Hahn, F. G. Klamer, U. Muller, W. M. Muller, C. Verhaelen, V. Vicinelli, F. Vogtle, *J. Am. Chem. Soc.* **2006**, *128*, 637.
- [35] L. G. Kuz'mina, A. I. Vedernikov, N. A. Lobova, J. A. K. Howard, Y. A. Strelenko, V. P. Fedin, M. V. Alfimov, S. P. Gromov, *New J. Chem.* **2006**, *30*, 458.
- [36] V. Martinez-Junza, A. Rizzi, K. A. Jolliffe, N. J. Head, M. N. Paddon-Row, S. E. Braslavsky, *Phys. Chem. Chem. Phys.* **2005**, *7*, 4114.
- [37] J. W. Park, S. Y. Lee, H. J. Song, K. K. Park, *J. Org. Chem.* **2005**, *70*, 9505.
- [38] A. Mirzoian, A. E. Kaifer, *Chem. Commun.* **1999**, 1603.
- [39] E. N. Ushakov, S. P. Gromov, A. I. Vedernikov, E. V. Malysheva, A. A. Botsmanova, M. V. Alfimov, B. Eliasson, U. G. Edlund, J. K. Whitesell, M. A. Fox, *J. Phys. Chem. A* **2002**, *106*, 2020.

Chapter IX: Pseudopolymorphism in Hexameric Pyrogallarenes[†]

1. Abstract.....	351
2. Introduction.....	352
3. Experimental Section.....	354
4. Results and Discussion.....	356
Single Crystal X-ray Diffraction (SCXRD) Structure of Clathrate 1	356
Structural Studies of Thermal Transformation Product 2a	359
TGA and SCXRD Studies of Recrystallization Product 2b	364
PXRD, SSNMR, and Microscopic Studies of 2b	369
5. Conclusion	372
6. References	374

1. Abstract

Recent studies have demonstrated that the *r-tctct* isomer of ethylpyrogall[6]arene (6EPGR) can be readily isolated as a minor product of the synthesis of the corresponding tetramer in the form of a 6 DMSO:1 6EPGR clathrate in the hexagonal space group *R*-3. Simultaneous studies in our group led to the isolation of said hexamer as a 12 DMSO:1 6EPGR clathrate in the same space group. Using powder x-ray diffraction (PXRD) and ¹³C cross polarization magic angle spinning (CP/MAS) NMR spectroscopy, it is demonstrated that this 12 DMSO:1 6EPGR pseudopolymorph is, in fact, the precursor to the 6 DMSO:1 6EPGR form. The 6 DMSO:1 6EPGR form can be obtained through simple heating of this 12 DMSO:1 6EPGR precursor, as well as recrystallization of the precursor from acetone. Furthermore, in light of the data obtained using these techniques, in conjunction with direct observation of the process using a microscope, it is suggested that the 6:1 inclusion as prepared by recrystallization from acetone is more appropriately modeled as containing acetone in addition to DMSO. Based on this, it is

[†] Portions of this chapter have been previously published: P.O. Brown, G.D. Enright, J.A. Ripmeester, *Cryst. Growth Des.* **2006**, *6*, 719.

possible to rationalize the relationship between these pseudopolymorphic forms and the impacts of the two methods of conversion on the structures of the clathrates.

2. Introduction

Given the pre-organized cavity found in the *rccc* isomers of tetrameric calixarenes, it is unsurprising that calixarene research has largely focused on these compounds.^[1-3] This is particularly prevalent for the resorcinarenes and pyrogallarenes. The pre-organization of the OH groups on the rim make them favoured targets for chemists interested in using supramolecular interactions to direct resorcinarene structural motifs. Hydrogen bonding to pyridyl-type moieties has been used to extend the calixarene cavity to allow it to take up aromatics and metallocenes.^[4-6] The hydroxyls also serve as binding sites for metals, and the key moieties for directing the formation of a variety of capsular assemblies.^[7-11] As a result, the synthesis of other resorcinarenes isomers and larger cyclic molecules have been reported much less frequently.^[12-15]

In the case of the pyrogallarenes, however, it is possible to easily isolate isomers which inherently favour the formation of channelled structures due to their lack of four fold symmetry, as demonstrated by the isolation of the *rctt* isomer of pyrogall[4]arene (see Chapter VIII)^[16, 17] Furthermore, investigations of comparable calixarenes have shown the increased conformational flexibility and larger cavities of the larger calixarenes gives rise to a richer inclusion and synthetic chemistry, while additional available isomers favour the formation of differing framework structures.^[18] In particular, the increased competition between hydrogen bonding and van der Waals

stabilization in pyrogallarenes makes them highly attractive targets for investigations as to how the structural motifs of larger calixarenes are governed.

As alluded to above, since the simple acid-catalyzed reaction used to synthesize most pyrogallarenes heavily favours the formation of the tetramer, there has been little research on the larger pyrogallarenes. However, Rissanen *et al.* recently reported the isolation of ethylpyrogall[6]arene (6EPGR) as a minor product of the synthesis of the corresponding tetramer.^[19] This compound was isolated as an unusual clathrate consisting of 6 DMSO molecules for each 6EPGR molecule, leaving several of the phenolic OH groups to form hydrogen bonds directly with each other. In the course of investigating the inclusion chemistry of pyrogallarenes for the purposes of creating ionic frameworks in our group, a synthesis of a DMSO/6EPGR clathrate as a distinct 12 guest :1 host pseudopolymorph where all phenolic OH groups are hydrogen bonded to DMSO was discovered.

This pseudopolymorphism, much like that observed for the 4tBC4A amine systems (see Chapters III-VI), is a consequence of competition between intermolecular interactions in guiding the structural motif. However, in this case, the competition is between differing modes of hydrogen bonding. In this chapter, structural and thermal studies are used to clarify the relationship between the 12 guest : 1 host and the 6:1 form. The 12 : 1 form appears to be the parent of the 6 : 1 form, which can be obtained through both thermal desorption and recrystallization from acetone. However, as we will see, these two different methods of obtaining the 6 : 1 form have significant implications for the crystal structure of the clathrates. These studies have also led to our proposal of a

revised crystallographic model for the 6:1 pseudopolymorph arising from recrystallization that eliminates the irregularities in the previously reported structure.

3. Experimental Section

General Note: Unless otherwise indicated, chemicals were obtained from EMD Chemicals and Sigma-Aldrich, and were used without further purification.

Synthesis of 6EPGR, 12(DMSO)*1(6EPGR) clathrate **1** (POB91), 6(DMSO)* 1(6EPGR) clathrate **2a** and 4.26(DMSO)*(1.74 Acetone)*1(6EPGR clathrate) **2b** (POB99): The title compound was synthesized using a modified version of the procedure previously reported by Rissanen *et al.*^[19] In a typical synthesis, 25.222 g (0.2000 mol) of pyrogallol was placed in a three necked round bottom flask and dissolved in a solution of 40.0 mL H₂O, 40.0 mL EtOH and 15.0 mL concentrated hydrochloric acid. The flask was fitted with a condenser, placed under an N₂ purge and cooled to 0°C with an ice bath. Over the course of approximately 40 minutes, 14.6 mL (0.202 mol) of propionaldehyde was added using a dropping funnel. The resulting mixture was then heated at 70°C for approximately 1 day, at which point an off-white precipitate was observed to have formed. This precipitate was filtered off by vacuum and washed with a chilled 1:1 solution of chilled water and EtOH.

The resulting crude product was recrystallized from DMSO, yielding 3.383 g (0.175×10^{-3} mol, 3.5% yield) of purple plate-like crystals of the 12 DMSO: 1 6EPGR clathrate (clathrate **1**) after one night.

The 6 DMSO: 1 6EPGR clathrate (clathrate **2a**) was prepared by heating crystals of **1** on a hot plate at $60 \pm 1^\circ\text{C}$ for 15-30 minute intervals. The 4.26 DMSO: 1.74

Acetone: 1 6EPGR clathrate (clathrate **2b**) was prepared by recrystallizing **1** from acetone, yielding clear block-like crystals. This recrystallization was carried out by allowing conversion over the course of several days at room temperature, as well as by heating the acetone to accelerate the process such that crystals formed overnight.

Single Crystal X-ray Diffraction data are summarized in Table 1. For **1**, all hydrogen atoms on the 6EPGR found from the difference electron density map, while for **2b**, hydrogens on the 6EPGR were placed in calculated positions and refined as riding atoms. In both cases, hydrogens on the individual solvent molecules were placed in calculated positions, and refined as riding atoms.

Thermogravimetric analysis was carried as described in Chapter III on pages 72-73, with the exception that samples were heated from room temperature to 300°C at a rate of 5°C/minute. Powder X-ray Diffraction (PXRD) data were collected on the Scintag X-2 Advanced diffractometer. ¹³C CP/MAS SSNMR spectra for **1** and **2b** were collected using the Bruker AMX-300 spectrometer. A pulse delay of 3 sec and a contact time of 2 msec were used, with samples being spun at 5.5-6 kHz. ¹³C CP/MAS spectra for **2a** were collected using the Tecmag Apollo 200 spectrometer.

Table 1 Single Crystal X-Ray Diffraction Data for clathrates **1** and **2b**.

Identification code	Clathrate 1 (POB91)	Clathrate 2b (POB99)
Empirical formula	C13 H22 O5 S2	C11.04 H15.67 O3.94 S0.79
Formula weight	322.43	236.91
Temperature	125(2) K	125(2) K
Wavelength	0.71073 Å	0.71073 Å
Crystal system	Trigonal (Hexagonal)	Trigonal (Hexagonal)
Space group	<i>R</i> -3	<i>R</i> -3
Unit cell dimensions	<i>a</i> = 28.4485(15) Å <i>b</i> = 28.4485(15) Å <i>c</i> = 9.9871(7) Å α = 90° β = 90° γ = 120°	<i>a</i> = 24.691(2) Å <i>b</i> = 24.691(2) Å <i>c</i> = 10.2849(13) Å α = 90° β = 90° γ = 120°
Volume	6999.8(7) Å ³	5430.1(9) Å ³
Z	18	18
ρ_{calc}	1.377 Mg/m ³	1.304 Mg/m ³
Abs. coefficient	0.357 mm ⁻¹	0.228 mm ⁻¹
F(000)	3096	2271
Crystal size	0.5 x 0.3 x 0.16 mm ³	0.15 x 0.125 x 0.20 mm ³
θ Range	1.43 to 29.61°.	1.65 to 26.43°.
Index ranges	-39 ≤ <i>h</i> ≤ 38, -39 ≤ <i>k</i> ≤ 39, -13 ≤ <i>l</i> ≤ 13	-30 ≤ <i>h</i> ≤ 30, -30 ≤ <i>k</i> ≤ 30, -12 ≤ <i>l</i> ≤ 12
Reflections collected	29429	15387
Ind. reflections	4353 [R(int) = 0.0225]	2479 [R(int) = 0.0701]
Completeness to $\theta = \text{max}$	99.2 %	99.8 %
Absorption correction	Multi-Scan	Multi-Scan
Refinement method	Full-matrix least-squares on F ²	Full-matrix least-squares on F ²
Data / restraints / parameters	4353 / 12 / 252	2479 / 16 / 199
Goodness-of-fit on F ²	1.026	1.021
Final R indices [I > 2σ(I)]	R1 = 0.0365, wR2 = 0.0977	R1 = 0.0461, wR2 = 0.0978
R indices (all data)	R1 = 0.0426, wR2 = 0.1030	R1 = 0.0815, wR2 = 0.1130
Largest diff. peak and hole (e.Å ⁻³)	0.888 and -0.433	0.302 and -0.394

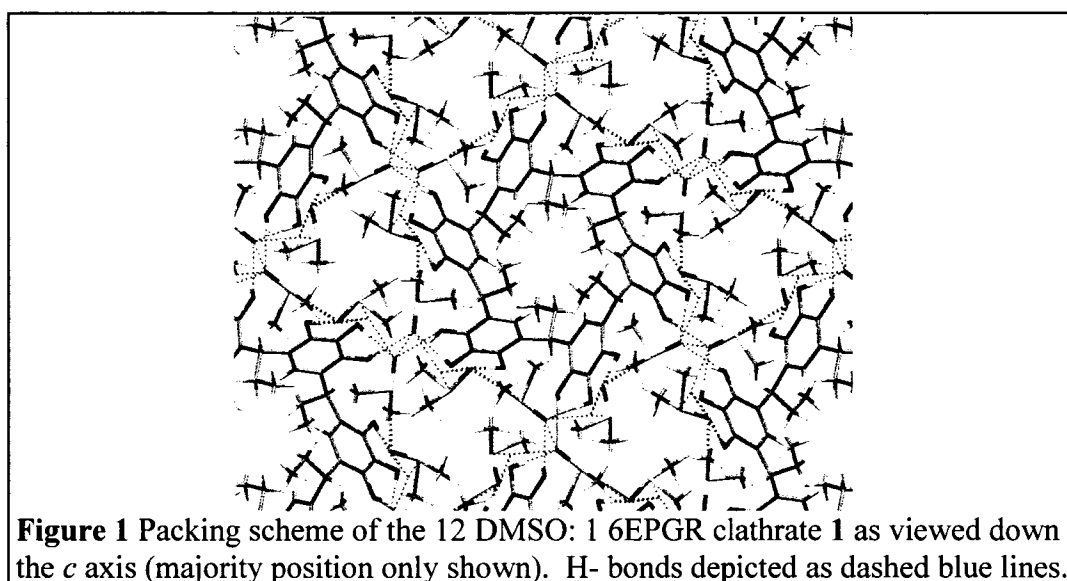
4. Results and Discussion

Single Crystal X-ray Diffraction (SCXRD) Structure of Clathrate **1**

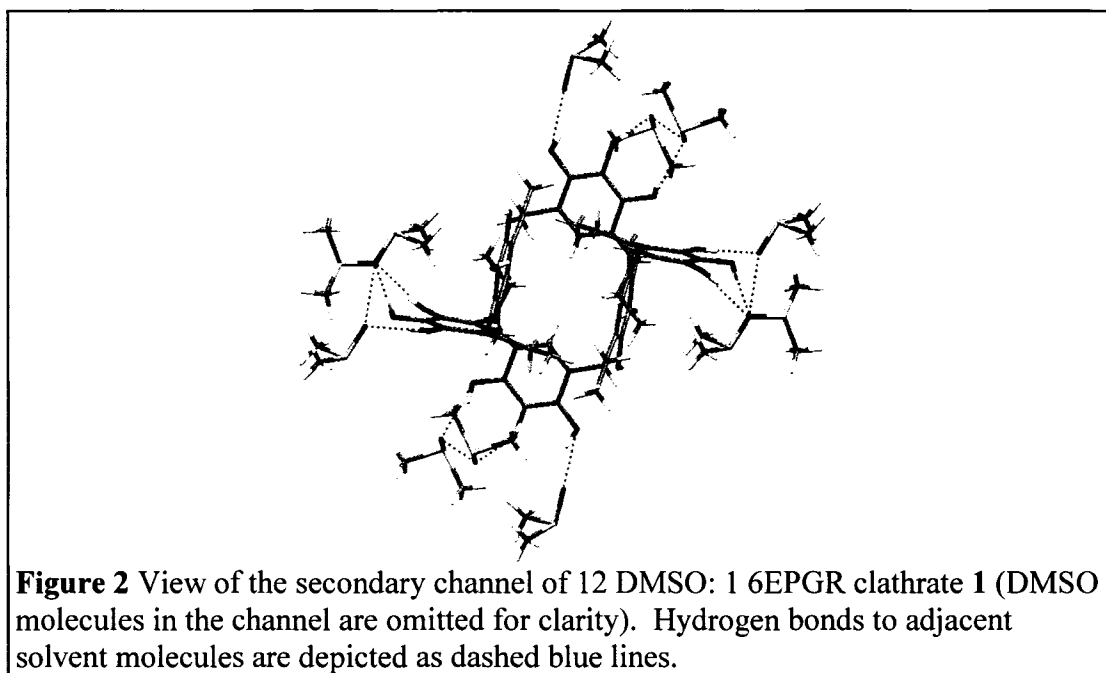
The details of the crystal structure and its refinement are summarized in Table 1.

The 12:1 inclusion scheme is analogous to that observed for resorcin[6]arene,^[20] with **1** crystallizing in a hexagonal space group with a threefold roto-inversion axis, such that the

axial ethyl groups alternate positions above and below the plane defined by the bridging methine carbons. The neighbouring phenyl rings are staggered in alternating directions, being nearly perpendicular to each other with a dihedral angle of 88.7° . In addition to the straight channel through the 6EPGR ring observed in the direction of the *c* axis (see Figure 1), there are several secondary channels filled with DMSO, such as the staggered 4.3 \AA rectangular channel formed by the 6EPGR at a 54° angle relative to the *ab* plane (see Figure 2).



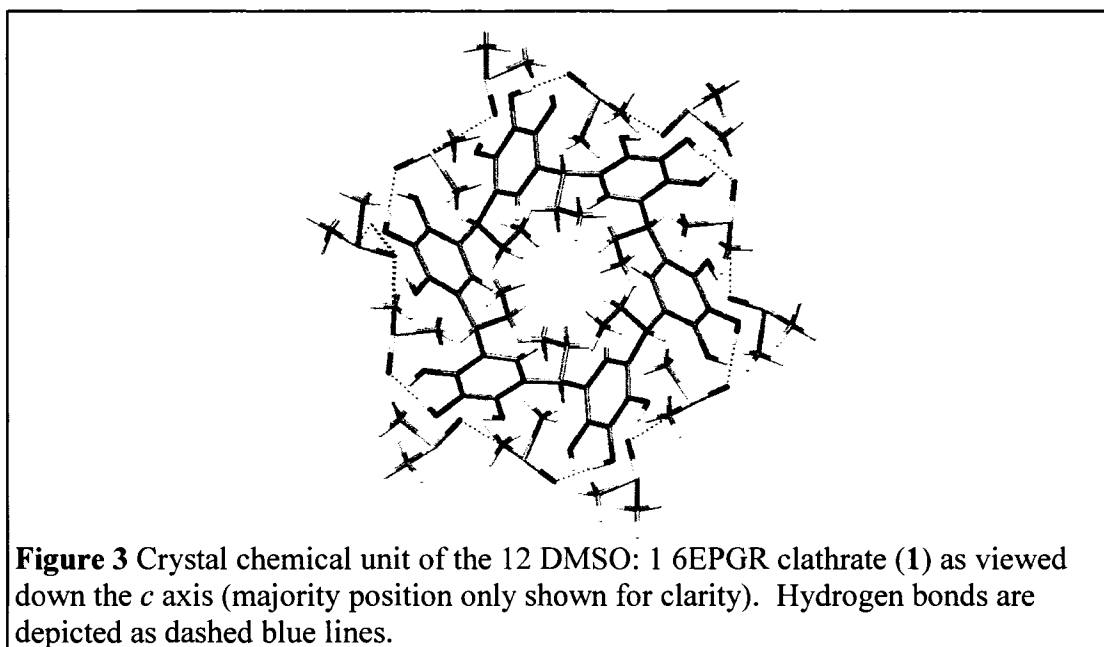
The distance between neighbouring phenolic hydroxyl groups on adjacent phenyl rings (3.79 \AA) is too long to allow for hydrogen bonding, with the resulting tubular structure being stabilized by an intricate series of intermolecular hydrogen bonds with two crystallographically distinct molecules of DMSO, such that there are 12 DMSO molecules per host (see Figure 3). One molecule is fully ordered, while the other is observed to be disordered over two sites with a 0.61:0.39 distribution. The fully ordered DMSO serves as a hydrogen bonding bridge between two pairs of phenolic hydroxyl moieties on adjacent 6EPGR phenyl rings (O...OH bond distances of 2.67 and 2.72 \AA



respectively). It also forms a single hydrogen bond to an adjacent disordered DMSO molecule. For the majority position, this results in the DMSO molecules forming a series of two molecule hydrogen bonded clusters in the spaces between the 6EPGR (S...O bond distance of 3.22 Å). For the minority position, the DMSO molecules form an infinite hydrogen bonding network consisting of a series of interconnected rings of composed of 12 solvent molecules each (S...O bond distances of 3.18 and 3.25 Å).

Despite the similarity of the inclusion scheme of **1** to that observed for the comparable resorcin[6]arene, the two compounds are not isostructural. The *a* axis of **1** is more than double that of the comparable resorcin[6]arene (28.448 vs. 11.455 Å), which is likely due to the presence of the additional phenolic hydroxyl. The additional bulk from the DMSO molecule introduced as a consequence prevents the tight packing observed for the resorcin[6]arene. Intriguingly, the 6EPGR 12:1 inclusion compound is nearly isostructural to the previously reported 6:1 resorcin[6]arene/acetone inclusion,^[20]

suggesting that the spatial arrangement of the guest molecules, as opposed to the specific degree of hydrogen bonding to the host dominates the selection of the structural motif.



Structural Studies of Thermal Transformation Product **2a**

In light of the fact that **1** is nearly isostructural to the corresponding 6:1 host:guest clathrates of resorcin[6]arene and pyrogall[6]arene, it immediately raised the question as to what the relationship between this 12:1 form and the forms with reduced guest content. Crystallographically, **1** has an *a* axis approximately 4 Å longer than that observed for the corresponding 6:1 clathrates. Given that this was the only reported difference between the 12:1 and 6:1 pyrogall[6]arene DMSO clathrates, one would presume that the two forms were related, and conversion of the 12:1 form into the 6:1 form should be possible.

TGA data for **1** shows three distinct transitions with onset temperatures of 69.5°C, 122.9°C and 159.5°C. The overall weight loss observed is 48.7%, which is consistent

with the loss of approximately 12 molecules of DMSO. The initial weight loss of 24.2% corresponds to a loss of ~6 DMSO molecules, with the subsequent transitions of 17.1 and 7.3 weight percent corresponding to losses of ~4.2 and ~1.8 DMSO molecules. Given the relatively large plateau of stability between the loss of the initial 6 DMSO molecules and the loss of the remaining DMSO, we were encouraged that it might be possible to monitor this transformation through crystallographic and spectroscopic techniques

Initial attempts focused on determining if this transformation could be carried out in a single crystal to single crystal fashion, not unlike the inclusion and desorption of vinyl bromide^[21] and toluene^[22] in of 4-*t*-butylcalix[4]arene. In those cases, the layers of the low density β *apo* form was observed to undergo a 6 Å shift to accommodate the guest. Unfortunately, despite varying the temperature and length of heating, all such attempts failed to produce such a transformation. Heating was observed to cause a conversion of the crystal from the outside in, as evidenced by the crystals becoming opaque on the surface, with the interior remaining a single crystal of **1** suitable for diffraction. As such, PXRD was initially used to monitor the transformation of **1**.

Figure 4 shows the transformation of **1** by heating for intervals of 15 minutes. The symmetry of the material makes it possible to readily index the powder pattern of **1** based on predictions from the SCXRD structure (see Table 2). As expected, the unit cell observed for **1** is larger than that observed with the SCXRD data, as one expects a degree of thermal expansion to be observed in the cell obtained at room temperature when compared with results obtained at 125 K.

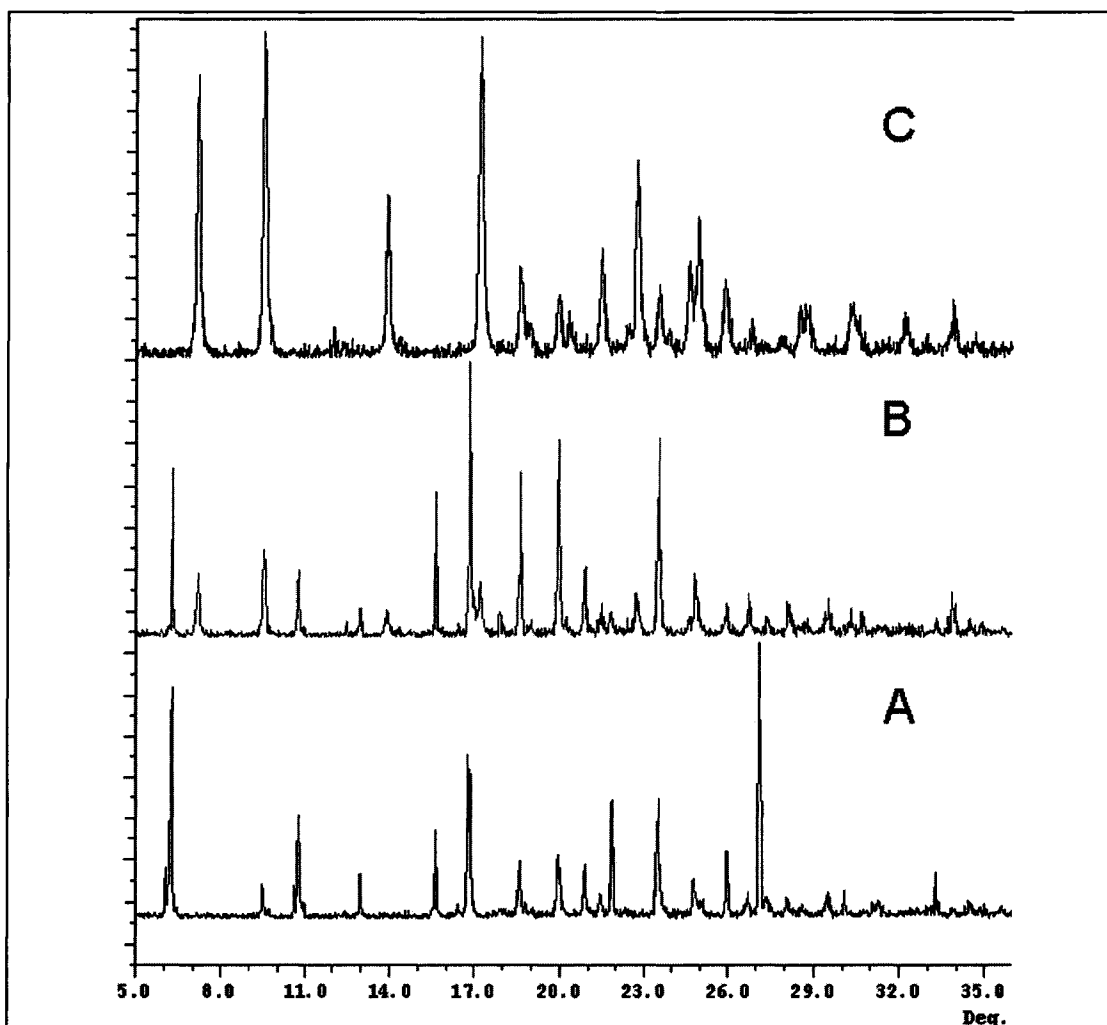


Figure 4 Powder X-Ray Diffractograms of the thermal conversion of the 12 DMSO: 1 6EPGR clathrate **1** to the 6 DMSO: 1 6EPGR clathrate **2a**. **A**: **1** prior to heating. **B**: Mixture of **1** and **2a** after 15 minutes at 60°C. **C**: Only **2a** is present after heating for a further 15 minutes at 60°C.

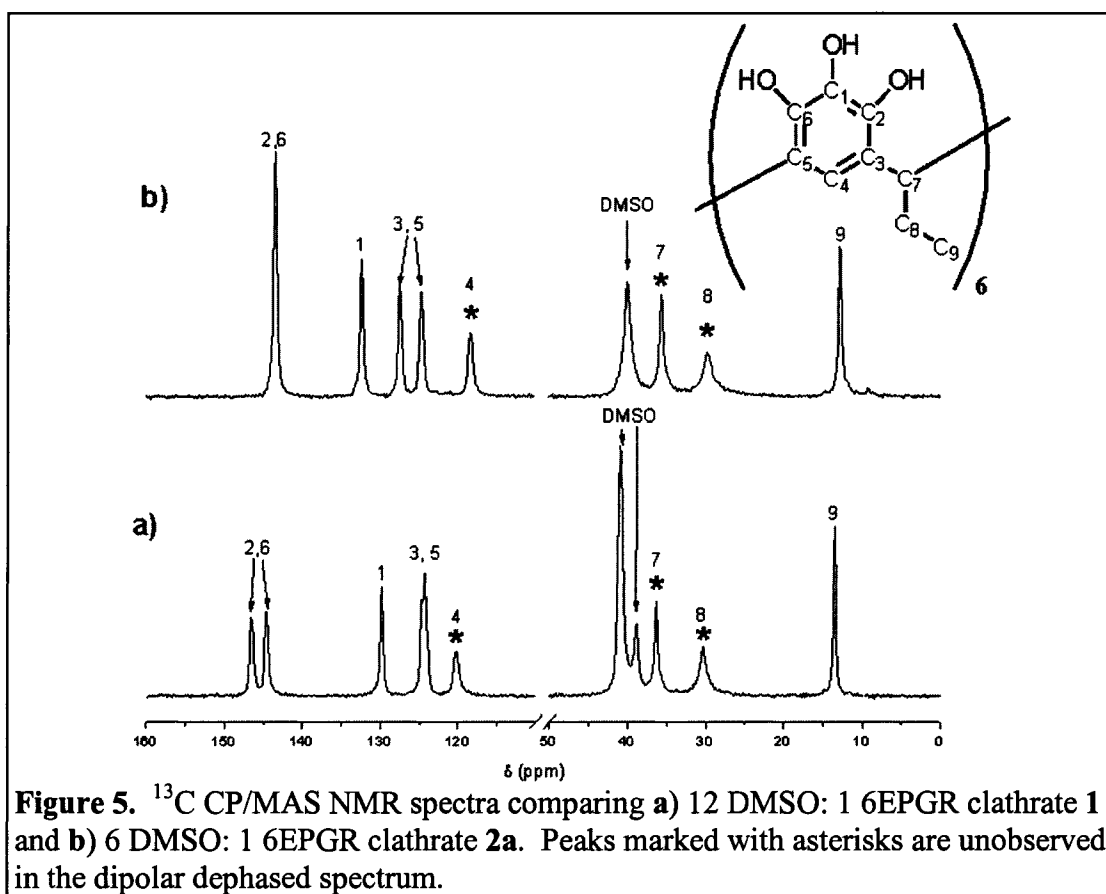
Table 2 Comparison of unit cell parameters for 6EPGR:12 DMSO clathrate **1** and 6EPGR:6 DMSO clathrate **2a**.

	1 (SCXRD @ 125 K)	1 (PXRD @ 293 K)	2 (SCXRD @ 173 K) ^[a]	2a (PXRD @ 293 K)
Space Group	<i>R</i> -3	<i>R</i> -3	<i>R</i> -3	<i>R</i> -3
<i>a, b</i> / Å	28.4485(15)	28.769	24.755(2)	24.985
<i>c</i> / Å	9.9871(7)	10.119	10.3010(4)	10.407
<i>V</i> / Å ³	6999.8(7)	7253.5	5466.7(7)	5626.1

^[a]From Rissanen *et al.*^[19]

After 15 minutes of heating, a number of peaks are observed to decrease in relative intensity, with new peaks beginning to appear. Visual examination of the resulting pattern suggests that it is a combination of **1** and the 6:1 clathrate (clathrate **2a**), such that the transformation is incomplete. The absence of any other reflections suggests that no intermediate form is involved in the transformation. However, with a further 15 minutes of heating, the peaks observed for **1** completely disappear, and the pattern now can be indexed to yield the unit cell parameters of **2a**, the 6:1 DMSO clathrate. TGA analysis confirms that **2a** is the 6:1 DMSO clathrate, with only two weight losses observed corresponding to ~4 and ~2 DMSO molecules being removed, with onsets at 128.8 and 167.9°C, which correspond closely to the temperatures observed for the loss of the final 6 DMSO molecules of **1**.

This transformation has also been monitored using ^{13}C CP/MAS solid state NMR (see Figure 5a). The spectrum of **1** is readily assigned in light of the solution spectrum for EPGR and the chemical shift for DMSO,^[19] along with the information provided by dipolar dephased spectra. Dipolar dephasing essentially consists of reintroducing the dipolar interaction between carbons and hydrogens for a brief period of time after cross polarization but before acquisition, such that CH and CH₂ carbons which are not experiencing high degrees of motion to disappear from ^{13}C spectrum. Upon dephasing, the three peaks marked in Figure 5a vanish, as would be expected for the aromatic CH group, the CH methine bridge and the CH₂ of the pendant ethyl group.



Information about the structural arrangement of each of the compounds can be obtained from the splitting observed in the ^{13}C CP/MAS spectrum, with each crystallographically inequivalent carbon theoretically giving rise to a distinct peak. Based on the asymmetric unit of **1** from the single crystal x-ray structure, the hydroxyl bearing carbons at positions 2 and 6 in the aromatic ring and the carbons linking to the methine unit at positions 3 and 5 should give rise to two peaks each. However, only the peaks due to the hydroxyl bearing carbons show discernable splitting, with the splitting of the peaks attributed to the carbons at positions 3 and 5 is nearly unobserved. Closer examination reveals that the carbons at positions 3 and 5 are nearly symmetric, and as such, only a very small difference in chemical shift would be expected, such that the

splitting is subsumed by the broadness of the peaks. Similarly, the dynamic motion and inherent symmetry of the DMSO molecules is such that only two peaks are observed, with further crystallographic splitting remaining concealed.

After thermal conversion (see Figure 5b), the peak positions for the methine bridge, ethyl substituents and enclathrated DMSO remain approximately the same, with a slight upfield shift of the peaks consistent with a structural shift to a smaller cell with closer contacts with adjacent aromatic moieties. Unsurprisingly, the peak due to the methine bridge shows some minor broadening, indicating a loss of crystallinity due to the heating process. A more dramatic change is observed in the aromatic region of the ^{13}C CP/MAS NMR spectrum, with the doublet due to the hydroxyl bearing carbons in positions 2 and 6 merging to produce a singlet, and the broad singlet due to the carbons in positions 3 and 5 resolving into a more distinct doublet. This strongly suggests a change in the asymmetric unit such that the two phenolic carbons are now equivalent, while the carbons attached to the methine linker are no longer pseudosymmetric such that their chemical shifts are indistinguishable. As we will see from the SCXRD evidence, such a change in arrangement arises from a shift in the positioning of the phenolic rings of 6EPGR relative to one another. As a result, both solid state NMR and PXRD can be used in determining the pseudopolymorph obtained, as well as to monitor the transformation.

TGA and SCXRD Studies of Recrystallization Product 2b

Upon failing to observe a single crystal to single crystal transformation from 1 to 2a, we turned our attention to the use of recrystallization from acetone to produce the 6:1 DMSO clathrate of 6EPGR. Since recrystallization under similar conditions of the

corresponding resorcin[6]arene 12:1 DMSO clathrate yields a 6:1 acetone clathrate, the absence of any acetone in the corresponding 6EPGR 6:1 clathrate structure is quite surprising.^[19, 20] This raises intriguing questions as to the role of acetone in the conversion of **1** to the 6:1 clathrate, and whether this process was a true recrystallization with the DMSO being retained due to particular constraints on the process, or if the acetone was simply stripping DMSO out of the crystals of a porous framework without actually completely dissolving them, causing the framework to contract.

In order to form a basis for studying the role of acetone in this process, a single crystal X-ray structure of the 6:1 clathrate was obtained for comparison with the previously reported structure.^[19] The resulting crystals selected for study diffracted extremely well, and we were easily able to collect a data set out to high angle. However, our initial attempts to solve and refine the resulting data using the model previously reported (consisting of one crystallographically unique DMSO disordered over two positions) proved to be highly frustrating. Despite the high quality of the data, with considerably better redundancy than the previously reported data set, we saw only marginal improvement in the resulting *R* value. As before, when modeling the minority solvent position as solely DMSO, the resulting thermal ellipsoids were found to be unstable. In light of the thermal transformation, a re-evaluation of the model used to resolve the solvent disorder in **2b** was clearly called for.

TGA of **2b** shows the same overall trend as that observed for **2a**, with two major transitions with the same ratios of weight lost (see Figure 6). It is important to note that the transitions observed for **2b** occur at approximately 20°C lower than those observed

for **2a**, with the initial transition of **2b** complicated by the presence of additional minor features. **2b** loses guest much more rapidly at low temperatures, with a more dramatic secondary transition starting at approximately 85°C. These data suggest the presence of a secondary, minority solvent component in single crystals of **2b**. In light of the difficulties in modeling the minority solvent position, the most reasonable possibility is that some acetone is included in the clathrate **2b**. Furthermore, with the SCXRD data in mind, we will see that the identical weight losses suggest that in the bulk material, the proportion of acetone present is even lower than in the single crystal.

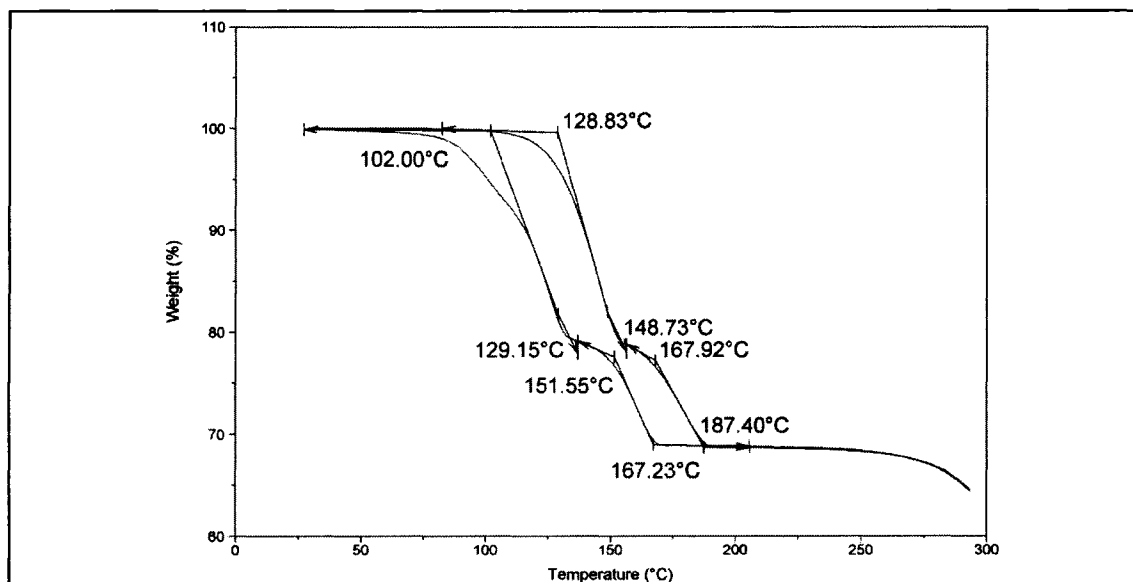
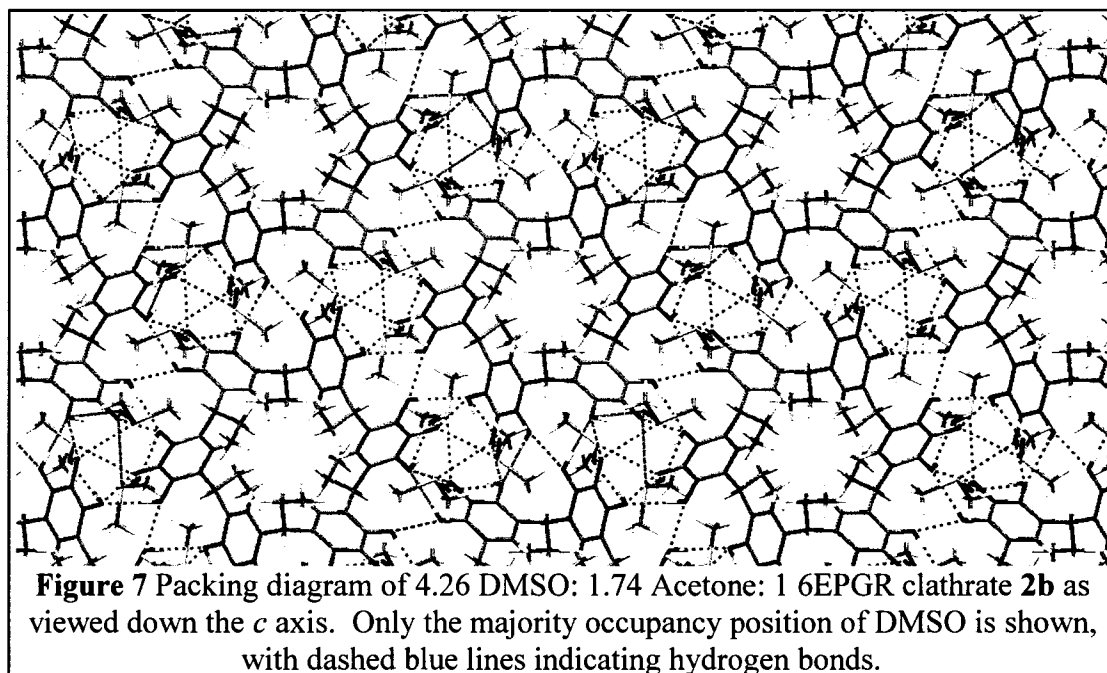


Figure 6 Comparison of TGAs for thermally converted 6 DMSO: 1 6EPGR clathrate **2a** (right) and recrystallized 4.26 DMSO: 1.74 Acetone: 1 6EPGR clathrate **2b** (left).

As previously mentioned, the overall packing scheme is quite similar to that of **1**, with a contraction of the *a* and *b* axes leading to direct interactions between adjacent 6EPGR units (see Table 1 and Figures 7 and 8). Our revised model for the solvent disorder in clathrate **2b** consists of four possible positions, with independently refined occupancies that add up to 100% total occupancy. As can be seen in Figure 9, each of the

two DMSO positions has a comparable position for acetone. Under this model, the DMSO positions show 0.63 and 0.08 occupancy, while the acetone positions are 0.15 and 0.14 occupied. No distortion in the conformation of the host 6EPGR due to the differing geometries of DMSO and acetone is observed, as the carbonyl oxygens and sulfonyl oxygens are oriented in the same directions, with only slight distances between each of the two positions (0.28 and 0.41 Å separation respectively).

In order to accommodate direct hydrogen bonding between 6EPGR units dictated by the reduced solvent content, the phenyl rings shift such that there is now only an angle of 83.1° between neighbouring units, introducing additional ripples into the secondary channels. The resulting asymmetric unit, as predicted from solid-state NMR results, only contains two crystallographically distinct aromatic carbons at positions 3 and 5, with the 2 and 6 positions now being nearly symmetrical and therefore not distinguishable by NMR.



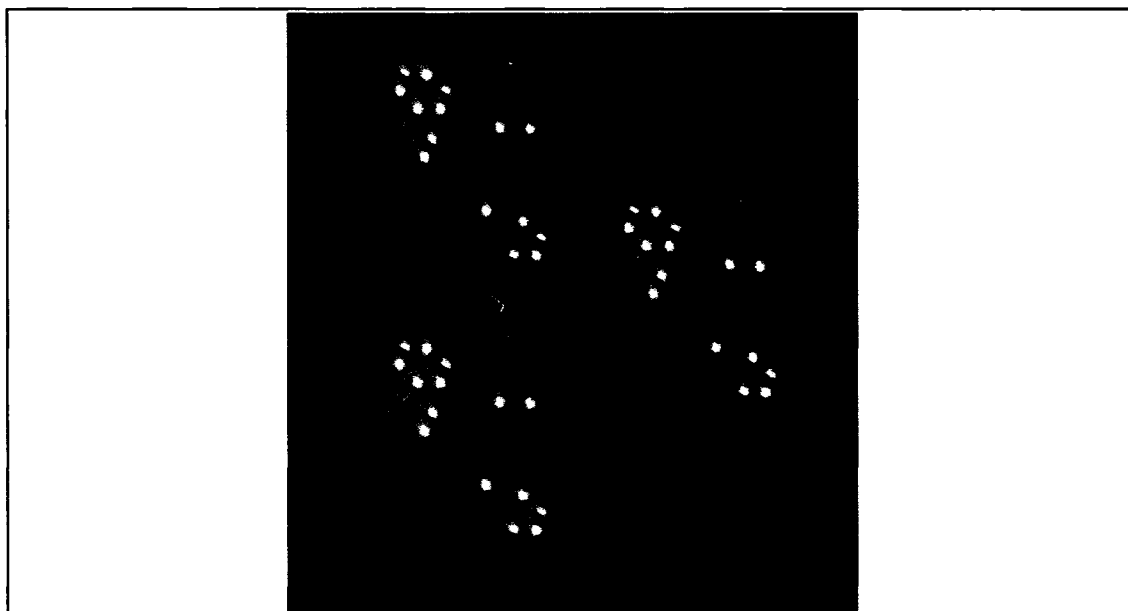


Figure 8 Packing diagram of 4.26 DMSO: 1.74 Acetone: 1 6EPGR clathrate **2b**. 6EPGR units are drawn in space-filling form, with a single DMSO molecule in the majority position shown for reference.

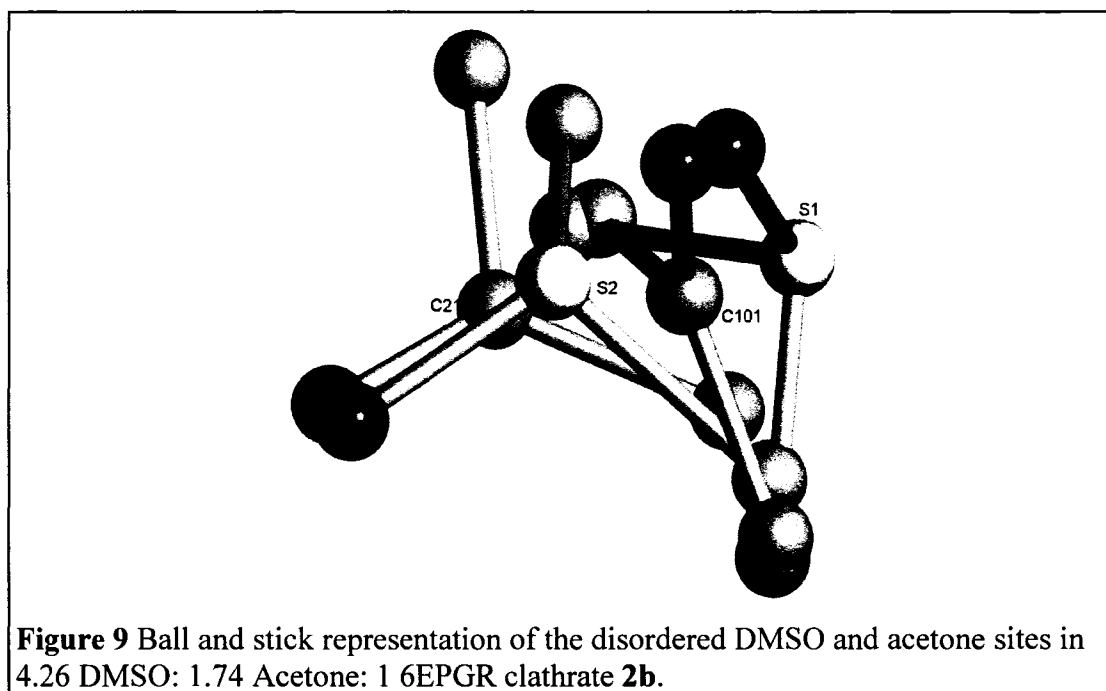
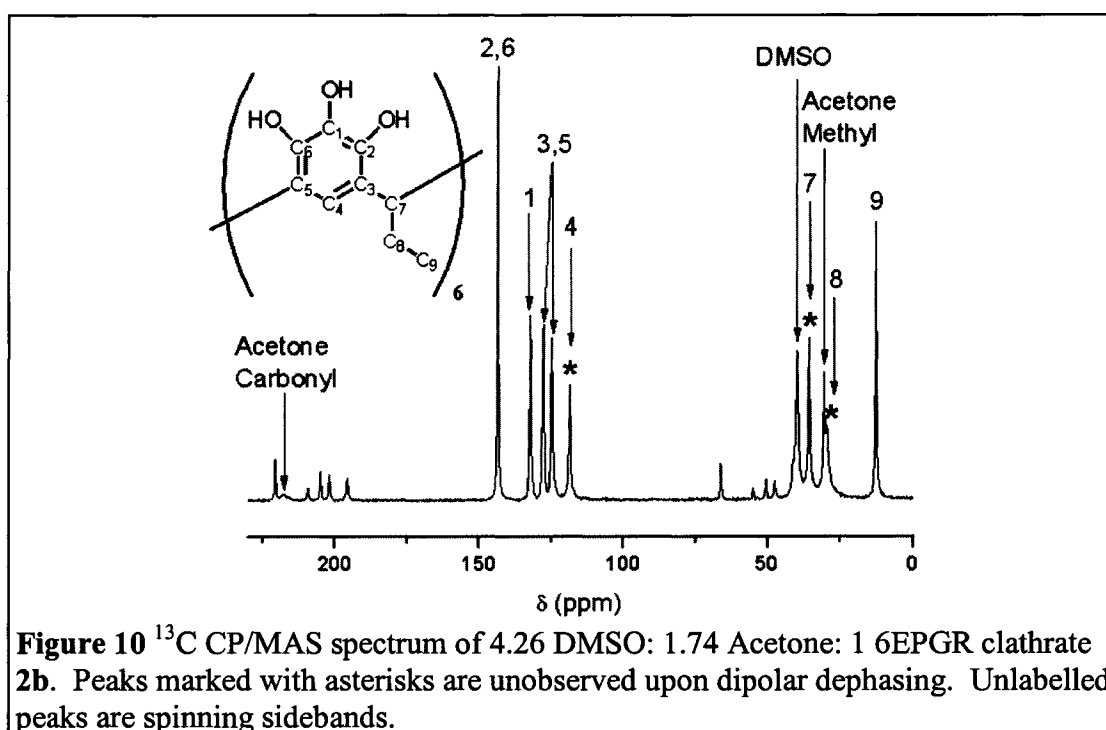


Figure 9 Ball and stick representation of the disordered DMSO and acetone sites in 4.26 DMSO: 1.74 Acetone: 1 6EPGR clathrate **2b**.

PXRD, SSNMR, and Microscopic Studies of 2b

In order to support this revised model for clathrate **2b**, we made use of solid state NMR and PXRD. The ^{13}C CP/MAS NMR spectrum of **2b** is shown in Figure 10, and is virtually identical to that of **2a**. However, two additional peaks at 30.5 ppm and at 217.4 ppm are observed, which are attributable to the methyl and carbonyl carbons of acetone. The methyl carbon is not significantly shifted from the solvent value (30.5 ppm in solid, 29.9 ppm in liquid), while the carbonyl carbon shows a ~ 10 ppm shift downfield from the solvent value of 206.7 ppm. This shift can be attributed to the carbonyl oxygen hydrogen bonding with the hydroxyl on the adjacent aromatic ring, leading to decreased electron density surrounding the carbon, deshielding it. Furthermore, since the cross polarization process is generally ineffective in liquids due to reliance on J coupling,^[23] the acetone is clearly included in the solid material.



The PXRD pattern clearly indicates that **1 2b** is isostructural to **2a**, with the major peaks appearing at the same 2θ values (see Figure 11). Along with the NMR results, this partially resolves the question as to the role of acetone in the transformation of **1** to **2b**, as it now appears that the acetone is partially displacing the DMSO from the two crystallographically unique positions in **1**, such that the equivalent of one molecule of DMSO ultimately remains. However, such a mechanism could be consistent with simple leaching of DMSO out the crystal as well as a recrystallization process. Microscopic investigations were used in order to fully clarify the nature of the transformation.

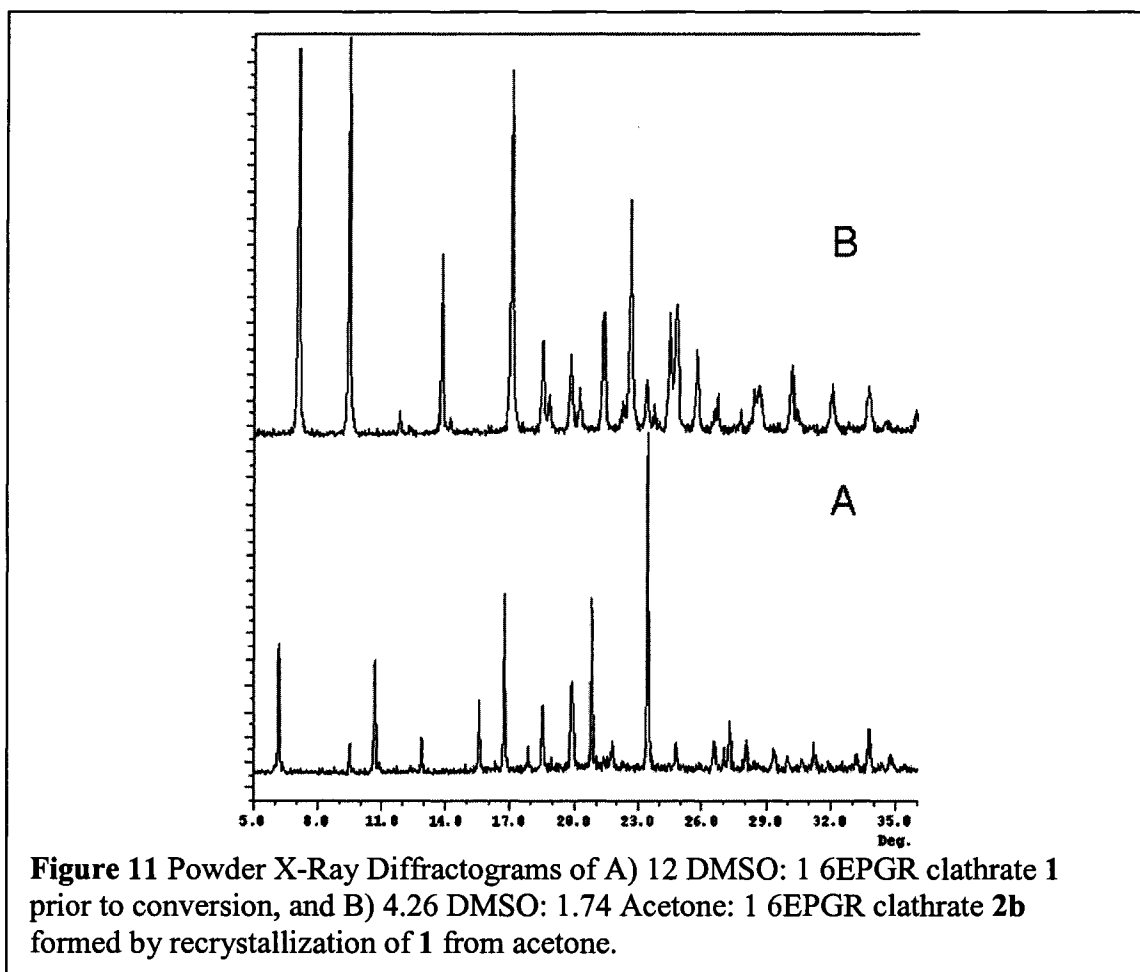
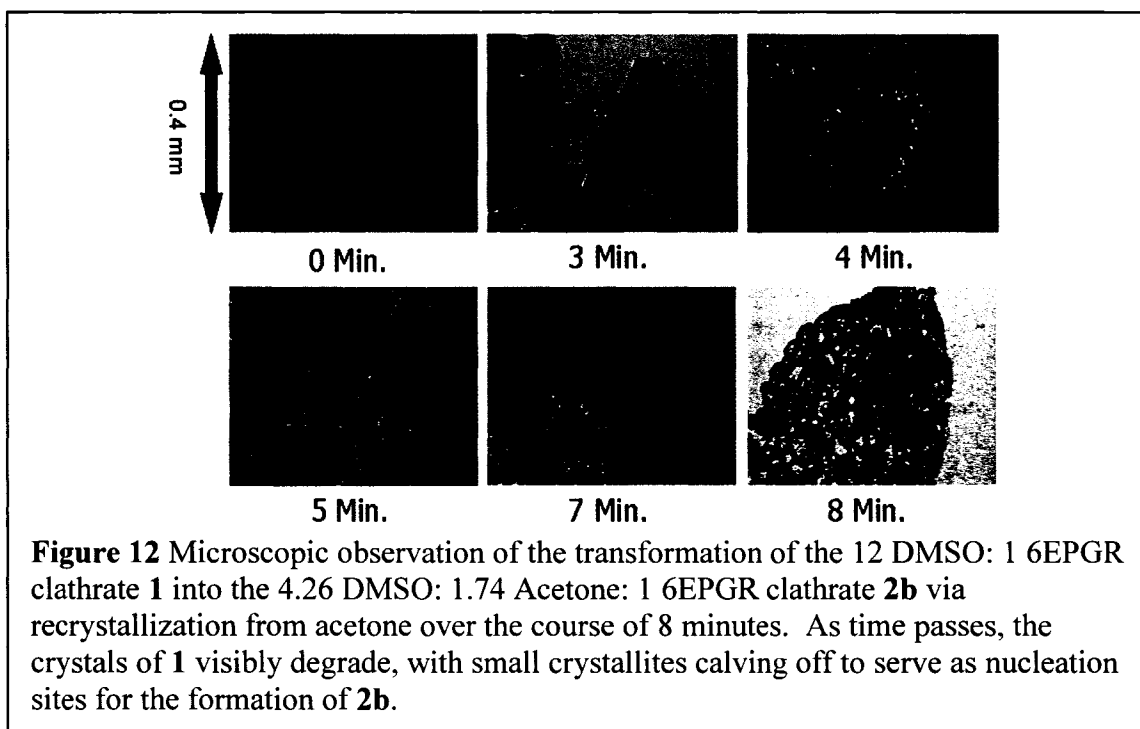


Figure 12 shows the transformation of crystals of **1** to **2b** by bathing with acetone as observed under a microscope. The process is quite rapid with such a small amount of material, and can be clearly seen to consist of dissolution followed by recrystallization. The crystals of **1** cleave into small fragments and nearly immediately recrystallize to form **2b**. The small fragments of **1** are quite likely serving as seeds for the formation of **2b**. As such, the DMSO is unlikely to be able to fully dissociate from the molecules of 6EPGR, and some acetone is in fact trapped within the new crystal, resulting in the mixed solvent crystals posited by our improved crystallographic model. However, the TGA results suggest that this acetone is readily lost from the bulk material, and is likely present in proportions less than that observed for the single crystal. Given this, extended storage in the atmosphere likely results in the formation of a clathrate structurally identical to **2a**. This is in fact the case, as SSNMR of **2b** left in air for a few days yields a spectrum identical to that observed for **2a**. Whether the acetone is replaced by DMSO through redistribution of solvent from the remaining bulk material or partial collapse of the framework (yielding small amounts of desolvated materials), or is present in such small quantities when prepared for TGA such that the influence on the desorption is negligible is unclear.



5. Conclusion

As with the *rctt* isomer of PGR (see Chapter VIII), the configuration rules out discrete inclusion motifs involving guest inclusion within the cavity of the calixarene,^[17] as the hydrogen bonding along the rim required to support the formation of such a cavity is physically impossible without isomerization. Instead, a channelled motif involving intermolecular hydrogen bond formation is favoured. Furthermore, by expanding the size of the host, the resulting symmetry of the inclusion compound is further adjusted to a hexagonal structure. Despite this, by disrupting the intermolecular hydrogen bonding scheme between adjacent molecules of the pyrogallarene, the channelled structure is again only adjusted, as opposed to forcing massive changes in the framework. While the structural motif is only adjusted a modest amount, the formation of DMSO clathrates with 6EPGR is clearly more complex than initially thought, with three distinct pseudopolymorphs existing.

Clathrate **1** is the parent inclusion compound, which can be transformed into both **2a** through heating and **2b** through recrystallization. Based on our observations, it is now clear that heating will not result in a single crystal to single crystal transformation as the shift in crystalline morphology is sufficient to cause the destruction of the original crystal. The recrystallization process, on the other hand, results in retention of DMSO despite massive excesses of acetone due to the fact that the new crystals of **2b** rapidly reform in the same vicinity as the original crystal, preventing a considerable proportion of the DMSO from diffusing away. The resulting compound contains both acetone and DMSO, with the acetone rapidly lost to yield a pseudo 6 guest :1 host clathrate. In both cases, the resulting reduction in hydrogen bonding intermediaries results in a contraction of the structure, with the overall structural motif being retained.

As a result, unlike the amines stabilized by 4-*t*-butylcalix[4]arene,^[24-26] the increased number of hydroxyl moieties allows for the formation of an intermediate structure, where hydrogen bonding still has a role to play. This clearly indicates that at least six of the hydrogen bonds formed by solvent with the 6EPGR are significantly stronger than the others. Presumably, this is because the structure only has to shift slightly to accommodate the more compact packing scheme, but detailed calorimetric studies of the transformation of **1** into **2** would be required to establish how the transformation proceeds. In conjunction with this, adsorption studies on the two pseudopolymorphs would serve to establish whether the resulting channels are accessible to gases, and exactly how dramatic the shift in the channel affects such properties.

6. References

- [1] C. D. Gutsche, *Calixarenes*, Royal Society of Chemistry, Cambridge, **1989**.
- [2] C. D. Gutsche, *Calixarenes Revisited*, Royal Society for Chemistry, Cambridge, **1998**.
- [3] L. Mandolini, R. Ungaro, *ed.*, *Calixarenes in Action*, Imperial College Press, London, **2000**.
- [4] L. R. MacGillivray, H. A. Spinney, J. L. Reid, J. A. Ripmeester, *Chem. Commun.* **2000**, 517.
- [5] L. R. MacGillivray, J. L. Atwood, *J. Am. Chem. Soc.* **1997**, *119*, 6931.
- [6] L. R. MacGillivray, P. R. Diamente, J. L. Reid, J. A. Ripmeester, *Chem. Commun.* **2000**, 359.
- [7] T. Gerkensmeier, W. Iwanek, C. Agena, R. Frohlich, S. Kotila, C. Nather, J. Mattay, *Eur. J. Org. Chem.* **1999**, 2257.
- [8] J. L. Atwood, L. J. Barbour, A. Jerga, *Chem. Commun.* **2001**, 2376.
- [9] L. R. MacGillivray, J. L. Atwood, *Nature* **1997**, *389*, 469.
- [10] A. Shivanyuk, J. Rebek Jr., *Chem. Commun.* **2001**, 2424.
- [11] A. Shivanyuk, J. C. Friese, S. Doring, J. Rebek Jr., *J. Org. Chem.* **2003**, *68*, 6489.
- [12] H. Konishi, T. Nakamura, K. Ohata, K. Kobayashi, O. Morikawa, *Tetrahedron Lett.* **1996**, *37*, 7383.
- [13] O. Morikawa, M. Yanagimoto, H. Sakakibara, K. Kobayashi, H. Konishi, *Tetrahedron Lett.* **2004**, *45*, 5731.
- [14] T. Klimova, E. Klimova, R. A. Vazquez, N. M. Gutierrez, M. Martinez, *Fuller. Nanotub. Carbon Nanostruct.* **2003**, *11*, 269.
- [15] C. Naumann, E. Roman, C. Peinador, T. Ren, B. O. Patrick, A. E. Kaifer, J. C. Sherman, *Chem. Eur. J.* **2001**, *7*, 1637.
- [16] T. Gerkensmeier, C. Agena, W. Iwanek, R. Frohlich, S. Kotila, C. Nather, J. Mattay, *Z. Natur. B Chem. Sci.* **2001**, *56*, 1063.
- [17] P. O. Brown, G. D. Enright, J. A. Ripmeester, *CrystEngComm* **2006**, DOI: 10.1039/b603883b.
- [18] M. Coruzzi, G. D. Andreotti, V. Bocchi, A. Pochini, R. Ungaro, *J. Chem. Soc. Perkin Trans. 2* **1982**, 1133.
- [19] M. Luostarinen, A. Ahman, M. Nissinen, K. Rissanen, *Supramol. Chem.* **2004**, *16*, 505.
- [20] B. W. Purse, A. Shivanyuk, J. Rebek Jr., *Chem. Commun.* **2002**, 2612.
- [21] J. L. Atwood, L. J. Barbour, A. Jerga, B. L. Schottel, *Science* **2002**, *298*, 1000.
- [22] G. D. Enright, I. L. Moudrakovski, J. A. Ripmeester, Unpublished Data, **2006**.
- [23] S. R. Hartmann, E. L. Hahn, *Phys. Rev. A* **1962**, *128*, 2042.
- [24] P. O. Brown, K. A. Udachin, G. D. Enright, J. A. Ripmeester, *Chem. Eur. J.* **2006**, in press.
- [25] P. O. Brown, K. A. Udachin, G. D. Enright, J. A. Ripmeester, *Chem. Commun.* **2005**, 4402.
- [26] K. A. Udachin, G. D. Enright, P. O. Brown, J. A. Ripmeester, *Chem. Commun.* **2002**, 2162.

Chapter X: Conclusions and Future Work

1. Supramolecular Frameworks based on 4- <i>t</i> -butylcalix[4]arene	375
2. Supramolecular Frameworks based on Resorcinarenes	377
3. Summary of Contributions	379

1. Supramolecular Frameworks based on 4-*t*-butylcalix[4]arene

In the course of studying the inclusion chemistry of 4-*t*-butylcalix[4]arene (4tBC4A) with amines, it has been demonstrated that complex, 3-dimensional frameworks can be derived from a simple host. Based principally on physical characterization by single crystal X-ray diffraction (SCXRD) and solid-state NMR (SSNMR) spectroscopy, it has been shown that the acid base chemistry of the amines and calixarenes gives rise to a disruption in the symmetry of the host molecule that leads to hydrogen bonding and stabilization through inclusion in the calixarene cavity competing with each other. This competition gives rise to a new family of structures that upon disruption of the hydrogen bonding through heating, give rise to related pseudopolymorphs and both *apo* forms of 4tBC4A.

This balance of forces can be tuned using other methods as well. The size of the alkyl tail of the amine, as well as its bulk, can be used to drive the formation of layered and constricted channelled structures. Conversely, difunctional amines, with their additional opportunities for hydrogen bonding, give rise to larger amine clusters with liquid-like characteristics. Even further tuning of these frameworks is possible by introducing additional hydrogen bonding intermediaries, such as water, or by coordination to a metal centre.

These amine clusters are accessible for the purposes of carrying out chemical reactions. They are available to serve as ligands to metal centres, with Ag^+ proving to be readily included in such structures. This is a consequence of the flexible coordination sphere of Ag^+ readily adapting to the secondary coordination offered by the calixarene framework. With isobutylamine, this allows for the formation of a solid solution, due to the near equivalence of the amine cluster and the amine- Ag^+ cluster. The amines are also accessible for gas adsorption, with both n-butylamine and ethanolamine exhibiting significant uptake of CO_2 when compared to similar systems.

The current work therefore represents a basis for further studies into how competition of forces in 4tBC4A might be used to further investigate non-covalent interactions in calixarenes, and how such systems can be used to produce functional materials. The role of concentration was only briefly examined for n-butylamine, and future studies involving other amines may indicate other pseudopolymorphs are favoured at reduced concentrations. Likewise, DSC studies may reveal undiscovered intermediate pseudopolymorphs. The dynamics of the various amine inclusion systems is only surveyed in the current work using ^{13}C SSNMR spectroscopy and SCXRD. Further investigations using techniques such as ^2H SSNMR spectroscopy would serve to further clarify the role that molecular motion of the guests play in some of the more disordered structures (particularly the large droplets observed for the difunctional amines). Similarly, further probing of the local symmetry of the amine clusters through ^{15}N SSNMR spectroscopy would help to resolve some of the dynamics and disorder in these systems.

In terms of the chemistry that might be carried out by amine clusters in 4tBC4A, the coordination chemistry of other metal centres should prove enlightening as to the relative strengths of the interactions at play. With regards to Ag, ^{109}Ag SSNMR could potentially clarify the nature of the reductive process at work in the calixarene. More detailed studies involving careful control of the time and silver loading would help to further clarify the formation of solid solutions and how much control can be exerted over the formation of the nanoparticles obtained by heating. Further TEM studies would help to clarify the nature of the resulting assemblies. Finally, practical applications of these frameworks as gas adsorbents and catalysts would entail more systematic studies of the kinetics and thermodynamics of gas adsorption, as well as spectroscopic studies to monitor the catalytic transformation of sample substrates, such as ethylene.

2. Supramolecular Frameworks based on Resorcinarenes

Competition between non-covalent interactions has also been shown to play a significant role in guiding the structural motifs of resorcinarenes. Under acidic conditions, organic cations prompt the formation of channelled structures by resorcinarenes and inorganic anions. The geometry of the cations and anions control the specific arrangement of these channels, while residual solvent serves to reinforce these networks. This dependence on solvent resulted in it not being possible at this time to carry out ion exchange or detailed structural studies of the desolvated frameworks. Future studies should therefore focus on using solvents that with decreased hydrogen bonding potential, along with guests that might serve to be flexible enough to displace solvent from secondary channels. Similarly, it would be of considerable interest if an *apo*

form of C-methylcalix[4]resorcinarene could be fully characterized through isolation of a single crystal by way of sublimation or through a molecular recognition phenomenon similar to that observed for C-methylpyrogall[4]arene.

The studies of alternate conformers of tetrameric and hexameric pyrogallarenes demonstrate that such materials also show potential for producing complex structures based on competition between non-directional interactions, and various hydrogen bonding possibilities. For C-methylpyrogall[4]arene, the difference in molecular recognition properties allowed for structural characterization of the first *apo* form of a resorcinarene. This *rctt* isomer appears to be well suited to the formation of channelled structures. Future studies of such a material could entail a closer examination of the potential porosity of this isomer (using He pycnometry and ^{129}Xe NMR spectroscopy to probe the void-space, along with gas adsorption studies). DSC studies of this *apo* form would also be interesting, to see if other phases similar to those observed for the guest free form of 4tBC4A exist. The geometry may also make such networks better suited to formation of ionic frameworks with higher stability in the absence of solvent.

In the case of C-ethylpyrogall[6]arene, the competition between different hydrogen bonding partners (DMSO, Acetone and adjacent hosts) gives rise to an array of pseudopolymorphs. Again, the combination of SSNMR and SCXRD was vital to fully modeling this system, clarifying how competition between forces of the same class was involved in guiding the structural motifs of such frameworks. In this case, the unusual conformation of the host results in an intriguing channelled structure that again calls for further study by spectroscopy and physical studies of adsorption. By the same token, the

persistence of DMSO suggests that recrystallization from other hydrogen bonding solvents might give rise to related pseudopolymorphs. The nature of the *apo* forms of this material also remains a subject for future investigations.

3. Summary of Contributions

In conclusion, the role of multiple non-covalent interactions in guiding the structural motifs in 4tBC4A and resorcinarenes has been examined. The chemistry of 4tBC4A and amines represent a new family of inclusion compounds unlike those previously examined, and the studies presented here demonstrate how such non-covalent assemblies can be used to produce functional materials capable of gas adsorption and formation of Ag nanoparticles. For the resorcinarenes, competition between cationic and anionic guests allows for conformation control of C-methylcalix[4]resorcinarene. Alternate conformers of pyrogallarenes produce channelled frameworks that can be mediated through competition between hydrogen bonding interactions, giving rise to pseudopolymorphism similar to that observed for 4tBC4A with amines. These studies provide a firm basis for the use of simple calixarenes to design non-covalent functional materials.